MULTI-OMICS BIOMARKERS OF METABOLIC HOMEOSTASIS OF RISK FACTORS ASSOCIATED TO NON-COMMUNICABLE DISEASES

Julia Hernandez Baixauli

UNIVERSITAT ROVIRA I VIRGILI
MULTI-OMICS BIOMARKERS OF METABOLIC HOMEOSTASIS OF RISK FACTORS ASSOCIATED TO NON-COMMUNICABLE DISEASES
Julia Hernandez Baixauli
UNIVERSITAT ROVIRA i VIRGILI

eurecat
Centre Tecnològic de Catalunya

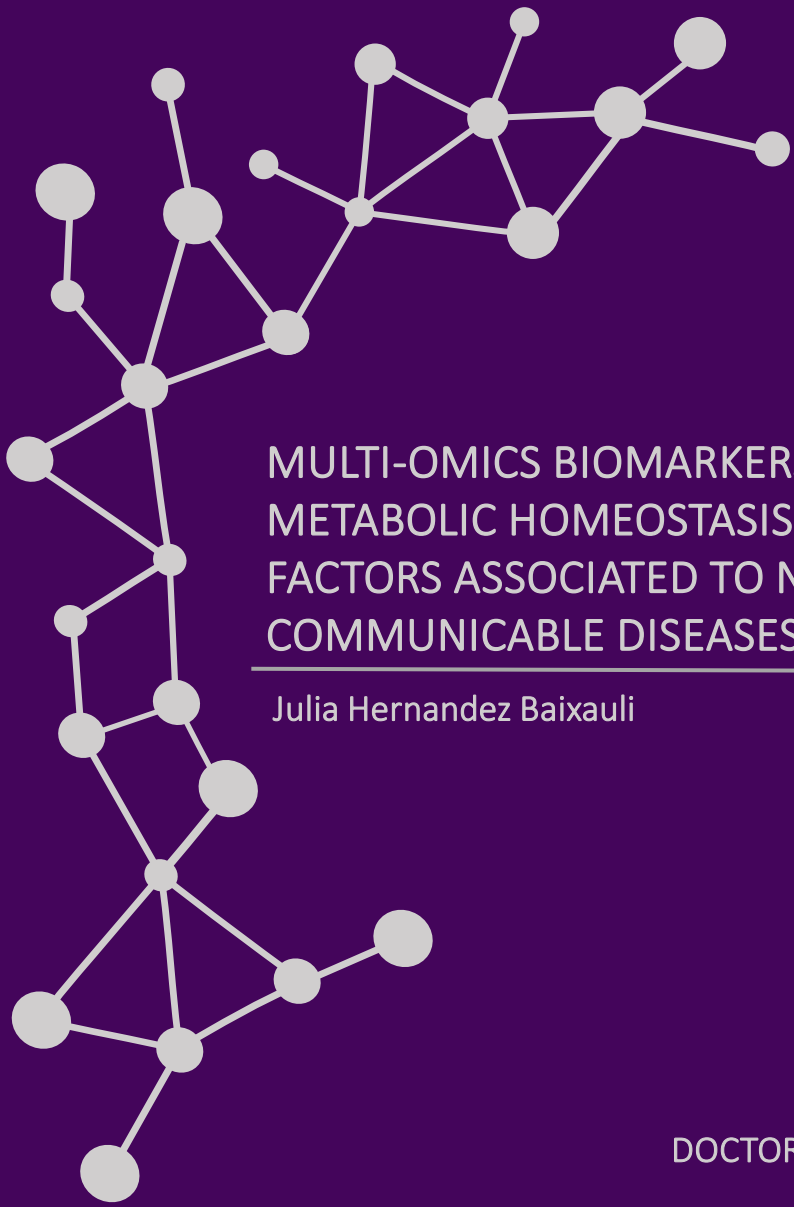

MULTI-OMICS BIOMARKERS OF METABOLIC HOMEOSTASIS OF RISK FACTORS ASSOCIATED TO NON-COMMUNICABLE DISEASES

Julia Hernandez Baixauli

DOCTORAL THESIS
2022

UNIVERSITAT ROVIRA I VIRGILI
MULTI-OMICS BIOMARKERS OF METABOLIC HOMEOSTASIS OF RISK FACTORS ASSOCIATED TO NON-COMMUNICABLE DISEASES
Julia Hernandez Baixauli

Julia Hernandez Baixauli

MULTI-OMICS BIOMARKERS OF METABOLIC HOMEOSTASIS OF RISK FACTORS ASSOCIATED TO NON-COMMUNICABLE DISEASES

DOCTORAL THESIS

Supervised by

Dr. Miquel Mulero Abellán

Dr. Josep Maria del Bas Prior

Department of Biochemistry and Biotechnology

Eurecat, Unitat de Nutrició i Salut

UNIVERSITAT ROVIRA i VIRGILI

eurecat

Reus 2022

UNIVERSITAT ROVIRA I VIRGILI
MULTI-OMICS BIOMARKERS OF METABOLIC HOMEOSTASIS OF RISK FACTORS ASSOCIATED TO NON-COMMUNICABLE DISEASES
Julia Hernandez Baixauli

UNIVERSITAT ROVIRA i VIRGILI

Departament de Bioquímica i Biotecnologia
Campus Sescelades (Edif. N4)
C/ Marcel·lí Domingo, 1
43007 Tarragona

Centre tecnològic de Catalunya
Unitat de Nutrició i salut
Av. Universitat, 1
43204 Reus

FAIG CONSTAR que aquest treball, titulat "**Multi-omics biomarkers of metabolic homeostasis of risk factors associated to non-communicable diseases**", que presenta **Julia Hernandez Baixauli** per a l'obtenció del títol de Doctor, ha estat realitzat sota la meva direcció al **Departament de Bioquímica i Biotecnologia** d'aquesta universitat i que compleix els requisits per poder optar a la Menció Internacional de Doctorat.

HAGO CONSTAR que el presente trabajo, titulado "**Multi-omics biomarkers of metabolic homeostasis of risk factors associated to non-communicable diseases**", que presenta **Julia Hernandez Baixauli** para la obtención del título de Doctor, ha sido realizado bajo mi dirección en el **Departamento de Bioquímica y Biotecnología** de esta universidad y que cumple con los requisitos para poder optar a la Mención Internacional de Doctorado.

I STATE that the present study, entitled "**Multi-omics biomarkers of metabolic homeostasis of risk factors associated to non-communicable diseases**", presented by **Julia Hernandez Baixauli** for the award of the degree of Doctor, has been carried out under my supervision at the **Department of Biochemistry and Biotechnology** of this university and that this thesis is eligible to apply for the International Doctorate Mention.

Reus, 9 de març del 2022
Reus, 9 de marzo del 2022
Reus, the 9th of March 2022

Els directors de la tesi doctoral
Los directores de la tesis doctoral
Doctoral Thesis Supervisors

Miguel Mulero Abellán - DNI 39885398V (SIG)
Signat digitalment per Miguel Mulero Abellán - DNI 39885398V (SIG)
Data: 2022.03.08 09:21:47 +01'00'

Firmado por DEL BAS PRIOR, JOSE MARIA (FIRMA) el día 08/03/2022 con un certificado emitido por AC DNIE 004

Dr. Miquel Mulero Abellán

Dr. Josep Maria del Bas Prior

UNIVERSITAT ROVIRA I VIRGILI
MULTI-OMICS BIOMARKERS OF METABOLIC HOMEOSTASIS OF RISK FACTORS ASSOCIATED TO NON-COMMUNICABLE DISEASES
Julia Hernandez Baixauli

"Nothing in life is to be feared,

it is only to be understood.

Now is the time to understand more,

so that we may fear less."

Marie Curie

UNIVERSITAT ROVIRA I VIRGILI
MULTI-OMICS BIOMARKERS OF METABOLIC HOMEOSTASIS OF RISK FACTORS ASSOCIATED TO NON-COMMUNICABLE DISEASES
Julia Hernandez Baixauli

Acknowledgements

"When eating fruit, remember

the one who planted the tree."

Vietnamese proverb

Pot ser aquesta és una de les parts més complicades de la tesi, ja que considere que és molt difícil agrair com voldria a tot el món. Podria començar per la senyoreta Rosa que quan tenia quatre anys va incentivar la meva part més curiosa, passant per totes les figures que han continuat alimentant i motivant el meu interès per la ciència, i finalment acabant pels meus directors de tesi. Sense oblidar tots els que han tingut un paper important a la meua vida personal. Per això, vull donar les gracies a tots i totes que ho heu fet possible.

En primer lloc, voldria agrair al Dr. Miquel Mulero tot el seu suport, dedicació i guia des del primer dia a l'últim, ja que has format part d'aquest llarg viatge des del principi. He après moltíssim durant les reunions revisant els articles i també ha sigut molt divertit treballar amb tu. En segon lloc, voldria agrair al Dr. Josep M. Del Bas la seva ajuda en aquesta etapa final de la tesi i sobretot la seva comprensió en determinats moments delicats d'aquests moments finals. Sempre tens moltes idees/consells que m'han fet reflexionar i m'han ajudat a millorar el meu treball. També, voldria agrair a la Dr. Laura Baselga que em va acompanyar pràcticament durant tota aquesta aventura i que em donés l'oportunitat de participar en aquest projecte.

Voldria agrair a tots els companys d'Eurecat el seu suport i ajuda durant tota aquesta etapa. Principalment voldria agrair a tot l'equip tècnic la seva ajuda en la meva formació. Heu invertit molt de temps em formar-me i ajudar-me amb els dubtes i problemes que he tingut al estabulari i laboratori. També a tots els investigadors que m'heu donat consells i ajudat en tot el que estava a la vostra mà. I a la resta de doctorands dels quals he après molt i em crescut junts. Al cap i a la fi, a tot l'equip d'Eurecat, sense vosaltres no hagués sigut possible!

I would like to thank Dr. Marnix Morissen for the opportunitty of doing my intership with his group in Nijmegen (The Netheerlands). Bedankt dat je me naar je lab hebt laten komen en me de fantastische wereld van zebrafia hebt laten zien, me hebt begeleid en me vrijelijk hebt laten leren en genieten. Bovenal wilde ik Jan Zethof bedanken voor zijn vriendelijkheid en zijn goede gevoel voor humor. Bedankt.

Finalment, voldria donar les gràcies als meus, la meua família i amics que sempre heu estat al meu costat. Tots els que heu patit al meu costat i heu confiat en mi durant tot aquest viatge. Gràcies infinites!

UNIVERSITAT ROVIRA I VIRGILI
MULTI-OMICS BIOMARKERS OF METABOLIC HOMEOSTASIS OF RISK FACTORS ASSOCIATED TO NON-COMMUNICABLE DISEASES
Julia Hernandez Baixauli

This research work performed in this PhD has been financially supported by the Catalan Government through the funding grant ACCIÓ-Eurecat (PRIV2019-PREVENTOMICS) and by the Centre for the Development of Industrial Technology (CDTI) of the Spanish Ministry of Science and Innovation under grant agreement: TECNOMIFOOD project. CER-20191010.

This thesis has been carried out in the Unit of Nutrition and Health of Eurecat in collaboration with Universitat Rovira i Virgili (URV) thanks to the Vicente Lopez fellowship (Eurecat).

An international phase has been completed in the Department of Animal Ecology & Physiology of the Radboud University in Nijmegen (The Netherlands) under the supervision of Dr. Marnix Gorissen to obtain the European PhD mention. This short stage was supported by a personal EMBO Short-Term Fellowship grant.

UNIVERSITAT ROVIRA I VIRGILI
MULTI-OMICS BIOMARKERS OF METABOLIC HOMEOSTASIS OF RISK FACTORS ASSOCIATED TO NON-COMMUNICABLE DISEASES
Julia Hernandez Baixauli

Index

UNIVERSITAT ROVIRA I VIRGILI
MULTI-OMICS BIOMARKERS OF METABOLIC HOMEOSTASIS OF RISK FACTORS ASSOCIATED TO NON-COMMUNICABLE DISEASES
Julia Hernandez Baixauli

Summary

Nowadays, common medical problems such as obesity, metabolic syndrome, cardiovascular diseases, cancer, and neurodegenerative diseases, which are non-communicable (NCD), are considered multifactorial diseases. This means that a cluster of risk factors, associated with disrupted metabolism, influence the development of NCDs. For this reason, as Van Ommen *et al*. proposed, the onset of NCDs arise from the imbalance of a few overarching processes that are mainly metabolic stress, inflammatory stress, oxidative stress, and psychological stress. Monitoring these overarching processes opens the door to the possibility of modulating them, therefore preventing the onset of different NCDs by designing more precise personalized interventions or treatments. Nevertheless, current disease biomarkers cannot assess the early alterations that might lead to the development of disease, highlighting the need to define new biomarkers to identify early deviations.

Thus, the present work presents a characteristic metabolic signature for the detection of specific processes using omic technologies. These include the deregulation of carbohydrate metabolism and lipid metabolism, hypertension, and gut dysbiosis, as representative of metabolic stress; inflammation stress; oxidative stress and psychological stress. For this purpose, different animal models were developed using different induction approaches to isolate the different risk factors of interest. After the validation of the animal models by classical biomarkers, homeostasis disturbances were defined through the characterisation of the systemic metabolism using omics approaches. To assess the metabolic profile, GC-qTOF and UHPLC-qTOF were performed to evaluate plasma metabolome; ^{1}H-NMR was used for the evaluation of urine metabolome; additionally, shotgun metagenomics sequencing was carried out for the characterization of the cecum microbiome.

Finally, a metabolic profile was assessed for each risk factor and a predictive model was achieved which can discriminate among the different risk factors. The results indicated that, lipids and tricarboxylic acid (TCA) cycle intermediates are the most promising components of the metabolic profile. The lipid profile is unique for each one of the risk factors. Nevertheless, in all the risk factors, diacylglycerols (DGs) are the lipidic metabolites with the greatest impact on metabolic profiles. Specifically, DG 36:4 and DG 34:2 are the common compounds that link arachidonic acid metabolism with the different risk factors. In inflammation, oxidative and psychological stress, the other key player is the TCA cycle which is the central mitochondrial energetic pathway. Particularly, alpha-ketoglutarate is one of the most promising intermediates as a biomarker due to its multiple roles in mitochondrial metabolism. In consequence, the presented metabolic profile is a potential tool for the monitoring of risk factors and could open a window to target the onset of diseases and try to prevent and treat them.

Resum

En la actualitat, els problemes mèdics més comuns com l'obesitat, la síndrome metabòlica, les malalties cardiovasculars, el càncer i les malalties neurodegeneratives, es consideren malalties multifactorials, a més a més de no ser transmissibles. Això significa que un grup de factors de risc, associats amb el metabolisme alterat, influeixen en el desenvolupament d'aquestes malalties. Per aquesta raó, com Van Ommen *et al.* va proposar, l'inici d'aquestes malalties es deu al desequilibri d'uns processos generals que són principalment estrès metabòlic, estrès inflamatori, estrès oxidatiu i estrès psicològic. El seguiment d'aquests processos obre la porta a la possibilitat de modular-los, evitant així l'inici de diferents malalties mitjançant el disseny d'intervencions o tractaments personalitzats més precisos. No obstant això, els biomarcadors de malalties actuals no poden avaluar les alteracions inicials que podrien portar al desenvolupament de la malaltia, destacant la necessitat de definir nous biomarcadors per identificar les desviacions primerenques.

Per tant, el treball actual presenta una signatura metabòlica característica per a la detecció d'aquests processos específics utilitzant tecnologies òmiques. Aquests inclouen la desregulació del metabolisme dels carbohidrats i el metabolisme dels lípids, la hipertensió i la dysbiosis intestinal, com a representant de l'estrès metabòlic; l'estrès inflamació; l'estrès oxidatiu i l'estrès psicològic. Per a aquest propòsit, es van desenvolupar diferents models animals utilitzant diferents aproximacions per tal d'aïllar els diferents factors de risc d'interès. Després de la validació dels models animals pels biomarcadors clàssics, les pertorbacions de l'homeòstasi es van definir a través de la caracterització del metabolisme sistèmic utilitzant enfocaments òmics. Per avaluar el perfil metabòlic, GC-qTOF i UHPLC-qTOF es van realitzar per avaluar el metaboloma del plasma; 1H-NMR es va utilitzar per a l'avaluació del metaboloma de l'orina; addicionalment, es va dur a terme la seqüenciació de la metagenòmica mitjançant shotgun per a la caracterització del microbioma cecal.

Finalment, es va avaluar un perfil metabòlic per a cada factor de risc i es va establir un model predictiu que pot discriminar entre els diferents factors de risc. Els resultats indicaven que, els lípids i els intermediaris del cicle de l'àcid tricarboxílic (TCA) són els components més prometedors del perfil metabòlic. El perfil lípid és únic per a cadascun dels factors de risc. En tots els factors de risc, els diacilglicerols (DG) són els metabòlits lipídics amb major impacte en els perfils metabòlics. Concretament, el DG 36:4 i el DG 34:2 són els compostos comuns que uneixen el metabolisme de l'àcid araquidònic amb els diferents factors de risc. En inflamació, estrès oxidatiu i psicològic, l'altre protagonista clau és el cicle del TCA, que és la ruta energètica mitocondrial central. En particular, l'alfa-cetoglutarat és un dels intermedis més prometedors com a biomarcador a causa dels seus múltiples rols en el metabolisme mitocondrial. En conseqüència, el perfil metabòlic presentat és una eina potencial per al seguiment dels factors de risc i podria obrir una finestra per apuntar a l'inici de les malalties i intentar prevenir-les i tractar-les.

Abbreviations

1C metabolism: one carbon metabolism

2-OGDD: 2-oxoglutarate-dependent dioxygenases

3d CUMS: 3 days Chronic Unpredictable Mild Stress

8-OHdG: 8-hydroxy-2'-deoxyguanosine

ALP: alkaline phosphatase

ALT: alanine transaminase

ALX: alloxan

ANGPTL3: angiopoietin-like 3

ANGPTL4: angiopoietin-like 4

ANOVA: analysis of variance

Apo: apolipoprotein

AST: aspartate transaminaseç

BCAA: branched-chain amino acid

CAT: catalase

CE: capillary electrophoresis

ChoE: cholesteryl ester

CMS: Chronic Mild Stress

COSY: correlated spectroscopy

COVID-19: coronavirus disease 2019

COX: cyclooxygenases

CRD: chronic respiratory disease

CRP: C-reactive protein

CUMS: Chronic Unpredictable Mild Stress

CVD: cardiovascular disease

DAMP: damage-associated molecular pattern

dB: decibel

DBP: diastolic blood pressure

DG: diacylglycerol

DIABLO: Data Integration Analysis for Biomarker discovery using Latent cOmponents

DNMT: DNA methyltransferase

DSS rats: Dahl salt-sensitive rats

EPM: elevated plus maze

ESI: Electrospray ionization

FFA: fatty acid

FHH: fawn-hooded hypertensive rats

FST: forced swim test

GABA: ɣ-aminobutyric acid

GC: gas chromatography

GDM: gestational diabetes mellitus

GGT: ɣ-glutamyl transferase

GPx: glutathione peroxidase

GUCY1A1: guanylate cyclase 1 soluble subunit alpha 1

GWAS: genome-wide association studies

H_2O_2: hydrogen peroxide

HbA1c: glycated haemoglobin

HDAC: histone deacetylase

HDL: high-density lipoprotein

HFD: high-fat diet

HMDB: Human Metabolome Database

HMG CoA reductase: 3-hydroxy-3-methylglutaryl coenzyme A reductase

$HO^{\bullet}$: hydroxyl radical

HOCl: hypochlorous acid

HPA axis: hypothalamic-pituitary-adrenocortical axis

HPLC: high performance liquid chromatography

HSD11B2: 11 beta-hydroxysteroid dehydrogenase 2

HSQC: heteronuclear single-quantum correlation

IDL: intermediate-density lipoprotein

IL-1β: interleukin-1β

IL-6: interleukin-6

IL-8: interleukin-8

IP: intraperitoneal

KEGG: Kyoto Encyclopaedia of Genes and Genomes

LC: liquid chromatography

LDH: lactate dehydrogenase

LDL: low-density lipoprotein

LOX: lipoxygenases

Lp(a): lipoprotein(a)

LPC: lysophospholipid

LPS: lipopolysaccharide

MetS: metabolic syndrome

MINT: Multivariate INTegration

miRNA: micro-RNA

MS: mass spectrometry

MTNR1B: melatonin receptor 1B

MWAS: microbiome wide association studies

NAFLD: non-alcoholic fatty liver disease

NCD: non-communicable disease

ncRNA: noncoding RNA

NEFA: non-esterified free fatty acid

NeuroD1: neurogenic differentiation 1

NMR: nuclear magnetic resonance

$O_2^{\bullet-}$: superoxide anion

OFT: open field test

OGTT: oral glucose test tolerance

OLPS-DA: Orthogonal Projections to Latent Structures Discriminant Analysis

$ONOO^-$: peroxynitrite anion

OUT: operational taxonomic unit

P407: poloxamer 407

PAMP: pathogen-associated molecular pattern

PC: phosphatidylcholine

PCA: principal components analysis

PCSK9: proprotein convertase subtilisin/kexin type 9

PLA_2: phospholipase A_2

PLC: phospholipase C

PLD: phospholipase D

PLS-DA: partial least squares-discriminant analysis

PQ: paraquat or 1,10-dimethyl-4,40-bipyridinium dichloride

REN: renine

RGD: Rat Genome Database

ROS: reactive oxygen species

rRNA: ribosomal RNA

SAM: sympathetic-adrenal-medullary system

SBP: systolic blood pressure

SHR rats: spontaneously hypertensive rats

SM: sphingomyelin

SMPDB: Small Molecule Pathway Database

SNP: single nucleotide polymorphisms

SOD: superoxide dismutase

SPT: sucrose preference test

STZ: streptozotocin

T1DM: type 1 diabetes mellitus

T2DM: type 1 diabetes mellitus

T3DM: type 3 diabetes mellitus

TC: total cholesterol

TCA cycle: tricarboxylic acid cycle

TG: triglycerides

TMAO: trimethylamine N-oxide

TNF-α: tumour necrosis factor-alpha

TOCSY: total correlation spectroscopy

TOFMS: time-of-flight mass spectrometry

TTM: total thiol molecules

VLDL: very low-density lipoprotein

WBC: white blood cells

WGS: whole genome shotgun sequencing

WHO: World Health Organization

WKY rats: Wistar Kyoto rats

UNIVERSITAT ROVIRA I VIRGILI
MULTI-OMICS BIOMARKERS OF METABOLIC HOMEOSTASIS OF RISK FACTORS ASSOCIATED TO NON-COMMUNICABLE DISEASES
Julia Hernandez Baixauli

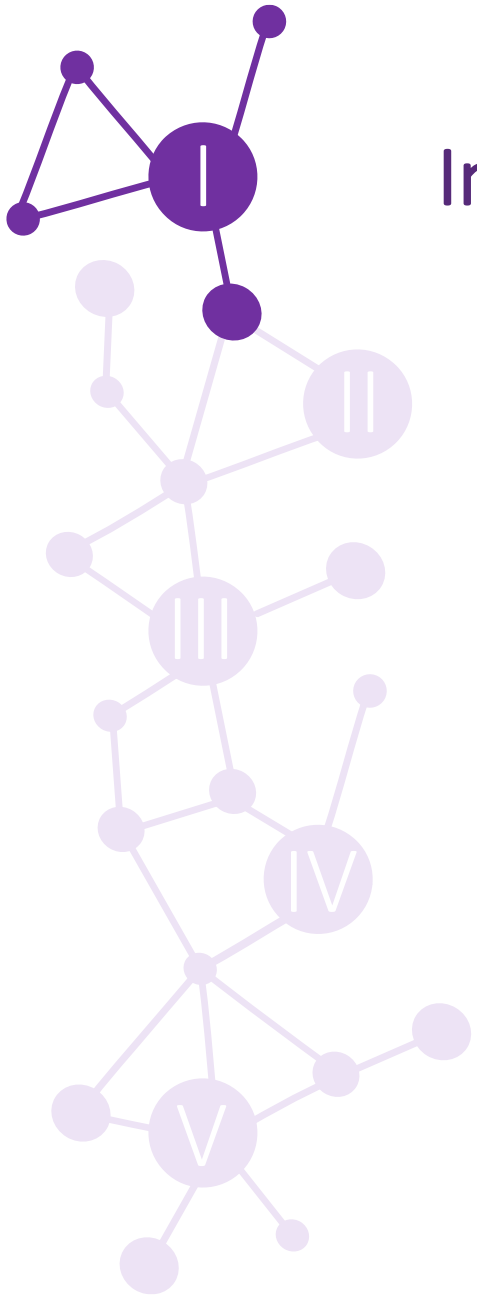

Introduction

UNIVERSITAT ROVIRA I VIRGILI
MULTI-OMICS BIOMARKERS OF METABOLIC HOMEOSTASIS OF RISK FACTORS ASSOCIATED TO NON-COMMUNICABLE DISEASES
Julia Hernandez Baixauli

I. Introduction

1. Non-communicable diseases (NCDs)

Non-communicable diseases (NCDs), also known as chronic diseases, are a group of diseases that are not spread from person to person (non-contagious origin) [1]. In fact, NCDs are the result of a combination of multiple risk factors (i.e., genetic, physiological, environmental and behavioural factors) [2]. This means that this kind of diseases tend to be both long-term and slow progressing. Thus, NCDs are a subset of unnoticed harmful diseases that threaten public health without showing any symptoms until the clinical debut of the disease. Patients with NCDs, or people who are more susceptible to developing one of them, need long-term prevention/care that is personalized, proactive, and ongoing [3]. According to the World Health Organization (WHO), the main NCDs are cardiovascular diseases (CVDs), diabetes, cancer, neurodegenerative disorders, and chronic respiratory diseases (CRDs). Evolving over time, the concept of NCDs has been widespread to cover a wider range of health problems, such as hepatic, renal, and gastroenterological diseases, endocrine, haematological, and neurological disorders, dermatological conditions, genetic disorders, trauma, mental disorders, and disabilities (e.g., blindness and deafness) [4].

1.1. Global impact of NCDs

This silent epidemic is an under-appreciated cause of poverty and hinders the economic development of many countries. The burden of NCDs is growing every year regarding the number of people, families and communities affected. Annually, the WHO compiles a list of the biggest threats to highlight the current global health problems. In 2019, NCDs were considered the second-highest threat regarding its severity order (**Figure 1**). In 2021, NCDs fell to the eighth-highest threat position due to the outbreak of the coronavirus disease 2019 (COVID-19) (**Figure 1**). However, the current pandemic has aggravated the previous mentioned situation about NCDs. In fact, having a NCDs is associated with an increased risk of severe COVID-19, and more likely to die from it [5].

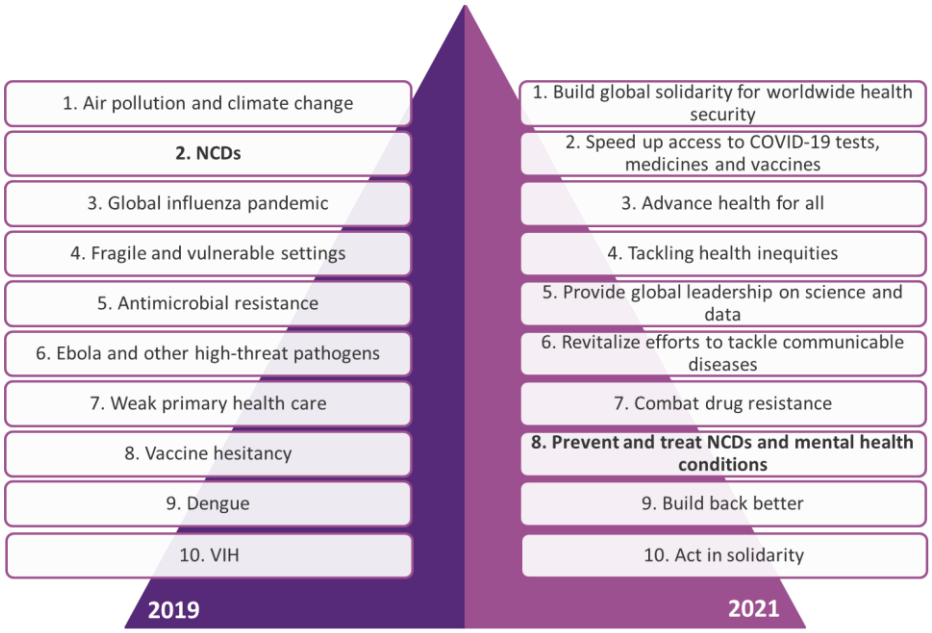

Figure 1. Global health issues to track in 2019 and 2021. List of the biggest threats to global health in 2019 and 2021 compiled by the World Health Organisation and ranked by a community of healthcare professionals [6]. NCDs (in bold) are listed as a serious threat despite the outbreak of COVID-19. Abbreviations: NCD, non-communicable disease; VIH, human immunodeficiency virus; COVID-19, coronavirus disease 2019.

These complex diseases are responsible for the death of 41 million people each year, which corresponds to 71% of global deaths. Focusing on the nature of people perished by NCDs, more than 15 million people die between the ages of 30 and 69 from premature deaths, 85% of which are concentrated in low- and middle-income countries (31.4 million people) [6]. The most harmful NCD in terms of annual deaths is CVD that account for 17.9 million people died annually; followed by cancer (9.3 million), CRD (4.1 million), and diabetes (1.5 million). Overall, the total amount of all premature deaths due to NCDs account are around the 80 % [6].

One of the increasing concerns associated to premature NCD deaths are suicides that are included in the eighth-highest threat that were tracked in 2021 (**Figure 1**). In fact, every year 703,000 people commit suicide and even more attempt suicide, making it the fourth leading cause of death for those aged 15-29 in 2019. Despite the notion that this issue only occurs in high-income countries, suicide is a global phenomenon in all regions of the world. In fact, over 77% of global suicides occurred in low- and middle-income countries in 2019 [6].

The NCD epidemic has devastating consequences on the health of individuals, families, and communities, and threatens to overwhelm national health systems. The socioeconomic costs associated with NCDs make the prevention and control of these diseases a hot topic for the 21st century [6]. In this regard, there are increasing initiatives to control and prevent these diseases as the NCD Countdown 2030 that aim

to reduce the worldwide burden of NCDs [7]. The data collected by the NCD Countdown 2030 highlights the importance of detect their risk factors and tailor interventions toward reducing the burden of NCDs.

1.2. Risk factors and metabolic risk factors for NCDs

A risk factor is an aspect of personal behaviour or lifestyle, an environmental exposure, or a hereditary characteristic that is associated with an increase in the occurrence of a particular disease, injury, or other health condition [8]. Thus, different risk factors can increase the possibilities to develop NCDs and can be classically classified in different ways. As it is shown in **Figure 2**, risk factors can be grouped as non-modifiable and modifiable ones: non-modifiable risk factors are the one that cannot be reduced or controlled by an external intervention (e.g., age, gender, and genetics). In consequence, the focus of the scientific community has been to point modifiable risk factors that can be reduced or controlled by an early intervention, reducing in consequence the probability of disease [9]. The modifiable risk factors can be also classified into three classes: (1) biological factors, including overweight, dyslipidaemia, hyperinsulinemia and hypertension; (2) behavioural factors, including diet, physical inactivity, smoking and alcohol consumption; (3) social factors, including complex combinations of interacting socioeconomic, cultural and environmental parameters [10].

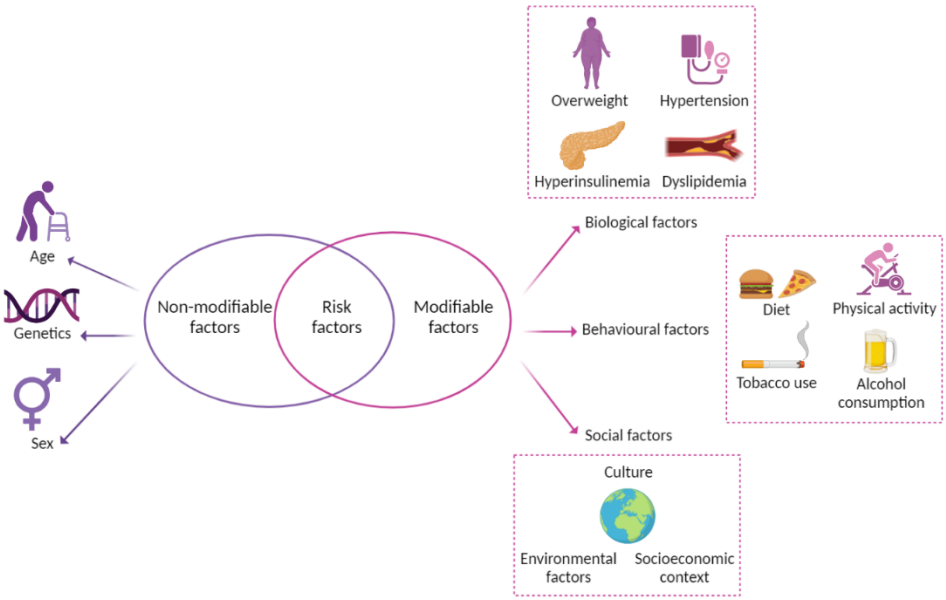

Figure 2. Modifiable and non-modifiable risk factors for NCDs.

Generally, unhealthy diets, physical inactivity, smoking and alcohol consumption, which are the main four behavioural risk factors, are the most important and influential in the context of NCDs [4]. In this sense, unhealthy diets and a lack of physical activity may be evidenced in the population as raised blood pressure, increased blood glucose, elevated blood lipids and obesity (biological factors), among

others. These aspects are also called metabolic risk factors because they are referred to the biochemical processes involved in the normal functioning of metabolism. Furthermore, these metabolic risk factors are enclosed by the metabolic syndrome concept (MetS). Thus, a more precise definition of MetS defines it as a cluster of altered conditions that includes abdominal obesity and hyperglycaemia or glucose metabolic disorder, hypertension, and heterogenic dyslipidaemia. A great amount of NCD burden is caused by CVDs and diabetes, as well as cancer and CRDs that are affected by the high prevalence of MetS [11].

Consequently, one of the critical challenges in the management of NCDs is to deal with MetS, which includes those common metabolic risk factors across the different diseases encompassed in the NCD term [12]. In fact, MetS has been considered by some researchers as a new NCD [13]. Nevertheless, in the context of NCDs, there are a complex pathophysiologic state that generates severe CVDs and diabetes [14,15]. In consequence, MetS represents a proper and suitable condition for detecting and diagnosing people that are threatened by NCDs. Therefore, the early detection of MetS among the population is pivotal for the public health systems.

1.3. Key diseases in NCDs

Different diseases associated with NCDs are interconnected through the risk factors. For this reason, it is of vital importance to accurately target each disease according to its own risk factors. In this section, the most common diseases are highlighted, and their main characteristics and their modifiable risk factors are discussed.

1.3.1. CVDs

As it has been previously discussed, CVDs are the main contributors to the global burden of disease among the NCDs; in fact, they are the major cause of deaths worldwide each year. In this sense, the sum of the number of deaths from cancer and CRDs are lower than the ones originated by CVDs [6]. Specifically, CVDs are a group of hearth disorders (i.e., rheumatic, and congenital heart disease) and blood vessels (i.e., deep vein thrombosis, pulmonary embolism, coronary heart, peripheral arterial, and cerebrovascular disease), together with acute events such as heart attacks and strokes. It represents a set of heterogeneous diseases whose underlying cause of development is most often atherosclerosis [16]. The most important metabolic risk factors of CVDs are behavioural risk factors that have been previously described for general NCDs [17]. Particularly, obesity is the main risk factor for CVDs; in fact over-weight is associated with a prevalence of comorbidities such as diabetes, hypertension, and MetS [18]. Another important risk factor gaining attention and relevance in recent times is psychological stress, which is often overlooked [19,20].

1.3.2. Cancer

Cancer is a complex aggrupation of diseases that are originated in almost any organ or tissue of the body when abnormal cells grow uncontrollably and go beyond their usual boundaries to invade adjoining tissues spreading to other organs

(metastasizing), which is the major cause of death from cancer (around 90%). Lung, prostate, colon, stomach and liver cancer are the most common types of cancer in men, while breast, colon, lung, cervical and thyroid cancer are the most common among women [21]. Cancer is the second leading cause of death globally [6], due to this disease is highly heterogeneous varying in its geographical distribution, etiologic and pathology. Therefore, the classical risk factors shared among NCDs are insufficient for the prevention of many important types of cancer, because it is a disease influenced by multiple other identified and unidentified factors [22]. Among the identified risk factors, smoking is considered to be the main cause of cancer, followed by unhealthy diets [10,23]. Moreover, both body weight gain and lack of physical activity are also associated with the most common cancers types, including breast, colon, endometrium, kidney, and esophagus cancers [24]. It has been suggested that between the 30% and 50% of cancer deaths could be prevented by modifying or avoiding key risk factors and implementing existing evidence-based prevention strategies as, for example, modifying dietary patterns [25].

1.3.3. CRDs

CRDs are a range of diseases related to airways and lungs, such as asthma and respiratory allergies, chronic obstructive pulmonary disease, occupational lung diseases, sleep apnea syndrome and pulmonary hypertension. Many risk factors for preventable CRDs have been identified being smoking and other forms of indoor air pollution the most dangerous, particularly in low- and middle-income countries [26]. Additionally, overweight associated with obesity has emerged as an important risk factor for these respiratory diseases, and in many instances weight loss is associated with important symptomatic improvements [27]. However, CRDs are not fully reversible, thus it is important to prevent the development and the progression of the disease managing the associated risk factors.

1.3.4. Diabetes

Diabetes occurs either when the pancreas does not produce insulin due to autoimmune issues (type 1 diabetes mellitus, T1DM) or when the body cannot effectively respond to the produced insulin and/or the pancreas produces it in lower amounts (type 2 diabetes mellitus, T2DM), leading to hyperglycaemia [28]. Other secondary types of diabetes are related to pregnant women with glucose intolerance (gestational diabetes mellitus, GDM) [29] and to a certain diabetic specific state, mainly associated with Alzheimer's disease, where neurons cannot adequately respond to brain insulin (type 3 diabetes mellitus, T3DM) [30]. Furthermore, diabetes mellitus may be associated with other serious diseases such as heart diseases, kidney failure, and eye damage, which may subsequently lead to blindness, and foot ulcers, which may require limb amputation. Although diabetes can be partially inherited, several risk common factors with CVDs, such as obesity, high sugar consumption, and lack of physical activity significantly contribute to the progress of the diabetic state.

1.3.5. Neurodegenerative disorders

Neurodegenerative disorders are a heterogeneous group of diseases generally characterized by progressive loss of neurons associated with deposition of proteins (showing altered physicochemical properties) in the brain and in peripheral organs, that induce effects on mobility, coordination, strength, emotion, and cognition [31]. The most frequent proteins involved in the pathogenesis of neurodegenerative diseases are amyloid-β, prion protein, tau, α-synuclein, TAR-DNA-binding protein 43 kDa, and fused-in sarcoma protein. Interestingly, the most common neurodegenerative diseases include Alzheimer's disease and Parkinson's disease. Nevertheless, the overlap and combination of neurodegenerative diseases is frequent. Additionally to sex and age, environmental, metabolic and behavioural risk factors increase the susceptibility to suffer from neurodegenerative disorders [32].

1.4. Prevention and managing of NCD: personalized nutrition

Nowadays, one of the most claimed ways of managing NCDs is through the regulation of the risk factors that lead to the disease development and can be largely preventable by several available mechanisms. The most promising approaches include an active and healthy lifestyle that implicates individual responsibility to manage the risk factors of NCDs [4]. The promotion of activities towards these goals are a low-cost way for countries and governments to reduce the number of NCD deaths. Tackling these risk factors cannot only save lives, but also reduce a significative economic burden for public health systems [33].

Since diet is a common component among most NCDs, it attracts more attention in the efforts to find more effective strategies to prevent their advancement [34]. Nevertheless, dietary habits of populations in low-to-middle income countries have rapidly shifted to unhealthy diets (consisting of processed foods, away-from-home food intake, and increased use of edible oils and sugar-sweetened beverages) in line with the global nutrition transition [35]. In this context, numerous observational studies have established the health-promoting effects of two European diets (i.e., Mediterranean and Nordic diet) based on the consumption of rich nutrient-dense foods (mostly plant-derived foods) and low energy-dense foods (mainly of animal origin), particularly regulating CVDs and T2DM [36]. In large epidemiological studies, higher adherence to a traditional Mediterranean diet was associated with a significant lower rate of all-causes mortality [37,38]. The health benefits of the Nordic diet have also been investigated (through to a lesser extent than those of the Mediterranean diet) and the results associate this diet with improvements in CVDs [39]. However, more studies are needed to determine the long-term effects of adherence to both dietary styles on disease prevalence and incidence.

Although health-promoting diets improve health, their results are not satisfactory enough to control risk factors because they neglect the variations inherent in the complexity of individual differences [40]. In this regard, over the past two decades, the scientific community has significantly advanced in analytical technologies, data science, molecular physiology, and nutritional knowledge to be able to stratify

populations at a more individual level [41]. This could be exemplified by the application of personalized nutrition, which is defined as tailor-made nutritional recommendations aimed at health promotion, health maintenance and disease prevention [42]. Personalized recommendations consider differential responses to different nutrients due to the interaction between nutrients and biological processes [43]. For this reason, different approaches such as genomics, epigenetics, metabolomics, and proteomics are used to target individual variability. The results of these methods generate a large amount of data that provides an overall picture at systemic level (systems biology). Therefore, the integration of this information is of paramount importance to obtain biomarkers, which are pivotal for developing a personalised nutritional approach [44].

One of the main challenges of nutritional studies is a valid and reliable assessment of metabolic state and its effects on the body. Measurement of food intake is usually based on questionnaires, which have inherent limitations. This issue can be overcome using health status biomarkers that are capable of objectively assess metabolic state without the bias of food intake and self-reported dietary assessment. Currently, there are no health status biomarkers available to address the metabolic deviations that ultimately lead to the development of NCDs. Altogether, the challenge is to have integrative health status biomarkers as well as early disease-state biomarkers that can be corrected/modulated by personalised nutrition [45].

Indeed, the goals of personalized nutrition go beyond prevention and mitigation of NCDs, and include multiple aspects of health, such as mood, weight maintenance, medical conditions (e.g., glucose control or blood pressure management) among other multiple well-being aspects. Interestingly, the Diabetes Prevention Program, which is established by the US National Institute of Diabetes and Digestive and Kidney Diseases, provided evidence that a multiyear lifestyle modification program is more effective than metformin treatment in reducing the incidence of diabetes in high-risk people [46].

2. Biomarkers of health status

As it has been previously highlighted, the limitation of the dietary assessment to estimate homeostatic status determines the need for biomarkers of health status. Therefore, these biomarkers of health need to be able to identify and quantify disease states and progression by unbiased and accurate quantification of the metabolic status. These types of biomarkers represent a new approach that reflect the maintenance of optimal health that is the main objective of diet and nutrition. For this reason, it is highly important to provide biomarkers of the early stages of alterations before the unbalanced health status (homeostasis disruption) [45]. Accordingly, those biomarkers should be considered as health status biomarkers instead of disease biomarkers.

With a focus on the general concept of health, the initial definition was “a state of complete physical, mental and social well-being and not merely the absence of

disease or infirmity" that was published in 1948 since the constitution of the WHO [47]. However, this concept has been evolving to be defined as a more flexible concept as the ability to adapt and self-manage to achieve homeostasis [48]. In the past decade, Van Ommen *et al*. proposed that many diseases emerge from the imbalance of a few overarching processes that are key in the maintenance of homeostasis [49]. Thus, they propose as key overarching processes: metabolic stress, inflammatory stress, oxidative stress and psychological stress [49]. This concept opens the door to new ways of interpreting the origin of prevalent NCDs and might provide the basis for quantifying health.

In line with the concept of health status, the management of health must be done by using biomarkers of health status. The biomarker concept refers to the concise measure used to perform a clinical assessment for monitoring and predicting health status in individuals or across populations, so that an appropriate therapeutic intervention can be planned [50]. Thus, biomarkers of health indicate an end-point reflecting the different intermediate disease phenotypes or the severity of the disease and are extensively used in the clinical practise [45].

Currently, the available technologies for the detection of these small changes are not powerful enough to elucidate these subtle deviations [45]. This is attributed to the fact that a functional, even suboptimal, homeostasis tends to maintain the levels of circulating molecules (i.e., hormones, cytokines, metabolites) within a certain range of values [45,51]. This means that these circulating molecules need great changes or the onset of disease to fall outside the boundaries of normality (when the homeostatic capacity of the individual has been overcome). Therefore, the measurement of the health status of a healthy individual without extensively stressing him is challenging. An alternative to target small deviations is the use of combinations of single biomarkers, which is known as biomarker profile, which is based on the additivity or multiplicity of effects [52]. This approach results in a more sensitive manner of assessing changes in the homeostasis of the overarching processes, since slight undetectable changes in different biomarkers might become detectable if the combination is considered. At the same time, important changes in a single, but relevant biomarker of the signature does not affect the capacity of detection.

To further explore this issue, it has been proposed that challenging homeostasis through different punctual stressors could be a useful strategy to measure the adaptive capacity of the individual to counteract the effects of the stressor [51,53]. Disruption in the homeostatic capacity can result in metabolic alterations leading to the development of an unbalanced physiological state [49]. However, the individual characterization might involve multiple functional tests that are difficult to apply and extend in current health systems or in a personalized nutrition approach. An alternative approach should be based on the idea that the overarching processes previously mentioned are associated to different pathways and physiological processes that can be assessed and quantified by means of biomarkers measured by omics technologies.

In the past decades, the improvement in omics technologies has opened new research avenues in the biomarkers research field and have provided unprecedented insights in the responses of the genome, epigenome, transcriptome, proteome, and metabolome (**Figure 3**). In fact, the technological development has been continuous improving, especially with regards to DNA and RNA sequencing [54], mass spectrometry (MS) [55], single-cell omics [56] and, of course, bioinformatics [57]. Furthermore, rather than a single deviation as is previously described, it is likely that there will be a profiling of different biomarkers and omics that, together with machine-learning tools will provide a more sensitive and specific diagnostic and prognostic approaches to NCDs [58]. In this regard, systems approach allows the assessment of a comprehensive and in-depth view of the physiology/pathology of an individual and open the possibility for the identification of new biomarkers or profiles of biomarkers that link overarching processes with health and homeostasis.

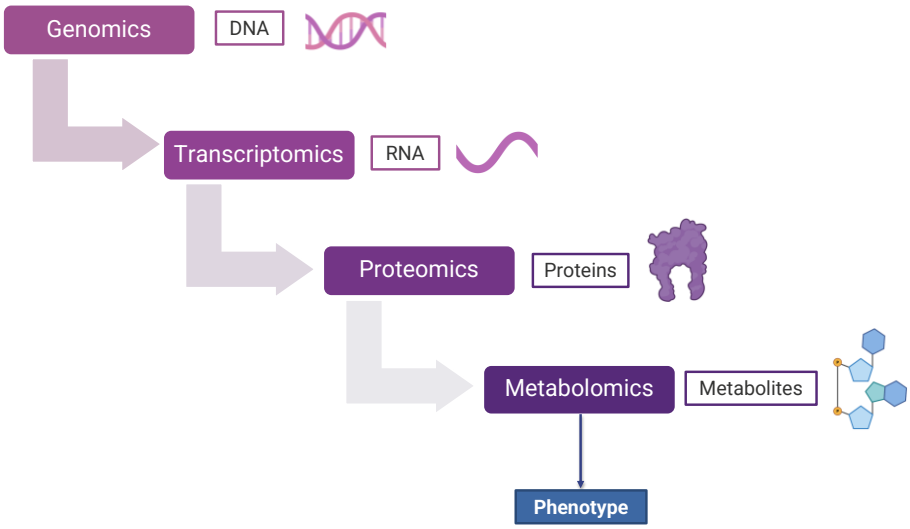

Figure 3. The omics cascade. This cascade represents from genomics (genes) to metabolomics (metabolites). Metabolomics represents the downstream output of the genome being the final step in the cascade, thus this omic is closer to the phenotype than the preceding omics.

2.1. Genomic biomarkers

A genomic biomarker is a measurable DNA or RNA feature that is an indicator of either anormal or pathogenic processes. Furthermore, it could be related to therapeutic or other kind of intervention [59]. Due to the publication of the human genome project data, thousands of genes contributing to human diseases have been discovered facilitating the characterisation of the different genotypes during the last years [60]. Those genes have provided a paramount tool for personalized medicine focusing on the genetic “architecture” of the diseases.

Many of these genomic biomarkers have been identified by genome-wide association studies (GWAS) [61]. For example, in the case of T2DM, 300 loci have been robustly associated with higher disease risk [62]. One of this important region is

related to the regulation of melatonin receptor 1B (*MTNR1B*), the neurogenic differentiation 1 (NeuroD1) binding site in a DNA islet enhancer upstream of *MTNR1B* that influences the expression of *MTNR1* [63]. In the case of CVDs, near 161 loci have been associated with the disease [64]. The first important biomarkers found in CVDs has been a single nucleotide polymorphisms (SNPs) on chromosome 9p21 and its variants [65]. In fact, several genes are presently targeted in a personalized therapy based on the genetic CVDs susceptibilities (e.g., proprotein convertase subtilisin/kexin type 9 (*PCSK9*), guanylate cyclase 1 soluble subunit alpha 1 (*GUCY1A1*), angiopoietin-like 3 and 4 (*ANGPTL3*, *ANGPTL4*)) [64].

The research of genomic biomarkers has been intensified in the last years revealing that a significant proportion of clinical studies have been inconclusive or non-replicable [66]. For example, the SNPs variants to be tested are often identified according to their appearance in defined populations (i.e., Caucasians, Hispanics, Asians, Arabs, Africans) leading to errors due to the different geographical origins. In general, there are some limitations on the studies involving genetics: (1) poor quality of test samples; (2) analysing somatic instead of germline DNA; (3) noisy data; (4) poor quality of analytical methods; (5) lack of phenotype identification; (6) inadequate study design and statistical analysis planning [67]. These problems could be attributed to the lack of standardization and the continuous development of these methodologies. However, the lack of the phenotype association is related to the kind of target, which is DNA or RNA, thus a possible solution to this limitation is to target other types of biomarkers that connect the genotype with the environment.

2.2. Epigenetic and transcriptional biomarkers

The connection between genotype and environment could be studied by the use of epigenetics that is the study of changes in gene function that are heritable and not attributed to alterations of the DNA sequence [68]. This epigenetic features can be employed as biomarkers, thus explaining differences among patient phenotypes with a clear genetic connection (endophenotypes) [69]. Epigenetic modifications include large-scale DNA methylation changes throughout the genome as well as alterations in the compendium of post-translational chromatin modifications. These modifications involve changes in gene expression that change the accessibility to DNA without changing its sequence, leading to silencing or downregulation/upregulation of gene expression [70].

Additionally, post-transcriptional regulation of gene expression by noncoding RNAs (ncRNAs) is also considered a part of the epigenetic machinery. Micro-RNAs (miRNAs) are small ncRNAs that contribute to regulation of the expression of different epigenetic regulators such as DNA methyltransferases (DNMTs) and histone deacetylases (HDACs), among others [71]. Similarly, DNA methylation and histone modifications can regulate the expression of miRNAs indicating a feedback mechanism.

For example, several epigenetic modifications have been detected in the progression of hypertension [72]: the 11 beta-hydroxysteroid dehydrogenase 2 (*HSD11B2*) promoter, whose low activity has been associated with the induction of hypertension, is highly methylated favouring its low transcription [73]; histone 3 (H3K4 or H3K9) demethylation is induced by lysine-specific demethylase-1 (LSD1) and modify, in consequence, gene transcription [74]. In the case of miRNAs, miRNA-9 and miRNA-126, they presented low expression levels in hypertensive patients and are related to hypertension prognosis and organ damage [75]. Therefore, although most of the epigenetic mechanisms are being intensively investigated, miRNAs are the most evaluated for their use as predictive biomarkers.

For instance, epigenetic biomarkers overcome the limitation of genetic biomarkers regarding the phenotype consideration. However, some limitations should be considered: (1) lack of large multicentre studies to provide convincing evidence for clinical applicability; (2) technical challenges; (3) noisy data (high background level); (4) shortcomings related to the DNA or miRNA quality. Some of these challenges must be solved before the efficacious use of epigenetic biomarkers in the clinical field [72].

2.3. Proteomic biomarkers

Proteomics involves the application of several technologies for the identification and quantification of overall present protein content of a cell, tissue or organism [76]. The use of proteins is widely carried out in reductionist approaches for clinical tests in the diagnosis and prognosis of diseases by Western blot, ELISA, or immunological assays. In this sense, proteomics provides a holistic view that offers high-throughput information on the global content of proteins, in contrast with the classical reductionist approximation [76]. Primarily, human diseases involve changes in the expression of normal proteins or the creation of abnormal proteins, which perturb the body homeostasis.

Proteomics approaches for the identification of biomarker are delimited by the protein characteristics and the current available techniques. The initial proteomics methodology used was two-dimensional electrophoresis that presents several limitations: (1) bias toward the most abundant proteins; (2) non- detection of proteins with extreme properties (e.g., extreme size or pH); (3) time consuming and costly [77]. Recent advances in MS have overcome the problems with two-dimensional electrophoresis providing results with greater sensitivity, specificity and resolution [78]. Furthermore, a promising proteomic approach is the protein array capable to detect changes in protein expression and post-translational modifications of thousands proteins at the same time [77]. An example of the use of proteomic biomarkers is the detection of advanced glycation end-products (post-translational modifications of proteins) that are considered potential biomarkers for changes in glucose metabolism related to diabetes [79]. The use of proteomics together with metabolomics has been increasing and the creation of combined data bases is expected to help the identification of new metabolic profiles [80].

2.4. Metabolomic biomarkers

2.4.1. Characteristics of metabolomic biomarkers

Metabolomics can be defined as the analysis or screening of small metabolites present in samples of biological origin [81]. In fact, metabolomic biomarkers are a downstream expression of the genome, the proteome, the transcriptome, and their modifications. Thus, metabolomics can closely represent the biochemical phenotype of an organism at any point in time, which is a notable advantage of the metabolome over the genome [82]. Another advantage is that current metabolomics tools offer some advantages like being faster, cheaper, and more sensitive compared to other techniques.

In this regard, there are many published articles on the metabolomics field for the assessment of metabolic profiles; this fact highlights the advantages of metabolomic biomarkers. Those studies are focused on different objectives of general interest in clinical problems: new drug discovery [83]; early disease diagnosis as CVDs [84]; inborn errors of metabolism [85] or Alzheimer disease [86]; monitoring cancer prognosis, diagnosis, and treatment [87]. For example, the emerging role of metabolomic biomarkers in obesity disease research has opened new opportunities to improve early diagnosis and the subsequent prognosis with the identification of key metabolites [88]. The list of potential metabolomic biomarkers has been evidenced by the integration of the past, present, and future studies leading to an accurate metabolomic profile of biomarkers. In this sense, the data generated by these tools must be properly analysed for the construction of biochemical pathways and for understanding how these pathways interact in different states between health and disease states [89]. In general, metabolome-based biomarkers, along with others identified, using the previously described omics techniques, are of great interest in nutrition, because they can be used to monitor intake in epidemiological or intervention studies, which could complement the results of dietary questionnaires.

2.4.2. Metabolomic pipeline

The general pipeline that is mainly followed in metabolomic studies contains the following steps (**Figure 4**) [90]: (1) experimental design; (2) sample collection, preparation and metabolite extraction; (3) data acquisition and processing; (4) data analysis; and (5) biomarker identification.

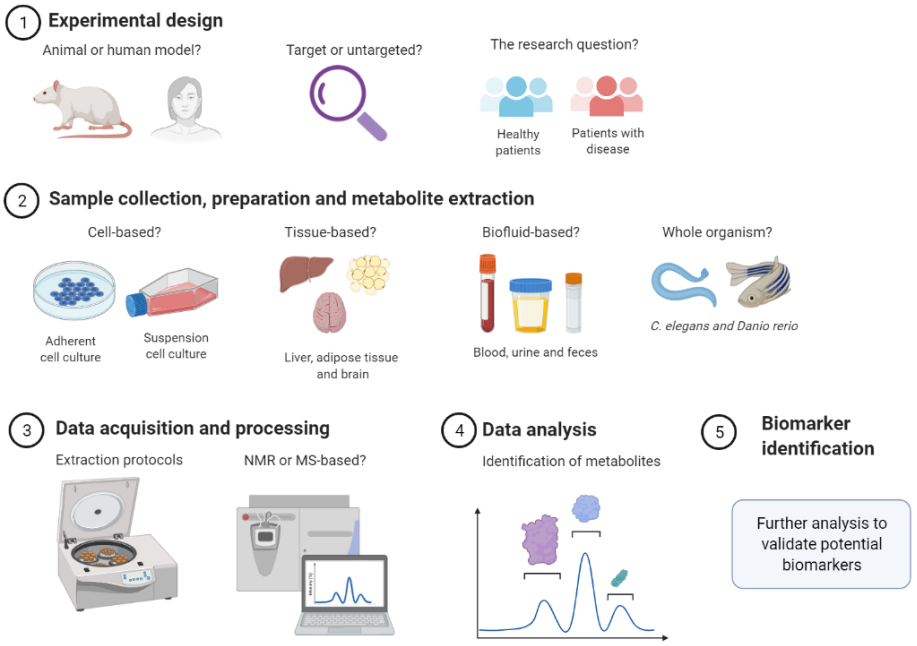

Figure 4. Pipeline of metabolomic process. The first stage involves experimental design, followed by sample collection, preparation, and metabolite extraction. Next is acquisition and processing of data, then data analysis, and finally, making sense of the data through biomarker discovery.

During the experimental design, different questions need to be answered before starting the procedure. The experimental design should start with a scientific question that need to be answered by the study. It is essential to choose the appropriate model to determine and examine the most influential factors that are relevant for the hypothesis under investigation. Therefore, some key questions need to be answered: (1) the type of model such as animal or human models, targeted or untargeted and healthy or unhealthy individuals; (2) whether to be cell based, tissue based (e.g., liver, adipose tissue, brain, muscular tissue), fluid-based (e.g., blood, urine, faeces, seminal fluid, saliva, bile, cerebrospinal fluid) or the whole organism [91].

One of the first technical questions is about targeted and untargeted approaches that will determine the experimental design, sample preparation, and analytical techniques. On the one hand, the targeted approach focus on the accurate identification and quantitation of a defined set of metabolites related to a predetermined scientific question [92]. Normally, this set of metabolites are predetermined by the scientific question, which could be selected manually and considering the available metabolite library. For example, a targeted approach identified a set of amino acids (i.e., isoleucine, leucine, valine, tyrosine and phenylalanine) that strongly predict T2DM [93]. On the other hand, untargeted or global approach is used to measure all the possible metabolites from a biological sample thought the identification of as many signals as possible across a sample set, followed by the assignment of these signal to a metabolite by using datasets [94]. Untargeted studies are highly dedicated to the identification of unknown metabolites,

especially in the discovery of novel biomarkers. Metabolomics strategies, both targeted and untargeted, have clearly contributed to biomarker discovery over the last twenty years and many reports provide the evidence of metabolomics as a key tool for biomarker discovery on biomedical research [95]. Recently, the trend in metabolomics research indicated the need for coupling the two main approaches to form a hybrid approach. Being the greatest challenge the maximization on the detection; as well as on the accuracy during the identification of thousands of metabolites [96].

Once this has been stablished, the next phase is the sample collection, preparation, and metabolite extraction. Sample should be quenched immediately after harvesting with liquid nitrogen to arrest metabolism and prevent induction of "stress" metabolites which can mislead the analysis [91]. Sample preparation typically entails metabolite extraction and enrichment, depletion of proteins and removal of sample matrix depending on the approach. After the extraction protocols, the analysis is performed by the two main analytical platforms used in metabolomics that are nuclear magnetic resonance (NMR) and MS. Both approaches are capable of high throughput reproducible measurement of several metabolites.

The fourth step is statistical analysis, which involves a univariate and a multivariate analytical approach. Finally, the last step of the pipeline is biomarker discovery using data libraries and bioinformatics tools.

2.4.3. Analytical platforms for data acquisition

Metabolomic biomarkers of health status can only be achieved by using powerful analytical tools, which are characterized by its high sensitivity, specificity, and precision, to obtain accurate metabolic profiles. In this context, many analytical platforms have been used in metabolomic studies. As has been previously described, the two predominant analytical platforms applied in this field are NMR and MS. In this sense, the global characterization of the metabolome requires the combination of different techniques, because both of these platforms have limitations in their applicability for the investigation of specific metabolites (as summarized in **Table 1**) [97].

Table 1. Comparison of the most common analytical platforms employed in metabolomics. Abbreviations: NMR, nuclear magnetic resonance; MS, mass spectrometry; GC, gas chromatography; LC, liquid chromatography; CE, capillary electrophoresis.

	NMR	MS		
		GC-MS	LC-MS	CE-MS
Sensitivity	Low (limited to high abundance metabolites)	High		
Resolution	Low	High		
Analysis time	Reduced analysis time (high-throughput analysis)	High (long separation step)		
Reproducibility	Very high	High	Relatively high	
Sample handling	Minimum	Derivatization step	Relatively simple	
Destructive	No	Yes		
Metabolic coverage	Limited to 100 metabolites	Low molecular weight (volatile) metabolites	Hydrophobic and hydrophilic metabolites	Polar and ionic metabolites
Metabolite identification	Easy (superior to MS)	Easy (spectral libraries)	Difficult (databases need to be improved)	
Targeted analysis	Not optimal	Better for targeted analysis than NMR		
Instrument cost	More expensive than MS	Cheaper than NMR		
Sample cost	Low cost per sample	High cost per sample		

Nuclear magnetic resonance (NMR)

The use of NMR is extensive in metabolomics due to its high reproducibility and short analysis time, which allows a high throughput analysis of samples in a few minutes [98]. In NMR spectroscopy, a compound is placed in a magnetic field, then isotopes within the compound (e.g., ^{1}H, ^{13}C, ^{14}N, ^{15}N, ^{17}O) absorb the radiation and resonate at a frequency which is dependent on its location in the small molecule [99]. Although the most common is the one dimensional ^{1}H-NMR approach, two dimensional methods can also be employed to enlarge metabolome coverage, including COSY (correlated spectroscopy), TOCSY (total correlation spectroscopy) and HSQC (heteronuclear single-quantum correlation) [100].

One advantage of NMR is that it is a non-destructive technique and requires a relatively simple sample preparation, thus those samples could be reused for further studies. Another advantage of NMR technique is its non-discriminant character, since its sensitivity does not depend on physicochemical characteristics of analytes, allowing the simultaneous determination of diverse metabolites. The NMR spectra provides important structural information and facilitates the identification of individual metabolites through the interpretation of chemical shifts and coupling constants. Nevertheless, some limitations must be considered like low spectral resolution and sensitivity, which limits its applicability to the detection of the highest

abundant metabolites in simple samples. These challenges are the focus of numerous research efforts to try to improve their performance like enhancing the sensitivity with the use of cryogenically cooled probes, micro probes and increasing magnetic field strength [101].

Mass spectrometry (MS)

MS is a more sensitive methodology that is capable to detect numerous classes of metabolites and identify them through fragmentation experiments using tandem MS. For this reason, there are multiple sample introduction systems and ionization sources that can be employed; expanding in consequence the analytical coverage of MS approaches [102]. Therefore, MS is the main methodology used for the metabolic characterization of complex systems despite its lower robustness compared to NMR. The simplest instrumental configuration is direct MS analysis without previous separation step as chromatographic or electrophoretic separation. Despite its high-throughput screening capability due to the reduced analysis time, this technique presents important drawbacks making the use of complementary hyphenated approaches mandatory. Anyway, direct MS analysis stands out as a suitable metabolomic platform for fast and comprehensive first step approach [97].

Hence, the mass spectrometer could be combined with chromatographic and electrophoretic separation techniques as gas chromatography (GC), liquid chromatography (LC) and capillary electrophoresis (CE). Those separation techniques improve the results of MS reducing the complexity of metabolic profiles and facilitating the identification of individual metabolites [103]. The incorporation of the separation step increases the total time of analysis, but these hyphenated approaches introduce the “retention time” in resulting data and that provides additional information about physicochemical properties of the measured metabolites and the metabolome coverage increases.

The combination of GC with MS provides a well-developed and robust tool presenting a high sensitivity and a good resolution [104]. The reproducibility of GC-MS is generally higher than the obtained with other hyphenated techniques as LC-MS and CE-MS in terms of ionization efficiency and chromatographic retention. Other advantage of GC-MS is the availability of spectral libraries due to the highly reproducible mass fragmentation observed under electronic impact (EI) ionization, which facilitates peak identification [105]. Additionally, dimensional GC (GC x GC) coupled to time-of-flight mass spectrometry (TOFMS) makes possible to detect more than 1200 compounds in a single analytical run increasing the sensitivity and separation efficiency [104]. In this case, metabolites are resolved according to their volatility in the first column and polarity in the second column. Despite their advantages, the derivatization step, which consists on the “methoximation” of carbonyl groups and substitution of active hydrogens with trimethylsilyl groups, can introduce technical variability and increases the data complexity [106]. This time-consuming sample treatment, together with the long chromatographic running times, makes GC-MS a less profitable high-throughput technique for metabolomic

application. However, GC-MS is widely used for the metabolomic profiling of low molecular weight metabolites including organic and amino acids, carbohydrates, amines, fatty acids, among others.

In fact, LC-MS covers a wide range of metabolites, extending from low molecular weight compounds detectable by GC-MS to non-volatile metabolites, without the derivatization step [103]. The coupling with MS is generally accomplished by using an atmospheric pressure ionization source, which allows the direct introduction of the liquid effluent from the LC system into the vacuum region of the mass spectrometer. Electrospray ionization (ESI) is the most common choice due to its high sensitivity and versatility, which is applicable for the detection of compounds with very different polarities and molecular weights. In this sense, there are other ionization sources specifically for different type of compounds, thus the combination of ionization sources is recommended to maximize the metabolome coverage. Conventional high performance liquid chromatography (HPLC) has been extensively employed in metabolomic research, but the resolution is usually not sufficient to resolve the huge complexity of the metabolome. Hence, numerous efforts have been made to improve analytical performance of LC [107]. A step forward has been done with capillary chromatography that provides a higher sensitivity and resolution than traditional HPLC and requires fewer amounts of sample and solvent consumption. Thus, the most employed platform is ultra-high-performance liquid chromatography (UHPLC) system that provides resolution equivalent to GC, as well as higher sensitivity, reproducibility and reduced time analysis compared to HPLC.

Finally, CE coupled to MS completes the metabolome showing great potential for the analysis of highly polar and ionic metabolites that are not resolved by GC or LC [108]. This separation method presents high separation efficiency and low volume per sample. Separations are usually performed in bare or surface coated fused-silica capillaries, operating under strongly acidic or alkaline conditions to ensure the complete ionization of weakly ionic metabolites and generate stable electroosmotic flows. However, the low robustness and reproducibility of this separation technique makes this method only used in specific cases. Moreover, the interfacing of CE with MS is a great challenge because of the electrical requirements of these analytical techniques

2.4.4. Data analysis

Data processing aims to extract biologically relevant information from the acquired data, and it includes many steps that are similar both for NMR and MS. Prior to the analysis, data sets should be normalised and pre-filtered using appropriate computing/analytical techniques specific to the type of platform used. Depending on the scientific question the data analysis can follow different approaches as descriptive, exploratory, inferential or include modelling and prediction.

Descriptive statistics precede the other type of analysis trying to anticipate future analytical challenges and obtaining a basic understanding of the data. These statistics include calculating the sample mean and standard deviation or plotting boxplots of

single variable (univariant analysis). Comparative analyses of the means can then be performed by calculating a fold change, F-ratios, t-tests, or ANOVA to assess the significance of the changes [109].

Due to the large number of variables and complexity of the metabolomics data sets, multivariate methods are also used for exploratory and comparative analyses. The purpose of these methods is to reduce the dimensionality of the data set to better enable classification of individual samples and/or visualization of similarities and differences between samples. The initial step does not require a specific data distribution due to the fact that these types of analysis are conducted to understand the major sources of variation in the data (multivariate), by using dimension reduction methods such as Principal Component Analysis (PCA) [110]. Ideally, the results of PCA analyses would be used to formulate an initial biological conclusion; then, there are supervised forms of discriminant analysis such as Partial Least Squares (PLS-DA; alternatively Partial Least Squares Projections to Latent Structures) [111] and Orthogonal Projections to Latent Structures (OPLS) that includes orthogonal projections, improving the PLS method [112]. Multivariate analyses are available in many commercial software packages, including XLSTAT (an add-on to Excel, Microsoft Corp), JMP (SAS Institute Inc.), Pirouette (InfoMetrix, Woodinville, WA, USA), MATLAB (The MathWorks, Inc.), and various R programming packages (http://www.r-project.org/).

Altogether, inferential statistics allows the assumption that conclusions obtained by univariant analysis can be generalize to the whole population. In the omics era, statistical inference is difficult to achieve, and it is often unreliable due to insufficient sample size. In fact, inferential statistics can be achieved with, multivariate methods, when the number of samples is much higher than the number of variables. In the past few years, machine learning or the concept of 'training' computational methods which can improve given more 'experience' or data has been a revolutionizing approach in many disciplines complementing statistical inference. In particular, machine and learning method based on artificial neural networks has been increasingly applied to problems in metabolomics, which are very difficult or infeasible to solve by using conventional algorithms [113].

The last step in data processing is data visualization within a biological context. This process is necessary to visualize and understand the qualitative and quantitative changes in metabolite profiles at a pathway and system levels. This challenging task can be done by the assistance of several exciting tools (data bases) that are now emerging and are allowing the contextualization of metabolomics within a pathway context. In this regard, there are different data bases that could be consulted as Kyoto Encyclopaedia of Genes and Genomes (KEGG) [114], Rat Genome Database (RGD) [115], Human Metabolome Database (HMDB) [116] and Small Molecule Pathway Database (SMPDB) [117].

2.5. Microbiome biomarkers

Microbiome analysis, also called Microbiome Wide Association Studies (MWAS) [118], are transforming clinical investigation through the improvement of patient stratification and are a source of new biomarkers for health. These studies focus on different aspects of microbes as: their identification, the assessment of their genetic variability and metabolic activities of microbes (bacteria, viruses, archaea, and eukaryotes) associated with numerous sites in the body. In line with the metabolome, variations in the gut microbiome can reflect host lifestyle and behaviours that could influence disease biomarker levels in blood. Despite the influence of host lifestyle, several studies have reported associations between host genetics and the microbiome making this a promising approach [119–121]. The understanding of the relationships between the host genome, the host phenotype and the genome of this microbiome is critical for the recognition of health and disease states. However, in the microbiome context, the mechanistic links between health and disease have not been yet satisfactorily established [122].

Microbiome studies have been possible in large part due to advances in next-generation sequencing, high-throughput sequencing and mass-spectrometry platforms [123]. Sequencing platforms allow the assessment of microbiota composition via gene analysis, as for example the sequencing and classification of 16S ribosomal RNA (rRNA). This method consists on the amplification by PCR of the 16S rRNA region with primers that recognize highly conserved regions of this bacterial gene sequence [124]. The annotation is based on the putative association of the 16S rRNA gene within the taxon, defined as an operational taxonomic unit (OTU) and it is capable to determine phyla or genera; but it is less precise at species level. Hence, as specific genes are not directly sequenced and they are based on the OTUs, the lack of direct identification limits the understanding of the microbiome [125]. An alternative approach to the 16S rRNA amplicon sequencing method is whole genome shotgun sequencing (WGS) that consist of the sequencing with random primers to sequence overlapping regions of genome [126]. The major advantage of the WGS method is the accuracy and the capacity to define until species level. However, WGS is more expensive, requires a high coverage of the genome and demands a complex data analysis [127]. In parallel, detection and identification of microbiome-associated products, including metabolites and proteins, have been facilitated by targeted and untargeted MS.

The emerging field of microbiome has been promising in relation to the future elucidation of the relations between microbiome and health. However, there are some challenges that should be achieved related to experimental, computational and conceptual issues [128]. In fact, researchers in the field of microbiome faces with a huge complexity when are trying to define specific microbes at different taxa levels and the subsequent healthy gut microbiome. One of the key successes of this effort has been the identification of gaps in our technologies that would need to be filled to uncover the full potential of microbiome science. Additionally, faeces are currently the most used sample, but additional information is likely to be obtained by studying

other samples along the gastrointestinal tract. Future studies measuring responses to an exposure or intervention need to combine validated microbiome-related biomarkers and omics characterization of the microbiome [122].

2.6. Systems biology approach

Once single omics approach has been performed, systems biology is the next step to integrate the different mechanisms involved in health and disease; as well as an opportunity to define a larger picture of the biochemistry and dynamics of biological systems. After the outbreak of genomics, the scientific community has been trying to establish a correlation between the genotype and the phenotype in living organisms. Despite the development of strategies that have generated improved information which is closer to the phenotype (e.g., metabolomics), the individualized data provided by each one of these omics in an isolated way do not answer how the different biological processes are correlated and how to explain its complexity. Therefore, data integration from different omic sciences is a promising tool which fulfils the gap of the single omics studies. In consequence, the proper integration of multi-omics approaches has allowed a deeper insight into disease development. For example, Poore *et al.* by using multi-omics and machine learning tools, detected that microbial biomarkers from blood and tissues are capable to discriminate between healthy and cancer-free individuals, as well as between multiple cancer types [129].

Several data integration methodologies have been developed to integrate certain types of omics data. Those methodologies are complex, and the available tools are not user-friendly for researchers with limited bioinformatics background. Many tools utilize the statistical language R, which requires programming expertise in addition to strong biostatistical knowledge. For example, the R package mixOmics uses multivariate analysis for data exploration, dimension reduction and visualization [130]. In this package, Data Integration Analysis for Biomarker discovery using Latent cOmponents (DIABLO) method stands out as an integration method that generalizes PLS for multiple matching datasets (same subjects, different omics) in order to evaluate the major sources of variation and to guide through the integration processes [131]. Other complementary tool in mixOmics is the Multivariate INTegration (MINT), which is a method based on multi-group PLS that includes information about samples belonging to independent groups o studies [130].

The addition of biological knowledge gained by omics integration increases the knowledge extracted from the available data. However, there is still a long way to go to get the maximum information from these data by discarding noise and redundant data. As discussed above, there is room for improvement in mathematics and bioinformatics, as well as the development of improved methodologies of high-throughput data. Additionally, new omics are also emerging that could be considered in data integration as the case of omics related to phenotype. This is the case of the exposome that capture the diversity and range of exposures to synthetic chemicals, dietary constituents, psychosocial stressors, and physical factors, as well as their corresponding biological responses [132].

3. Epidemiology, pathology, and animal models of NCDs risk factors

This section describes the risk factors explored in this research for biomarker profiling, based on the concept of overarching processes placed by Van Ommen research *et al*. [49]. They are based on their characteristics that make them important for the development of NCDs (**Figure 5**). The selected risk factors are carbohydrate metabolism dysfunction, hyperlipidaemia, hypertension, and gut microbiota dysbiosis for metabolic stress; inflammation stress; oxidative stress; and psychological stress. The main characteristics of the biomarker profile is that each one recapitulates different and complementary aspects of the metabolic disruption. Thus, the biomarker profile can be conceived as an independent profile of different metabolites and proteins that are currently recognized as established clinical biomarkers or biomarkers from advanced research stages. In this section, the state of the art of these risk factors will be discussed focusing on epidemiology, pathology, and the available animal models. In the following section, studies using metabolomics will be reviewed to have an idea of the current potential as health status biomarkers.

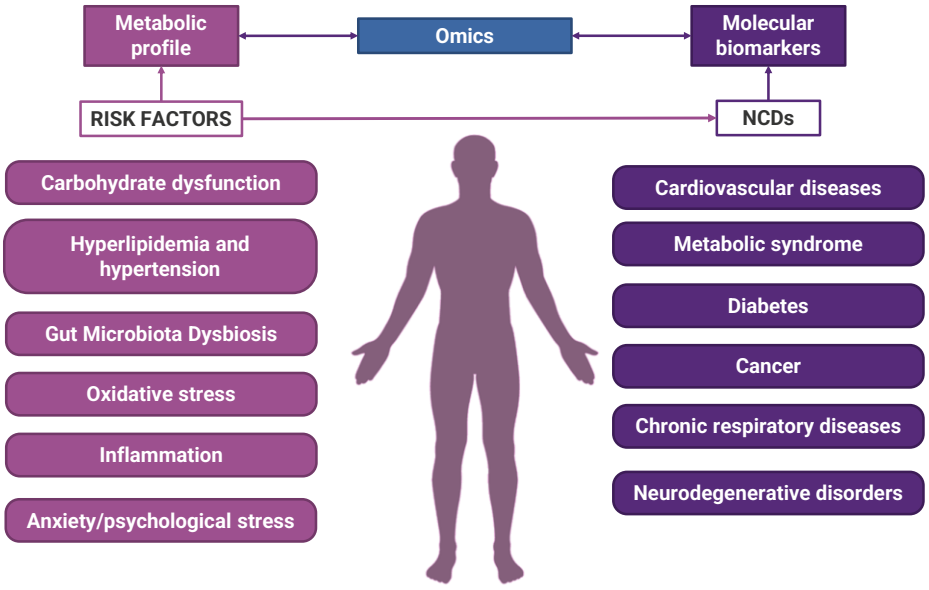

Figure 5. Summary of the relationship between risk factors, NCDs, and omics for health state biomarker discovery. The accumulation and persistence during time of different risk factors (e.g., carbohydrate dysfunction, hyperlipidaemia, hypertension, inflammation, oxidative stress, gut microbiota dysbiosis and anxiety or psychological stress) induces the development of diseases. The detection of these risk factors can be done by omic profiling and biomarkers obtained from omic approaches.

3.1. Carbohydrate metabolism dysfunction

3.1.1. Epidemiology

Carbohydrate metabolism dysfunction could be considered a main risk factor that directly influences many disorders such as obesity, insulin resistance and T2DM and other risk factors (e.g., hyperlipidaemia or hypertension). The assessment of this carbohydrate dysfunction as a risk factor and not as a disease state is complex because it has not been usually monitored at non-pathogenic levels. Furthermore, carbohydrate metabolism dysfunction is highly related to diabetes, which represents approximately the 95% of cases worldwide [133]. Thus, the only way to study the impact of this risk factor would be to look at the prevalence of obesity, diabetes and CVDs which is very high as previously mentioned. Indeed, Mustafina *et al*. highlighted that the epidemiological trends of glucose metabolism disorders especially in obese persons are understudied [134].

3.1.2. Pathogenesis

Carbohydrate metabolism dysfunction occur in many forms. However, the most common deficiencies are rare inborn errors of metabolism (i.e., genetic alterations). In fact, carbohydrate metabolism is a fundamental biochemical process that ensures a constant supply of energy to living cells. Currently, the uncontrolled intake of carbohydrates induces long-term alterations in carbohydrate metabolism. The complex hormonal control of nutrient homeostasis involves numerous tissues and organs, including liver, skeletal muscle, adipose, endocrine pancreas, and central nervous system.

In general, fasting plasma glucose level higher than 7 mmol/L and fasting plasma insulin below 110 pmol/L are related to the carbohydrate metabolism pre-disease [135,136]. We are going to focus on the alterations of glucose metabolism in fasting and post-prandial hyperglycaemia in T2DM, because is one of the main hallmarks of carbohydrate metabolism dysfunction [137]. A peculiarity of the regulation of glucose metabolism is that many hormones exert a net hyperglycaemic effect, but only one, insulin, displays a direct hypoglycaemic action [138].

In an altered carbohydrate metabolism, during the fasting state, gluconeogenesis along with other metabolic reactions proceeds at a high rate, producing an increased level of endogenous glucose output. Thus, reduced glucose homeostatic efficiency, both in glucose output and glucose utilisation, amplifies the degree of hyperglycaemia. A great proportion of glucose is channelled towards three-carbon glucose precursors, which fuels gluconeogenesis in the liver. Additionally, glucotoxicity and lipotoxicity may play a role in both directly maintaining endogenous glucose production and decreasing glucose efficiency [137].

In an altered carbohydrate metabolism, during the postprandial state, the disrupted response of both endogenous glucose output and glucose utilization to hyperglycaemia and/or hyperinsulinemia are responsible for altered glucose tolerance. Gluconeogenesis, glucose transport, glucose phosphorylation and glucose

oxidation are insulin-resistant and play quantitative roles. Impaired glucose efficiency abrogates the ability of glucose to limit the degree of hyperglycaemia. It is also suggested that lipotoxicity play a major role in the pathogenesis of these defects. An additional direct hyperglycaemic effect can be attributed to hyperglucagonemia [137].

3.1.3. Animal models

Currently, the animal models used for the study of carbohydrate dysfunction are diabetes-based models, but more specific models are needed. Indeed, rodent animals are by far the most commonly used species for experimental studies of glucose homeostasis [139]. In fact, many rodent models already exist for the study of diabetes, with various mechanisms for inducing either T1DM or T2DM. These murine models can be classified into two categories: (1) genetically induced spontaneous diabetes models; and (2) experimentally induced non-spontaneous diabetes models [140].

The popularity of using experimentally induced models compared to the genetically induced ones is due to their comparatively lower cost, ease of induction, ease of maintenance and wider availability. Different experimental approaches based on induced models are summarized in **Table 2**. The most commonly used diabetes model involves the administration of a single high dose of streptozotocin (STZ) or alloxan (ALX), which leads to the destruction of pancreatic β cells and causes hyperglycaemia as a direct consequence of deficient insulin production [140]. The understanding of changes in β cells of the pancreas as well as in the whole organism after ALX or STZ treatment is essential for using these compounds as diabetogenic agents [141]. The cytotoxic action of these diabetogenic agents is mediated by the generation of reactive oxygen species (ROS), however, the source of its generation is different in the case of STZ compared to ALX. In the case of ALX, the alteration produced is associated to T1DM and in our case the target of carbohydrate dysfunction is T2DM [142]. In fact, classically ALX induction of diabetes was administered alone [143] and trying to overcome the limitation of T1DM is also administrated together with high-fat diet (HFD) [144]. Indeed, STZ is the preferred inductor of carbohydrate disfunction and it is widely used experimentally to produce a model of T1DM and T2DM depending on the dose and the combination with other agents [145]. Normally, the induction by multiple [146] or single [147–149] administration of STZ is associated with T1DM. However, the combination of STZ together with other strategies as feeding the animals with HFD [150,151] and previous administration with nicotinamide [152–154] fits better with a T2DM condition.

Table 2. Animal-based studies of carbohydrate metabolism dysfunction. In this table a summary of the most used animal models for carbohydrate metabolism dysfunction research are represented, including the induction by streptozotocin (STZ), alloxan (ALX), high-fat diet (HFD). Abbreviations: HFD, high fat diet; OGTT, oral glucose test tolerance; IP, intraperitoneal injection; HbA1c, glycated haemoglobin; TG, triglycerides; TC, total cholesterol.

Model	Induction	Year	Subject	Biomarkers	Ref
ALX	Single subcutaneous injection of 120 mg/kg	2002	Male Sprague-Dawley rats	Glucose	[143]
ALX + HFD	Single injection of 105 mg/kg + HFD	2017	Male Sprague-Dawley rats	OGTT, glucose, insulin, level of antioxidants, and β-cell function	[144]
STZ	Single IP 180 or 100 mg/kg and multiple IP of 40 mg/kg/day for 5 days	2009	Swiss albino mice	Glucose	[146]
	Single IP of 70 mg/kg	2013	Male Wistar rats	Glucose, insulin and HbA1c	[147]
	Single IP of 45 mg/kg	2017	Male Wistar rats	Glucose, insulin, HbA1c and level of antioxidants	[148]
	Single tail vein injection of 60 mg/kg	2018	Male Sprague-Dawley rats	Glucose	[149]
STZ + HFD	HFD + after 2 weeks 35 mg/kg of STZ	2005	Male Sprague-Dawley rats	Glucose, insulin, TG and TC	[150]
	HFD + after 2 weeks single IP of 40 mg/kg of STZ	2019	Male Wistar rats	OGTT, glucose, insulin, glucagon	[151]
STZ + Nicotinamide	Single IP of STZ (55 mg/kg) after 15 min of nicotinamide injection (210 mg/kg IP)	2012	Sprague-Dawley rats	Glucose and level of antioxidants	[152]
		2019	Male Sprague-Dawley rats	Glucose, TG, TC, and level of antioxidants	[153]
	Single IP of STZ (65 mg/kg) after 15 min of nicotinamide injection (230 mg/kg IP)	2017	Male Wistar rats	Glucose, insulin, TG, and TC	[154]

3.2. Hyperlipidaemia and hypertension

3.2.1. Epidemiology

Hyperlipidaemia and hypertension are well-established risk factors for the development of NCDs, these risk factors are especially associated with cardiovascular disease susceptibility. For instance, the European Society of Cardiology states in their guidelines of management of dyslipidaemias [155] and hypertension [156] that the preventive targeting of these above mentioned risk factors could elude further CVD; avoiding in consequence billions of dead's worldwide. Additionally, epidemiological studies have reported a 15-31% rate of coexistence of hyperlipidaemia and hypertension [157,158]. The coexistence of these risk factors has been suggested to multiply the development of diseases compared to the sum of the individual risk factors [159].

The prevalence of hyperlipidaemia increases constantly at a drastic pace, in fact there are over three million adults that are diagnosed for hyperlipidaemia. In 2018, according to the WHO, the prevalence of hyperlipidaemia was the highest in Europe (54% for both sexes), followed by North and South America (48% for both sexes), whereas Africa and Southeast Asia had the lowest prevalence (22.6% and 29.0%, respectively) [155]. Globally, no change has been observed between 1980 and 2018, but several regions presented notable changes. In this case, high-income countries, which had the highest plasma cholesterol (TC) levels in 1980, underwent a substantial reduction in population plasma TC levels, whereas low-income and middle-income countries underwent a large increase in both population plasma TC and triglyceride (TG) levels. Indeed, the change of lifestyle habits and the use of statins has considerably impacted in high-income countries [160].

The prevalence of hypertension, as in the case of hyperlipidaemia, is rising globally possibly due to ageing of the population and increases in the exposition to lifestyle risk factors. In 2019, the global age-standardised prevalence of hypertension in adults (aged 30–79 years) was 32% in women and 34% in men [161]. Unlike the popular belief that hypertension is more important for high-income countries, people in low- and middle-income countries have more than two-fold the risk of dying from hypertension [162]. This fact may be attributed to some recent measures in high-income countries as the increase on the availability and affordability of fresh fruits and vegetables, lowering the sodium content, and improving the offer of dietary salt substitutes that can help to lower blood pressure in the entire population [161].

3.2.2. Pathogenesis

Hyperlipidaemia is a condition that includes various genetic and acquired disorders that describe elevated plasmatic lipid levels within the human body. In line with this, lipoproteins transport lipids from plasma to tissues for energy utilization, lipid deposition, steroid hormone production, and bile acid formation. There are six major lipoproteins in blood including chylomicrons, very low-density lipoprotein (VLDL), intermediate-density lipoprotein (IDL), low-density lipoprotein (LDL), high-density lipoprotein (HDL) and LP(a) (**Table 3**). All the lipoproteins containing ApoB with <70 nm in diameter and rich TG lipoproteins can cross the endothelial barrier leading to the growth and progression of atherosclerotic plaques during long-term circulation in the system [163]. Particularly elevated plasma LDL-cholesterol level (hypercholesterolaemia) is a major risk factors for CVDs, but some forms, such as elevated TGs level (hypertriglyceridemia) are associated with severe pathological consequences in other organ systems, including non-alcoholic fatty liver disease (NAFLD) and acute pancreatitis [160]. Furthermore, the combination of high TGs level and low HDL-cholesterol level (together with the presence of small, dense LDL particles), referred to as atherogenic dyslipidaemia, is highly prevalent in patients with T2DM or MetS and increases their risk to develop CVDs.

Table 3. Physical and chemical characteristics of human plasma lipoproteins. Adapted from the European Society of Cardiology reports of management of dyslipidaemias [155]. Abbreviations: TG, triglyceride; ChoE, cholesteryl ester; PL, phospholipids; VLDL, very low-density lipoprotein; IDL, intermediate-density lipoprotein; LDL, low-density lipoprotein; HDL, high-density lipoprotein; Lp(a), lipoprotein(a); Apo, apolipoprotein.

	Density (g/mL)	Diameter (nm)	TG (%)	ChoE (%)	PL (%)	CT (%)	Apolipoproteins	
							Major	Others
Chylomicrons	<0.95	80-100	90-95	2-4	2-6	1	ApoB-48	ApoA-I, A-II, A-IV, A-V
VLDL	0.95-1.006	30-80	50-65	8-14	12-16	4-7	ApoB-100	ApoA-I, C-II, C-III, E, A-V
IDL	1.006-1.019	25-30	25-40	20-35	16-24	7-11	ApoB-100	ApoC-II, C-III, E
LDL	1.019-1.063	20-25	4-6	34-35	22-26	6-15	ApoB-100	
HDL	1.063-1.210	8-13	7	10-20	55	5	ApoA-I	ApoA-II, C-III, E, M
LP(a)	1.006-1.125	25-30	4-8	35-46	17-24	6-9	Apo(a)	ApoB-100

On the other hand, hypertension arises when the blood pressure is abnormally high, and it comprises a spectrum from uncontrolled hypertension to heart failure. This occurs when the arterioles narrow, causing the blood to exert excessive pressure against the vessel walls and forcing the heart to work harder to maintain the blood pressure. Despite the flexibility of the hearth and blood vessels, the heart may eventually enlarge (hypertrophy) and be weakened to the point of heart failure [164]. In fact, hypertension is diagnosed if the systolic blood pressure (SBP) is ≥ 140 mmHg and/or the diastolic blood pressure (DBP) is ≥ 90 mmHg and the health and pathology state could be divided in different categories, as summarized in **Table 4** [156]. Hypertension rarely occurs as an isolated factor, and often clusters with hyperlipemia as well as carbohydrate metabolism dysfunction [165,166].

Table 4. Classification of blood pressure and definitions of hypertension grade. Adapted from the European Society of Cardiology reports of management of hypertension [156]. This classification is used for all ages from 16 years. For the case of the optimal category, both values are needed, while for the rest of the categories, if one is fulfilled, it is enough to assign it to that grade. Abbreviations: SBP, systolic blood pressure; DBP, diastolic blood pressure.

Category	SBP (mmHg)	DBP (mmHg)
Optimal	<120	<80
Normal	120-129	80-84
High normal	130-139	85-89
Grade 1 hypertension	140-159	90-99
Grade 2 hypertension	160-179	100-109
Grade 3 hypertension	≥180	≥110

3.2.3. Animal models

In the case of hyperlipidaemia, different approaches have been carried out to obtain animal models that allow the elucidation of hyperlipidaemia metabolic impact. However, there is no clear scientific consensus. In this regard, there are different approaches depending on the objective, the grade of hyperlipidaemia (from low grade of hyperlipidaemia to atherosclerosis) and the desired alteration (e.g., hypercholesterolemia and hypertriglyceridemia), as summarized in **Table 5**. The classical models are induced by high fat diet [167] that are low-cost, easy to obtain and robust, but when using this approach other problems as obesity and related complications appears. Nevertheless, there are also spontaneous genetic variants as Zucker (fa/fa) rats [168]. Additionally, in the field/era of genetic editing, due to the outbreak of CRISPR/Cas 9 recent transgenic rodent variants have been developed like animals deficient in apolipoprotein-E (apoE$^{-/-}$) and LDL receptor (LDLr$^{-/-}$) genes [169–172]. However, genetic models, as already mentioned for carbohydrate dysfunction, are experimental methods that have several technical disadvantages compared to other models that are easier to obtain and manipulate.

On the other hand, hyperlipidaemia could be also induced by administration of chemical compounds as poloxamer 407 (P407), thus the degree of hyperlipidaemia can be controlled through the regulation of the dosing of P407 [173]. For instance, P407 is one of the most interesting models of hyperlipidaemia characterized by the elevation of TG levels, which is attributed to: (1) the inhibition of lipoprotein lipase; (2) the elevation of TC levels, which is linked to indirect stimulation of the activity of 3-hydroxy-3-methylglutaryl coenzyme A reductase (HMG CoA reductase), the rate-limiting enzyme in TC biosynthesis; and (3) the decreased LDL receptor expression in all synthesizing cholesterol cells [173]. The P407 animal model may be modulated by the selection of: (1) different rodent species [173–177], (2) dose concentrations between 300 mg/Kg [175] to 1500 mg/kg of body weight [178], being the former the popular one for low-grade hyperlipidaemia; and (3) single treatment [179] or chronic treatment [177,180] of an intraperitoneal (IP) injection have been also selected according to the expected effect [181].

Table 5. Animal-based studies of hyperlipidaemia. In this table a summary of the most used animal models for hyperlipidaemia research are represented, including the induction by high fat diet, genetic models, transgenic models, and administration of poloxamer-407 (P407). Abbreviations: HFD, high fat diet; TC, cholesterol; TG, triglycerides; NEFAs, Non-esterified free fatty acids; PL, phospholipids; HDL, high-density lipoprotein; LDL, low-density lipoprotein; LCAT, lecithin-cholesterol acyltransferase; sPLA2-IIA, group IIA secreted phospholipase A2; PON1, paraoxonase-1; IP, intraperitoneal injection; HMG-CoA, 3-hydroxy-3-methylglutaryl coenzyme A.

Model	Induction	Year	Subject	Biomarkers	Ref
High fat diet	HFD	1996	Male Wistar rats	TC, TG, PL, NEFAs and glucose	[182]
	HFD	1998	C57BL/6 mice	TC, TG, NEFAs, glucose and insulin	[183]
	HFD (360 kcal/kg/day)	2017	Male Golden Syrian hamsters	PL, NEFAs, TC, HDL, LDL, LCAT, sPLA2-IIA, PON1	[177]
Genetic models	Spontaneous mutated leptin receptor (fa/fa)	1992	Zucker rats	TC, TG, LDL, and lipid peroxides	[168]
Transgenic models	LDLr-/- (CRISPR/Cas 9)	2017	Male Sprague-Dawley rats	All alipoproteins	[170]
	ApoE-/- (CRISPR/Cas 9)	2018	Bama miniature pigs	TC, TG, HDL, and LDL	[171]
	$ApoE^{-/-}$ and LDLr-/- (CRISPR/Cas 9)	2018	Male Sprague-Dawley rats	TC, TG, HDL, and LDL	[172]
P407	Single IP of 0.3 g/kg	1997	Male Sprague-Dawley rats	TC and HMG-CoA reductase activity	[175]
	Single IP of 0.5 and 1 g/kg	2013	Male Sprague-Dawley rats	TC, TG, HDL, adiponectin, and leptin	[179]
	IP of 0.5 g/kg twice per week for 1 month	2013	Male CBA mice	TC, TG, HDL, and LDL	[180]
	Periodically IP of 50 mg/kg every 72 h until 4 and 30 days	2017	Male Golden Syrian hamsters	PL, NEFAs, TC, HDL, LDL, LCAT, sPLA2-IIA, PON1	[177]
	Single IP of 0.5 g/kg	2017	Male Wistar rats	TC, TG, HDL, and LDL	[184]
	Single IP of 0.4 g/kg	2018	Male Sprague-Dawley rats	TC, TG, HDL, and LDL	[185]

In the case of hypertension, the complex nature of hypertensive phenotypes complicates the establishment of an animal model for primary hypertension. For this reason, rat genetic models of hypertension have been widely used in the study of high blood pressure levels, as summarized in **Table 6**: spontaneously hypertensive (SHR) rats, Dahl salt-sensitive (DSS) rats, fawn-hooded hypertensive (FHH) rat, Milan hypertensive strain and Lyon hypertensive rat, among others [186,187]. Among these, the most studied model is the SHR, which is widely used in different studies as a rat

model of primary or essential hypertension [187–189]; the second one is the DSS rat [190] followed by other rat strains [191–193]. Additionally, there are transgenic models as the renin 2 (REN 2) that presents the overexpression of *REN* gene [194].

Table 6. Animal models of hypertension. In this table a summary of the most used animal models for hypertension research are represented, including genetic and transgenic models. Abbreviations: SHR rats, spontaneously hypertensive rat; DSS rat, Dahl salt-sensitive rats; FHH rat, fawn-hooded hypertensive rat; BP, blood pressure; TC, total cholesterol; SBP, systolic blood pressure; REN, renin.

Model	Induction	Year 1st publication	Subject	Biomarkers	Ref
Genetic models	Spontaneously hypertension	1977	SHR rats	SBP >150 mm Hg	[188,189]
	Salt-sensitive hypertension	1990	DSS rat	Elevated BP	[190]
	Spontaneously hypertension	1986	FHH rat	Elevated BP compared to Wistar rats	[191]
	Spontaneously hypertension	1986	Milan hypertensive strain	Renal abnormality	[192]
	Low renin release and salt-sensitive	1979	Lyon hypertensive rat	Elevated BP and TC	[193]
Transgenic model	Overexpression REN gene	1990	REN2 transgenic rats	Elevated BP	[194]

3.3. Gut microbiome dysbiosis

3.3.1. Epidemiology

Hundreds of clinical studies have demonstrated associations between the human microbiome and disease [195], but fundamental questions remain unanswered about how we can generalise this knowledge and how it can be traced epidemiologically. Some diseases are associated with more than 50 genera, while most show only 10-15 changes at the genus level [196]. Some diseases are marked by the presence of potentially pathogenic microbes, while others are characterised by a decrease in health-associated bacteria [196]. In addition, about a half of the genera associated with individual studies are from bacteria that respond to more than one disease. Although we have a lot of information about microbiota dysfunction, the challenge will be to discover the key changes that are of paramount importance due to its effect on disease development.

3.3.2. Pathogenesis

The gut is composed of large microbial communities including bacteria, fungi, archaea and viruses [197]. The distribution of this microbial population is the lowest in the upper intestine (stomach, duodenum and jejunum), with approximately 10^3 bacteria per mL, while there are approximately 10^7-10^{12} bacteria per mL in the lower intestine (ileum and proximal colon) [198]. The gut microbiome performs diverse functions such as helping on food digestion, production of essential vitamins, synthesis of metabolites, prevention of colonisation by pathogenic bacteria, intestinal

immune regulation, drug metabolism, detoxification and maintenance of physiological homeostasis of the gastrointestinal tract [199]. Therefore, the maintaining of a healthy proportion of beneficial microbes, also called eubiosis, is essential for human well-being and health.

In contrast, gut microbial imbalance, known as dysbiosis, can include: (1) an increased ratio of small intestinal bacteria; (2) an alteration of the relative ratio of beneficial to pathogenic microbes; as well as (3) a translocation of colonic bacteria [200]. Fundamentally, there are several factors that contribute to the progression towards a pathologic state, including microbe-microbe interactions, microbial metabolites, host immune response, host physiology, diet and host environment [201,202].

In a healthy host, *Bacteroidetes* and *Firmicutes* are the predominant phyla in the gut, while *Proteobacteria*, *Verrucomicrobia*, *Actinobacteria*, *Fusobacteria* and *Cyanobacteria* are found in much lower proportions [203]. In general, if it occurs changes in the proportions of these phyla then a disturbance of microbial homeostasis could be assumed.

3.3.3. Animal models

Increasing evidence indicates that the gut microbiome responds to diet, antibiotics, and other external stimuli (**Table 7**). In consequence, these changes on the microbiome could have consequences on metabolism. Despite decades of research in the field of gut dysbiosis, the development of successful animal models remains very challenging and has been found to involve multiple challenges. Therefore, the existing models are usually associated with a disease-related dysfunction of the gut microbiome as for example in the case of obesity [204]. Dietary habits, which could be related to obesity and associated complications, are fundamental for the modulation of the gut microbiome, for this reason changes in healthy diet in favour of HFD or cafeteria diet leads to gut microbiome dysbiosis. Therefore, some animal models are based on the feeding for long periods (i.e., 4-6 months) with this type of diets [205,206]. Moreover, specific fetal surgeries have been used to mimic neonatal gut dysbiosis through the isolation of intestinal segments before birth [207].

A classical inductor of gut microbiome dysbiosis are antibiotics that alters the composition and function of microbiota through its direct effect on bacteria. Different treatments can be performed using different antibiotics (e.g., penicillin, vancomycin, chlortetracycline, gentamicin, metronidazole) or a combination of them during short or long periods and the administration can be done via oral gavage or via drinking water depending on the desired effect [208–210].

In line with this, the antibiotic treatment could be combined with microbial transplant leading to gut microbiome dysbiosis. This type of transplant involves transferring microbiota from a diseased (i.e., obese) donor to a healthy recipient to generate gut microbiome dysbiosis in the recipient. Interestingly, there are also opposite approaches, which involves the treatment of diseased recipients with

microbes from healthy donors, to revert the disbiotic condition as a treatment for related diseases. Focusing on the transplant leading to gut microbiome dysbiosis, there are mainly two approaches: (1) the use as a donor microbiota of the same animal species with disrupted microbiome[211] or (2) inter-species transplantation were the donors can be human [212].

Table 7. Animal-based studies of gut microbiome dysfunction. In this table a summary of the most suitable animal models for gut microbiome dysfunction research are represented. Abbreviations: AB, antibiotic; LFD, low fat diet; HFD, high fat diet; CAF diet, cafeteria diet; OG, oral gavage.

Model	Induction	Year	Subject	Effect	Ref
Diet	CAF diet for 12 weeks	2018	Male Wistar rats	↓bacteria diversity	[205]
	HFD for 9 weeks	2019	Male Wistar rats	↓bacteria diversity: specially *Firmicutes*	[206]
Fetal surgeries	Isolated intestinal segments 15–20 cm before birth	2019	Lambs	↓bacteria diversity: specially ↑*Proteobacteria*	[207]
AB Treatment	Penicillin, vancomycin, penicillin plus vancomycin, or chlortetracycline via drinking water	2012	Female C57BL/6J mice	Metabolome changes	[208]
	Amoxicillin, gentamicin and Metronidazole in water for 14 days	2019	Male Sprague-Dawley rats	↓bacteria diversity: specially *Bifidobacterium* spp., *Lactobacillus* spp.	[209]
	Moxifloxacin and clindamycin by subcutaneous injection for 5 days	2018	Syrian hamster	-	[210]
Microbial transplantation	AB treatment for 3 days and transplantation of a pool of cecum content from Wistar and Sprague-Dawley rats	2010	Lewis rats	-	[211]
	Inoculated with human faeces by OG to germ-free rats (Sterile pelleted feed)	2013	Male Sprague-Dawley rats	↓bacteria diversity: ↓Firmicutes and ↑ in Actinobacteria and Proteobacteria	[212]

3.4. Chronic inflammation

3.4.1. Epidemiology

Although occasional increases in inflammation are critical for survival during physical injury and/or infection, recent research has revealed that certain social, environmental and lifestyle factors can promote chronic systemic inflammation, [213]. Furthermore, chronic inflammatory diseases have been recognized as the most significant cause of death in the world today, with more than 50% of all deaths being attributable to inflammation-related diseases (e.g., CVDs, obesity, cancer or NAFLD) [214]. Indeed, it is difficult to assess the chronic inflammation overall impact on health

systems because it has been considered as a “silent” risk factor since it is arduous to track without the development of an associated disease linked to inflammation

3.4.2. Pathogenesis

In general, inflammation is a combination of biological processes characterized by the activation of immune and non-immune cells that protect the host from bacteria, viruses, toxins and infections by eliminating pathogens and promoting tissue repair and recovery [215]. Furthermore, there is also a long-term low-grade inflammation which can last for prolonged periods (from several months to years) and is characterized by the sustained elevation of inflammatory cytokines in serum due to the failure to resolve acute inflammation [216]. Even though acute and chronic inflammation share common mechanisms, there are some interesting differences. Initially, chronic inflammation is typically triggered by damage-associated molecular patterns (DAMPs) in the absence of activation of pathogen-associated molecular patterns (PAMPs) [217]. It is observed that chronic inflammation increases with age as it has been shown a higher circulating levels of cytokines, chemokines and genes involved in inflammation in elderly [218]. Additionally, chronic inflammation is a low-grade and persistent type of inflammatory process, and subsequently it is the prolongation and accumulation during the time that causes collateral damage to tissues and organs until the development of NCDs. Despite the link between the disease and chronic inflammation, there are currently non-standard fully accepted biomarkers to indicate the presence of chronic inflammation [213].

3.4.3. Animal models

Despite the need for a deeper understanding of the underlying chronic inflammation, there are few models that study this alteration from an isolated point of view. In general, animal models used to mimic acute and chronic inflammation are based on its induction by a chemical or biological stimuli [219,220], as summarized in **Table 8**. On the one hand, different chemical stimuli are used as magnesium silicate [221] or indomethacin [222]. On the other hand, lipopolysaccharide (LPS), which is a structure found in the outer membrane of gram-negative bacteria, is the preferred stimulus for acute as well as chronic inflammation [220,223–230]. Furthermore, different degrees of inflammation and related pathologies can be obtained by regulating the LPS administration (i.e., type administration, dosage, and frequency). However, it has been observed that repeated administration of LPS induces the development of tolerance to the endotoxin, thereby decreasing the inflammatory response [231]. For this reason, different procedures have been explored to overcome the endotoxin resistance generated by the animals. Several approaches have been developed: one of the most cutting-edge approaches consists of administering LPS via slow-release pellets for at least 30 days [226–229]; intermittent injection of LPS on different days is also quite effective in rats [223,230]; administration of IP three times a week with increasing dosage [220].

Table 8. Animal-based studies of chronic inflammation. In this table a summary of the most suitable animal models for chronic inflammation research are represented. Abbreviations: LPS, lipopolysaccharide; COX2, cyclooxygenase-2; TNF-α, tumour necrosis factor-alpha; IL-1β, and interleukin-1β; WBC, white blood cells; IP, intraperitonially injection; CRP, C-reactive protein; IL-6, interleukin-6; IL-8, interleukin-8.

Model	Induction	Year	Subject	Biomarkers	Ref
Magnesium silicate	Injection of 1 g	1988	Female Wistar rats	Granulocytes, macrophages, and giant cells	[221]
Indomethacin	Two subcutaneous injections of Indomethacin (7.5 mg/kg)	1993	Male Sprague-Dawley rats	-	[222]
LPS	Slow-release pellets (1.33 μg LPS/day) for 30 days	2007	Female C57BL/6J mice	TNF-α	[226]
	Slow-release pellets (0, 3.3, or 33.3 μg LPS/day) for 90 days	2006, 2009	Male Sprague-Dawley rats	COX2, TNF-α, IL-1β	[227,228]
	Slow-release pellets (44.4 μg LPS/day) for 90 days	2012	Male C57/BL6J mice	WBC and neutrophils	[229]
	Periodically IP of 0.25 mg/kg twice weekly for up to 25 weeks	2016	Male C57/BL6J mice	TNF-α and IL-6	[230]
	Periodically IP of 0.1 mg/kg	2017	Male Wistar rats	Insulin resistance	[223]
	Periodically and intermittent IP (0.5, 1, 2 mg/kg) thrice a week for 30 days	2018	Male Sprague-Dawley rats	CRP, TNF-α, IL-6, IL-1β and IL-8	[220]

3.5. Oxidative stress

3.5.1. Epidemiology

In line with other risk factors, the epidemiological monitorization of oxidative stress is difficult because it is not clinically diagnosed as an isolated risk factor, because it is rather associated with other related diseases. For example, many human epidemiological studies have demonstrated a close association between chronically oxidative conditions and carcinogenesis [232]. Additionally, the increase of environmental pollutants has been directly related to oxidative stress and has been considered as a growing threat for the global health [233].

3.5.2. Pathogenesis

Oxidative stress is the homeostatic disruption that occurs when there is an imbalance between ROS generation and the body's antioxidant defence systems [234]. Many types of agents (chemical, physical and microbial) can cause oxidative stress in tissues and cells. In addition, oxidative stress is involved in many fundamental aspects of life processes, such as cellular respiration (mitochondria), lipid synthesis, cytochrome activities, lysosomes, phagocytosis of foreign bodies (immunity and

inflammation) and xenobiotic biotransformation of organic compounds. Oxidative stress could be related to the production of reactive species during oxidative stress such as hydroxyl radical ($HO^{\bullet}$), peroxynitrite anion ($ONOO^{-}$) or hypochlorous acid (HOCl).

ROS are mainly produced by mitochondria under both physiological and pathological conditions. Indeed, superoxide anion ($O_2^{\bullet -}$) is formed by cellular respiration through the activity of lipoxygenases (LOX) and cyclooxygenases (COX) during arachidonic acid metabolism, and by endothelial and inflammatory cells [235]. Although these organelles have an intrinsic ROS scavenging capacity [236], it should be noted that this is not sufficient enough to cope with the cellular needs to remove the ROS amount produced by mitochondria [237]. ROS have divergent effects on cellular function and contribute to disease through different mechanism [238]. The first mechanism involves is associated with the oxidation of important biomolecules (e.g., proteins, lipids, and nucleic acids) leading to disrupted homeostasis of cell function and death. The second mechanism involves aberrant redox signalling as the case of the oxidant hydrogen peroxide (H_2O_2) which could normally act as second messenger [239].

On the other hand, the antioxidant system of cells is based mainly on enzymatic components, such as superoxide dismutase (SOD), catalase (CAT) and glutathione peroxidase (GPx), to protect cellular systems from ROS-induced cellular damage [240].

3.5.3. Animal models

The animal models of oxidative stress rely on the rate of prooxidant generation and the effects of antioxidants. Consequently, experimental oxidative stress models can target either production of ROS or suppression of antioxidants [241]. Indeed, treatments that increase ROS production are particularly useful to evaluate oxidative stress. Among the most common chemicals for inducing oxidative stress through increased ROS (either by ingestion or injection), there are a group of oxidative stress generating molecules such as diazinon [242], diquat [243] or paraquat (PQ) [244–250], as summarized in **Table 9**. For example, diquat is a powerful inducer of oxidative stress, being the liver its main target organ, thus in this case the goal is mainly the hepatic oxidative stress study and it is mostly used in piglets or chickens [243].

In fact, PQ (paraquat or 1,10-dimethyl-4,40-bipyridinium dichloride) is the most commonly used oxidative stress inducer, it should be noted that this herbicide is very toxic when is absorbed by ingestion, skin contact or inhalation [251–253]. The molecular effect of PQ is related to the induction of oxidative stress by generating ROS through redox cycling by microsomal NADPH-cytochrome P-450 reductase, xanthine oxidase and mitochondrial NADH-quinone oxidoreductase [252]. The high ROS production induces a non-selective oxidation of biomolecules such as lipids, proteins and nucleic acids that lead to cell damage and eventually result in death [253]. The administration of PQ by intragastric administration (IG) is widely related to PQ poisoning [244]. However, single or periodically IP of PQ induce oxidative stress in different degree depending on the rodent model and the dosage that has been used

[245–250]. Currently, PQ oxidative stress model is the most suitable experimental approach, but it should be evaluated with caution as it is associated with a high number of complications such as: (1) localized damage to lungs; (2) interaction with microglia to induce increased neural damage, particularly to dopaminergic neurons; and (3) researchers must take precautions to prevent their exposure [241].

Table 9. Animal-based studies of oxidative stress. In this table a summary of the most suitable animal models for oxidative stress research are represented. Abbreviations: PQ, paraquat; IP, intraperitonially injection; IG, intragastric administration; LPO, lipid peroxidation; GSH-Px, glutathione peroxidase; AST, aspartate transaminase; ALT, alanine transaminase; ALP, alkaline phosphatase; TAC, total antioxidant capacity; GGT, ɣ-glutamyl transferase; TTM, total thiol molecules; 8-OHdG, 8-hydroxy-2'-deoxyguanosine; CAT, catalase; SOD activity, superoxide dismutase activity; LDH, lactate dehydrogenase

Model	Induction	Year	Subject	Biomarkers	Ref
Diazinon	Periodically IG 10 mg/kg per day for 7 weeks	2018	Male Wistar rats	LPO, TTM, TAC, SOD and GSH-Px	[242]
Diquat	Single IP of 10 mg/kg	2020	Male piglets	ALT, AST, 8-OHdG, LPO, GSH-Px, SOD, CAT and TTM	[243]
PQ	Single IP of 30 mg/kg	2012	Male Wistar rats	Glucose, AST, ALT, ALP, GGT, LPO, CAT SOD	[245]
	Single IG of 36 mg/kg	2015	Male Sprague-Dawley rats	-	[244]
	Single IP of 10, 20 or 30 mg/kg	2016	Male Wistar rats	LPO, AST, ALT, 8-OHdG, CAT and SOD	[246]
	Single IP of 50 mg/kg	2017	Male Swiss albino mice	LPO, AST, ALT	[247]
	Periodically IP of 50 mg/kg for 14 days	2018	Male Wistar rats	LPO, TAC, TTM and 8-OHdG	[249]
	Single IP of 10 mg/kg	2019	Female C57BL/6 mice	-	[250]
	Single IP of 30 mg/kg	2019	Male Wistar rats	LDH, SOC, TAC, LPO	[248]

3.6. Psychological stress, anxiety, and related disorders

3.6.1. Epidemiology

Although psychological stress disorders have increased dramatically in recent decades, their importance as a global health problem has not received the attention it deserves until recent years. Nowadays, it affects the lives of almost 300 million people worldwide suffering from a range of different stress disorders [254]. Indeed, psychological disorders could lead to suicide, which its global annual mortality rate has been estimated to be around 10.7 per 100,000 individuals (with variations across age groups and countries) [255]. In fact, the WHO estimates that psychological disorders cost to the global economy around USD 1 trillion each year due to lost productivity [254]. Generally, stressful events are thought to influence the pathogenesis of other NCDs by causing negative affective states (e.g., feelings of anxiety and depression) [256,257].

3.6.2. Pathogenesis

Physiological stress can be defined as any external or internal condition that challenges the homeostasis of a an organism [258]. In fact, psychological stress itself is not pathological as it is an adaptative mechanism of the animal to deal with stressful events. During stressful events, two endocrine response systems are activated: the hypothalamic-pituitary-adrenocortical (HPA) axis and the sympathetic-adrenal-medullary (SAM) system. Thus, prolonged or repeated activation of the HPA and SAM systems can interfere with a broad range of physiological processes, resulting in anxiety or depression as an increased risk of NCDs [259]. Psychological disorders are complex conditions including genetic, neurological, neurochemical, and psychological factors involved in their development [260]. Among psychological disorders, the most common is anxiety, which occurs when the individual is not under a real danger/threat, but the body responds as if this stimulus would be real (stress).

3.6.3. Animal models

There are several animal models of stress disorders, although it should be noted that mimicking these disorders in animals is far from the real global condition in humans. Particularly rodent models, can only model specific aspects of stress disorders and not their full pathological characteristics [261]. Therefore, animal models do not intend to replicate all the features and symptoms of a specific disorder but rather generate a state of stress or anxiety that could be related to these disorders. For example, there are models that do not involve a direct stressor such as fear conditioning that involves learning the association of a neutral stimulus, such as a light, tone, or setting; with an aversive stimulus, such as an electric shock [262] [263]. Re-exposure to the neutral stimulus will activate a conditioned fear response which resembles the responses that occur in the real presence of danger. This type of models mimics traumatic memories representing a psychological stress without physical stimuli [264].

Furthermore, there are different types of stressors that have been used to mimic acute and chronic stress inducing phycological and/or physical stress, as summarized in **Table 10**. Predator stress is an effective stressor used in rodents that can be manipulated by presenting the odours of the predator such as introducing bobcat urine into a test cage with the rat [265,266]. Early-life stressful experiences, such as neonatal isolation or early induction of stressors, promote long-lasting neural and behavioural effects and have profound consequences on subsequent quality of life [267,268]. Alterations in circadian rhythm changes consist of unexpected changes in the day-night light cycle inducing short-term stress related to melatonin secretion, as the case of continuous light [269]. Furthermore, in animal models, noisy stress can be induced by using loudspeakers to generate a noise exposure that exceeds 90 decibels (dB) for at least two weeks [270,271]. Changes in body temperature lead to stressful responses due to activation of the thermoregulatory centre and, subsequently, of the HPA axis through the immersion of the animals in cold water for a short period of time (5-30 min) or placing the animals (in their home cages) in a cold or isolated environment (4°C for 5-30 min) during one to several days [272,273]. Restraint stress

is usually induced by keeping the animals in a cylindrical or semi-cylindrical tube with ventilation holes; while in immobilisation stress protocol, the animals are restrained by gently wrapping their upper and lower limbs with adhesive tape for short periods of time [274]. The social defeat stress protocol consists of the introduction of a single mouse (known as the intruder) in the home cage of a resident male mouse (known as the aggressor) [275].

Currently, the most commonly experimental approach to simulate the core behavioural characteristics of human depression for investigating the pathophysiology and assisting in diagnosis is the Chronic Unpredictable Mild Stress (CUMS) [276]. It involves presenting different randomly stressors to rodents daily to avoid the stress adaptation process observed in other chronic stress models. In this model, animals are exposed for 2-5 weeks to a wide range of stressors, including some of those previously exposed (e.g., electric foot shocks, restraint stress, light-dark cycle reversal, unpleasant noises, changes in the home cage) [277,278]. After several days of exposure to this regime, animals show a gradual increase in HPA axis sensitivity and a decrease in responses to pleasant stimuli, but no change in exploratory activity. This protocol has good face validity and seems to more realistically represent the stressors that humans face in everyday life.

Table 10. Animal-based studies on psychological stress, anxiety, and related disorders. In this table a summary of the most suitable animal models for anxiety, psychological stress and related disorders are represented. Abbreviations: IP, intraperitoneal injection; OFT, open field test; EPM, elevated plus maze; SPT, sucrose preference test; FST, forced swim test; dB, decibel; CMS, Chronic Mild Stress; CUMS, Chronic Unpredictable Mild Stress.

Model	Induction	Year	Subject	Detection	Ref
Fear conditioning	Source of shock + Electric foot shock	1980	Female Long-Evans rats	Post-shock freezing	[262]
	Tone stimulus + Electric foot shock	2020	Male CHF and CLF rats	Post-shock freezing	[263]
Predator stress	Bobcat urine	2014	Male Wistar rats	Acoustic startle response and operant alcohol oral self-administration	[265]
		2019	Male Wistar rats	SPT, corticosterone and glucocorticoids assays	[266]
Neonatal stress	1 h per day isolation on postnatal days 2-9	2000	Sprague-Dawley rats	Locomotor activity, food training and corticosterone assay	[267]
	IP saline after 22h of birth	2014	Wistar rats	OFT, EPM, SPT, social investigation and corticosterone assay	[268]
Circadian rhythm changes	Constant light	2009	Male Swiss-Webster mice	OFT, EPM, SPT and FST	[269]
Noisy stimulus	100 dB for 4 h/day for 15 days	2005	Male Wistar rats	Norepinephrine, epinephrine, dopamine and 5-hydroxytryptamine	[270]
	95 dB for 4 h/day for 28 days	2019	Male Sprague-Dawley rats	Glucose, insulin, and corticosterone	[271]
Low temperature	Immerse in cold water at 4 °C for 5 min	2002	Male Sprague-Dawley rats	-	[273]
	Immerse in cold water at 15 °C for 5 min for 1 day or 5 days	2011	Male Wistar rats	Locomotor activity, hole board test, OFT and social interaction test	[272]
Restraint and immobilization	Single restrained for 2 h or immobilized 2 h/day for 7 days	2000	Male Wistar rats	EPM	[274]
Social defeat	Chronic psychosocial defeat protocol	2018	Male C57BL/6J mice	Locomotor activity	[275]
Depression	CMS protocol for 8 weeks	2019	Male Sprague-Dawley rats	SPT, FST and EPM	[279]
	CUMS protocol for 6 weeks	2019	Male Wistar rats	SPT and FST	[277]
	CUMS protocol for 6 weeks	2020	Male Wistar rats	SPT and FST	[278]

3.6.4. Biomarkers of psychological stress, anxiety, and related disorders

As for the rest of the previously mentioned factors, in the following section a compilation of the most promising metabolomic biomarkers will be made for this specific risk factor. Currently, the diagnosis and detection of these disorders is based on a symptom checklist, and there is a need to complement the current diagnose with objective laboratory analyses. For this reason, important efforts have been made to differentiate healthy from anxious subjects by the analysis of metabolomics (**Table 11**). To date, the metabolites related to psychological disorders seem to be involved in oxidative stress, alteration in lipid and energy metabolism, and neurotransmission (i.e., glutamate-glutamine cycle or ɣ-aminobutyric acid (GABA) metabolism) [280].

Table 11. Metabolic biomarkers involved in psychological stress, anxiety, and related disorders, identified in clinical studies. Abbreviations: GlycA, glycoprotein acetylation; TMAO, trimethylamine N-oxide; BCAA, branched-chain amino acid.

Biofluid	Study	Metabolite	Ref
Plasma	Netherlands Study for Depression and Anxiety (NESDA)	↑ GlycA ↓ Omega-3 fatty acids	[281]
	The Brazilian longitudinal study of adult health (ELSA-Brazil)	↑ GlycA	[282]
	Bipolar depression and healthy control participants	↑ Lactate ↓ Glucose, TMAO and GlycA	[283]
	Psychological suboptimal health status	↑ Glutamine, GlycA, TMAO, citrate, tyrosine, and phenylalanine ↓ Valine, isoleucine, and glucose	[284]
Serum	Anxiety related to anorexia nervosa	↑ Glutamine ↓ Threonine, methanol, glucose, and GlycA	[285]
	Environmental stress on subjects of sea-voyage and Antarctic-stay	↑ Ketone bodies (3-hydoxybutyrate and acetone), glucose, arginine, BCAA, phosphoric acid, and D-galactose ↓ Lactate and choline	[286]

Many early stress psychological disorders studies have focused on lipids (lipidomics) based on the fact that it has been postulated a connection between lipids and neuronal signalling disease [287]. Indeed, the brain is particularly enriched with PUFAs, which are mainly represented by omega-6 and omega-3 fatty acids. In a cohort of depressive and anxious subjects, the decrease of omega-3 fatty acids in plasma is proposed as a potential biomarker [281]. Interestingly, omega-3 have a neuroprotective effect [288]. Accumulating evidence situates GlycA, a robust

inflammatory biomarker, as a biomarker for anxiety and depression, and may drive to associate psychological stress with systemic inflammation [281–284]. However, this association varies depending on gender and age, which might also contribute to the association of lipid metabolism and inflammation with stress symptoms.

Furthermore, glutamine, as the most abundant amino acid circulating in blood, is not only essential as a neurotransmitter but it is also a precursor for other neurotransmitters as glutamate and GABA, and might be considered as a biomarker for anxiety and depression [289]. Other amino acids have also been detected by metabolomic approaches in stressed subjects such as tyrosine, phenylalanine, branched-chain amino acid (BCAAs), arginine or choline, among others. However, glutamine stands out among other amino acids, because it shows an effect on the disruption of brain glutamate-glutamine cycle, which is suggested to be involved in different forms of anxieties and it is easily and abundantly detected by NMR [284,285].

Related to carbohydrate dysfunction, altered glucose levels are found in neurological disorders such as bipolar depression [283], psychological unhealthy health status [284], anxiety related to anorexia nervosa [285] or environmental stress [286]. The commonly assessed stress factor is the alteration of glucose levels; but this metabolite highly fluctuates in contrast with healthy subjects, which is a disadvantage for being reliable. However, this metabolite may be considered a key factor for psychological disorders as well as a potential biomarker, considering other metabolites to complete the profile of this risk factor.

References

1. Tulchinsky, T.H.; Varavikova, E.A. Chapter 5 - Non-Communicable Diseases and Conditions. In; Tulchinsky, T.H., Varavikova, E.A.B.T.-T.N.P.H. (Third E., Eds.; Academic Press: San Diego, 2014; pp. 237–309 ISBN 978-0-12-415766-8.

2. Meetoo, D. Chronic diseases: the silent global epidemic. *Br. J. Nurs.* **2008**, *17*, 1320–1325, doi:10.12968/bjon.2008.17.21.31731.

3. Budreviciute, A.; Damiati, S.; Sabir, D.K.; Onder, K.; Schuller-Goetzburg, P.; Plakys, G.; Katileviciute, A.; Khoja, S.; Kodzius, R. Management and Prevention Strategies for Non-communicable Diseases (NCDs) and Their Risk Factors. *Front. public Heal.* **2020**, *8*, 574111, doi:10.3389/fpubh.2020.574111.

4. WHO Global action plan for the prevention and control of noncommunicable diseases 2013-2020. 2013.

5. Nikoloski, Z.; Alqunaibet, A.M.; Alfawaz, R.A.; Almudarra, S.S.; Herbst, C.H.; El-Saharty, S.; Alsukait, R.; Algwizani, A. Covid-19 and non-communicable diseases: evidence from a systematic literature review. *BMC Public Health* **2021**, *21*, 1068, doi:10.1186/s12889-021-11116-w.

6. WHO *Noncommunicable diseases: Progress monitor.*; 2020;

7. Bennett, J.E.; Stevens, G.A.; Mathers, C.D.; Bonita, R.; Rehm, J.; Kruk, M.E.; Riley, L.M.; Dain, K.; Kengne, A.P.; Chalkidou, K.; et al. NCD Countdown 2030: worldwide trends in non-communicable disease mortality and progress towards Sustainable Development Goal target 3.4. *Lancet* **2018**, *392*, 1072–1088, doi:https://doi.org/10.1016/S0140-6736(18)31992-5.

8. Dicker, R.C.; Coronado, F.; Koo, D.; Parrish, R.G. Principles of epidemiology in public health practice; an introduction to applied epidemiology and biostatistics. **2006**.

9. WHO *European food and nutrition action plan 2015–2020.*; World Health Organization. Regional Office for Europe, 2015;

10. WHO *Diet, nutrition and the prevention of chronic diseases.*; Switzerland, 2003; Vol. 916;.

11. Grundy, S.M.; Cleeman, J.I.; Daniels, S.R.; Donato, K.A.; Eckel, R.H.; Franklin, B.A.; Gordon, D.J.; Krauss, R.M.; Savage, P.J.; Smith, S.C.J.; et al. Diagnosis and management of the metabolic syndrome: an American Heart Association/National Heart, Lung, and Blood Institute Scientific Statement. *Circulation* **2005**, *112*, 2735–2752, doi:10.1161/CIRCULATIONAHA.105.169404.

12. Eckel, R.H.; Grundy, S.M.; Zimmet, P.Z. The metabolic syndrome. *Lancet (London, England)* **2005**, *365*, 1415–1428, doi:10.1016/S0140-6736(05)66378-7.

13. Saklayen, M.G. The Global Epidemic of the Metabolic Syndrome. *Curr. Hypertens. Rep.* **2018**, *20*, 12, doi:10.1007/s11906-018-0812-z.

14. Esmailnasab, N.; Moradi, G.; Delaveri, A. Risk factors of non-communicable diseases and metabolic syndrome. *Iran. J. Public Health* **2012**, *41*, 77–85.

15. Heidari-Beni, M. Early Life Nutrition and Non Communicable Disease. *Adv. Exp. Med. Biol.* **2019**, *1121*, 33–40, doi:10.1007/978-3-030-10616-4_4.

16. CDC Million hearts: strategies to reduce the prevalence of leading cardiovascular disease risk factors--United States, 2011. *MMWR. Morb. Mortal. Wkly. Rep.* **2011**, *60*, 1248–1251.

17. Francula-Zaninovic, S.; Nola, I.A. Management of Measurable Variable Cardiovascular Disease' Risk Factors. *Curr. Cardiol. Rev.* **2018**, *14*, 153–163, doi:10.2174/1573403X14666180222102312.

18. Flora, G.D.; Nayak, M.K. A Brief Review of Cardiovascular Diseases, Associated Risk Factors and Current Treatment Regimes. *Curr. Pharm. Des.* **2019**, *25*, 4063–4084, doi:10.2174/1381612825666190925163827.

19. Wirtz, P.H.; von Känel, R. Psychological Stress, Inflammation, and Coronary Heart Disease. *Curr. Cardiol. Rep.* **2017**, *19*, 111, doi:10.1007/s11886-017-0919-x.

20. Satyjeet, F.; Naz, S.; Kumar, V.; Aung, N.H.; Bansari, K.; Irfan, S.; Rizwan, A. Psychological Stress as a Risk Factor for Cardiovascular Disease: A Case-Control Study. *Cureus* **2020**, *12*, e10757, doi:10.7759/cureus.10757.

21. WHO *Cancer Control: Knowledge into Action: WHO Guide for Effective Programmes*; Geneva, 2007;

22. Wild, C.P. The Role of Cancer Research in Noncommunicable Disease Control. *JNCI J. Natl. Cancer Inst.* **2012**, *104*, 1051–1058, doi:10.1093/jnci/djs262.

23. Vineis, P.; Alavanja, M.; Buffler, P.; Fontham, E.; Franceschi, S.; Gao, Y.T.; Gupta, P.C.; Hackshaw, A.; Matos, E.; Samet, J.; et al. Tobacco and Cancer: Recent Epidemiological Evidence. *JNCI J. Natl. Cancer Inst.* **2004**, *96*, 99–106, doi:10.1093/jnci/djh014.

24. Sung, H.; Siegel, R.L.; Torre, L.A.; Pearson-Stuttard, J.; Islami, F.; Fedewa, S.A.; Goding Sauer, A.; Shuval, K.; Gapstur, S.M.; Jacobs, E.J.; et al. Global patterns in excess body weight and the associated cancer burden. *CA. Cancer J. Clin.* **2019**, *69*, 88–112, doi:10.3322/caac.21499.

25. McGuire, S. World Cancer Report 2014. Geneva, Switzerland: World Health Organization, International Agency for Research on Cancer, WHO Press, 2015. *Adv. Nutr.* **2016**, *7*, 418–419, doi:10.3945/an.116.012211.

26. Rabe, K.F.; Hurd, S.; Anzueto, A.; Barnes, P.J.; Buist, S.A.; Calverley, P.; Fukuchi, Y.; Jenkins, C.; Rodriguez-Roisin, R.; van Weel, C.; et al. Global strategy for the diagnosis, management, and prevention of chronic obstructive pulmonary disease: GOLD executive summary. *Am. J. Respir. Crit. Care Med.* **2007**, *176*, 532–555, doi:10.1164/rccm.200703-456SO.

27. Poulain, M.; Doucet, M.; Major, G.C.; Drapeau, V.; Sériès, F.; Boulet, L.-P.; Tremblay, A.; Maltais, F. The effect of obesity on chronic respiratory diseases: pathophysiology and therapeutic strategies. *CMAJ* **2006**, *174*, 1293–1299, doi:10.1503/cmaj.051299.

28. Bellou, V.; Belbasis, L.; Tzoulaki, I.; Evangelou, E. Risk factors for type 2 diabetes mellitus: An exposure-wide umbrella review of meta-analyses. *PLoS One* **2018**, *13*, e0194127, doi:10.1371/journal.pone.0194127.

29. McIntyre, H.D.; Catalano, P.; Zhang, C.; Desoye, G.; Mathiesen, E.R.; Damm, P. Gestational diabetes mellitus. *Nat. Rev. Dis. Prim.* **2019**, *5*, 47, doi:10.1038/s41572-019-0098-8.

30. de la Monte, S.M.; Wands, J.R. Alzheimer's disease is type 3 diabetes-evidence reviewed. *J. Diabetes Sci. Technol.* **2008**, *2*, 1101–1113, doi:10.1177/193229680800200619.

31. Kovacs, G.G. Concepts and classification of neurodegenerative diseases. *Handb. Clin. Neurol.* **2017**, *145*, 301–307, doi:10.1016/B978-0-12-802395-2.00021-3.

32. Ahmed, R.M.; Devenney, E.M.; Irish, M.; Ittner, A.; Naismith, S.; Ittner, L.M.; Rohrer, J.D.; Halliday, G.M.; Eisen, A.; Hodges, J.R.; et al. Neuronal network disintegration: common pathways linking neurodegenerative diseases. *J. Neurol. Neurosurg. Psychiatry* **2016**, *87*, 1234–1241, doi:10.1136/jnnp-2014-308350.

33. Nugent, R.; Bertram, M.Y.; Jan, S.; Niessen, L.W.; Sassi, F.; Jamison, D.T.; Pier, E.G.; Beaglehole, R. Investing in non-communicable disease prevention and management to advance the Sustainable Development Goals. *Lancet* **2018**, *391*, 2029–2035, doi:https://doi.org/10.1016/S0140-6736(18)30667-6.

34. Billingsley, H.E.; Carbone, S.; Lavie, C.J. Dietary Fats and Chronic Noncommunicable Diseases. *Nutr.* 2018, *10*.

35. Popkin, B.M.; Adair, L.S.; Ng, S.W. Global nutrition transition and the pandemic of obesity in developing countries. *Nutr. Rev.* **2012**, *70*, 3–21, doi:10.1111/j.1753-4887.2011.00456.x.

36. Iriti, M.; Varoni, E.M.; Vitalini, S. Healthy Diets and Modifiable Risk Factors for Non-Communicable Diseases—The European Perspective. *Foods* 2020, *9*.

37. Trichopoulou, A.; Costacou, T.; Bamia, C.; Trichopoulos, D. Adherence to a Mediterranean diet and survival in a Greek population. *N. Engl. J. Med.* **2003**, *348*, 2599–2608, doi:10.1056/NEJMoa025039.

38. Knoops, K.T.B.; de Groot, L.C.P.G.M.; Kromhout, D.; Perrin, A.-E.; Moreiras-Varela, O.; Menotti, A.; van Staveren, W.A. Mediterranean diet, lifestyle factors, and 10-year mortality in elderly European men and women: the HALE project. *JAMA* **2004**, *292*, 1433–1439, doi:10.1001/jama.292.12.1433.

39. Kanerva, N.; Kaartinen, N.E.; Rissanen, H.; Knekt, P.; Eriksson, J.G.; Sääksjärvi, K.; Sundvall, J.; Männistö, S. Associations of the Baltic Sea diet with cardiometabolic risk factors--a meta-analysis of three Finnish studies. *Br. J. Nutr.* **2014**, *112*, 616–626, doi:10.1017/S0007114514001159.

40. Schulze, M.B.; Martínez-González, M.A.; Fung, T.T.; Lichtenstein, A.H.; Forouhi, N.G. Food based dietary patterns and chronic disease prevention. *BMJ* **2018**, *361*, k2396, doi:10.1136/bmj.k2396.

41. van Ommen, B.; van den Broek, T.; de Hoogh, I.; van Erk, M.; van Someren, E.; Rouhani-Rankouhi, T.; Anthony, J.C.; Hogenelst, K.; Pasman, W.; Boorsma, A.; et al. Systems biology of personalized nutrition. *Nutr. Rev.* **2017**, *75*, 579–599, doi:10.1093/nutrit/nux029.

42. Betts, J.A.; Gonzalez, J.T. Personalised nutrition: What makes you so special? *Nutr. Bull.* **2016**, *41*, 353–359, doi:https://doi.org/10.1111/nbu.12238.

43. Celis-Morales, C.; Lara, J.; Mathers, J.C. Personalising nutritional guidance for more effective behaviour change. *Proc. Nutr. Soc.* **2015**, *74*, 130–138, doi:10.1017/S0029665114001633.

44. Verma, M.; Hontecillas, R.; Tubau-Juni, N.; Abedi, V.; Bassaganya-Riera, J. Challenges in Personalized Nutrition and Health. *Front. Nutr.* 2018, *5*, 117.

45. Picó, C.; Serra, F.; Rodríguez, A.M.; Keijer, J.; Palou, A. Biomarkers of nutrition and health: New tools for new approaches. *Nutrients* **2019**, *11*, 1–30, doi:10.3390/nu11051092.

46. Knowler, W.C.; Barrett-Connor, E.; Fowler, S.E.; Hamman, R.F.; Lachin, J.M.; Walker, E.A.; Nathan, D.M. Reduction in the incidence of type 2 diabetes with lifestyle intervention or metformin. *N. Engl. J. Med.* **2002**, *346*, 393–403, doi:10.1056/NEJMoa012512.

47. Grad, F.P. The preamble of the constitution of the World Health Organization. *Bull. World Health Organ.* **2002**, *80*, 981.

48. Huber, M.; Knottnerus, J.A.; Green, L.; van der Horst, H.; Jadad, A.R.; Kromhout, D.; Leonard, B.; Lorig, K.; Loureiro, M.I.; van der Meer, J.W.M.; et al. How should we define health? *BMJ* **2011**, *343*, d4163, doi:10.1136/bmj.d4163.

49. van Ommen, B.; Keijer, J.; Heil, S.G.; Kaput, J. Challenging homeostasis to define biomarkers for nutrition related health. *Mol. Nutr. Food Res.* **2009**, *53*, 795–804, doi:10.1002/mnfr.200800390.

50. Strimbu, K.; Tavel, J.A. What are biomarkers? *Curr. Opin. HIV AIDS* **2010**, *5*, 463–466, doi:10.1097/COH.0b013e32833ed177.

51. B, van O.; J, van der G.; JM, O.; H, D. Phenotypic flexibility as key factor in the human nutrition and health relationship. *Genes Nutr.* **2014**, *9*, doi:10.1007/S12263-014-0423-5.

52. Sinclair, K.; Dudley, E. Metabolomics and Biomarker Discovery. *Adv. Exp. Med. Biol.* **2019**, *1140*, 613–633, doi:10.1007/978-3-030-15950-4_37.

53. Broek, T.J. van den; Bakker, G.C.M.; Rubingh, C.M.; Bijlsma, S.; Stroeve, J.H.M.; Ommen, B. van; Erk, M.J. van; Wopereis, S. Ranges of phenotypic flexibility in healthy subjects. *Genes Nutr.* **2017**, *12*, doi:10.1186/S12263-017-0589-8.

54. Qiu, C.; Kaplan, C.D. Functional assays for transcription mechanisms in high-throughput. *Methods*

2019, *159–160*, 115–123, doi:10.1016/j.ymeth.2019.02.017.

55. Carneiro, G.; Radcenco, A.L.; Evaristo, J.; Monnerat, G. Novel strategies for clinical investigation and biomarker discovery: a guide to applied metabolomics. *Horm. Mol. Biol. Clin. Investig.* **2019**, *38*, doi:10.1515/hmbci-2018-0045.

56. Stuart, T.; Satija, R. Integrative single-cell analysis. *Nat. Rev. Genet.* **2019**, *20*, 257–272, doi:10.1038/s41576-019-0093-7.

57. Orlov, Y.L.; Baranova, A. V Editorial: Bioinformatics of Genome Regulation and Systems Biology . *Front. Genet.* 2020, *11*, 625.

58. Fitó, M.; Melander, O.; Martínez, J.A.; Toledo, E.; Carpéné, C.; Corella, D. Advances in Integrating Traditional and Omic Biomarkers When Analyzing the Effects of the Mediterranean Diet Intervention in Cardiovascular Prevention. *Int. J. Mol. Sci.* 2016, *17*.

59. Novelli, G.; Ciccacci, C.; Borgiani, P.; Papaluca Amati, M.; Abadie, E. Genetic tests and genomic biomarkers: regulation, qualification and validation. *Clin. cases Miner. bone Metab. Off. J. Ital. Soc. Osteoporosis, Miner. Metab. Skelet. Dis.* **2008**, *5*, 149–154.

60. Green, E.D.; Watson, J.D.; Collins, F.S. Human Genome Project: Twenty-five years of big biology. *Nature* **2015**, *526*, 29–31, doi:10.1038/526029a.

61. Buniello, A.; MacArthur, J.A.L.; Cerezo, M.; Harris, L.W.; Hayhurst, J.; Malangone, C.; McMahon, A.; Morales, J.; Mountjoy, E.; Sollis, E.; et al. The NHGRI-EBI GWAS Catalog of published genome-wide association studies, targeted arrays and summary statistics 2019. *Nucleic Acids Res.* **2019**, *47*, D1005–D1012, doi:10.1093/nar/gky1120.

62. Ingelsson, E.; McCarthy, M.I. Human Genetics of Obesity and Type 2 Diabetes Mellitus: Past, Present, and Future. *Circ. Genomic Precis. Med.* **2018**, *11*, e002090, doi:10.1161/CIRCGEN.118.002090.

63. Gaulton, K.J.; Ferreira, T.; Lee, Y.; Raimondo, A.; Mägi, R.; Reschen, M.E.; Mahajan, A.; Locke, A.; William Rayner, N.; Robertson, N.; et al. Genetic fine mapping and genomic annotation defines causal mechanisms at type 2 diabetes susceptibility loci. *Nat. Genet.* **2015**, *47*, 1415–1425, doi:10.1038/ng.3437.

64. Erdmann, J.; Kessler, T.; Munoz Venegas, L.; Schunkert, H. A decade of genome-wide association studies for coronary artery disease: the challenges ahead. *Cardiovasc. Res.* **2018**, *114*, 1241–1257, doi:10.1093/cvr/cvy084.

65. Helgadottir, A.; Thorleifsson, G.; Manolescu, A.; Gretarsdottir, S.; Blondal, T.; Jonasdottir, A.; Jonasdottir, A.; Sigurdsson, A.; Baker, A.; Palsson, A.; et al. A common variant on chromosome 9p21 affects the risk of myocardial infarction. *Science* **2007**, *316*, 1491–1493, doi:10.1126/science.1142842.

66. Manjang, K.; Yli-Harja, O.; Dehmer, M.; Emmert-Streib, F. Limitations of Explainability for Established Prognostic Biomarkers of Prostate Cancer. *Front. Genet.* **2021**, *12*, 649429, doi:10.3389/fgene.2021.649429.

67. Novelli, G.; Biancolella, M.; Latini, A.; Spallone, A.; Borgiani, P.; Papaluca, M. Precision Medicine in Non-Communicable Diseases. *High-throughput* **2020**, *9*, doi:10.3390/ht9010003.

68. Weinhold, B. Epigenetics: the science of change. *Environ. Health Perspect.* **2006**, *114*, A160–A167, doi:10.1289/ehp.114-a160.

69. García-Giménez, J.L.; Seco-Cervera, M.; Tollefsbol, T.O.; Romá-Mateo, C.; Peiró-Chova, L.; Lapunzina, P.; Pallardó, F. V Epigenetic biomarkers: Current strategies and future challenges for their use in the clinical laboratory. *Crit. Rev. Clin. Lab. Sci.* **2017**, *54*, 529–550, doi:10.1080/10408363.2017.1410520.

70. Baccarelli, A.; Rienstra, M.; Benjamin, E.J. Cardiovascular epigenetics: basic concepts and results

from animal and human studies. *Circ. Cardiovasc. Genet.* **2010**, *3*, 567–573, doi:10.1161/CIRCGENETICS.110.958744.

71. Backes, C.; Meese, E.; Keller, A. Specific miRNA Disease Biomarkers in Blood, Serum and Plasma: Challenges and Prospects. *Mol. Diagn. Ther.* **2016**, *20*, 509–518, doi:10.1007/s40291-016-0221-4.

72. Soler-Botija, C.; Gálvez-Montón, C.; Bayés-Genís, A. Epigenetic Biomarkers in Cardiovascular Diseases. *Front. Genet.* **2019**, *10*, 950, doi:10.3389/fgene.2019.00950.

73. Friso, S.; Pizzolo, F.; Choi, S.-W.; Guarini, P.; Castagna, A.; Ravagnani, V.; Carletto, A.; Pattini, P.; Corrocher, R.; Olivieri, O. Epigenetic control of 11 beta-hydroxysteroid dehydrogenase 2 gene promoter is related to human hypertension. *Atherosclerosis* **2008**, *199*, 323–327, doi:10.1016/j.atherosclerosis.2007.11.029.

74. Pojoga, L.H.; Williams, J.S.; Yao, T.M.; Kumar, A.; Raffetto, J.D.; do Nascimento, G.R.A.; Reslan, O.M.; Adler, G.K.; Williams, G.H.; Shi, Y.; et al. Histone demethylase LSD1 deficiency during high-salt diet is associated with enhanced vascular contraction, altered NO-cGMP relaxation pathway, and hypertension. *Am. J. Physiol. Heart Circ. Physiol.* **2011**, *301*, H1862-71, doi:10.1152/ajpheart.00513.2011.

75. Kontaraki, J.E.; Marketou, M.E.; Zacharis, E.A.; Parthenakis, F.I.; Vardas, P.E. MicroRNA-9 and microRNA-126 expression levels in patients with essential hypertension: potential markers of target-organ damage. *J. Am. Soc. Hypertens.* **2014**, *8*, 368–375, doi:10.1016/j.jash.2014.03.324.

76. Aslam, B.; Basit, M.; Nisar, M.A.; Khurshid, M.; Rasool, M.H. Proteomics: Technologies and Their Applications. *J. Chromatogr. Sci.* **2017**, *55*, 182–196, doi:10.1093/chromsci/bmw167.

77. Zhang, X.; Yap, Y.; Wei, D.; Chen, G.; Chen, F. Novel omics technologies in nutrition research. *Biotechnol. Adv.* **2008**, *26*, 169–176, doi:10.1016/j.biotechadv.2007.11.002.

78. Cominetti, O.; Núñez Galindo, A.; Corthésy, J.; Oller Moreno, S.; Irincheeva, I.; Valsesia, A.; Astrup, A.; Saris, W.H.M.; Hager, J.; Kussmann, M.; et al. Proteomic Biomarker Discovery in 1000 Human Plasma Samples with Mass Spectrometry. *J. Proteome Res.* **2016**, *15*, 389–399, doi:10.1021/acs.jproteome.5b00901.

79. Chiu, C.-J.; Rabbani, N.; Rowan, S.; Chang, M.-L.; Sawyer, S.; Hu, F.B.; Willett, W.; Thornalley, P.J.; Anwar, A.; Bar, L.; et al. Studies of advanced glycation end products and oxidation biomarkers for type 2 diabetes. *Biofactors* **2018**, *44*, 281–288, doi:10.1002/biof.1423.

80. Marshall, J.; Bowden, P.; Schmit, J.C.; Betsou, F. Creation of a federated database of blood proteins: a powerful new tool for finding and characterizing biomarkers in serum. *Clin. Proteomics* **2014**, *11*, 3, doi:10.1186/1559-0275-11-3.

81. Newgard, C.B. Metabolomics and Metabolic Diseases: Where Do We Stand? *Cell Metab.* **2017**, *25*, 43–56, doi:10.1016/j.cmet.2016.09.018.

82. Manzoni, C.; Kia, D.A.; Vandrovcova, J.; Hardy, J.; Wood, N.W.; Lewis, P.A.; Ferrari, R. Genome, transcriptome and proteome: the rise of omics data and their integration in biomedical sciences. *Brief. Bioinform.* **2018**, *19*, 286–302, doi:10.1093/bib/bbw114.

83. Wishart, D.S. Emerging applications of metabolomics in drug discovery and precision medicine. *Nat. Rev. Drug Discov.* **2016**, *15*, 473–484, doi:10.1038/nrd.2016.32.

84. Li, X.S.; Wang, Z.; Cajka, T.; Buffa, J.A.; Nemet, I.; Hurd, A.G.; Gu, X.; Skye, S.M.; Roberts, A.B.; Wu, Y.; et al. Untargeted metabolomics identifies trimethyllysine, a TMAO-producing nutrient precursor, as a predictor of incident cardiovascular disease risk. *JCI insight* **2018**, *3*, doi:10.1172/jci.insight.99096.

85. Ismail, I.T.; Showalter, M.R.; Fiehn, O. Inborn Errors of Metabolism in the Era of Untargeted Metabolomics and Lipidomics. *Metabolites* **2019**, *9*, 242, doi:10.3390/metabo9100242.

86. Wilkins, J.M.; Trushina, E. Application of Metabolomics in Alzheimer's Disease. *Front. Neurol.* **2017**, *8*, 719, doi:10.3389/fneur.2017.00719.

87. Armitage, E.G.; Ciborowski, M. Applications of Metabolomics in Cancer Studies BT - Metabolomics: From Fundamentals to Clinical Applications. In; Sussulini, A., Ed.; Springer International Publishing: Cham, 2017; pp. 209–234 ISBN 978-3-319-47656-8.

88. Zhang, A.; Sun, H.; Wang, X. Emerging role and recent applications of metabolomics biomarkers in obesity disease research. *RSC Adv.* **2017**, *7*, 14966–14973, doi:10.1039/c6ra28715h.

89. Hasin, Y.; Seldin, M.; Lusis, A. Multi-omics approaches to disease. *Genome Biol.* **2017**, *18*, 83, doi:10.1186/s13059-017-1215-1.

90. Aderemi, A. V; Ayeleso, A.O.; Oyedapo, O.O.; Mukwevho, E. Metabolomics: A Scoping Review of Its Role as a Tool for Disease Biomarker Discovery in Selected Non-Communicable Diseases. *Metab.* 2021, *11*.

91. Wishart, D.S. Metabolomics: the principles and potential applications to transplantation. *Am. J. Transplant. Off. J. Am. Soc. Transplant. Am. Soc. Transpl. Surg.* **2005**, *5*, 2814–2820, doi:10.1111/j.1600-6143.2005.01119.x.

92. Weljie, A.M.; Newton, J.; Mercier, P.; Carlson, E.; Slupsky, C.M. Targeted profiling: quantitative analysis of 1H NMR metabolomics data. *Anal. Chem.* **2006**, *78*, 4430–4442, doi:10.1021/ac060209g.

93. Wang, T.J.; Larson, M.G.; Vasan, R.S.; Cheng, S.; Rhee, E.P.; McCabe, E.; Lewis, G.D.; Fox, C.S.; Jacques, P.F.; Fernandez, C.; et al. Metabolite profiles and the risk of developing diabetes. *Nat. Med.* **2011**, *17*, 448–453, doi:10.1038/nm.2307.

94. Gertsman, I.; Barshop, B.A. Promises and pitfalls of untargeted metabolomics. *J. Inherit. Metab. Dis.* **2018**, *41*, 355–366, doi:10.1007/s10545-017-0130-7.

95. Mastrangelo, A.; Barbas, C. Chronic Diseases and Lifestyle Biomarkers Identification by Metabolomics. *Adv. Exp. Med. Biol.* **2017**, *965*, 235–263, doi:10.1007/978-3-319-47656-8_10.

96. Chen, L.; Zhong, F.; Zhu, J. Bridging Targeted and Untargeted Mass Spectrometry-Based Metabolomics via Hybrid Approaches. *Metabolites* **2020**, *10*, doi:10.3390/metabo10090348.

97. González-Domínguez, R.; Sayago, A.; Fernández-Recamales, Á. Direct infusion mass spectrometry for metabolomic phenotyping of diseases. *Bioanalysis* **2017**, *9*, 131–148, doi:10.4155/bio-2016-0202.

98. Emwas, A.-H.M.; Salek, R.M.; Griffin, J.L.; Merzaban, J. NMR-based metabolomics in human disease diagnosis: applications, limitations, and recommendations. *Metabolomics* **2013**, *9*, 1048–1072, doi:10.1007/s11306-013-0524-y.

99. Wang, J.H.; Byun, J.; Pennathur, S. Analytical approaches to metabolomics and applications to systems biology. *Semin. Nephrol.* **2010**, *30*, 500–511, doi:10.1016/j.semnephrol.2010.07.007.

100. Gonzalez-Dominguez, A.; Duran-Guerrero, E.; Fernandez-Recamales, A.; Lechuga-Sancho, A.M.; Sayago, A.; Schwarz, M.; Segundo, C.; Gonzalez-Dominguez, R. An Overview on the Importance of Combining Complementary Analytical Platforms in Metabolomic Research. *Curr. Top. Med. Chem.* **2017**, *17*, 3289–3295, doi:10.2174/1568026618666171211144918.

101. Ardenkjaer-Larsen, J.-H.; Boebinger, G.S.; Comment, A.; Duckett, S.; Edison, A.S.; Engelke, F.; Griesinger, C.; Griffin, R.G.; Hilty, C.; Maeda, H.; et al. Facing and Overcoming Sensitivity Challenges in Biomolecular NMR Spectroscopy. *Angew. Chem. Int. Ed. Engl.* **2015**, *54*, 9162–9185, doi:10.1002/anie.201410653.

102. Theodoridis, G.; Gika, H.G.; Wilson, I.D. Mass spectrometry-based holistic analytical approaches for metabolite profiling in systems biology studies. *Mass Spectrom. Rev.* **2011**, *30*, 884–906, doi:10.1002/mas.20306.

103. Kuehnbaum, N.L.; Britz-McKibbin, P. New Advances in Separation Science for Metabolomics: Resolving Chemical Diversity in a Post-Genomic Era. *Chem. Rev.* **2013**, *113*, 2437–2468, doi:10.1021/cr300484s.

104. Pasikanti, K.K.; Ho, P.C.; Chan, E.C.Y. Gas chromatography/mass spectrometry in metabolic profiling of biological fluids. *J. Chromatogr. B, Anal. Technol. Biomed. life Sci.* **2008**, *871*, 202–211, doi:10.1016/j.jchromb.2008.04.033.

105. Schauer, N.; Steinhauser, D.; Strelkov, S.; Schomburg, D.; Allison, G.; Moritz, T.; Lundgren, K.; Roessner-Tunali, U.; Forbes, M.G.; Willmitzer, L.; et al. GC-MS libraries for the rapid identification of metabolites in complex biological samples. *FEBS Lett.* **2005**, *579*, 1332–1337, doi:10.1016/j.febslet.2005.01.029.

106. Moldoveanu, S.C.; David, V. Derivatization methods in GC and GC/MS. *Gas Chromatogr. Sample Prep. Appl.* **2018**.

107. Rainville, P.D.; Theodoridis, G.; Plumb, R.S.; Wilson, I.D. Advances in liquid chromatography coupled to mass spectrometry for metabolic phenotyping. *TrAC Trends Anal. Chem.* **2014**, *61*, 181–191, doi:https://doi.org/10.1016/j.trac.2014.06.005.

108. Barbas, C.; Moraes, E.P.; Villaseñor, A. Capillary electrophoresis as a metabolomics tool for non-targeted fingerprinting of biological samples. *J. Pharm. Biomed. Anal.* **2011**, *55*, 823–831, doi:10.1016/j.jpba.2011.02.001.

109. Brereton, R.G.; Jansen, J.; Lopes, J.; Marini, F.; Pomerantsev, A.; Rodionova, O.; Roger, J.M.; Walczak, B.; Tauler, R. Chemometrics in analytical chemistry-part I: history, experimental design and data analysis tools. *Anal. Bioanal. Chem.* **2017**, *409*, 5891–5899, doi:10.1007/s00216-017-0517-1.

110. Jolliffe, I. Principal Component Analysis. *Encycl. Stat. Behav. Sci.* 2005.

111. Wold, S.; Sjöström, M.; Eriksson, L. PLS-regression: a basic tool of chemometrics. *Chemom. Intell. Lab. Syst.* **2001**, *58*, 109–130, doi:https://doi.org/10.1016/S0169-7439(01)00155-1.

112. Bylesjö, M.; Rantalainen, M.; Cloarec, O.; Nicholson, J.K.; Holmes, E.; Trygg, J. OPLS discriminant analysis: combining the strengths of PLS-DA and SIMCA classification. *J. Chemom.* **2006**, *20*, 341–351, doi:https://doi.org/10.1002/cem.1006.

113. Pomyen, Y.; Wanichthanarak, K.; Poungsombat, P.; Fahrmann, J.; Grapov, D.; Khoomrung, S. Deep metabolome: Applications of deep learning in metabolomics. *Comput. Struct. Biotechnol. J.* **2020**, *18*, 2818–2825, doi:https://doi.org/10.1016/j.csbj.2020.09.033.

114. Kanehisa, M.; Goto, S. KEGG: kyoto encyclopedia of genes and genomes. *Nucleic Acids Res.* **2000**, *28*, 27–30, doi:10.1093/nar/28.1.27.

115. Smith, J.R.; Hayman, G.T.; Wang, S.-J.; Laulederkind, S.J.F.; Hoffman, M.J.; Kaldunski, M.L.; Tutaj, M.; Thota, J.; Nalabolu, H.S.; Ellanki, S.L.R.; et al. The Year of the Rat: The Rat Genome Database at 20: a multi-species knowledgebase and analysis platform. *Nucleic Acids Res.* **2020**, *48*, D731–D742, doi:10.1093/nar/gkz1041.

116. Wishart, D.S.; Feunang, Y.D.; Marcu, A.; Guo, A.C.; Liang, K.; Vázquez-Fresno, R.; Sajed, T.; Johnson, D.; Li, C.; Karu, N.; et al. HMDB 4.0: the human metabolome database for 2018. *Nucleic Acids Res.* **2018**, *46*, D608–D617, doi:10.1093/nar/gkx1089.

117. Frolkis, A.; Knox, C.; Lim, E.; Jewison, T.; Law, V.; Hau, D.D.; Liu, P.; Gautam, B.; Ly, S.; Guo, A.C.; et al. SMPDB: The Small Molecule Pathway Database. *Nucleic Acids Res.* **2010**, *38*, D480-7, doi:10.1093/nar/gkp1002.

118. Gilbert, J.A.; Quinn, R.A.; Debelius, J.; Xu, Z.Z.; Morton, J.; Garg, N.; Jansson, J.K.; Dorrestein, P.C.; Knight, R. Microbiome-wide association studies link dynamic microbial consortia to disease. *Nature* **2016**, *535*, 94–103, doi:10.1038/nature18850.

119. Blekhman, R.; Goodrich, J.K.; Huang, K.; Sun, Q.; Bukowski, R.; Bell, J.T.; Spector, T.D.; Keinan, A.; Ley, R.E.; Gevers, D.; et al. Host genetic variation impacts microbiome composition across human body sites. *Genome Biol.* **2015**, *16*, 191, doi:10.1186/s13059-015-0759-1.

120. Bonder, M.J.; Kurilshikov, A.; Tigchelaar, E.F.; Mujagic, Z.; Imhann, F.; Vila, A.V.; Deelen, P.; Vatanen, T.; Schirmer, M.; Smeekens, S.P.; et al. The effect of host genetics on the gut microbiome. *Nat. Genet.* **2016**, *48*, 1407–1412, doi:10.1038/ng.3663.

121. Proctor, D.M.; Relman, D.A. The Landscape Ecology and Microbiota of the Human Nose, Mouth, and Throat. *Cell Host Microbe* **2017**, *21*, 421–432, doi:10.1016/j.chom.2017.03.011.

122. McBurney, M.I.; Davis, C.; Fraser, C.M.; Schneeman, B.O.; Huttenhower, C.; Verbeke, K.; Walter, J.; Latulippe, M.E. Establishing What Constitutes a Healthy Human Gut Microbiome: State of the Science, Regulatory Considerations, and Future Directions. *J. Nutr.* **2019**, *149*, 1882–1895, doi:10.1093/jn/nxz154.

123. Durack, J.; Lynch, S. V The gut microbiome: Relationships with disease and opportunities for therapy. *J. Exp. Med.* **2019**, *216*, 20–40, doi:10.1084/jem.20180448.

124. Sanschagrin, S.; Yergeau, E. Next-generation sequencing of 16S ribosomal RNA gene amplicons. *J. Vis. Exp.* **2014**, 51709, doi:10.3791/51709.

125. Poretsky, R.; Rodriguez-R, L.M.; Luo, C.; Tsementzi, D.; Konstantinidis, K.T. Strengths and limitations of 16S rRNA gene amplicon sequencing in revealing temporal microbial community dynamics. *PLoS One* **2014**, *9*, e93827, doi:10.1371/journal.pone.0093827.

126. Kuczynski, J.; Lauber, C.L.; Walters, W.A.; Parfrey, L.W.; Clemente, J.C.; Gevers, D.; Knight, R. Experimental and analytical tools for studying the human microbiome. *Nat. Rev. Genet.* **2012**, *13*, 47–58, doi:10.1038/nrg3129.

127. Sims, D.; Sudbery, I.; Ilott, N.E.; Heger, A.; Ponting, C.P. Sequencing depth and coverage: key considerations in genomic analyses. *Nat. Rev. Genet.* **2014**, *15*, 121–132, doi:10.1038/nrg3642.

128. Biteen, J.S.; Blainey, P.C.; Cardon, Z.G.; Chun, M.; Church, G.M.; Dorrestein, P.C.; Fraser, S.E.; Gilbert, J.A.; Jansson, J.K.; Knight, R.; et al. Tools for the Microbiome: Nano and Beyond. *ACS Nano* **2016**, *10*, 6–37, doi:10.1021/acsnano.5b07826.

129. Poore, G.D.; Kopylova, E.; Zhu, Q.; Carpenter, C.; Fraraccio, S.; Wandro, S.; Kosciolek, T.; Janssen, S.; Metcalf, J.; Song, S.J.; et al. Microbiome analyses of blood and tissues suggest cancer diagnostic approach. *Nature* **2020**, *579*, 567–574, doi:10.1038/s41586-020-2095-1.

130. Rohart, F.; Gautier, B.; Singh, A.; Lê Cao, K.-A. mixOmics: An R package for 'omics feature selection and multiple data integration. *PLOS Comput. Biol.* **2017**, *13*, e1005752.

131. Singh, A.; Shannon, C.P.; Gautier, B.; Rohart, F.; Vacher, M.; Tebbutt, S.J.; Le Cao, K.-A. DIABLO: an integrative approach for identifying key molecular drivers from multi-omics assays. *Bioinformatics* **2019**, *35*, 3055–3062, doi:10.1093/bioinformatics/bty1054.

132. Vermeulen, R.; Schymanski, E.L.; Barabási, A.-L.; Miller, G.W. The exposome and health: Where chemistry meets biology. *Science* **2020**, *367*, 392–396, doi:10.1126/science.aay3164.

133. Ali, M.K.; Siegel, K.R.; Chandrasekar, E.; Tandon, N.; Montoya, P.A.; Mbanya, J.-C.; Chan, J.; Zhang, P.; Narayan, K.M.V. Diabetes: An Update on the Pandemic and Potential Solutions. In; Prabhakaran, D., Anand, S., Gaziano, T.A., Mbanya, J.-C., Wu, Y., Nugent, R., Eds.; Washington (DC), 2017 ISBN 9781464805189.

134. Mustafina, V.S.; Rymar, O.D.; Shcherbakova, L.V.; Voevoda, M.I. The epidemiology of obesity and the development of disorders of glucose metabolism according to a prospective study in Siberia. *Obe. Metab.* **2015**, *12*, 14–28.

135. Cosentino, F.; Grant, P.J.; Aboyans, V.; Bailey, C.J.; Ceriello, A.; Delgado, V.; Federici, M.; Filippatos, G.; Grobbee, D.E.; Hansen, T.B.; et al. 2019 ESC Guidelines on diabetes, pre-diabetes, and

cardiovascular diseases developed in collaboration with the EASD. *Eur. Heart J.* **2019**, *41*, 255–323, doi:10.1093/eurheartj/ehz486.

136. Aleksandrova, K.; Mozaffarian, D.; Pischon, T. Addressing the Perfect Storm: Biomarkers in Obesity and Pathophysiology of Cardiometabolic Risk. *Clin. Chem.* **2018**, *64*, 142–153, doi:10.1373/clinchem.2017.275172.

137. Bonadonna, R.C. Alterations of glucose metabolism in type 2 diabetes mellitus. An overview. *Rev. Endocr. Metab. Disord.* **2004**, *5*, 89–97, doi:10.1023/B:REMD.0000021429.89218.c6.

138. Titchenell, P.M.; Lazar, M.A.; Birnbaum, M.J. Unraveling the Regulation of Hepatic Metabolism by Insulin. *Trends Endocrinol. Metab.* **2017**, *28*, 497–505, doi:10.1016/j.tem.2017.03.003.

139. Bowe, J.E.; Franklin, Z.J.; Hauge-Evans, A.C.; King, A.J.; Persaud, S.J.; Jones, P.M. Metabolic phenotyping guidelines: assessing glucose homeostasis in rodent models. *J. Endocrinol.* **2014**, *222*, G13-25, doi:10.1530/JOE-14-0182.

140. Islam, M.S.; Loots, D.T. Experimental rodent models of type 2 diabetes: a review. *Methods Find. Exp. Clin. Pharmacol.* **2009**, *31*, 249–261, doi:10.1358/mf.2009.31.4.1362513.

141. Szkudelski, T. The mechanism of alloxan and streptozotocin action in B cells of the rat pancreas. *Physiol. Res.* **2001**, *50*, 537–546.

142. Rohilla, A.; Ali, S. Alloxan induced diabetes: mechanisms and effects. *Int. J. Res. Pharm. Biomed. Sci.* **2012**, *3*, 819–823.

143. Mansour, H.A.; Newairy, A.-S.A.; Yousef, M.I.; Sheweita, S.A. Biochemical study on the effects of some Egyptian herbs in alloxan-induced diabetic rats. *Toxicology* **2002**, *170*, 221–228, doi:https://doi.org/10.1016/S0300-483X(01)00555-8.

144. Xu, M.; Sun, B.; Li, D.; Mao, R.; Li, H.; Li, Y.; Wang, J. Beneficial Effects of Small Molecule Oligopeptides Isolated from Panax ginseng Meyer on Pancreatic Beta-Cell Dysfunction and Death in Diabetic Rats. *Nutrients* **2017**, *9*, doi:10.3390/nu9101061.

145. Furman, B.L. Streptozotocin-Induced Diabetic Models in Mice and Rats. *Curr. Protoc. Pharmacol.* **2015**, *70*, 5.47.1-5.47.20, doi:10.1002/0471141755.ph0547s70.

146. Arora, S.; Ojha, S.K.; Vohora, D. Characterisation of streptozotocin induced diabetes mellitus in swiss albino mice. *Glob. J. Pharmacol.* **2009**, *3*, 81–84.

147. George, G.S.; Uwakwe, A.A.; Ibeh, G.O. Glycated haemoglobin, glucose and insulin levels in diabetic treated rats. *Can J Pure Appl Sci* **2013**, *7*, 2223–2226.

148. Sadek, K.M.; Lebda, M.A.; Nasr, S.M.; Shoukry, M. Spirulina platensis prevents hyperglycemia in rats by modulating gluconeogenesis and apoptosis via modification of oxidative stress and MAPK-pathways. *Biomed. Pharmacother.* **2017**, *92*, 1085–1094, doi:10.1016/j.biopha.2017.06.023.

149. Tojo, A.; Hatakeyama, S.; Nangaku, M.; Ishimitsu, T. H(+)-ATPase blockade reduced renal gluconeogenesis and plasma glucose in a diabetic rat model. *Med. Mol. Morphol.* **2018**, *51*, 89–95, doi:10.1007/s00795-017-0175-6.

150. Srinivasan, K.; Viswanad, B.; Asrat, L.; Kaul, C.L.; Ramarao, P. Combination of high-fat diet-fed and low-dose streptozotocin-treated rat: A model for type 2 diabetes and pharmacological screening. *Pharmacol. Res.* **2005**, *52*, 313–320, doi:https://doi.org/10.1016/j.phrs.2005.05.004.

151. Magalhães, D.A.D.E.; Kume, W.T.; Correia, F.S.; Queiroz, T.S.; Allebrandt Neto, E.W.; Santos, M.P. Dos; Kawashita, N.H.; França, S.A.D.E. High-fat diet and streptozotocin in the induction of type 2 diabetes mellitus: a new proposal. *An. Acad. Bras. Cienc.* **2019**, *91*, e20180314, doi:10.1590/0001-3765201920180314.

152. Arya, A.; Cheah, S.C.; Looi, C.Y.; Taha, H.; Rais Mustafa, M.; Mohd, M.A. The methanolic fraction of Centratherum anthelminticum seed downregulates pro-inflammatory cytokines, oxidative stress, and hyperglycemia in STZ-nicotinamide-induced type 2 diabetic rats. *Food Chem. Toxicol.*

2012, *50*, 4209–4220, doi:https://doi.org/10.1016/j.fct.2012.08.012.

153. Rashid, U.; Khan, M.R.; Sajid, M. Antioxidant, anti-inflammatory and hypoglycemic effects of Fagonia olivieri DC on STZ-nicotinamide induced diabetic rats - In vivo and in vitro study. *J. Ethnopharmacol.* **2019**, *242*, 112038, doi:https://doi.org/10.1016/j.jep.2019.112038.

154. Kaur, N.; Kishore, L.; Singh, R. Therapeutic effect of Linum usitatissimum L. in STZ-nicotinamide induced diabetic nephropathy via inhibition of AGE's and oxidative stress. *J. Food Sci. Technol.* **2017**, *54*, 408–421, doi:10.1007/s13197-016-2477-4.

155. Mach, F.; Baigent, C.; Catapano, A.L.; Koskinas, K.C.; Casula, M.; Badimon, L.; Chapman, M.J.; De Backer, G.G.; Delgado, V.; Ference, B.A.; et al. 2019 ESC/EAS Guidelines for the management of dyslipidaemias: lipid modification to reduce cardiovascular risk. *Eur. Heart J.* **2020**, *41*, 111–188, doi:10.1093/eurheartj/ehz455.

156. Williams, B.; Mancia, G.; Spiering, W.; Rosei, E.A.; Azizi, M.; Burnier, M.; Clement, D.L.; Coca, A.; De Simone, G.; Dominiczak, A.; et al. *2018 ESC/ESH Guidelines for the management of arterial hypertension*; 2018; Vol. 39; ISBN 0000000000.

157. Chobanian, A. V; Bakris, G.L.; Black, H.R.; Cushman, W.C.; Green, L.A.; Izzo, J.L.J.; Jones, D.W.; Materson, B.J.; Oparil, S.; Wright, J.T.J.; et al. The Seventh Report of the Joint National Committee on Prevention, Detection, Evaluation, and Treatment of High Blood Pressure: the JNC 7 report. *JAMA* **2003**, *289*, 2560–2572, doi:10.1001/jama.289.19.2560.

158. Eaton, C.B.; Feldman, H.A.; Assaf, A.R.; McPhillips, J.B.; Hume, A.L.; Lasater, T.M.; Levinson, P.; Carleton, R.A. Prevalence of hypertension, dyslipidemia, and dyslipidemic hypertension. *J. Fam. Pract.* **1994**, *38*, 17–23.

159. Dalal, J.J.; Padmanabhan, T.N.C.; Jain, P.; Patil, S.; Vasnawala, H.; Gulati, A. LIPITENSION: Interplay between dyslipidemia and hypertension. *Indian J. Endocrinol. Metab.* **2012**, *16*, 240–245, doi:10.4103/2230-8210.93742.

160. Pirillo, A.; Casula, M.; Olmastroni, E.; Norata, G.D.; Catapano, A.L. Global epidemiology of dyslipidaemias. *Nat. Rev. Cardiol.* **2021**, *18*, 689–700, doi:10.1038/s41569-021-00541-4.

161. Worldwide trends in hypertension prevalence and progress in treatment and control from 1990 to 2019: a pooled analysis of 1201 population-representative studies with 104 million participants. *Lancet (London, England)* **2021**, *398*, 957–980, doi:10.1016/S0140-6736(21)01330-1.

162. Mills, K.T.; Stefanescu, A.; He, J. The global epidemiology of hypertension. *Nat. Rev. Nephrol.* **2020**, *16*, 223–237, doi:10.1038/s41581-019-0244-2.

163. Tabas, I.; Williams, K.J.; Borén, J. Subendothelial lipoprotein retention as the initiating process in atherosclerosis: update and therapeutic implications. *Circulation* **2007**, *116*, 1832–1844, doi:10.1161/CIRCULATIONAHA.106.676890.

164. Slivnick, J.; Lampert, B.C. Hypertension and Heart Failure. *Heart Fail. Clin.* **2019**, *15*, 531–541, doi:10.1016/j.hfc.2019.06.007.

165. Bhatt, D.L.; Steg, P.G.; Ohman, E.M.; Hirsch, A.T.; Ikeda, Y.; Mas, J.-L.; Goto, S.; Liau, C.-S.; Richard, A.J.; Röther, J.; et al. International prevalence, recognition, and treatment of cardiovascular risk factors in outpatients with atherothrombosis. *JAMA* **2006**, *295*, 180–189, doi:10.1001/jama.295.2.180.

166. Mancia, G.; Facchetti, R.; Bombelli, M.; Polo Friz, H.; Grassi, G.; Giannattasio, C.; Sega, R. Relationship of office, home, and ambulatory blood pressure to blood glucose and lipid variables in the PAMELA population. *Hypertens. (Dallas, Tex. 1979)* **2005**, *45*, 1072–1077, doi:10.1161/01.HYP.0000165672.69176.ed.

167. Sullivan, M.P.; Cerda, J.J.; Robbins, F.L.; Burgin, C.W.; Beatty, R.J. The gerbil, hamster, and guinea pig as rodent models for hyperlipidemia. *Lab. Anim. Sci.* **1993**, *43*, 575–578.

168. Kasiske, B.L.; O'Donnell, M.P.; Keane, W.F. The Zucker rat model of obesity, insulin resistance, hyperlipidemia, and renal injury. *Hypertens. (Dallas, Tex. 1979)* **1992**, *19*, I110-5, doi:10.1161/01.hyp.19.1_suppl.i110.

169. Zhao, Y.; Qu, H.; Wang, Y.; Xiao, W.; Zhang, Y.; Shi, D. Small rodent models of atherosclerosis. *Biomed. Pharmacother.* **2020**, *129*, 110426, doi:https://doi.org/10.1016/j.biopha.2020.110426.

170. Sithu, S.D.; Malovichko, M. V; Riggs, K.A.; Wickramasinghe, N.S.; Winner, M.G.; Agarwal, A.; Hamed-Berair, R.E.; Kalani, A.; Riggs, D.W.; Bhatnagar, A.; et al. Atherogenesis and metabolic dysregulation in LDL receptor-knockout rats. *JCI insight* **2017**, *2*, doi:10.1172/jci.insight.86442.

171. Fang, B.; Ren, X.; Wang, Y.; Li, Z.; Zhao, L.; Zhang, M.; Li, C.; Zhang, Z.; Chen, L.; Li, X.; et al. Apolipoprotein E deficiency accelerates atherosclerosis development in miniature pigs. *Dis. Model. Mech.* **2018**, *11*, dmm036632, doi:10.1242/dmm.036632.

172. Zhao, Y.; Yang, Y.; Xing, R.; Cui, X.; Xiao, Y.; Xie, L.; You, P.; Wang, T.; Zeng, L.; Peng, W.; et al. Hyperlipidemia induces typical atherosclerosis development in Ldlr and Apoe deficient rats. *Atherosclerosis* **2018**, *271*, 26–35, doi:10.1016/j.atherosclerosis.2018.02.015.

173. Johnston, T.P. The P-407-induced murine model of dose-controlled hyperlipidemia and atherosclerosis: a review of findings to date. *J. Cardiovasc. Pharmacol.* **2004**, *43*, 595–606, doi:10.1097/00005344-200404000-00016.

174. Korolenko, T.A.; Johnston, T.P.; Tuzikov, F. V; Tuzikova, N.A.; Pupyshev, A.B.; Spiridonov, V.K.; Goncharova, N. V; Maiborodin, I. V; Zhukova, N.A. Early-stage atherosclerosis in poloxamer 407-induced hyperlipidemic mice: pathological features and changes in the lipid composition of serum lipoprotein fractions and subfractions. *Lipids Health Dis.* **2016**, *15*, 16, doi:10.1186/s12944-016-0186-7.

175. Johnston, T.P.; Palmer, W.K. The effect of pravastatin on hepatic 3-hydroxy-3-methylglutaryl CoA reductase obtained from poloxamer 407-induced hyperlipidemic rats. *Pharmacotherapy* **1997**, *17*, 342–347.

176. Blonder, J.M.; Baird, L.; Fulfs, J.C.; Rosenthal, G.J. Dose-dependent hyperlipidemia in rabbits following administration of poloxamer 407 gel. *Life Sci.* **1999**, *65*, PL261-6, doi:10.1016/s0024-3205(99)00495-6.

177. Suárez-García, S.; Caimari, A.; del Bas, J.M.; Suárez, M.; Arola, L. Serum lysophospholipid levels are altered in dyslipidemic hamsters. *Sci. Rep.* **2017**, *7*, 10431, doi:10.1038/s41598-017-10651-0.

178. Tanko, Y.; Kabiru, A.; Abdulrasak, A.; Mohammed, K.A.; Salisu, A.I.; Jimoh, A.; Gidado, N.M.; Sada, N.M. Effects of Fermented Ginger Rhizome (Zingiber officinale) and Fenu Greek (Trigonella foenum-graceum) Supplements on Oxidative stress and Lipid Peroxidation Biomarkers in Poloxamer-407 Induced -Hyperlipidemic Wistar Rats. *Niger. J. Physiol. Sci.* **2017**, *32*, 137–143.

179. Chaudhary, H.R.; Brocks, D.R. The single dose poloxamer 407 model of hyperlipidemia; systemic effects on lipids assessed using pharmacokinetic methods, and its effects on adipokines. *J. Pharm. Pharm. Sci.* **2013**, *16*, 65–73, doi:10.18433/j37g7m.

180. Korolenko, T.A.; Johnston, T.P.; Dubrovina, N.I.; Kisarova, Y.A.; Zhanaeva, S.Y.; Cherkanova, M.S.; Filjushina, E.E.; Alexeenko, T. V; Machova, E.; Zhukova, N.A. Effect of poloxamer 407 administration on the serum lipids profile, anxiety level and protease activity in the heart and liver of mice. *Interdiscip. Toxicol.* **2013**, *6*, 18–25, doi:10.2478/intox-2013-0004.

181. Korolenko, T.A.; Tuzikov, F. V; Johnston, T.P.; Tuzikova, N.A.; Kisarova, Y.A.; Zhanaeva, S.Y.; Alexeenko, T. V; Zhukova, N.A.; Brak, I. V; Spiridonov, V.K.; et al. The influence of repeated administration of poloxamer 407 on serum lipoproteins and protease activity in mouse liver and heart. *Can. J. Physiol. Pharmacol.* **2012**, *90*, 1456–1468, doi:10.1139/y2012-118.

182. Akiyama, T.; Tachibana, I.; Shirohara, H.; Watanabe, N.; Otsuki, M. High-fat hypercaloric diet induces obesity, glucose intolerance and hyperlipidemia in normal adult male Wistar rat. *Diabetes Res. Clin. Pract.* **1996**, *31*, 27–35, doi:https://doi.org/10.1016/0168-8227(96)01205-3.

183. Schreyer, S.A.; Wilson, D.L.; LeBoeuf, R.C. C57BL/6 mice fed high fat diets as models for diabetes-accelerated atherosclerosis. *Atherosclerosis* **1998**, *136*, 17–24, doi:https://doi.org/10.1016/S0021-9150(97)00165-2.

184. Ruchel, J.B.; Braun, J.B.S.; Adefegha, S.A.; Guedes Manzoni, A.; Abdalla, F.H.; de Oliveira, J.S.; Trelles, K.; Signor, C.; Lopes, S.T.A.; da Silva, C.B.; et al. Guarana (Paullinia cupana) ameliorates memory impairment and modulates acetylcholinesterase activity in Poloxamer-407-induced hyperlipidemia in rat brain. *Physiol. Behav.* **2017**, *168*, 11–19, doi:https://doi.org/10.1016/j.physbeh.2016.10.003.

185. Yeom, M.; Park, J.; Lee, B.; Lee, H.S.; Park, H.-J.; Won, R.; Lee, H.; Hahm, D.-H. Electroacupuncture ameliorates poloxamer 407-induced hyperlipidemia through suppressing hepatic SREBP-2 expression in rats. *Life Sci.* **2018**, *203*, 20–26, doi:10.1016/j.lfs.2018.04.016.

186. Pinto, Y.M.; Paul, M.; Ganten, D. Lessons from rat models of hypertension: from Goldblatt to genetic engineering. *Cardiovasc. Res.* **1998**, *39*, 77–88, doi:10.1016/s0008-6363(98)00077-7.

187. Lerman, L.O.; Kurtz, T.W.; Touyz, R.M.; Ellison, D.H.; Chade, A.R.; Crowley, S.D.; Mattson, D.L.; Mullins, J.J.; Osborn, J.; Eirin, A.; et al. Animal Models of Hypertension: A Scientific Statement From the American Heart Association. *Hypertension* **2019**, *73*, e87–e120, doi:10.1161/HYP.0000000000000090.

188. Doris, P.A. Genetics of hypertension: an assessment of progress in the spontaneously hypertensive rat. *Physiol. Genomics* **2017**, *49*, 601–617, doi:10.1152/physiolgenomics.00065.2017.

189. Hallbäck, M.; Weiss, L. Mechanisms of spontaneous hypertension in rats. *Med. Clin. North Am.* **1977**, *61*, 593–609, doi:10.1016/s0025-7125(16)31319-0.

190. Morgan, D.A.; DiBona, G.F.; Mark, A.L. Effects of interstrain renal transplantation on NaCl-induced hypertension in Dahl rats. *Hypertens. (Dallas, Tex. 1979)* **1990**, *15*, 436–442, doi:10.1161/01.hyp.15.4.436.

191. Kuijpers, M.H.; de Jong, W. Spontaneous hypertension in the fawn-hooded rat: a cardiovascular disease model. *J. Hypertens. Suppl. Off. J. Int. Soc. Hypertens.* **1986**, *4*, S41-4.

192. Bianchi, G.; Ferrari, P.; Salvati, P.; Salardi, S.; Parenti, P.; Cusi, D.; Guidi, E. A renal abnormality in the Milan hypertensive strain of rats and in humans predisposed to essential hypertension. *J. Hypertens. Suppl. Off. J. Int. Soc. Hypertens.* **1986**, *4*, S33-6.

193. Biol, M.C.; Vincent, M.; Sassard, J. Ouabain-sensitive and -insensitive ATPase activities in the kidney and the liver of spontaneously hypertensive rats. *Arch. Int. Physiol. Biochim.* **1979**, *87*, 291–296, doi:10.3109/13813457909070501.

194. Mullins, J.J.; Peters, J.; Ganten, D. Fulminant hypertension in transgenic rats harbouring the mouse Ren-2 gene. *Nature* **1990**, *344*, 541–544, doi:10.1038/344541a0.

195. Vijay, A.; Valdes, A.M. Role of the gut microbiome in chronic diseases: a narrative review. *Eur. J. Clin. Nutr.* **2021**, doi:10.1038/s41430-021-00991-6.

196. Duvallet, C.; Gibbons, S.M.; Gurry, T.; Irizarry, R.A.; Alm, E.J. Meta-analysis of gut microbiome studies identifies disease-specific and shared responses. *Nat. Commun.* **2017**, *8*, 1784, doi:10.1038/s41467-017-01973-8.

197. Brody, H. The gut microbiome. *Nature* 2020, *577*, S5.

198. Ghoshal, U.C.; Ghoshal, U. Small Intestinal Bacterial Overgrowth and Other Intestinal Disorders. *Gastroenterol. Clin. North Am.* **2017**, *46*, 103–120, doi:10.1016/j.gtc.2016.09.008.

199. Eisenstein, M. The hunt for a healthy microbiome. *Nature* 2020, *577*, S6–S8.

200. Cani, P.D. Gut microbiota: Changes in gut microbes and host metabolism: squaring the circle? *Nat. Rev. Gastroenterol. Hepatol.* **2016**, *13*, 563–564, doi:10.1038/nrgastro.2016.135.

201. Shreiner, A.B.; Kao, J.Y.; Young, V.B. The gut microbiome in health and in disease. *Curr. Opin. Gastroenterol.* **2015**, *31*, 69–75, doi:10.1097/MOG.0000000000000139.

202. Schroeder, B.O.; Bäckhed, F. Signals from the gut microbiota to distant organs in physiology and disease. *Nat. Med.* **2016**, *22*, 1079–1089, doi:10.1038/nm.4185.

203. Eckburg, P.B.; Bik, E.M.; Bernstein, C.N.; Purdom, E.; Dethlefsen, L.; Sargent, M.; Gill, S.R.; Nelson, K.E.; Relman, D.A. Diversity of the human intestinal microbial flora. *Science* **2005**, *308*, 1635–1638, doi:10.1126/science.1110591.

204. Maruvada, P.; Leone, V.; Kaplan, L.M.; Chang, E.B. The Human Microbiome and Obesity: Moving beyond Associations. *Cell Host Microbe* **2017**, *22*, 589–599, doi:10.1016/j.chom.2017.10.005.

205. Del Bas, J.M.; Guirro, M.; Boqué, N.; Cereto, A.; Ras, R.; Crescenti, A.; Caimari, A.; Canela, N.; Arola, L. Alterations in gut microbiota associated with a cafeteria diet and the physiological consequences in the host. *Int. J. Obes. (Lond).* **2018**, *42*, 746–754, doi:10.1038/ijo.2017.284.

206. Guirro, M.; Costa, A.; Gual-Grau, A.; Herrero, P.; Torrell, H.; Canela, N.; Arola, L. Effects from diet-induced gut microbiota dysbiosis and obesity can be ameliorated by fecal microbiota transplantation: A multiomics approach. *PLoS One* **2019**, *14*, e0218143, doi:10.1371/journal.pone.0218143.

207. Malmuthuge, N.; Griebel, P.J. A Novel Animal Model for Regional Microbial Dysbiosis of the Pioneer Microbial Community. *Front. Microbiol.* **2019**, *10*, 1706, doi:10.3389/fmicb.2019.01706.

208. Cho, I.; Yamanishi, S.; Cox, L.; Methé, B.A.; Zavadil, J.; Li, K.; Gao, Z.; Mahana, D.; Raju, K.; Teitler, I.; et al. Antibiotics in early life alter the murine colonic microbiome and adiposity. *Nature* **2012**, *488*, 621–626, doi:10.1038/nature11400.

209. Butts, C.A.; Paturi, G.; Stoklosinski, H.; Martell, S.; Hedderley, D.; Carpenter, E. Animal Model of Antibiotic Induced Gut Microbiota Dysbiosis. *Proc.* 2019, *8*.

210. Charles, B.; Sakina, S.-J.; Thuy, N.T.; Perrine, H.; Frédérique, S.-G.; Nathalie, S.-L.; Tanguy, C.; Stéphanie, F.; Mark, P.; William, W.; et al. Antibiotic-Induced Dysbiosis Predicts Mortality in an Animal Model of Clostridium difficile Infection. *Antimicrob. Agents Chemother.* **2021**, *62*, e00925-18, doi:10.1128/AAC.00925-18.

211. Manichanh, C.; Reeder, J.; Gibert, P.; Varela, E.; Llopis, M.; Antolin, M.; Guigo, R.; Knight, R.; Guarner, F. Reshaping the gut microbiome with bacterial transplantation and antibiotic intake. *Genome Res.* **2010**, *20*, 1411–1419, doi:10.1101/gr.107987.110.

212. Saint-Cyr, M.J.; Perrin-Guyomard, A.; Houée, P.; Rolland, J.-G.; Laurentie, M. Evaluation of an oral subchronic exposure of deoxynivalenol on the composition of human gut microbiota in a model of human microbiota-associated rats. *PLoS One* **2013**, *8*, e80578–e80578, doi:10.1371/journal.pone.0080578.

213. Furman, D.; Campisi, J.; Verdin, E.; Carrera-Bastos, P.; Targ, S.; Franceschi, C.; Ferrucci, L.; Gilroy, D.W.; Fasano, A.; Miller, G.W.; et al. Chronic inflammation in the etiology of disease across the life span. *Nat. Med.* **2019**, *25*, 1822–1832, doi:10.1038/s41591-019-0675-0.

214. Global, regional, and national age-sex-specific mortality for 282 causes of death in 195 countries and territories, 1980-2017: a systematic analysis for the Global Burden of Disease Study 2017. *Lancet (London, England)* **2018**, *392*, 1736–1788, doi:10.1016/S0140-6736(18)32203-7.

215. Netea, M.G.; Balkwill, F.; Chonchol, M.; Cominelli, F.; Donath, M.Y.; Giamarellos-Bourboulis, E.J.; Golenbock, D.; Gresnigt, M.S.; Heneka, M.T.; Hoffman, H.M.; et al. A guiding map for inflammation. *Nat. Immunol.* **2017**, *18*, 826–831, doi:10.1038/ni.3790.

216. Bennett, J.M.; Reeves, G.; Billman, G.E.; Sturmberg, J.P. Inflammation-Nature's Way to Efficiently Respond to All Types of Challenges: Implications for Understanding and Managing "the Epidemic" of Chronic Diseases. *Front. Med.* **2018**, *5*, 316, doi:10.3389/fmed.2018.00316.

217. Liston, A.; Masters, S.L. Homeostasis-altering molecular processes as mechanisms of inflammasome activation. *Nat. Rev. Immunol.* **2017**, *17*, 208–214, doi:10.1038/nri.2016.151.

218. Franceschi, C.; Garagnani, P.; Vitale, G.; Capri, M.; Salvioli, S. Inflammaging and "Garb-aging". *Trends Endocrinol. Metab.* **2017**, *28*, 199–212, doi:10.1016/j.tem.2016.09.005.

219. Hamesch, K.; Borkham-Kamphorst, E.; Strnad, P.; Weiskirchen, R. Lipopolysaccharide-induced inflammatory liver injury in mice. *Lab. Anim.* **2015**, *49*, 37–46, doi:10.1177/0023677215570087.

220. Ranneh, Y.; Akim, A.M.; Hamid, H.A.; Khazaai, H.; Mokhtarrudin, N.; Fadel, A.; Albujja, M.H.K. Induction of Chronic Subclinical Systemic Inflammation in Sprague-Dawley Rats Stimulated by Intermittent Bolus Injection of Lipopolysaccharide. *Arch. Immunol. Ther. Exp. (Warsz).* **2019**, *67*, 385–400, doi:10.1007/s00005-019-00553-6.

221. Krempien, B.; Vukičević, S.; Vogel, M.; Stavljenić, A.; Böchele, R. Cellular basis of inflammation-induced osteopenia in growing rats. *J. Bone Miner. Res.* 1988, *3*, 573–582.

222. Yamada, T.; Deitch, E.; Specian, R.D.; Perry, M.A.; Sartor, R.B.; Grisham, M.B. Mechanisms of acute and chronic intestinal inflammation induced by indomethacin. *Inflammation* **1993**, *17*, 641–662, doi:10.1007/BF00920471.

223. Rorato, R.; Borges, B. de C.; Uchoa, E.T.; Antunes-Rodrigues, J.; Elias, C.F.; Kagohara Elias, L.L. LPS-induced low-grade inflammation increases hypothalamic JNK expression and causes central insulin resistance irrespective of body weight changes. *Int. J. Mol. Sci.* **2017**, *18*, 1–14, doi:10.3390/ijms18071431.

224. Asgharzadeh, F.; Bargi, R.; Hosseini, M.; Farzadnia, M.; Khazaei, M. Cardiac and renal fibrosis and oxidative stress balance in lipopolysaccharide-induced inflammation in male rats. *ARYA Atheroscler.* **2018**, *14*, 71–77, doi:10.22122/arya.v14i2.1550.

225. Kudo, K.; Hagiwara, S.; Hasegawa, A.; Kusaka, J.; Koga, H.; Noguchi, T. Cepharanthine exerts anti-inflammatory effects via NF-κB inhibition in a LPS-induced rat model of systemic inflammation. *J. Surg. Res.* **2011**, *171*, 199–204, doi:10.1016/j.jss.2010.01.007.

226. Droke, E.A.; Hager, K.A.; Lerner, M.R.; Lightfoot, S.A.; Stoecker, B.J.; Brackett, D.J.; Smith, B.J. Soy isoflavones avert chronic inflammation-induced bone loss and vascular disease. *J. Inflamm.* **2007**, *4*, 1–12, doi:10.1186/1476-9255-4-17.

227. Smith, B.J.; Lerner, M.R.; Bu, S.Y.; Lucas, E.A.; Hanas, J.S.; Lightfoot, S.A.; Postier, R.G.; Bronze, M.S.; Brackett, D.J. Systemic bone loss and induction of coronary vessel disease in a rat model of chronic inflammation. *Bone* **2006**, *38*, 378–386, doi:10.1016/j.bone.2005.09.008.

228. Smith, B.J.; Lightfoot, S.A.; Lerner, M.R.; Denson, K.D.; Morgan, D.L.; Hanas, J.S.; Bronze, M.S.; Postier, R.G.; Brackett, D.J. Induction of cardiovascular pathology in a novel model of low-grade chronic inflammation. *Cardiovasc. Pathol.* **2009**, *18*, 1–10, doi:10.1016/j.carpath.2007.07.011.

229. Arimura, K.; Aoshiba, K.; Tsuji, T.; Tamaoki, J. Chronic low-grade systemic inflammation causes dna damage in the lungs of mice. *Lung* **2012**, *190*, 613–620, doi:10.1007/s00408-012-9414-8.

230. Saritha Krishnaa, Celia A. Dodda,1, and Nikolay M. Filipova, * Behavioral and monoamine perturbations in adult male mice with chronic inflammation induced by repeated peripheral lipopolysaccharide administration. **2016**, *131*, 1796–1803, doi:10.1161/CIRCULATIONAHA.114.010270.Hospital.

231. Liu, D.; Cao, S.; Zhou, Y.; Xiong, Y. Recent advances in endotoxin tolerance. *J. Cell. Biochem.* **2019**, *120*, 56–70, doi:10.1002/jcb.27547.

232. Toyokuni, S. Molecular mechanisms of oxidative stress-induced carcinogenesis: from epidemiology to oxygenomics. *IUBMB Life* **2008**, *60*, 441–447, doi:10.1002/iub.61.

233. Kim, D.; Chen, Z.; Zhou, L.-F.; Huang, S.-X. Air pollutants and early origins of respiratory diseases. *Chronic Dis. Transl. Med.* **2018**, *4*, 75–94, doi:https://doi.org/10.1016/j.cdtm.2018.03.003.

234. Sies, H.; Cadenas, E. Oxidative stress: damage to intact cells and organs. *Philos. Trans. R. Soc. London. Ser. B, Biol. Sci.* **1985**, *311*, 617–631, doi:10.1098/rstb.1985.0168.

235. Al-Gubory, K.H.; Garrel, C.; Faure, P.; Sugino, N. Roles of antioxidant enzymes in corpus luteum rescue from reactive oxygen species-induced oxidative stress. *Reprod. Biomed. Online* **2012**, *25*, 551–560, doi:10.1016/j.rbmo.2012.08.004.

236. Hansen, J.M.; Go, Y.-M.; Jones, D.P. Nuclear and mitochondrial compartmentation of oxidative stress and redox signaling. *Annu. Rev. Pharmacol. Toxicol.* **2006**, *46*, 215–234, doi:10.1146/annurev.pharmtox.46.120604.141122.

237. Glasauer, A.; Chandel, N.S. Targeting antioxidants for cancer therapy. *Biochem. Pharmacol.* **2014**, *92*, 90–101, doi:10.1016/j.bcp.2014.07.017.

238. Forman, H.J.; Zhang, H. Targeting oxidative stress in disease: promise and limitations of antioxidant therapy. *Nat. Rev. Drug Discov.* **2021**, *20*, 689–709, doi:10.1038/s41573-021-00233-1.

239. Forman, H.J.; Maiorino, M.; Ursini, F. Signaling functions of reactive oxygen species. *Biochemistry* **2010**, *49*, 835–842, doi:10.1021/bi9020378.

240. Deponte, M. Glutathione catalysis and the reaction mechanisms of glutathione-dependent enzymes. *Biochim. Biophys. Acta* **2013**, *1830*, 3217–3266, doi:10.1016/j.bbagen.2012.09.018.

241. Koch, R.E.; Hill, G.E. An assessment of techniques to manipulate oxidative stress in animals. *Funct. Ecol.* **2017**, *31*, 9–21.

242. Karimani, A.D.V.M.; Mamashkhani, Y.D.V.M.; Moghadam Jafari, A.P.; Akbarabadi, M.D.V.M.; Heidarpour, M.P. Captopril Attenuates Diazinon-Induced Oxidative Stress: A Subchronic Study in Rats. *Iran. J. Med. Sci.* **2018**, *43*, 514–522.

243. Zhang, H.; Chen, Y.; Chen, Y.; Jia, P.; Ji, S.; Xu, J.; Li, Y.; Wang, T. Comparison of the effects of resveratrol and its derivative pterostilbene on hepatic oxidative stress and mitochondrial dysfunction in piglets challenged with diquat. *Food Funct.* **2020**, *11*, 4202–4215, doi:10.1039/d0fo00732c.

244. Wang, Z.; Ma, J.; Zhang, M.; Wen, C.; Huang, X.; Sun, F.; Wang, S.; Hu, L.; Lin, G.; Wang, X. Serum Metabolomics in Rats after Acute Paraquat Poisoning. *Biol. Pharm. Bull.* **2015**, *38*, 1049–1053, doi:10.1248/bpb.b15-00147.

245. Novaes, R.D.; Gonçalves, R.V.; Marques, D.C.S.; Cupertino, M. do C.; Peluzio, M. do C.G.; Leite, J.P.V.; Maldonado, I.R.D.S.C. Effect of bark extract of Bathysa cuspidata on hepatic oxidative damage and blood glucose kinetics in rats exposed to paraquat. *Toxicol. Pathol.* **2012**, *40*, 62–70, doi:10.1177/0192623311425059.

246. Novaes, R.D.; Gonçalves, R. V; Cupertino, M.C.; Santos, E.C.; Bigonha, S.M.; Fernandes, G.J.M.; Maldonado, I.R.S.C.; Natali, A.J. Acute paraquat exposure determines dose-dependent oxidative injury of multiple organs and metabolic dysfunction in rats: impact on exercise tolerance. *Int. J. Exp. Pathol.* **2016**, *97*, 114–124, doi:10.1111/iep.12183.

247. El-Boghdady, N.A.; Abdeltawab, N.F.; Nooh, M.M. Resveratrol and Montelukast Alleviate Paraquat-Induced Hepatic Injury in Mice: Modulation of Oxidative Stress, Inflammation, and Apoptosis. *Oxid. Med. Cell. Longev.* **2017**, *2017*, 9396425, doi:10.1155/2017/9396425.

248. Ahmed, M.A.E.; El Morsy, E.M.; Ahmed, A.A.E. Protective effects of febuxostat against paraquat-induced lung toxicity in rats: Impact on RAGE/PI3K/Akt pathway and downstream inflammatory cascades. *Life Sci.* **2019**, *221*, 56–64, doi:10.1016/j.lfs.2019.02.007.

249. Ranjbar, A.; Soleimani Asl, S.; Firozian, F.; Heidary Dartoti, H.; Seyedabadi, S.; Taheri Azandariani, M.; Ganji, M. Role of Cerium Oxide Nanoparticles in a Paraquat-Induced Model of Oxidative Stress: Emergence of Neuroprotective Results in the Brain. *J. Mol. Neurosci.* **2018**, *66*, 420–427, doi:10.1007/s12031-018-1191-2.

250. Liu, M.-W.; Su, M.-X.; Tang, D.-Y.; Hao, L.; Xun, X.-H.; Huang, Y.-Q. Ligustrazin increases lung cell autophagy and ameliorates paraquat-induced pulmonary fibrosis by inhibiting PI3K/Akt/mTOR and hedgehog signalling via increasing miR-193a expression. *BMC Pulm. Med.* **2019**, *19*, 35, doi:10.1186/s12890-019-0799-5.

251. Dasta, J.F. Paraquat poisoning: a review. *Am. J. Hosp. Pharm.* **1978**, *35*, 1368–1372.

252. Bismuth, C.; Garnier, R.; Baud, F.J.; Muszynski, J.; Keyes, C. Paraquat poisoning. An overview of the current status. *Drug Saf.* **1990**, *5*, 243–251, doi:10.2165/00002018-199005040-00002.

253. Blanco-Ayala, T.; Andérica-Romero, A.C.; Pedraza-Chaverri, J. New insights into antioxidant strategies against paraquat toxicity. *Free Radic. Res.* **2014**, *48*, 623–640, doi:10.3109/10715762.2014.899694.

254. World Health Organization Mental Health in the Workplace Available online: http://www.who.int/mental_health/world-mental-health-day/2017/en/ (accessed on Apr 12, 2021).

255. Bachmann, S. Epidemiology of Suicide and the Psychiatric Perspective. *Int. J. Environ. Res. Public Heal.* 2018, *15*.

256. Cohen, S.; Kessler, R.C.; Gordon, L.U. Strategies for measuring stress in studies of psychiatric and physical disorders. In *Measuring stress: A guide for health and social scientists.*; Oxford University Press: New York, NY, US, 1995; pp. 3–26 ISBN 0-19-508641-4 (Hardcover).

257. Tang, F.; Wang, G.; Lian, Y. Association between anxiety and metabolic syndrome: A systematic review and meta-analysis of epidemiological studies. *Psychoneuroendocrinology* **2017**, *77*, 112–121, doi:https://doi.org/10.1016/j.psyneuen.2016.11.025.

258. Cohen, S.; Janicki-Deverts, D.; Miller, G.E. Psychological Stress and Disease. *JAMA* **2007**, *298*, 1685–1687, doi:10.1001/jama.298.14.1685.

259. Turner, A.I.; Smyth, N.; Hall, S.J.; Torres, S.J.; Hussein, M.; Jayasinghe, S.U.; Ball, K.; Clow, A.J. Psychological stress reactivity and future health and disease outcomes: A systematic review of prospective evidence. *Psychoneuroendocrinology* **2020**, *114*, 104599, doi:https://doi.org/10.1016/j.psyneuen.2020.104599.

260. DeMartini, J.; Patel, G.; Fancher, T.L. Generalized Anxiety Disorder. *Ann. Intern. Med.* **2019**, *170*, ITC49–ITC64, doi:10.7326/AITC201904020.

261. Freudenberg, F.; O'Leary, A.; Aguiar, D.C.; Slattery, D.A. Challenges with modelling anxiety disorders: a possible hindrance for drug discovery. *Expert Opin. Drug Discov.* **2018**, *13*, 279–281, doi:10.1080/17460441.2018.1418321.

262. Fanselow, M.S. Conditional and unconditional components of post-shock freezing. *Pavlov. J. Biol. Sci. Off. J. Pavlov.* **1980**, *15*, 177–182, doi:10.1007/BF03001163.

263. Macêdo-Souza, C.; Maisonnette, S.S.; Filgueiras, C.C.; Landeira-Fernandez, J.; Krahe, T.E. Cued Fear Conditioning in Carioca High- and Low-Conditioned Freezing Rats. *Front. Behav. Neurosci.* **2019**, *13*, 285, doi:10.3389/fnbeh.2019.00285.

264. Mineka, S.; Oehlberg, K. The relevance of recent developments in classical conditioning to understanding the etiology and maintenance of anxiety disorders. *Acta Psychol. (Amst).* **2008**, *127*, 567–580, doi:10.1016/j.actpsy.2007.11.007.

265. Roltsch, E.A.; Baynes, B.B.; Mayeux, J.P.; Whitaker, A.M.; Baiamonte, B.A.; Gilpin, N.W. Predator odor stress alters corticotropin-releasing factor-1 receptor (CRF1R)-dependent behaviors in rats. *Neuropharmacology* **2014**, *79*, 83–89, doi:10.1016/j.neuropharm.2013.11.005.

266. Albrechet-Souza, L.; Gilpin, N.W. The predator odor avoidance model of post-traumatic stress disorder in rats. *Behav. Pharmacol.* **2019**, *30*, 105–114, doi:10.1097/FBP.0000000000000460.

267. Kosten, T.A.; Miserendino, M.J.; Kehoe, P. Enhanced acquisition of cocaine self-administration in

adult rats with neonatal isolation stress experience. *Brain Res.* **2000**, *875*, 44–50, doi:10.1016/s0006-8993(00)02595-6.

268. Girardi, C.E.N.; Zanta, N.C.; Suchecki, D. Neonatal stress-induced affective changes in adolescent Wistar rats: early signs of schizophrenia-like behavior . *Front. Behav. Neurosci.* 2014, *8*, 319.

269. Fonken, L.K.; Finy, M.S.; Walton, J.C.; Weil, Z.M.; Workman, J.L.; Ross, J.; Nelson, R.J. Influence of light at night on murine anxiety- and depressive-like responses. *Behav. Brain Res.* **2009**, *205*, 349–354, doi:10.1016/j.bbr.2009.07.001.

270. Ravindran, R.; Rathinasamy, S.D.; Samson, J.; Senthilvelan, M. Noise-stress-induced brain neurotransmitter changes and the effect of Ocimum sanctum (Linn) treatment in albino rats. *J. Pharmacol. Sci.* **2005**, *98*, 354–360, doi:10.1254/jphs.fp0050127.

271. Morakinyo, A.O.; Samuel, T.A.; Awobajo, F.O.; Adekunbi, D.A.; Olatunji, I.O.; Binibor, F.U.; Oni, A.F. Adverse effects of noise stress on glucose homeostasis and insulin resistance in Sprague-Dawley rats. *Heliyon* **2019**, *5*, e03004, doi:https://doi.org/10.1016/j.heliyon.2019.e03004.

272. Agrawal, A.; Jaggi, A.S.; Singh, N. Pharmacological investigations on adaptation in rats subjected to cold water immersion stress. *Physiol. Behav.* **2011**, *103*, 321–329, doi:10.1016/j.physbeh.2011.02.014.

273. Lee, K.-S.; Lim, B.-V.; Jang, M.-H.; Shin, M.-C.; Lee, T.-H.; Kim, Y.-P.; Shin, H.-S.; Cho, S.-Y.; Kim, H.; Shin, M.-S.; et al. Hypothermia inhibits cell proliferation and nitric oxide synthase expression in rats. *Neurosci. Lett.* **2002**, *329*, 53–56, doi:10.1016/s0304-3940(02)00591-8.

274. Padovan, C.M.; Guimarães, F.S. Restraint-induced hypoactivity in an elevated plus-maze. *Brazilian J. Med. Biol. Res. = Rev. Bras. Pesqui. medicas e Biol.* **2000**, *33*, 79–83, doi:10.1590/s0100-879x2000000100011.

275. Coccurello, R.; Romano, A.; Giacovazzo, G.; Tempesta, B.; Fiore, M.; Giudetti, A.M.; Marrocco, I.; Altieri, F.; Moles, A.; Gaetani, S. Increased intake of energy-dense diet and negative energy balance in a mouse model of chronic psychosocial defeat. *Eur. J. Nutr.* **2018**, *57*, 1485–1498, doi:10.1007/s00394-017-1434-y.

276. Antoniuk, S.; Bijata, M.; Ponimaskin, E.; Wlodarczyk, J. Chronic unpredictable mild stress for modeling depression in rodents: Meta-analysis of model reliability. *Neurosci. Biobehav. Rev.* **2019**, *99*, 101–116, doi:10.1016/j.neubiorev.2018.12.002.

277. Aricioglu, F.; Ozkartal, C.S.; Bastaskin, T.; Tüzün, E.; Kandemir, C.; Sirvanci, S.; Kucukali, C.I.; Utkan, T. Antidepressant-like Effects Induced by Chronic Blockade of the Purinergic 2X7 Receptor through Inhibition of Non-like Receptor Protein 1 Inflammasome in Chronic Unpredictable Mild Stress Model of Depression in Rats. *Clin. Psychopharmacol. Neurosci. Off. Sci. J. Korean Coll. Neuropsychopharmacol.* **2019**, *17*, 261–272, doi:10.9758/cpn.2019.17.2.261.

278. Aricioğlu, F.; Yalcinkaya, C.; Ozkartal, C.S.; Tuzun, E.; Sirvanci, S.; Kucukali, C.I.; Utkan, T. NLRP1-Mediated Antidepressant Effect of Ketamine in Chronic Unpredictable Mild Stress Model in Rats. *Psychiatry Investig.* **2020**, *17*, 283–291, doi:10.30773/pi.2019.0189.

279. Tang, M.; Huang, H.; Li, S.; Zhou, M.; Liu, Z.; Huang, R.; Liao, W.; Xie, P.; Zhou, J. Hippocampal proteomic changes of susceptibility and resilience to depression or anxiety in a rat model of chronic mild stress. *Transl. Psychiatry* **2019**, *9*, 260, doi:10.1038/s41398-019-0605-4.

280. Humer, E.; Pieh, C.; Probst, T. Metabolomic Biomarkers in Anxiety Disorders. *Int. J. Mol. Sci.* **2020**, *21*, 4784, doi:10.3390/ijms21134784.

281. de Kluiver, H.; Jansen, R.; Milaneschi, Y.; Bot, M.; Giltay, E.J.; Schoevers, R.; Penninx, B.W.J.H. Metabolomic profiles discriminating anxiety from depression. *Acta Psychiatr. Scand.* **2021**, doi:10.1111/acps.13310.

282. Brunoni, A.R.; Salum, G.A.; Hoffmann, M.S.; Goulart, A.C.; Barreto, S.M.; Canhada, S.; Carvalho, A.F.; Koyanagi, A.; Calice-Silva, V.; Lotufo, P.A.; et al. Prospective associations between hsCRP and

GlycA inflammatory biomarkers and depression: The Brazilian longitudinal study of adult health (ELSA-Brasil). *J. Affect. Disord.* **2020**, *271*, 39–48, doi:https://doi.org/10.1016/j.jad.2020.03.074.

283. Ren, Y.; Bao, S.; Jia, Y.; Sun, X.-L.; Cao, X.-X.; Bai, X.-Y.; Tian, J.-S.; Yang, H. Metabolic Profiling in Bipolar Disorder Patients During Depressive Episodes. *Front. psychiatry* **2020**, *11*, 569612, doi:10.3389/fpsyt.2020.569612.

284. Tian, J.; Xia, X.; Wu, Y.; Zhao, L.; Xiang, H.; Du, G.; Zhang, X.; Qin, X. Discovery, screening and evaluation of a plasma biomarker panel for subjects with psychological suboptimal health state using 1H-NMR-based metabolomics profiles. *Sci. Rep.* **2016**, *6*, 33820, doi:10.1038/srep33820.

285. Salehi M., A.; Nilsson, I.A.K.; Figueira, J.; Thornton, L.M.; Abdulkarim, I.; Pålsson, E.; Bulik, C.M.; Landén, M. Serum profiling of anorexia nervosa: A 1H NMR-based metabolomics study. *Eur. Neuropsychopharmacol.* **2021**, *49*, 1–10, doi:https://doi.org/10.1016/j.euroneuro.2021.02.015.

286. Yadav, A.P.; Chaturvedi, S.; Mishra, K.P.; Pal, S.; Ganju, L.; Singh, S.B. Evidence for altered metabolic pathways during environmental stress: 1H-NMR spectroscopy based metabolomics and clinical studies on subjects of sea-voyage and Antarctic-stay. *Physiol. Behav.* **2014**, *135*, 81–90, doi:https://doi.org/10.1016/j.physbeh.2014.05.045.

287. Tracey, T.J.; Steyn, F.J.; Wolvetang, E.J.; Ngo, S.T. Neuronal Lipid Metabolism: Multiple Pathways Driving Functional Outcomes in Health and Disease. *Front. Mol. Neurosci.* **2018**, *11*, 10, doi:10.3389/fnmol.2018.00010.

288. Larrieu, T.; Layé, S. Food for Mood: Relevance of Nutritional Omega-3 Fatty Acids for Depression and Anxiety. *Front. Physiol.* **2018**, *9*, 1047, doi:10.3389/fphys.2018.01047.

289. Chen, Y.-P.; Wang, C.; Xu, J.-P. Chronic unpredictable mild stress induced depression-like behaviours and glutamate-glutamine cycling dysfunctions in both blood and brain of mice. *Pharm. Biol.* **2019**, *57*, 280–286, doi:10.1080/13880209.2019.1598445.

MANUSCRIPT 1

DETECTION OF EARLY DISEASE RISK FACTORS ASSOCIATED WITH METABOLIC SYNDROME: A NEW ERA WITH THE NMR METABOLOMICS ASSESSMENT

Julia Hernandez-Baixauli [1,†], Sergio Quesada-Vázquez [1,†], Roger Mariné-Casadó [1,2], Katherine Gil Cardoso [1,2], Antoni Caimari [1], Josep M. Del Bas [1], Xavier Escoté [1,*] and Laura Baselga-Escudero [1,*]

[1] Eurecat, Centre Tecnològic de Catalunya, Unitat de Nutrició i Salut, 43204 Reus, Spain
[2] Universitat Rovira i Virgili; Department of Biochemistry and Biotechnology, Campus Sescelades, Tarragona, Spain
***** Correspondence: xavier.escote@eurecat.org and laura.baselga@eurecat.org

[†] Both authors contributed equally to this work as first authors.

Published by Nutrients

Nutrients 2020, 12(3), 806; https://doi.org/10.3390/nu12030806

Received: 14 February 2020; Revised: 11 March 2020; Accepted: 17 March 2020; Published: 18 March 2020

UNIVERSITAT ROVIRA I VIRGILI
MULTI-OMICS BIOMARKERS OF METABOLIC HOMEOSTASIS OF RISK FACTORS ASSOCIATED TO NON-COMMUNICABLE DISEASES
Julia Hernandez Baixauli

4. Biomarkers associated to different risk factors.

MANUSCRIPT 1. Literature review.

Abstract: The metabolic syndrome is a multifactorial disease developed due to accumulation and chronification of several risk factors associated with disrupted metabolism. The early detection of the biomarkers by nuclear magnetic resonance (NMR) could be helpful to prevent multifactorial diseases. The exposure of each risk factor can be detected by traditional molecular markers, but the current biomarkers have not been enough precise to detect the primary stages of disease. Thus, there is a need to obtain novel molecular markers of pre-disease stages. A promising source of new molecular markers are metabolomics standing out the research of biomarkers in NMR approaches. An increasing number of nutritionists integrate metabolomics into their study design, making nutrimetabolomics one of the most promising avenues for improving personalized nutrition. This review highlights the major five risk factors associated with metabolic syndrome and related diseases including carbohydrate dysfunction, dyslipidemia, oxidative stress, inflammation and gut microbiota dysbiosis. Together, it is proposed a profile of metabolites of each risk factor obtained from NMR approaches to target them using personalized nutrition, which will improve the quality of life for these patients.

Keywords: metabolic syndrome, metabolism deregulation, molecular biomarker, prevention, metabolomics, nutritional habits, carbohydrate dysfunction, dyslipidemia, oxidative stress, inflammation, gut microbiota.

1. Introduction

Metabolic syndrome (MetS) is considered a multifactorial disease, which means that a cluster of risk factors associated with disrupted metabolism may influence in their development [1]. Multifactorial diseases are caused by different single factors but also by a combination of altered metabolic situations (genetic, environmental, physiological, metabolic, cellular and molecular elements) that working together and extended over time eventually lead to a pathologic state [2,3]. However, these processes are not fully understood yet and MetS has emerged as a worldwide health concern in the recent decades, which prevalence is growing in parallel with the incidence of obesity, type 2 diabetes (T2D) or insulin resistance (IR). Thus, MetS is mainly attributed to changes in lifestyle that may impact genetic and phenotypic susceptibility [4–6]. Subsequently, the opportunity to prevent this disease is presented as a medical challenge for the whole facultative and research community.

Nowadays, there is a lack of efficient tools to prevent the development of MetS, obesity and their metabolic disarrangements, which essentially includes carbohydrate and lipid metabolism, inflammation, oxidative stress and gut microbiota [7]. Nevertheless, there are several lifestyle aspects that can be modified to prevent the development of these risk factors associated to MetS such as diet, nutritional habits and physical activity [8]. However, nutrition is probably the most important adaptable factor that regulates the expression of genes involved in several metabolic pathways [9]. Thus, driven changes in diet and nutritional habits, known as personalized nutrition, have been increasing as a promising tool and are taking more relevance in society to control and prevent metabolic diseases [10].

The classical concept of personalized nutrition is assisted by genetic assessment through an analysis of single nucleotide polymorphisms (SNPs), which may provide useful information about the genetically programmed response of a subject to a given food or nutrient (nutrigenomics) [11]. The phenotypic traits are dynamic markers and hence, more appropriate for defining the effects of lifestyle variables on the organism (diet, nutritional habits, physical activity, daylight rhythmicity, etc.). Advances in omics technologies have led to the possibility of characterizing the metabolism of every subject from a holistic point of view, thus opening a wide array of possibilities for phenotypic characterization and providing a more accurate health assessment contributing to improve quality of life [8].

Recently, the concept of nutrigenomics has evolved to incorporate many integrative methods concerning high-throughput omics technologies such as genomics, transcriptomics, proteomics, metabolomics, metagenomics and epigenomics [12] because the personalized nutrition based in nutrigenomics is limited. Ideally, the optimal personalized nutrition should be based in this modern concept of nutrigenomics, but is reasonless in a practical way due to the methodology high cost and the technical difficulties [13].

An alternative of the classical and modern concept of nutrigenomics is the study of the metabolomic profile [14]. An increasing number of nutritionists integrate metabolomics into their study design, nutrimetabolomics, achieving to be one of the most promising avenues for improving personalized nutrition [15,16]. Personalized nutrition can target small deviations of the metabolism associated with the risk factors, before the onset of the disease. When the disease is finally developed, the problem escapes the field of personalized nutrition and medical drugs administration are required. Therefore, there is a real need for an early detection of the slight changes on different metabolic parameters that combined triggers the disease development. At present, the lack of robust health status biomarkers for the principal clusters of MetS and obesity is a bottleneck that slows down the personalized nutrition in metabolomics [17]. This fact has been taken up by the scientific community. For example, the BIOCLAIMS project (FP7-244995) which has established the principles to obtain robust biomarkers for health status, or the PREVENTOMICS project (DT-SFS-14-2018-818318) which aims to use health biomarkers in applications for consumers.

In order to introduce the advantages of metabolomics in the research of biomarkers, the common techniques used in metabolomics should be known. The two most common techniques used are nuclear magnetic resonance (NMR) spectroscopy and mass spectrometry (MS) hyphened to chromatographic techniques such as gas chromatography (GC), capillary electrophoresis (CE), liquid chromatography (LC) and ultra-high performance liquid chromatography (UHPLC). Each analytical platform has its own advantages and disadvantages, thus the choice of the platform principally depends on the objective of the study, the accessibility and expertise of the platform [18]. The NMR platform is proposed as an emerging tool for large-scale metabolomics studies in the personalized nutrition field. The NMR characteristics which make it a unique platform include its high level of experimental reproducibility, its simplicity in sample pre-processing and preparation, its capacity to handle diverse biofluids, its quantitative capabilities (with a high coverage and low detection limits [19]), and its utility in identifying unknown metabolites along with its non-destructive nature [20]. The inherent limitation of NMR is the low sensitivity compared to MS but there are emerging new NMR technologies that suggest a huge improvement in the NMR spectroscopy [21]. In order to highlight one of the NMR-approaches, quantitative proton ^{1}H-NMR is the most useful NMR-based platform for metabolomics and has been successfully applied to early diagnostic and prognostic purposes [22,23]. The most popular biological fluids used in metabolomics are plasma, serum, urine and faeces, while other fluids and tissues are not yet well explored. Plasma and serum are the most common biofluids used in human metabolomic studies, because they are relatively easy to collect with minimal invasive procedures and their metabolome reflects individual changes in metabolism. On the other hand, the advantages of urine and faeces samples are that they are biological samples easy-to-access, which can be obtained using non-invasive procedures [15]. Between urine and faeces, urine is preferable as biofluid because the NMR techniques are optimized for early disease detection [24].

Taking into account these necessities, the present review addresses the demand to have a list of the potential molecular markers obtained by NMR metabolomics to be targeted in personalized nutrition in plasma/serum and urine (Table 1). We propose five clusters of molecular markers associated with five of the most relevant risk factors associated with MetS and related diseases. Then we will discuss the involvement of new biomarkers in the early stages of MetS distributed in the following list of molecular clusters: carbohydrate metabolism, dyslipidaemia, inflammation, oxidative stress and gut microbiota dysbiosis.

Table 1. Metabolomic biomarkers risk factors of MetS and related diseases by NMR approaches. Abbreviations: S, serum; P, plasma; U, urine; BCAA, branched chain amino acids; AAA, aromatic amino acids; TMAO, trimethylamine N-oxide; TCA cycle, tricarboxylic acid; TMA, trimethylamine; DMA, dimethylamine; NAG, N-acetylglycoprotein; LPC, lysophosphatidilcholine; SFA, saturated fatty acids; MUFA, monounsaturated fatty acids; PUFA, polyunsaturated fatty acids; DHA, docosahexaenoic acid; EPA, eicosapentaenoic acid; ALA, alpha linoleic acid; AA, arachidonic acid; 1C metabolism, one-carbon metabolism.

Biomarker	Level	Biofluid	Risk factor	Metabolic pathway	Pre-clinical evidence	Clinical evidence
Glucose	↑	S, U	Carbohydrate disruption	Glycolysis, gluconeogenesis, pyruvate metabolism	[25,26]	[19,27,28]
Lactate	↑	S, U	Carbohydrate disruption	Gluconeogenesis, Pyruvate metabolism	[29,30]	[27,31,32]
	↑	U	Gut microbiota metabolism		-	[33]
Uric acid	↑	S, U	Carbohydrate disruption	Purine metabolism	[34,35]	[36]
Propionylcarnitine	↑	P	Carbohydrate disruption	Lipid metabolism	-	[37–40]
Leucine (BCAA)	↑	S/P, U	Carbohydrate disruption	Amino acid metabolism	[25,26]	[32,41–43]
Isoleucine (BCAA)	↑	S/P, U	Carbohydrate disruption	Amino acid metabolism	[25,26]	[32,41–44]
Valine (BCAA)	↑	S/P, U	Carbohydrate disruption	Amino acid metabolism	[25,26]	[32,41–43,45,46]
Phenylalanine (AAA)	↑	S/P, U	Carbohydrate disruption	Amino acid metabolism	[25,26]	[32,41–43,47]
Tyrosine (AAA)	↑	S/P, U	Carbohydrate disruption	Amino acid metabolism	[25,26]	[32,41–44,48]
Glutamate	↑	S	Carbohydrate disruption	Amino acid metabolism	[49]	[39,50,51]
Glutamine	↓	S, U	Carbohydrate disruption	Amino acid metabolism	[30]	[39,50]
Citrate	↑/↓	S	Carbohydrate disruption	TCA cycle	[29,52]	[53]
TMAO	↑	P/ U	Gut microbiota metabolism	Choline metabolism	[54]	[55,56]

Acetate	↑	P	Gut microbiota metabolism	Pyruvate metabolism	[57]	[58]
TMA	↑/↓	P/ U	Gut microbiota metabolism	Choline metabolism	[59–61]	-
DMA	↑/ ↓	P/ U	Gut microbiota metabolism	Choline metabolism	[59,62]	[27]
Succinate	↑	P	Gut microbiota metabolism	Succinate metabolism	[63]	[64]
NAG	↑	P/ S	Inflammation pathway	Protein Glycosylation	-	[65–67],
LPCs	↑	P/ S	Inflammation pathway	Phospholipid hydrolysis	-	[68]
SFA, MUFAs PUFAs: DHA, EPA / ALA, AA	↑/ ↓	U/ S	Inflammation pathway	Lipid metabolism	[69]	-
		S	Dyslipidemia		[70]	[43]
3-hydroxybutirate	↑	U/P	Dyslipidemia	Ketogenesis	[71]	[72]
Choline	↓	S	Dyslipidemia	Choline metabolism	[73,74]	[27]
Allantoin	↑	U	Oxidative stress	Purine metabolism	[26,75–77]	-
Pseudouridine	↑	U	Oxidative stress	Nucleic acid metabolism	-	[78–80]
Glycine	↓	P/S	Oxidative stress	1C metabolism	-	[81,82]
Serine	↓	P/S	Oxidative stress	1C metabolism	-	[81,82]

2. Carbohydrate dysfunction

Carbohydrate metabolism dysfunction is highly related with IR and T2D, which represents approximately 95% of diabetes cases worldwide [83]. The standard clinical determinations of carbohydrate dysfunction include glucose and insulin determinations; HOMA-IR (homeostasis model assessment of IR) calculated by fasting plasma glucose and insulin levels; glycated hemoglobin (HbA1c) determination; and adiponectin and leptin levels, and the ratio of both, as hormones produced predominantly by adipocytes involved in carbohydrate dysfunction [84].

Fasting plasma glucose levels upper 7 mmol/L and fasting plasma insulin below 110 pmol/L are related to the carbohydrate metabolism pre-disease [85,86]. HOMA-IR, which is a widely accepted method to calculate IR state, determines the IR using the fasting glucose and insulin levels as described in different clinical guidelines [87,88], following the formula [HOMA-IR= Insulin (µU/ml) x Glucose (mmol/l) / 22.5] [89]. A higher value of HOMA-IR corresponds to a more severe IR [90]. Additionally, the HOMA-B index has been used as a robust measure of beta cell function [HOMA-B = Insulin (µU/ml) / (Glucose (mmol/l) -3.5)] [89], as well as the QUICKI index [QUICKI =1/ [Log Insulin (µU/ml) + Log Glucose (mmol/l)] , which is considered a measure of

insulin sensitivity [91]. As a conclusion, nowadays HOMA-IR is the most frequently used index to determine IR using fasting blood levels of glucose and insulin [92].

Other typical determination in T2D diagnosis is HbA1c, which was initially identified as an "unusual" hemoglobin, and has been correlated with glucose in several studies, suggesting the idea that HbA1c could be used as an objective measure of glycemic control [93]. HbA1c values represent the average glycemic control over the past 2-3 months and account for both, pre-prandial and post-prandial blood glucose levels [94]. Moreover, regular HbA1c measurement is recommended by different international guidelines for all patients with diabetes for the assessment of glycemic control [95]. Although the HbA1c concentration is used for diagnosis, the biological variation and non-standardized procedure limits its application [96].

In addition, some hormones secreted by the adipose tissue, such as the adipokines leptin and adiponectin, interact in modulating T2D risk, being adiponectin more strongly associated with T2D risk [97]. Specifically, the circulating levels of adiponectin are inversely associated with pre-diabetes and other metabolic traits [98–100]. In the case of leptin, higher circulating levels are directly contributing to the development of IR. Moreover, the leptin/adiponectin (L/A) ratio is related with preventive measures in MetS [101] and highly associated with IR in non-diabetic patients [102]. In the ARIRANG study, low ratio of L/A is a predictor for the regression of MetS and L/A was proposed as a clinical biomarker to measure the risk to develop the syndrome [103]. Finally, L/A ratio and HOMA-IR index has been demonstrated that both can be used to identify obese patients with IR [104,105].

Regrettably, insulin, HbA1c, leptin and adiponectin levels detected by traditional methods are only useful when the disease is well-stablished and not in the preliminary states of the pathology. Thus, we propose different metabolites, that are detected by NMR approaches, as molecular markers of carbohydrate metabolism dysfunction that can be detected in the pre-disease state. Specifically, we propose glucose and lactate as principal bioenergetics molecules and, new emerging biomarkers, such as plasmatic levels of uric acid; branched chain amino acids (BCAA); aromatic amino acids (AAA); other amino acids as glutamate and glutamine; or propionylcarnitine.

2.1. Glucose

Glucose is a classic carbohydrate used as a biomarker for the diagnostic for carbohydrate dysfunction metabolism [106]. In the absence of more specific biological marker to define T2D, glucose has been used as a marker for diagnostic criteria for T2D and pre-diabetes according to the 2006/2013 World Health Organization (WHO) [84,107] and 2019 American Diabetes Association (ADA) recommendations [108]. Carbohydrate metabolism is important in the development of T2D, where insulin regulates the blood levels of glucose and its metabolism helping cells to take glucose or store it as glycogen, depending on the needed. To sum up, high blood levels of glucose finally results in alteration of pancreatic β-cell function carrying on with IR [109]. Moreover, glucose, which is the primary source of energy for living organisms,

could be broken down via glycolysis, enter into the TCA cycle and oxidative phosphorylation to generate nucleotide adenosine triphosphate (ATP). Other important pathways in carbohydrate metabolism are glycogenesis, glycogenolysis (conversion of glycogen polymers into glucose, stimulated by glucagon) and gluconeogenesis (*de novo* glucose synthesis) [110].

There are several pre-clinical and clinical evidence about the potential of glucose as early biomarker of disease using NMR method. However, it is difficult to identify other metabolites in samples with an imbalance of glucose because the glucose signals (including other metabolites that overlap with the glucose region) suppress the other metabolite signals in the NMR spectrum [111]. In animal studies, high levels of glucose are shown in the metabolic profile. For example, Abu Bakar Sajak *et al*. [26] and Mulidiani *et al*. [25] detected and quantified glucose in urine in streptozotocin (STZ)-induced diabetic rats. In recent clinical studies, glucose is significantly increased in adults with risk to develop MetS or related diseases [95]. In forty-six young adults of normal weight and overweight, the serum metabolite profile was analysed by NMR and high levels of glucose were detected in overweight adults compared to normal weight volunteers [27]. Moreover, the importance of using glucose in the profiling of a pre-disease state was stablished in another clinical trial, where healthy people and patients with different levels of T2D presented an increase on glucose concentration depending on the disease state (T2D and its complications) [28]. In addition, Zhang *et al* [19] aimed to identify the biomarker signature of pre-states in metabolic diseases by serum profiling with NMR. Principal components analysis and orthogonal partial least squares-discriminant analysis were used to distinguish between samples from patients and healthy controls. In this study, glucose was highly expressed and included in the suggested metabolic profile for the early prediction [19]. However, taking into account the wide and easy extended use of glucometers to measure glycaemia, measure glucose levels with NMR analysis will be not justified unless additional parameters would be obtained in the same NMR profile.

2.2. Lactate

Focus on carbohydrate metabolism dysfunction, lactate has been considered a disease biomarker but also a marker for the pre-disease stage [112]. It plays a role in several biochemical processes and it is also an end-product of bacterial fermentation, produced by lactic acid bacteria of the genera *Lactobacillus* and *Bifidobacterium* [113] (discussed below). Lactate is formed in mammalian cells predominantly from glucose and alanine through their conversion into pyruvate, which is reduced to lactate by lactate dehydrogenase. Besides, the same enzyme removes lactate via its oxidation to pyruvate. Pyruvate could be oxidized to carbon dioxide producing energy or transformed glucose. Lactate metabolism is directly implicated in the gluconeogenesis, indirectly in the TCA cycle and in the respiratory chain, which are metabolic pathways implicated in carbohydrate metabolism [114]. Changes in plasma lactate during an oral glucose tolerance test (OGTT) are inversely correlated with fasting insulin, indicating that IR can be reflected through this metabolite response to a glucose challenge [115,116]. Lactate homeostasis is related to glucose metabolism

and, therefore, diseases associated with glucose disruption, as MetS, obesity or diabetes, are associated with disturbed lactate metabolism [114,117]. Failures in the mitochondrial energy-generating system in the pancreatic β-cells may also lead to the abnormal accumulation of lactate in urine, blood, and cerebrospinal fluids [118].

The first metabolomic approach to quantify lactate urinary level, which determined lactate as a risk marker for T2D, was done by Chou and their colleagues [31]. In animal studies, high levels of lactate were shown in urine NMR metabolomic profile in rats feed with a high fat diet (HFD) and in obese rats [29,30]. In these studies, lactate was selected as key metabolite in the carbohydrate's disruption. In overweight volunteers, lactate was increased compared with normal weight patients in the serum metabolite profile [27]. In a longitudinal clinical study, OGTT was assessed in two Finnish population-based studies consisting of 1,873 individuals and re-examined after 6.5 years. Metabolites were quantified by NMR from fasting serum samples and the associations were studied by linear regression models adjusted for established risk factors. Lactate was determined as potential marker for long-term IR that could be related to glucose tolerance later in life [32]. Consequently, changes in lactate levels are a promising tool to monitor early disarrangements in the carbohydrate metabolism.

2.3. Uric acid

Uric acid, generated during ATP metabolism, is the end product of the exogenous pool of purines and endogenous purine metabolism [119]. In the purine metabolism, adenosine monophosphate (AMP) deaminase promotes fat storage and IR, whereas activation of AMP activated protein kinase stimulates fat degradation and decreases gluconeogenesis. Uric acid is a key factor that appears to promote the mechanism implicated in imbalanced carbohydrate metabolism [120,121]. Overproduction of uric acid has been implicated in chronic diseases states including MetS, pre-diabetes, hypertension and non-alcoholic fatty liver disease (NAFLD) [122–125]. In addition, uric acid has been described as an antioxidant molecule [126] which will be discussed in the oxidative stress section. Elevated uric acid may become one of the most important molecular markers for early-phase mechanisms in the development of MetS and other metabolic diseases [127,128].

In pre-clinical studies, elevated serum levels of uric acid, determined by NMR approach, were found in STZ rats [34] and in obese mice [35], compared to control animals, associating this metabolite with diabetes and obesity. In a clinical work focused on an NMR-based metabolomic investigation of the serum profiles of diabetic, higher concentration of uric acid was detected in T2M subjects [36]. All these evidence place uric acid as a promising new biomarker for the early detection of metabolic alterations.

2.4. Propionylcarnitine

Acylcarnitines play an essential role in the regulation of carbohydrate and lipid metabolism balance. They are esters of L-carnitine and fatty acids formed in the

cytosol to transport fatty acids into the mitochondrial matrix for β-oxidation as a major source of energy for cell activities. The involvement of acylcarnitines in the intermediary metabolism is essential to mammalian bioenergetics process, and it is needed for the carnitine-dependent production of energy from different fatty acids and for the cell membrane structure maintenance [129] Disruption in fatty acid oxidation results in elevated acylcarnitine concentrations, suggesting that more fatty acids are entering into the mitochondria [130]. It has been described that concentrations of some acylcarnitines are associated with MetS, obesity and pre-diabetes [131–134]. The mechanisms by which acylcarnitines contribute to mitochondrial dysfunction have yet to be fully elucidated [135].

The acylcarnitines, which have been related to a pre-disease state, are not clear markers but, among the different types of acylcarnitines, the propionylcarnitine (C3) is the most promising short chain acylcarnitine to become a pre-disease biomarker. In general, the levels of blood acylcarnitines inadequately reflect tissue acylcarnitine metabolism [37], but C3 is one of them overcoming this impediment. In some studies of short-chain carnitine esters, C3 has been positively associated with T2D risk and IR [136]. On the other hand, the combination of C3 with other metabolites of interest as BCAAs, glutamate/glutamine and methionine, was particularly most robust to differentiate metabolically lean from obese patients [38,39]. In other clinical study, twenty-four acylcarnitines were measured in more than thousand subjects which were grouped by normal glucose tolerance, isolated impaired fasting glycaemia, impaired glucose tolerance or T2D [40]. Serum levels of C3 stood out significantly among the groups, proving its relevance as a robust biomarker of early stages of carbohydrate metabolism disorders [40]. Finally, the accuracy of MS in acylcarnitine profile determination is the main reason why most of the studies analysing acylcarnitines are performed by using this approach. In the latest years the NMR techniques have been improving to screen the acylcarnitine profile [137], what will allow to obtain a more precise vision of the early involvement of C3 in the development of metabolic diseases, and at the same time, to detect the contribution of other acylcarnitines in these critical phases that have so far gone unnoticed.

2.5. BCAAs and AAAs

BCAAs (isoleucine, leucine and valine) and AAAs (including phenylalanine and tyrosine) are essential amino acids; this means that they cannot be synthesized *de novo* by human cells, forcing to be obtained from the diet. Once inside the body, the levels of are relatively stable in blood and tissues (table 2 shows normal levels of these amino acids). BCAAs and AAAs are mainly regulated by their catabolic pathways (which are mainly localized in the mitochondria of all tissues), then higher plasma levels of these amino acids are well correlated with several pathologies. Consequently, BCAAs and AAAs are potential biomarkers which have been shown to be associated with a ~5-fold increased risk of developing T2D [138,139].

Table 2. Standard levels of BCAAs and AAAs as essential amino acids in serum.

BCAAs	Valine	mmol/L	<0.2492	[140]
	Leucine	mmol/L	<0.1236	[141]
	Isoleucine	mmol/L	<0.0602	[141]
AAAs	Tyrosine	mmol/L	<0.0545	[142]
	Phenylalanine	mmol/L	<0.0781	[142]

BCAAs cluster has been more exploited as a health marker than AAAs in the literature. An overwhelming number of publications and multiple studies support that concentrations of BCAAs in plasma and urine are associated with IR [143]. BCAAs play an important role in the regulation of energy homeostasis, nutrition metabolism, gut microbiome health, immunity and disease in humans and animals [144]. As the most abundant of essential amino acids, BCAAs are not only the substrates for synthesis of nitrogenous compounds, they also serve as signalling molecules regulating glucose, lipid, and protein synthesis [144]. Metabolomic profile of obese *vs.* lean subjects reveals a BCAA-related metabolite signature that is suggestive of increased catabolism of BCAAs and it is positively correlated with IR. The increased BCAAs was reported to stimulate gluconeogenesis and glucose intolerance via glutamate transamination to alanine [140]. In addition, BCCAs detection and quantification are highly correlated using both NMR and MS methods, becoming BCAAs as a suitable new biomarkers for disease prevention [145].

AAAs cluster has been less exploited but there is real evidence of two amino acids, phenylalanine and tyrosine, implicated in the pre-disease stages. Both amino acids are involved, as BCAAs, in protein synthesis. Tyrosine is considered a semi-essential amino acid because it can be synthesized from phenylalanine, and both are the initial precursors for the biosynthesis of fundamental neurotransmitters or hormones in animals and humans [146]. BCAAs and AAAs have been related to MetS, obesity and T2D in animal models and in human studies, both longitudinal and cross-sectional studies, having in common the usage of NMR metabolic profiles. For example, elevated levels of BCAAs and AAAs have been reported between diabetes and control group in STZ rat model [25,26]. In a longitudinal human studies, BCAAs were associated with higher glycaemia and IR and post-challenge glucose levels using NMR approach [32]. A recent meta-analysis of four groups of patients with pre-diabetes and diabetes showed that BCAAs were elevated by approximately 40% in the setting of poor glycemic control [41]. Moreover, BCAAs and AAAs were significantly different between metabolically healthy overweight/obese and MetS women, independent of other risk factors [43]. In other study of women transitioning from gestational diabetes mellitus to T2D, the BCAAs-related metabolite cluster was tightly associated with the incidence of T2D in the different groups [42].

Altogether, the studies using NMR approaches have reported an increase level of circulating BCAAs and AAAs consequently of the dysfunction of carbohydrate metabolism. Some studies include BCAAs and AAAs together representing a profile biomarker, and others only use a specific BCAA or AAA. For example, isoleucine and

tyrosine were different between women who develop gestational diabetes and those who remained normal glucose tolerant [44]. Tyrosine was suggested as a particularly strong predictor of metabolic and obesity traits in South Asian individuals determined in a unique healthy cohort with follow-up during nineteen years by NMR approach between nine amino acids [48]. In some studies, valine stands out with an increase predisposition to develop T2D in the future. This fact is showed in the study of the relation between circulating metabolites and abdominal obesity in twin's brothers [45] or the study revealing the predisposition to develop T2D in Chinese population [46]. Moreover, in 263 healthy men with MetS and their control counterparts, Siomkajło *et al.* proposed a diagnostic model consisted of phenylalanine as a marker obtained from omics technologies and other classical determinations [47].

All in all, the selection of the best option would be the utilization of BCAAs and AAAs as two clusters because the choice of one specific amino acid is controversial. There is a need of more robust studies using NMR methods to elucidate the implication of each amino acid in health metabolism and to elucidate a common outline.

2.6. Glutamate family: glutamine and glutamate

Besides BCAAs and AAAs, other common amino acids are potential biomarkers, as glutamine and glutamate, of the dysregulation of carbohydrates metabolism. In recent studies, the profile of amino acids, including BCAAs, AAAs and glutamine and glutamate, has been linked with risk factors related to T2D [28,147]. In this section, plasma glutamine, glutamate and their ratio will be discussed as potential biomarkers for T2D as it is showed in several studies [148]. Glutamine and glutamate are key amino acids in the mammal intermediary metabolism and, they are also associated with aerobic metabolism via the TCA cycle and with ammonia metabolism [149].

Glutamine plays a crucial role in various cellular processes, such as in energy balance, apoptosis, and cell proliferation and, its deprivation can activate the fatty acid β-oxidation pathway [150,151]. For instance, there has been a controversy linking glutamine with the prediction of the T2D. An inverse association of glutamine with the risk of T2D has been hugely observed in the literature but some studies reported a positive association. This inconsistency was solved by Guasch-Ferré *et al*. after a systematic review. They concluded that the strongest association of glutamine is the inverse with the risk to develop T2D [50]. In a recent animal study, changed levels of glutamine were shown in HFD-fed rats compared with control group in urine NMR metabolomic profile [30].

Glutamate is produced in the first step of BCAAs catabolism [152]. Different authors have proposed that glutamate likely stimulates glucagon release from pancreatic α cells and increases transamination of pyruvate to alanine, which strongly promotes gluconeogenesis in obesity [153]. Thus, circulating glutamate is positively related to visceral obesity and posterior development of MetS [154]. In a pre-clinical study, IR was correlated with glutamate in mice treated with monosodium glutamate

to develop obesity [49]. Moreover, in obese morbid patients, those with pre-diabetes were found to have higher serum glutamate levels compared to non-diabetic controls. It was speculated that glutamate was elevated in morbidly obese patients due to an increased need for α-ketoglutarate in the TCA cycle to compensate the IR. This same study also found that morbidly obese non-pre-diabetic group had increased levels of glutamate compared to non-obese and non-pre-diabetic groups, suggesting that obesity plays a role in glutamate metabolism [51]. As other amino acids, the detection and quantification of glutamine and glutamate by NMR methodology is evident and accessible as it has been shown. Therefore, they are promising metabolites for the prevention of carbohydrate metabolism dysfunction.

2.7. Citrate

Currently citrate has been studied as a metabolite that could be a good biomarker to detect carbohydrate dysfunction [29,52]. Citrate is an intermediary of the TCA cycle, being synthetized from fatty acids and glucose, and it is regulated by glucose levels and insulin [52]. It is mostly analysed in urine as a key metabolite contributing to the detection of metabolic disruptions. In a preclinical study, rats were fed with HFD or control diet and their urine was analysed by NMR. The results showed higher levels of citrate in the HFD group. The authors also found differences between high gainers and low gainers. Thus, citrate variation is associated to diet and physical constitution, being higher in these animals with obesity and a gainer constitution [29]. E-Y, Won *et al.* also showed an increase on citrate levels in the urine of obese mice in comparison with control group, analysed by NMR [52]. Corroborating this study, an increased levels of citrate were observed in other study of HFD-induced obese animals due to hyperglycaemia and IR [71]. These alterations in different studies of citrate levels suggest a closed relation with the disturbances in glucose and insulin in obesity [52]. Inversely, it was reported a depletion of the citrate levels in urine associated with a higher level of IR in humans [53]. Furthermore, in obese and IR animals a decrease on citrate urinary levels was also observed, and the opposite result was seen in obese animals without IR [155]. More clinical studies using NMR approach should be done to have more information about the possibility of citrate as a biomarker of MetS. It is hypothesized that the increase on citrate concentration might be originated through increased free fatty acid (FFA) oxidation due to higher levels of FFAs. This oxidation cause an elevation of acetyl-CoA:CoA and NADH: NAD^+ ratios in the mitochondria, where pyruvate hydrogenase is inactivated, rising the levels of citrate, which inhibits phosphofructokinase activity, causing an accumulation of glucose-6-phosphate. The glucose-6-phosphate may inhibit hexokinase II, decreasing glucose uptake [156]. Thus, citrate became a key player in the carbohydrate and lipid metabolism as well a potential new biomarker for the metabolic syndrome.

3. Dyslipidemia

One of the main consequences of the MetS is cardiovascular disease (CVD), which remains as the leading cause of morbidity and mortality in the western countries and whose incidence is increasing daily mainly due to diet and lifestyle [157]. Numerous

risk scores have been developed to predict CVD risk (Atherogenic Index of Plasma –AIF–; Framingham and Reynolds scores; etc.) [158,159]. These scores are based on clinical observations of individual traditional biomarkers of serum lipids, glucose and hormone profile [159]. Indeed, dyslipidemia is an abnormal amount of lipids in the blood that it is generally characterized by an elevation of triglycerides (TG), non-high-density lipoprotein-cholesterol (non-HDL-C), and low-density lipoprotein-cholesterol (LDL-C), and in parallel, a reduction in the high-density lipoprotein-cholesterol (HDL-C) [160]. In addition, dyslipidemia is also promoted in obesity, T2D and IR by a prolonged elevation of insulin levels. The association between obesity and CVD risk factors may be mediated by the ability of adipose tissue to synthesize and secrete several hormones with a systemic influence, including leptin and adiponectin. Leptin plays an important role in the regulation of feeding behaviour and their levels reflect the amount of energy reserves stored in adipose tissue [158]. On the other hand, adiponectin levels are inversely associated with body fat mass, inflammation, dyslipidemia, T2D and MetS; and their levels may be increased by healthy dietary patterns [161]. However, conventional algorithms to detect CVD risk factors are stablished in diseased population [159] and not in the preliminary stages of disease.

Unfortunately, these traditional biomarkers are not enough to evaluate the disease progression and status of emerging risks in apparently healthy patients. Hence, other biomarkers, alone or in combination, should be incorporated into risk prediction models to determine whether their addition increases the model's predictive accuracy and reliable estimation of CVD risk related to dyslipidemia. Thus, an early identification and treatment of risk factors are much needed to accelerate disease prevention and morbidity improvement. Consequently, in the absence of disease and, therefore, without pharmaceutical treatment, the robustness of this prediction model will allow to reduce the potential cardiovascular risk by acting on specific dyslipidemia cluster using precise nutritional recommendations.

3.1. Fatty acids: saturated, monounsaturated and polyunsaturated

Lipid and carbohydrates metabolism are closely interconnected. In fact, altered fatty acid profile affects IR and T2D; and *vice versa* [162]. Structurally, fatty acids can be splitted by the presence of double bounds in their backbone as saturated (SFA; absence of double bound) and unsaturated fatty acids [162]. Unsaturated fatty acids can be further divided by the number of double bounds as mono- (MUFAs; a single double bound) and poly-unsaturated fatty acids (PUFAs; more than one double bound) [163]. SFAs, MUFAs and PUFAs present different biological properties. The types of fatty acids present in various food groups are thought to play a pivotal role in whether or not such food is considered beneficial, neutral, or detrimental with respect to developing MetS and related diseases. It is well established an implication of dietary fats as risk factors for T2D and MetS, especially for long chain SFA (C14:0, C16:0 and C18:0) which could induce IR, whereas increased circulating levels of very long-chain SFA (C20:0, C22:0 and C24:0) are associated with reduced T2D risk [164,165]. In the

case of palmitate, its presence activates receptor FFA from beta-cells initiating a cascade with cell stress responses as ceramide formation, lipid droplets formation, endoplasmic reticulum stress, mitochondrial dysfunction and autophagy triggering an impairment of insulin secretion and damage in beta-cells [166]. PUFAs include some subgroups identified by the position of the last double bond in their molecular structure [164]. PUFA n-3 include mainly alpha linoleic acid (ALA), eicosapentaenoic acid (EPA) and docosahexaenoic acid (DHA), while PUFA n-6 include linoleic acid (LA) and arachidonic acid (AA) [162]. Thus, both MUFA and PUFA have been related to an improvement of insulin sensitivity.

Numerous beneficial healthy effects have been attributed to unsaturated fatty acids, including protection from obesity, diabetes, cancer, and atherosclerosis [162,164]. The most abundant MUFA in typical diets is oleic acid (C18:1n-9) which is effective in lowering the inflammatory response and LDL levels; that together contribute in the reduction of CVD risk [162,163]. High levels of MUFAs were described in the prevention of abdominal fat accumulation. Moreover, the substitution of carbohydrates with MUFA cause a decrease on total blood cholesterol an TGs, reducing the levels of HDL-C [162,163]. The mechanism involved in the anti-inflammatory effect of MUFAs is the inhibition of NF-kB activity [167]. In an animal study, Guo *et al*. demonstrated with NMR that high fat fed animals presented a significant increase on TG, LDL/VDL and SFAs levels and a decrease in the PUFA/MUFA ratio[168]. However, in a NMR study of hundred three obese women divided by the absence or presence of MetS, several species of PUFAs were associated with MetS[70]. In addition, different studies have been done to associate PUFAs with inflammatory parameters. EPA and DHA have been seen to exhibit anti-inflammatory properties and are also important to produce eicosanoids from the n-6 fatty acid like arachidonic acid [43]. Thus, even the generally beneficial effects attributed to PUFAs, deeper research is necessary to identify the relevance of every fatty acid species levels in the context of dyslipidemia as in the development of metabolic and CVD.

3.2. 3-hydroxybutyrate

Acetoacetate, 3-hydroxybutyrate (3-OHB) and acetone are ketone bodies, emerging as crucial regulators of metabolic health and produced in the liver from fatty acids that serve as a circulating energy in situations of glucose deprivation (i.e. fasting, carbohydrate restrictive diets, prolonged intense exercise, ketogenic diets, etc.) [169]. Ketone bodies have a characteristic smell, which can easily be detected in the breath of persons in ketosis and ketoacidosis [170]. 3-hydroxybutyrate (or β-hydroxybutyrate) serum levels can increase thousands of times in their concentrations after a prolonged fasting and present a broad range of signalling and regulatory effects including inhibition of many deacetylases [170]. Moreover, 3-hydroxybutyrate is described to induce resistance to oxidative stress via deacetylases inhibition that may explain, at least partially, the therapeutic value of low-carbohydrate and ketogenic diets [170]. Mitochondrial β-oxidation of FFAs results in the production of Acetyl-CoA, which might go into the TCA cycle for further oxidation. Acetyl-coA is condensed to ketone bodies in the liver by ketogenic enzymes, for example 3-OHB [171]. Bugianesi

et al. [172] found in NAFLD patients increased 3-OHB circulatory levels associated with hyperinsulinemia. Taken together, application of new diagnostic tools based in NMR will contribute to understand the uses of 3-hidroxybutirate as biomarker for MetS. Thus, hamsters fed with high-fat high-cholesterol diet showed an increase in the urine levels of 3-hydroxybutirate [173]. These results were corroborated at serum level, observing that high fat–fed mice showed an increase in 3-hydroxybutirate concentration [174] Similar results were observed at plasma, where T2D patients presented increased 3-hydroxybutirate levels [71]. Therefore, these evidences point 3-hydroxybutirate as an important biomarker to taken in consideration for an early metabolic disarrangements' detection.

3.3. Choline

Choline is an essential nutrient for maintaining human health which is involved in the mobilization of fat from liver [72]. In animals, the 95% of the total choline in tissues is used for the formation of phosphatidylcholine (PC) via the Kennedy pathway. It was described circulatory PC levels were increased in high-fat diet fed animals. PC is essential for the packaging, exporting and secreting of TG in VLDL, and acts as an intermediary to maintain a balance between fat in plasma and in the liver [175]. Choline deficiency results in various disorders, as fatty liver and liver dysfunction, which leads to elevations in serum concentrations of the liver aminotransferases [27]. Moreover, choline is a precursor of the neurotransmitter acetylcholine and it is essential in the membrane phospholipids and lipoproteins structure [175]. Consequently, it performs important functions in signal transduction, neurotransmitter synthesis or lipid transport. Moreover, plasma choline levels exhibited a positive correlation with serum TG and glucose levels, showing its involvement in the pathogenesis of several diseases, including MetS, fatty liver, obesity or cardiovascular disease [175]. Indeed, monkeys fed with high fat and high cholesterol diet showed lower serum level of choline and an inverse correlation with TG levels, explaining the relation between the lack of choline and the accumulation of TG in the liver [74]. A clinical study based in the differences between overweight patients and control subjects about metabolites levels. In the case of choline, was decreased in overweight patients in comparison with healthy subjects, showing a relationship between choline and a disruption in the lipid metabolism [73]. Although thse evidence, more studies with NMR are necessary to decipher the specific contribution of choline as a new biomarker for the early MetS detection.

4. Inflammation

Obesity and MetS are described as risk factors for T2D and CVD, which are viewed as inflammatory diseases. One of the main causes of chronic inflammation is the constant overload of glucose and FFAs, that promote the production of pro-inflammatory signals or elevates reactive oxygen species (ROS) levels. Chronic inflammation and immune cells are related to the pathogenesis of IR in obesity [27]. The best described markers of inflammation are cytokines released by immune cells, C-reactive protein (CRP) and monocyte chemoattractant protein 1 (MCP-1),

interleukin (IL)-6, IL-8, or tumour necrosis factor α (TNFα) [176]. As it happens with other common biomarkers, these cytokines are analysed by ELISA methods, which are time-consuming, laboured and less reproducible in comparison with NMR analysis. Therefore, to extract levels of other reliably biomarkers of inflammation from the NMR profiles it would be beneficial for the early detection of metabolic alterations. In this section we will focus on the role of N- acetylglycoproteins and lysophospholipids in the inflammation cluster, but other metabolites such as PUFAs (including EPA; DHA or ARA) also develop important inflammation roles as pointed in previous sections.

4.1. N-acetylglycoproteins

Glycosylation is one of the most common post-translational modification of secreted proteins and their misregulation is related with inflammation and multiple diseases (CVD, T2D, cancer, etc.) [177,178]. Therefore, human glycome is a novel tool to identify biomarkers and potential mechanistic mediators of pathogenesis. Indeed, increased serum glycoproteins levels are positively correlated with CRP levels [179]. The interest to study glycans, as an early biomarker of disease, is due to an altered glycosylation pattern might reflect the development of diseases [66]. Lawler *et al*. identified a glycoprotein-N-acetyl methyl group signature measured by NMR (GlycA) associated with CVD and T2D [66]. The two major contributors of the GlycA signal are α1-acid glycoprotein and haptoglobin, synthesized and secreted by neutrophils granules, as well by the liver [66]. The potential risk associated with elevated GlycA would relate to activation of systemic inflammatory pathways, because GlycA identifies aggregates of glycan moieties on circulating glycoproteins, which the majority of them are acute phase reactants and immunologic proteins [62,180]. In a large study with apparently healthy individuals, CVD mortality was significantly associated with elevated levels of GlycA [66]. The development of IR and β-cell dysfunction is triggered by low grade chronic systemic inflammation. Increased circulating levels of acute phase reactants are related to clinical expression of T2D, but is still unknown whether GlycA will be a proper marker for early detection of disease development [66]. 26,508 apparently healthy women described the first evidence for the potential role of GlycA as a biomarker predictor in development of T2D [181], providing evidence of the potential role of glycans in the development of the disease. Moreover, it was suggested that elevated high GlycA might be correlated with a chronic inflammatory state [65]. Bervoets *et al.* [67] studied the plasma metabolic profile of obese children with NMR, and found N-acetyl glycoprotein increased in obese children in comparison with healthy children, and it could be traduced in an activation of the hexosamine pathway related to lower levels of glutamine and glucose. These proofs pointed GlycA as a better biomarker option for a systemic inflammatory response compared to traditional inflammatory cytokines, which often exhibit high intra-individual variability. Therefore, GlycA integrates the protein levels and glycosylation states of the most abundant acute phase proteins in serum [182], allowing a more stable measure of inflammation with lower variability.

4.2. Lysophospholipids

Lysophospholipids are molecules derived from the hydrolysis of phospholipids, which transport fatty acids, phosphatidylglycerol, and choline between different tissues [183]. They are signalling molecules which modulate processes such as insulin production, insulin sensitivity and inflammation through interactions with G protein–coupled receptors [184], and are related to fatty liver, steatohepatitis, diabetes and obesity [184]. Different lysophospholipids species, mainly lysophosphatidilcholines (LPCs), have been identified as being altered in the plasma of obese individuals [185]. Significant amounts of circulatory levels of LPCs are synthetized by a specific enzyme activity lecithin, and lipoprotein-associated phospholipase A2 (Lp-PLA2), an inflammatory marker which has pro-inflammatory properties hydrolysing oxidized phospholipids generating LPC under inflammatory conditions [186]. LPCs activate signalling pathways promoting the release of second messengers, related to G protein-coupled receptors [186]. In obesity, significantly lower concentrations of most of the LPCs are detected [68], whereas LPCs concentrations were inversely correlated with the increased CRP levels [184]. Therefore, LPC could be useful early biomarkers to detect inflammatory states associated with MetS and related disorders.

5. Oxidative stress

Oxidative stress appears as a risk factor when an imbalance of homeostasis happens between oxidant and antioxidant agents. The oxidant agents, mainly ROS and reactive nitrogen species (RNS), are constantly produced in the aerobic organism by normal metabolic processes (cellular respiration, antibacterial defence, etc.) and external exposures (smoking, toxins, ionizing radiation, etc.). In order to regulate the reactive species, organism has endogenous antioxidant systems, or it obtains exogenous antioxidants from diet, that neutralizes these species and keeps the homeostasis of the body [68]. Production of free radicals and the resulting oxidative stress are part of the energy metabolism, emphasizing mitochondrial dysfunction in the development of disease. Finally, the oxidative stress accumulation leads to the development of pathological condition as MetS, obesity and diabetes [187]. The inference of oxidative stress in T2D is done by the alteration in enzymatic systems, lipid peroxidation, dysfunction in glutathione metabolism and decreased vitamin C level [188]. The recommended biomarkers for monitoring oxidative status over time are 8-hydroxy-2'-deoxyguanosine (8-OHdG), F2-isoprostane 8-iso-prostaglandin F2α (8-iso-PGF2α), 3-nitrotyrosine, malondialdehyde (MDA) and oxidized low-density lipoprotein (oxLDL) [189]. These determinations are performed by ELISA kits. One of the most used is 8-iso-PGF2α, which are products of free radical-mediated oxidation of arachidonic acid. It has been detected to be altered in T2D, hypercholesterolemia, hypertension and MetS. The main biofluid in where it is determined is urine [190]. Other widely used is 8-OHdG, which represents the oxidative DNA damages [191]. However, the most popular determinations in plasma are 3-nitrotyrosine and MDA. 3-nitrotyrosine, the main product of tyrosine oxidation, has been described as a stable marker of ROS/RNS stress in inflammatory related diseases [192]. MDA, a small

reactive aldehyde end product of the lipid peroxidation pathway, is a frequently used biomarker that can also be determined in urine, or tissue as thiobarbituric acid-reactive (TBAR) material, but the method is unstable and non-specific [193]. The last determination considered as classical is the oxLDL, which is the quantification of the oxidized LDL-C, but it is not stable in samples stored longer than a month [194]. All these determinations until the date are performed with expensive ELISA kits and sometimes the fine-tune determination depends on the storage time. Thus, it is essential to find different metabolites determined by NMR methods as new potential biomarkers in the risk factor of oxidative stress as allantoin, pseudouridine and finally GSH (reduced glutathione)/ GSSG (oxidized glutathione) ratio, glycine and serine as metabolites of the one-carbon metabolism.

5.1. Uric acid and allantoin

Uric acid is accepted as the major antioxidant in plasma that protects cardiac, vascular and neural cells from oxidative injury [195]. Uric acid, despite being a major antioxidant in the human plasma, it correlates and predicts positively and negatively the development of obesity and related diseases, conditions associated with oxidative stress and carbohydrate metabolism disruption as it is described in its section. Sautin & Johnson [196] tried to explain the paradox proposing that uric acid may function either as an antioxidant (primarily in plasma) or pro-oxidant (primarily within the cell). Therefore, considering the duality of the uric acid as a biomarker, we propose the end product of the uric acid oxidation from purine metabolism which is the allantoin as an alternative biomarker to uric acid [126]. Allantoin has been considered an oxidative stress biomarker as it also can be produced through non-enzymatic processes, especially when the levels of ROS are elevated [197]. While uric acid is considered antioxidant, allantoin is considered an pro-oxidant agent [198]. Urinary allantoin has been validated in a clinical model of oxidative stress, standing out its stability over different storage conditions as an oxidant biomarker [199].

There are several animal studies that determined allantoin as a biomarker in pre-disease using NMR metabolomic approach. In STD-rats, allantoin levels in urine stand out, among other metabolites, in T2D and obesity risk factor [196]. In a project characterizing biomarkers associated with T2D in eighteen biological matrices in *db*/*db* mouse model, allantoin was elevated in urine and plasma [26]. In other study characterizing the urine metabolome between lean and overweight dogs during a feed-challenge, overweight dogs had higher postprandial allantoin concentrations compared with lean dogs [76]. However, there is a need for more studies in humans and NMR approaches because the evidence of the association in several animal studies should be confirmed with clinical studies. To date, only one study determined allantoin as a biomarker in humans, which aimed to predict gestational diabetes development using MS approach. This study showed higher levels of allantoin in the group of women with higher risk to develop diabetes [77].

5.2. Pseudouridine

Urinary excreted nucleic acids catabolites are used as non-invasive markers for oxidative processes related to resting metabolic rate and energy intake: 8-OHdG represents oxidative stress to DNA (considered a classical biomarker) and pseudouridine, the metabolite considered as a potential metabolic biomarker, determines oxidative stress to RNA [200]. Pseudouridine is an isomer of the nucleoside uridine in which the uracil is attached via a carbon-carbon instead of a nitrogen-carbon glycosidic bond. It is the most prevalent of the over one hundred different modified nucleosides found in RNA, being a marker of RNA degradation and damage in oxidative stress [201].

The trace of pseudouridine in NMR metabolic approaches had not been precise enough but nowadays there are promising studies in pseudouridine. For example, in a NMR metabolomics study trying to optimize quantitative urine metabolomics, urine and plasma samples from 1004 individuals correlated high levels of glucose and circulating amino acids with pseudouridine [202]. In a randomized controlled trial of VSL-based intervention (unknown product due to industrial interest) *vs.* control in children obesity complication leading to NAFLD, the pseudouridine was identified as a potential non-invasive metabolic biomarker by a urinary NMR metabolic profiling. Pseudouridine decreased in the VSL *vs*. the placebo group, concluding that pseudouridine may be increased in metabolic diseases as an oxidative risk factor [78].

5.3. One-carbon metabolism intermediates: GSH/GSSG ratio, glycine and serine

One-carbon (1C) metabolism is associated with metabolic disease, overweight and obesity; higher levels of metabolites implicated in 1C metabolism are shown in healthy individuals [80]. The 1C metabolism consists on the transfer of one-carbon group and also, it is implicated in redox defence. The 1C metabolism is a reliable source of potential biomarkers as the selected, which are GSH/GSSG ratio, glycine and serine; thus, there are other with high probability to consider as betaine, dimethylglycine, methionine or cysteine [203]. One handicap to detect biomarkers of oxidative stress is the perception of oxidized metabolites, because the redox reactions could change the state of the metabolite (oxidized/reduced) during the manipulation of the sample and the redox ratio is difficult to determine. The GSH/GSSG ratio, which is an example in the 1C metabolism as an indicator of cellular health, is composed principally of reduced GSH constituting up to 98% of cellular GSH under normal conditions. The total quantification could be performed but the redox ratio calculation leads to more technical complications [204].

In order to avoid the problems in the determinations of redox ratio, an alternative to GSH/GSSG ratio is the selection of other metabolites of 1C metabolism. Glycine and serine, which are key amino acids in 1C metabolism, are proposed as a potential alternative to classical biomarkers [205]. For one hand, chronic glycine deficiency may impact health status, because glycine was found to have a strong negative association

with IR when measured as HOMA-IR score [206], or by other methods (hyperinsulinemic/euglycemic clamp) [140]. This amino acid of lowest molecular weight, incorporates a hydrogen atom as a side-chain [207]. Glycine is a precursor for many pathways as glutathione synthesis, which has been related with oxidative stress as the master antioxidant, but it participates in other metabolic processes being an unstable measure to detect the risk factor of interest [204]. Some glycine derivatives have also been found to be associated with IR and the risk of T2D, one of them with the strongest relation is serine. Serine and glycine are very related. Loss of the mitochondrial pathway, renders cells dependent on extracellular serine to make 1C units and on extracellular glycine to make GSH [208,209].

There are some studies standing out some metabolites implicated in the 1C metabolism related to oxidative stress and metabolism disorder by NMR approaches. Specifically, serum glycine and serine were found in lower concentrations in participants with more MetS risk factors and greater adiposity, using modifiable lifestyle factors to attenuate health effects of obesity [210]. Further, plasma glycine and serine level were lower in obese diabetic African-American women compared to obese non-diabetic African-American women [81].

6. Gut microbiota dysbiosis

100 trillion microbes exist in a symbiotic relationship with human cells, and the metabolic state of the human is related, in many cases, with the composition of the gut microbiota [82]. Numerous studies have shown that the gut microbiota composition may differ between lean and obese individuals or between pre-diabetic, T2D and normoglycemic individuals [211]. Dysbiosis of the gut microbiota, which is an alteration of the bacterial intestinal composition, reflexed a decreasing number of species related to an increased intestinal barrier permeability, thus allowing the bacterial translocation and causing endotoxemia [212], which is an important risk factor for obesity development and related metabolic diseases, as it is confirmed in different studies [213]. The constant flow in the composition of the gut microbiota is due to changes in diet, environmental factors and lifestyle [214]. As an intrinsic factor, the immune system health may cause changes in gut microbiota composition that may promote the proliferation of specific bacterial species which could be harmful due to the immune deficiency or hyperimmunity [215]. Genetics, age or gender are factors that also affects in the human homeostasis [215]. The decrease of microbial diversity is triggered by different factors, such as the psychological stress, the type of diet or the higher sedentary lifestyle, causing dysbiosis [203]. Thus, this altered gut microbiota metabolizes different molecules, spreading metabolites in the blood, urine or faeces which would be detected and used as biomarkers [216].

6.1. Lactate

Lactate, as it has been mentioned before, independent of participating in several biochemical processes is also an end-product of bacterial fermentation [217], produced by lactic acid bacteria of the genera *Lactobacillus* and *Bifidobacterium* [113].

Lactate is an intermediate metabolite, such as succinate, from the carbohydrate fermentation of some bacterial species. Moreover, it contributes to the maintenance of diversity within the colonic microbiota and the synthesis of the principal short chain fatty acids (SCFAs) [113]. Lactate is not accumulated in colon of healthy subjects, although a big proportion of intestinal bacteria can synthetize this metabolite, which is metabolized in butyrate or propionate [218]. In NAFLD patients was studied the composition of gut microbiota and selected bacterial products related with the fermentation of SCFAs in serum and faeces by NMR analysis. The results showed higher levels of lactate in NAFLD patients, compared to control individuals, which was associated with reduced abundance of several bacterial species (*Ruminococcus, Coprococcus* and *F. prausnitzii*) [218]. The amount and type of products can vary depending on species [33]. If the number of bacteria which metabolize lactate is decreased, excessive lactate production could end in its accumulation in the colon, where the absorption of lactate is low, lowering colonic pH and inhibiting the activity of microorganisms that metabolize lactate, for example propionate-producing bacteria or butyrate-producing. Butyrate is an inhibitor of acetate synthesis and the main energy source for colonocytes, could prevent the accumulation of lactate, which could be a potential toxic metabolite [33].

6.2. Acetate

Acetate, together with butyrate and propionate, is one of the three most common short chain fatty acid (SCFA) [219]. It is derived from intestinal microbial fermentation of dietary fibres in the colon [220] and acts as signalling ligand between host metabolism and the gut microbiome at different levels [221]. Acetate contribution leads to energy harvest participating in the human energy balance, with an important role in lipogenesis, cholesterol synthesis and accumulation in adipocytes [222]. Acetate affects substrate metabolism and host energy via an increase in energy expenditure and fat oxidation [223]. Via cross-feeding mechanisms branched-chain and aromatic amino acids might be produced and further metabolized, altering gut integrity and impairing insulin sensitivity. That is to say gut-derived acetate production is determined by the balance in gut between saccharolytic and proteolytic fermentation which is determined by the presence of acetogenic fibres [224]. *Firmicutes* are positive related to acetate, thus when dysbiosis cause an increase of *Firmicutes* in obese rats, plasma acetate levels increase, and it is linked to insulin action in morbidly obese individuals through circulating acetate. Fat cells release leptin in higher concentration by the presence of acetate [224]. In a human study with thirty-four morbidly obese women and men through NMR analysis, increased plasma levels of acetate were found, with a positive correlation with gut *Firmicutes*, and negatively correlated with HOMA-IR and fasting TG [224,225]. In a study with NAFLD patients, acetate was found increased in circulatory level and faecal level, analysed by NMR. This increase was correlated with the reduction of the abundance of several bacterial species as *Ruminococcus, Coprococcus* and *F. prausnitzii* [58]. HFD-induced obesity and IR in rats is associated with increased plasma concentration of acetate metabolized by the gut microbiota measured with GS-MS [33]. Less than 0.005% of

the SCFAs were excreted into urine because they are excreted via the lungs after oxidation, that is why acetate is mostly identified in blood and faeces [226]. Zang *et al*. studied female rats with diabetes by NMR urine analysis. It described acetate increased in diabetes group against control groups. The increase in the levels of acetate was correlated with higher levels of ethanol, and that suggested that the origin of this metabolites could be from microbial production, as in the case of *K. pneumoniae* [227].

6.3. Succinate

Succinate, a metabolite produced in the human body but also by the gut microbiota, is described as the major intermediary in the citric acid cycle, where it stands between succinyl-CoA and fumarate in the carbohydrate metabolism but the gut-microbiota produced succinate is classically described as an intermediate of the propionate synthesis [57]. Succinate has been increased in hypertension, ischemic heart disease, and T2D, but also in obesity, which is associated with elevated plasma levels of succinate concomitant with impaired glucose metabolism [228] Alterations in circulating succinate levels were associated with specific metagenomics signatures linked to energy production and carbohydrate metabolism [64]. It has been related with a antilipolytic action in adipose tissue through the succinate receptor 1 (SUCNR1), inhibiting the release of fatty acid from adipocytes. Thus, succinate has been related to cardiovascular diseases and obesity. In humans is found a strong association between microbial community, gene composition, and metabolism and plasma levels of succinate. In a study of a cohort of ninety-one patients stratified according to obesity and T2D, plasma succinate levels, analysed by NMR and LC-MS, were significantly higher in obese than in lean individuals. A positive association was found between plasma levels of succinate and BMI, but also glucose, insulin, TG and HOMA-IR [64]. This increase in circulating succinate levels was associated with specific changes in gut microbiota related to succinate metabolism. *Prevotellaceae* and *Veillonellaceae*, succinate-producing bacteria, increased their relative abundance level in obese individuals. On the other hand, *Odoribacteraceae* and *Clostridaceae*, succinate-consuming bacteria, decrease their relative abundance level in obese individual. A significant increase of glycaemia was presented in these patients who present high circulatory levels of succinate, related to changes in gut microbiota associated to higher barrier permeability. Therefore, it explains the association of succinate as a microbiota-derived metabolite with an important role in obesity and metabolic-associated cardiovascular disorders [64]. It is also described a study with diabetic mice analysed by NMR and the result was an increase of the succinate levels in urine [64]. Succinate has seen increased in faecal NMR analysis in NAFLD patients correlated to decreasing abundance of *Ruminococcus, Coprococcus* and *F. prausnitzii* bacteria in comparison with healthy individuals [63].

6.4. TMAO, TMA and DMA

Trimethylamine (TMA) and trimethylamine N-oxide (TMAO) are metabolites which come from the choline metabolic pathway and L-carnitine [33]. Choline

deficiency, which might cause microbial dysbiosis, is modulated by the conversion of dietary choline in TMA by gut bacteria, reducing the bioavailability of choline to synthesize phosphatidylcholine [229]. This TMA is released in the liver and is transformed in TMAO by the enzyme flavin-containing monooxygenase 3 (FMO3) [62]. These metabolites are seen to be related to the development of metabolic diseases, modulating the glucose metabolism in the liver and causing obesity [230], triggering inflammation in the adipose tissue and influencing lipid absorption and cholesterol homeostasis [231]. The fundamental role of the microbiota is evidenced in TMA production is derived from germ-free mice, which do not excrete TMA [232]. Using the urine of obese mice analysed by NMR, TMA reflects metabolic changes related to HFD that follow body fat deposit [233]. An *et al*. studied the metabolic changes in HFD rats by NMR faecal analysis. HFD rats showed a level reduction of faecal TMA, which its origin is mostly from gut microbiota, probably resulted from its transportation to the liver, where is transformed in TMAO [59]. TMA showed positive correlation with gut microbiota from the genera *Allobaculum* and *Clostridium* [60,61].

TMAO present in urine and plasma is considered a biomarker for NAFLD, IR, and CVD [61]. Large perturbations in TMAO levels may result from dietary differences, and intestinal microbiota are suggested as playing a prominent role in the variation of TMAO levels. Some studies reinforced the importance of diet and microbiota in cardio-metabolic health, with the TMAO level emerging as a possible target for therapeutic interventions. Given that CVD risk in humans is linked to circulating levels of TMAO [234], and dietary supplementation with TMAO promotes atherosclerotic CVD in mice [235], a key opportunity for therapeutic research leads to blocking the ability of plasma TMAO to obtain a biological response. More than five hundred Finnish men with MetS was studied, the serum obtained was analysed by NMR, and the results described a positive correlation between plasma TMAO concentrations and gut microbiota *Prevotella* and *Peptococcaceae*, however a negative correlation with *Faecalibacterium prausnitzii* was detected. These correlations are linked to dysbiosis in human disorders, as obesity and diabetes [54]. A study analysed by HPLC in diabetic patients, high levels of TMAO were found as a strong marker of all cardiovascular events, like in diabetic patients who tend to have elevated TMAO plasma levels. Thus, diabetes disease accentuates the relationship of elevated levels of TMAO and increased cardiovascular risk [56].

Dimethylamine (DMA) is also a metabolite generated from the TMA absorbed in the liver. High plasma and/or urine levels of DMA was described to be related to HFD induced IR, fatty liver and T2D in mice [236]. In a mice study compared urinary metabolites of gut microbiota between HFD mice and control mice, this product of dietary choline processing by gut microbiota had a statistically significant result by NMR, showing a significant reverse correlation with total body fat. Thus, DMA could be considered a possible prospective biomarkers indicative of accumulation of body fat in obesity, being converted by the host liver to TMAO [62].

7. Relation between the proposed metabolites and related metabolic pathways

To further characterize the metabolic pathways affected by the proposed metabolites, the metabolites were first annotated with Kyoto Encyclopedia of Genes and Genomes (KEGG) [59]. Then, the MetaboAnalyst (v4.0) software was used for metabolic pathway analysis and interpretation [237]. Eight pathways were statistically affected (FDR<0.05) by the proposed profile of metabolites (see table 3), thus five pathways stand out with high impact: the aminoacyl-tRNA biosynthesis; the glyoxylate and dicarboxylate metabolism; the alanine, aspartate and glutamate metabolism; the phenylalanine, tyrosine and tryptophan biosynthesis; and the D-Glutamine and D-glutamate metabolism. These five pathways with high impact mainly affect amino acid biosynthesis and metabolism, except the glyoxylate/dicarboxylate metabolism and the aminoacyl-tRNA biosynthesis. Besides being involved in the different discussed clusters in the review, the metabolites proposed as early biomarkers for MetS are closely related to amino acid pathways and protein synthesis, suggesting that amino acid metabolism and associated pathways may be fundamental to the biologic processes that may underline prevention of MetS and associated diseases [238].

Table 3. Metabolic pathways significantly affected by the proposed metabolites. Adapted from the MetaboAnalyst results. Pathway name, match status (number of metabolites implicated in each pathway *vs.* the total implicated), metabolites involved, FDR and Impact are shown in the table.

Pathway Name	Match Status	Metabolites involved	FDR	Impact
Aminoacyl-tRNA biosynthesis	9/48	Phenylalanine, Glutamine, Glycine, Serine, Valine, Isoleucine, Leucine, Tyrosine, Glutamate	1.4304E-6	0.167
Glyoxylate and dicarboxylate metabolism	6/32	Citrate, Serine, Glycine, Glutamate, Acetate, Glutamine	2.6791E-4	0.179
Valine, leucine and isoleucine biosynthesis	3/8	Leucine, Isoleucine, Valine	0.0055	0.0
Alanine, aspartate and glutamate metabolism	4/28	Glutamate, Glutamine, Citrate, Succinate	0.0175	0.311
Phenylalanine, tyrosine and tryptophan biosynthesis	2/4	Phenylalanine, Tyrosine	0.0208	1.0
Butanoate metabolism	3/15	3-Hydroxybutirate, Glutamate, Succinate	0.0208	0.0
Glutamine and glutamate metabolism	2/6	Glutamate, Glutamine	0.0378	0.5
Glutathione metabolism	3/28	Glutathione disulfide, Glycine, Glutamate	0.0869	0.135
Phenylalanine metabolism	2/10	Phenylalanine, Tyrosine	0.0873	0.357

8. Future perspectives and conclusions

In this review, the detection of early molecular biomarkers has been highlighted as a promising strategy to prevent the development of MetS. Indeed, the finding of alterations in these metabolic parameters, which are closely related with robust clinical biomarkers such as glucose, triglycerides and cholesterol through several signaling pathways, could avoid the deregulation of metabolic pathways directly related with the development of MetS. However, the analysis of the described biomarkers would be relevant not only for the prevention of this multifactorial disease, but also for a large number of diseases, as there is a complex crosstalk between most of the metabolic parameters described in this review and several diseases, such as cancer, diabetes and neuro-related diseases.

As an example, the gut microbiome product TMAO has been considered a shared risk factor between numerous diseases, such as IR, cancer, Alzheimer Disease (AD) and schizophrenia, among others [239,240]. Clinical studies have described that higher circulating levels of TMAO are correlated with a higher inflammatory response (↑ C-reactive protein, ↑ TNF-α, ↑ IL-6) [241]. Moreover, it is related to the synthesis of N-Nitroso compounds, which are involved in epigenetic alterations and DNA-damage that can lead to the induction of cancer [242]. As another example, BCAA have been described to be altered in human diabetes, a risk factor for Alzheimer's disease [243]. Preclinical studies have shown that the accumulation of these amino acids in brain promotes the phosphorylation of Tau proteins, which are involved in the development of Alzheimer [244]. Thus, the identification of alterations in these biomarkers and their precursors would be of high relevance.

Although the detection of molecular biomarkers by NMR techniques is very promising, there are several factors that must be taken into consideration. As a clear example, the selection of the analysed biofluids is crucial. Blood and urine have been the preferred source of metabolites used by NMR analysis, but there are other useful and potential biofluids (Figure 1). One of them is faeces, which might be a suitable biofluid for NMR analysis. In this case, the recollection is non-invasive and neither need a specialized person to acquire the biofluid via needle extraction. The challenge is to extract useful information from a complex sample that contains end products of human metabolism, different species of bacteria, end products from bacterial processes and epithelial cells from the colorectal mucosa via faecal NMR metabolomics [245]. Other fluid of interest, which has the same advantages as faeces, is saliva, as it is also easy to obtain, and it could inform about several metabolic processes. As an example, saliva biomarkers in AD early diagnostic were detected in a pilot study with NMR metabolomics. The development of accurate and sensitive salivary biomarkers would be ideal for screening those individuals at greatest risk of developing disease, translating the AD example to other diseases as MetS, obesity and T2D [246]. Thus, there is a need to promote the use of these promising biofluids to improve the detection of new biomarkers.

Another factor that has a sharp influence on the detection and interpretation of new biomarkers is sample processing, which requires specific conditions depending on the analysed biomarkers. As an example, several oxidative stress biomarkers, such as glutathione, are unstable and unreliable to detect by NMR due to its oxidation during sample processing. Moreover, other biomarkers such as acetate, can be easily overestimated in different biofluids because of the contamination of samples during its manipulation. Therefore, specific extraction and quantification procedures must be taken into consideration depending on the analysed biomarkers and their chemical properties.

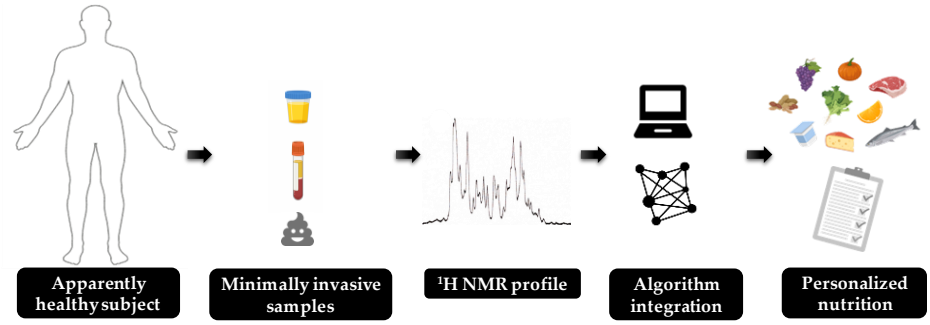

Figure 1. Scheme of the research of biomarkers of health. Pipeline explaining the steps that should be followed for an early detection of pre-diseases states and prevention of the development of cardiometabolic diseases through the ^{1}H NMR analysis of minimal invasive samples, thus getting metabolomics profile of the potential patients. Therefore, using this metabolomics information, we will be able to find a personalized interventional nutrition through the integration of studied algorithms to finally reduce or stop the development of the different cardiometabolic diseases.

Several molecular biomarkers involved in metabolic disorders have been excluded from this review as there is not enough evidence to be considered as biomarkers of early stages of disease. Despite the fact that further research is needed in order to enlarge the list of robust biomarkers exposed in this review, identification and aggrupation of early biomarkers in different risk factor clusters can be of great help to *a*) make it easier to identify altered metabolic pathways when more than one early biomarker placed in the same cluster is changed; and *b*) design personalized diets with ingredients that are described to target the identified metabolic alterations.

To sum up, from the identification and quantification of early biomarkers, different metabolic diseases could be treated in early states of the development of the diseases, before they could not be reversed. NMR metabolomics assessment is a reproducible and economic analysis of these metabolites which could be useful to detect these early disease development stages. This review summarizes some potential biomarkers that have been described in the literature related to different clusters which have been associated with metabolic diseases (carbohydrates metabolism, dyslipidemia, oxidative stress, inflammation and gut microbiota), and have been used to achieve health information about the patients who may have symptoms related to metabolic disorders. If these biomarkers are assessed together instead of individually, the information obtained would be more complete and it

would be a good strategy to detect cardiometabolic diseases in their early stages. However, the lack of qualitative analysis through NMR assessments take us to improve the methods used to process the samples and the way to analyse the recently known metabolites. Besides, it is necessary to find more metabolites related to these early stages of development of diseases, being characterized and intensively studied. When these further studies advance, we will be able to establish a fast and accurate method to prevent cardiometabolic and metabolic syndrome diseases in pre-stages of their development.

References

1. Grundy, S.M. Metabolic syndrome update. *Trends Cardiovasc. Med.* **2016**, *26*, 364–373, doi:https://doi.org/10.1016/j.tcm.2015.10.004.

2. Stolk, R.P.; Rosmalen, J.G.M.; Postma, D.S.; de Boer, R.A.; Navis, G.; Slaets, J.P.J.; Ormel, J.; Wolffenbuttel, B.H.R. Universal risk factors for multifactorial diseases. *Eur. J. Epidemiol.* **2008**, *23*, 67–74, doi:10.1007/s10654-007-9204-4.

3. Vassallo, P.; Driver, S.L.; Stone, N.J. Metabolic Syndrome: An Evolving Clinical Construct. *Prog. Cardiovasc. Dis.* **2016**, *59*, 172–177, doi:https://doi.org/10.1016/j.pcad.2016.07.012.

4. Marti, A.; Martinez-González, M.A.; Martinez, J.A. Interaction between genes and lifestyle factors on obesity. *Proc. Nutr. Soc.* **2008**, *67*, 1–8, doi:10.1017/S002966510800596X.

5. Oladejo, A.O. Overview of the metabolic syndrome; an emerging pandemic of public health significance. *Ann. Ibadan Postgrad. Med.* **2011**, *9,2*, 78–82.

6. Hossain, P.; Kawar, B.; El Nahas, M. Obesity and diabetes in the developing world--a growing challenge. *N. Engl. J. Med.* **2007**, *356*, 213–215, doi:10.1056/NEJMp068177.

7. James, P.T.; Rigby, N.; Leach, R. The obesity epidemic, metabolic syndrome and future prevention strategies. *Eur. J. Cardiovasc. Prev. Rehabil.* **2004**, *11*, 3–8, doi:10.1097/01.hjr.0000114707.27531.48.

8. van Ommen, B.; Keijer, J.; Heil, S.G.; Kaput, J. Challenging homeostasis to define biomarkers for nutrition related health. *Mol. Nutr. Food Res.* **2009**, *53*, 795–804, doi:10.1002/mnfr.200800390.

9. Kohlmeier, M.; De Caterina, R.; Ferguson, L.R.; Gorman, U.; Allayee, H.; Prasad, C.; Kang, J.X.; Nicoletti, C.F.; Martinez, J.A. Guide and Position of the International Society of Nutrigenetics/Nutrigenomics on Personalized Nutrition: Part 2 - Ethics, Challenges and Endeavors of Precision Nutrition. *J. Nutrigenet. Nutrigenomics* **2016**, *9*, 28–46, doi:10.1159/000446347.

10. Kussmann, M.; Fay, L. Nutrigenomics and personalized nutrition. *Nestle Res. Cent.* **2008**, *5*, 447–455.

11. Bouchard, C.; Ordovas, J.M. Fundamentals of Nutrigenetics and Nutrigenomics. In *Recent Advances in Nutrigenetics and Nutrigenomics*; Bouchard, C., Ordovas, J.M.B.T.-P. in M.B. and T.S., Eds.; Academic Press, 2012; Vol. 108, pp. 1–15 ISBN 1877-1173.

12. Chirita-Emandi, A.; Niculescu, M. Chapter 7 - Methods for Global Nutrigenomics and Precision Nutrition. In; Caterina, R.D.E., Martinez, J.A., Kohlmeier, M.B.T.-P. of N. and N., Eds.; Academic Press, 2020; pp. 49–58 ISBN 978-0-12-804572-5.

13. Misra, B.B.; Langefeld, C.; Olivier, M.; Cox, L.A. Integrated omics: tools, advances and future approaches. *J. Mol. Endocrinol.* **2018**, R21–R45, doi:10.1530/jme-18-0055.

14. Gomez-Casati, D.F.; Busi, M. V Chapter 3 - Molecular basis of clinical metabolomics. In; Kumar, D.B.T.-C.M.M., Ed.; Academic Press, 2020; pp. 47–55 ISBN 978-0-12-809356-6.

15. Ulaszewska, M.M.; Weinert, C.H.; Trimigno, A.; Portmann, R.; Andres Lacueva, C.; Badertscher, R.; Brennan, L.; Brunius, C.; Bub, A.; Capozzi, F.; et al. Nutrimetabolomics: An Integrative Action for Metabolomic Analyses in Human Nutritional Studies. *Mol. Nutr. Food Res.* **2019**, *63*, e1800384, doi:10.1002/mnfr.201800384.

16. Zhang, A.; Sun, H.; Wang, X. Emerging role and recent applications of metabolomics biomarkers in obesity disease research. *RSC Adv.* **2017**, *7*, 14966–14973, doi:10.1039/c6ra28715h.

17. Picó, C.; Serra, F.; Rodríguez, A.M.; Keijer, J.; Palou, A. Biomarkers of nutrition and health: New tools for new approaches. *Nutrients* **2019**, *11*, 1–30, doi:10.3390/nu11051092.

18. Emwas, A.-H.M. The strengths and weaknesses of NMR spectroscopy and mass spectrometry with particular focus on metabolomics research. *Methods Mol. Biol.* **2015**, *1277*, 161–193, doi:10.1007/978-1-4939-2377-9_13.

19. Zhang, Y.; Zhang, H.; Chang, D.; Guo, F.; Pan, H.; Yang, Y. Metabolomics approach by 1 H NMR spectroscopy of serum reveals progression axes for asymptomatic hyperuricemia and gout. *Arthritis Res. Ther.* **2018**, *20*, 1–11, doi:10.1186/s13075-018-1600-5.

20. Rhee, E.P.; Gerszten, R.E. Metabolomics and Cardiovascular Biomarker Discovery. *Clin. Chem.* **2020**, *58*, 139–147, doi:10.1373/clinchem.2011.169573.

21. Emwas, A.-H.; Roy, R.; McKay, T.R.; Tenori, L.; Saccenti, E.; Gowda, A.N.G.; Raftery, D.; Alahmari, F.; Jaremko, L.; Jaremko, M.; et al. NMR Spectroscopy for Metabolomics Research. *Metabolites* **2019**, *9*, 123, doi:10.3390/metabo9070123.

22. Mancano, G.; Mora-Ortiz, M.; Claus, S.P. Recent developments in nutrimetabolomics: from food characterisation to disease prevention. *Curr. Opin. Food Sci.* **2018**, *22*, 145–152, doi:https://doi.org/10.1016/j.cofs.2018.03.012.

23. Silva, R.A.; Pereira, T.C.S.; Souza, A.R.; Ribeiro, P.R. 1H NMR-based metabolite profiling for biomarker identification. *Clin. Chim. Acta* **2020**, *502*, 269–279, doi:https://doi.org/10.1016/j.cca.2019.11.015.

24. Gao, Y. *Urine: Promising Biomarker Source for Early Disease Detection*; Springer, 2019; ISBN 9811391092.

25. Maulidiani, M.; Abas, F.; Rudiyanto, R.; Kadir, N.H.A.; Zolkeflee, N.K.Z.; Lajis, N.H. Analysis of urinary metabolic alteration in type 2 diabetic rats treated with metformin using the metabolomics of quantitative spectral deconvolution 1H NMR spectroscopy. *Microchem. J.* **2020**, *153*, 104513, doi:https://doi.org/10.1016/j.microc.2019.104513.

26. Abu Bakar Sajak, A.; Mediani, A.; Maulidiani; Ismail, A.; Abas, F. Metabolite Variation in Lean and Obese Streptozotocin (STZ)-Induced Diabetic Rats via 1H NMR-Based Metabolomics Approach. *Appl. Biochem. Biotechnol.* **2017**, *182*, 653–668, doi:10.1007/s12010-016-2352-9.

27. Pasanta, D.; Chancharunee, S.; Tungjai, M.; Kim, H.J.; Kothan, S. Effects of obesity on the lipid and metabolite profiles of young adults by serum (1)H-NMR spectroscopy. *PeerJ* **2019**, *7*, e7137, doi:10.7717/peerj.7137.

28. Rawat, A.; Misra, G.; Saxena, M.; Tripathi, S.; Dubey, D.; Saxena, S.; Aggarwal, A.; Gupta, V.; Khan, M.Y.; Prakash, A. 1H NMR based serum metabolic profiling reveals differentiating biomarkers in patients with diabetes and diabetes-related complication. *Diabetes Metab. Syndr. Clin. Res. Rev.* **2019**, *13*, 290–298, doi:https://doi.org/10.1016/j.dsx.2018.09.009.

29. Kim, S.-H.; Yang, S.-O.; Kim, H.-S.; Kim, Y.; Park, T.; Choi, H.-K. 1H-nuclear magnetic resonance spectroscopy-based metabolic assessment in a rat model of obesity induced by a high-fat diet. *Anal. Bioanal. Chem.* **2009**, *395*, 1117–1124, doi:10.1007/s00216-009-3054-8.

30. Abdul Ghani, Z.D.F.; Ab Rashid, A.H.; Shaari, K.; Chik, Z. Urine NMR Metabolomic Study on Biochemical Activities to Investigate the Effect of P. betle Extract on Obese Rats. *Appl. Biochem. Biotechnol.* **2019**, *189*, 690–708, doi:10.1007/s12010-019-03042-w.

31. Chou, C.K.; Lee, Y.T.; Chen, S.M.; Hsieh, C.W.; Huang, T.C.; Li, Y.C.; Lee, J.A. Elevated urinary d-lactate levels in patients with diabetes and microalbuminuria. *J. Pharm. Biomed. Anal.* **2015**, *116*, 65–70, doi:10.1016/j.jpba.2015.06.014.

32. Würtz, P.; Tiainen, M.; Mäkinen, V.-P.; Kangas, A.J.; Soininen, P.; Saltevo, J.; Keinänen-Kiukaanniemi, S.; Mäntyselkä, P.; Lehtimäki, T.; Laakso, M.; et al. Circulating metabolite predictors of glycemia in middle-aged men and women. *Diabetes Care* **2012**, *35*, 1749–1756, doi:10.2337/dc11-1838.

33. Da Silva, H.E.; Teterina, A.; Comelli, E.M.; Taibi, A.; Arendt, B.M.; Fischer, S.E.; Lou, W.; Allard, J.P. Nonalcoholic fatty liver disease is associated with dysbiosis independent of body mass index and insulin resistance. *Sci. Rep.* **2018**, *8*, 1–12, doi:10.1038/s41598-018-19753-9.

34. Liu, J.; Wang, C.; Liu, F.; Lu, Y.; Cheng, J. Metabonomics revealed xanthine oxidase-induced oxidative stress and inflammation in the pathogenesis of diabetic nephropathy. *Anal. Bioanal. Chem.* **2015**, *407*, 2569–2579, doi:10.1007/s00216-015-8481-0.

35. Kim, H.-J.; Kim, J.H.; Noh, S.; Hur, H.J.; Sung, M.J.; Hwang, J.-T.; Park, J.H.; Yang, H.J.; Kim, M.-S.; Kwon, D.Y.; et al. Metabolomic Analysis of Livers and Serum from High-Fat Diet Induced Obese Mice. *J. Proteome Res.* **2011**, *10*, 722–731, doi:10.1021/pr100892r.

36. Gogna, N.; Krishna, M.; Oommen, A.M.; Dorai, K. Investigating correlations in the altered metabolic profiles of obese and diabetic subjects in a South Indian Asian population using an NMR-based metabolomic approach. *Mol. Biosyst.* **2015**, *11*, 595–606, doi:10.1039/C4MB00507D.

37. Schooneman, M.G.; Achterkamp, N.; Argmann, C.A.; Soeters, M.R.; Houten, S.M. Plasma acylcarnitines inadequately reflect tissue acylcarnitine metabolism. *Biochim. Biophys. Acta - Mol. Cell Biol. Lipids* **2014**, *1841*, 987–94, doi:10.1016/j.bbalip.2014.04.001.

38. Dorcely, B.; Katz, K.; Jagannathan, R.; Chiang, S.S.; Oluwadare, B.; Goldberg, I.J.; Bergman, M. Novel biomarkers for prediabetes, diabetes, and associated complications. *Diabetes. Metab. Syndr. Obes.* **2017**, *10*, 345–361, doi:10.2147/DMSO.S100074.

39. Gonzalez-Franquesa, A.; Burkart, A.M.; Isganaitis, E.; Patti, M.E. What Have Metabolomics Approaches Taught Us About Type 2 Diabetes? *Curr. Diab. Rep.* **2016**, *16*, doi:10.1007/s11892-016-0763-1.

40. Mai, M.; Tönjes, A.; Kovacs, P.; Stumvoll, M.; Fiedler, G.M.; Leichtle, A.B. Serum levels of acylcarnitines are altered in prediabetic conditions. *PLoS One* **2013**, *8*, e82459, doi:10.1371/journal.pone.0082459.

41. 't Hart, L.M.; Vogelzangs, N.; Mook-Kanamori, D.O.; Brahimaj, A.; Nano, J.; van der Heijden, A.A.W.A.; Willems van Dijk, K.; Slieker, R.C.; Steyerberg, E.W.; Ikram, M.A.; et al. Blood Metabolomic Measures Associate With Present and Future Glycemic Control in Type 2 Diabetes. *J. Clin. Endocrinol. Metab.* **2018**, *103*, 4569–4579, doi:10.1210/jc.2018-01165.

42. Andersson-Hall, U.; Gustavsson, C.; Pedersen, A.; Malmodin, D.; Joelsson, L.; Holmang, A. Higher Concentrations of BCAAs and 3-HIB Are Associated with Insulin Resistance in the Transition from Gestational Diabetes to Type 2 Diabetes. *J. Diabetes Res.* **2018**, *2018*, 4207067, doi:10.1155/2018/4207067.

43. Cheng, S.; Wiklund, P.K.; Pekkala, S.; Autio, R.; Munukka, E.; Xu, L.; Saltevo, J.; Cheng, S.; Kujala, U.M.; Alen, M. Serum metabolic profiles in overweight and obese women with and without metabolic syndrome. *Diabetol. Metab. Syndr.* **2014**, *6*, 1–9, doi:10.1186/1758-5996-6-40.

44. Jiang, R.; Wu, S.; Fang, C.; Wang, C.; Yang, Y.; Liu, C.; Hu, J.; Huang, Y. Amino acids levels in early pregnancy predict subsequent gestational diabetes. *J. Diabetes* **2019**, doi:10.1111/1753-0407.13018.

45. Bogl, L.H.; Kaye, S.M.; Rämö, J.T.; Kangas, A.J.; Soininen, P.; Hakkarainen, A.; Lundbom, J.; Lundbom, N.; Ortega-Alonso, A.; Rissanen, A.; et al. Abdominal obesity and circulating metabolites: A twin study approach. *Metabolism.* **2016**, *65*, 111–121, doi:10.1016/j.metabol.2015.10.027.

46. Chen, T.; Ni, Y.; Ma, X.; Bao, Y.; Liu, J.; Huang, F.; Hu, C.; Xie, G.; Zhao, A.; Jia, W.; et al. Branched-chain and aromatic amino acid profiles and diabetes risk in Chinese populations. *Sci. Rep.* **2016**, *6*, 20594, doi:10.1038/srep20594.

47. Siomkajło, M.; Rybka, J.; Mierzchała-Pasierb, M.; Gamian, A.; Stankiewicz-Olczyk, J.; Bolanowski, M.; Daroszewski, J. Specific plasma amino acid disturbances associated with metabolic syndrome. *Endocrine* 2017, *58*, 553–562.

48. Tillin, T.; Hughes, A.D.; Wang, Q.; Würtz, P.; Ala-Korpela, M.; Sattar, N.; Forouhi, N.G.; Godsland, I.F.; Eastwood, S. V.; McKeigue, P.M.; et al. Diabetes risk and amino acid profiles: cross-sectional and prospective analyses of ethnicity, amino acids and diabetes in a South Asian and European cohort from the SABRE (Southall And Brent REvisited) Study. *Diabetologia* **2015**, *58*, 968–979, doi:10.1007/s00125-015-3517-8.

49. Araujo, T.R.; da Silva, J.A.; Vettorazzi, J.F.; Freitas, I.N.; Lubaczeuski, C.; Magalhaes, E.A.; Silva, J.N.; Ribeiro, E.S.; Boschero, A.C.; Carneiro, E.M.; et al. Glucose intolerance in monosodium glutamate obesity is linked to hyperglucagonemia and insulin resistance in alpha cells. *J. Cell. Physiol.* **2019**, *234*, 7019–7031, doi:10.1002/jcp.27455.

50. Guasch-Ferré, M.; Hruby, A.; Toledo, E.; Clish, C.B.; Martínez-González, M.A.; Salas-Salvadó, J.; Hu, F.B. Metabolomics in prediabetes and diabetes: A systematic review and meta-analysis. *Diabetes Care* **2016**, *39*, 833–46, doi:10.2337/dc15-2251.

51. Tulipani, S.; Palau-Rodriguez, M.; Minarro Alonso, A.; Cardona, F.; Marco-Ramell, A.; Zonja, B.; Lopez de Alda, M.; Munoz-Garach, A.; Sanchez-Pla, A.; Tinahones, F.J.; et al. Biomarkers of Morbid Obesity and Prediabetes by Metabolomic Profiling of Human Discordant Phenotypes. *Clin. Chim. Acta.* **2016**, *463*, 53–61, doi:10.1016/j.cca.2016.10.005.

52. Won, E.Y.; Yoon, M.K.; Kim, S.W.; Jung, Y.; Bae, H.W.; Lee, D.; Park, S.G.; Lee, C.H.; Hwang, G.S.; Chi, S.W. Gender-Specific Metabolomic Profiling of Obesity in Leptin-Deficient ob/ob Mice by 1H NMR Spectroscopy. *PLoS One* **2013**, *8*, e75998, doi:10.1371/journal.pone.0075998.

53. Cupisti, A.; Meola, M.; D'Alessandro, C.; Bernabini, G.; Pasquali, E.; Carpi, A.; Barsotti, G. Insulin resistance and low urinary citrate excretion in calcium stone formers. *Biomed. Pharmacother.* **2007**, *61*, 86–90, doi:10.1016/j.biopha.2006.09.012.

54. Wang, Z.; Klipfell, E.; Bennett, B.J.; Koeth, R.; Levison, B.S.; Dugar, B.; Feldstein, A.E.; Britt, E.B.; Fu, X.; Chung, Y.M.; et al. Gut flora metabolism of phosphatidylcholine promotes cardiovascular disease. *Nature* **2011**, *472*, 57–65, doi:10.1038/nature09922.

55. Graessler, J.; Qin, Y.; Zhong, H.; Zhang, J.; Licinio, J.; Wong, M.L.; Xu, A.; Chavakis, T.; Bornstein, A.B.; Ehrhart-Bornstein, M.; et al. Metagenomic sequencing of the human gut microbiome before and after bariatric surgery in obese patients with type 2 diabetes: Correlation with inflammatory and metabolic parameters. *Pharmacogenomics J.* **2013**, *13*, 514–522, doi:10.1038/tpj.2012.43.

56. Org, E.; Blum, Y.; Kasela, S.; Mehrabian, M.; Kuusisto, J.; Kangas, A.J.; Soininen, P.; Wang, Z.; Ala-Korpela, M.; Hazen, S.L.; et al. Relationships between gut microbiota, plasma metabolites, and metabolic syndrome traits in the METSIM cohort. *Genome Biol.* **2017**, *18*, 1–14, doi:10.1186/s13059-017-1194-2.

57. Shucha Zhang, G.A. Nagana Gowda, Vincent Asiago, Narasimhamurthy Shanaiah; Coral Barbas,*, and D.R. Correlative and quantitative 1H NMR-based metabolomics reveals specific metabolic pathway disturbances in diabetic rats. *Anal Biochem* **2008**, *1*, 383, doi:10.1038/jid.2014.371.

58. Moreno-Navarrete, J.M.; Serino, M.; Blasco-Baque, V.; Azalbert, V.; Barton, R.H.; Cardellini, M.; Latorre, J.; Ortega, F.; Sabater-Masdeu, M.; Burcelin, R.; et al. Gut Microbiota Interacts with Markers of Adipose Tissue Browning, Insulin Action and Plasma Acetate in Morbid Obesity. *Mol. Nutr. Food Res.* **2018**, *62*, 1–9, doi:10.1002/mnfr.201700721.

59. Stec, D.F.; Henry, C.; Stec, D.E.; Voziyan, P. Changes in urinary metabolome related to body fat involve intermediates of choline processing by gut microbiota. *Heliyon* **2019**, *5*, e01497, doi:10.1016/j.heliyon.2019.e01497.

60. An, Y.; Xu, W.; Li, H.; Lei, H.; Zhang, L.; Hao, F.; Duan, Y.; Yan, X.; Zhao, Y.; Wu, J.; et al. High-fat diet induces dynamic metabolic alterations in multiple biological matrices of rats. *J. Proteome Res.* **2013**, *12*, 3755–3768, doi:10.1021/pr400398b.

61. Lin, H.; An, Y.; Hao, F.; Wang, Y.; Tang, H. Correlations of Fecal Metabonomic and Microbiomic Changes Induced by High-fat Diet in the Pre-Obesity State. *Sci. Rep.* **2016**, *6*, 1–14, doi:10.1038/srep21618.

62. Hernández-Alonso, P.; Cañueto, D.; Giardina, S.; Salas-Salvadó, J.; Cañellas, N.; Correig, X.; Bulló, M. Effect of pistachio consumption on the modulation of urinary gut microbiota-related metabolites in prediabetic subjects. *J. Nutr. Biochem.* **2017**, *45*, 48–53, doi:10.1016/j.jnutbio.2017.04.002.

63. Connor, S.C.; Hansen, M.K.; Corner, A.; Smith, R.F.; Ryan, T.E. Integration of metabolomics and transcriptomics data to aid biomarker discovery in type 2 diabetes. *Mol. Biosyst.* **2010**, *6*, 909–921, doi:10.1039/b914182k.

64. Serena, C.; Ceperuelo-Mallafré, V.; Keiran, N.; Queipo-Ortuño, M.I.; Bernal, R.; Gomez-Huelgas, R.; Urpi-Sarda, M.; Sabater, M.; Pérez-Brocal, V.; Andrés-Lacueva, C.; et al. Elevated circulating levels of succinate in human obesity are linked to specific gut microbiota. *ISME J.* **2018**, *12*, 1642–1657, doi:10.1038/s41396-018-0068-2.

65. Akinkuolie, A.O.; Pradhan, A.D.; Buring, J.E.; Ridker, P.M.; Mora, S. Novel Protein Glycan Side-Chain Biomarker and Risk of Incident Type 2 Diabetes Mellitus. *Arterioscler. Thromb. Vasc. Biol.* **2015**, *35*, 1544–1550, doi:10.1161/ATVBAHA.115.305635.

66. Lawler, P.R.; Akinkuolie, A.O.; Chandler, P.D.; Moorthy, M.V.; Vandenburgh, M.J.; Schaumberg, D.A.; Lee, I.M.; Glynn, R.J.; Ridker, P.M.; Buring, J.E.; et al. Circulating N-Linked Glycoprotein Acetyls and Longitudinal Mortality Risk. *Circ. Res.* **2016**, *118*, 1106–1115, doi:10.1161/CIRCRESAHA.115.308078.

67. Ritchie, S.C.; Würtz, P.; Nath, A.P.; Abraham, G.; Havulinna, A.S.; Fearnley, L.G.; Sarin, A.P.; Kangas, A.J.; Soininen, P.; Aalto, K.; et al. The Biomarker GlycA is Associated with Chronic Inflammation and Predicts Long-Term Risk of Severe Infection. *Cell Syst.* **2015**, *1*, 293–301, doi:10.1016/j.cels.2015.09.007.

68. Pietzner, M.; Kaul, A.; Henning, A.K.; Kastenmüller, G.; Artati, A.; Lerch, M.M.; Adamski, J.; Nauck, M.; Friedrich, N. Comprehensive metabolic profiling of chronic low-grade inflammation among generally healthy individuals. *BMC Med.* **2017**, *15*, 1–12, doi:10.1186/s12916-017-0974-6.

69. Vinaixa, M.; Ángel Rodríguez, M.; Rull, A.; Beltrán, R.; Bladé, C.; Brezmes, J.; Cañellas, N.; Joven, J.; Correig, X. Metabolomic assessment of the effect of dietary cholesterol in the progressive development of fatty liver disease. *J. Proteome Res.* **2010**, *9*, 2527–2538, doi:10.1021/pr901203w.

70. Guo, W.; Jiang, C.; Yang, L.; Li, T.; Liu, X.; Jin, M.; Qu, K.; Chen, H.; Jin, X.; Liu, H.; et al. Quantitative Metabolomic Profiling of Plasma, Urine, and Liver Extracts by 1H NMR Spectroscopy Characterizes Different Stages of Atherosclerosis in Hamsters. *J. Proteome Res.* **2016**, *15*, 3500–3510, doi:10.1021/acs.jproteome.6b00179.

71. Shearer, J.; Duggan, G.; Weljie, A.; Hittel, D.S.; Wasserman, D.H.; Vogel, H.J. Metabolomic profiling of dietary-induced insulin resistance in the high fat-fed C57BL/6J mouse. *Diabetes, Obes. Metab.* **2008**, *10*, 950–958, doi:10.1111/j.1463-1326.2007.00837.x.

72. Suhre, K.; Meisinger, C.; Döring, A.; Altmaier, E.; Belcredi, P.; Gieger, C.; Chang, D.; Milburn, M. V.; Gall, W.E.; Weinberger, K.M.; et al. Metabolic footprint of diabetes: A multiplatform metabolomics study in an epidemiological setting. *PLoS One* **2010**, *5*, e13953, doi:10.1371/journal.pone.0013953.

73. Li, X.; Chen, Y.; Liu, J.; Yang, G.; Zhao, J.; Liao, G.; Shi, M.; Yuan, Y.; He, S.; Lu, Y.; et al. Serum metabolic variables associated with impaired glucose tolerance induced by high-fat-high-cholesterol diet in Macaca mulatta. *Exp. Biol. Med.* **2012**, *237*, 1310–1321, doi:10.1258/ebm.2012.012157.

74. Gao, X.; Randell, E.; Tian, Y.; Zhou, H.; Sun, G. Low serum choline and high serum betaine levels are associated with favorable components of metabolic syndrome in Newfoundland population. *J. Diabetes Complications* **2019**, *33*, 107398, doi:10.1016/j.jdiacomp.2019.06.003.

75. Azam, A.A.; Pariyani, R.; Ismail, I.S.; Ismail, A.; Khatib, A.; Abas, F.; Shaari, K. Urinary metabolomics study on the protective role of Orthosiphon stamineus in Streptozotocin induced diabetes mellitus in rats via 1H NMR spectroscopy. *BMC Complement. Altern. Med.* **2017**, *17*, 1–13, doi:10.1186/s12906-017-1777-1.

76. Mora-Ortiz, M.; Nuñez Ramos, P.; Oregioni, A.; Claus, S.P. NMR metabolomics identifies over 60 biomarkers associated with Type II Diabetes impairment in db/db mice. *Metabolomics* **2019**, *15*, 1–16, doi:10.1007/s11306-019-1548-8.

77. Söder, J.; Hagman, R.; Dicksved, J.; Lindåse, S.; Malmlöf, K.; Agback, P.; Moazzami, A.; Höglund, K.; Wernersson, S. The urine metabolome differs between lean and overweight Labrador Retriever dogs during a feed-challenge. *PLoS One* **2017**, *12*, e0180086–e0180086, doi:10.1371/journal.pone.0180086.

78. Tynkkynen, T.; Wang, Q.; Ekholm, J.; Anufrieva, O.; Ohukainen, P.; Vepsäläinen, J.; Männikkö, M.; Keinänen-Kiukaanniemi, S.; Holmes, M. V; Goodwin, M.; et al. Proof of concept for quantitative urine NMR metabolomics pipeline for large-scale epidemiology and genetics. *Int. J. Epidemiol.* **2019**, *48*, 978–993, doi:10.1093/ije/dyy287.

79. Westhof, E. Pseudouridines or how to draw on weak energy differences. *Biochem. Biophys. Res. Commun.* **2019**, *520*, 702–704, doi:https://doi.org/10.1016/j.bbrc.2019.10.009.

80. Miccheli, A.; Capuani, G.; Marini, F.; Tomassini, A.; Praticò, G.; Ceccarelli, S.; Gnani, D.; Baviera, G.; Alisi, A.; Putignani, L.; et al. Urinary 1H-NMR-based metabolic profiling of children with NAFLD undergoing VSL#3 treatment. *Int. J. Obes.* **2015**, *39*, 1118–1125, doi:10.1038/ijo.2015.40.

81. Palmnäs, M.S.A.; Kopciuk, K.A.; Shaykhutdinov, R.A.; Robson, P.J.; Mignault, D.; Rabasa-Lhoret, R.; Vogel, H.J.; Csizmadi, I. Serum metabolomics of activity energy expenditure and its relation to metabolic syndrome and obesity. *Sci. Rep.* **2018**, *8*, 1–12.

82. Zhao, H.; Shen, J.; Djukovic, D.; Daniel-MacDougall, C.; Gu, H.; Wu, X.; Chow, W.-H. Metabolomics-identified metabolites associated with body mass index and prospective weight gain among Mexican American women. *Obes. Sci. Pract.* **2016**, *2*, 309–317, doi:10.1002/osp4.63.

83. Ali, M.K.; Siegel, K.R.; Chandrasekar, E.; Tandon, N.; Montoya, P.A.; Mbanya, J.-C.; Chan, J.; Zhang, P.; Narayan, K.M.V. Diabetes: An Update on the Pandemic and Potential Solutions. In; Prabhakaran, D., Anand, S., Gaziano, T.A., Mbanya, J.-C., Wu, Y., Nugent, R., Eds.; Washington (DC), 2017 ISBN 9781464805189.

84. WHO Global action plan for the prevention and control of noncommunicable diseases 2013-2020. *World Heal. Organ.* **2013**, doi:978 92 4 1506236.

85. Cosentino, F.; Grant, P.J.; Aboyans, V.; Bailey, C.J.; Ceriello, A.; Delgado, V.; Federici, M.; Filippatos, G.; Grobbee, D.E.; Hansen, T.B.; et al. 2019 ESC Guidelines on diabetes, pre-diabetes, and cardiovascular diseases developed in collaboration with the EASD. *Eur. Heart J.* **2019**, *41*, 255–323, doi:10.1093/eurheartj/ehz486.

86. Aleksandrova, K.; Mozaffarian, D.; Pischon, T. Addressing the Perfect Storm: Biomarkers in Obesity and Pathophysiology of Cardiometabolic Risk. *Clin. Chem.* **2018**, *64*, 142–153, doi:10.1373/clinchem.2017.275172.

87. E, G. Guideline for the Management of Insulin Resistance. *Int. J. Endocrinol. Metab. Disord.* **2015**, *1*, 1–10, doi:10.16966/2380-548x.115.

88. Bloomgarden, Z.T. American Association of Clinical Endocrinologists (AACE) consensus conference on the insulin resistance syndrome: 25-26 August 2002, Washington, DC. In Proceedings of the Diabetes Care; 2003.

89. Matthews, D.R.; Hosker, J.P.; Rudenski, A.S.; Naylor, B.A.; Treacher, D.F.; Turner, R.C. Homeostasis model assessment: insulin resistance and beta-cell function from fasting plasma glucose and insulin concentrations in man. *Diabetologia* **1985**, *28*, 412–419.

90. Shashaj, B.; Luciano, R.; Contoli, B.; Morino, G.S.; Spreghini, M.R.; Rustico, C.; Sforza, R.W.; Dallapiccola, B.; Manco, M. Reference ranges of HOMA-IR in normal-weight and obese young Caucasians. *Acta Diabetol.* **2016**, *53*, 251–60, doi:10.1007/s00592-015-0782-4.

91. Katz, A.; Nambi, S.S.; Mather, K.; Baron, A.D.; Follmann, D.A.; Sullivan, G.; Quon, M.J. Quantitative insulin sensitivity check index: A simple, accurate method for assessing insulin sensitivity in humans. *J. Clin. Endocrinol. Metab.* **2000**, *85*, 2402–2410, doi:10.1210/jcem.85.7.6661.

92. van der Aa, M.P.; Knibbe, C.A.J.; Boer, A. de; van der Vorst, M.M.J. Definition of insulin resistance affects prevalence rate in pediatric patients: a systematic review and call for consensus. *J. Pediatr. Endocrinol. Metab.* **2017**, *30*, 123–131, doi:10.1515/jpem-2016-0242.

93. Organization, W.H. *Use of glycated haemoglobin (HbA1c) in diagnosis of diabetes mellitus: abbreviated report of a WHO consultation*; World Health Organization, 2011;

94. Schnell, O.; Crocker, J.B.; Weng, J. Impact of HbA1c Testing at Point of Care on Diabetes Management. *J. Diabetes Sci. Technol.* **2017**, *11*, 611–617, doi:10.1177/1932296816678263.

95. Dennedy, M.C.; Rizza, R.A.; Dinneen, S.F. Classification and Diagnosis of Diabetes Mellitus. *Endocrinol. Adult Pediatr.* **2015**, *1–2*, 662-671.e2, doi:10.1016/B978-0-323-18907-1.00038-X.

96. Weykamp, C. HbA1c: a review of analytical and clinical aspects. *Ann. Lab. Med.* **2013**, *33*, 393–400.

97. Thorand, B.; Zierer, A.; Baumert, J.; Meisinger, C.; Herder, C.; Koenig, W. Associations between leptin and the leptin/adiponectin ratio and incident Type 2 diabetes in middle-aged men and women: Results from the MONICA/KORA Augsburg Study 1984-2002. *Diabet. Med.* **2010**, *27*, 1004–11, doi:10.1111/j.1464-5491.2010.03043.x.

98. Dastani, Z.; Hivert, M.F.; Timpson, N.; Perry, J.R.B.; Yuan, X.; Scott, R.A.; Henneman, P.; Heid, I.M.; Kizer, J.R.; Lyytikäinen, L.P.; et al. Novel loci for adiponectin levels and their influence on type 2 diabetes and metabolic traits: A multi-ethnic meta-analysis of 45,891 individuals. *PLoS Genet.* **2012**, *8*, e1002607, doi:10.1371/journal.pgen.1002607.

99. Liu, C.; Feng, X.; Li, Q.; Wang, Y.; Li, Q.; Hua, M. Adiponectin, TNF-α and inflammatory cytokines and risk of type 2 diabetes: A systematic review and meta-analysis. *Cytokine* **2016**, *86*, 100–109, doi:10.1016/j.cyto.2016.06.028.

100. Wang, Y.; Meng, R.W.; Kunutsor, S.K.; Chowdhury, R.; Yuan, J.M.; Koh, W.P.; Pan, A. Plasma adiponectin levels and type 2 diabetes risk: A nested case-control study in a Chinese population and an updated meta-analysis. *Sci. Rep.* **2018**, *8*, 406, doi:10.1038/s41598-017-18709-9.

101. Lopez-Jaramillo, P.; Gomez-Arbelaez, D.; Lopez-Lopez, J.; Lopez-Lopez, C.; Martinez-Ortega, J.; Gomez-Rodriguez, A.; Triana-Cubillos, S. The role of leptin/adiponectin ratio in metabolic syndrome and diabetes. *Horm. Mol. Biol. Clin. Investig.* **2014**, *18*, 37–45, doi:10.1515/hmbci-2013-0053.

102. Finucane, F.M.; Luan, J.; Wareham, N.J.; Sharp, S.J.; O'Rahilly, S.; Balkau, B.; Flyvbjerg, a.; Walker, M.; Højlund, K.; Nolan, J.J.; et al. Correlation of the leptin:adiponectin ratio with measures of insulin resistance in non-diabetic individuals. *Diabetologia* **2009**, *52*, 2345–2349, doi:10.1007/s00125-009-1508-3.

103. Kang, D.R.; Yadav, D.; Koh, S.B.; Kim, J.Y.; Ahn, S.V. Impact of Serum Leptin to Adiponectin Ratio on Regression of Metabolic Syndrome in High-Risk Individuals: The ARIRANG Study. *Yonsei Med. J.* **2017**, *58*, 339–346, doi:10.3349/ymj.2017.58.2.339.

104. Larsen, M.A.; Isaksen, V.T.; Moen, O.S.; Wilsgaard, L.; Remijn, M.; Paulssen, E.J.; Florholmen, J.; Goll, R. Leptin to adiponectin ratio – A surrogate biomarker for early detection of metabolic disturbances in obesity. *Nutr. Metab. Cardiovasc. Dis.* **2018**, *28*, 1114–1121, doi:https://doi.org/10.1016/j.numecd.2018.06.020.

105. Madeira, I.R.; Carvalho, C.N.M.; Gazolla, F.M.; de Matos, H.J.; Borges, M.A.; Bordallo, M.A.N. [Cut-off point for Homeostatic Model Assessment for Insulin Resistance (HOMA-IR) index established from Receiver Operating Characteristic (ROC) curve in the detection of metabolic syndrome in overweight pre-pubertal children]. *Arq. Bras. Endocrinol. Metabol.* **2008**, *52*, 1466–1473, doi:10.1590/s0004-27302008000900010.

106. Gabir, M.M.; Hanson, R.L.; Dabelea, D.; Imperatore, G.; Roumain, J.; Bennett, P.H.; Knowler, W.C. The 1997 American Diabetes Association and 1999 World Health Organization criteria for hyperglycemia in the diagnosis and prediction of diabetes. *Diabetes Care* **2000**, doi:10.2337/diacare.23.8.1108.

107. WHO *Definition and Diagnosis of Diabetes Mellitus and Intermediate Hyperglycemia: report of a WHO/IDF consultation*; 2006;

108. Ovalle, F. American Diabetes Association 2019 Conference Podcast With the Editor-in-Chief: What Are the Outcomes from ADA This Year and What Are the Future Developments in Diabetes? *Diabetes Ther.* **2019**, *10*, 1177–1179, doi:10.1007/s13300-019-0661-z.

109. Brereton, M.F.; Rohm, M.; Shimomura, K.; Holland, C.; Tornovsky-Babeay, S.; Dadon, D.; Iberl, M.; Chibalina, M. V; Lee, S.; Glaser, B.; et al. Hyperglycaemia induces metabolic dysfunction and glycogen accumulation in pancreatic β-cells. *Nat. Commun.* **2016**, *7*, 13496, doi:10.1038/ncomms13496.

110. Bessesen, D.H. The Role of Carbohydrates in Insulin Resistance. *J. Nutr.* **2001**, *131*, 2782S-2786S, doi:10.1093/jn/131.10.2782S.

111. Sébédio, J.-L.; Pujos-Guillot, E.; Ferrara, M. Metabolomics in evaluation of glucose disorders. *Curr. Opin. Clin. Nutr. Metab. Care* **2009**, *12*, 412–8.

112. Okorie, O.N.; Dellinger, P. Lactate: Biomarker and Potential Therapeutic Target. *Crit. Care Clin.* **2011**, *27*, 299–326, doi:10.1016/j.ccc.2010.12.013.

113. Flint, H.J.; Duncan, S.H.; Scott, K.P.; Louis, P. Links between diet, gut microbiota composition and gut metabolism. *Proc. Nutr. Soc.* **2014**, *760*, 13–22, doi:10.1017/S0029665114001463.

114. Adeva-Andany, M.; López-Ojén, M.; Funcasta-Calderón, R.; Ameneiros-Rodríguez, E.; Donapetry-García, C.; Vila-Altesor, M.; Rodríguez-Seijas, J. Comprehensive review on lactate metabolism in human health. *Mitochondrion* **2014**, *17*, 76–100, doi:https://doi.org/10.1016/j.mito.2014.05.007.

115. Berhane, F.; Fite, A.; Daboul, N.; Al-Janabi, W.; Msallaty, Z.; Caruso, M.; Lewis, M.K.; Yi, Z.; Diamond, M.P.; Abou-Samra, A.B.; et al. Plasma lactate levels increase during hyperinsulinemic euglycemic clamp and oral glucose tolerance test. *J. Diabetes Res.* **2015**, *2015*, 102054, doi:10.1155/2015/102054.

116. Shaham, O.; Wei, R.; Wang, T.J.; Ricciardi, C.; Lewis, G.D.; Vasan, R.S.; Carr, S.A.; Thadhani, R.; Gerszten, R.E.; Mootha, V.K. Metabolic profiling of the human response to a glucose challenge reveals distinct axes of insulin sensitivity. *Mol. Syst. Biol.* **2008**, *4*, 214, doi:10.1038/msb.2008.50.

117. Crawford, S.O.; Hoogeveen, R.C.; Brancati, F.L.; Astor, B.C.; Ballantyne, C.M.; Schmidt, M.I.; Young, J.H. Association of blood lactate with type 2 diabetes: the Atherosclerosis Risk in Communities Carotid MRI Study. *Int. J. Epidemiol.* **2010**, *39*, 1647–1655, doi:10.1093/ije/dyq126.

118. Abu Bakar, M.H.; Sarmidi, M.; Cheng, K.-K.; Khan, A.; Chua, L.S.; Zaman Huri, H.; Yaakob, H. Metabolomics – The Complementary Field in Systems Biology: A Review on Obesity and Type 2 Diabetes. *Mol. BioSyst.* **2015**, *11*, 1742–1774, doi:10.1039/C5MB00158G.

119. Maiuolo, J.; Oppedisano, F.; Gratteri, S.; Muscoli, C.; Mollace, V. Regulation of uric acid metabolism and excretion. *Int. J. Cardiol.* **2016**, *213*, 8–14, doi:https://doi.org/10.1016/j.ijcard.2015.08.109.

120. Cicerchi, C.; Li, N.; Kratzer, J.; Garcia, G.; Roncal-Jimenez, C.A.; Tanabe, K.; Hunter, B.; Rivard, C.J.; Sautin, Y.Y.; Gaucher, E.A.; et al. Uric acid-dependent inhibition of AMP kinase induces hepatic glucose production in diabetes and starvation: evolutionary implications of the uricase loss in hominids. *FASEB J. Off. Publ. Fed. Am. Soc. Exp. Biol. Off. Publ. Fed. Am. Soc. Exp. Biol.* **2014**, *28*, 3339–3350, doi:10.1096/fj.13-243634.

121. Choi, Y.-J.; Shin, H.-S.; Choi, H.S.; Park, J.-W.; Jo, I.; Oh, E.-S.; Lee, K.-Y.; Lee, B.-H.; Johnson, R.J.; Kang, D.-H. Uric acid induces fat accumulation via generation of endoplasmic reticulum stress and SREBP-1c activation in hepatocytes. *Lab. Invest.* **2014**, *94*, 1114–1125, doi:10.1038/labinvest.2014.98.

122. Shani, M.; Vinker, S.; Dinour, D.; Leiba, M.; Twig, G.; Holtzman, E.J.; Leiba, A. High Normal Uric Acid Levels Are Associated with an Increased Risk of Diabetes in Lean, Normoglycemic Healthy Women. *J. Clin. Endocrinol. Metab.* **2016**, *101*, 3772–3778, doi:10.1210/jc.2016-2107.

123. Bombelli, M.; Quarti-Trevano, F.; Tadic, M.; Facchetti, R.; Cuspidi, C.; Mancia, G.; Grassi, G. Uric acid and risk of new-onset metabolic syndrome, impaired fasting glucose and diabetes mellitus in a general Italian population: data from the Pressioni Arteriose Monitorate E Loro Associazioni study. *J. Hypertens.* **2018**, *36*, 1492–1498, doi:10.1097/HJH.0000000000001721.

124. Barragan, M.; Luna, V.; Vargas-Morales, J.M.; Aradillas-Garcia, C.; Teran-Garcia, M. Uric Acid: An Overlooked, Inexpensive Biomarker of Metabolic Syndrome (P10-068-19). *Curr. Dev. Nutr.* **2019**, *3*, nzz034-P10., doi:10.1093/cdn/nzz034.P10-068-19.

125. Han, T.; Lan, L.; Qu, R.; Xu, Q.; Jiang, R.; Na, L.; Sun, C. Temporal Relationship Between Hyperuricemia and Insulin Resistance and Its Impact on Future Risk of Hypertension. *Hypertens. (Dallas, Tex. 1979)* **2017**, *70*, 703–711, doi:10.1161/HYPERTENSIONAHA.117.09508.

126. Sautin, Y.Y.; Johnson, R.J. Uric Acid: The Oxidant-Antioxidant Paradox. *Nucleosides. Nucleotides Nucleic Acids* **2008**, *27*, 608–619, doi:10.1080/15257770802138558.

127. van der Schaft, N.; Brahimaj, A.; Wen, K.-X.; Franco, O.H.; Dehghan, A. The association between serum uric acid and the incidence of prediabetes and type 2 diabetes mellitus: The Rotterdam Study. *PLoS One* **2017**, *12*, e0179482, doi:10.1371/journal.pone.0179482.

128. Kanbay, M.; Jensen, T.; Solak, Y.; Le, M.; Roncal-Jimenez, C.; Rivard, C.; Lanaspa, M.A.; Nakagawa, T.; Johnson, R.J. Uric acid in metabolic syndrome: From an innocent bystander to a central player. *Eur. J. Intern. Med.* **2016**, *29*, 3–8, doi:https://doi.org/10.1016/j.ejim.2015.11.026.

129. Reuter, S.E.; Evans, A.M. Carnitine and Acylcarnitines. *Clin. Pharmacokinet.* **2012**, *51*, 553–572, doi:10.1007/BF03261931.

130. Koves, T.R.; Li, P.; An, J.; Akimoto, T.; Slentz, D.; Ilkayeva, O.; Dohm, G.L.; Yan, Z.; Newgard, C.B.; Muoio, D.M. Peroxisome proliferator-activated receptor-gamma co-activator 1alpha-mediated metabolic remodeling of skeletal myocytes mimics exercise training and reverses lipid-induced mitochondrial inefficiency. *J. Biol. Chem.* **2005**, *280*, 33588–33598, doi:10.1074/jbc.M507621200.

131. Mihalik, S.J.; Goodpaster, B.H.; Kelley, D.E.; Chace, D.H.; Vockley, J.; Toledo, F.G.S.; Delany, J.P. Increased levels of plasma acylcarnitines in obesity and type 2 diabetes and identification of a marker of glucolipotoxicity. *Obesity* **2010**, doi:10.1038/oby.2009.510.

132. Huffman, K.M.; Shah, S.H.; Stevens, R.D.; Bain, J.R.; Muehlbauer, M.; Slentz, C.A.; Tanner, C.J.; Kuchibhatla, M.; Houmard, J.A.; Newgard, C.B.; et al. Relationships between circulating metabolic intermediates and insulin action in overweight to obese, inactive men and women. *Diabetes Care* **2009**, *32*, 1678–1683, doi:10.2337/dc08-2075.

133. Ha, C.Y.; Kim, J.Y.; Paik, J.K.; Kim, O.Y.; Paik, Y.-H.; Lee, E.J.; Lee, J.H. The association of specific metabolites of lipid metabolism with markers of oxidative stress, inflammation and arterial stiffness in men with newly diagnosed type 2 diabetes. *Clin. Endocrinol. (Oxf).* **2012**, *76*, 674–682, doi:10.1111/j.1365-2265.2011.04244.x.

134. Zhang, X.; Zhang, C.; Chen, L.; Han, X.; Ji, L. Human serum acylcarnitine profiles in different glucose tolerance states. *Diabetes Res. Clin. Pract.* **2014**, *104*, 376–382, doi:10.1016/j.diabres.2014.04.013.

135. Beger, R.D.; Bhattacharyya, S.; Gill, P.S.; James, L.P. Acylcarnitines as Translational Biomarkers of Mitochondrial Dysfunction. *Mitochondrial Dysfunct. Caused by Drugs Environ. Toxicants* **2018**, *1–2*, 383–393, doi:10.1002/9781119329725.ch24.

136. Bene, J.; Szabo, A.; Komlosi, K.; Melegh, B. Mass Spectrometric Analysis of L-carnitine and Its Esters: Potential Biomarkers of Disturbances in Carnitine Homeostasis. *Curr. Mol. Med.* **2019**, doi:10.2174/1566524019666191113120828.

137. Saito, N.; Saito, T.; Yamazaki, T.; Fujimine, Y.; Ihara, T. Establishment of an analytical method for accurate purity evaluations of acylcarnitines by using quantitative 1H NMR spectroscopy. *Accredit. Qual. Assur.* **2017**, *22*, 171–178, doi:10.1007/s00769-017-1263-y.

138. Wang, T.J.; Larson, M.G.; Vasan, R.S.; Cheng, S.; Rhee, E.P.; McCabe, E.; Lewis, G.D.; Fox, C.S.; Jacques, P.F.; Fernandez, C.; et al. Metabolite profiles and the risk of developing diabetes. *Nat. Med.* **2011**, *17*, 448–453, doi:10.1038/nm.2307.

139. Newgard, C.B. Metabolomics and Metabolic Diseases: Where Do We Stand? *Cell Metab.* **2017**, *25*, 43–56, doi:10.1016/j.cmet.2016.09.018.

140. Newgard, C.B.; An, J.; Bain, J.R.; Muehlbauer, M.J.; Stevens, R.D.; Lien, L.F.; Haqq, A.M.; Shah, S.H.; Arlotto, M.; Slentz, C.A.; et al. A branched-chain amino acid-related metabolic signature that differentiates obese and lean humans and contributes to insulin resistance. *Cell Metab.* **2009**, *9*, 311–326, doi:10.1016/j.cmet.2009.02.002.

141. Takashina, C.; Tsujino, I.; Watanabe, T.; Sakaue, S.; Ikeda, D.; Yamada, A.; Sato, T.; Ohira, H.; Otsuka, Y.; Oyama-Manabe, N.; et al. Associations among the plasma amino acid profile, obesity, and glucose metabolism in Japanese adults with normal glucose tolerance. *Nutr. Metab. (Lond).* **2016**, *13*, 5, doi:10.1186/s12986-015-0059-5.

142. Psychogios, N.; Hau, D.D.; Peng, J.; Guo, A.C.; Mandal, R.; Bouatra, S.; Sinelnikov, I.; Krishnamurthy, R.; Eisner, R.; Gautam, B.; et al. The human serum metabolome. *PLoS One* **2011**, *6*, 1–2, doi:10.1371/journal.pone.0016957.

143. Zheng, Y.; Li, Y.; Qi, Q.; Hruby, A.; Manson, J.E.; Willett, W.C.; Wolpin, B.M.; Hu, F.B.; Qi, L. Cumulative consumption of branched-chain amino acids and incidence of type 2 diabetes. *Int. J. Epidemiol.* **2016**, *45*, 1482–1492, doi:10.1093/ije/dyw143.

144. Nie, C.; He, T.; Zhang, W.; Zhang, G.; Ma, X. Branched chain amino acids: Beyond nutrition metabolism. *Int. J. Mol. Sci.* 2018, *19*.

145. Wolak-Dinsmore, J.; Gruppen, E.G.; Shalaurova, I.; Matyus, S.P.; Grant, R.P.; Gegen, R.; Bakker, S.J.L.; Otvos, J.D.; Connelly, M.A.; Dullaart, R.P.F. A novel NMR-based assay to measure circulating concentrations of branched-chain amino acids: Elevation in subjects with type 2 diabetes mellitus and association with carotid intima media thickness. *Clin. Biochem.* **2018**, *54*, 92–99, doi:10.1016/j.clinbiochem.2018.02.001.

146. Parthasarathy, A.; Cross, P.J.; Dobson, R.C.J.; Adams, L.E.; Savka, M.A.; Hudson, A.O. A Three-Ring Circus: Metabolism of the Three Proteogenic Aromatic Amino Acids and Their Role in the Health of Plants and Animals. *Front. Mol. Biosci.* **2018**, *5*, 29, doi:10.3389/fmolb.2018.00029.

147. Chen, S.; Akter, S.; Kuwahara, K.; Matsushita, Y.; Nakagawa, T.; Konishi, M.; Honda, T.; Yamamoto, S.; Hayashi, T.; Noda, M.; et al. Serum amino acid profiles and risk of type 2 diabetes among Japanese adults in the Hitachi Health Study. *Sci. Rep.* **2019**, *9*, 7010, doi:10.1038/s41598-019-43431-z.

148. Rhee, S.Y.; Jung, E.S.; Park, H.M.; Jeong, S.J.; Kim, K.; Chon, S.; Yu, S.Y.; Woo, J.T.; Lee, C.H. Plasma glutamine and glutamic acid are potential biomarkers for predicting diabetic retinopathy. *Metabolomics* **2018**, doi:10.1007/s11306-018-1383-3.

149. Kvamme, E. *Glutamine and Glutamate Mammals: Volume I*; CRC Press, 2018; ISBN 1351080741.

150. Long, B.; Muhamad, R.; Yan, G.; Yu, J.; Fan, Q.; Wang, Z.; Li, X.; Purnomoadi, A.; Achmadi, J.; Yan, X. Quantitative proteomics analysis reveals glutamine deprivation activates fatty acid β-oxidation pathway in HepG2 cells. *Amino Acids* **2016**, *48*, 1297–1307, doi:10.1007/s00726-016-2182-7.

151. Carlessi, R.; Rowlands, J.; Ellison, G.; de Oliveira Alves, H.H.; Newsholme, P.; Mamotte, C. Glutamine deprivation induces metabolic adaptations associated with beta cell dysfunction and exacerbate lipotoxicity. *Mol. Cell. Endocrinol.* **2019**, *491*, 110433, doi:https://doi.org/10.1016/j.mce.2019.04.013.

152. Bhagavan, N. V; Ha, C.-E. Chapter 15 - Protein and Amino Acid Metabolism. In; Bhagavan, N. V, Ha, C.-E.B.T.-E. of M.B., Eds.; Academic Press: San Diego, 2011; pp. 169–190 ISBN 978-0-12-095461-2.

153. Sookoian, S.; Pirola, C.J. Alanine and aspartate aminotransferase and glutamine-cycling pathway: their roles in pathogenesis of metabolic syndrome. *World J. Gastroenterol.* **2012**, *18*, 3775–3781, doi:10.3748/wjg.v18.i29.3775.

154. Maltais-Payette, I.; Boulet, M.-M.; Prehn, C.; Adamski, J.; Tchernof, A. Circulating glutamate concentration as a biomarker of visceral obesity and associated metabolic alterations. *Nutr. Metab. (Lond).* **2018**, *15*, 78, doi:10.1186/s12986-018-0316-5.

155. Xie, B.; Waters, M.J.; Schirra, H.J. Investigating potential mechanisms of obesity by metabolomics. *J. Biomed. Biotechnol.* **2012**, *2012*, 10, doi:10.1155/2012/805683.

156. Abranches, M.V.; De Oliveira, F.C.E.; Da Conceição, L.L.; Peluzio, M.D.C.G. Obesity and diabetes: The link between adipose tissue dysfunction and glucose homeostasis. *Nutr. Res. Rev.* **2015**, *28*, 121–132, doi:10.1017/S0954422415000098.

157. Upadhyay, R.K. Emerging Risk Biomarkers in Cardiovascular Diseases and Disorders. *J. Lipids* **2015**, *2015*, 1–50, doi:10.1155/2015/971453.

158. Irrakhimov, E.M.; Kerimkulova, A.S.; Lunegova, O.S.; Mirrakhimov, A.E.; Nabiev, M.P.; Neronova, K. V.; Bayramukova, A.A.; Alibaeva, N.T.; Satarov, N. The association of leptin with dyslipidemia, arterial hypertension and obesity in Kyrgyz (Central Asian nation) population. *BMC Res. Notes* **2014**, *7*, 1–7, doi:10.1186/1756-0500-7-411.

159. Nimmanapalli, H.; Kasi, A.; Devapatla, P.; Nuttakki, V. Lipid ratios, atherogenic coefficient and atherogenic index of plasma as parameters in assessing cardiovascular risk in type 2 diabetes mellitus. *Int. J. Res. Med. Sci.* **2016**, *4*, 2863–2869, doi:10.18203/2320-6012.ijrms20161966.

160. Grundy, S.M. Hypertriglyceridemia, insulin resistance, and the metabolic syndrome. *Am. J. Cardiol.* **1999**, *83*, 25–29, doi:10.1016/S0002-9149(99)00211-8.

161. Izadi, V.; Farabad, E.; Azadbakht, L. Epidemiologic evidence on serum adiponectin level and lipid profile. *Int. J. Prev. Med.* **2013**, *4*, 133–140.

162. Suiter, C.; Singha, S.K.; Khalili, R.; Shariat-Madar, Z. Free Fatty Acids: Circulating Contributors of Metabolic Syndrome. *Cardiovasc. Hematol. Agents Med. Chem.* **2018**, *16*, 20–34, doi:10.2174/1871525716666180528100002.

163. Elmsjo, A.; Rosqvist, F.; Engskog, M.K.R.; Haglof, J.; Kullberg, J.; Iggman, D.; Johansson, L.; Ahlstrom, H.; Arvidsson, T.; Riserus, U.; et al. NMR-based metabolic profiling in healthy individuals overfed different types of fat: Links to changes in liver fat accumulation and lean tissue mass. *Nutr. Diabetes* **2015**, *5*, doi:10.1038/nutd.2015.31.

164. Sobczak, A.I.S.; Blindauer, C.A.; Stewart, A.J. Changes in plasma free fatty acids associated with type-2 diabetes. *Nutrients* **2019**, *11*, 1–42, doi:10.3390/nu11092022.

165. Ardisson Korat, A. V; Malik, V.S.; Furtado, J.D.; Sacks, F.; Rosner, B.; Rexrode, K.M.; Willett, W.C.; Mozaffarian, D.; Hu, F.B.; Sun, Q. Circulating Very-Long-Chain SFA Concentrations Are Inversely Associated with Incident Type 2 Diabetes in US Men and Women. *J. Nutr.* **2019**, *150*, 340–349, doi:10.1093/jn/nxz240.

166. Janikiewicz, J.; Hanzelka, K.; Dziewulska, A.; Kozinski, K.; Dobrzyn, P.; Bernas, T.; Dobrzyn, A. Inhibition of SCD1 impairs palmitate-derived autophagy at the step of autophagosome-lysosome fusion in pancreatic β-cells. *J. Lipid Res.* **2015**, *56*, 1901–1911, doi:10.1194/jlr.M059980.

167. Postic, C.; Girard, J. The role of the lipogenic pathway in the development of hepatic steatosis. *Diabetes Metab.* **2008**, *34*, 643–648, doi:10.1016/S1262-3636(08)74599-3.

168. Keapai, W.; Apichai, S.; Amornlerdpison, D.; Lailerd, N. Evaluation of fish oil-rich in MUFAs for anti-diabetic and antiinflammation potential in experimental type 2 diabetic rats. *Korean J. Physiol. Pharmacol.* **2016**, *20*, 581–593, doi:10.4196/kjpp.2016.20.6.581.

169. Calder, P.C. Omega-3 fatty acids and inflammatory processes: from molecules to man. *Biochem. Soc. Trans.* **2017**, *45*, 1105–1115, doi:10.1042/BST20160474.

170. Newman, J.C.; Verdin, E. β-hydroxybutyrate: Much more than a metabolite. *Diabetes Res. Clin. Pract.* **2014**, *106*, 173–181, doi:10.1016/j.diabres.2014.08.009.

171. Du, Z.; Shen, A.; Huang, Y.; Su, L.; Lai, W.; Wang, P.; Xie, Z.; Xie, Z.; Zeng, Q.; Ren, H.; et al. 1H-NMR-based metabolic analysis of human serum reveals novel markers of myocardial energy expenditure in heart failure patients. *PLoS One* **2014**, *9*, doi:10.1371/journal.pone.0088102.

172. Kotronen, A.; Seppälä-Lindroos, A.; Vehkavaara, S.; Bergholm, R.; Frayn, K.N.; Fielding, B.A.; Yki-Järvinen, H. Liver fat and lipid oxidation in humans. *Liver Int.* **2009**, *29*, 1439–1446, doi:10.1111/j.1478-3231.2009.02076.x.

173. Bugianesi, E. EASL–EASD–EASO Clinical Practice Guidelines for the management of non-alcoholic fatty liver disease: disease mongering or call to action? *Diabetologia* **2016**, *59*, 1145–1147, doi:10.1007/s00125-016-3930-7.

174. Jiang, C. ying; Yang, K. min; Yang, L.; Miao, Z. xia; Wang, Y. hong; Zhu, H. bo A 1H NMR-Based Metabonomic Investigation of Time-Related Metabolic Trajectories of the Plasma, Urine and Liver Extracts of Hyperlipidemic Hamsters. *PLoS One* **2013**, *8*, e66786, doi:10.1371/journal.pone.0066786.

175. Gao, X.; Randell, E.; Zhou, H.; Sun, G. Higher serum choline and betaine levels are associated with better body composition in male but not female population. *PLoS One* **2018**, *13*, 1–15, doi:10.1371/journal.pone.0193114.

176. Esser, N.; Legrand-Poels, S.; Piette, J.; Scheen, A.J.; Paquot, N. Inflammation as a link between obesity, metabolic syndrome and type 2 diabetes. *Diabetes Res. Clin. Pract.* **2014**, *105*, 141–150, doi:10.1016/j.diabres.2014.04.006.

177. Vykoukal, D.; Davies, M.G. Vascular biology of metabolic syndrome. *J. Vasc. Surg.* **2011**, *54*, 819–831, doi:10.1016/j.jvs.2011.01.003.

178. Sprague, A.H.; Khalil, R.A. Inflammatory cytokines in vascular dysfunction and vascular disease. *Biochem. Pharmacol.* **2009**, *78*, 539–552, doi:10.1016/j.bcp.2009.04.029.

179. Akinkuolie, A.O.; Buring, J.E.; Ridker, P.M.; Mora, S. A novel protein glycan biomarker and future cardiovascular disease events. *J. Am. Heart Assoc.* **2014**, *3*, doi:10.1161/JAHA.114.001221.

180. Lent-Schochet, D.; McLaughlin, M.; Ramakrishnan, N.; Jialal, I. Exploratory metabolomics of metabolic syndrome: A status report. *World J. Diabetes* **2019**, *10*, 23–36, doi:10.4239/wjd.v10.i1.23.

181. Lontchi-Yimagou, E.; Sobngwi, E.; Matsha, T.E.; Kengne, A.P. Diabetes mellitus and inflammation. *Curr. Diab. Rep.* **2013**, *13*, 435–444, doi:10.1007/s11892-013-0375-y.

182. Bervoets, L.; Massa, G.; Guedens, W.; Reekmans, G.; Noben, J.P.; Adriaensens, P. Identification of metabolic phenotypes in childhood obesity by H NMR metabolomics of blood plasma. *Futur. Sci. OA* **2018**, *4*, doi:10.4155/fsoa-2017-0146.

183. Connelly, M.A.; Otvos, J.D.; Shalaurova, I.; Playford, M.P.; Mehta, N.N. GlycA, a novel biomarker of systemic inflammation and cardiovascular disease risk. *J. Transl. Med.* **2017**, *15*, 1–5, doi:10.1186/s12967-017-1321-6.

184. Bas, J.M.D.; Caimari, A.; Rodriguez-Naranjo, M.I.; Childs, C.E.; Chavez, C.P.; West, A.L.; Miles, E.A.; Arola, L.; Calder, P.C. Impairment of lysophospholipid metabolism in obesity: Altered plasma profile and desensitization to the modulatory properties of n-3 polyunsaturated fatty acids in a randomized controlled trial. *Am. J. Clin. Nutr.* **2016**, *104*, 266–279, doi:10.3945/ajcn.116.130872.

185. Cantero, I.; Abete, I.; Del Bas, J.M.; Caimari, A.; Arola, L.; Zulet, M.A.; Martinez, J.A. Changes in lysophospholipids and liver status after weight loss: the RESMENA study. *Nutr. Metab.* **2018**, *15*, 1–11, doi:10.1186/s12986-018-0288-5.

186. Alkan, Berna; Mungan, S. Lipoprotein-Associated Phospholipase A2 : A Risk Factor for Ischemic Stroke ? *ASHD* **2018**, *17*, 28–35.

187. Halliwell, B.; Gutteridge, J.M.C. *Free radicals in biology and medicine*; Oxford University Press, USA, 2015;

188. Newsholme, P.; Cruzat, V.F.; Keane, K.N.; Carlessi, R.; de Bittencourt, P.I.H.J. Molecular mechanisms of ROS production and oxidative stress in diabetes. *Biochem. J.* **2016**, *473*, 4527–4550, doi:10.1042/BCJ20160503C.

189. Asmat, U.; Abad, K.; Ismail, K. Diabetes mellitus and oxidative stress—A concise review. *Saudi Pharm. J.* **2016**, *24*, 547–553, doi:https://doi.org/10.1016/j.jsps.2015.03.013.

190. Furukawa, S.; Fujita, T.; Shimabukuro, M.; Iwaki, M.; Yamada, Y.; Nakajima, Y.; Nakayama, O.; Makishima, M.; Matsuda, M.; Shimomura, I. Increased oxidative stress in obesity and its impact on metabolic syndrome. *J. Clin. Invest.* **2004**, *114*, 1752–1761, doi:10.1172/JCI21625.

191. Milne, G.L.; Musiek, E.S.; Morrow, J.D. F2-isoprostanes as markers of oxidative stress in vivo: an overview. *Biomarkers* **2005**, *10 Suppl 1*, S10-23, doi:10.1080/13547500500216546.

192. Di Minno, A.; Turnu, L.; Porro, B.; Squellerio, I.; Cavalca, V.; Tremoli, E.; Di Minno, M.N.D. 8-Hydroxy-2-Deoxyguanosine Levels and Cardiovascular Disease: A Systematic Review and Meta-Analysis of the Literature. *Antioxid. Redox Signal.* **2016**, *24*, 548–55, doi:10.1089/ars.2015.6508.

193. Thomson, L. 3-nitrotyrosine modified proteins in atherosclerosis. *Dis. Markers* **2015**, *2015*, 708282, doi:10.1155/2015/708282.

194. Tsikas, D. Assessment of lipid peroxidation by measuring malondialdehyde (MDA) and relatives in biological samples: Analytical and biological challenges. *Anal. Biochem.* **2017**, *524*, 13–30, doi:https://doi.org/10.1016/j.ab.2016.10.021.

195. Itabe, H. Oxidized low-density lipoprotein as a biomarker of in vivo oxidative stress: from atherosclerosis to periodontitis. *J. Clin. Biochem. Nutr.* **2012**, *51*, 1–8, doi:10.3164/jcbn.11-00020R1.

196. Il'yasova, D.; Scarbrough, P.; Spasojevic, I. Urinary biomarkers of oxidative status. *Clin. Chim. Acta* 2012, *413*, 1446–1453.

197. Allantoin as a marker of oxidative stress in human erythrocytes . *Clin. Chem. Lab. Med.* 2008, *46*, 1270.

198. Zhao, L.; Gao, H.; Lian, F.; Liu, X.; Zhao, Y.; Lin, D. 1H-NMR-based metabonomic analysis of metabolic profiling in diabetic nephropathy rats induced by streptozotocin. *Am. J. Physiol. Physiol.* **2011**, *300*, F947–F956, doi:10.1152/ajprenal.00551.2010.

199. Kand'ár, R.; Žáková, P.; Mužáková, V. Monitoring of antioxidant properties of uric acid in humans for a consideration measuring of levels of allantoin in plasma by liquid chromatography. *Clin. Chim. Acta* **2006**, *365*, 249–256, doi:https://doi.org/10.1016/j.cca.2005.09.002.

200. Bentley-Lewis, R.; Huynh, J.; Xiong, G.; Lee, H.; Wenger, J.; Clish, C.; Nathan, D.; Thadhani, R.; Gerszten, R. Metabolomic profiling in the prediction of gestational diabetes mellitus. *Diabetologia* **2015**, *58*, 1329–1332, doi:10.1007/s00125-015-3553-4.

201. Topp, H.; Fusch, G.; Schoch, G.; Fusch, C. Noninvasive markers of oxidative DNA stress, RNA degradation and protein degradation are differentially correlated with resting metabolic rate and energy intake in children and adolescents. *Pediatr. Res.* **2008**, *64*, 246–250, doi:10.1203/PDR.0b013e31817cfca6.

202. Zhang, W.; Zhang, X.-A. A Novel Urinary Metabolite Signature for Non-invasive Post-stroke Depression Diagnosis. *Cell Biochem. Biophys.* **2015**, *72*, 661–667, doi:10.1007/s12013-014-0472-9.

203. DAS, B.; Nair, G.B. Homeostasis and dysbiosis of the gut microbiome in health and disease. *J. Biosci.* **2019**, *44*, 1–8, doi:10.1007/s12038-019-9926-y.

204. Ducker, G.S.; Rabinowitz, J.D. One-Carbon Metabolism in Health and Disease. *Cell Metab.* **2017**, *25*, 27–42, doi:https://doi.org/10.1016/j.cmet.2016.08.009.

205. Owen, J.B.; Butterfield, D.A. Measurement of oxidized/reduced glutathione ratio. *Methods Mol. Biol.* **2010**, *648*, 269–277, doi:10.1007/978-1-60761-756-3_18.

206. Ducker, G.S.; Rabinowitz, J.D. One-Carbon Metabolism in Health and Disease. *Cell Metab.* **2017**, *25*, 27–42, doi:https://doi.org/10.1016/j.cmet.2016.08.009.

207. Thalacker-Mercer, A.E.; Ingram, K.H.; Guo, F.; Ilkayeva, O.; Newgard, C.B.; Garvey, W.T. BMI, RQ, diabetes, and sex affect the relationships between amino acids and clamp measures of insulin action in humans. *Diabetes* **2014**, *63*, 791–800, doi:10.2337/db13-0396.

208. Teskey, G.; Abrahem, R.; Cao, R.; Gyurjian, K.; Islamoglu, H.; Lucero, M.; Martinez, A.; Paredes, E.; Salaiz, O.; Robinson, B.; et al. Chapter Five - Glutathione as a Marker for Human Disease. In *Advances in Clinical Chemistry*; Makowski, G.S.B.T.-A. in C.C., Ed.; Elsevier, 2018; Vol. 87, pp. 141–159.

209. Alves, A.; Bassot, A.; Bulteau, A.-L.; Pirola, L.; Morio, B. Glycine Metabolism and Its Alterations in Obesity and Metabolic Diseases. *Nutrients* **2019**, *11*, 1356, doi:10.3390/nu11061356.

210. Ducker, G.S.; Chen, L.; Morscher, R.J.; Ghergurovich, J.M.; Esposito, M.; Teng, X.; Kang, Y.; Rabinowitz, J.D. Reversal of Cytosolic One-Carbon Flux Compensates for Loss of the Mitochondrial Folate Pathway. *Cell Metab.* **2016**, *23*, 1140–1153, doi:10.1016/j.cmet.2016.04.016.

211. Rosenbaum, M.; Knight, R.; Leibel, R.L. The gut microbiota in human energy homeostasis and obesity. *Trends Endocrinol. Metab.* **2015**, *26*, 493–501, doi:10.1016/j.tem.2015.07.002.

212. Plovier, H.; Cani, P.D. Microbial Impact on Host Metabolism: Opportunities for Novel Treatments of Nutritional Disorders? *Microbiol. Spectr.* **2017**, *5*, 1–13, doi:10.1128/microbiolspec.bad-0002-2016.

213. Gottardi, A. De; McCoy, K.D. Evaluation of the gut barrier to intestinal bacteria in non-alcoholic fatty liver disease. *J. Hepatol.* **2011**, *55*, 1181–1183, doi:10.1016/j.jhep.2011.05.003.

214. Quesada-Vázquez, S.; Aragonès, G.; Del Bas, J.M.; Escoté, X. Diet, Gut Microbiota and Non-Alcoholic Fatty Liver Disease: Three Parts of the Same Axis. *Cells* **2020**, *9*, 1–17, doi:10.3390/cells9010176.

215. Donaldson, G.P.; Lee, S.M.; Mazmanian, S.K. Gut biogeography of the bacterial microbiota. *Nat. Rev. Microbiol.* **2015**, *14*, 20–32, doi:10.1038/nrmicro3552.

216. Weiss, G.A.; Hennet, T. Mechanisms and consequences of intestinal dysbiosis. *Cell. Mol. Life Sci.* **2017**, *74*, 2959–2977, doi:10.1007/s00018-017-2509-x.

217. Holmes, E.; Li, J. V.; Athanasiou, T.; Ashrafian, H.; Nicholson, J.K. Understanding the role of gut microbiome-host metabolic signal disruption in health and disease. *Trends Microbiol.* **2011**, *19*, 349–359, doi:10.1016/j.tim.2011.05.006.

218. Bernalier-Donadille, A. Activités métaboliques du microbiote intestinal humain. *Gastroenterol. Clin. Biol.* **2010**, *34*, S16–S22, doi:10.1016/S0399-8320(10)70016-6.

219. Gomes, J.M.G.; Costa, J.A.; Alfenas, R.C. Could the beneficial effects of dietary calcium on obesity and diabetes control be mediated by changes in intestinal microbiota and integrity? *Br. J. Nutr.* **2015**, *114*, 1756–1765, doi:10.1017/S0007114515003608.

220. Abed-Meraim, F.; Combescure, A. New prismatic solid-shell element: Assumed strain formulation and hourglass mode analysis. *Struct. Eng. Mech.* **2011**, *37*, 253–256, doi:10.12989/sem.2011.37.2.253.

221. Parekh, P.J.; Balart, L.A.; Johnson, D.A. The influence of the gut microbiome on obesity, metabolic syndrome and gastrointestinal disease. *Clin. Transl. Gastroenterol.* **2015**, *6*, e91-12, doi:10.1038/ctg.2015.16.

222. Kim, K.N.; Yao, Y.; Ju, S.Y. Short chain fatty acids and fecal microbiota abundance in humans with obesity: A systematic review and meta-analysis. *Nutrients* 2019, *11*.

223. Diamant, M.; Blaak, E.E.; de Vos, W.M. Do nutrient-gut-microbiota interactions play a role in human obesity, insulin resistance and type 2 diabetes? *Obes. Rev.* **2011**, *12*, 272–281, doi:10.1111/j.1467-789X.2010.00797.x.

224. Hernández, M.A.G.; Canfora, E.E.; Jocken, J.W.E.; Blaak, E.E. The short-chain fatty acid acetate in body weight control and insulin sensitivity. *Nutrients* **2019**, *11*, 1943, doi:10.3390/nu11081943.

225. Kimura, I.; Inoue, D.; Hirano, K.; Tsujimoto, G. The SCFA receptor GPR43 and energy metabolism. *Front. Endocrinol. (Lausanne).* **2014**, *5*, 3–5, doi:10.3389/fendo.2014.00085.

226. Perry, R.J.; Peng, L.; Barry, N.A.; Cline, G.W.; Zhang, D.; Cardone, R.L.; Petersen, K.F.; Kibbey, R.G.; Goodman, A.L. Acetate mediates a microbiome-brain-B cell axis promoting metabolic Syndrome. *Nature* 2016, *534*, 213–217.

227. Boets, E.; Gomand, S. V.; Deroover, L.; Preston, T.; Vermeulen, K.; De Preter, V.; Hamer, H.M.; Van den Mooter, G.; De Vuyst, L.; Courtin, C.M.; et al. Systemic availability and metabolism of colonic-derived short-chain fatty acids in healthy subjects: a stable isotope study. *J. Physiol.* **2017**, *595*, 541–555, doi:10.1113/JP272613.

228. de Vadder, F.; Mithieux, G. Gut-brain signaling in energy homeostasis: The unexpected role of microbiota-derived succinate. *J. Endocrinol.* **2018**, *236*, R105–R108, doi:10.1530/JOE-17-0542.

229. Sonnenburg, J.L.; Xu, J.; Leip, D.D.; Chen, C.H.; Westover, B.P.; Weatherford, J.; Buhler, J.D.; Gordon, J.I. Glycan foraging in vivo by an intestine-adapted bacterial symbiont. *Science (80-.).* **2005**, *307*, 1955–1959, doi:10.1126/science.1109051.

230. Chiang, J.Y.L. Regulation of bile acid synthesis: Pathways, nuclear receptors, and mechanisms. *J. Hepatol.* **2004**, *40*, 539–551, doi:10.1016/j.jhep.2003.11.006.

231. AF, H. THe continuing importance of bile acids in liver and intestinal disease. *Arch. Intern. Med.* **1999**, *159*, 2647–2658.

232. Turnbaugh, P.J. Microbiology: Fat, bile and gut microbes. *Nature* **2012**, *486*, 47–48, doi:10.1038/487047a.

233. Wang, Z.; Zhao, Y. Gut microbiota derived metabolites in cardiovascular health and disease. *Protein Cell* **2018**, *9*, 416–431, doi:10.1007/s13238-018-0549-0.

234. Tan, X.; Liu, Y.; Long, J.; Chen, S.; Liao, G.; Wu, S.; Li, C.; Wang, L.; Ling, W.; Zhu, H. Trimethylamine N-Oxide Aggravates Liver Steatosis through Modulation of Bile Acid Metabolism and Inhibition of Farnesoid X Receptor Signaling in Nonalcoholic Fatty Liver Disease. *Mol. Nutr. Food Res.* **2019**, *63*, 1–10, doi:10.1002/mnfr.201900257.

235. Wang, Z.; Tang, W.H.W.; Buffa, J.A.; Fu, X.; Britt, E.B.; Koeth, R.A.; Levison, B.S.; Fan, Y.; Wu, Y.; Hazen, S.L. Prognostic value of choline and betaine depends on intestinal microbiota-generated metabolite trimethylamine-N-oxide. *Eur. Heart J.* **2014**, *35*, 904–910, doi:10.1093/eurheartj/ehu002.

236. Lever, M.; George, P.M.; Slow, S.; Bellamy, D.; Young, J.M.; Ho, M.; McEntyre, C.J.; Elmslie, J.L.; Atkinson, W.; Molyneux, S.L.; et al. Betaine and trimethylamine-N-oxide as predictors of cardiovascular outcomes show different patterns in diabetes mellitus: An observational study. *PLoS One* **2014**, *9*, 1–19, doi:10.1371/journal.pone.0114969.

237. Kanehisa, M.; Goto, S. KEGG: kyoto encyclopedia of genes and genomes. *Nucleic Acids Res.* **2000**, *28*, 27–30, doi:10.1093/nar/28.1.27.

238. Chong, J.; Wishart, D.S.; Xia, J. Using MetaboAnalyst 4.0 for Comprehensive and Integrative Metabolomics Data Analysis. *Curr. Protoc. Bioinforma.* **2019**, *68*, e86, doi:10.1002/cpbi.86.

239. Roberts, J.A.; Varma, V.R.; Huang, C.-W.; An, Y.; Oommen, A.; Tanaka, T.; Ferrucci, L.; Elango, P.; Takebayashi, T.; Harada, S.; et al. Blood Metabolite Signature of Metabolic Syndrome Implicates Alterations in Amino Acid Metabolism: Findings from the Baltimore Longitudinal Study of Aging (BLSA) and the Tsuruoka Metabolomics Cohort Study (TMCS). *Int. J. Mol. Sci.* **2020**, *21*, E1249, doi:10.3390/ijms21041249.

240. Reddy, P.; Leong, J.; Jialal, I. Amino acid levels in nascent metabolic syndrome: A contributor to the pro-inflammatory burden. *J. Diabetes Complications* **2018**, *32*, 465–469, doi:10.1016/j.jdiacomp.2018.02.005.

241. Janeiro, M.H.; Ramírez, M.J.; Milagro, F.I.; Martínez, J.A.; Solas, M. Implication of trimethylamine n-oxide (TMAO) in disease: Potential biomarker or new therapeutic target. *Nutrients* 2018, *10*.

242. Rohrmann, S.; Linseisen, J.; Allenspach, M.; von Eckardstein, A.; Müller, D. Plasma Concentrations of Trimethylamine-N-oxide Are Directly Associated with Dairy Food Consumption and Low-Grade Inflammation in a German Adult Population. *J. Nutr.* **2016**, *146*, 283–289, doi:10.3945/jn.115.220103.

243. Oellgaard, J.; Winther, S.A.; Hansen, T.S.; Rossing, P.; von Scholten, B.J. Trimethylamine N-oxide (TMAO) as a New Potential Therapeutic Target for Insulin Resistance and Cancer. *Curr. Pharm. Des.* **2017**, *23*, doi:10.2174/1381612823666170622095324.

244. Bloomgarden, Z. Diabetes and branched-chain amino acids: What is the link? *J. Diabetes* 2018, *10*, 350–352.

245. Griffin, J.W.D.; Bradshaw, P.C. Amino Acid Catabolism in Alzheimer's Disease Brain: Friend or Foe? *Oxid. Med. Cell. Longev.* **2017**, *2017*, 5472792, doi:10.1155/2017/5472792.

246. Lin, Y.; Ma, C.; Liu, C.; Wang, Z.; Yang, J.; Liu, X.; Shen, Z.; Wu, R. NMR-based fecal metabolomics fingerprinting as predictors of earlier diagnosis in patients with colorectal cancer. *Oncotarget* **2016**, *7*, 29454–29464, doi:10.18632/oncotarget.8762.

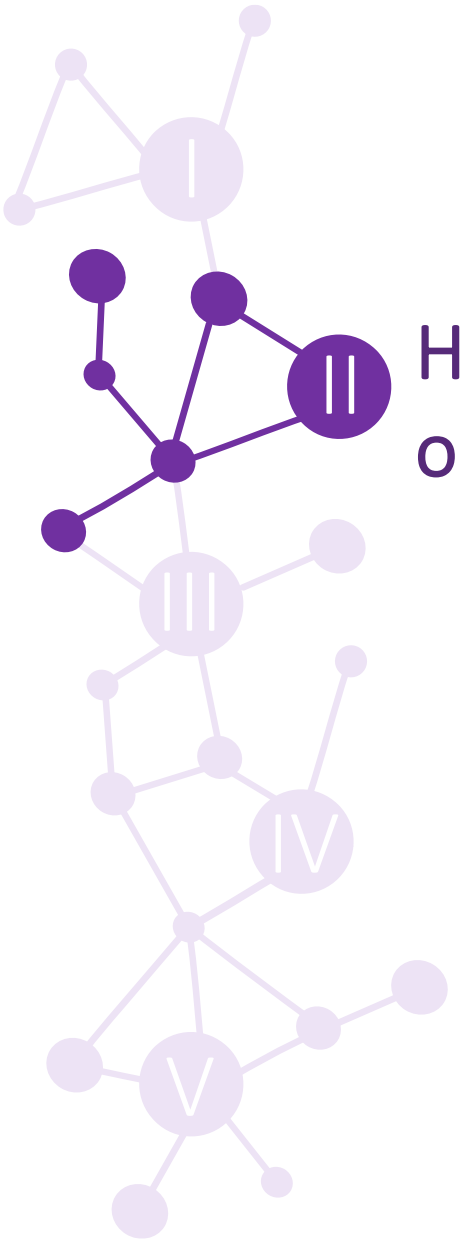

Hypothesis & objectives

UNIVERSITAT ROVIRA I VIRGILI
MULTI-OMICS BIOMARKERS OF METABOLIC HOMEOSTASIS OF RISK FACTORS ASSOCIATED TO NON-COMMUNICABLE DISEASES
Julia Hernandez Baixauli

II. Hypothesis & Objectives

Nowadays, common medical problems such as obesity, MetS, CVD diseases, cancer and neurodegenerative diseases, are considered multifactorial diseases and/or non-communicable (i.e., NCDs) [1]. This means that a cluster of risk factors associated with disrupted metabolism influence the development of NCDs [2]. A decade ago, Van Ommen *et al*., proposed that the onset of diseases arise from the imbalance of a few overarching processes, namely metabolic stress, inflammatory stress, oxidative stress and psychological stress [3]. These general processes can be subdivided into different risk factors. In fact, the accumulation and combination of the risk factors working together and extended over time, eventually lead to a pathologic state [1,4]. Monitoring these overarching processes opens the door to the possibility of modulating them, therefore preventing the onset of different NCDs by designing more precise personalized interventions or treatments. Nevertheless, current disease biomarkers cannot capture the early alterations in these overarching processes that might lead to the development of disease. Thus, the opportunity to provide biomarkers to prevent these diseases is presented as a medical challenge for the whole facultative and research community.

During the last decade, advances in high-throughput analytical platforms, mainly ^{1}H-NMR and MS coupled to different chromatographic techniques, either gas or liquid chromatography (GC-MS and LC-MS respectively), have provided advanced tools to study the human metabolome with an unprecedented detail. This has opened the window to a growing number of applications in biological and biomedical sciences. In the field of nutrition, metabolomics, together with other omics such as metagenomics, are proposed as an invaluable tool for providing nutritional recommendations based on the state of the metabolism at a stratified and a personalized level [5,6]. These new approaches have led to the definition of the so called precision nutrition, which has the final goal of providing nutritional recommendations based on specific traits of the individual metabolism [6]. To do so, a reliable strategy is to interrogate the metabolome of the person by omics such as metabolomics or proteomics in order to detect points of malfunction or altered homeostasis in order to restore them by means of nutritional interventions [7]. In fact, precision nutrition can target small deviations of the metabolism associated with the risk factors, before the onset of the disease. When the disease is finally developed, the problem escapes the field of nutrition and medical interventions are required. Therefore, there is a real need for an early detection of the slight changes on different metabolic parameters that combined triggers the development of disease. At present, the lack of robust health status biomarkers is a bottleneck that slows down the prevention based on metabolomics [8]. Thus, in parallel with the increasing knowledge on human metabolism, the use of these technologies allows to map elements of different metabolic pathways that are altered in human diseases.

The present work hypothesizes that each risk factor presents a characteristic metabolic signature that can be measured in standard conditions (i.e., in a basal fasted state) by means of omics technologies. To unravel this specific signature, the different overarching processes should be isolated to obtain pure biomarkers of each risk factor. Nevertheless, this is currently challenging since they appear concomitantly in humans. It is therefore proposed that preclinical models aimed to reproduce early alterations of the overarching processes separately might represent an opportunity to discover their metabolic signatures.

With this premises, the main objective of the present work is to identify a metabolomic signature that can be used to detect early alterations in different risk factors.

To achieve this main goal, the following specific objectives were set:

- **Selection, induction, and characterization of pre-clinical models of risk factors.** A state-of-the-art study was carried out to define which risk factors are characteristics of the overarching processes. These include the deregulation of carbohydrate and lipid metabolism, hypertension, and gut dysbiosis, as representative of metabolic stress; chronic inflammation; oxidative stress and psychological stress. From here, rodent models were considered to study each risk factor individually in a controlled way, thus the most suitable models were selected to simulate these factors. Once the rodent models were established, they were characterised to assess the reproducibility and the degree of isolation (biochemical, analytical, and molecular analyses). Thus, the selected risk factors and their induction and further characterization are listed below:

  - **Carbohydrate dysfunction.** This model was based on a single IP injection of STZ mimicking a diabetic state in male Wistar rats. To characterise this model, the analysis of glucose and insulin was performed to establish the degree of dysfunction.

  - **Hyperlipidaemia (manuscript 2).** This model was based on a single IP injection of P407 in male Wistar rats. To characterise this model, the analysis of the main lipids altered in hyperlipidaemia were carried out in plasma and liver (TC, TGs, NEFAs).

  - **Hypertension (manuscript 2).** SHR rodent animals, which at 16 weeks-old are spontaneously hypertensive, and their normotensive control (WKY) were used.

  - **Gut dysbiosis (manuscript 3)**. This model was carried out in two stages in male Wistar rats: (1) Obtention of microbes from donor rats that were fed with cafeteria diet and control diet; (2) Transplant microbiota from donor rats to recipient rats that have been previously treated with antibiotics for microbiota depletion. This model was characterized by the analysis of the microbiome.

- **Chronic inflammation (manuscript 4)**. Chronic inflammation was induced by the intermittent and increasing IP injection of LPS in male Wistar rats. To characterise this model, the main mediators of inflammation were measured as id the case of IL-6, MCP-1, TNF-α and PGE2.

- **Oxidative stress (manuscript 5).** Based on a single IP injection of PQ (15 and 30 mg/kg) in male Wistar rats. We measured the markers of lipid oxidative damage with evaluation of MDA and 8-isoprostanes. To know the antioxidant capacity of the subjects, SOD activity was measured.

- **Early psychological stress (manuscript 6).** A combination of protocols based on CUMS from the literature was used to induce the early psychological stress model. To evaluate the stress grade, behavioural and biochemical tests were performed: (1) behavioural test (OFT) was performed before the end of the study; (2) and after the study, serotonin and corticosterone were measured in plasma.

- **Characterization of the metabolic profile of the risk factors using omic approaches (manuscript 2-6)**. To accomplish this goal, cutting-edge omic tools were applied: (1) for plasma profiling, the abundance of almost 200 well-characterised metabolites were obtained from GC-MS and LC-MS approaches; (2) for urine profiling, ^{1}H-NMR was selected to detect general metabolite signals; (3) for microbiome analysis, 16S and shotgun sequencing was carried out. Thee above methodologies involve the generation of a large volume of data that requires the capacity of perform analysis at different levels.

- **Data integration and pathway analysis of the different risk to evaluate the metabolic profile (manuscript 2-6).** Data integration was performed to elucidate the metabolic profile and the subsequent biomarkers implicated in the development of NCDs.

II. Hipòtesis i Objectius

Actualment, els problemes mèdics més comuns com l'obesitat, la síndrome metabòlica, les CVDs, el càncer i les malalties neurodegeneratives es consideren malalties multifactorials i a més a més són no transmissibles [1]. Això significa que un grup de factors de risc associats amb el mal funcionament del metabolisme afavoreix el desenvolupament d'aquestes malalties [2]. Fa unes dècades, Van Ommen *et al.*, va proposar que l'aparició de malalties sorgeix del desequilibri d'uns processos generals, es a dir, l'estrès metabòlic, l'estrès inflamatori, l'estrès oxidatiu i l'estrès psicològic [3]. Aquests processos generals poden subdividir-se en diferents factors de risc. De fet, la combinació i l'acumulació al llarg del temps dels factors de risc condueixen a un estat patològic [1,4]. El seguiment d'aquests processos generals podria obrir la porta a la possibilitat de modular-los, evitant així l'inici de diferents malalties mitjançant el disseny d'intervencions o tractaments personalitzats més precisos. No obstant això, els biomarcadors de malalties actuals no són capaços de capturar les alteracions primerenques que podrien portar al desenvolupament de la malaltia. Per tant, l'oportunitat de proporcionar biomarcadors per prevenir aquestes malalties es presenta com un desafiament per a la comunitat científica.

Durant l'última dècada, els avenços en plataformes analítiques d'alt rendiment, principalment ^{1}H-NMR i MS acoblat a diferents cromatografies, com la cromatografia de gas i líquida (GC-MS i LC-MS respectivament), han proporcionat eines avançades per estudiar el metaboloma humà amb un detall sense precedents. Aquestes metodologies han obert la finestra a un nombre creixent d'aplicacions en ciències biològiques i biomèdiques. En el camp de la nutrició, la metabolòmica i la proteòmica juntament amb altres òmiques com la metagenòmica, es proposen com una eina inestimable per proporcionar recomanacions nutricionals basades en l'estat del metabolisme a un nivell estratificat i personalitzat [5,6]. Aquests nous enfocaments han donat lloc a la definició de l'anomenada nutrició de precisió, que té com a objectiu final proporcionar recomanacions nutricionals basades en trets específics del metabolisme individual [6]. Per fer-ho, una estratègia fiable és interrogar el metaboloma individual mitjançant òmiques, per tal de detectar alteracions en la homeòstasi i corregir-les mitjançant intervencions nutricionals [7]. De fet, la nutrició de precisió pot corregir petites desviacions del metabolisme associat amb els factors de risc, abans de l'aparició de la malaltia. Quan finalment es desenvolupa la malaltia, el problema escapa a l'àmbit de la nutrició i les intervencions farmacològiques són necessàries. Per tant, existeix una necessitat real d'una detecció precoç dels lleugers canvis en els diferents paràmetres metabòlics que combinats desencadenen el desenvolupament de les malalties no transmissibles. En l'actualitat, la manca de biomarcadors robustos és un coll d'ampolla que alenteix la prevenció basada en la metabolòmica [8]. Per tant, en paral·lel amb el creixent del coneixement sobre el metabolisme humà, l'ús d'aquestes tecnologies permet cartografiar elements de diferents vies metabòliques que s'alteren en malalties humanes.

La tesi actual planteja la hipòtesi de que cada factor de risc presenta una signatura metabòlica característica que es pot mesurar en condicions estàndard (és a dir, en un estat de dejuni basal) per mitjà de tecnologies òmiques. Per a desenvolupar aquesta signatura específica, en un marc ideal s'haurien d'aïllar els diferents factors de risc de l'individu per tal d'obtindre biomarcadors purs. De fet, aïllar els diferents factors de risc és un repte, ja que apareixen de manera concomitant en humans. Per tant, s'utilitzen models pre-clínics destinats a reproduir aquestes alteracions i obtindré un perfil metabòlic.

Amb aquestes premisses, l'objectiu principal d'aquest projecte és identificar una signatura metabolòmica per a detectar alteracions primerenques en diferents factors de risc.

Per aconseguir aquest objectiu principal, es van establir els següents objectius específics:

- **Selecció, inducció i caracterització de models pre-clínics de factors de risc.** Es va dur a terme un estudi de l'estat de l'art per definir quins factors de risc són característics dels processos generals. Aquests inclouen la desregulació del metabolisme dels carbohidrats i dels lípids, la hipertensió i la dysbiosis intestinal, com a representants de l'estrès metabòlic; inflamació crònica; l'estrès oxidatiu i l'estrès psicològic. A partir d'aquí, es va determinar quins models de rosegadors estudiaven cada factor de risc individualment d'una manera controlada, de manera que els models més adequats van ser seleccionats per estudiar aquests factors. Una vegada es van establir els models de rosegadors, es van caracteritzar per avaluar la seva reproductibilitat i el seu grau d'aïllament (bioquímica, analítica i anàlisi molecular). Així, els factors de risc seleccionats, la seva inducció i posterior caracterització s'enumeren a continuació:

  - **Disfunció de carbohidrats.** Aquest model es basa en una única administració IP de STZ imitant un estat diabètic en rates de Wistar mascles. Per caracteritzar aquest model, es va realitzar l'anàlisi de la glucosa i la insulina per establir el grau d'hiperglucèmia.

  - **Hiperlipèmia (manuscrit 2).** Aquest model es basa en una única administració IP de P407 en rates Wistar mascles. Per caracteritzar aquest model, l'anàlisi dels lípids principals alterats en la hiperlipèmia es va dur a terme en plasma i fetge (TC, TGs, NEFAs).

  - **Hipertensió (manuscrit 2).** S'utilitzaren les rates SHR, que amb 16 setmanes d'edat són hipertenses espontàniament, i el seu control nomo-tensiu (WKY).

  - **Dysbiosis intestinal (manuscrit 3).** Aquest model es va dur a terme en dues etapes en rates Wistar mascles: (1) obtenció de microbiota de rates donants que s'alimentaven amb dieta cafeteria i dieta control; (2) transplantament de microbiota de rates donants a rates receptores que

anteriorment havien estat tractades amb antibiòtics per a eliminar la microbiota de l'hoste. Aquest model es va caracteritzar per l'anàlisi del microbioma.

- **Inflamació crònica (manuscrit 4).** La inflamació crònica va ser induïda per l'administració intermitent i incrementada IP de LPS en rates Wistar mascles. Per caracteritzar aquest model, els principals mediadors de la inflamació es van mesurar com a cas de MCP-1, IL-6, TNF-2 i PGE_2.

- **Estrès oxidatiu (manuscrit 5).** Basat en una única IP de PQ (15 i 30 mg/kg) en rates Wistar mascles. Caracteritzat per marcadors oxidatius lipídics amb l'avaluació de MDA i 8-isoprostans. Per conèixer la capacitat antioxidant dels subjectes, quantifiquem l'activitat de SOD.

- **Estrès psicològic (manuscrit 6).** Es va utilitzar una combinació de protocols basats en el model CUMS de depressió per tal d'induir un model d'estrès psicològic. Per tal d'avaluar el grau d'estrès, es van utilitzar test de comportament i bioquímics: (1) la prova de comportament (OFT) es va realitzar abans del sacrifici de rates; (2) i al final del estudi, la serotonina i la corticosterona es van mesurar a plasma.

- **Caracterització del perfil metabòlic dels factors de risc utilitzant aproximacions òmiques (manuscrit 2-6).** Per aconseguir aquest objectiu, s'han utilitzat eines òmiques d'avantguarda: (1) per a l'elaboració de perfils de plasma, l'abundància de gairebé 200 metabòlits ben caracteritzats van ser obtinguts a partir d'aproximacions basades en GC-MS i LC-MS; (2) per a l'elaboració de perfils metabolòmics d'orina, es va utilitzar ^{1}H-NMR per detectar senyals generals de metabòlits; (3) per a l'anàlisi de microbis, la seqüenciació mitjançant 16S i shotgun es va utilitzar. Les metodologies anteriors impliquen la generació d'un gran volum de dades que requereixen la capacitat de realitzar anàlisi a diferents nivells.

- **Integració de les dades i anàlisi de les rutes metabòliques afectades als diferent factors de risc per avaluar el perfil metabòlic (manuscrit 2-6).** La integració de dades es va realitzar per dilucidar el perfil metabòlic i els possibles biomarcadors implicats en el desenvolupament i inici de les malalties no transmissibles.

References

1. Stolk, R.P.; Rosmalen, J.G.M.; Postma, D.S.; de Boer, R.A.; Navis, G.; Slaets, J.P.J.; Ormel, J.; Wolffenbuttel, B.H.R. Universal risk factors for multifactorial diseases. *Eur. J. Epidemiol.* **2008**, *23*, 67–74, doi:10.1007/s10654-007-9204-4.

2. Grundy, S.M. Metabolic syndrome update. *Trends Cardiovasc. Med.* **2016**, *26*, 364–373, doi:https://doi.org/10.1016/j.tcm.2015.10.004.

3. van Ommen, B.; Keijer, J.; Heil, S.G.; Kaput, J. Challenging homeostasis to define biomarkers for nutrition related health. *Mol. Nutr. Food Res.* **2009**, *53*, 795–804, doi:10.1002/mnfr.200800390.

4. Vassallo, P.; Driver, S.L.; Stone, N.J. Metabolic Syndrome: An Evolving Clinical Construct. *Prog. Cardiovasc. Dis.* **2016**, *59*, 172–177, doi:https://doi.org/10.1016/j.pcad.2016.07.012.

5. Ordovas, J.M.; Ferguson, L.R.; Tai, E.S.; Mathers, J.C. Personalised nutrition and health. *BMJ* **2018**, *361*, doi:10.1136/bmj.k2173.

6. Tebani, A.; Bekri, S. Paving the way to precision nutrition through metabolomics. *Front. Nutr.* **2019,** *6*.

7. Suárez, M.; Caimari, A.; del Bas, J.M.; Arola, L. Metabolomics: An emerging tool to evaluate the impact of nutritional and physiological challenges. *TrAC - Trends Anal. Chem.* **2017**, *96*, 79–88.

8. Picó, C.; Serra, F.; Rodríguez, A.M.; Keijer, J.; Palou, A. Biomarkers of nutrition and health: New tools for new approaches. *Nutrients* **2019**, *11*, 1–30, doi:10.3390/nu11051092.

UNIVERSITAT ROVIRA I VIRGILI
MULTI-OMICS BIOMARKERS OF METABOLIC HOMEOSTASIS OF RISK FACTORS ASSOCIATED TO NON-COMMUNICABLE DISEASES
Julia Hernandez Baixauli

MANUSCRIPT 2

METABOLOMIC PROFILING FOR THE CHARACTERIZATION OF HYPERLIPIDEMIA AND HYPERTENSION RISK FACTORS ACROSS SPECIES IN WISTAR RATS AND HEALTHY HUMAN POPULATION

Julia Hernandez-Baixauli [1], Nerea Abasolo [2], Hector Palacios-Jordan [2], Vicent J. Ribas Ripoll [3], Anna Pedret [4], Rosa M. Valls [4], Rosa Solà [4,5], Antoni Caimari [1], Laura Baselga-Escudero [1], Josep M. Del Bas [1,*], and Miquel Mulero [6,*]

[1] Eurecat, Centre Tecnològic de Catalunya, Unitat de Nutrició i Salut, 43204 Reus, Spain
[2] Eurecat, Centre Tecnològic de Catalunya, Centre for Omic Sciences (COS), Joint Unit Universitat Rovira i Virgili–EURECAT, 43204 Reus, Spain
[3] Eurecat, Centre Tecnològic de Catalunya, Digital Health Unit, 08005 Barcelona, Spain
[4] Functional Nutrition, Oxidation and Cardiovascular Diseases Group (NFOC-Salut), Facultat de Medicina iCiències de la Salut, Universitat Rovira i Virgili, C/Sant Llorenç, 21, 43201 Reus, Spain
[5] Internal Medicine Service, Hospital Universitari Sant Joan de Reus, Av/del Doctor Josep Laporte, 2,43204 Reus, Spain
[6] Nutrigenomics Research Group, Department of Biochemistry and Biotechnology, Universitat Rovira i Virgili, 43007 Tarragona, Spain

* Correspondence: josep.delbas@eurecat.org; miquel.mulero@urv.cat

Pending submission to Molecular Nutrition & Food Research

UNIVERSITAT ROVIRA I VIRGILI
MULTI-OMICS BIOMARKERS OF METABOLIC HOMEOSTASIS OF RISK FACTORS ASSOCIATED TO NON-COMMUNICABLE DISEASES
Julia Hernandez Baixauli

Abstract: Currently, hyperlipidemia and hypertension are coexisting risk factors, for a diverse type of non-communicable diseases (NCD), that have been emerged as an important health problem worldwide. In this sense, the actual clinical standards to detect hyperlipidemia and hypertension lack the required sensitivity in early/prodromal stages, thus a pressing need to shift the focus to detect accurately the onset of these risks have been increasing. Therefore, the aim of this study was to identify a metabolic pattern in the prodromal stage of hyperlipidemia and hypertension across species in preclinical and clinical studies. The preclinical studies were composed by the hyperlipidemia rat model, which was induced by a single intraperitoneal injection of 150 mg/kg of poloxamer 407 (P407) in male Wistar rats, and the hypertension rat model, which was based in the spontaneous hypertensive rats (SHR) and its normotensive control (WKY). In the clinical study, 140 healthy subjects were divided into normal and moderate group according to their risk to suffer hyperlipidemia and hypertension. Metabolomic approach on plasma (UHPLC-qTOF) and urine (1H-NMR) were performed to explore the metabolome and find early key biomarkers. On the one hand, 11 metabolites were identified as potential biomarkers of hyperlipidemia in the preclinical model. Translating those results to the clinic, 5 metabolites were considered potential biomarkers for men (i.e., DG 34:2, TG 46:0, ChoE (17:0), PC 36:4 and PC 38:4) and 4 for woman (i.e., DG 34:2, DG 34:3, ChoE (17:0), ChoE (18:0)). On the other hand, 52 metabolites were identified as potential biomarkers of hypertension in the preclinical model. In the clinical study, 7 metabolites were considered potential biomarkers for moderate hypertension for men [i.e., SM 34:1, SM 34:2, SM 40:1, SM 41:1, LPC 16:0 e, ChoE (22:6) and 3-hydroxybutiric acid] and 6 for woman (i.e., SM 32:1, SM 33:1, SM 38:1, SM 40:1, SM 41:1 and LPC 16:0 e). The identified potential biomarkers were lipid metabolites in hyperlipidemia and hypertension, mainly involved in lipid signalling pathway. These findings provide further insights into the prodromal stage and, consequently potential biomarkers in early hyperlipidemia and hypertension using metabolomic approaches.

Keywords: hyperlipidaemia, hypertension, metabolomics, biomarker, metabolic profiling, metabolic pathway.

1. Introduction

Hyperlipidaemia and hypertension are a well-established risk factors for the development of non-communicable diseases (NCDs), which are considered multifactorial diseases, thus the accumulation during long periods of these risk factors drive to complex diseases, as cardiovascular diseases (CVD), diabetes and metabolic syndrome (MetS), among others. For instance, the European Society of Cardiology reports in their guidelines of management of dyslipidaemias [1] and hypertension [2] that the prevention targeting these risk factors could elude further CVD, avoiding billions of dead's worldwide. In fact, epidemiological studies have reported a 15-31% rate of coexistence of hyperlipidaemia and hypertension [3,4]. In this line, the coexistence of these risk factors has been suggested to multiplicate the development of diseases compared with the sum of the individual risk factors [5].

In this context, the metabolic impact of hyperlipidaemia and hypertension and their early detection has not been completely elucidated. There is an interest to prevent the development of hyperlipidaemia and hypertension exploring new early biomarkers to characterise the prodromal stage of this health problem. Currently, prodromal stage has only been related to fully developed diseases, such as CVD, but has not considered within early stages of risk factors. The prodromal phase connotes a time interval between the early symptoms and signs that differ from those of acute clinical phase [6]. Essentially, monitoring circulating lipids for hyperlipidaemia and blood pressure for hypertension provides an invaluable tool for the tracking of these risk factors [1,2]. Unfortunately, these current clinical biomarkers lack the required sensibility to evaluate the degree of the risk factors [7].

In the case of hyperlipidaemia, different approaches have been carried out to obtain isolated animal models trying to elucidate its metabolic impact without a scientific consensus: some of them are genetic variants as Zucker rats [8], induced by high fat diet [9,10] or treated by chemical compounds as poloxamer 407 (P407) [11]. For instance, P407 is one of the most interesting models of hyperlipidaemia inducing hypertriglyceridemia and hypercholesterolemia that acts through the inhibition of the heparin-releasable fraction of lipoprotein lipase (LPL) and the cholesterol 7α-hydroxylase (CYP7A1), respectively [11]. The P407 animal model has been extensively selected by different researchers to study lipidemic alterations presenting different characteristics: different rodent species [11–15], concentrations between 300 mg/Kg [14] to 1500 mg/kg of body weight [16], being the lowest the popular one; and single dose [17] or chronic dose [13] of an intraperitoneal (IP) injection have been also selected according to the expected effect [18].

In the case of hypertension, the complex nature of hypertensive phenotypes complicates the establishment of an animal model for the study of metabolism. For this reason, rat genetic models of hypertension have been widely used in the study of high blood pressure levels (e.g., spontaneously hypertensive rats (SHR), Dahl salt-

sensitive (DSS) rats) [19,20]. Of these, the most studied model is the SHR with more than 4,600 articles indexed in PubMed under the term spontaneously hypertensive rats in the past 10 years. The SHR model is widely used in different studies as a rat model of primary or essential hypertension [20].

In this context, metabolomics have been increasing as a powerful tool for the prognosis, and diagnosis, of early stages, by investigating the endogenous levels of small metabolites in clinical practice from different biofluids (i.e., plasma/serum and urine) [21,22]. In this context, omics-based strategies allowed us to provide a global characterization of the changes in the metabolic profile associated with hyperlipidaemia and hypertension prodromal stage, being a possible solution to the lack of sensitivity of classical clinical biomarkers in prodromal stages [23]. Numerous metabolomic studies have been focus on hyperlipidaemia and hypertension in animal models and profiling human samples [24–26]. However, none of these metabolomic studies have focused on the prodromal stage of these risk factors in animals and the posterior translation to healthy human subjects to evaluate their risk.

Therefore, we performed two murine models of hyperlipidaemia and hypertension to profile their metabolome in plasma and urine, trying to elucidate the metabolic profile and potential biomarkers of early stages. Once the metabolic profile was stabilised in rats, the plasma metabolome of a cohort of 140 healthy humans was studied to compare the metabolic profile of the risk factors. Novel potential biomarkers and metabolic pathways of hyperlipidaemia and hypertension were stand out that could underlie the pathological foundation and the metabolic profile of early stages. Furthermore, similarities and differences of the metabolic profiles are highlighted to understand their relationships and mutual interactions.

2. Methods

2.1. Hyperlipidaemic and hypertensive rat models

Animals were housed individually under a fully controlled condition including temperature (22 ± 2°C), humidity (55± 5%) and light (12 h-light-dark cycle and lights on at 9:00 a.m.). All rats were fed with a standard rat chow diet *ad libitum* (Teklad Global 18% Protein Rodent Diet 2014, Harlan, Barcelona, Spain). The Animal Ethics Committee of the University Rovira i Virgili (URV,Tarragona, Spain) approved all the procedures for the hyperlipidaemic model (code 10025) and the hypertensive model (code 10522). The experimental protocol followed the “Principles of Laboratory Care” and was carried out in accordance with the European Communities Council Directive (86/609/EEC).

The hyperlipidaemic rat model consists of twenty 8-week-old male Wistar rats (Harlan Laboratories, Barcelona, Spain). After a 1-week acclimation period, the animals were weighted and randomly divided into two experimental groups (n = 10):

control group (CON) or P407-induced hyperlipidaemic group. The P407 group received a single IP injection of a 150 mg dose of P407 (Fluka/Sigma-Aldrich, Madrid, Spain) per kg body weight in a sterile solution of cold NaCl at 0.9%. The CON group received a single IP injection with the same volume of vehicle (sterile cold 0.9% NaCl). Body weight was recorded at the day of IP injection and at the end of the study. Food intake was estimated once, the weight of chow was recorded before the IP injection and 24 h after.

The hypertensive rat model consists into two experimental groups (n = 8): 20-week-old male spontaneously hypertensive (SHR) rats and their control consisting of 20-week-old male Wistar Kyoto (WKY) rats (Janvier Labs, Saint-Berthevin, France). The blood pressure of SHR rats increase at 6-7 weeks of age and reach a stable level of hypertension by 17-19 weeks of age [19]. The rats arrive at the age of 15 weeks and the samples were collected at the age of 20 weeks. Body weight was recorded to monitor the state of the animals and food intake was estimated before the sacrifice.

2.2. Sample collection

Urine samples were collected the day before the end of the study with the hydrophobic sand method, which is less stressful for the animals [27]. For each rat, 300 g of hydrophobic sand was spread (LabSand, Coastline Global, Palo Alto, CA) on the bottom of a mouse plastic micro-isolation cage. Urine was collected with sodium azide (Sigma, St Louis, MO, USA) as preservative every half hour for 6 hours and was pooled at the end of the session. On the day of the sacrifice, animals were euthanized by guillotine under anaesthesia (pentobarbital sodium, 50 mg/kg per body weight) after 7 hours of fasting. Blood was collected and centrifuged at 3,000 g at 4 °C for 15 min to recover plasma. Tissues were rapidly removed, weighted and snap-frozen in liquid nitrogen (i.e., RWAT, MWAT, muscle, liver, and cecum). All the samples were stored at -80°C until further analysis.

2.3. Plasma and liver measurements

Enzymatic colorimetric kits were used for the plasma determination of TC, TG, glucose (QCA, Barcelona, Spain), non-esterified free fatty acids (NEFAs) (WAKO, Neuss, Germany) and LPL enzymatic activity (Roar Biomedical, New York, USA). Circulating insulin levels were measured using rat ELISA kits (Merck, Madrid, Spain). Monocyte chemoattractant protein-1 (MCP-1), as an inflammatory biomarker, was measured by the Rat MCP-1 Instant ELISA Kit (Invitrogen, Vienna, Austria). The oxidative stress was evaluated by the determination of aspartate aminotransferase (AST) and alanine aminotransferase (ALT) activity in plasma (Sigma-Aldrich, St. Louis, USA) and 8-isoprostane in urine (Cayman chemical, Ann Arbor, MI, USA).

Liver lipids were extracted and quantified from a tissue piece of approximately 100 mg from the frozen liver following a method previously described in the literature [28]. Briefly, lipids were extracted with 1 ml of hexane/isopropanol (3:2, v/v),

degassed with gas nitrogen before left overnight under orbital agitation at room temperature protected from light. After an extraction with 0.3 ml of Na2SO4 (0.47 M), the lipid phase was dried with nitrogen gas and total lipids quantified gravimetrically before emulsifying as described previously [29]. TG, TC and phospholipids were assayed with commercial enzymatic kits (QCA, Barcelona, Spain).

2.4. Study population

The volunteer's data was provided by the biobank of the URV from arbitrary subjects (*n* = 140) that were men and women from 43 to 65 years. At the time of sampling, all subjects were defined as healthy with no diagnosis of any significant disease. On the one hand , the subjects were divided according to their TG levels in normal and moderate group following the guidelines for the management of dyslipidaemia [1]: (1) normal: less than 150 mg/dL, or less than 1.7 mmol/L; (2) moderate risk of hyperlipidaemia: above 150 mg/dL or above 1.7 mmol/L. On the other hand, the blood pressure was categorized based on systolic blood pressure (SBP) and diastolic blood pressure (DBP) following the guidelines for the management of hypertension [2]: (1) normal blood pressure: SBP < 129 mmHg and DBP < 84 mmHg; (2) moderate blood pressure/risk of hypertension: SBP 130 to 159 mmHg and DBP 85 to 99 mmHg. The plasma samples were profiled using classical determinations and metabolomics.

2.5. Plasma metabolomics

Plasma metabolites were analysed by gas Chromatography coupled with Quadrupole Time-of-Flight (GC-qTOF). For the extraction, a protein precipitation extraction was performed by adding eight volumes of methanol:water (8:2, v/v) containing internal standard mixture (succinic acid-d4, myristic acid-d27, glicerol-13C3 and D-glucose-13C6) to plasma samples. Then, the samples were mixed and incubated at 4 °C for 10 min, centrifuged at 21.420 g and supernatant was evaporated to dryness before compound derivatization (metoximation and silylation). The derivatized compounds were analysed by GC-qTOF (model 7200 of Agilent, USA). The chromatographic separation was based on the Fiehn Method, using a J&W Scientific HP5-MS (30 m x 0.25 mm i.d.), 0.25 µm film capillary column and helium as carrier gas using an oven program from 60ºC to 325ºC. Ionization was done by electronic impact (EI), with electron energy of 70eV and operated in full Scan mode. The identification of metabolites was performed by matching their EI mass spectrum and retention time to metabolomic Fiehn library (Agilent, Santa Clara, CA, USA) which contains more than 1.400 metabolites. After putative identification of metabolites, these were semi-quantified in terms of internal standard response ratio.

Plasma lipids were analysed by Ultra High Perfomance Liquid Chromatography coupled with Quadrupole Time-of-Flight (UHPLC-qTOF). For the extraction of the hydrophobic lipids, a liquid-liquid extraction based on the Folch procedure was performed by adding four volumes of chloroform:methanol (2:1, *v*/*v*) containing

internal standard mixture (Lipidomic SPLASH®, Avanti Polar Lipids, Inc., Alabaster, AL, USA) to plasma. Then, the samples were mixed and incubated at -20 °C for 30 min. Afterwards, water with NaCl (0.8 %) was added and the mixture was centrifuged at 21.420 g. Lower phase was recovered, evaporated to dryness and reconstituted with methanol:methyl-tert-butyl ether (9:1, v/v) and analyzed by UHPLC-qTOF (model 6550 of Agilent, USA) in positive electrospray ionization mode. The chromatographic consists in an elution with a ternary mobile phase containing water, methanol, and 2-propanol with 10 mM ammonium formate and 0.1% formic acid. The stationary phase was a C18 column (Kinetex EVO C18 Column, 2.6 µm, 2.1 mm X 100 mm) that allows the sequential elution of the more hydrophobic lipids such as TG, diacylglycerols (DGs), phosphatidylcholines (PCs), cholesterol esters (ChoEs), lysophospholipids (LPCs) and sphingomyelins (SMs), among others. The identification of lipid species was performed by matching their accurate mass and tandem mass spectrum, when available, to Metlin-PCDL from Agilent containing more than 40,000 metabolites and lipids. In addition, chromatographic behaviour of pure standards for each family and bibliographic information was used to ensure their putative identification. After putative identification of lipids, these were semi quantified in terms of internal standard response ratio using one internal standard for each lipid family.

A pooled matrix of samples was generated by taking a small volume of each experimental sample to serve as a technical replicate throughout the data set. As the study took multiple days, a data normalization step was performed to correct variation resulting from instrument inter-day tuning differences. Essentially, each compound was corrected in run-day blocks through quality controls, normalizing each data point proportionately

2.6. Urine metabolomics

Urine metabolites were analysed by proton Nuclear Magnetic Resonance (^{1}H-NMR). The urine sample was mixed (1:1, *v*/*v*) with phosphate buffered saline containing with 3-(Trimethylsilyl)propionic-2,2,3,3-d4 acid sodium salt (TSP) (Sigma Aldrich) and placed on a 5 nm NMR tube for direct analysis by ^{1}H-NMR. ^{1}H-NMR spectra were recorded at 300 K on an Avance III 600 spectrometer (Bruker®, Bremen, Germany) operating at a proton frequency of 600.20 MHz using a 5 mm PBBO gradient probe. Diluted urine aqueous samples were measured and recorded in procno 11 using a One-dimensional ^{1}H pulse experiments were carried out using the nuclear Overhauser effect spectroscopy (NOESY). NOESY presaturation sequence (RD–90°–t1–90°–tm–90° ACQ) to suppress the residual water peak, and the mixing time was set at 100 ms. Solvent presaturation with irradiation power of 150 µW was applied during recycling delay (RD = 5 s) and mixing time. (noesypr1d pulse program in Bruker®, Bremen, Germany) to eliminate the residual water. The 90° pulse length was calibrated for each sample and varied from 11.21 to 11.38 ms. The spectral width was 9.6 kHz (16 ppm), and a total of 128 transients were collected into 64 k data points for each ^{1}H spectrum. The exponential line broadening applied before Fourier

transformation was of 0.3 Hz. The frequency domain spectra were manually phased and baseline-corrected using TopSpin software (version 3.2, Bruker, Bremen, Germany). Data has been normalized by two different ways, by probabilistic to avoid differences between sample due to different urine concentration, and by ERETIC. The acquired ^{1}H-NMR were compared to references of pure compounds from the metabolic profiling AMIX spectra database (Bruker®, Bremen, Germany), HMDB, and Chenomx databases for metabolite identification. In addition, we assigned metabolites by ^{1}H-^{1}H homonuclear correlation (COSY and TOCSY) and ^{1}H-^{13}C heteronuclear (HSQC) 2D NMR experiments and by correlation with pure compounds run in-house. After pre-processing, specific ^{1}H-NMR regions identified in the spectra were integrated using MATLAB scripts run in house. Curated identified regions across the spectra were exported to excel spreadsheet to evaluate robustness of the different ^{1}H-NMR signals and to give relative concentrations.

2.7. Statistical analysis

Statistical analysis was performed using the R software (version 4.0.1, R Core Team 2021) and different libraries, included in Bioconductor (version 3.11, Bioconductor project), were used. All data was expressed as the mean ± standard error of the mean (SEM). For the animal model, after the normality study, parametric unpaired t-test was used for single statistical comparisons, thus a two-tailed value of $p < 0.05$ was considered. For metabolomic data, the Mann-Whitney (MW) test was performed in this case because the variables follow the assumption of a non-parametric. The *p*-value adjustment for multiple comparisons was carried out according to the Benjamin-Hochberg (BH) correction considering a 5% of false discovery rate (FDR). The magnitude of difference between populations are presented as fold change (FC) relative to the control groups [30]. Multivariate analysis, both an unsupervised method (Principal Component Analysis, PCA) and a supervised method (Orthogonal Partial Least-Squares Discriminant Analysis, OPLS-DA) were employed to reveal the global metabolic changes between groups using the ropls R package (version 1.19.16) [31]. The predictive performance of the test set was estimated by the Q2Y parameter calculated through cross-validation. The values of $Q2 < 0$ suggests a model with no predictive ability, $0 < Q2 < 0.5$ suggests some predictive character and $Q2 > 0.5$ indicates good predictive ability [32]. The corresponding Variable Importance in the Projection (VIP) value was calculated to select the metabolites responsible of the difference between groups. Using the criteria of FDR < 0.05 and VIP > 1, metabolites were ultimately selected as biomarkers of hyperlipaemia and hypertension in the animal model. After the selection of the potential biomarkers in rats, those metabolites were studied in human subjects performing one-way ANOVA test to evaluate the effect of sex and the Tukey's test for post-hoc analysis. The resulting significant differential features were analysed through different data bases to identify related pathways and elucidate the global effect in the metabolism of the study. The main data bases consulted are listed below: Kyoto Encyclopaedia of Genes

and Genomes (KEGG) [33], Rat Genome Database (RGD) [34], Human Metabolome Database (HMDB) [35] and Small Molecule Pathway Database (SMPDB) [36].

3. Results

3.1. Characterization of the hyperlipidemic rat model

Biometric measurements, plasma parameters and liver biochemistry were determined to confirm the success of the P407-induced hyperlipidaemic rat model (Table 1). Food intake was higher in the P407 group, although no differences were observed in body weight. In addition, P407 group showed a tendency to increase muscle and liver weight (Table 1). The hypertriglyceridemia and hypercholesterolemia were confirmed by the significant increase of TG and TC in plasma, additionally increased liver TC was confirmed in the P407 group without noticing other significant changes in liver (i.e., total lipids, TC, and phospholipids). As it is described before, according to the TG increase in plasma, the LPL activity was decreased significantly in the P407 group. Different parameters related to carbohydrate dysfunction were also analysed to discard other related metabolic alterations; no significant differences were found in glucose, non-esterified fatty acids (NEFAs) and insulin resistance parameters [i.e., Homeostatic Model Assessment Insulin Resistance (HOMA-IR), Homeostatic Model Assessment β-cells (HOMA-β) and Revised - Quantitative Insulin Sensitivity Check Index (R-QUICKI)]. Additionally, the inflammation level and the oxidative stress was evaluated presenting an increase of MCP-1 in the P407 group, and no significant differences were found in AST, ALT and 8-isoprostane.

Table 1. Characteristics of the P407-induced hyperlipidaemic rat model. The results are presented as the mean ± SEM (n = 10). The statistical comparisons among groups were conducted using Student's t test. * Denotes $p < 0.1$ (tendency), ** $p < 0.05$ (significantly different) and *** $p < 0.01$ (high significantly different) compared with control. Abbreviations: RWAT, retroperitoneal white adipose tissue; MWAT, mesenteric white adipose tissue; TG, triglycerides; TC, total cholesterol; NEFAs, non-esterified fatty acids; HOMA-IR, Homeostatic Model Assessment Insulin Resistance; HOMA-β, Homeostatic Model Assessment β-cells: R-QUICKI, Revised - Quantitative Insulin Sensitivity Check Index; au, arbitrary units; LPL activity, lipoprotein lipase activity (Δ nmol/ 0.2 mL per 15 min); MCP-1, monocyte chemoattractant protein-1; AST, aspartate aminotransferase (one unit of AST is the amount of enzyme that will generate 1.0 µmole of glutamate per minute at pH 8.0 at 37 °C); ALT, alanine aminotransferase (one milliunit of ALT is defined as the amount of enzyme that generates 1.0 nmole of pyruvate per minute at 37 °C).

		CON	P407	*p*-value
Biometric parameters	Initial body weight (g)	300.28 ± 4.09	300.33 ± 3.06	0,99
	Final body weight (g)	302.09 ± 3.85	304.57 ± 3.28	0,63
	Food intake (g)	18.49 ± 0.70	20.49 ± 0.48	0.03**
	RWAT weight (g)	3.52 ± 0.34	3.59 ± 0.27	0,87
	MWAT weight (g)	2.58 ± 0.21	2.54 ± 0.17	0,89
	Muscle weight (g)	1.78 ± 0.03	1.86 ± 0.04	0.09*
	Liver weight (g)	9.28 ± 0.54	10.38 ± 0.25	0.09*

	Cecum weight (g)	4.35 ± 0.18	4.15 ± 0.19	0,44
Plasma parameters	Glucose (mM)	132.45 ± 2.22	130.21 ± 4.73	0,68
	TG (mM)	92.84 ± 9.71	157.11 ± 18.26	0.01***
	TC (mM)	73.02 ± 2.58	81.10 ± 2.74	0.04**
	NEFAs (mM)	0.48 ± 0.04	0.50 ± 0.05	0,67
	Insulin (µg/L)	1.04 ± 0.18	0.91 ± 0.11	0,54
	HOMA-IR (au)	0.34 ± 0.06	0.30 ± 0.04	0,5
	HOMA-β (au)	5.34 ± 0.89	4.95 ± 0.64	0,75
	R-QUICKI (au)	0.59 ± 0.03	0.60 ± 0.04	0,89
	LPL activity (Δ)	1.64 ± 0.02	1.57 ± 0.02	0.03**
	MCP-1 (ng/mL)	9.78 ± 0.83	11.40 ± 0.44	0.10*
	AST (mU/mL)	1.25 ± 0.62	1.35 ± 0.67	0.29
	ALT (mU/mL)	2.57 ± 0.16	2.67 ± 0.17	0.82
Urine parameters	8-isoprostanes (ng/mL)	2.5 ± 0.78	2.66 ± 0.44	0.87
Liver biochemistry	Total lipids (mg/g)	41.48 ± 2.01	43.27 ± 3.18	0,64
	TC (mg/g)	1.31 ± 0.07	1.48 ± 0.13	0,3
	Phospholipids (mg/g)	11.56 ± 0.48	11.97 ± 0.78	0,66
	TG (mg/g)	3.70 ± 0.18	4.77 ± 0.43	0.04**

3.2. Characterization of the hypertension rat model

The SHR rats differed from their control in terms of increased body weight, food intake and tissue weight (Table 2). In this line, SHR group had increase TC levels without showng other significant changes in plasma TG and liver-specific lipids (i.e., TC, and phospholipids). Additionally, different parameters related to other related metabolic alterations were analysed: no significant differences were found in glucose and non-esterified fatty acids (NEFAs); while significant differences were found in insulin levels and insulin resistance parameters (i.e., HOMA-IR, HOMA-β and R-QUICKI). Moreover, no significant differences were observed in MCP-1, a biomarker of inflammation, although significant differences were observed in 8-isoprostane, a biomarker of oxidative stress.

Table 2. Characteristics of the SHR/WKY hypertension rat model. The results are presented as the mean ± SEM (n = 10). The statistical comparisons among groups were conducted using Student's t test. * Denotes $p < 0.1$ (tendency), ** $p < 0.05$ (significantly different) and *** $p < 0.01$ (high significantly different). Abbreviations: RWAT, retroperitoneal white adipose tissue; MWAT, mesenteric white adipose tissue; TG, triglycerides; TC, total cholesterol; NEFAs, non-esterified fatty acids; HOMA-IR, Homeostatic Model Assessment Insulin Resistance; HOMA-β, Homeostatic Model Assessment β-cells: R-QUICKI, Revised - Quantitative Insulin Sensitivity Check Index; AU, arbitrary units; LPL activity, lipoprotein lipase activity (Δ nmol/ 0.2 mL per 15 min); MCP-1, monocyte chemoattractant protein-1; AST, aspartate aminotransferase (one unit of AST is the amount of enzyme that will generate 1.0 µmole of glutamate per minute at pH 8.0 at 37 °C); ALT, alanine aminotransferase (one milliunit of ALT is defined as the amount of enzyme that generates 1.0 nmole of pyruvate per minute at 37 °C).

		WKY	SHR	*p*-value
Biometric parameters	Initial body weight 15w (g)	293.35 ± 3,42	307.77 ± 1.89	0.004***
	Final body weight 20w (g)	368.32 ± 4.62	405.69 ± 5.40	0.001***
	Food intake (g)	18.56 ± 0.74	21.56 ± 0.42	0.005***
	RWAT weight (g)	4.28 ± 0.32	6.71 ± 0.33	0.001***
	MWAT weight (g)	3.35 ± 0.26	4.18 ± 0.13	0.01**
	Muscle weight (g)	2.01 ± 0.13	2.41 ± 0.07	0.01**
	Liver weight (g)	10.38 ± 0.18	12.19 ± 0.38	0.01**
	Cecum weight (g)	3.56 ± 0.28	4.98 ± 0.41	0.01**
Plasma parameters	Glucose (mM)	103.40 ± 7.33	114.86 ± 2.27	0,16
	TG (mM)	106.27 ± 9.82	98.49 ± 3.65	0,47
	TC (mM)	76 ± 3.54	116.12 ± 3.05	0.001***
	NEFAs (mM)	0.59 ± 0.04	0.52 ± 0.04	0,22
	Insulin (µg/L)	1.62 ± 0.25	2.65 ± 0.18	0,01**
	HOMA-IR (AU)	0.42 ± 0.07	0.75 ± 0.05	0.004***
	HOMA-β (AU)	11.33 ± 1.45	18.79 ± 1.61	0.006***
	R-QUICKI (AU)	0.55 ± 0.03	0.45 ± 0.01	0.02**
	MCP-1 (ng/mL)	6.26 ± 0.48	7.37 ± 0.80	0.26
	AST (mU/mL)	2.57 ± 0.16	2.63 ± 0.17	0.82
	ALT (mU/mL)	3.11 ± 0.09	3.33 ± 0.12	0.15
Urine parameters	8-isoprostanes (ng/ml)	0.58 ± 0.18	2.15 ± 0.30	0.002***
Liver biochemistry	Total lipids (mg/g)	32.08 ± 0.69	38.07 ± 2.60	0.06*
	TC (mg/g)	1.99 ± 0.08	2.29 ± 0.21	0.22
	Phospholipids (mg/g)	10.72 ± 0.40	11.86 ± 0.79	0.22
	TG (mg/g)	7.06 ± 0.34	7.69 ± 0.70	0.44

3.3. Metabolomic profiling and biomarker identification of the hyperlipidemic rat model

The metabolome of the hyperlipidemic rat model consisted of 130 metabolites from plasma and 43 from urine. A preliminary univariate analysis was performed on the plasma (Table S1) and urine data set (Table S2) to obtain a preliminary list of altered metabolites prior to multivariate analysis. Focusing on plasma, 44 out 130 metabolites were significantly altered between groups after MW test. After the BH correction, 11 specific lipids prevailed among the 44 metabolites, including DGs, TGs, ChoEs, PCs and LPCs, which were mainly overrepresented in the P407 group. On the other hand, 4 out 43 metabolites were significantly different between groups in urine after the MW test (i.e., trimethylamine N-oxide (TMAO), phenylacetylglycine (PAG), 2-

deoxycytidine and leucine). Although, after BH correction none of these metabolites remain altered, the changes in magnitude were distinctive.

Unsupervised analysis (PCA) was performed to find intrinsic variation in the plasma (Figure S1) and urine datasets (Figure S2). The P407 and CON groups were not separated in either plasma or urine in the PCA. In plasma, the OPLS-DA model was able to differentiate between the two groups (Figure 1a). The fitness and prediction accuracy of the plasma model were established by the values of $R2X(_{cum})$ = 0.377, $R2Y(_{cum})$ = 0.862, and $Q2Y(_{cum})$ = 0.567. Since the Q2Y value (0.567) was greater than the pQ2 value (0.01) and 0.5, we can conclude that the OPLS-DA model has a good predictive capacity (Figure 1b). These results indicate that it is possible to predict if an animal has a hyperlipidaemic profile, based on the analysis of plasma lipidomics and metabolomics. Specifically, it was found 39 significantly altered plasma features with a VIP threshold of 1 (Table 2). Specifically, the main altered lipid metabolites were PC 36:4 and PC 38:4 (VIP > 2 and *q*-value < 0.01 in univariate analysis) (Table 2). In urine, although both groups were partially separated in the OPLS-DA analysis (Figure 1c), the low value of Q2Y (-0.029) and the higher value of pQ2 in the permutation test (Figure 1d) suggest that this model is overfitted.

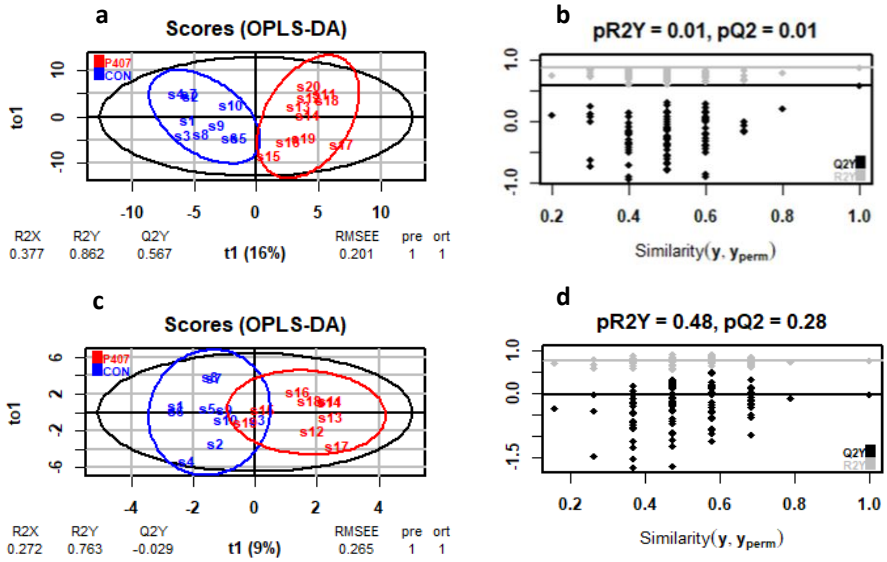

Figure 1. OPLS-DA of plasma and urine metabolomics of the P407-induced hyperlipidaemic rat model. Blue represents CON group and red P407 group. Plasma (**a**) and urine (**c**) X-score plot (OPLS-DA). The number of components and the cumulative R2X, R2Y and Q2Y are indicated below the plot. Plasma (**b**) and urine (**d**) significance diagnostic: The R2Y and Q2Y of the model are compared with the corresponding values obtained after random permutation of the y response.

Given the above, 11 plasma metabolites pointed out the metabolic profile of hyperlipidaemic subjects in plasma, which are TG 46:0, PC 38:4, PC 36:4, LPC 18:0, DG 36:4, DG 34:3, DG 34:2, ChoE (18:1), ChoE (18:0) and ChoE (17:0) and ChoE (16:0) (Table 2). Additionally, urine metabolites were not considered because the analysis were not enough robust.

Table 3. Summary of the potential biomarkers in the P407-induced hyperlipidaemic rat model in plasma. The results are presented as the mean ± SEM per group (n = 10); summary of univariant analysis include p-value, q-value (pFDR) and FC (P407/CON); VIP values of OPLS-DA (multivariant analysis); and metabolism pathway (KEGG). Metabolites are listed by q-value. * Denotes $p < 0.05$ (significantly different) and ** $p < 0.01$ (high significantly different). Abbreviations: TG, triglyceride; PC, phosphatidylcholine; LPC, lysophospholipid; DG, diacylglycerol; ChoE, cholesterol ester.

Metabolite	CON	P407	p-value	q-value	FC	VIP	Pathway
DG 36:4	1.53 ± 0.05	2.02 ± 0.03	<0.01**	<0.01**	1.33	1.81	Glycerolipid metabolism
PC 38:4	14.02 ± 0.61	20.4 ± 0.88	<0.01**	<0.01**	1.46	2.05	Glycerophospholipid metabolism
DG 34:3	0.2 ± 0.01	0.31 ± 0.02	<0.01**	0.01*	1.50	1.45	Glycerolipid metabolism
ChoE (17:0)	0.13 ± 0	0.16 ± 0.01	<0.01**	0.01*	1.28	1.79	Steroid biosynthesis
PC 36:4	13.76 ± 0.61	17.73 ± 0.7	<0.01**	0.01*	1.29	1.81	Glycerolipid metabolism
ChoE (18:0)	0.12 ± 0.01	0.18 ± 0.01	<0.01**	0.02*	1.51	1.73	Steroid biosynthesis
LPC 18:0	50.4 ± 1.83	58.86 ± 1.39	<0.01**	0.03*	1.17	1.88	Glycerophospholipid metabolism
DG 34:2	0.85 ± 0.04	1.05 ± 0.05	<0.01**	0.03*	1.24	1.71	Glycerolipid metabolism
TG 46:0	0.84 ± 0.05	1.16 ± 0.07	<0.01**	0.03*	1.37	1.21	Glycerolipid metabolism
ChoE (18:1)	2.52 ± 0.11	3.54 ± 0.25	<0.01**	0.03*	1.41	1.74	Steroid biosynthesis
ChoE (16:0)	2.02 ± 0.09	2.39 ± 0.07	<0.01**	0.04*	1.18	1.7	Steroid biosynthesis

3.4. Metabolomic profiling and biomarker identification of the hypertension rat model

The metabolome of the hypertension rat model was composed by 128 metabolites from plasma and 32 from urine. A preliminary univariate analysis was performed in plasma (Table S3) and urine data set (Table S4) to obtain a preliminary list of altered metabolites before multivariate analysis. On the one hand, 62 out 128 plasma metabolites were significant altered between the groups after the MW test.

After the BH correction, 52 metabolites prevailed among the 62 metabolites (i.e., threonic acid, PCs, LPC, ChoEs, SMs, among other metabolites). On the other hand, 10 out 32 urine metabolites were significantly different between groups after the MW test and 2 out 10 remain significative altered after de BH correction (i.e., fumarate and 4-Guanidinobutanoate).

The multivariate analysis presented differences in the unsupervised analysis (PCA) in the plasma data set (Figure S3) and urine data set (Figure S4). In this case, groups were separated by the PCA at the first components analyzed. In the plasma data set, the OPLS-DA model was able to differentiate between both groups (Figure 2a). The fitness and prediction accuracy of the plasma model were established by the values of $R2X(_{cum})$ = 0.493, $R2Y(_{cum})$ = 0.95, and $Q2Y(_{cum})$ = 0.826. Since the Q2Y value (0.826) was greater than the pQ2 value (0.01) (Figure 2b). Specifically, it was found 56 plasma features with a VIP threshold of 1. In the urine data set, the OPLS-DA model was also able to differentiate between both groups (Figure 2c). The fitness and prediction accuracy of the plasma model were established by the values of $R2X(_{cum})$ = 0.38, $R2Y(_{cum})$ = 0.905, and $Q2Y(_{cum})$ = 0.613. Since the Q2Y value (0.6013) was greater than the pQ2 value (0.01) (Figure 2d). Specifically, it was found 14 urine features with a VIP threshold of 1. These results indicate that it is possible to predict if an animal is classified in the group of SHR or WKY based on the analysis of plasma and urine metabolomics.

The metabolites selected as potential biomarkers considering the statistical analysis and the prediction power are constituted by 50 plasma metabolites and 2 urine metabolites (Table 2) which are mainly implicated in lipid metabolism.

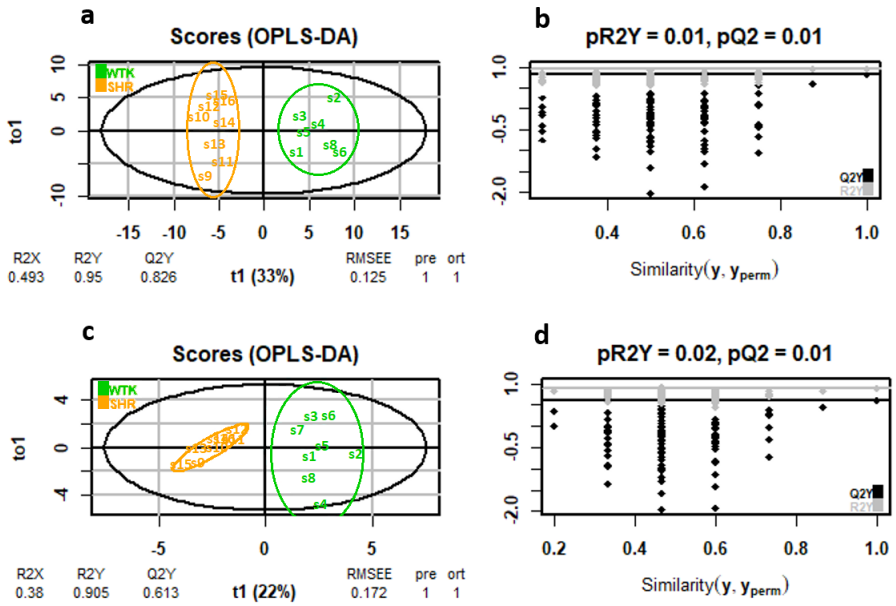

Figure 2. OPLS-DA of plasma and urine metabolomics of the SHR/WKY hypertension rat model. Green represents WKY group and orange SHR group. Plasma (**a**) and urine (**c**) X-score plot (OPLS-DA). The number of components and the cumulative R2X, R2Y and Q2Y are indicated below the plot. Plasma (**b**) and urine (**d**) significance diagnostic: The R2Y and Q2Y of the model are compared with the corresponding values obtained after random permutation of the y response.

Table 4. Summary of the potential biomarkers of the SHR/WKY hypertension rat model in plasma and urine. The results are presented as the mean ± SEM per group (*n* = 8); summary of univariant analysis include *p*-value, *q*-value (pFDR) and FC (SHR/WKY); VIP values of OPLS-DA (multivariant analysis); and metabolism pathway (KEGG). Metabolites are listed by *q*-value. * Denotes p < 0.05 (significantly different) and ** p < 0.01 (high significantly different). Abbreviations: PC, phosphatidylcholine; LPC, lysophospholipid; ChoE, cholesterol ester; SM, sphingomyelin; DG, diacylglycerol.

Metabolite	WKY	SHR	*p*-value	*q*-value	FC	VIP	Pathway
Threonic acid	3.19 ± 0.15	1.07 ± 0.07	<0.01**	<0.01**	0.34	1.62	Ascorbate and aldarate metabolism
PC 32:0	0.98 ± 0.03	1.44 ± 0.04	<0.01**	<0.01**	1.47	1.62	Glycerophospholipid metabolism
PC 36:4	30.51 ± 1.27	43.46 ± 1.1	<0.01**	<0.01**	1.42	1.54	Glycerophospholipid metabolism
PC 34:1	5.36 ± 0.29	8.87 ± 0.37	<0.01**	<0.01**	1.66	1.53	Glycerophospholipid metabolism
LPC 16:1 e	0.13 ± 0	0.18 ± 0.01	<0.01**	<0.01**	1.38	1.49	Glycerophospholipid metabolism
ChoE (18:3)	1.45 ± 0.11	3.05 ± 0.22	<0.01**	<0.01**	2.10	1.59	Steroid biosynthesis
ChoE (20:2)	3 ± 0.46	6.58 ± 0.21	<0.01**	<0.01**	2.20	1.44	Steroid biosynthesis
SM 34:1	22.65 ± 1.16	31.41 ± 1.03	<0.01**	<0.01**	1.39	1.53	Sphingolipid metabolism

SM 34:2	1.72 ± 0.05	2.36 ± 0.09	<0.01**	<0.01**	1.37	1.56	Sphingolipid metabolism
SM 41:1	7.36 ± 0.16	8.87 ± 0.2	<0.01**	<0.01**	1.20	1.58	Sphingolipid metabolism
SM 41:2	1.57 ± 0.07	2.09 ± 0.05	<0.01**	<0.01**	1.33	1.52	Sphingolipid metabolism
ChoE (22:5)	1.8 ± 0.29	3.78 ± 0.19	<0.01**	<0.01**	2.10	1.43	Steroid biosynthesis
PC 34:0	0.5 ± 0.02	0.63 ± 0.01	<0.01**	<0.01**	1.26	1.47	Glycerophospholipid metabolism
SM 40:2	1.03 ± 0.05	1.36 ± 0.04	<0.01**	<0.01**	1.32	1.50	Sphingolipid metabolism
ChoE (22:4)	18.21 ± 2.96	37.47 ± 1.3	<0.01**	<0.01**	2.06	1.37	Steroid biosynthesis
PC 30:0	0.06 ± 0	0.11 ± 0.01	<0.01**	<0.01**	1.84	1.46	Glycerophospholipid metabolism
ChoE (20:4)	64.55 ± 4.42	97.45 ± 5.14	<0.01**	<0.01**	1.51	1.36	Steroid biosynthesis
ChoE (16:1)	0.28 ± 0.03	0.62 ± 0.06	<0.01**	<0.01**	2.17	1.42	Steroid biosynthesis
SM 42:1	23.82 ± 0.55	28.34 ± 0.76	<0.01**	<0.01**	1.19	1.46	Sphingolipid metabolism
Glutamine	0.23 ± 0.02	0.09 ± 0.02	<0.01**	<0.01**	0.49	1.31	Arginine biosynthesis
LPC 16:0 e	0.37 ± 0.02	0.46 ± 0.01	<0.01**	<0.01**	0.41	1.39	Glycerophospholipid metabolism
PC 32:1	0.57 ± 0.07	1.26 ± 0.13	<0.01**	<0.01**	1.24	1.38	Glycerophospholipid metabolism
PC 32:2	0.24 ± 0.02	0.37 ± 0.02	<0.01**	<0.01**	2.19	1.30	Glycerophospholipid metabolism
PC 38:4	33.55 ± 1.24	40.71 ± 1.08	<0.01**	<0.01**	1.55	1.34	Glycerophospholipid metabolism
PC 40:5	1.26 ± 0.05	1.67 ± 0.07	<0.01**	<0.01**	1.21	1.37	Glycerophospholipid metabolism
SM 32:1	0.23 ± 0.02	0.32 ± 0.01	<0.01**	<0.01**	1.32	1.34	Sphingolipid metabolism
Asparagine	0.43 ± 0.04	0.24 ± 0.03	<0.01**	<0.01**	1.36	1.28	Alanine, aspartate and glutamate metabolism
SM 36:2	0.52 ± 0.01	0.67 ± 0.03	<0.01**	0.01*	0.55	1.49	Sphingolipid metabolism
Tyrosine	0.91 ± 0.07	0.54 ± 0.06	<0.01**	0.01*	1.30	1.23	Phenylalanine, tyrosine and tryptophan metabolism
LPC 16:0	88.34 ± 3.31	105.66 ± 2.98	<0.01**	0.01*	0.59	1.26	Glycerophospholipid metabolism
PC 31:0	0.06 ± 0	0.08 ± 0	<0.01**	0.01*	1.20	1.26	Glycerophospholipid metabolism
DG 36:4	3.45 ± 0.19	2.63 ± 0.06	<0.01**	0.01*	1.32	1.26	Lipid metabolism
SM 33:1	0.45 ± 0.01	0.51 ± 0.01	<0.01**	0.01*	0.76	1.37	Sphingolipid metabolism
Glyceric acid	0.84 ± 0.04	1.15 ± 0.08	<0.01**	0.02*	1.15	1.29	Glycine, serine and threonine metabolism

ChoE (18:2)	19.66 ± 1.2	25.35 ± 1.24	0.01*	0.02**	1.38	1.17	Steroid biosynthesis
PC 33:1	0.09 ± 0.01	0.13 ± 0.01	0.01*	0.02*	1.29	1.09	Glycerophospholipid metabolism
LPC 18:1	16.17 ± 0.98	20.26 ± 0.86	0.01*	0.02*	1.41	1.07	Glycerophospholipid metabolism
Serine	0.48 ± 0.05	0.66 ± 0.03	0.01*	0.02*	1.25	1.04	Glycine, serine and threonine metabolism
Glycine	7.35 ± 0.13	8.39 ± 0.29	0.01*	0.03*	1.38	1.18	Glycine, serine and threonine metabolism
3-hydroxybutiric acid	2.76 ± 0.3	1.76 ± 0.08	0.01*	0.03*	1.14	1.08	Synthesis and degradation of ketone bodies
Beta-alanine	0.11 ± 0.01	0.16 ± 0.01	0.01*	0.03*	0.64	1.19	Pyrimidine metabolism
ChoE (22:6)	3.57 ± 0.2	4.58 ± 0.27	0.01*	0.03*	1.45	1.17	Steroid biosynthesis
Citric acid	4.88 ± 0.21	4.18 ± 0.07	0.01*	0.03*	1.28	1.07	Citrate cycle (TCA cycle)
Ribose	15.87 ± 1.61	31.01 ± 4.47	0.01*	0.03*	0.86	1.23	Pentose phosphate pathway
SM 40:1	7.56 ± 0.27	8.69 ± 0.27	0.01*	0.03*	1.95	1.27	Sphingolipid metabolism
PC 40:4	0.35 ± 0.02	0.51 ± 0.05	0.01*	0.03*	1.15	1.21	Glycerophospholipid metabolism
DG 36:2	1.19 ± 0.06	1.52 ± 0.1	0.01*	0.03*	1.45	1.03	Lipid metabolism
SM 38:1	0.71 ± 0.04	0.85 ± 0.03	0.02*	0.04*	0.84	1.25	Sphingolipid metabolism
Valine	1.8 ± 0.05	1.55 ± 0.07	0.02*	0.04*	1.28	1.06	Valine, leucine and isoleucine metabolism
ChoE (17:0)	0.03 ± 0.01	0.07 ± 0.01	0.02*	0.04*	1.19	0.95	Steroid biosynthesis
Fumarate (Urine)	5.62 ± 0.34	3.11 ± 0.42	<0.01**	0.01*	0.55	1.63	Citrate cycle (TCA cycle)
4-Guanidinobutanoate (Urine)	6.1 ± 1.23	13.17 ± 0.33	<0.01**	0.01*	2.16	1.86	Arginine and proline metabolism

3.5. Characteristics of the human population

Subjects were divided according to two independent criteria: (1) the hyperlipidemia and the hypertension risk; (2) gender as sex-differences were observed. In this sense, Table 3 shows the characterisation of the subjects divided by the hyperlipidaemia risk and hypertension risk that includes age, body mass index (BMI), blood pressure levels (SPB/DBP), TG, TC, LDL, HDL, APOB and LPL activity. Regarding the risk of hyperlipidemia, the increase in TG correlates with the significant decrease in HDL in both genders. Additionally, an increase in apolipoprotein B-100 (APOB) was observed in the moderate hyperlipidaemic man, as it is widely known that

lipids levels are lower in women than in men. Those facts correspond with our results. The other parameters were similar between the normal and moderate hyperlipidaemic men and women groups. Regarding the risk of hypertension, the population showing moderate risk to develop hypertension were older than the population without risk. Both genders presented significant differences in SBP and DBP. Thus, men were also presenting a significant increase in the BMI, TC, LDL and APOB, while woman were showing a significant increase in LPL activity.

Table 3. Characteristics of the of human population divided their risk to suffer hyperlipidemia and hypertension. The results are presented as the mean ± SEM. The statistical comparisons among groups were conducted using one-way ANOVA and the post-hoc Tukey. * Denotes $p < 0.1$ (tendency), ** $p < 0.05$ (significantly different) and *** $p < 0.01$ (high significantly different). Abbreviations: BMI, body mass index; SBP, systolic blood pressure; DBP, diastolic blood pressure; TG, triglycerides; TC, total cholesterol; LDL, low-density lipoprotein cholesterol; HDL, high-density lipoprotein cholesterol; APOB, apolipoprotein B-100; LPL activity, lipoprotein lipase activity (Δ nmol/ 0.2 mL per 15 min); N, normal; M, moderate.

	Hyperlipidaemia						Hypertension					
	Men			Women			Men			Women		
	N (*n* = 51)	M (*n* = 23)	*p*-value	N (*n* = 55)	M (*n* = 11)	*p*-value	N (*n* = 51)	M (*n* = 23)	*p*-value	N (*n* = 55)	M (*n* = 11)	*p*-value
Age	45.12 ± 2.21	52.65 ± 2.73	0.13	54.6 ± 1.64	56.64 ± 2.89	0.97	34.33 ± 9.96	53.76 ± 13.30	<0.01***	40.29 ± 11.84	58.88 ± 8.04	<0.01***
BMI	26.02 ± 0.42	26.3 ± 0.48	0.97	26.82 ± 0.3	27.7 ± 0.99	0.74	24.20 ± 2.29	27.02 ± 2.53	<0.01***	26.93 ± 1.82	26.98 ± 2.54	1
SBP (mmHg)	132.31 ± 2.11	131.57 ± 3.44	1.00	139.02 ± 2.28	140.18 ± 5.23	1.00	116.67 ± 5.79	139.48 ± 12.89	<0.01***	114.28 ± 10.51	145.92 ± 10.88	<0.01***
DBP (mmHg)	80.23 ± 1.5	82.63 ± 2.04	0.74	86.25 ± 1.11	87.82 ± 1.73	0.96	71.46 ± 8.29	85.54 ± 7.97	<0.01***	76.86 ± 5.90	89.12 ± 6.11	<0.01***
TG (mmol/L)	1.13 ± 0.04	2.55 ± 0.16	<0.01***	0.94 ± 0.05	2.06 ± 0.13	<0.01***	1.44 ± 0.50	1.63 ± 0.94	0.71	0.94 ± 0.48	1.18 ± 0.55	0.67
TC (mmol/L)	5.39 ± 0.15	5.88 ± 0.1	0.12	5.82 ± 0.11	5.68 ± 0.2	0.96	4.94 ± 1.08	5.83 ± 0.74	<0.01***	5.94 ± 1.10	5.76 ± 0.72	0.88
LDL (mmol/L)	3.47 ± 0.13	3.51 ± 0.11	1.00	3.79 ± 0.11	3.59 ± 0.25	0.87	3.09 ± 0.92	3.66 ± 0.72	0.02**	4.06 ± 0.97	3.67 ± 0.73	0.37
HDL (mmol/L)	1.32 ± 0.05	1.1 ± 0.06	0.04**	1.44 ± 0.05	1.12 ± 0.08	0.03**	1.20 ± 0.32	1.27 ± 0.36	0.82	1.27 ± 0.30	1.42 ± 0.39	0.49
APOB (mmol/L)	0.99 ± 0.03	1.19 ± 0.03	<0.01***	1.07 ± 0.03	1.1 ± 0.06	0.97	0.88 ± 0.22	1.13 ± 0.19	<0.01***	1.12 ± 0.23	1.07 ± 0.17	0.86
LPL activity (Δ)	1.47 ± 0.01	1.45 ± 0.01	0.52	1.44 ± 0.01	1.45 ± 0.02	0.94	1.47 ± 0.04	1.46 ± 0.05	0.82	1.41 ± 0.04	1.45 ± 0.07	0.03**

3.6. Hyperlipidemia biomarkers in the human population

The hyperlipidemia biomarker's validation was focused on the above preselected metabolites in the hyperlipidemic rat model to check their discriminatory potential (Table S5). In this sense, the altered metabolites in both species were higligted in Figure 3. Specifically, ChoE (17:0) levels were increased 4-fold as well as DG 34:2 levels that were also increased of moderate group. Thus, ChoE (17:0) and DG 34:2 were discriminative in hiperlipidemia across species and gender. Furthermore, TG 46:0 was increased almost 2-fold in moderate group, which is significantly different in man and presents a tendency in woman. Following the trend of TG 46:0, PC 36:4 and PC 38:4 were significantly increased in moderate in man. Other potential DG is DG 34:3 that was higher in moderate hyperlipidemic, and the increase was more pronounced in woman. Regarding ChoEs, ChoE (18:0) was the only metabolite significantly decreased in the case of woman.

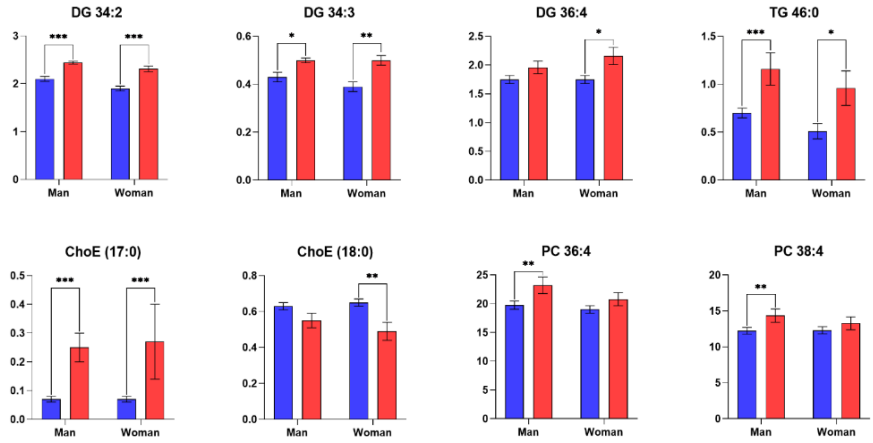

Figure 3. Changes in the preselected metabolites to evaluate hyperlipidaemia in human plasma. The results are presented as the mean ± SEM per gender (men and women) and the level of TG (normal and moderate). The statistical comparisons among groups were conducted using one-way ANOVA and the post-hoc Tukey's test. * Denotes $p < 0.1$ (tendency), ** $p < 0.05$ (significantly different) and *** $p < 0.01$ (high significantly different). Abbreviations: DG, diacylglycerol; TG, triglyceride; ChoE, cholesterol ester; PC, phosphatidylcholine.

3.7. Hypertension biomarkers in the human population

The hypertension biomarker's validation was focused on the above preselected metabolites in the hypertension rat model to doble check their discriminatory potential (Table S6). In men, 14 metabolites differentiate between normal and moderate risk to suffer hypertension, while in women this number decrease to 8 metabolites (Figure 4). Specifically, LPC 16:0 was decreased in moderate hypertensive individuals. Additionally, the metabolites related to SM metabolism were altered in the population with higher risk to suffer hypertension.

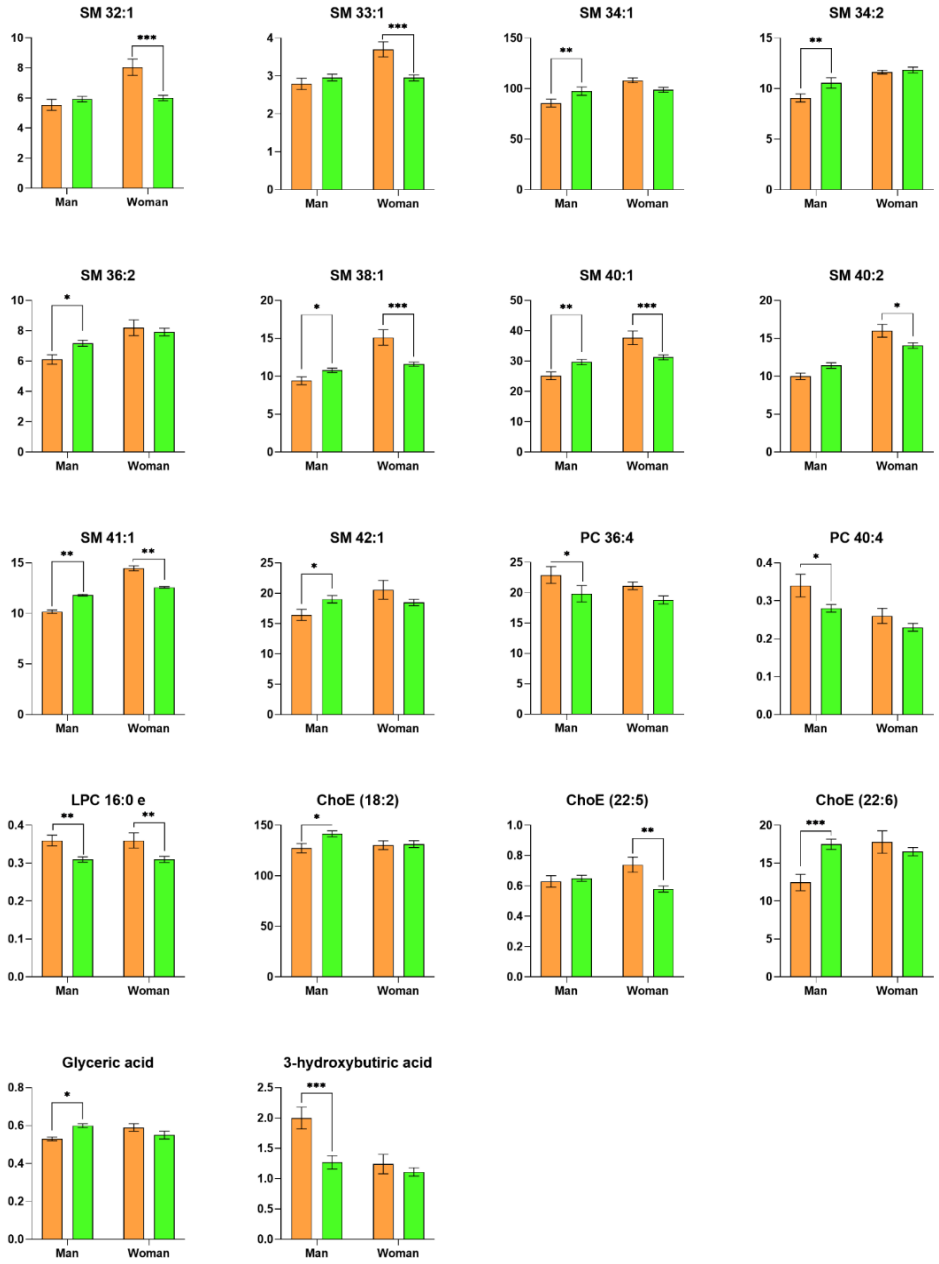

Figure 4. Changes in the preselected metabolites to evaluate hypertension in human plasma. The results are presented by the mean ± S.E.M per sex (men and women) and the level of hypertension risk (normal and moderate). The statistical comparisons among groups were conducted using one-way ANOVA and the post-hoc Tukey's test. * Denotes $p < 0.1$ (tendency), ** $p < 0.05$ (significantly different) and *** $p < 0.01$ (high significantly different). Abbreviations: PC, phosphatidylcholine; SM, sphingomyelin; ChoE, cholesterol ester.

4. Discussion

This study explored the metabolic signature associated with hyperlipidemia and hypertension across species in preclinical and clinical studies. On the one hand, 11 metabolites, involved in glycerolipid, glycerophospholipid and steroid metabolism, were identified as potential biomarkers of hyperlipidemia in the preclinical model. Translating those results to the clinic, 5 metabolites were consistent for moderate hyperlipidemia for men and 4 for woman. On the other hand, 52 metabolites, involved in glycerophospholipid, steroid and sphingolipid metabolism among others, were identified as potential biomarkers of hypertension in the preclinic model. In the clinic study, 7 metabolites were considered potential biomarkers for moderate hypertension for men and 6 for woman. The identified and proposed as potential biomarkers were lipid metabolites, mainly involved in lipid signalling pathway, in hyperlipidemia and hypertension.

4.1. Metabolic profiling in hyperlipidemia

To date, the single dose of 150 mg/kg P407 is the lowest dose used in the literature [11–18,37] that is capable to induce low levels of hyperlipidemia and the subsequent changes in the metabolic signature. The mechanism of action was effective inhibiting LPL as it could be observed a decrease of this lipase in the P407 group, which is characteristic of P407 models [11]. The main characteristics defining this early hyperlipidemia model were slightly high plasma levels of TG and TC in the P407 group, without reaching values described in other models of P407, highlighting that the classical biomarkers were 10-fold lower than other studies with doses between 300 mg/Kg to 1500 mg/kg [14,16] and single or multiple injections [38–40]. Interestingly, these clinical biomarkers do not reach the characteristic elevated levels associated with pathological states [1]. To complete the overall picture of the model, carbohydrate alterations, inflammation and oxidative stress were not detected in the hyperlipidemic group, which are also associated to the development of CVD and are considered risk factors for NCDs [41,42]. These allows us to consider this model suitable for monitoring and explore potential biomarkers in the hyperlipidemia prodromal stage. In this line, the healthy population with moderate risk to suffer hyperlipidemia presented higher levels of TG, as well as lower levels of HDL compared to the subjects with normal risk in concordance with the guidelines [1]. Those parameters allowed us to discriminate between individual with normal and moderate risk to suffer hyperlipidaemia, with low level of overweight according the BMI (24.9 to 39.9 BMI), which is not the best index to assess the health status [43]. However, the BMI together with other classical biomarkers lack the enough sensitivity to discriminate between the development of early risk factors and healthy stages.

Focusing on the need of the assessment of metabolic health and offering an alternative to BMI index and other classical determinations, metabolomic profiling has been increasing as a tool for early assessment and prevention of early hyperlipidaemia

among others risk factors as hypertension [44]. In the hyperlipidemic animal model, many specific lipids were found to be up regulated in plasma (e.g., DGs, PCs, ChoEs, LPCs and TGs), these specific lipids may help to elucidate key biomarkers for the early assessment of prodromal stages of hyperlipidemia. Translating those lipids to the healthy population, some DGs, TG, ChoEs and PCs stand out as discriminatory lipids across species. The vast majority of long-chain DGs were increased in hyperlipidemic subjects in concordance with other metabolomic studies [26]. In fact, those specific lipids are precursors of TGs which are the main lipids determined in classical determinations characteristics of hyperlipidemia, thus those results suggests that the determination of DGs are key metabolites of prodromal lipid alteration [45]. In this case, DG 34:2 was the metabolite with the highest discriminative power across species and genera. In this line, DG 34:4 was found elevated in preclinical and clinical studies related to hyperlipidemia, as the case of animals with transplanted microbiota from cafeteria diet induced-obesity [46] and patients with MetS [47]. In the case of other specific DGs, woman presented more differences regarding DGs than men (DG 34:3 and DG 36:4). Despite, men and women presented the same tendencies, the magnitude and tendency of some metabolites were different due to gender-differences. In fact, women have a higher percent body fat of their body weight compared to men from puberty onward due to physiological events and genetic composition and women also tend to gain more fat during adult life than men. Additionally, women may experience persistent increases in body weight and fat distribution after pregnancy or gain weight due to menopause [43]. This data helps to elucidate gender-differences in lipid metabolism, which are complex and involve hormonal effects that are distributed across tissues and involve effects in gene expression of X-chromosome [48].

Following with TGs, the total sum of TG was higher in the hyperlipidaemic animals, although only the specific TG 46:0 presented a significantly increased in the model. In previous studies, several long chain TGs were increased in hyperlipidaemic subjects [49], thus, it was expected to obtain more individual TG altered in this model, in contrast, precursors of TG (DGs) had presented greater impact in early stages instead the levels of specific TGs. In different studies focused on hyperlipidemia, several ChoEs were increased as the main characters of fatty acid metabolism [26,50]. A number of experimental investigations have revealed that unsaturated and saturated fatty acids metabolism are disturbed in hyperlipidemia as well as fatty acids with carbon chain lengths from 14 to 24 carbon atoms [51,52]. According those previous studies, ChoE 17:0 was increased almost 3-fold in the P407 model in line with other studies [53]. In prior metabolomic characterization, specific PCs (PC 36:4 and PC 38:4) has been specifically reported as potential biomarkers in hyperlipidemia and healthy subjects [26,49,50,54]. Elevated PCs, which are precursors of DGs implicated in lipid signaling, can cause the autoimmune response and inflammation in hyperlipidemia-related diseases [55].

To complement the metabolic profiling of hyperlipidemia, urine metabolome was elucidated by NMR approaches, highlighting that TMAO and PAG were decreased by a half and increased almost twice in the P407 group, correspondently. Interestingly, TMAO and PAG were key metabolites in urine produced by gut bacteria and the increase of those metabolites are related to obesity, CVD and MetS [56][57]. Nevertheless, some limitations should be considered in the urine metabolic profiling: (1) the collection method implicated 6 hours of collection with an hour of fasting, while in plasma all the samples were collected at the same time with 7 hours of fasting; (2) the NMR method is often 10 to 100 times less sensitive compared to mass spectroscopy [58]. Thus, there is a need to optimize the procedure to collect urine and perform further experiments with metabolomic approaches more sensitive. Consequently, only the plasma metabolites were studied in humans.

4.2. Metabolic profiling in hypertension

In hypertension research, the SHR animal model has been used as the popular genetic model to study hypertension, thus, in the current study, we interrogated this model as their pathophysiological processes have been recognized to be related to essential hypertension [19]. The SHR rats blood pressure gradually rises with aging and becomes significantly increased after approximately 17-19 weeks of age compared with healthy matched normotensive pairs (WTK) [19]. The characterization of SHR rats presented several differences disturbances in body weight and plasma parameters corresponding to hypercholesterolemia, carbohydrate dysfunction and oxidative stress which are previously described in this model [59]. In line with the SHR model, individual volunteers presenting moderate risk were older than those without apparent risk of hypertension, due to this condition is a metabolic disorder being the actual causes unclear though the risk appears to increase with age, usually influenced by unhealthy lifestyles, obesity and physical inactivity [2]. In the case of men, the risk to suffer hypertension is associated with overweight, while in women these differences were not observed presenting low degree of overweight in both groups regarding our clinical studies [48].

Several plasma metabolites from the SHR model were significantly altered including lipids (e.g., PCs, LPCs, ChoEs, SMs), amino acids (threonic acid, glutamine, asparagine, tyrosine, serine, glycine, beta-alanine, valine), 3-hydroxybutiric acid, citric acid and ribose. In consistence with previous research, those metabolites were found to be significantly altered in SHR compared to WKY rats [60]. In addition, fumarate and 4-guanidinobutanoate, which are related to urea metabolism, were altered in urine. Urea has become an independent predictor of hypertension, and those metabolites are implicated in the urea metabolism and could be key biomarkers for hypertension in early stages [45]. However, the efforts to find biomarkers in humans remain in plasma biofluid due to the limitations previously outlined in hyperlipidemia. Specifically, the remaining metabolites were only lipids discarding amino acids and

carbohydrates that were related to other risk factors associated to CVD, which were also pointed by other studies without clarifying the nature of the alteration [60].

In our study, sphingolipids and glycerolipids were associated with blood pressure, supporting the major role of sphingolipid and glycerolipid metabolism in blood pressure regulation [61,62]. Interestingly, an increasing number of studies has emerged revealing associations of long-chain circulating sphingolipids (i.e., more than 30 total carbons) with pathological conditions as hypertension or further complications as atherosclerosis and CVD [63]. The elevation of vascular SMs in SHR induces a marked endothelium-dependent release of thromboxane A_2 that may contribute to endothelial dysfunction in hypertension [64]. Integrating that tendency with our results, the main significantly altered circulating metabolites were unsaturated long-chain SMs in both rats and human studies including men and woman: (1) SM 34:1, SM 34:2, SM 40:1, SM 41:1 were up-regulated in men as in the hypertensive rat model; (2) SM 32:1, SM 33:1, SM 38:1, SM 40:1, SM 41:1 were down-regulated in woman presenting a different bias compared to the rat model; (3) SM 40:1 and SM 41:1 were different in all the studies and genera. Previous investigations had focus on gender differences in the association of SMs concluding that SMs concentrations increase more rapidly in women than in men, although younger age women have lower levels of SMs than men and this fact tends to reverse in older age [65]. This fact supports the idea of performing hypertension studies and treatment strategies for hypertension and CVD that are tailored according to sex and age [66].

In preceding studies, higher levels of PCs and LPCs were identified in hypertensive subjects compared with normal controls in consistency with our results [26]. In contrast to those preliminary results, the population with moderate hypertension risk presented a tendency to decrease the levels of PCs (e.g., PC 36:4 and PC 40:0) and a significantly decrease of LPC 16:0 e. In addition, LPC potentially plays an important role in atherosclerosis and inflammatory diseases by altering various functions in a number of cell-types [67]. In the rat model, ChoEs were up regulated in SHR animals compared to the normotensive group. In the human population, the up regulation prevails in ChoE (18:2) and ChoE (22:6) in men, while the tendency is to decrease in women as in the case of ChoE (22:6). Furthermore, glyceric acid was up regulated in the animal model and a tendency to increase was shown in humans. This metabolite is obtained from the oxidation of glycerol and it is related to carbohydrate metabolism alterations in hypertension playing an important role through sodium retention, renal tubular sodium reabsorption, sympathetic nervous system and adverse effects of anti-hypertensive drugs [45]. One ketone body, the 3-hydroxybutiric acid was significantly down-regulated in the animal model and in men in the line with other studies identifying a protective effect of this ketone body on salt-sensitive hypertension [68].

4.3. Comparison between hyperlipidemia and hypertension

The metabolic profiling of hyperlipidemia and hypertension confirm the clear link between these metabolism disorders which have been described by many epidemiological studies in different diseases [26]. Indeed, prospective cohorts have reported that hyperlipidemia can serve as a predictor for future risk of hypertension [69,70], as well as the treatment of hyperlipidemia has been reported to be beneficial on blood pressure and vice versa [5]. The fact that the coexistence of the two risk factors has more than an additional adverse effect indicate that hyperlipidemia and hypertension may develop and progress both independently and collaborative [3–5].

We observed in our approach between species that the remaining metabolites were lipids, mainly implicated in signalling pathways, discarding other metabolites described in other studies as amino acids or intermediate metabolites of the TCA cycle. Dysregulation of the signalling pathway contribute to the pathogenesis of human diseases as CVDs and MetS [71]. In fact, the lipid signalling pathway consists on the breakdown of SMs that generate PCs and LPCs, which may accelerate the formation of DGs and the posterior synthesis of TGs, the key lipids implicated in lipid alteration in hyperlipidemia and hypertension [45]. Thus, direct metabolic similarities include up-regulated glycerolipids implicated in signalling pathways, while the changing trends in some lipids suggest different mechanisms of hyperlipidemia and hypertension together with inflammation and oxidative stress that has been implicated in multiple pathologies.

5. Conclusions

To sum up, we systematically explored the metabolic signatures associated with a prodromal hyperlipidemia animal model, achieved successfully by a single low dose of P407 (150 mg/kg) in male Wistar rats, and an hypertense animal model, which is the extensively used the SHR model and its normotensive control (WKY). Due to the key role of lipids in the development of different multifactorial diseases, hyperlipidemia and hypertension are considerate primary risk factors being asymptomatically for years. Therefore, we propose in this article an early hyperlipidemia and hypertension metabolic profile across species in plasma using UHPLC/GC-qTOF approach, discarding urine as a source of metabolites due to the high variability. In hyperlipidemia, 11 metabolites were identified as potential biomarkers of the P407-induced hyperlipidaemic rat model. Translating those results to the clinic, 5 metabolites were considered potential biomarkers for men [i.e., DG 34:2, TG 46:0, ChoE (17:0), PC 36:4 and PC 38:4] and 4 for woman [i.e., DG 34:2, DG 34:3, ChoE (17:0), ChoE (18:0)]. In hypertension, 52 metabolites were identified as potential biomarkers of SHR/WTK model. In the clinical study, 7 metabolites were considered potential biomarkers for moderate hypertension for men [i.e., SM 34:1, SM 34:2, SM 40:1, SM 41:1, LPC 16:0 e, ChoE (22:6) and 3-hydroxybutiric acid] and 6 for woman (i.e., SM 32:1, SM 33:1, SM 38:1, SM 40:1, SM 41:1 and LPC 16:0 e). This metabolic profile could

assist the exhaustive diagnosis and management of lipid and blood pressure disorders since they provide information about the stage of the alteration and, furthermore, allow researchers to determine the stage of the risk factor. Further extensive validation of this metabolic profile in different cluster of subjects are needed to verify the suitability of the biomarkers described here for use in the general population. In the future, prospective cohort studies deserve to be conducted to establish the causal relationship between metabolite biomarkers and hyperlipidaemia/hypertension.

References

1. Mach, F.; Baigent, C.; Catapano, A.L.; Koskinas, K.C.; Casula, M.; Badimon, L.; Chapman, M.J.; De Backer, G.G.; Delgado, V.; Ference, B.A.; et al. 2019 ESC/EAS Guidelines for the management of dyslipidaemias: lipid modification to reduce cardiovascular risk. *Eur. Heart J.* **2020**, *41*, 111–188, doi:10.1093/eurheartj/ehz455.

2. Williams, B.; Mancia, G.; Spiering, W.; Rosei, E.A.; Azizi, M.; Burnier, M.; Clement, D.L.; Coca, A.; De Simone, G.; Dominiczak, A.; et al. *2018 ESC/ESH Guidelines for the management of arterial hypertension*; 2018; Vol. 39; ISBN 0000000000.

3. Chobanian, A. V; Bakris, G.L.; Black, H.R.; Cushman, W.C.; Green, L.A.; Izzo, J.L.J.; Jones, D.W.; Materson, B.J.; Oparil, S.; Wright, J.T.J.; et al. The Seventh Report of the Joint National Committee on Prevention, Detection, Evaluation, and Treatment of High Blood Pressure: the JNC 7 report. *JAMA* **2003**, *289*, 2560–2572, doi:10.1001/jama.289.19.2560.

4. Eaton, C.B.; Feldman, H.A.; Assaf, A.R.; McPhillips, J.B.; Hume, A.L.; Lasater, T.M.; Levinson, P.; Carleton, R.A. Prevalence of hypertension, dyslipidemia, and dyslipidemic hypertension. *J. Fam. Pract.* **1994**, *38*, 17–23.

5. Dalal, J.J.; Padmanabhan, T.N.C.; Jain, P.; Patil, S.; Vasnawala, H.; Gulati, A. LIPITENSION: Interplay between dyslipidemia and hypertension. *Indian J. Endocrinol. Metab.* **2012**, *16*, 240–245, doi:10.4103/2230-8210.93742.

6. Mosby *Mosby's Medical Dictionary*; 10th Editi.; Elsevier, 2016; ISBN 9780323414258.

7. van Ommen, B.; Keijer, J.; Heil, S.G.; Kaput, J. Challenging homeostasis to define biomarkers for nutrition related health. *Mol. Nutr. Food Res.* **2009**, *53*, 795–804, doi:10.1002/mnfr.200800390.

8. Kasiske, B.L.; O'Donnell, M.P.; Keane, W.F. The Zucker rat model of obesity, insulin resistance, hyperlipidemia, and renal injury. *Hypertens. (Dallas, Tex. 1979)* **1992**, *19*, I110-5, doi:10.1161/01.hyp.19.1_suppl.i110.

9. Gawronska-Szklarz, B.; Drozdzik, M.; Wojcicki, J.; Zakrzewski, J. Effect of experimental hyperlipidemia on the pharmacokinetics of digoxin. *Acta Pol. Pharm.* **1994**, *51*, 271–274.

10. Sullivan, M.P.; Cerda, J.J.; Robbins, F.L.; Burgin, C.W.; Beatty, R.J. The gerbil, hamster, and guinea pig as rodent models for hyperlipidemia. *Lab. Anim. Sci.* **1993**, *43*, 575–578.

11. Johnston, T.P. The P-407-induced murine model of dose-controlled hyperlipidemia and atherosclerosis: a review of findings to date. *J. Cardiovasc. Pharmacol.* **2004**, *43*, 595–606, doi:10.1097/00005344-200404000-00016.

12. Suárez-García, S.; Caimari, A.; del Bas, J.M.; Suárez, M.; Arola, L. Serum lysophospholipid levels are altered in dyslipidemic hamsters. *Sci. Rep.* **2017**, *7*, 10431, doi:10.1038/s41598-017-10651-0.

13. Korolenko, T.A.; Johnston, T.P.; Tuzikov, F. V; Tuzikova, N.A.; Pupyshev, A.B.; Spiridonov, V.K.; Goncharova, N. V; Maiborodin, I. V; Zhukova, N.A. Early-stage atherosclerosis in poloxamer 407-induced hyperlipidemic mice: pathological features and changes in the lipid composition of serum lipoprotein fractions and subfractions. *Lipids Health Dis.* **2016**, *15*, 16, doi:10.1186/s12944-016-0186-7.

14. Johnston, T.P.; Palmer, W.K. The effect of pravastatin on hepatic 3-hydroxy-3-methylglutaryl CoA reductase obtained from poloxamer 407-induced hyperlipidemic rats. *Pharmacotherapy* **1997**, *17*, 342–347.

15. Blonder, J.M.; Baird, L.; Fulfs, J.C.; Rosenthal, G.J. Dose-dependent hyperlipidemia in rabbits following administration of poloxamer 407 gel. *Life Sci.* **1999**, *65*, PL261-6, doi:10.1016/s0024-3205(99)00495-6.

16. Tanko, Y.; Kabiru, A.; Abdulrasak, A.; Mohammed, K.A.; Salisu, A.I.; Jimoh, A.; Gidado, N.M.; Sada, N.M. Effects of Fermented Ginger Rhizome (Zingiber officinale) and Fenu Greek (Trigonella foenum-graceum) Supplements on Oxidative stress and Lipid Peroxidation Biomarkers in Poloxamer-407 Induced -Hyperlipidemic Wistar Rats. *Niger. J. Physiol. Sci.* **2017**, *32*, 137–143.

17. Chaudhary, H.R.; Brocks, D.R. The single dose poloxamer 407 model of hyperlipidemia; systemic effects on lipids assessed using pharmacokinetic methods, and its effects on adipokines. *J. Pharm. Pharm. Sci.* **2013**, *16*, 65–73, doi:10.18433/j37g7m.

18. Korolenko, T.A.; Tuzikov, F. V; Johnston, T.P.; Tuzikova, N.A.; Kisarova, Y.A.; Zhanaeva, S.Y.; Alexeenko, T. V; Zhukova, N.A.; Brak, I. V; Spiridonov, V.K.; et al. The influence of repeated administration of poloxamer 407 on serum lipoproteins and protease activity in mouse liver and heart. *Can. J. Physiol. Pharmacol.* **2012**, *90*, 1456–1468, doi:10.1139/y2012-118.

19. Pinto, Y.M.; Paul, M.; Ganten, D. Lessons from rat models of hypertension: from Goldblatt to genetic engineering. *Cardiovasc. Res.* **1998**, *39*, 77–88, doi:10.1016/s0008-6363(98)00077-7.

20. Lerman, L.O.; Kurtz, T.W.; Touyz, R.M.; Ellison, D.H.; Chade, A.R.; Crowley, S.D.; Mattson, D.L.; Mullins, J.J.; Osborn, J.; Eirin, A.; et al. Animal Models of Hypertension: A Scientific Statement From the American Heart Association. *Hypertension* **2019**, *73*, e87–e120, doi:10.1161/HYP.0000000000000090.

21. Kaddurah-Daouk, R.; Kristal, B.S.; Weinshilboum, R.M. Metabolomics: A Global Biochemical Approach to Drug Response and Disease. *Annu. Rev. Pharmacol. Toxicol.* **2008**, *48*, 653–683, doi:10.1146/annurev.pharmtox.48.113006.094715.

22. Ulaszewska, M.M.; Weinert, C.H.; Trimigno, A.; Portmann, R.; Andres Lacueva, C.; Badertscher, R.; Brennan, L.; Brunius, C.; Bub, A.; Capozzi, F.; et al. Nutrimetabolomics: An Integrative Action for Metabolomic Analyses in Human Nutritional Studies. *Mol. Nutr. Food Res.* **2019**, *63*, e1800384, doi:10.1002/mnfr.201800384.

23. Hernandez-Baixauli, J.; Quesada-Vazquez, S.; Marine-Casado, R.; Gil Cardoso, K.; Caimari, A.; Del Bas, J.M.; Escote, X.; Baselga-Escudero, L. Detection of Early Disease Risk Factors Associated with Metabolic Syndrome: A New Era with the NMR Metabolomics Assessment. *Nutrients* **2020**, *12*, doi:10.3390/nu12030806.

24. Nikolic, S.B.; Sharman, J.E.; Adams, M.J.; Edwards, L.M. Metabolomics in hypertension. *J. Hypertens.* **2014**, *32*, 1159–1169, doi:10.1097/HJH.0000000000000168.

25. Chen, J.; Ye, C.; Hu, X.; Huang, C.; Yang, Z.; Li, P.; Wu, A.; Xue, X.; Lin, D.; Yang, H. Serum metabolomics model and its metabolic characteristics in patients with different syndromes of dyslipidemia based on nuclear magnetic resonance. *J. Pharm. Biomed. Anal.* **2019**, *167*, 100–113, doi:10.1016/j.jpba.2018.12.042.

26. Ke, C.; Zhu, X.; Zhang, Y.; Shen, Y. Metabolomic characterization of hypertension and dyslipidemia. *Metabolomics* **2018**, *14*, 117, doi:10.1007/s11306-018-1408-y.

27. Hoffman, J.F.; Fan, A.X.; Neuendorf, E.H.; Vergara, V.B.; Kalinich, J.F. Hydrophobic Sand Versus Metabolic Cages: A Comparison of Urine Collection Methods for Rats (Rattus norvegicus). *J. Am. Assoc. Lab. Anim. Sci.* **2018**, *57*, 51–57.

28. Caimari, A.; del Bas, J.M.; Crescenti, A.; Arola, L. Low doses of grape seed procyanidins reduce adiposity and improve the plasma lipid profile in hamsters. *Int. J. Obes. (Lond).* **2013**, *37*, 576–583, doi:10.1038/ijo.2012.75.

29. Rodriguez-Sureda, V.; Peinado-Onsurbe, J. A procedure for measuring triacylglyceride and cholesterol content using a small amount of tissue. *Anal. Biochem.* **2005**, *343*, 277–282, doi:10.1016/j.ab.2005.05.009.

30. Vinaixa, M.; Samino, S.; Saez, I.; Duran, J.; Guinovart, J.J.; Yanes, O. A Guideline to Univariate

Statistical Analysis for LC/MS-Based Untargeted Metabolomics-Derived Data. *Metabolites* **2012**, *2*, 775–795, doi:10.3390/metabo2040775.

31. Thévenot, E.A.; Roux, A.; Xu, Y.; Ezan, E.; Junot, C. Analysis of the Human Adult Urinary Metabolome Variations with Age, Body Mass Index, and Gender by Implementing a Comprehensive Workflow for Univariate and OPLS Statistical Analyses. *J. Proteome Res.* **2015**, *14*, 3322–3335, doi:10.1021/acs.jproteome.5b00354.

32. Llorach-Asunción, R.; Jauregui, O.; Urpi-Sarda, M.; Andres-Lacueva, C. Methodological aspects for metabolome visualization and characterization: a metabolomic evaluation of the 24 h evolution of human urine after cocoa powder consumption. *J. Pharm. Biomed. Anal.* **2010**, *51*, 373–381, doi:10.1016/j.jpba.2009.06.033.

33. Kanehisa, M.; Goto, S. KEGG: kyoto encyclopedia of genes and genomes. *Nucleic Acids Res.* **2000**, *28*, 27–30, doi:10.1093/nar/28.1.27.

34. Smith, J.R.; Hayman, G.T.; Wang, S.-J.; Laulederkind, S.J.F.; Hoffman, M.J.; Kaldunski, M.L.; Tutaj, M.; Thota, J.; Nalabolu, H.S.; Ellanki, S.L.R.; et al. The Year of the Rat: The Rat Genome Database at 20: a multi-species knowledgebase and analysis platform. *Nucleic Acids Res.* **2020**, *48*, D731–D742, doi:10.1093/nar/gkz1041.

35. Wishart, D.S.; Feunang, Y.D.; Marcu, A.; Guo, A.C.; Liang, K.; Vázquez-Fresno, R.; Sajed, T.; Johnson, D.; Li, C.; Karu, N.; et al. HMDB 4.0: the human metabolome database for 2018. *Nucleic Acids Res.* **2018**, *46*, D608–D617, doi:10.1093/nar/gkx1089.

36. Frolkis, A.; Knox, C.; Lim, E.; Jewison, T.; Law, V.; Hau, D.D.; Liu, P.; Gautam, B.; Ly, S.; Guo, A.C.; et al. SMPDB: The Small Molecule Pathway Database. *Nucleic Acids Res.* **2010**, *38*, D480-7, doi:10.1093/nar/gkp1002.

37. Johnston, T.P.; Palmer, W.K. Mechanism of poloxamer 407-induced hypertriglyceridemia in the rat. *Biochem. Pharmacol.* **1993**, *46*, 1037–1042, doi:10.1016/0006-2952(93)90668-m.

38. Joo, I.W.; Ryu, J.H.; Oh, H.J. The influence of Sam-Chil-Geun (Panax notoginseng) on the serum lipid levels and inflammations of rats with hyperlipidemia induced by poloxamer-407. *Yonsei Med. J.* **2010**, *51*, 504–510, doi:10.3349/ymj.2010.51.4.504.

39. Yeom, M.; Park, J.; Lee, B.; Lee, H.S.; Park, H.-J.; Won, R.; Lee, H.; Hahm, D.-H. Electroacupuncture ameliorates poloxamer 407-induced hyperlipidemia through suppressing hepatic SREBP-2 expression in rats. *Life Sci.* **2018**, *203*, 20–26, doi:10.1016/j.lfs.2018.04.016.

40. Hor, S.; Farsi, E.; Yam, M.; Nuyah, N.; Abdullah, M. Lipid-lowering effects of Coriolus versicolor extract in poloxamer 407-induced hypercholesterolaemic rats and high cholesterol-fed rats. *J. Med. Plants Res.* **2011**, *5*.

41. Steven, S.; Frenis, K.; Oelze, M.; Kalinovic, S.; Kuntic, M.; Bayo Jimenez, M.T.; Vujacic-Mirski, K.; Helmstädter, J.; Kröller-Schön, S.; Münzel, T.; et al. Vascular Inflammation and Oxidative Stress: Major Triggers for Cardiovascular Disease. *Oxid. Med. Cell. Longev.* **2019**, *2019*, 7092151, doi:10.1155/2019/7092151.

42. Zhazykbayeva, S.; Pabel, S.; Mügge, A.; Sossalla, S.; Hamdani, N. The molecular mechanisms associated with the physiological responses to inflammation and oxidative stress in cardiovascular diseases. *Biophys. Rev.* **2020**, *12*, 947–968, doi:10.1007/s12551-020-00742-0.

43. Weir, C.B.; Jan, A. *BMI Classification Percentile And Cut Off Points*; StatPearls Publishing, Treasure Island (FL): Michigan State University/Mclaren, 2020;

44. Hernandez-Baixauli, J.; Quesada-Vázquez, S.; Mariné-Casadó, R.; Cardoso, K.G.; Caimari, A.; Del Bas, J.M.; Escoté, X.; Baselga-Escudero, L. Detection of early disease risk factors associated with metabolic syndrome: A new era with the NMR metabolomics assessment. *Nutrients* **2020**, *12*, 1–34, doi:10.3390/nu12030806.

45. Au, A.; Cheng, K.-K.; Wei, L.K. Metabolomics, Lipidomics and Pharmacometabolomics of Human Hypertension. *Adv. Exp. Med. Biol.* **2017**, *956*, 599–613, doi:10.1007/5584_2016_79.

46. Hernandez-Baixauli, J.; Puigbò, P.; Torrell, H.; Palacios-Jordan, H.; Ripoll, V.J.R.; Caimari, A.; Del Bas, J.M.; Baselga-Escudero, L.; Mulero, M. A Pilot Study for Metabolic Profiling of Obesity-Associated Microbial Gut Dysbiosis in Male Wistar Rats. *Biomolecules* **2021**, *11*, doi:10.3390/biom11020303.

47. Jové, M.; Naudí, A.; Portero-Otin, M.; Cabré, R.; Rovira-Llopis, S.; Bañuls, C.; Rocha, M.; Hernández-Mijares, A.; Victor, V.M.; Pamplona, R. Plasma lipidomics discloses metabolic syndrome with a specific HDL phenotype. *FASEB J. Off. Publ. Fed. Am. Soc. Exp. Biol.* **2014**, *28*, 5163–5171, doi:10.1096/fj.14-253187.

48. Palmisano, B.T.; Zhu, L.; Eckel, R.H.; Stafford, J.M. Sex differences in lipid and lipoprotein metabolism. *Mol. Metab.* **2018**, *15*, 45–55, doi:https://doi.org/10.1016/j.molmet.2018.05.008.

49. Castro-Perez, J.M.; Roddy, T.P.; Shah, V.; McLaren, D.G.; Wang, S.-P.; Jensen, K.; Vreeken, R.J.; Hankemeier, T.; Johns, D.G.; Previs, S.F.; et al. Identifying Static and Kinetic Lipid Phenotypes by High Resolution UPLC–MS: Unraveling Diet-Induced Changes in Lipid Homeostasis by Coupling Metabolomics and Fluxomics. *J. Proteome Res.* **2011**, *10*, 4281–4290, doi:10.1021/pr200480g.

50. Miao, H.; Chen, H.; Pei, S.; Bai, X.; Vaziri, N.D.; Zhao, Y.-Y. Plasma lipidomics reveal profound perturbation of glycerophospholipids, fatty acids, and sphingolipids in diet-induced hyperlipidemia. *Chem. Biol. Interact.* **2015**, *228*, 79–87, doi:10.1016/j.cbi.2015.01.023.

51. Yin, W.; Carballo-Jane, E.; McLaren, D.G.; Mendoza, V.H.; Gagen, K.; Geoghagen, N.S.; McNamara, L.A.; Gorski, J.N.; Eiermann, G.J.; Petrov, A.; et al. Plasma lipid profiling across species for the identification of optimal animal models of human dyslipidemia. *J. Lipid Res.* **2012**, *53*, 51–65, doi:10.1194/jlr.M019927.

52. Miao, H.; Zhao, Y.-H.; Vaziri, N.D.; Tang, D.-D.; Chen, H.; Chen, H.; Khazaeli, M.; Tarbiat-Boldaji, M.; Hatami, L.; Zhao, Y.-Y. Lipidomics Biomarkers of Diet-Induced Hyperlipidemia and Its Treatment with Poria cocos. *J. Agric. Food Chem.* **2016**, *64*, 969–979, doi:10.1021/acs.jafc.5b05350.

53. Kwan, H.Y.; Hu, Y.-M.; Chan, C.L.; Cao, H.-H.; Cheng, C.Y.; Pan, S.-Y.; Tse, K.W.; Wu, Y.C.; Yu, Z.-L.; Fong, W.F. Lipidomics identification of metabolic biomarkers in chemically induced hypertriglyceridemic mice. *J. Proteome Res.* **2013**, *12*, 1387–1398, doi:10.1021/pr3010327.

54. DU, H.; RAO, Y.; LIU, R.; DENG, K.; GUAN, Y.; LUO, D.; MAO, Q.; YU, J.; BO, T.; FAN, Z.; et al. Proteomic And Metabolomic Analyses Reveal The Full Spectrum of Inflammatory and Lipid Metabolic Abnormalities In Dyslipidemia. *28 December 2020, Prepr. (Version 1) available Res. Sq.*, doi:10.21203/rs.3.rs-135087/v1.

55. Frostegård, J. Low level natural antibodies against phosphorylcholine: A novel risk marker and potential mechanism in atherosclerosis and cardiovascular disease. *Clin. Immunol.* **2010**, *134*, 47–54, doi:https://doi.org/10.1016/j.clim.2009.08.013.

56. Yu, D.; Shu, X.-O.; Rivera, E.S.; Zhang, X.; Cai, Q.; Calcutt, M.W.; Xiang, Y.-B.; Li, H.; Gao, Y.-T.; Wang, T.J.; et al. Urinary Levels of Trimethylamine-N-Oxide and Incident Coronary Heart Disease: A Prospective Investigation Among Urban Chinese Adults. *J. Am. Heart Assoc.* **2019**, *8*, e010606, doi:10.1161/JAHA.118.010606.

57. Kim, S.-H.; Yang, S.-O.; Kim, H.-S.; Kim, Y.; Park, T.; Choi, H.-K. 1H-nuclear magnetic resonance spectroscopy-based metabolic assessment in a rat model of obesity induced by a high-fat diet. *Anal. Bioanal. Chem.* **2009**, *395*, 1117–1124, doi:10.1007/s00216-009-3054-8.

58. Emwas, A.-H.; Roy, R.; McKay, T.R.; Tenori, L.; Saccenti, E.; Gowda, A.N.G.; Raftery, D.; Alahmari, F.; Jaremko, L.; Jaremko, M.; et al. NMR Spectroscopy for Metabolomics Research. *Metabolites*

2019, *9*, 123, doi:10.3390/metabo9070123.

59. Pravenec, M.; Křen, V.; Landa, V.; Mlejnek, P.; Musilová, A.; Šilhavý, J.; Šimáková, M.; Zídek, V. Recent progress in the genetics of spontaneously hypertensive rats. *Physiol. Res.* **2014**, *63*, S1-8, doi:10.33549/physiolres.932622.

60. Onuh, J.O.; Aliani, M. Metabolomics profiling in hypertension and blood pressure regulation: a review. *Clin. Hypertens.* **2020**, *26*, 23, doi:10.1186/s40885-020-00157-9.

61. Meikle, P.J.; Summers, S.A. Sphingolipids and phospholipids in insulin resistance and related metabolic disorders. *Nat. Rev. Endocrinol.* **2017**, *13*, 79–91, doi:10.1038/nrendo.2016.169.

62. Hannun, Y.A.; Obeid, L.M. Sphingolipids and their metabolism in physiology and disease. *Nat. Rev. Mol. Cell Biol.* **2018**, *19*, 175–191, doi:10.1038/nrm.2017.107.

63. Cogolludo, A.; Villamor, E.; Perez-Vizcaino, F.; Moreno, L. Ceramide and Regulation of Vascular Tone. *Int. J. Mol. Sci.* **2019**, *20*, doi:10.3390/ijms20020411.

64. Spijkers, L.J.A.; van den Akker, R.F.P.; Janssen, B.J.A.; Debets, J.J.; De Mey, J.G.R.; Stroes, E.S.G.; van den Born, B.-J.H.; Wijesinghe, D.S.; Chalfant, C.E.; MacAleese, L.; et al. Hypertension is associated with marked alterations in sphingolipid biology: a potential role for ceramide. *PLoS One* **2011**, *6*, e21817, doi:10.1371/journal.pone.0021817.

65. Muilwijk, M.; Callender, N.; Goorden, S.; Vaz, F.M.; van Valkengoed, I.G.M. Sex differences in the association of sphingolipids with age in Dutch and South-Asian Surinamese living in Amsterdam, the Netherlands. *Biol. Sex Differ.* **2021**, *12*, 13, doi:10.1186/s13293-020-00353-0.

66. Colafella, K.M.M.; Denton, K.M. Sex-specific differences in hypertension and associated cardiovascular disease. *Nat. Rev. Nephrol.* **2018**, *14*, 185–201, doi:10.1038/nrneph.2017.189.

67. Matsumoto, T.; Kobayashi, T.; Kamata, K. Role of lysophosphatidylcholine (LPC) in atherosclerosis. *Curr. Med. Chem.* **2007**, *14*, 3209–3220, doi:10.2174/092986707782793899.

68. Chakraborty, S.; Galla, S.; Cheng, X.; Yeo, J.-Y.; Mell, B.; Singh, V.; Yeoh, B.; Saha, P.; Mathew, A. V; Vijay-Kumar, M.; et al. Salt-Responsive Metabolite, β-Hydroxybutyrate, Attenuates Hypertension. *Cell Rep.* **2018**, *25*, 677-689.e4, doi:10.1016/j.celrep.2018.09.058.

69. Otsuka, T.; Takada, H.; Nishiyama, Y.; Kodani, E.; Saiki, Y.; Kato, K.; Kawada, T. Dyslipidemia and the Risk of Developing Hypertension in a Working-Age Male Population. *J. Am. Heart Assoc.* **2016**, *5*, e003053, doi:10.1161/JAHA.115.003053.

70. He, D.; Fan, F.; Jia, J.; Jiang, Y.; Sun, P.; Wu, Z.; Li, J.; Huo, Y.; Zhang, Y. Lipid profiles and the risk of new-onset hypertension in a Chinese community-based cohort. *Nutr. Metab. Cardiovasc. Dis.* **2021**, *31*, 911–920, doi:10.1016/j.numecd.2020.11.026.

71. Wymann, M.P.; Schneiter, R. Lipid signalling in disease. *Nat. Rev. Mol. Cell Biol.* **2008**, *9*, 162–176, doi:10.1038/nrm2335.

Annex. Supplementary Material of Manuscript 2

Supplementary table 1. **Plasma univariate analysis of the P407-induced hyperlipidemic rat model.** 139 metabolites are presented by the mean ± S.E.M per group; the summary of univariant analysis includes p-value, q-value (pFDR) and FC (P407/CON). Metabolites are listed by q-value. * Denotes p < 0.1 (tendency), ** p < 0.05 (significantly different) and *** p < 0.01 (high significantly different). DG, diacylglycerol; PC, phosphatidylcholine; ChoE, cholesterol ester; LPC, lysophospholipid; TG, triglyceride; SM, sphingomyelin.

Metabolite	CON	P407	p-value	q-value	FC
DG 36:4	1.53 ± 0.05	2.02 ± 0.03	<0.01***	<0.01***	1.33
PC 38:4	14.02 ± 0.61	20.4 ± 0.88	<0.01***	<0.01***	1.46
DG 34:3	0.2 ± 0.01	0.31 ± 0.02	<0.01***	0.01**	1.50
ChoE (17:0)	0.13 ± 0	0.16 ± 0.01	<0.01***	0.01**	1.28
PC 36:4	13.76 ± 0.61	17.73 ± 0.7	<0.01***	0.01**	1.29
ChoE (18:0)	0.12 ± 0.01	0.18 ± 0.01	<0.01***	0.02**	1.51
LPC 18:0	50.4 ± 1.83	58.86 ± 1.39	<0.01***	0.03**	1.17
DG 34:2	0.85 ± 0.04	1.05 ± 0.05	<0.01***	0.03**	1.24
TG 46:0	0.84 ± 0.05	1.16 ± 0.07	<0.01***	0.03**	1.37
ChoE (18:1)	2.52 ± 0.11	3.54 ± 0.25	<0.01***	0.03**	1.41
ChoE (16:0)	2.02 ± 0.09	2.39 ± 0.07	<0.01***	0.04**	1.18
PC 36:2	11.88 ± 0.63	14.81 ± 0.67	<0.01***	0.06*	1.25
ChoE (20:4)	65.98 ± 1.98	74.78 ± 2.06	<0.01***	0.06*	1.13
PC 31:0	0.03 ± 0	0.04 ± 0	<0.01***	0.06*	1.19
TG 54:6	15.66 ± 1.84	32.62 ± 4.94	<0.01***	0.07*	2.08
PC 34:3 e	0.02 ± 0	0.02 ± 0	0.01**	0.13	1.00
TG 48:0	1.26 ± 0.11	2.19 ± 0.31	0.01**	0.13	1.73
TG 46:2	0.37 ± 0.03	0.5 ± 0.04	0.01**	0.13	1.34
Fructose	0.4 ± 0.02	0.34 ± 0.01	0.01**	0.13	0.86
TG 54:4	10.76 ± 1.6	25.48 ± 5.24	0.02**	0.13	2.37
TG 54:2	0.69 ± 0.07	1.36 ± 0.24	0.02**	0.13	1.97
TG 52:1	0.65 ± 0.06	1.22 ± 0.21	0.02**	0.13	1.88
TG 50:2	10.73 ± 1.62	22 ± 4.08	0.02**	0.13	2.05
TG 50:1	3.12 ± 0.45	6.46 ± 1.23	0.02**	0.13	2.07
PC 35:2	0.35 ± 0.02	0.42 ± 0.02	0.02**	0.13	1.19
TG 54:3	3.84 ± 0.45	7.75 ± 1.47	0.02**	0.13	2.02
TG 52:3	40.05 ± 6.14	81.4 ± 15.33	0.02**	0.13	2.03
TG 50:0	0.42 ± 0.03	0.74 ± 0.12	0.02**	0.13	1.77
PC 34:0	0.29 ± 0.01	0.32 ± 0.01	0.03**	0.13	1.13

TG 54:7	6.06 ± 0.92	12.67 ± 2.51	0.03**	0.13	2.09
TG 52:2	10.05 ± 1.59	20.73 ± 4.05	0.03**	0.13	2.06
PC 38:6 e	0.05 ± 0	0.04 ± 0	0.03**	0.14	0.83
Phenylalanine	0.58 ± 0.04	0.44 ± 0.04	0.03**	0.14	0.77
PC 40:4	0.14 ± 0.01	0.18 ± 0.01	0.03**	0.14	1.26
TG 51:2	0.76 ± 0.07	1.34 ± 0.24	0.03**	0.15	1.77
TG 52:5	8.05 ± 1.17	16.74 ± 3.57	0.04**	0.15	2.08
TG 50:4	1.7 ± 0.27	3.21 ± 0.61	0.04**	0.15	1.89
LPC 18:2	33.17 ± 1.34	29.66 ± 0.86	0.04**	0.15	0.89
SM 36:1	1.09 ± 0.05	0.93 ± 0.05	0.04**	0.15	0.85
TG 52:6	1.25 ± 0.2	2.32 ± 0.45	0.04**	0.16	1.87
TG 48:2	1.4 ± 0.15	2.18 ± 0.33	0.05**	0.16	1.56
LPC 16:0 e	0.51 ± 0.02	0.47 ± 0.01	0.05**	0.18	0.91
ChoE (22:4)	3.88 ± 0.24	4.49 ± 0.17	0.05**	0.18	1.16
TG 50:3	5.61 ± 0.98	10 ± 1.87	0.05**	0.18	1.78
Malic Acid	0.38 ± 0.05	0.28 ± 0.02	0.06*	0.20	0.74
PE 36:4	4.39 ± 0.37	5.73 ± 0.6	0.07*	0.23	1.30
TG 48:3	0.48 ± 0.05	0.68 ± 0.09	0.07*	0.23	1.42
ChoE (20:2)	0.79 ± 0.05	0.93 ± 0.06	0.08*	0.23	1.18
SM 39:1	0.14 ± 0.01	0.11 ± 0.01	0.08*	0.23	0.78
Hydroxyproline	0.87 ± 0.08	1.1 ± 0.1	0.08*	0.24	1.27
Lactic Acid	7.79 ± 0.31	6.92 ± 0.39	0.09*	0.25	0.89
2-hydroxyglutaric	0.54 ± 0.05	0.44 ± 0.03	0.10	0.27	0.82
LPC 16:1 e	0.14 ± 0.01	0.13 ± 0	0.10	0.27	0.89
Threonine	1.18 ± 0.08	1.01 ± 0.05	0.11	0.28	0.86
Beta-Alanine	0.05 ± 0	0.06 ± 0.01	0.11	0.28	1.24
ChoE (22:5)	0.58 ± 0.07	0.71 ± 0.03	0.11	0.28	1.23
SM 42:3	4.71 ± 0.28	4.15 ± 0.19	0.11	0.28	0.88
TG 48:1	1.63 ± 0.16	2.18 ± 0.3	0.12	0.29	1.34
PC 38:3	0.78 ± 0.09	0.97 ± 0.08	0.13	0.30	1.24
Lysine	0.66 ± 0.04	0.76 ± 0.05	0.13	0.30	1.15
Alpha-Tocopherol	0.66 ± 0.05	0.55 ± 0.05	0.13	0.30	0.84
TG 46:1	0.68 ± 0.07	0.84 ± 0.07	0.13	0.30	1.23
LPC 18:0 e	0.1 ± 0	0.09 ± 0	0.14	0.31	0.92
Glycolic Acid	2.99 ± 0.13	2.68 ± 0.16	0.14	0.31	0.90
Alpha-Ketoglutarate	1.12 ± 0.05	1 ± 0.06	0.15	0.32	0.90

LPC 20:0	0.29 ± 0.02	0.33 ± 0.02	0.15	0.32	1.12
Glyceric Acid	1.15 ± 0.1	0.96 ± 0.08	0.16	0.33	0.84
3-Hydroxybutiric Acid	1.61 ± 0.08	1.44 ± 0.08	0.15	0.33	0.90
Methionine	0.1 ± 0.01	0.12 ± 0.01	0.17	0.35	1.15
PC 36:2 e	0.01 ± 0	0.02 ± 0	0.17	0.35	1.25
PC 38:4 e	0.04 ± 0	0.05 ± 0	0.18	0.35	1.12
LPC 18:1	13.89 ± 0.48	13.02 ± 0.42	0.18	0.35	0.94
Glucose-6-phosphate	0.15 ± 0.01	0.18 ± 0.02	0.19	0.35	1.21
Proline	0.24 ± 0.01	0.27 ± 0.01	0.19	0.35	1.09
Glycerol	3.68 ± 0.22	4.2 ± 0.32	0.19	0.35	1.14
PC 33:1	0.06 ± 0	0.07 ± 0	0.20	0.36	1.13
SM 35:1	0.16 ± 0.01	0.15 ± 0.01	0.20	0.36	0.90
SM 42:2	9.81 ± 0.63	8.8 ± 0.46	0.21	0.37	0.90
Glycine	2.02 ± 0.07	2.16 ± 0.09	0.22	0.38	1.07
Alanine	0.31 ± 0.04	0.39 ± 0.05	0.22	0.38	1.25
DG 34:1	1.02 ± 0.04	1.11 ± 0.06	0.22	0.38	1.09
PC 32:0	0.59 ± 0.02	0.62 ± 0.01	0.24	0.41	1.06
SM 42:1	13.11 ± 0.53	12.31 ± 0.41	0.25	0.41	0.94
ChoE (18:2)	16.99 ± 0.99	18.25 ± 0.4	0.25	0.41	1.07
Glucose	0.71 ± 0.01	0.75 ± 0.03	0.25	0.41	1.06
Asparagine	0.15 ± 0.02	0.18 ± 0.01	0.26	0.42	1.18
Fructose-6-phosphate	0.15 ± 0.02	0.18 ± 0.02	0.28	0.44	1.20
PC 38:5 e	0.08 ± 0.01	0.09 ± 0	0.28	0.44	1.10
SM 38:1	0.47 ± 0.02	0.44 ± 0.02	0.28	0.44	0.93
Serine	0.26 ± 0.01	0.29 ± 0.03	0.29	0.44	1.13
SM 32:1	0.22 ± 0.01	0.2 ± 0.01	0.29	0.44	0.94
SM 34:2	1.53 ± 0.08	1.44 ± 0.02	0.29	0.44	0.94
Glutamic Acid	0.1 ± 0.01	0.11 ± 0	0.29	0.44	1.09
PC 30:0	0.04 ± 0	0.04 ± 0	0.30	0.45	1.07
SM 43:1	0.97 ± 0.04	0.92 ± 0.04	0.31	0.46	0.94
PC 32:1	0.29 ± 0.03	0.26 ± 0.01	0.36	0.51	0.89
PC 36:0	0.07 ± 0	0.07 ± 0	0.38	0.54	1.07
PC 40:5	0.16 ± 0.02	0.19 ± 0.02	0.40	0.56	1.15
PC 36:3 e	0.05 ± 0	0.05 ± 0	0.40	0.56	1.07
ChoE (18:3)	1.32 ± 0.08	1.4 ± 0.06	0.41	0.56	1.06
SM 34:1	15.83 ± 0.76	15.09 ± 0.48	0.42	0.56	0.95

LPC 15:0	0.91 ± 0.04	0.87 ± 0.02	0.42	0.56	0.96
PC 34:1 e	0.1 ± 0.01	0.1 ± 0	0.42	0.56	0.94
SM 41:1	3.54 ± 0.17	3.37 ± 0.13	0.45	0.60	0.95
PC 32:2	0.19 ± 0.01	0.2 ± 0.01	0.46	0.60	1.06
Histidine	0.12 ± 0.01	0.14 ± 0.03	0.46	0.60	1.18
Citric Acid	3.87 ± 0.11	3.75 ± 0.12	0.47	0.61	0.97
SM 36:2	0.4 ± 0.02	0.38 ± 0.02	0.48	0.62	0.96
PC 42:4 e	0.01 ± 0	0.01 ± 0	0.50	0.63	1.25
PC 34:1	3.59 ± 0.21	3.78 ± 0.18	0.50	0.64	1.05
SM 40:1	3.3 ± 0.16	3.16 ± 0.13	0.51	0.64	0.96
Pyruvic Acid	15.87 ± 1.01	14.88 ± 1.19	0.53	0.66	0.94
ChoE (16:1)	0.56 ± 0.05	0.52 ± 0.05	0.56	0.68	0.93
Ribose	3.69 ± 0.23	4.03 ± 0.56	0.58	0.71	1.09
Tryptophan	1.24 ± 0.06	1.29 ± 0.05	0.59	0.71	1.04
Urea	2.18 ± 0.1	2.11 ± 0.1	0.59	0.71	0.96
Succinic Acid	0.64 ± 0.03	0.62 ± 0.03	0.60	0.71	0.97
PC 38:2	0.11 ± 0.01	0.12 ± 0.02	0.62	0.74	1.10
Ornithine	2.4 ± 0.22	2.55 ± 0.21	0.64	0.74	1.06
SM 41:2	0.56 ± 0.03	0.58 ± 0.03	0.64	0.74	1.04
Valine	0.48 ± 0.02	0.46 ± 0.03	0.65	0.74	0.97
ChoE (17:1)	0.09 ± 0.01	0.1 ± 0.01	0.67	0.76	1.04
Tyrosine	0.59 ± 0.04	0.61 ± 0.03	0.67	0.76	1.03
DG 36:2	1.26 ± 0.09	1.31 ± 0.05	0.68	0.76	1.03
Leucine	0.05 ± 0.0	0.04 ± 0.0	0.69	0.76	0.96
Aspartic Acid	0.55 ± 0.04	0.57 ± 0.04	0.73	0.79	1.04
ChoE (22:6)	2.03 ± 0.14	1.97 ± 0.12	0.74	0.80	0.97
SM 40:2	0.66 ± 0.04	0.68 ± 0.03	0.76	0.82	1.02
LPC 16:0	78.98 ± 1.7	79.45 ± 1.23	0.82	0.88	1.01
Glutamine	1.19 ± 0.22	1.14 ± 0.2	0.85	0.90	0.95
Fumaric Acid	0.86 ± 0.09	0.84 ± 0.1	0.92	0.97	0.98
Threonic Acid	2.08 ± 0.13	2.07 ± 0.08	0.93	0.97	0.99
Isoleucine	0.12 ± 0.01	0.12 ± 0.01	0.93	0.97	1.01
SM 33:1	0.31 ± 0.01	0.31 ± 0.01	0.94	0.97	1.00
Oleic Acid	1.6 ± 0.12	1.6 ± 0.08	0.96	0.98	1.00
PE 38:5 e	1.47 ± 0.4	1.46 ± 0.25	0.98	0.99	0.99
Aconitic Acid	0.01 ± 0	0.01 ± 0	1.00	1.00	1.00

PC 33:0	0.03 ± 0	0.03 ± 0	1.00	1.00	1.00

Supplementary table 2. **Urine univariate analysis of the P407-induced hyperlipidemic rat model.** 43 metabolites are presented by the mean ± SEM per group; the summary of univariant analysis includes p-value, q-value (pFDR) and FC (P407/CON). Metabolites are listed by q-value. * Denotes p < 0.1 (tendency), ** p < 0.05 (significantly different) and *** p < 0.01 (high significantly different). TMAO, trimethylamine N-oxide; PAG, phenylacetylglycine; DG, diacylglycerol; PC, phosphatidylcholine; ChoE, cholesterol ester; LPC, lysophospholipid; TG, triglyceride; sphingomyelin, SM.

Metabolite	CON	P407	p-value	q-value	FC
TMAO	2.31 ± 0.26	1.28 ± 0.09	<0.01***	0.15	0.55
PAG	39.07 ± 3.42	63.78 ± 7.31	0.01**	0.23	1.63
2-deoxycytidine	1.89 ± 0.19	1.36 ± 0.11	0.03**	0.35	0.72
Leucine	11.97 ± 1.03	9.23 ± 0.38	0.03**	0.35	0.77
3-hydroxyisovalerate	3.38 ± 0.15	2.9 ± 0.16	0.06*	0.55	0.86
Betaine	25.78 ± 2.25	21.36 ± 0.62	0.09*	0.62	0.83
HPPA sulfate	6.98 ± 1.77	14.91 ± 3.68	0.10*	0.62	2.14
o-Coumaric acid	3.48 ± 0.58	4.99 ± 0.75	0.13	0.67	1.44
Creatinine	126.44 ± 6.22	114.02 ± 4.64	0.13	0.67	0.90
Trimethylamine	0.91 ± 0.12	1.37 ± 0.26	0.18	0.79	1.50
Malate	1.92 ± 0.12	2.84 ± 0.65	0.20	0.79	1.48
Tyrosine	14.15 ± 3.39	21.75 ± 4.56	0.21	0.79	1.54
N,N-Dimethylglycine	6.09 ± 1.19	4.53 ± 0.52	0.26	0.79	0.74
2-Hydroxyisobutyrate	0.004 ± 0.001	0.003 ± 0.0007	0.27	0.79	0.62
Formate	1.6 ± 0.25	2.14 ± 0.39	0.27	0.79	1.34
Glycine	10.24 ± 0.78	9.21 ± 0.5	0.28	0.79	0.90
4-PY	2.98 ± 0.55	2.31 ± 0.34	0.32	0.81	0.78
3-HPPA	9.9 ± 2.38	14.22 ± 3.47	0.35	0.81	1.44
Fumarate	3.78 ± 0.52	3.1 ± 0.39	0.36	0.81	0.82
Allantoin	230.44 ± 5.54	222.16 ± 7.86	0.41	0.81	0.96
Sarcosine	3.99 ± 0.36	4.36 ± 0.26	0.43	0.87	1.09
Indoxyl Sulphate	7.5 ± 0.73	8.39 ± 1.01	0.48	0.87	1.12
Tryptophan	7.52 ± 0.74	8.4 ± 1.02	0.49	0.87	1.12
Alanine	3.97 ± 0.28	3.74 ± 0.16	0.50	0.87	0.94
Methylamine	5.17 ± 0.21	4.97 ± 0.2	0.52	0.87	0.96
N-acetylglycoproteins	73.29 ± 8.32	66.48 ± 5.35	0.54	0.87	0.91
2-Oxoglutarate	142.06 ± 13.08	129.55 ± 15.72	0.56	0.87	0.91
3-methyl-2-oxovalerate	4.2 ± 0.39	3.95 ± 0.2	0.59	0.87	0.94
Hippurate	267.88 ± 27.15	245.29 ± 32.31	0.60	0.87	0.92

Acetate	4.74 ± 0.58	5.07 ± 0.39	0.64	0.87	1.07
1-methylnicotinamide	0.02 ± 0.01	0.03 ± 0.01	0.65	0.87	1.24
Pseudouridine	10.38 ± 0.73	10.14 ± 0.5	0.79	0.88	0.98
α-hydroxyhippurate	1.09 ± 0.11	1.12 ± 0.09	0.82	0.88	1.03
Succinate	43.05 ± 3.57	43.96 ± 2.8	0.84	0.95	1.02
Taurine	417.08 ± 39.53	428.39 ± 40.02	0.84	0.95	1.03
Dimethylamine	49.3 ± 2.54	48.57 ± 2.33	0.86	0.95	0.99
N-Acetylglycine	29.61 ± 2.69	29.02 ± 1.87	0.87	0.95	0.98
Citrate	252.17 ± 20.74	258.04 ± 28.6	0.88	0.95	1.02
Fucose	10.19 ± 0.38	10.26 ± 0.54	0.92	0.95	1.01
NAD+	0.3 ± 0.04	0.3 ± 0.04	0.92	0.95	0.98
Valine	1.11 ± 0.12	1.1 ± 0.02	0.93	0.95	0.99
N6-Acetyllysine	16.84 ± 0.91	16.72 ± 1.02	0.93	0.95	0.99
Lactate	10.19 ± 0.97	10.17 ± 0.76	0.99	0.95	1.00

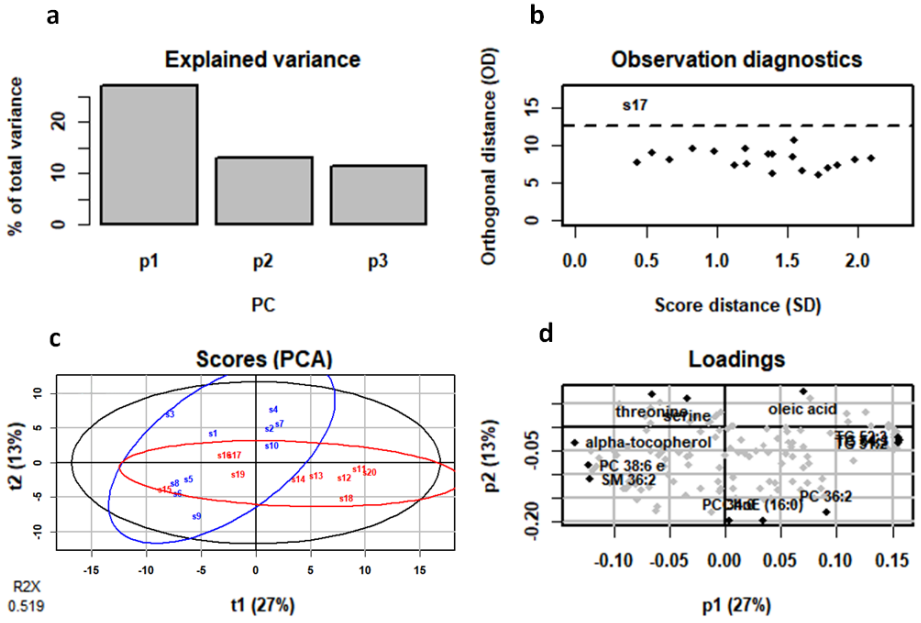

Supplementary figure 1. Plasma multivariate analysis of the P407-induced hyperlipidemic rat model: PCA summary plot. (a) Explained variance. The scree plot suggests that 3 components may be sufficient to capture most of the variance. (b) Observation diagnostics. This graphics shows the distances within and orthogonal to the projection plane the name of the samples with a high value for at least one of the distances is indicated. (c) Score plot (PCA). The total variance explained is 40%: PC1 explains the 27 % and the PC2 explains the 13%, represented the CON group in blue and P407 group in red. (d) The variables with most extreme values (positive and negative) for each loading are black coloured and labelled.

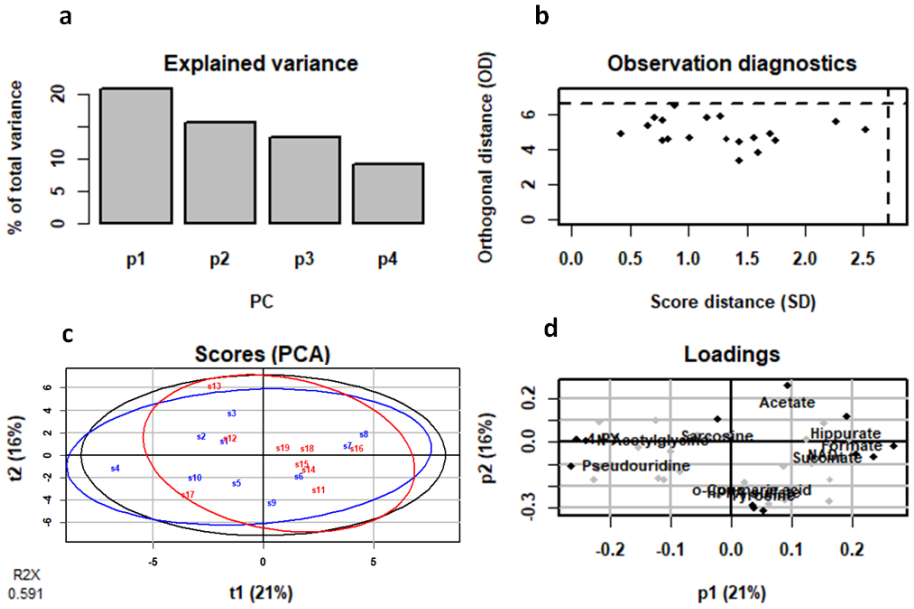

Supplementary figure 2. Urine multivariate analysis of the P407-induced hyperlipidemic rat model: PCA summary plot. (**a**) Explained variance. The scree plot suggests that 4 components may be sufficient to capture most of the variance. (**b**) Observation diagnostics. This graphics shows the distances within and orthogonal to the projection plane the name of the samples with a high value for at least one of the distances are indicated. (**c**) Score plot (PCA). The total variance explained is 37%: PC1 explains the 21 % and the PC2 explains the 16%, represented the CON group in blue and P407 group in red. (**d**) The variables with most extreme values (positive and negative) for each loading are black coloured and labelled.

Supplementary table 3. Plasma univariate analysis of the SHR/WKY model. 128 metabolites are presented as the mean ± S.E.M per group; the summary of univariant analysis include p-value, q-value (pFDR) and FC (SHR/WKY). Metabolites are listed by q-value. * Denotes $p < 0.1$ (tendency), ** $p < 0.05$ (significantly different) and *** $p < 0.01$ (high significantly different). DG, diacylglycerol; PC, phosphatidylcholine; ChoE, cholesterol ester; LPC, lysophospholipid; TG, triglyceride; SM, sphingomyelin.

Metabolite	WKY	SHR	*p*-value	*q*-value	FC
Threonic acid	3.19 ± 0.15	1.07 ± 0.07	<0.01***	<0.01***	0.34
PC 32:0	0.98 ± 0.03	1.44 ± 0.04	<0.01***	<0.01***	1.47
PC 36:4	30.51 ± 1.27	43.46 ± 1.1	<0.01***	<0.01***	1.42
PC 34:1	5.36 ± 0.29	8.87 ± 0.37	<0.01***	<0.01***	1.66
LPC 16:1 e	0.13 ± 0	0.18 ± 0.01	<0.01***	<0.01***	1.38
ChoE (18:3)	1.45 ± 0.11	3.05 ± 0.22	<0.01***	<0.01***	2.10
ChoE (20:2)	3 ± 0.46	6.58 ± 0.21	<0.01***	<0.01***	2.20
SM 34:1	22.65 ± 1.16	31.41 ± 1.03	<0.01***	<0.01***	1.39
SM 34:2	1.72 ± 0.05	2.36 ± 0.09	<0.01***	<0.01***	1.37
SM 41:1	7.36 ± 0.16	8.87 ± 0.2	<0.01***	<0.01***	1.20

SM 41:2	1.57 ± 0.07	2.09 ± 0.05	<0.01***	<0.01***	1.33
ChoE (22:5)	1.8 ± 0.29	3.78 ± 0.19	<0.01***	<0.01***	2.10
PC 34:0	0.5 ± 0.02	0.63 ± 0.01	<0.01***	<0.01***	1.26
SM 40:2	1.03 ± 0.05	1.36 ± 0.04	<0.01***	<0.01***	1.32
ChoE (22:4)	18.21 ± 2.96	37.47 ± 1.3	<0.01***	<0.01***	2.06
PC 30:0	0.06 ± 0	0.11 ± 0.01	<0.01***	<0.01***	1.84
ChoE (20:4)	64.55 ± 4.42	97.45 ± 5.14	<0.01***	<0.01***	1.51
ChoE (16:1)	0.28 ± 0.03	0.62 ± 0.06	<0.01***	<0.01***	2.17
SM 42:1	23.82 ± 0.55	28.34 ± 0.76	<0.01***	<0.01***	1.19
Glutamine	0.23 ± 0.02	0.09 ± 0.02	<0.01***	<0.01***	0.41
LPC 16:0 e	0.37 ± 0.02	0.46 ± 0.01	<0.01***	<0.01***	1.24
PC 32:1	0.57 ± 0.07	1.26 ± 0.13	<0.01***	<0.01***	2.19
PC 32:2	0.24 ± 0.02	0.37 ± 0.02	<0.01***	<0.01***	1.55
PC 38:4	33.55 ± 1.24	40.71 ± 1.08	<0.01***	<0.01***	1.21
PC 40:5	1.26 ± 0.05	1.67 ± 0.07	<0.01***	<0.01***	1.32
SM 32:1	0.23 ± 0.02	0.32 ± 0.01	<0.01***	<0.01***	1.36
Asparagine	0.43 ± 0.04	0.24 ± 0.03	<0.01***	<0.01***	0.55
SM 36:2	0.52 ± 0.01	0.67 ± 0.03	<0.01***	0.01**	1.30
Tyrosine	0.91 ± 0.07	0.54 ± 0.06	<0.01***	0.01**	0.59
LPC 16:0	88.34 ± 3.31	105.66 ± 2.98	<0.01***	0.01**	1.20
PC 31:0	0.06 ± 0	0.08 ± 0	<0.01***	0.01**	1.32
DG 36:4	3.45 ± 0.19	2.63 ± 0.06	<0.01***	0.01**	0.76
SM 33:1	0.45 ± 0.01	0.51 ± 0.01	<0.01***	0.01**	1.15
Glyceric acid	0.84 ± 0.04	1.15 ± 0.08	<0.01***	0.02**	1.38
ChoE (18:2)	19.66 ± 1.2	25.35 ± 1.24	0.01**	0.02***	1.29
PC 33:1	0.09 ± 0.01	0.13 ± 0.01	0.01**	0.02**	1.41
LPC 18:1	16.17 ± 0.98	20.26 ± 0.86	0.01**	0.02**	1.25
Serine	0.48 ± 0.05	0.66 ± 0.03	0.01**	0.02**	1.38
Glycine	7.35 ± 0.13	8.39 ± 0.29	0.01**	0.03**	1.14
3-hydroxybutiric acid	2.76 ± 0.3	1.76 ± 0.08	0.01**	0.03**	0.64
Beta-alanine	0.11 ± 0.01	0.16 ± 0.01	0.01**	0.03**	1.45
ChoE (22:6)	3.57 ± 0.2	4.58 ± 0.27	0.01**	0.03**	1.28
Citric acid	4.88 ± 0.21	4.18 ± 0.07	0.01**	0.03**	0.86
Ribose	15.87 ± 1.61	31.01 ± 4.47	0.01**	0.03**	1.95
SM 40:1	7.56 ± 0.27	8.69 ± 0.27	0.01**	0.03**	1.15
PC 40:4	0.35 ± 0.02	0.51 ± 0.05	0.01**	0.03**	1.45

Urea	0.94 ± 0.04	0.79 ± 0.02	0.01**	0.03**	0.84
DG 36:2	1.19 ± 0.06	1.52 ± 0.1	0.02**	0.04**	1.28
SM 38:1	0.71 ± 0.04	0.85 ± 0.03	0.02**	0.04**	1.19
Valine	1.8 ± 0.05	1.55 ± 0.07	0.02**	0.05*	0.87
ChoE (17:0)	0.03 ± 0.01	0.07 ± 0.01	0.02**	0.05*	2.12
SM 39:1	0.28 ± 0.02	0.34 ± 0.01	0.02**	0.06*	1.21
Methionine	0.22 ± 0.01	0.19 ± 0.01	0.03**	0.07*	0.86
PC 33:0	0.05 ± 0	0.06 ± 0	0.03**	0.07*	1.23
SM 43:1	1.39 ± 0.14	1.77 ± 0.04	0.03**	0.07*	1.27
Succinic acid	0.46 ± 0.01	0.43 ± 0.01	0.03**	0.07*	0.93
TG 52:5	10.79 ± 1.32	7.26 ± 0.54	0.03**	0.08*	0.67
Fructose-6-phosphate	0.52 ± 0.09	0.29 ± 0.04	0.04**	0.10	0.56
Alpha-tocopherol	0.31 ± 0.02	0.43 ± 0.05	0.05*	0.10	1.40
SM 35:1	0.26 ± 0.02	0.3 ± 0.01	0.05*	0.10	1.18
Glutamic acid	0.2 ± 0.01	0.18 ± 0.01	0.05*	0.10	0.88
TG 52:3	65.43 ± 7.39	47.77 ± 3.27	0.05*	0.11	0.73
LPC 18:0 e	0.07 ± 0	0.09 ± 0	0.06*	0.11	1.17
DG 34:1	1.27 ± 0.1	1.56 ± 0.1	0.06*	0.12	1.23
LPC 15:0	0.88 ± 0.04	1.01 ± 0.05	0.06*	0.13	1.14
TG 50:4	1.8 ± 0.25	1.23 ± 0.11	0.07*	0.13	0.68
PC 38:2	0.24 ± 0.02	0.28 ± 0.02	0.07*	0.13	1.19
SM 42:3	6.78 ± 0.18	7.41 ± 0.27	0.08*	0.15	1.09
SM 36:1	1.47 ± 0.12	1.73 ± 0.07	0.08*	0.15	1.18
PC 35:2	0.52 ± 0.04	0.6 ± 0.02	0.09*	0.16	1.16
PC 36:2	14.82 ± 0.8	16.57 ± 0.5	0.09*	0.16	1.12
DG 34:3	0.55 ± 0.04	0.63 ± 0.02	0.10	0.18	1.15
LPC 20:0	0.32 ± 0.02	0.36 ± 0.02	0.10	0.18	1.12
Histidine	0.16 ± 0.01	0.13 ± 0.02	0.11	0.18	0.80
Lysine	0.53 ± 0.04	0.43 ± 0.04	0.11	0.18	0.80
TG 54:7	6.96 ± 0.84	5.33 ± 0.43	0.11	0.18	0.77
TG 52:6	1.45 ± 0.18	1.11 ± 0.07	0.12	0.20	0.77
Malic acid	0.43 ± 0.04	0.36 ± 0.01	0.12	0.20	0.84
Fumaric acid	0.82 ± 0.07	0.69 ± 0.03	0.12	0.20	0.84
Ornithine	6.5 ± 0.34	5.46 ± 0.54	0.13	0.20	0.84
Lactic acid	4.86 ± 0.11	4.5 ± 0.19	0.13	0.21	0.93
ChoE (18:1)	2.5 ± 0.15	2.78 ± 0.09	0.13	0.21	1.11

PC 38:3	0.68 ± 0.07	0.83 ± 0.07	0.14	0.22	1.21
Glycolic acid	11.31 ± 0.57	12.27 ± 0.26	0.16	0.24	1.08
TG 52:1	0.86 ± 0.1	0.68 ± 0.07	0.17	0.25	0.79
SM 42:2	23.85 ± 0.75	26.03 ± 1.28	0.17	0.25	1.09
TG 54:4	16.78 ± 2.34	12.94 ± 1.24	0.18	0.26	0.77
Threonine	2.64 ± 0.1	2.84 ± 0.1	0.19	0.27	1.08
Isoleucine	0.99 ± 0.12	0.79 ± 0.08	0.19	0.28	0.80
Glucose-6-phosphate	0.8 ± 0.12	0.6 ± 0.08	0.20	0.28	0.75
ChoE (18:0)	0.13 ± 0.01	0.19 ± 0.04	0.20	0.28	1.44
Cholesterol	0.15 ± 0	0.15 ± 0	0.21	0.29	0.96
TG 48:1	0.98 ± 0.15	1.24 ± 0.13	0.21	0.29	1.27
ChoE (16:0)	1.03 ± 0.09	1.17 ± 0.06	0.22	0.29	1.14
Leucine	0.29 ± 0.03	0.25 ± 0.02	0.28	0.37	0.86
TG 51:2	0.75 ± 0.1	0.63 ± 0.05	0.30	0.40	0.84
TG 50:0	0.31 ± 0.08	0.21 ± 0.04	0.32	0.42	0.69
Alpha-ketoglutarate	2.43 ± 0.16	2.63 ± 0.12	0.35	0.44	1.08
Aspartic acid	1.19 ± 0.03	1.26 ± 0.07	0.35	0.44	1.06
Tryptophan	3.01 ± 0.2	2.77 ± 0.18	0.37	0.47	0.92
TG 54:6	29.61 ± 2.43	27.31 ± 1.11	0.41	0.51	0.92
Fructose	1.69 ± 0.07	1.55 ± 0.17	0.43	0.54	0.91
2-hydroxyglutaric	0.75 ± 0.06	0.84 ± 0.1	0.45	0.56	1.12
TG 46:1	0.07 ± 0.01	0.07 ± 0.01	0.49	0.59	1.12
Hydroxyproline	3.34 ± 0.28	3.12 ± 0.15	0.50	0.61	0.93
DG 34:2	2.38 ± 0.07	2.3 ± 0.09	0.52	0.62	0.97
TG 48:0	0.88 ± 0.08	0.8 ± 0.08	0.53	0.63	0.92
Phenylalanine	2.14 ± 0.05	2.09 ± 0.08	0.56	0.64	0.97
Pyruvic acid	24.34 ± 2.58	22.24 ± 2.35	0.56	0.64	0.91
TG 50:3	7.8 ± 1.26	6.95 ± 0.61	0.56	0.64	0.89
TG 54:3	6.09 ± 0.76	5.54 ± 0.49	0.55	0.64	0.91
ChoE (17:1)	0.02 ± 0.01	0.02 ± 0.01	0.65	0.73	1.21
TG 50:2	14.25 ± 1.92	13.3 ± 1.1	0.67	0.75	0.93
TG 54:2	3.36 ± 0.41	3.15 ± 0.26	0.67	0.75	0.94
TG 48:3	0.24 ± 0.04	0.22 ± 0.02	0.69	0.76	0.92
Glucose	0.25 ± 0.01	0.24 ± 0.02	0.70	0.77	0.97
Oleic acid	1.81 ± 0.07	1.85 ± 0.09	0.72	0.78	1.02
TG 46:0	0.09 ± 0.01	0.09 ± 0.01	0.74	0.79	0.95

LPC 18:0	51.64 ± 2.31	52.59 ± 1.73	0.75	0.80	1.02
Alanine	1.08 ± 0.09	1.11 ± 0.05	0.77	0.81	1.03
Glycerol	2.98 ± 0.29	2.86 ± 0.26	0.76	0.81	0.96
LPC 18:2	51.01 ± 2.66	52.13 ± 2.65	0.77	0.81	1.02
TG 48:2	0.77 ± 0.12	0.8 ± 0.08	0.85	0.87	1.04
TG 50:1	4.04 ± 0.58	4.14 ± 0.36	0.89	0.91	1.02
Proline	1.01 ± 0.05	1.01 ± 0.05	0.90	0.92	0.99
TG 46:2	0.04 ± 0.01	0.04 ± 0	0.93	0.94	0.98
TG 52:2	15.55 ± 2.31	15.67 ± 1.31	0.97	0.97	1.01

Supplementary table 4. **Urine univariate analysis of the SHR/WKY model.** 32 metabolites are presented as the mean ± SEM per group; the summary of univariant analysis include p-value, q-value (pFDR) and FC (SHR/WKY). Metabolites are listed by q-value. * Denotes p < 0.1 (tendency), ** p < 0.05 (significantly different) and *** p < 0.01 (high significantly different). TMAO, trimethylamine N-oxide; PAG, phenylacetylglycine; DG, diacylglycerol; PC, phosphatidylcholine; ChoE, cholesterol ester; LPC, lysophospholipid; TG, triglyceride; sphingomyelin, SM.

Metabolite	WKY	SHR	p-value	q-value	FC
Fumarate	5.62 ± 0.34	3.11 ± 0.42	<0.01***	0.01**	0.55
4-Guanidinobutanoate	6.1 ± 1.23	13.17 ± 0.33	<0.01***	0.01**	2.16
Pyruvate	8.61 ± 1.13	4.2 ± 0.25	0.01**	0.08*	0.49
Alanine	8.98 ± 0.59	7.01 ± 0.39	0.02**	0.10	0.78
2-Oxoglutarate	370.5 ± 38.42	235.97 ± 31.6	0.02**	0.10	0.64
3-HPPA	11.01 ± 1.35	26.41 ± 5.21	0.02**	0.10	2.40
Lactate	28.09 ± 4.13	15.71 ± 2.06	0.03**	0.10	0.56
Phenylacetylglycine	96.34 ± 9.9	135.46 ± 11.92	0.03**	0.10	1.41
Choline	6.93 ± 0.53	8.82 ± 0.57	0.03**	0.11	1.27
3-HPPA Sulfate	3.21 ± 0.25	8.34 ± 2.02	0.04**	0.12	2.60
Trigonelline	0.63 ± 0.14	0.97 ± 0.08	0.05*	0.15	1.56
Citrate	354.81 ± 41.9	246.6 ± 30.65	0.06*	0.16	0.70
Betaine	9.4 ± 1.68	12.86 ± 0.77	0.10	0.24	1.37
1-Methylnicotinamide	0.08 ± 0.03	0.03 ± 0.01	0.16	0.36	0.35
Allantoin	204.41 ± 8.15	225.61 ± 13.96	0.22	0.44	1.10
Hippurate	59.91 ± 7.85	48.21 ± 4.03	0.22	0.44	0.80
Acetate	26.44 ± 16.81	4.77 ± 1.03	0.25	0.46	0.18
N-Acetylglycoproteins	86.39 ± 8.23	96.01 ± 3.1	0.31	0.54	1.11
Glucose	4.44 ± 0.44	3.83 ± 0.39	0.32	0.54	0.86
Dimethylsulfone	16.44 ± 1.97	14.34 ± 0.65	0.34	0.55	0.87
Glyoxylic acid	0.26 ± 0.09	0.36 ± 0.05	0.36	0.55	1.39

Creatinine	358.31 ± 21.53	335.86 ± 15.78	0.42	0.57	0.94
Taurine	341.46 ± 77.14	274.59 ± 22.27	0.43	0.57	0.80
Isoleucine	18.87 ± 1.77	17.02 ± 1.44	0.43	0.57	0.90
Pseudouridine	8.24 ± 0.45	8.75 ± 0.46	0.45	0.57	1.06
N,N-Dimethylglycine	7.28 ± 1.26	6.46 ± 0.74	0.59	0.72	0.89
Formate	2.28 ± 0.61	1.92 ± 0.27	0.60	0.72	0.84
Succinate	40.88 ± 5.66	38.42 ± 4.49	0.74	0.85	0.94
Fucose	7.61 ± 1.5	8.26 ± 1.95	0.80	0.87	1.09
Indoxyl sulfate	10.68 ± 0.68	10.44 ± 0.87	0.83	0.87	0.98
Methylamine	8.13 ± 1.14	7.8 ± 1.15	0.84	0.87	0.96
Glycine	15.98 ± 1.23	15.99 ± 2.04	1.00	1.00	1.00

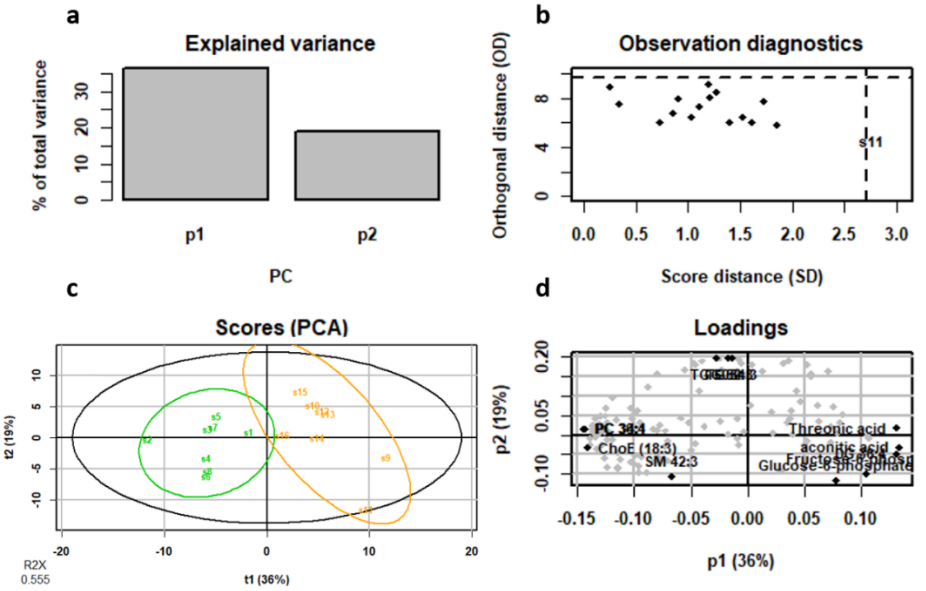

Supplementary figure 3. Plasma multivariate analysis of the SHR/WKY model: PCA summary plot. (**a**) Explained variance. The scree plot suggests that 2 components may be sufficient to capture most of the variance. (**b**) Observation diagnostics. This graphics shows the distances within and orthogonal to the projection plane the name of the samples with a high value for at least one of the distances is indicated. (**c**) Score plot (PCA). The total variance explained is 55%: PC1 explains the 36 % and the PC2 explains the 19%, represented the WKY group in green and SHR group in orange. (**d**) The variables with most extreme values (positive and negative) for each loading are black coloured and labelled.

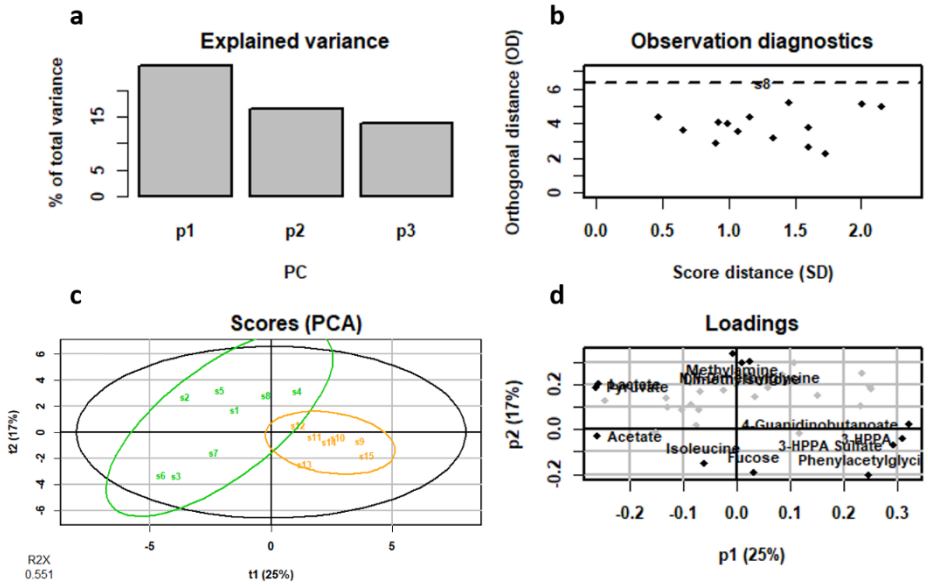

Supplementary figure 4. Urine multivariate analysis of the SHR/WKY model: PCA summary plot. (**a**) Explained variance. The scree plot suggests that 3 components may be sufficient to capture most of the variance. (**b**) Observation diagnostics. This graphics shows the distances within and orthogonal to the projection plane the name of the samples with a high value for at least one of the distances is indicated. (**c**) Score plot (PCA). The total variance explained is 42%: PC1 explains the 25 % and the PC2 explains the 17%, represented the WKY group in green and SHR group in orange. (**d**) The variables with most extreme values (positive and negative) for each loading are black coloured and labelled.

Supplementary table 5. Summary of the analysis of the preselected metabolites in human plasma grouped by sex (men and women) and the hyperlipidemia risk (normal and moderate). The statistical comparisons among groups were conducted using one-way ANOVA and the post-hoc Tukey. * Denotes p or q < 0.1 (tendency), ** p or q < 0.05 (significantly different) and *** p or q < 0.01 (high significantly different). DG, diacylglycerol; TG, triglyceride; ChoE, cholesterol ester; PC, phosphatidylcholine; LPC, lysophospholipid; N, normal; M, moderate.

	Men			Women		
Metabolite	**N (*n* = 24)**	**M (*n* = 50)**	***p*-value**	**N (*n* = 14)**	**M (*n* = 52)**	***p*-value**
DG 34:2	2.10 ± 0.05	2.44 ±0.03	<0.01***	1.90 ± 0.05	2.31 ± 0.06	<0.01***
DG 34:3	0.43 ± 0.02	0.50 ± 0.01	0.08*	0.39 ± 0.02	0.50 ± 0.02	0.01**
TG 46:0	0.70 ± 0.05	1.16 ± 0.17	<0.01***	0.51 ± 0.08	0.96 ± 0.18	0.07*
ChoE (17:0)	0.07 ± 0.01	0.25 ± 0.05	<0.01***	0.07 ± 0.01	0.27 ± 0.13	<0.01***
ChoE (18:0)	0.63 ± 0.02	0.55 ± 0.04	0.34	0.65 ± 0.02	0.49 ± 0.05	0.04**
PC 36:4	19.76 ± 0.70	23.21 ± 1.45	0.05**	19.00 ± 0.65	20.79 ± 1.13	0.73
DG 36:4	1.75 ± 0.07	1.96 ± 0.11	0.42	1.75 ± 0.07	2.16 ± 0.15	0.10*
PC 38:4	12.23 ± 0.48	14.35 ± 0.92	0.05**	12.30 ± 0.50	13.29 ± 0.89	0.73
LPC 18:0	13.81 ± 0.37	15.51 ± 0.70	0.17	14.12 ± 0.52	13.45 ± 0.73	0.93
ChoE (16:0)	6.45 ± 0.17	7.12 ± 0.28	0.11	6.86 ± 0.15	6.44 ± 0.34	0.72
ChoE (18:1)	27.09 ± 0.63	27.49 ± 0.91	0.99	27.35 ± 0.66	26.58 ± 1.55	0.96

Supplementary table 6. Summary of the analysis of the preselected metabolites in human plasma grouped by sex (men and women) and the hypertension risk (normal and moderate). The statistical

comparisons among groups were conducted using one-way ANOVA and the post-hoc Tukey. * Denotes p or q <0.1 (tendency), ** p or q<0.05 (significantly different) and *** p or q<0.01 (high significantly different). PC, phosphatidylcholine; LPC, lysophospholipid; ChoE, cholesterol ester; SM, sphingomyelin; DG, diacylglycerol; N, normal; M, moderate.

	Men			Women		
Metabolite	**N (*n* = 24)**	**M (*n* = 50)**	***p*-value**	**N (*n* = 14)**	**M (*n* = 52)**	***p*-value**
Threonic acid	1.45 ± 0.08	1.66 ± 0.06	0.45	1.58 ± 0.12	1.64 ± 0.07	0.99
PC 32:0	1.4 ± 0.06	1.48 ± 0.04	0.59	1.4 ± 0.05	1.39 ± 0.02	1.00
PC 36:4	22.92 ± 0.29	19.82 ± 0.16	0.08*	21.13 ± 0.2	18.81 ± 0.16	0.46
PC 34:1	26.15 ± 0.22	28.1 ± 0.17	0.55	24.17 ± 0.2	26.79 ± 0.16	0.46
LPC 16:1 e	0.32 ± 0.02	0.3 ± 0.02	0.54	0.32 ± 0.04	0.29 ± 0.02	0.15
ChoE (18:3)	15.63 ± 0.46	18.14 ± 0.18	0.35	20.82 ± 0.3	18.56 ± 0.16	0.61
ChoE (20:2)	0.33 ± 0.05	0.37 ± 0.04	0.65	0.35 ± 0.06	0.36 ± 0.04	0.99
SM 34:1	85.73 ± 0.42	97.57 ± 0.22	0.03**	108.09 ± 0.44	98.78 ± 0.24	0.27
SM 34:2	9.08 ± 0.14	10.56 ± 0.09	0.02**	11.64 ± 0.11	11.84 ± 0.09	0.99
SM 41:1	10.17 ± 0.17	11.81 ± 0.08	0.03**	14.47 ± 0.25	12.57 ± 0.08	0.04**
SM 41:2	5.03 ± 0.11	5.58 ± 0.07	0.30	7.83 ± 0.13	7.01 ± 0.07	0.14
ChoE (22:5)	0.63 ± 0.05	0.65 ± 0.03	0.92	0.74 ± 0.06	0.58 ± 0.03	0.03**
PC 34:0	0.28 ± 0.03	0.31 ± 0.01	1.00	0.31 ± 0.03	0.37 ± 0.14	0.94
SM 40:2	10 ± 0.14	11.42 ± 0.11	0.14	16 ± 0.21	14.05 ± 0.1	0.08
ChoE (22:4)	0.18 ± 0.06	0.15 ± 0.04	0.59	0.16 ± 0.06	0.14 ± 0.04	0.96
PC 30:0	0.22 ± 0.05	0.22 ± 0.03	1.00	0.22 ± 0.06	0.23 ± 0.03	0.99
ChoE (20:4)	70.95 ± 0.59	69.56 ± 0.26	0.99	73.71 ± 0.4	67.08 ± 0.27	0.57
ChoE (16:1)	3.38 ± 0.25	3.81 ± 0.14	0.75	3.07 ± 0.11	3.36 ± 0.11	0.94
SM 42:1	16.42 ± 0.23	19.02 ± 0.14	0.08*	20.56 ± 0.35	18.47 ± 0.12	0.38
Glutamine	1.86 ± 0.06	1.47 ± 0.08	0.64	1.45 ± 0.13	1.96 ± 0.2	0.59
LPC 16:0 e	0.36 ± 0.02	0.31 ± 0.01	0.02**	0.36 ± 0.04	0.31 ± 0.02	0.03**
PC 32:1	1.61 ± 0.13	1.81 ± 0.12	0.81	1.35 ± 0.14	1.68 ± 0.08	0.63
PC 32:2	0.34 ± 0.05	0.37 ± 0.03	0.85	0.45 ± 0.1	0.43 ± 0.03	0.97
PC 38:4	14.09 ± 0.23	12.31 ± 0.14	0.21	14.06 ± 0.17	12.03 ± 0.15	0.26
PC 40:5	0.6 ± 0.04	0.65 ± 0.03	0.65	0.59 ± 0.06	0.57 ± 0.02	0.97
SM 32:1	5.54 ± 0.16	5.92 ± 0.08	0.75	8.04 ± 0.19	5.99 ± 0.08	<0.01***
Asparagine	0.15 ± 0.03	0.14 ± 0.03	1.00	0.22 ± 0.05	0.3 ± 0.14	0.86
SM 36:2	6.11 ± 0.13	7.18 ± 0.08	0.05*	8.2 ± 0.18	7.92 ± 0.09	0.95
Tyrosine	2.23 ± 0.12	2.1 ± 0.08	1.00	2.36 ± 0.1	3.21 ± 0.29	0.65

LPC 16:0	48.73 ± 0.26	48.51 ± 0.19	1.00	47.85 ± 0.38	43.93 ± 0.16	0.45
PC 31:0	0.07 ± 0.02	0.07 ± 0.01	0.86	0.07 ± 0.03	0.07 ± 0.01	0.99
DG 36:4	1.9 ± 0.06	1.78 ± 0.06	0.80	1.79 ± 0.09	1.83 ± 0.06	1.00
SM 33:1	2.79 ± 0.09	2.96 ± 0.06	0.75	3.7 ± 0.11	2.95 ± 0.05	<0.01***
Glyceric acid	0.53 ± 0.02	0.6 ± 0.02	0.08*	0.59 ± 0.03	0.55 ± 0.03	0.70
ChoE (18:2)	127.4 ± 0.4	141.57 ± 0.25	0.05*	130.33 ± 0.38	131.4 ± 0.29	1.00
PC 33:1	0.25 ± 0.02	0.25 ± 0.02	1.00	0.22 ± 0.03	0.25 ± 0.02	0.48
LPC 18:1	11.56 ± 0.15	10.86 ± 0.11	0.72	9.8 ± 0.26	10.07 ± 0.12	0.99
Serine	0.21 ± 0.03	0.18 ± 0.03	0.92	0.26 ± 0.03	0.29 ± 0.09	0.96
Glycine	8.37 ± 0.14	7.41 ± 0.16	1.00	9.01 ± 0.21	26.3 ± 1.96	0.57
3-hydroxybutiric acid	2 ± 0.13	1.27 ± 0.1	<0.01***	1.24 ± 0.15	1.12 ± 0.07	0.93
Beta-alanine	0.73 ± 0.05	0.52 ± 0.06	0.96	0.55 ± 0.33	1.09 ± 0.39	0.75
ChoE (22:6)	12.45 ± 0.3	17.49 ± 0.16	<0.01***	17.79 ± 0.36	16.52 ± 0.14	0.81
Citric acid	6.43 ± 0.1	5.73 ± 0.09	0.27	5.21 ± 0.12	5.8 ± 0.1	0.60
Ribose	0.23 ± 0.03	0.27 ± 0.03	0.35	0.23 ± 0.05	0.23 ± 0.03	1.00
SM 40:1	25.15 ± 0.26	29.67 ± 0.16	0.03**	37.74 ± 0.37	31.25 ± 0.15	0.01**
PC 40:4	0.34 ± 0.05	0.28 ± 0.03	0.05*	0.27 ± 0.04	0.23 ± 0.02	0.72
DG 36:2	6.69 ± 0.11	6.71 ± 0.08	1.00	5.7 ± 0.17	6.59 ± 0.1	0.29
SM 38:1	9.42 ± 0.17	10.8 ± 0.09	0.09*	15.12 ± 0.26	11.6 ± 0.08	<0.01***
Valine	3.63 ± 0.09	3.11 ± 0.12	1.00	3.45 ± 0.23	6.63 ± 0.96	0.77
ChoE (17:0)	0.12 ± 0.07	0.13 ± 0.08	1.00	0.02 ± 0.02	0.13 ± 0.09	0.26

MANUSCRIPT 2

A PILOT STUDY FOR METABOLIC PROFILING OF OBESITY-ASSOCIATED MICROBIAL GUT DYSBIOSIS IN MALE WISTAR RATS

Julia Hernandez-Baixauli [1], Pere Puigbò [1,2,3], Helena Torrell [4], Hector Palacios-Jordan [4], Vicent J. Ribas Ripoll [5], Antoni Caimari [1], Josep M. Del Bas [1,*], Laura Baselga-Escudero [1] and Miquel Mulero [6,*]

[1] Eurecat, Centre Tecnològic de Catalunya, Unitat de Nutrició i Salut, 43204 Reus, Spain
[2] Department of Biochemistry and Biotechnology, Universitat Rovira i Virgili, 43007, Tarragona, Spain
[3] Department of Biology, University of Turku, 20014 Turku, Finland
[4] Eurecat, Centre Tecnològic de Catalunya, Centre for Omic Sciences (COS), Joint Unit Universitat Rovira i Virgili–EURECAT, 43204 Reus, Spain
[5] Eurecat, Centre Tecnològic de Catalunya, eHealth Unit, 08005 Barcelona, Spain
[6] Nutrigenomics Research Group, Department of Biochemistry and Biotechnology, Universitat Rovira i Virgili, 43007 Tarragona, Spain

* Correspondence: josep.delbas@eurecat.org; miquel.mulero@urv.cat

Published by Biomolecules

Biomolecules 2021, 11(2), 303; https://doi.org/10.3390/biom11020303

Received: 29 November 2020; Revised: 6 February 2021; Accepted: 13 February 2021; Published: 18 February 2021

(This article belongs to the Collection Metabolomics and Integrated Multi-Omics in Health and Disease)

UNIVERSITAT ROVIRA I VIRGILI
MULTI-OMICS BIOMARKERS OF METABOLIC HOMEOSTASIS OF RISK FACTORS ASSOCIATED TO NON-COMMUNICABLE DISEASES
Julia Hernandez Baixauli

Abstract: Obesity is one of the most incident and concerning disease worldwide. Definite strategies to prevent obesity and related complications remain elusive. Among the risk factors of the onset of obesity, gut microbiota might play an important role in the pathogenesis of the disease, and it has received extensive attention because it affects the host metabolism. In this study, we aimed to define a metabolic profile of the segregated obesity-associated gut dysbiosis risk factor. The study of the metabolome, in an obesity-associated gut dysbiosis model, provides a relevant way for the discrimination on the different biomarkers in the obesity onset. Thus, we developed a model of this obesity risk factors through the transference of gut microbiota from obese to non-obese male Wistar rats and performed a subsequent metabolic analysis in the receptor rats. Our results showed alterations in the lipid metabolism in plasma and in the phenylalanine metabolism in urine. In consequence, we have identified metabolic changes characterized by: (1) an increase in DG:34:2 in plasma, a decrease in hippurate, (2) an increase in 3-HPPA, and (3) an increase in o-coumaric acid. Hereby, we propose these metabolites as a metabolic profile associated to a segregated dysbiosis state related to obesity disease.

Keywords: microbial dysbiosis, gut microbiota, metagenomics, metabolomics, dysbiosis biomarkers, metabolic profile, diacylglycerol 34:2, hippurate, 3-HPPA, o-coumaric acid.

1. Introduction

Obesity has been defined as an excessive or abnormal accumulation of fat that represents a significant health risk [1]. The dramatical increase in the incidence of obesity worldwide, during the last 20 years across all ages, has changed the health perspective regarding this condition [2]. In fact, the term has evolved to "globesity," referring to the acquired pandemic characteristic of this condition due to globalization [3].

Lots of efforts have been devoted to try to decrease the incidence and prevalence, as well as the health complications associated to obesity [4]. For instance, obesity-associated risk factors have been associated with a large number of chronic diseases, including cardiovascular diseases (e.g., heart disease or stroke), which are the leading causes of death worldwide [5]. Furthermore, being obese can also lead to important disorders, including diabetes and its associated conditions [6] and musculoskeletal disorders, such as osteoarthritis [7]. In accordance to that, since 1980, the rates of diabetes have quadrupled around the world [8]. Finally, even some cancers (including endometrial, breast, ovarian, prostate, liver, gallbladder, kidney, and colon cancers) have also been associated with obesity [9], [10]. Interestingly, the risk of these noncommunicable diseases significantly increases even when a person is only slightly overweight and grows more seriously as the body mass index (BMI) rises [11], [12].

Unfortunately, definite strategies to tackle the prevention of obesity, and its related complications, remain elusive. In this regard, epidemiological studies have highlighted some potential environmental exposures, including diet, energy expenditure, early life influences, sleep deprivation, endocrine disruptors, chronic inflammation, and altered gut microbiota (GM) status, as important contributors to a higher obesity risk [13]–[15]. Among these, the GM has received extensive attention during the previous decade because it has been shown that manipulation of the GM may affect the host metabolism. In this sense, it has been proved that obesity is accompanied by a deep alteration of the host microbiota, and such condition has been defined as intestinal or gut dysbiosis [16]–[18].

In consequence, it has been demonstrated that the variation in GM might play an important role in the pathogenesis of obesity [19]. Although in healthy individuals the composition of intestinal microbiota is highly diverse, those exhibiting obesity, insulin resistance, and dyslipidaemia are characterized by low bacterial richness [20]. Moreover, the GM composition differs between obese and lean individuals [20], e.g., *Bacteroidetes* abundance is lower in obese individuals [20], and this proportion increases along with weight loss based on a low-calorie diet [21]. *Lactobacillus* and *Clostridium* spp. are associated with insulin resistance, being *Lactobacillus* positively correlated with fasting glucose and HbA1c levels, whereas *Clostridium* showed a negative correlation with these parameters [22], [23]. These data suggest that specific bacteria, as well as certain microbial metabolic activities, could be beneficial or

detrimental to the onset of obesity. Therefore, the GM has been suggested to be a driving force in the pathogenesis of obesity [24].

Although the evidence for many classical obesity biomarkers (i.e., adiponectin and C-reactive protein) has been initially promising in disease ethology, the evidence for a clear causal role in humans remains limited [25]. Furthermore, the ability to improve disease prediction has been little demonstrated beyond classical biomarkers. Hereby, it is time to focus on the risk factors of the onset of obesity to open to novel biomarkers discerning between health and disease. Consequently, in the "precision medicine" era, there is an increasing demand of novel and growing sources of potentially promising biomarkers, such as adipokines, cytokines, metabolites, and microRNAs, which are related to obesity and could bring new improvement to personalized prevention [26]. The field of metabolomics has been increasing as an important tool for the prognosis, and diagnosis, of different diseases stages, by investigating the endogenous levels of small metabolites in clinical practice from different biofluids standing out plasma/serum and urine [27], [28]. Furthermore, the scientific community has been called to use these tools to obtain information about the metabolism and potential biomarkers of obesity-associated risk factors [29].

Importantly, reshaping the GM has been shown as an effective strategy in weight loss and metabolic diseases amelioration [30]. To illustrate this fact, in a recent study with obese participants for avoiding weight gain after a weight reduction treatment, an autologous fecal microbiota transplantation was proposed to prevent weight regain (instead to modify the diet). The experimental approach focused on the idea that microbiota is more important to modulate obesity than diet [31]. Interestingly, the results showed that the autologous fecal microbiota transplantation preserved weight loss, and it was useful for glycemic control [31].

However, the gradual changes in the GM during weight gain and the related onset of metabolic abnormalities is still unclear in obesity [32]. In this sense, due to the urgent need of development of new and more effective strategies for disease prevention, a better understanding of the obesity pathophysiology, as well as new obesity-related biomarkers, are constantly demanded. In consequence, as GM plays such important role in obesity, a myriad of GM obesity associated biomarkers has been discovered. For example, it has been shown that the size and composition of bile acid pool can change due to GM's alterations, and this may evolve with subsequent altered signalling and activation of bile acid receptors such as farnesoid X receptor (FXR) and Takeda G protein-coupled receptor 5 (TGR5) and perturb, in consequence, lipid and glucose homeostasis [33], [34]. Moreover, dysbiosis alters short-chain fatty acids (SCFA) production with a consequent altered secretion of gut peptide YY(PYY) and glucagon-like peptide 1 (GLP-1), thus affecting appetite and satiety [35], [36]. Similarly, biomarkers for GM metabolites and by-products may increase gut permeability and nutrient absorption and therefore, additionally contribute to obesity. On the other hand, the main factor responsible for inducing increased gut permeability and microbiota translocation into host interior is the bacterial by-

product lipopolysaccharide. Nevertheless, due to the diverse outcomes of obesity-related complications (e.g., insulin resistance, inflammation, or gut dysbiosis), that are intimately related to each other, there is a lack of knowledge about the segregated effect of each obesity-related complications on metabolism and its specific biomarkers.

In this study, we have stablished a pilot study for metabolic profiling of obesity-associated microbial gut dysbiosis. In this sense, the transference of GM from obese to non-obese rats could allow us the discovery of novel discriminatory biomarkers related to this GM alterations, providing valuable information about the origin of obesity-associated biomarkers.

2. Materials and Methods

2.1. Animal Procedure

The Animal Ethics Committee of the Universitat Rovira i Virgili (Tarragona, Spain) approved all the procedures (code 10454). The experimental protocol followed the "Principles of Laboratory Care" and was carried out in accordance with the European Communities Council Directive (86/609/EEC). All animals were housed individually at 22 °C with a light/dark cycle of 12 h (lights on at 9 a.m.) and were given access to food and water ad libitum during all the experiment. Individual housing allows to determine an accurate estimation of food intake and to avoid crossed effects on microbiota because of the "coprophagy effect" usually shown in rats. Animals were randomly assigned to the different groups considering similar average body weight. Body weight and food intake were recorded weekly. For food intake estimation, the chow weight was assessed before and after 24 h of the consumption.

The whole study was planned in two differentiated steps: in the first experimental part, the CEC of cafeteria diet donors (CAF-D) and standard diet donors (STD-D) groups were obtained to collect the cecal content, and in the second experimental part, healthy rats corresponding to the cafeteria receptors (CAF-R) and the standard receptors (STD-R) groups received the cecal content of the donors, including a control group receiving the vehicle (CNT-R) (Figure 1).

2.1.1. Obtention of Cecal Donors Induced by Cafeteria Diet and Standard Diet

The first part of the experiment was performed using 14 male 8-week-old Wistar rats (Harlan Laboratories, Barcelona, Spain), which were randomly distributed into two experimental groups (n = 7). Afterwards, they were fed with two different diets depending on the group for 12 weeks (Figure 1a): the animals from the STD-D group were fed with standard chow diet (Tecklad Global 18% Protein Rodent Diet 2014, Harlan, Barcelona, Spain), and the animals from the CAF-D group were fed with a cafeteria diet with the following components (quantity per rat): bacon (8–12 g), biscuit with pâté (12–15 g), biscuit with cheese (10–12 g), muffins (pastry) (8–10 g), carrots (6–8 g), milk with sugar (220 g/L; 50 mL), water (ad libitum), and also with standard chow. Sample size and nutrient compositions of CAF-D and STD-D used herein have

been previously described in the literature [37]. The day before the sacrifice, feces (FCS) were collected to perform metagenomics. The animals were killed after 7 h of fasting by guillotine under anaesthesia (pentobarbital sodium, 50 mg/kg per body weight), and cecum (CEC) was rapidly removed, weighed, frozen in liquid nitrogen, and stored at −80 °C for GM preservation. For the preparation of the second part of the experiment, the cecal content of each group was pooled and diluted in 0.5% PBS-cys (4 g of CEC/15 mL of 0.5% PBS-cys). The cecal mixture was centrifuged to eliminate solid residues and to facilitate the subsequent administration by oral gavage. Finally, the mixture of each group was aliquoted (single-dose of 1.1 mL) and stored at −80 °C for further treatment.

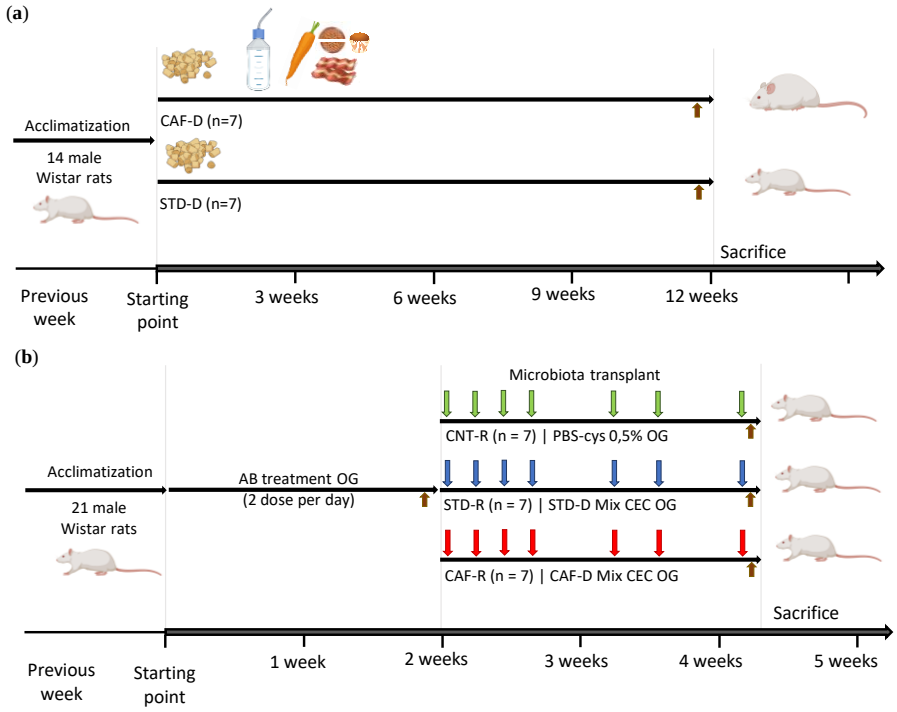

Figure 1. Schematic representation of the experimental design. (a) Obtention of cecum (CEC) donors induced by a cafeteria diet (CAF-D) and a standard diet (STD-D) (b) Obesity-associated gut dysbiosis with a healthy phenotype induced by cecal donors transplantation, including the previous depletion of host microbiota and the cecal content transplantation in healthy population. Brown arrow, feces (FCS) collection; green arrow, control group (CNT-R); blue arrow, standard receptors (STD-R); red arrow, cafeteria receptors (CAF-R). Abbreviations: OG, oral gavage; AB, antibiotic.

2.1.2. Model of Obesity-Associated Gut Dysbiosis with a Healthy Phenotype Induced by Cecal Transplantation

The second part of the experiment was carried out using 21 8-week-old male Wistar rats (Harlan Laboratories, Barcelona, Spain) and the procedure consisted into two parts (Figure 1b). First, all the rats were treated with an antibiotic cocktail to deplete the host microbiota. After the antibiotic treatment, the rats were randomly distributed into three experimental groups (n = 7) for the restoration of the microbiota

by the administration of the vehicle or the external GM (CNT-R, STD-R, and CAF-R groups). The animals were fed with a standard chow diet ad libitum (Teklad Global 18% Protein Rodent Diet 2014, Harlan, Barcelona, Spain). All the procedure was carried out with the maximum sterility.

The antibiotic cocktail was administered by oral gavage twice daily for 13 consecutive days to all groups (at 10:00 a.m. and 5:00 p.m.). It included a mixture of vancomycin (50 mg/kg), neomycin, and metronidazole (each at 100 mg/kg). In addition, the drinking water was supplemented with ampicillin (1 g/L) during the antibiotic treatment to avoid the growing of microorganism during the treatment [38]. At the end of the antibiotic treatment, FCS were collected to check the depletion of the host microbiota.

All animals received omeprazole (20 mg/kg) by oral gavage 24 h after the last antibiotic treatment and 4–5 h before every transplant to reduce the acidification of the environment and to allow the survival of microorganisms through the gastrointestinal tract. All the treatments were administered by oral gavage, and they consisted of following treatments: the CNT group was treated with 0.5% PBS-cys and the STD-R and CAF-R groups with STD-D and CAF-D cecal mix prepared in the first experiment, respectively. The microbiota transplant consisted of 4 consecutive days of treatment during the first week, 2 reminders on the second week, and finally, a weekly reminder over the last 2 weeks with 4 weeks of total duration. The day before the sacrifice, FCS and urine were collected to perform metagenomics and metabolomics, respectively. Urine was collected following the recommended hydrophobic sand method (avoiding stress and metabolic changes) [39]. For each rat, a single 300 g pack of hydrophobic sand was spread (LabSand, Coastline Global, Palo Alto, CA, USA) on the bottom of a mouse plastic microisolation cage. Urine was gathered with sodium azide (Sigma, St Louis, MO, USA) as preservative every half hour for 6 h and was subsequently pooled at the end of the session. The FCS and pooled urine samples for each animal were stored at − 80 °C until further analysis. At the end of the study, rats were killed under anaesthesia (pentobarbital sodium, 50 mg kg^{-1} body weight) by guillotine after 7 h of fasting to avoid interferences of the early postprandial state in plasma metabolites. Blood was collected, and plasma was obtained by centrifugation (2000× *g* for 15 min at 4 °C) and stored at −80 °C until analysis. Tissues were rapidly removed, weighted, snap-frozen in liquid nitrogen, and stored at −80 °C until further analyses.

2.2. Biochemical Parameters

2.2.1. Plasma Parameters

Enzymatic colorimetric kits were used for the determination of plasma total cholesterol, triglycerides, and glucose (QCA, Barcelona, Spain) and non-esterified free fatty acids (NEFAs) (WAKO, Neuss, Germany).

2.2.2. Liver Lipid Parameters

Liver lipids were extracted and quantified from a 100–120 mg liver piece using a method previously described in the literature [40]. Briefly, lipids were extracted with 1 mL of hexane/isopropanol (3:2, *v*/*v*) and degassed with gas nitrogen before leaving overnight under orbital agitation at room temperature protected from light. After an extraction with 0.3 mL of Na_2SO_4 (0.47 M), the lipid phase was dried with nitrogen gas and total lipids were quantified gravimetrically before emulsifying as described previously [41]. Triglycerides, cholesterol, and phospholipids were measured with commercial enzymatic kits (QCA, Barcelona, Spain).

2.3. Metagenomic Analysis

The genomic bacterial DNA was obtained from 700 to 1000 mg of FCS and CEC of previously collected with the QIAamp DNA stool kit (Qiagen, Hilden, Germany; cat. no. 51504) following the manufacturer's protocol. Partial 16S ribosomal RNA gene sequences were amplified from 20 ng of extracted DNA using three primer pairs, which target the V3, V4, and V6 regions, respectively. Equimolar pools of each fragment were combined to create the DNA library, which was subjected to a clonal amplification by an emulsion PCR. After an Ion Sphere Particle enrichment process, samples were loaded onto 318 chips and sequenced using the Ion Torrent PGM (Life Technologies, Carlsbad, CA, USA). The individual sequence reads were filtered by the PGM software (Life Technologies, Carlsbad, CA, USA) to remove low-quality and polyclonal sequences. Those reads were processed using QIIME [42], selecting only sequences with 150–200 bp and omitting homopolymers. 16S ribosomal RNA operational taxonomic units (OTUs) were assigned using uclust (>97% sequence homology) and a reference data set from Greengenes (Lawrence Berkeley National Laboratory, Berkeley, CA, USA).

2.4. Metabolomic Analysis: Plasma and Urine Approach

The method for the extraction of plasma lipids was ultrahigh performance liquid chromatography coupled with quadrupole time-of-flight (UHPLC-qTOF). For the extraction of the hydrophobic lipids, a liquid–liquid extraction based on the Folch procedure was performed by adding four volumes of chloroform:methanol (2:1, *v*/*v*) containing internal standard mixture (Lipidomic SPLASH®) to plasma. Then, the samples were mixed and incubated at −20 °C for 30 min. Afterwards, water with NaCl (0.8%) was added, and the mixture was centrifuged at 21.420× *g*. Lower phase was recovered, evaporated to dryness, reconstituted with methanol:methyl-tert-butyl ether (9:1, *v*/*v*), and analysed by UHPLC-qTOF (model 6550 of Agilent, Santa Clara, CA, USA) in positive electrospray ionization mode. The chromatographic consists in an elution with a ternary mobile phase containing water, methanol, and 2-propanol with 10 mM ammonium formate and 0.1% formic acid. The stationary phase was a C18 column (Kinetex EVO C18 Column, 2.6 µm, 2.1 mm × 100 mm) that allows the sequential elution of the more hydrophobic lipids such as TG, diacylglycerols (DG), phosphatidylcholines (PC), cholesterol esters (ChoE), lysophospholipids (LPC), and sphingomyelins (SM), among others. The identification of lipid species was performed

by matching their accurate mass and tandem mass spectrum, when available, to Metlin-PCDL from Agilent containing more than 40,000 metabolites and lipids. In addition, chromatographic behaviour of pure standards for each family and bibliographic information was used to ensure their putative identification. After putative identification of lipids, these were semiquantified in terms of internal standard response ratio using one internal standard for each lipid family.

The methodology followed for the extraction of plasma metabolites was gas chromatography coupled with quadrupole time-of-flight (GC-qTOF). For the extraction, a protein precipitation extraction was performed by adding eight volumes of methanol:water (8:2, *v*/*v*) containing internal standard mixture (succinic acid-d4, myristic acid-d27, glicerol-^{13}C3, and D-glucose-^{13}C6) to plasma samples. Then, the samples were mixed and incubated at 4 °C for 10 min and centrifuged at 21.420× *g*, and supernatant was evaporated to dryness before compound derivatization (metoximation and silylation). The derivatized compounds were analysed by GC-qTOF (model 7200 of Agilent, Santa Clara, CA, USA). The chromatographic separation was based on the Fiehn method, using a J&W Scientific HP5-MS (30 m × 0.25 mm i.d.), 0.25 µm film capillary column, and helium as carrier gas using an oven program from 60 to 325 °C. Ionization was done by electronic impact (EI), with electron energy of 70 eV and operated in full scan mode. The identification of metabolites was performed by matching their EI mass spectrum and retention time to metabolomic Fiehn library (Agilent, Santa Clara, CA, USA), which contains more than 1400 metabolites. After putative identification of metabolites, these were semiquantified in terms of internal standard response ratio.

The methodology followed for the extraction of urine metabolites was proton nuclear magnetic resonance (^{1}H-NMR). The urine sample was mixed (1:1, *v*/*v*) with phosphate buffered saline containing with 3-(Trimethylsilyl)propionic-2,2,3,3-d4 acid sodium salt (TSP) (Sigma Aldrich) and placed on a 5 nm NMR tube for direct analysis by ^{1}H-NMR. ^{1}H-NMR spectra were recorded at 300 K on an Avance III 600 spectrometer (Bruker®, Karlsruhe, Germany) operating at a proton frequency of 600.20 MHz using a 5 mm PBBO gradient probe. Diluted urine aqueous samples were measured and recorded in procno 11 using a one-dimensional ^{1}H pulse. Experiments were carried out using the nuclear Overhauser effect spectroscopy (NOESY). NOESY presaturation sequence (RD–90–t1–90–tm–90 ACQ) was used to suppress the residual water peak, and the mixing time was set at 100 ms. Solvent presaturation with irradiation power of 150 µW was applied during recycling delay (RD = 5 s) and mixing time (noesypr1d pulse program in Bruker®) to eliminate the residual water. The 90-pulse length was calibrated for each sample and varied from 11.21 to 11.38 ms. The spectral width was 9.6 kHz (16 ppm), and a total of 128 transients were collected into 64 k data points for each ^{1}H spectrum. The exponential line broadening applied before Fourier transformation was of 0.3 Hz. The frequency domain spectra were manually phased and baseline-corrected using TopSpin software (version 3.2, Bruker). Data was normalized by two different ways, by probabilistic method, to avoid differences between sample due to different urine concentration, and by ERETIC software. The

acquired 1H-NMR spectra were compared to references of pure compounds from the metabolic profiling AMIX spectra database (Bruker®), HMDB, and Chenomx databases for metabolite identification. In addition, we assigned metabolites by ^{1}H-^{1}H homonuclear correlation (COSY and TOCSY) and ^{1}H-^{13}C heteronuclear (HSQC) 2D NMR experiments and by correlation with pure compounds run in-house. After pre-processing, specific ^{1}H-NMR regions identified in the spectra were integrated using MATLAB scripts run in house. Curated identified regions across the spectra were exported to excel spreadsheet to evaluate robustness of the different ^{1}H-NMR signals and to give relative concentrations.

2.5. Pathway Analysis

The KEGG (Kyoto Encyclopedia of Genes and Genomes) pathway map was used to interpret the metabolomic data in the context of biological processes, pathways, and networks [43]. The most important features were analysed through KEGG to elucidate the global effect in metabolism.

2.6. Statistical Analysis

The statistical analysis was performed using the R software (version 4.0.1) and different libraries included in Bioconductor (version 3.11). The biochemical data are expressed as the mean ± standard error of the mean (SEM). Parametric unpaired *t*-test after a normality study was used for single statistical comparisons, thus a two-tailed value of $p < 0.05$ was considered. After parametric unpaired *t*-test, *p*-value adjustment for multiple comparisons was performed according to the Benjamin-Hochberg (B-H) correction considering a 5% of false discovery rate (FDR). The magnitude of difference between populations was determined by the determination of Fold Change (FC). For metagenomics, the number of OTUs per sample were scaled so each sample had the same mean and were filtered to only include OTUs that were present at 0.1% of the total counts in at least 3 samples [44]. Further, the random forest classifier was calculated to sort the most important metabolites that distinguish between the control (STD-R) and obesity-associated gut dysbiosis (CAF-R) group. Finally, correlation analysis between metagenomics and metabolomics were performed by kernel density plot and the correspondent test of equal densities.

2.7. Limitations

However, this research is limited by several shortcomings. As occurs in some studies, the design of the current study must be considered as a “pilot study” because the number of the animals is not high enough ($n = 7$ per group) to provide a strong statistical conclusion about the biomarkers. In addition, females must be included for further studies. Nonetheless, these metagenomic results must be interpreted with caution because 16S sequencing was performed. These issues should be considered to perform further experiments.

3. Results

3.1. Characterization and Metagenomic Analysis of Donor Animals: Induced by Cafeteria Diet and Standard Diet

Animals fed with an obesogenic diet presented a significant increase in body weight (g) (CAF-D = 550.09 ± 18.17 and STD-D = 443.05 ± 24.92; $p = 0.005$) and a huge decrease in CEC weight (g) (CAF-D = 4.34 ± 0.17 and STD-D = 5.59 ± 0.19; $p < 0.001$), respect those fed with a standard diet, in agreement with other researchers [45], [46].

To study the metabolic alterations of obesity-associated gut dysbiosis with a healthy phenotype, the previous step was the obtention of CEC donors for further transplant. Therefore, a metagenomic analysis was performed in donor groups (CAF-D and STD-D) in CEC and FCS to check the success on the obesity-associated gut dysbiosis. The reads count in 16S rRNA gene sequencing were 200.624–988.148 per sample.

Results from CEC showed a significant change in the two major phyla of the GM: *Firmicutes* (STD-D: 85.26%, CAF-D: 49.39%; $q = 0.001$) decreased and *Bacteroidetes* (STD-D: 12.83%, CAF-D: 34.77%; $q = 0.025$) increased in CAF-D group. Thus, there was an increase of the ratio of *Bacteroidetes/Firmicutes* in the CAF-D group (STD-D = 0.16 ± 0.04 and CAF-D = 0.81 ± 0.21; $p = 0.009$). Nevertheless, these alterations were not observed in FCS. Moreover, the results showed some changes in less represented phyla, e.g., the phylum *Tenericutes* was significantly decreased in the CAF-D group (STD-D: 0.29%, CAF-D: 0.11%; $q = 0.034$), the *Proteobacteria* (STD-D: 0.31%, CAF-D: 3.47%; $q = 0.034$) was increased, and the phylum *Verrucomicrobia* was almost significantly increased (STD-D: 1.21%, CAF-D: 12.01%; $q = 0.053$).

Focusing on genera, the differences between donor groups were summarized in Table S1 standing out that *Clostridiales* and *Bacteroidales* were the most altered taxa representing the main differences in *Firmicutes* and *Bacteroidetes* phyla, respectively. In the CAF-D group, some genera experienced changes as well: there was a significant increase of *Ruminococcus, Blautia*, and *Parabacteroides*. Some differences were common between FCS and CEC at genus level, as both experienced a significant decrease in an uncharacterized genus belonging to of *Clostridiales* (STD-D: 29.73%, CAF-D: 5.59%; $q = 0.019$) and an increase of *Parabacteroides* genus (STD-D: 0.42%, CAF-D: 3.44%; $q = 0.047$) in the CAF-D group. Other genus significantly decreased in CAF-D FCS group were, e.g., two *Clostridiales*, *Oscillospira* (STD-D: 5.03%, CAF-D: 1.93%; $q = 0.027$), and *Dehalobacterium* (STD-D: 0.16%, CAF-D: 0.05%; $q = 0.047$), and an uncharacterized genus of the *Rikenellaceae* family in the *Bacteroidales* order (STD-D: 2.17%, CAF-D: 0.83%; $q = 0.019$).

Alpha diversity values, which are measures of variability within a sample, were calculated with a variety of indices that measure richness and variation (including Shannon, Simpson, chao1, observed OTUs index, and phylogenetic diversity) (Figure S1). Shannon and Simpson indices showed evenness in the population of both groups.

The observed OTUs index was significantly decreased in FCS in the CAF-D group, though it was non-significantly decreased in CEC (FCS p = 0.036; CEC p = 0.066). However, chao1 was significantly lower in both, FCS and CEC (FCS p = 0.036; CEC p = 0.048). In addition, the phylogenetic diversity was significantly lower in CAF-D (FCS p = 0.030; CEC p = 0.012). The estimation of beta diversity, i.e., an indication of variability among groups, by means of a Principal Coordinate Analysis (PCoA) (Figure 2b) showed a clear and statistically significant separation between the STD-D and CAF-D groups (q < 0.001).

3.2. Depletion of Microbiota in Receptor Animals after the Antibiotic Treatment

After the obtention of the donors cecal content, the transplant in healthy animals was performed. Previously, the experimental procedure required a previous depletion of the host microbiota by means of an antibiotic treatment, and a subsequent metagenomic analysis of the FCS to evaluate the success of the depletion. The reads count in 16S rRNA gene sequencing were 188–342.242 per sample. The low minimum reads corresponds with a low quantity of bacterial DNA, which was also difficult to amplify. Data from the STD-D group were used to compare the microbiota after the antibiotic treatment. At the phylum level, all FCS samples had similar taxonomic relative abundance, composed mainly by *Firmicutes* (57%) and *Bacteroidetes* (30.09%) (Figure S2a). Other less abundant phyla included *Proteobacteria* (3.8%), *Verrumicomicrobia* (2.6%), *Spirochaetes* (1.6%), *Actinobacteria* (1%), *Cyanobacteria* (1%), and additional phyla not listed due to represent <1%. Thus, there is an emergence of less abundant phyla and a decrease in most abundant phyla (Figure S2b). Alpha diversity indices confirmed the decrease in bacteria after the treatment (Figure S2c). More concisely: (1) FCS samples showed lower levels of OTUs index per genus compared to the STD-D group; (2) Shannon and Simpson indices were 6.63 ± 0.12 and 0.99 ± 0.002, respectively; (3) the average of observed OTUs (124 ± 5.90) and chao 1 (465.65 ± 55.86) in the FCS were three orders of magnitude lower compared to the STD-D group; and 4) the phylogenetic diversity was 14.69 ± 1.38, being values too low compared to other studies. Moreover, the PCoA confirmed the homogeneity of the beta diversity of the host microbiota after the depletion treatment with antibiotics (Figure S2d).

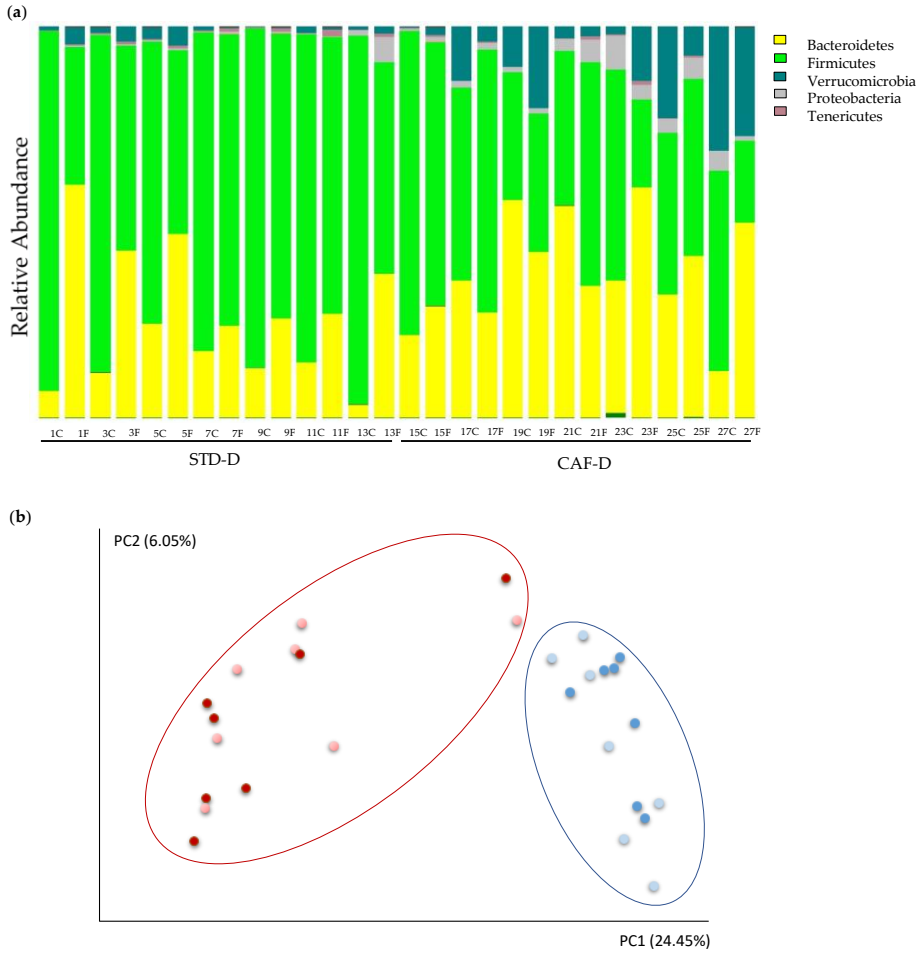

Figure 2. Changes in the metagenome of rats fed with cafeteria diet (CAF-D) and chow diet (STD-D). (a) the 5 phyla represented by relative abundance and (b) analysis of beta diversity represented by scores of each STD-D (blue) and CAF-D (red) groups in FCS (light color) and CEC (dark color) after Principal Coordinate Analysis (PCoA) with unweighted UniFrac.

3.3. Metagenomic Characterization of the Model of Obesity-Associated Gut Dysbiosis with a Healthy Phenotype

The biometric and biochemical parameters, plasma parameters, and liver biochemistry, which are summarized in Table S2, were carried out to better characterize the model of obesity-associated gut dysbiosis in the context of a healthy phenotype. Focusing on biometric parameters, the total white adipose tissue weight (gr.) increased in CAF-R group compared to the STD-R group; concretely a tendency to increase in MWAT (STD-R: 4.04 ± 0.26, CAF-R: 5.16 ± 0.52; p = 0.09) was observed and a slight increase in RWAT (STD-R: 7.14 ± 0.90, CAF-R: 9.70 ± 1.70; p = 0.22) was also assessed. Once the transplant was done, the effect of the cecal content transplant was mainly observed by a significant decrease in CEC weight (gr.) in the cecal content receptors groups versus the control group (CNT-R: 8.43 ± 0.63, STD-R + CAF-R: 5.28 ±

0.32; $p = 0.002$). Some plasma parameters presented a tendency to increase, including TG (STD-R: 80.91 ± 14.01, CAF-R: 117.30 ± 17.12; $p = 0.1$), TC (STD-R: 44.81 ± 9, CAF-R: 68.19 ± 11; $p = 0.1$), and NEFAs (STD-R: 0.37 ± 0.02, CAF-R: 0.43 ± 0.03; $p = 0.1$), while glucose remained unaltered. However, total liver lipids (STD-R: 38.57 ± 2.20, CAF-R: 28.99 ± 2.22; $p = 0.01$) significantly decreased in the CAF-R group, and specifically phospholipids (STD-R: 12.85 ± 0.60, CAF-R: 10.67 ± 0.67; $p = 0.03$) presented the highest decrease.

The reads count in 16S rRNA gene sequencing were 151.796–522.785 per sample. After the microbiota transplant, the composition of the communities showed a separation of the FCS and CEC samples in the second component (PC2) of the PCoA (Figure 3). The first component (PC1) of the PCoA clearly separates CNT-R and the transplanted rats (STD-R and CAF-D) (Figure 3). Thus, PC1 and PC2 explain 13.42% and 7.65% of the variability, respectively. Furthermore, the CNT-R group versus the transplanted microbiota rats (STD-R and CAF-D) had a smaller number of species, as shown by a significant decrease in the alpha diversity indices in CEC, i.e., chao1, observed OTUs and phylogenetic diversity. This decrease was not-significantly decreased in FCS (Figure S3).

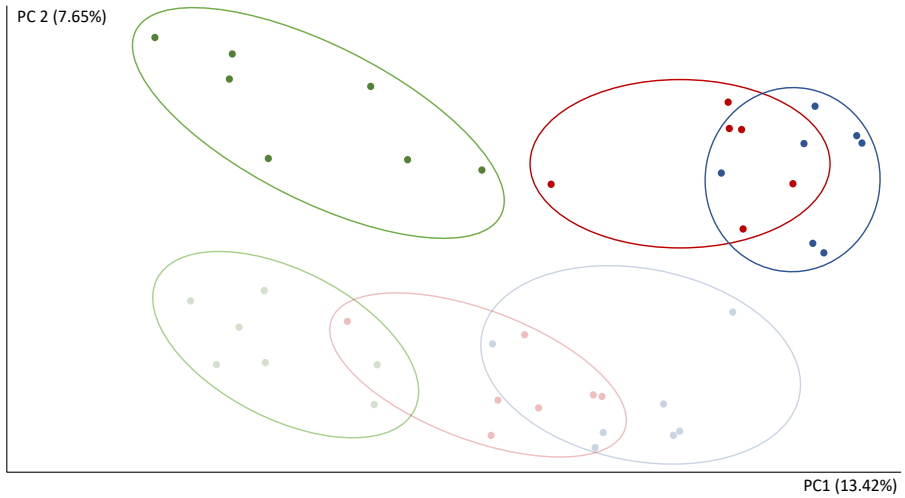

Figure 3. Analysis of beta diversity after the transplant represented by scores after PCoA (unweighted UniFrac). Green, CEC CNT-R; light green, FCS CNT-R; blue, CEC STD-R; light blue, FCS STD-R; red, CEC CAF-R; light red, FCS CAF-R.

At phylum level, the effect of the transplant in STD-R promoted an establishment of *Firmicutes* in CEC (CNT-R: 71.82% vs. STD-R: 91.02%; $p = 0.05$; $q = 0.09$) and in FCS (CNT-R: 40.5% vs. STD-R: 52.59%; $p = 0.14$; $q = 0.28$), whereas *Bacteroidetes* remained low in CEC (CNT-R: 18.86% vs. STD-R: 7.86%; $p = 0.15$; $q = 0.18$) and almost unaltered in FCS (CNT-R: 44.88% vs. STD-R: 43.2%; $p = 0.79$; $q = 0.79$). Otherwise, minor represented phyla such as *Verrucomicrobia* (CNT-R: 8.46% vs. STD-R: 0.78%; $p = 0.02$; $q = 0.07$), *Proteobacteria* (CNT-R: 0.66% vs. STD-R: 0.21%; $p = 0.05$; $q = 0.09$), and

Actinobacteria (CNT-R: 0.14% vs. STD-R: 0.03%; $p = 0.008$; $q = 0.05$) were decreased in CEC. The sorted minor phyla had more presence in CNT-R CEC instead of STD-R CEC compensating the non-establishment of the two major phyla (Figure 4a). Focusing on genera, the differences between CNT-R and STD-R are summarized in Table S3. Thus, the differences in *Firmicutes* were characterized in the cecum of STD-R group by the significative alteration of *Ruminococcus*, *Oscillospira*, and *Coprococcus* and an uncharacterized genus in the *Clostridiales* order (Figure 4d). Moreover, some differences were also found in feces of STD-R group characterized by changes in *rc4-4* genus and an uncharacterized genus.

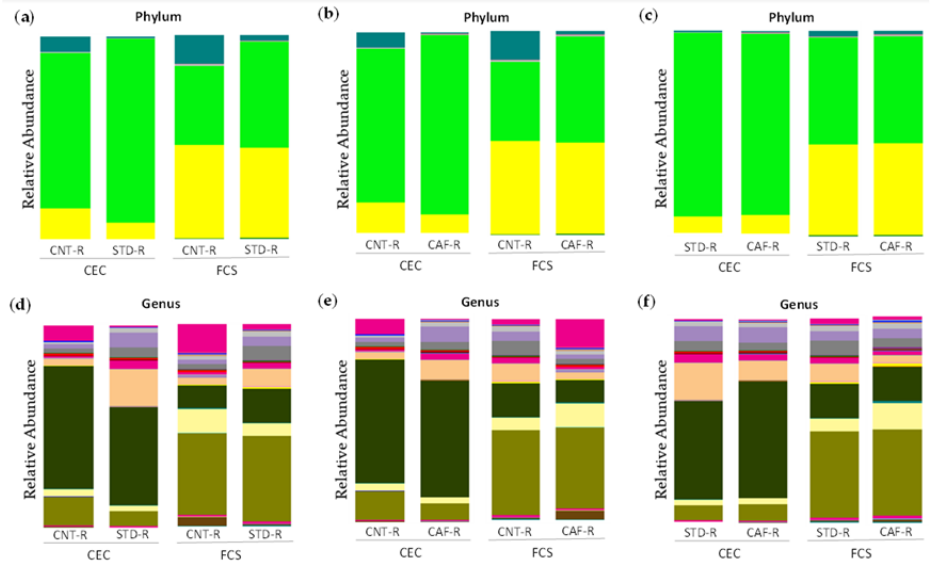

Figure 4. Microbiota composition between CNT-R, STD-R, and CAF-R groups represented by abundance. (a) phylum level in CNT-R vs. STD-R, (b) phylum level in CNT-R vs. CAF-R, (c) phylum level in STD-R vs. CAF-R, (d) genus level in CNT-R vs. STD-R, (e) genus level in CNT-R vs. CAF-R, (f) genus level in STD-R vs. CAF-R.

Regarding the CAF-R group, the differences were similar as previously described for the STD-R group with the establishment of *Firmicutes* in CEC (CNT-R: 71.82% and CAF-R: 89.3%) and in FCS (CNT-R: 40.5% and CAF-R: 52.05%), while *Bacteroidetes* remain low in CEC (CNT-R: 18.86% and CAF-R: 9.14%) and almost equal in FCS (CNT-R: 44.88% and STD-R: 43.89%). Besides, *Verrucomicrobia* phylum was increased in the CNT-R group having more differences in CEC than in FCS group (Figure 4b). Focusing on genera, the differences between CNT-R and CAF-R are summarized in Table S4. Thus, *Oscillospira* genus was the main altered genus presenting a significative increase in both sample types among other interesting changes in CEC genera as *Coprococcus* and *Ruminococcus* (Figure 4e).

The receptors of cecal content, the STD-R and the CAF-R groups, had a similar phyla composition (Figure 4c). Focusing on genera, the statistical analysis between STD-R and CAF-R are summarized in Table S5. Although the animals presented a similar phyla composition, some differences could be observed in genera as it is shown

in Figure 4f. In this case, more differences were observed in FCS than in CEC. In the case of CEC, an uncharacterized genus of *Lachnospiraceae* family presented a significant one-half decrease in CAF-R. Although there were not any more statistically significant differences, there were some genera with interesting fold changes as the case of *Parabacteroides*.

3.4. Metabolomic Characterization of the Model of Obesity-Associated Gut Dysbiosis with a Healthy Phenotype

The plasma metabolomic approach was based on a multiplatform global analysis including 139 metabolites belonging to: the metabolism of lipids as a wide diversity of different triglycerides (TG), ester cholesterols (ChoE), diacylglycerols (DG), sphingomyelins (SM), phosphatidylcholines (PC), and lysophospholipids (LPC); metabolism of carbohydrates as the main metabolites of citric acid pathway were included; and metabolism of the main amino acids affecting the microbiota and diet were included among other interesting metabolites. The analysis showed differences on the lipid metabolism in the CAF-R group in comparison to the STD-R group (Table S6). After the parametric unpaired *t*-test, 7 different significant lipids were determined as potential biomarkers in plasma (DG 34:2, DG 34:3, DG 36:2, DG 36:4, LPC 20:0, DG 34:1, and PC 31:0). However, only one plasma metabolite was significantly differentiated after the multivariate correction, which was the DG 34:2. Specifically, the DG 34:2 was significantly increased in CAF-R compared to CNT-R (q = 0.009) and STD-R (q = 0.045) (Table 1). Moreover, DG 34:2 is the most important feature in the model after applying the Random Forest classifier presenting the highest value by far in comparison to the second metabolite in the list (Table S7).

The urine metabolomic approach was based on untargeted ^{1}H-NMR methodology detecting 45 metabolites belonging, mainly, to the metabolism of amino acids (e.g., phenylalanine, tyrosine, and tryptophan metabolism; glycine, serine, and threonine metabolism; alanine, aspartate, and glutamate metabolism; glutathione metabolism; and taurine and hypotaurine metabolism) and the energetic metabolism (e.g., citrate cycle, pyruvate metabolism, and glycolysis/gluconeogenesis) (Table S8). After the parametric unpaired *t*-test, 6 different significant metabolites were determined as potential biomarkers in urine (hippurate, *o*-coumaric acid, 3-HPPA, HPPA sulfate, tyrosine, and phenylacetylglycine). After the multivariate correction, the results pointed out three metabolites involved in the phenylalanine metabolism that were significantly altered in the CAF-R group compared to the STD-R group (hippurate, *o*-coumaric acid, 3-HPPA). On the one hand, the *o*-coumaric acid (q = 0.035) and the 3-hydroxyphenylpropionate (3-HPPA) (q = 0.039) were significantly increased in the CAF-R group compared with the STD-R group, almost 3 and 10 times more elevated, respectively. On the other hand, the hippurate (q = 0.013) was significantly decreased by a half in the CAF-R group in comparison to the STD-R group (Table 1). Moreover, those metabolites are the most important features in the model after applying the Random Forest classifier being the top metabolites to discern between the STD-R and CAF-R groups (Table S9).

Table 1. Metabolites significantly altered affected by the microbiota transplant in plasma and urine. The statistically significant *p*-values ($p < 0.05$) and *q*-values ($q < 0.05$) are highlighted in bold. Abbreviations: DG 34:2, diacylglycerol 34:2; 3-HPPA, 3-hydroxyphenylpropionate. Bold figures mean significant.

	Biofluid	**Plasma**	**Urine**	**Urine**	**Urine**
	Metabolite	**DG 34:2**	**Hippurate**	***o*-Coumaric Acid**	**3-HPPA**
Mean ± SEM	CNT-R	0.40 ± 0.03	192.13 ± 48.87	4.36 ± 0.84	15.58 ± 5.87
	STD-R	0.42 ± 0.04	295.91 ± 20.55	2.16 ± 0.20	2.31 ± 0.60
	CAF-R	0.72 ± 0.05	145.49 ± 21.45	6.14 ± 0.76	21.30 ± 3.91
CNT-R vs STD-R	*p*-value	0.549	0.086	**0.039**	0.064
	q-value	0.963	0.351	0.290	0.290
	FC	1.07	1.54	0.50	0.15
CNT-R vs CAF-R	*p*-value	**<0.001**	0.407	0.141	0.435
	q-value	**0.009**	0.770	0.770	0.783
	FC	1.82	0.77	1.41	1.37
STD-R vs CAF-R	*p*-value	**<0.001**	**<0.001**	**0.002**	**0.003**
	q-value	**0.045**	**0.013**	**0.035**	**0.039**
	FC	1.69	0.49	2.84	9.24

3.5. Correlation between Metagenomics and Metabolomics in the Obesity-Associated Gut Dysbiosis

Focusing on the metabolic differences between the STD-R and the CAF-R groups, none of the metabolites ($n = 4$) used in this study were correlated with values of metagenomic diversity (Table S10). Nevertheless, we focused on specific genus. In this case, the Kernel density distribution of altered metabolites was correlated with some genus normalizing the relative values of the metabolites by the different genus, discerning between STD-R and CAF-R groups. Thus, 28 genera with a higher abundance of 0.1% were selected to study the density distribution. Interestingly, the density distribution of the STD-R and the CAF-R groups was significantly different in 3 genera for DG 34:2, 19 genera for 3-HPPA, 9 genera for Hippurate, and 14 genera for *o*-coumaric acid (Table S11). Indeed, *Firmicutes* was the phylum with the great part of genus affecting the distribution between groups. For example, the *Oscillospira* genus was differently distributed between groups in the four selected metabolites (Figure 5), and differences were found in donors and receptors. In addition, besides *Oscillospira* genus, other genera from the *Clostridiales* order have at least 3 altered metabolites (i.e., *Coprococcus* and an uncharacterized genus of *Lachnospiraceae* family; *Dehalobacterium* genus of *Dehalobacteriaceae* family; and an uncharacterized genus of uncharacterized family) (Figure 5).

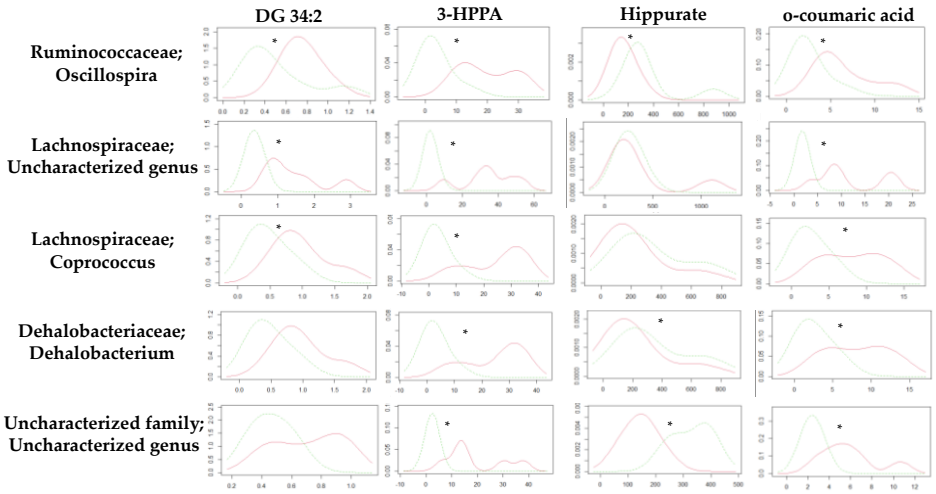

Figure 5. Kernel density plot of the altered metabolites normalized by genus for the STD-R and CAF-R group. The statistical comparisons between metabolites normalized by genus were conducted using test of equal densities. The X axis represents the values of Kernel density while the Y axis represents the metabolite values. Each row represents the metabolites normalized by one selected genus. Each column shows the metabolites represented in the Kernel density plot. The significant differences are highlighted by an asterisk. Green line: STD-R; red line: CAF-R.

4. Discussion

In the present study, a pilot metabolomic approach in healthy rats, that received cecal microbiota from obese ones, has been carried out to find a metabolic profile of obesity-associated GM with a healthy phenotype, avoiding metabolic disturbances related to other risk factors. Importantly, the transference of GM from obese to non-obese rats could help to discover new biomarkers exclusively related to this GM alterations that could provide interesting information about the metabolic profile of a segregated obesity-associated gut disbiotic state.

Interestingly, focusing on biometric parameters, a huge significant decrease in CEC weight was observed which could be directly induced by the effect of the cecal content. Additionally, there was a tendency to increase in the total weight of white adipose tissue, which was more evident in MWAT although a slight increase was also observed in RWAT. Thus, the transplanted cecal content affected the weight of the white adipose tissue. Focusing on plasma biochemistry, the glucose levels remained unaltered but TG, TC, and NEFAs presented a clear tendency to increase in the CAF-R group supporting the changes observed in MWAT and RWAT. On the other hand, the total liver lipids decreased in the CAF-R group, and specifically the phospholipids were the representative lipid species that also correlated with this decrease. Globally, all these changes demonstrate the impact of the different cecal donors' content in transplant on some biometric and biochemical parameters.

In our study, the depletion of host microbiota after the antibiotic treatment, which produces a decrease in the number of microbes, was characterized by an

emergence of less abundant phyla and a decrease in most abundant phyla in receptors animals (CNT-R, STD-R, and CAF-R). In our pilot model of obesity-associated gut dysbiosis in rats, we altered the microbiota of cecal receptors (STD-R and CAF-R) by oral gavage of cecal donors content (STD-D and CAF-D), which were fed with a standard diet. First, to determine the success of the transplant, the control group (CNT-R) and CEC receptors groups were compared (STD-R and CAF-R). Results showed an increase of bacteria and diversity in CEC receptors groups, as well as a decrease in CEC weight. Moreover, we observed slight differences between STD-R and CAF-R, where there was a change in the distribution of bacteria. Significant increases in genera of the STD-R group were induced in the *Clostridiales* spp.; *Ruminococcus*, *Oscillospira*, *Coprococcus*; and an uncharacterized genus (which were increased in CEC). On the other hand, an uncharacterized genus of *Ruminococcaceae* and *rc4-4* genus was significantly increased in FCS. In the case of CAF-R versus CNT-R, *Oscillospira* genus was increased either in CEC or FCS following the trend of STD-R. The differences in *Oscillospira* genus were maintained between the donors and receptors, which has been defined as a component of the GM related to leanness or lower BMI, confirming our model of obesity-associated to GM in a healthy phenotype [47]. Finally, some minor changes in the genera could be observed, including some important genera in the development of obesity (e.g., changes in the composition of *Clostridiales* spp.). Although, clear statistical differences between STD-R and CAF-R groups were not observed in metagenomics analysis, if we consider all these changes together with the biometric and biochemical parameters, we could sense a segregated model of obesity-associated gut dysbiosis.

In addition, some metabolic changes were observed in the host, induced by the alteration of the complexity microbial biofilm. In fact, the most interesting altered metabolites included those in plasma (e.g., DG 34:2) and urine (e.g., Hippurate, 3-HPPA, and *o*-coumaric acid), pointing out urine as a fundamental part of the metabolic profile of our model. These metabolic variations provide another hint to prove the achievement of the segregated dysbiosis between STD-R and CAF-R groups. In this sense, taking together the biometric and biochemical parameters, the metagenomics and, finally, the metabolomics, the general picture of the model would be elucidated. Thus, we can consider the experiment as a successful pilot model of obesity-associated gut dysbiosis.

DG were the main metabolites with altered circulating plasma levels that were found in transplanted rats; being increased in CAF-R compared to CNT-R and STD-R. However, after the multivariate correction, only the DG 34:2 was statistically significant. DG are glycerides consisting of two fatty acid chains covalently bonded to a glycerol molecule through ester linkages [48] and, apart from being the central intermediate in the synthesis of membrane phospholipids and the lipid storage [49], they are key regulators of cell physiology, controlling the membrane recruitment and activation of signalling molecules [50]. For example, Backhed and collaborators have suggested that because of dysbiosis, GM can stimulate the levels of TG and DG through the suppression of the intestinal epithelial expression of the fasting-induced

adipose factor (Fiaf), a natural inhibitor of circulating lipoprotein lipase (LPL) [51], which is the main rate-limiting enzyme in lipid metabolism, catalysing the hydrolysis of TGs and DG [52]. Our results suggest that microbial alteration associated to obesity could stimulate Fiaf expression, potentiating the inhibition of LPL and therefore, increasing the circulating levels of DG, specifically the DG 34:2. In this sense, the DG 34:2 is a diacylglycerol with fatty acids containing a total of 34 carbons and 2 double bonds joined via ester linkages at unknown positions (sn1, sn2, or sn3), it is mainly implicated in the novo triacylglycerol biosynthesis of several TG as other DG [53]. This specific lipid has been attracting attention in studies of lipidomics in diverse fields focusing on, e.g., diabetic kidney tissue of diabetic rats [54] and liver tissue of hypertensive rats [55]. Despite this metabolite was found as a biomarker in several pathologies and tissues in rats as it has been described before, we also propose this specific lipid to do further studies in obesity-associated to gut dysbiosis. Although the first lipidomic biomarkers are entering in the clinic, certain analytical standards need to be established in order to make lipidomic measurements generally accepted in clinical settings [56]. However, tissues responsible for DG levels in plasma are still unknown. Several authors have pointed out the utility of increased levels of plasma DG, as well as its composition, as biomarkers of metabolic syndrome and obesity in rodents [57], [58], rhesus monkeys [59], and humans [60], although without specifying the type/s of DG.

On the other hand, a relevant finding in our pilot study is the alteration on hepatic lipids observed in transplanted animals. CAF-R group showed decreased levels of total hepatic lipids and phospholipids compared to STD-R and CNT-R groups. Interestingly, it has been recently shown [61] that the transfer of disbiotic gut microbiota from obese to antibiotic-free conventional mice changes gut microbiota and microbiome of recipient mice, ameliorates hepatic gluconeogenesis, and prevents high-fat diet-induced dysmetabolism. These results agree with our present results and point out the potential success of our dysbiosis model. Additionally, despite not directly related to microbiota transfer, another interesting study [62], where the connection of the antifungal carbendazim (CBZ) on lipid metabolism was studied discovered that CBZ chronic treatment induced gut microbiota dysbiosis in mice and such dysbiosis was associated with a reduced lipid liver synthesis and an increased lipid storage in the fat. More concisely, regarding the liver, some genes involved in TG synthesis, such as Dgat1 and Gpat, were significantly downregulated by the CBZ chronic treatment.

Furthermore, there are, mainly, two enzymes, the diacylglycerol acyltransferase (DGAT) and ethanolamine phosphotransferase, which control the use of DG for lipid synthesis, suggesting the presence of a common DG pool for lipid synthetic pathways [63]. Another DG pool is also available for glycerolipid synthesis because DG that is released from TG stores in human fibroblasts can be converted to phospholipids [64]. Segregation of DG toward different metabolic routes seems to occur according to the cell's needs. For instance, the DG originally destined to form phospholipids is re-directed toward TG when phospholipid synthesis is inhibited [65]. In our animal model, the obesity-associated gut dysbiosis model produces a significant increase in

plasma DG levels, as the DG 34:2, and a decrease in hepatic phospholipids. Thus, it would be expected an increase in plasma or liver TG, although they were not changed. Further studies are needed to elucidate the relation between microbes, DG 34:2, and liver phospholipids.

The obesity-associated to gut dysbiosis in a healthy phenotype also produced the alteration of three main metabolites, i.e., hippurate, *o*-coumaric acid, and 3-HPPA, in urine. These metabolites, which belong to the phenylalanine metabolism, have also been related to the degradation of phenolic compounds that have been traditionally associated with the ingestion of polyphenols-rich food [66]. In this sense, diet is one of the major environmental factor that modulates the composition and the metabolic activity of GM, forming the food–gut axis [67]. Polyphenols are plant secondary metabolites, and there are many studies that support the idea that phenolic compounds modulate the composition and metabolic activities of GM, as well as GM metabolize polyphenols into bioactive compounds that produce clinical benefits [68], [69]. Hence, it has been postulated that changes in the species population or GM activities result in changes in the metabolic processing of polyphenolic compounds that can be observed in the derived urinary metabolites [70].

In our case, the changes in urine metabolomics are explained by the microbiota transplant and not by the modulation of dietary polyphenols, because all the animals received the same diet (without differences in trace polyphenols). The phenolic compounds that have been found altered in our urine model are included in the group of chlorogenic acids, standing out the contradictory information in literature about the bioavailability and effects of these type of polyphenols [66]. Interestingly, Clayton and collaborators proposed two distinct rat urinary compositional phenotypes, i.e., these may arise from differences in the gut microbially mediated metabolism of phenylalanine that are characterized by differences in hippurate and 3-HPPA, among other metabolites [71].

Hippurate is a glycine conjugate of benzoic acid formed in the mitochondria of the liver and kidneys and then excreted in the urine [72] and is considered a gut microbial-mammalian co-metabolite that can be made by *Clostridium* spp., primarily from polyphenols [73]. In our study, hippurate was reduced by a half in the CAF-R group compared to the STD-R group. In this sense, hippurate excreted in urine has been found as a distinguishing feature of different range on physiological and pathological conditions (e.g., obese phenotypes [74], [75], metabolic syndrome [76], Crohn's disease [77], psychological disorders [78], among others). Additionally, many studies have shown an increased excretion of hippurate resulted from the ingestion of specific dietary components containing phenolic molecules, as teas [79], [80] or edible fruits [81]. Considering the previous information, hippurate could be considered as a biomarker of health but this concept is ambiguous, since the source has not been robustly addressed. Thus, the wide associations of hippurate to different conditions support the idea of our findings that the changes in its excretion are caused by the GM and not by the disease. These results are in agreement with a recent review

showing that the differences in hippurate excretion are due, at least in part, to functional or compositional differences in GM, regardless of the specific diet [70].

Related to hippurate, the 3-HPPA is a phenol derivative formed through fermentation of tyrosine by *Clostridium* spp., that could be further metabolized to benzoic acid and excreted as hippurate [82], [83]. Interestingly, related to chlorogenic acids availability, 3-HPPA has been shown to be able to freely cross the gut epithelium [84] into the blood and brain [85]. In our animal model, 3-HPPA was increased almost 10 times in the CAF-R group compared to the STD-R. In a recent study, the effect of procyanidin A2, and its major colonic metabolite 3-HPPA, was investigated on the suppression of macrophage foam cell formation. The results showed a significant reduction in the cellular lipid accumulation and the inhibition of foam cell formation by both compounds [86]. According to our study, we speculate that the increased level of 3-HPPA urine excretion in CAF-R could be related to the reduction in lipid accumulation because CAF-R showed a lower 3-HPPA compared to STD-R. However, this mechanism would not directly explain the reduction in total lipids in liver showed in CAF-R animals. Altogether, we hypothesize that 3-HPPA could be a direct explanation of the decrease in hippurate because of elevated excretion levels in the urine profile. In agreement, there was no 3-HPPA availability in the CAF-R animals to metabolize hippurate. Furthermore, dietary modulation was found to cause a change in the excretion of 3-HPPA, which was replaced by hippurate in Wistar rats [87]. Surprisingly, the excretion of hippurate persisted when the animals returned to the original diet. It was proposed that, in addition to the precursors available in the diet, the absence or presence of urinary hippurate and 3-HPPA was influenced by variation on the GM. Additionally, this research proposed that a change in diet could potentially have caused a redistribution of the microbiota, resulting in the production of hippurate as the primary excretion product, regardless of the specific diet [87].

o-coumaric acid, which is an hydroxycinnamic acid, has been described to act as powerful antioxidant and as an important biological protector from oxidation [88]. Interestingly, our findings showed that *o*-coumaric acid excretion in urine was increased three times in the CAF-R group compared to the STD-R. Related to this, a research performed in rats fed with high-fat diet (HFD) showed that supplementing the HFD with *o*-coumaric acid for 8 weeks suppressed the increases in body weight, liver weight, and adipose tissue weights of peritoneal and epididymal fat induced by the hypercaloric diet [89]. Thus, in our case, the high increase in the *o*-coumaric secretion in urine may be hypothetically related to a decreased systemic protective effect in the CAF-R group, having, in consequence, a predisposition to develop obesity in the future. As far as we know, this is the first time that *o*-coumaric acid is proposed as a dysbiosis biomarker.

Finally, some correlations will be discussed to directly connect the obesity-associated gut dysbiosis with the host metabolism. There was a significant correlation between some genera in *Clostridiales* order and the metabolites included in the profile of metabolic changes. The *Oscillospira* genus was highly correlated with the selected

metabolites followed by other genus with three out of four metabolites including the following genera: *Coprococcus* and an uncharacterized genus of *Lachnospiraceae* family, *Dehalobacterium* genus of *Dehalobacteriaceae* family, and an uncharacterized genus of uncharacterized family. Previous intervention studies in humans showed minor effect on the metabolism of phospholipids and cholesterol (in large VLDL), after changes in the metagenomic composition induced by moderate exercise [90]. Other studies have shown correlation of metagenomics with imbalanced metabolome, resulting in a source of potential biomarkers of obesity [91], chronic obstructive disease in humans [92], the dietary effect of the insulin feeding in pigs [93], the quantifying diet effect in humans [94], or tracking a healthy dietary pattern [95]. Thus, external factors that induce changes in the microbial community, lead to changes in the metabolism.

Previous studies have found that changes in the microbiota produce metabolic alterations, however, to the best of our knowledge, this is the first study that focuses on changes in the metabolism caused by obesity-associated gut dysbiosis with a healthy phenotype. This study, under controlled experimental conditions, elucidates the metabolic changes caused by an obesity-associated gut dysbiosis. This fact opened a window of opportunities to propose metabolic biomarkers of segregated obesity-associated gut dysbiosis in a healthy population.

5. Conclusions

The important point in the present study is that we have developed a pilot experiment trying to isolate dysbiosis from the rest of obesity-associated complications (e.g., hyperglycemia, hyperinsulinemia, hyperlipidemia, hypercoagulable state, etc.). In this sense, we have been able to discriminate the alterations induced by the dysbiosis component of obesity in a relative isolated way. Our model of obesity-associated microbial gut dysbiosis in healthy rats produced biometric and biochemical changes, as well as metabolic changes, mainly in the lipid (DG 34:2 in plasma) and phenylalanine (hippurate, 3-HPPA, and *o*-coumaric acid in urine) metabolism. In consequence, we propose that external factors that induce changes in the microbial community may trigger the mechanism of obesity by altering mainly the lipid and phenylalanine metabolism of the host. To the best of our knowledge, this is the first study proposing this model of a segregated risk factor of obesity, expanding, in consequence, the knowledge about the metabolism on obesity-associated microbial gut dysbiosis as well as the determination of a metabolic profile of the risk factor. Hereby, we propose an obesity-associated metabolic profile, including DG 34:2, hippurate, 3-HPPA, and *o*-coumaric, that can be utilized as tentative biomarkers of an obesity-prone state mainly related to a disbiotic state. These pilot approach and associated results provide the basis for a better understanding of the biological role played by GM and for the discovery of novel biomarkers in future obesity studies.

References

[1] M. J. Müller and C. Geisler, "Defining obesity as a disease," 2017, doi: 10.1038/ejcn.2017.155.

[2] A. Hruby and F. B. Hu, "The Epidemiology of Obesity: A Big Picture," *PharmacoEconomics*, vol. 33, no. 7. pp. 673–689, 2015, doi: 10.1007/s40273-014-0243-x.

[3] R. Sturm and R. An, "Obesity and Economic Environments," *CA Cancer J Clin*, vol. 64, pp. 337–350, 2014, doi: 10.3322/caac.21237.

[4] W. T. Cefalu *et al.*, "Advances in the science, treatment, and prevention of the disease of obesity: Ref lections from a diabetes care editors' expert forum," *Diabetes Care*, vol. 38, no. 8, pp. 1567–1582, Aug. 2015, doi: 10.2337/dc15-1081.

[5] D. Okin and R. Medzhitov, "Evolution of inflammatory diseases," *Current Biology*. 2012, doi: 10.1016/j.cub.2012.07.029.

[6] A. S. Al-Goblan, M. A. Al-Alfi, and M. Z. Khan, "Mechanism linking diabetes mellitus and obesity.," *Diabetes. Metab. Syndr. Obes.*, vol. 7, pp. 587–91, 2014, doi: 10.2147/DMSO.S67400.

[7] S. P. Messier, "Obesity and Osteoarthritis: Disease Genesis and Nonpharmacologic Weight Management," *Rheumatic Disease Clinics of North America*, vol. 34, no. 3. NIH Public Access, pp. 713–729, Aug. 2008, doi: 10.1016/j.rdc.2008.04.007.

[8] M. A. Woldu, J. L. Lenjisa, and G. D. Satessa, "Recent Advancements in Diabetes Pharmacotherapy," 2014, doi: 10.4172/2167-0501.1000143.

[9] T. W. Stone, M. McPherson, and L. Gail Darlington, "Obesity and Cancer: Existing and New Hypotheses for a Causal Connection," *EBioMedicine*, vol. 30. Elsevier B.V., pp. 14–28, Apr. 2018, doi: 10.1016/j.ebiom.2018.02.022.

[10] K. Basen-Engquist and M. Chang, "Obesity and cancer risk: Recent review and evidence," *Current Oncology Reports*, vol. 13, no. 1. NIH Public Access, pp. 71–76, Feb. 2011, doi: 10.1007/s11912-010-0139-7.

[11] S. M. Chopra, A. Misra, S. Gulati, and R. Gupta, "Overweight, obesity and related non-communicable diseases in Asian Indian girls and women," *European Journal of Clinical Nutrition*, vol. 67, no. 7. Nature Publishing Group, pp. 688–696, Jul. 2013, doi: 10.1038/ejcn.2013.70.

[12] J. Banjare and S. Bhalerao, "Obesity associated noncommunicable disease burden," *Int. J. Heal. Allied Sci.*, vol. 5, no. 2, p. 81, 2016, doi: 10.4103/2278-344x.180429.

[13] A. Nirmala, C. Kanniammal, P. Venkataraman, and J. Arulappan, "Predisposing factors associated with obesity among adolescents-A case control study," *Biomed. Res.*, vol. 29, no. 18, pp. 3497–3501, 2018, doi: 10.4066/biomedicalresearch.29-18-1016.

[14] M. L. Endalifer and G. Diress, "Epidemiology, Predisposing Factors, Biomarkers, and Prevention Mechanism of Obesity: A Systematic Review," *Journal of Obesity*, vol. 2020. Hindawi Limited, 2020, doi: 10.1155/2020/6134362.

[15] G. Musso, R. Gambino, and M. Cassader, "Interactions Between Gut Microbiota and Host Metabolism Predisposing to Obesity and Diabetes," *Annu. Rev. Med.*, vol. 62, no. 1, pp. 361–380, Feb. 2011, doi: 10.1146/annurev-med-012510-175505.

[16] R. Nagpal, T. M. Newman, S. Wang, S. Jain, J. F. Lovato, and H. Yadav, "Obesity-Linked Gut Microbiome Dysbiosis Associated with Derangements in Gut Permeability and Intestinal Cellular Homeostasis Independent of Diet," *J. Diabetes Res.*, vol. 2018, 2018, doi: 10.1155/2018/3462092.

[17] F. F. Anhê *et al.*, "Gut Microbiota Dysbiosis in Obesity-Linked Metabolic Diseases and Prebiotic Potential of Polyphenol-Rich Extracts," *Current obesity reports*, vol. 4, no. 4. Springer, pp. 389–400, Dec. 2015, doi: 10.1007/s13679-015-0172-9.

[18] K. B. Martinez, V. Leone, and E. B. Chang, "Western diets, gut dysbiosis, and metabolic diseases:

Are they linked?," *Gut Microbes*, vol. 8, no. 2. Taylor and Francis Inc., pp. 130–142, Mar. 2017, doi: 10.1080/19490976.2016.1270811.

[19] K. Al-Assal, A. C. Martinez, R. S. Torrinhas, C. Cardinelli, and D. Waitzberg, "Gut microbiota and obesity," *Clinical Nutrition Experimental*, vol. 20. Elsevier Ltd, pp. 60–64, Aug. 2018, doi: 10.1016/j.yclnex.2018.03.001.

[20] O. Castaner *et al.*, "The gut microbiome profile in obesity: A systematic review," *Int. J. Endocrinol.*, vol. 2018, 2018, doi: 10.1155/2018/4095789.

[21] S. F. Clarke *et al.*, "The gut microbiota and its relationship to diet and obesity:New insights," *Gut Microbes*, vol. 3, no. 3. Landes Bioscience, pp. 186–202, 2012, doi: 10.4161/gmic.20168.

[22] K. Adachi *et al.*, "Gut microbiota disorders cause type 2 diabetes mellitus and homeostatic disturbances in gutrelated metabolism in Japanese subjects," *J. Clin. Biochem. Nutr.*, vol. 64, no. 3, pp. 231–238, 2019, doi: 10.3164/jcbn.18-101.

[23] Y. Yamaguchi *et al.*, "Association of Intestinal Microbiota with Metabolic Markers and Dietary Habits in Patients with Type 2 Diabetes," *Digestion*, vol. 94, no. 2, pp. 66–72, Oct. 2016, doi: 10.1159/000447690.

[24] M. Million, J. C. Lagier, D. Yahav, and M. Paul, "Gut bacterial microbiota and obesity," *Clinical Microbiology and Infection*, vol. 19, no. 4. Blackwell Publishing Ltd, pp. 305–313, Apr. 2013, doi: 10.1111/1469-0691.12172.

[25] S. Musaad and E. N. Haynes, "Biomarkers of obesity and subsequent cardiovascular events," *Epidemiologic Reviews*, vol. 29, no. 1. NIH Public Access, pp. 98–114, May 2007, doi: 10.1093/epirev/mxm005.

[26] K. Aleksandrova, D. Mozaffarian, and T. Pischon, "Addressing the Perfect Storm: Biomarkers in Obesity and Pathophysiology of Cardiometabolic Risk," *Clin. Chem.*, vol. 64, no. 1, pp. 142–153, Jan. 2018, doi: 10.1373/clinchem.2017.275172.

[27] R. Kaddurah-Daouk, B. S. Kristal, and R. M. Weinshilboum, "Metabolomics: A Global Biochemical Approach to Drug Response and Disease," *Annu. Rev. Pharmacol. Toxicol.*, vol. 48, no. 1, pp. 653–683, Jan. 2008, doi: 10.1146/annurev.pharmtox.48.113006.094715.

[28] M. M. Ulaszewska *et al.*, "Nutrimetabolomics: An Integrative Action for Metabolomic Analyses in Human Nutritional Studies.," *Mol. Nutr. Food Res.*, vol. 63, no. 1, p. e1800384, Jan. 2019, doi: 10.1002/mnfr.201800384.

[29] J. Hernandez-Baixauli *et al.*, "Detection of Early Disease Risk Factors Associated with Metabolic Syndrome: A New Era with the NMR Metabolomics Assessment.," *Nutrients*, vol. 12, no. 3, Mar. 2020, doi: 10.3390/nu12030806.

[30] M. Roberfroid *et al.*, "Prebiotic effects: Metabolic and health benefits," *British Journal of Nutrition*, vol. 104, no. SUPPL.2. Br J Nutr, Aug. 2010, doi: 10.1017/S0007114510003363.

[31] E. Rinott *et al.*, "Effects of Diet-Modulated Autologous Fecal Microbiota Transplantation on Weight Regain," *Gastroenterology*, 2020, doi: 10.1053/j.gastro.2020.08.041.

[32] E. Esteve, W. Ricart, and J. M. Fernández-Real, "Gut microbiota interactions with obesity, insulin resistance and type 2 diabetes: Did gut microbiote co-evolve with insulin resistance?," *Current Opinion in Clinical Nutrition and Metabolic Care*, vol. 14, no. 5. Curr Opin Clin Nutr Metab Care, pp. 483–490, Sep. 2011, doi: 10.1097/MCO.0b013e328348c06d.

[33] E. J. Kuipers, V. W. Yang, F. J. Gonzalez, C. Jiang, and A. D. Patterson, "REVIEWS IN BASIC AND CLINICAL GASTROENTEROLOGY AND HEPATOLOGY An Intestinal Microbiota-Farnesoid X Receptor Axis Modulates Metabolic Disease," *Gastroenterology*, vol. 151, pp. 845–859, 2016, doi: 10.1053/j.gastro.2016.08.057.

[34] A. Parséus *et al.*, "Microbiota-induced obesity requires farnesoid X receptor," *Gut*, vol. 66, no. 3,

pp. 429–437, Mar. 2017, doi: 10.1136/gutjnl-2015-310283.

[35] I. Kaji, S. Karaki, and A. Kuwahara, "Short-Chain Fatty Acid Receptor and Its Contribution to Glucagon-Like Peptide-1 Release," *Digestion*, vol. 89, no. 1, pp. 31–36, Jan. 2014, doi: 10.1159/000356211.

[36] C. B. Christiansen, M. B. N. Gabe, B. Svendsen, L. O. Dragsted, M. M. Rosenkilde, and J. J. Holst, "The impact of short-chain fatty acids on glp-1 and pyy secretion from the isolated perfused rat colon," *Am. J. Physiol. - Gastrointest. Liver Physiol.*, vol. 315, no. 1, pp. G53–G65, Jul. 2018, doi: 10.1152/ajpgi.00346.2017.

[37] I. Cigarroa *et al.*, "Treadmill Intervention Attenuates the Cafeteria Diet-Induced Impairment of Stress-Coping Strategies in Young Adult Female Rats.," *PLoS One*, vol. 11, no. 4, p. e0153687, 2016, doi: 10.1371/journal.pone.0153687.

[38] D. H. Reikvam *et al.*, "Depletion of murine intestinal microbiota: effects on gut mucosa and epithelial gene expression.," *PLoS One*, vol. 6, no. 3, p. e17996, Mar. 2011, doi: 10.1371/journal.pone.0017996.

[39] J. F. Hoffman, A. X. Fan, E. H. Neuendorf, V. B. Vergara, and J. F. Kalinich, "Hydrophobic Sand Versus Metabolic Cages: A Comparison of Urine Collection Methods for Rats (Rattus norvegicus)," *J. Am. Assoc. Lab. Anim. Sci.*, vol. 57, no. 1, pp. 51–57, Jan. 2018, [Online]. Available: https://pubmed.ncbi.nlm.nih.gov/29402352.

[40] A. Caimari, J. M. del Bas, A. Crescenti, and L. Arola, "Low doses of grape seed procyanidins reduce adiposity and improve the plasma lipid profile in hamsters.," *Int. J. Obes. (Lond).*, vol. 37, no. 4, pp. 576–583, Apr. 2013, doi: 10.1038/ijo.2012.75.

[41] V. Rodriguez-Sureda and J. Peinado-Onsurbe, "A procedure for measuring triacylglyceride and cholesterol content using a small amount of tissue.," *Anal. Biochem.*, vol. 343, no. 2, pp. 277–282, Aug. 2005, doi: 10.1016/j.ab.2005.05.009.

[42] J. G. Caporaso *et al.*, "QIIME allows analysis of high-throughput community sequencing data.," *Nature methods*, vol. 7, no. 5. United States, pp. 335–336, May 2010, doi: 10.1038/nmeth.f.303.

[43] M. Kanehisa and S. Goto, "KEGG: kyoto encyclopedia of genes and genomes," *Nucleic Acids Res.*, vol. 28, no. 1, pp. 27–30, Jan. 2000, doi: 10.1093/nar/28.1.27.

[44] S. Fujisaka *et al.*, "Diet, Genetics, and the Gut Microbiome Drive Dynamic Changes in Plasma Metabolites.," *Cell Rep.*, vol. 22, no. 11, pp. 3072–3086, Mar. 2018, doi: 10.1016/j.celrep.2018.02.060.

[45] L. Baselga-Escudero *et al.*, "Long-term supplementation with a low dose of proanthocyanidins normalized liver miR-33a and miR-122 levels in high-fat diet-induced obese rats.," *Nutr. Res.*, vol. 35, no. 4, pp. 337–345, Apr. 2015, doi: 10.1016/j.nutres.2015.02.008.

[46] A. Gual-Grau, M. Guirro, J. Mayneris-Perxachs, L. Arola, and N. Boqué, "Impact of different hypercaloric diets on obesity features in rats: a metagenomics and metabolomics integrative approach," *J. Nutr. Biochem.*, vol. 71, pp. 122–131, 2019, doi: https://doi.org/10.1016/j.jnutbio.2019.06.005.

[47] T. Konikoff and U. Gophna, "Oscillospira: a Central, Enigmatic Component of the Human Gut Microbiota.," *Trends Microbiol.*, vol. 24, no. 7, pp. 523–524, Jul. 2016, doi: 10.1016/j.tim.2016.02.015.

[48] S. Carrasco and I. Mérida, "Diacylglycerol, when simplicity becomes complex.," *Trends Biochem. Sci.*, vol. 32, no. 1, pp. 27–36, Jan. 2007, doi: 10.1016/j.tibs.2006.11.004.

[49] D. M. Erion and G. I. Shulman, "Diacylglycerol-mediated insulin resistance.," *Nat. Med.*, vol. 16, no. 4, pp. 400–402, Apr. 2010, doi: 10.1038/nm0410-400.

[50] G. Baldanzi, "Inhibition of diacylglycerol kinases as a physiological way to promote diacylglycerol

signaling," *Adv. Biol. Regul.*, vol. 55, pp. 39–49, 2014, doi: https://doi.org/10.1016/j.jbior.2014.02.001.

[51] F. Bäckhed, R. E. Ley, J. L. Sonnenburg, D. A. Peterson, and J. I. Gordon, "Host-bacterial mutualism in the human intestine.," *Science*, vol. 307, no. 5717, pp. 1915–1920, Mar. 2005, doi: 10.1126/science.1104816.

[52] L. Lichtenstein *et al.*, "Angptl4 upregulates cholesterol synthesis in liver via inhibition of LPL- and HL-dependent hepatic cholesterol uptake.," *Arterioscler. Thromb. Vasc. Biol.*, vol. 27, no. 11, pp. 2420–2427, Nov. 2007, doi: 10.1161/ATVBAHA.107.151894.

[53] D. S. Wishart *et al.*, "HMDB 4.0: the human metabolome database for 2018.," *Nucleic Acids Res.*, vol. 46, no. D1, pp. D608–D617, Jan. 2018, doi: 10.1093/nar/gkx1089.

[54] H.-M. Bergman, L. Lindfors, F. Palm, J. Kihlberg, and I. Lanekoff, "Metabolite aberrations in early diabetes detected in rat kidney using mass spectrometry imaging.," *Anal. Bioanal. Chem.*, vol. 411, no. 13, pp. 2809–2816, May 2019, doi: 10.1007/s00216-019-01721-5.

[55] Z. Tian *et al.*, "Intervention of Uncaria and Its Components on Liver Lipid Metabolism in Spontaneously Hypertensive Rats.," *Front. Pharmacol.*, vol. 11, p. 910, 2020, doi: 10.3389/fphar.2020.00910.

[56] M. J. Gerl *et al.*, "Machine learning of human plasma lipidomes for obesity estimation in a large population cohort," *PLoS Biol.*, vol. 17, no. 10, pp. e3000443–e3000443, Oct. 2019, doi: 10.1371/journal.pbio.3000443.

[57] M. Popović Hadžija, Z. Siketić, M. Hadžija, M. Barac, and I. Bogdanović Radović, "Study of the diacylglycerol composition in the liver and serum of mice with prediabetes and diabetes using MeV TOF-SIMS.," *Diabetes Res. Clin. Pract.*, vol. 159, p. 107986, Jan. 2020, doi: 10.1016/j.diabres.2019.107986.

[58] F. Magkos *et al.*, "Intrahepatic diacylglycerol content is associated with hepatic insulin resistance in obese subjects.," *Gastroenterology*, vol. 142, no. 7, pp. 1444–6.e2, Jun. 2012, doi: 10.1053/j.gastro.2012.03.003.

[59] M. A. Polewski *et al.*, "Plasma diacylglycerol composition is a biomarker of metabolic syndrome onset in rhesus monkeys.," *J. Lipid Res.*, vol. 56, no. 8, pp. 1461–1470, Aug. 2015, doi: 10.1194/jlr.M057562.

[60] M. Jové *et al.*, "Plasma lipidomics discloses metabolic syndrome with a specific HDL phenotype.," *FASEB J. Off. Publ. Fed. Am. Soc. Exp. Biol.*, vol. 28, no. 12, pp. 5163–5171, Dec. 2014, doi: 10.1096/fj.14-253187.

[61] S. Nicolas *et al.*, "Transfer of dysbiotic gut microbiota has beneficial effects on host liver metabolism.," *Mol. Syst. Biol.*, vol. 13, no. 3, p. 921, 2017, doi: 10.15252/msb.20167356.

[62] C. Jin *et al.*, "Insights into a Possible Mechanism Underlying the Connection of Carbendazim-Induced Lipid Metabolism Disorder and Gut Microbiota Dysbiosis in Mice.," *Toxicol. Sci.*, vol. 166, no. 2, pp. 382–393, Dec. 2018, doi: 10.1093/toxsci/kfy205.

[63] H. K. Stals, W. Top, and P. E. Declercq, "Regulation of triacylglycerol synthesis in permeabilized rat hepatocytes. Role of fatty acid concentration and diacylglycerol acyltransferase.," *FEBS Lett.*, vol. 343, no. 1, pp. 99–102, Apr. 1994, doi: 10.1016/0014-5793(94)80615-2.

[64] R. A. Igal and R. A. Coleman, "Neutral lipid storage disease: a genetic disorder with abnormalities in the regulation of phospholipid metabolism.," *J. Lipid Res.*, vol. 39, no. 1, pp. 31–43, Jan. 1998.

[65] S. Jackowski, J. Wang, and I. Baburina, "Activity of the phosphatidylcholine biosynthetic pathway modulates the distribution of fatty acids into glycerolipids in proliferating cells," *Biochim. Biophys. Acta*, vol. 1483, no. 3, p. 301—315, 2000, doi: 10.1016/s1388-1981(99)00203-6.

[66] L. Marín, E. M. Miguélez, C. J. Villar, and F. Lombó, "Bioavailability of Dietary Polyphenols and Gut

Microbiota Metabolism: Antimicrobial Properties," *Biomed Res. Int.*, vol. 2015, p. 905215, 2015, doi: 10.1155/2015/905215.

[67] M. De Angelis, G. Garruti, F. Minervini, L. Bonfrate, P. Portincasa, and M. Gobbetti, "The Food-gut Human Axis: The Effects of Diet on Gut Microbiota and Metabolome," *Curr. Med. Chem.*, vol. 26, no. 19, pp. 3567–3583, 2017, doi: 10.2174/0929867324666170428103848.

[68] Y. T. Loo, K. Howell, M. Chan, P. Zhang, and K. Ng, "Modulation of the human gut microbiota by phenolics and phenolic fiber-rich foods," *Compr. Rev. Food Sci. Food Saf.*, vol. 19, no. 4, pp. 1268–1298, Jul. 2020, doi: https://doi.org/10.1111/1541-4337.12563.

[69] T. Ozdal, D. A. Sela, J. Xiao, D. Boyacioglu, F. Chen, and E. Capanoglu, "The Reciprocal Interactions between Polyphenols and Gut Microbiota and Effects on Bioaccessibility," *Nutrients*, vol. 8, no. 2, p. 78, Feb. 2016, doi: 10.3390/nu8020078.

[70] H. J. Lees, J. R. Swann, I. D. Wilson, J. K. Nicholson, and E. Holmes, "Hippurate: The natural history of a mammalian-microbial cometabolite," *J. Proteome Res.*, vol. 12, no. 4, pp. 1527–1546, 2013, doi: 10.1021/pr300900b.

[71] T. A. Clayton, "Metabolic differences underlying two distinct rat urinary phenotypes, a suggested role for gut microbial metabolism of phenylalanine and a possible connection to autism," *FEBS Lett.*, vol. 586, no. 7, pp. 956–961, 2012, doi: https://doi.org/10.1016/j.febslet.2012.01.049.

[72] A. Temellini, S. Mogavero, P. C. Giulianotti, A. Pietrabissa, F. Mosca, and G. M. Pacifici, "Conjugation of benzoic acid with glycine in human liver and kidney: a study on the interindividual variability.," *Xenobiotica.*, vol. 23, no. 12, pp. 1427–1433, Dec. 1993, doi: 10.3109/00498259309059451.

[73] H. S. Ejtahed, P. Angoorani, A. R. Soroush, S. Hasani-Ranjbar, S. D. Siadat, and B. Larijani, "Gut microbiota-derived metabolites in obesity: A systematic review," *Biosci. Microbiota, Food Heal.*, vol. 39, no. 3, pp. 65–76, 2020, doi: 10.12938/bmfh.2019-026.

[74] M. S. Ahmad *et al.*, "Metabolic Phenotype of Obesity in a Saudi Population," *J. Proteome Res.*, vol. 16, no. 2, pp. 635–644, 2017, doi: 10.1021/acs.jproteome.6b00710.

[75] R. Calvani *et al.*, "Gut microbiome-derived metabolites characterize a peculiar obese urinary metabotype," *Int. J. Obes.*, vol. 34, no. 6, pp. 1095–1098, 2010, doi: 10.1038/ijo.2010.44.

[76] T. Pallister *et al.*, "Hippurate as a metabolomic marker of gut microbiome diversity: Modulation by diet and relationship to metabolic syndrome," *Sci. Rep.*, vol. 7, no. 1, pp. 1–9, 2017, doi: 10.1038/s41598-017-13722-4.

[77] H. R. T. Williams *et al.*, "Differences in gut microbial metabolism are responsible for reduced hippurate synthesis in Crohn's disease," *BMC Gastroenterol.*, vol. 10, p. 108, Sep. 2010, doi: 10.1186/1471-230X-10-108.

[78] F. Zhang *et al.*, "Metabonomics study of urine and plasma in depression and excess fatigue rats by ultra fast liquid chromatography coupled with ion trap-time of flight mass spectrometry.," *Mol. Biosyst.*, vol. 6, no. 5, pp. 852–861, May 2010, doi: 10.1039/b914751a.

[79] Y. Wang, H. Tang, J. K. Nicholson, P. J. Hylands, J. Sampson, and E. Holmes, "A metabonomic strategy for the detection of the metabolic effects of chamomile (Matricaria recutita L.) ingestion.," *J. Agric. Food Chem.*, vol. 53, no. 2, pp. 191–196, Jan. 2005, doi: 10.1021/jf0403282.

[80] M. N. Clifford, E. L. Copeland, J. P. Bloxsidge, and L. A. Mitchell, "Hippuric acid as a major excretion product associated with black tea consumption," *Xenobiotica*, vol. 30, no. 3, pp. 317–326, Jan. 2000, doi: 10.1080/004982500237703.

[81] J. Toromanović *et al.*, "Urinary hippuric acid after ingestion of edible fruits.," *Bosn. J. basic Med. Sci.*, vol. 8, no. 1, pp. 38–43, Feb. 2008, doi: 10.17305/bjbms.2008.2994.

[82] I. Rowland *et al.*, "Gut microbiota functions: metabolism of nutrients and other food

components," *Eur. J. Nutr.*, vol. 57, no. 1, pp. 1–24, 2018, doi: 10.1007/s00394-017-1445-8.

[83] I. Manso *et al.*, "3-Hydroxyphenylpropionate and phenylpropionate are synergistic activators of the MhpR transcriptional regulator from Escherichia coli.," *J. Biol. Chem.*, vol. 284, no. 32, pp. 21218–21228, Aug. 2009, doi: 10.1074/jbc.M109.008243.

[84] Y. Konishi and S. Kobayashi, "Microbial metabolites of ingested caffeic acid are absorbed by the monocarboxylic acid transporter (MCT) in intestinal Caco-2 cell monolayers.," *J. Agric. Food Chem.*, vol. 52, no. 21, pp. 6418–6424, Oct. 2004, doi: 10.1021/jf049560y.

[85] G. M. Pasinetti, R. Singh, S. Westfall, F. Herman, J. Faith, and L. Ho, "The Role of the Gut Microbiota in the Metabolism of Polyphenols as Characterized by Gnotobiotic Mice," *J. Alzheimer's Dis.*, vol. 63, pp. 409–421, 2018, doi: 10.3233/JAD-171151.

[86] Y.-Y. Zhang *et al.*, "3-(4-Hydroxyphenyl)propionic acid, a major microbial metabolite of procyanidin A2, shows similar suppression of macrophage foam cell formation as its parent molecule," *RSC Adv.*, vol. 8, no. 12, pp. 6242–6250, 2018, doi: 10.1039/C7RA13729J.

[87] A. N. Phipps, J. Stewart, B. Wright, and I. D. Wilson, "Effect of diet on the urinary excretion of hippuric acid and other dietary-derived aromatics in rat. A complex interaction between diet, gut microflora and substrate specificity.," *Xenobiotica.*, vol. 28, no. 5, pp. 527–537, May 1998, doi: 10.1080/004982598239443.

[88] H. Abramovič, "Chapter 93 - Antioxidant Properties of Hydroxycinnamic Acid Derivatives: A Focus on Biochemistry, Physicochemical Parameters, Reactive Species, and Biomolecular Interactions," V. R. B. T.-C. in H. and D. P. Preedy, Ed. San Diego: Academic Press, 2015, pp. 843–852.

[89] C.-L. Hsu, C.-H. Wu, S.-L. Huang, and G.-C. Yen, "Phenolic Compounds Rutin and o-Coumaric Acid Ameliorate Obesity Induced by High-Fat Diet in Rats," *J. Agric. Food Chem.*, vol. 57, no. 2, pp. 425–431, Jan. 2009, doi: 10.1021/jf802715t.

[90] E. Munukka *et al.*, "Six-Week Endurance Exercise Alters Gut Metagenome That Is not Reflected in Systemic Metabolism in Over-weight Women.," *Front. Microbiol.*, vol. 9, p. 2323, 2018, doi: 10.3389/fmicb.2018.02323.

[91] N. Shen *et al.*, "Longitudinal changes of microbiome composition and microbial metabolomics after surgical weight loss in individuals with obesity," *Surg. Obes. Relat. Dis.*, vol. 15, no. 8, pp. 1367–1373, 2019, doi: https://doi.org/10.1016/j.soard.2019.05.038.

[92] K. L. Bowerman *et al.*, "Disease-associated gut microbiome and metabolome changes in patients with chronic obstructive pulmonary disease," *Nat. Commun.*, vol. 11, no. 1, p. 5886, 2020, doi: 10.1038/s41467-020-19701-0.

[93] W. Wu *et al.*, "Bioregional Alterations in Gut Microbiome Contribute to the Plasma Metabolomic Changes in Pigs Fed with Inulin," *Microorganisms*, vol. 8, no. 1, p. 111, Jan. 2020, doi: 10.3390/microorganisms8010111.

[94] S. Shoaie *et al.*, "Quantifying Diet-Induced Metabolic Changes of the Human Gut Microbiome.," *Cell Metab.*, vol. 22, no. 2, pp. 320–331, Aug. 2015, doi: 10.1016/j.cmet.2015.07.001.

[95] R. Landberg and K. Hanhineva, "Biomarkers of a Healthy Nordic Diet-From Dietary Exposure Biomarkers to Microbiota Signatures in the Metabolome.," *Nutrients*, vol. 12, no. 1, Dec. 2019, doi: 10.3390/nu12010027.

Annex. Supplementary Material of Manuscript 3

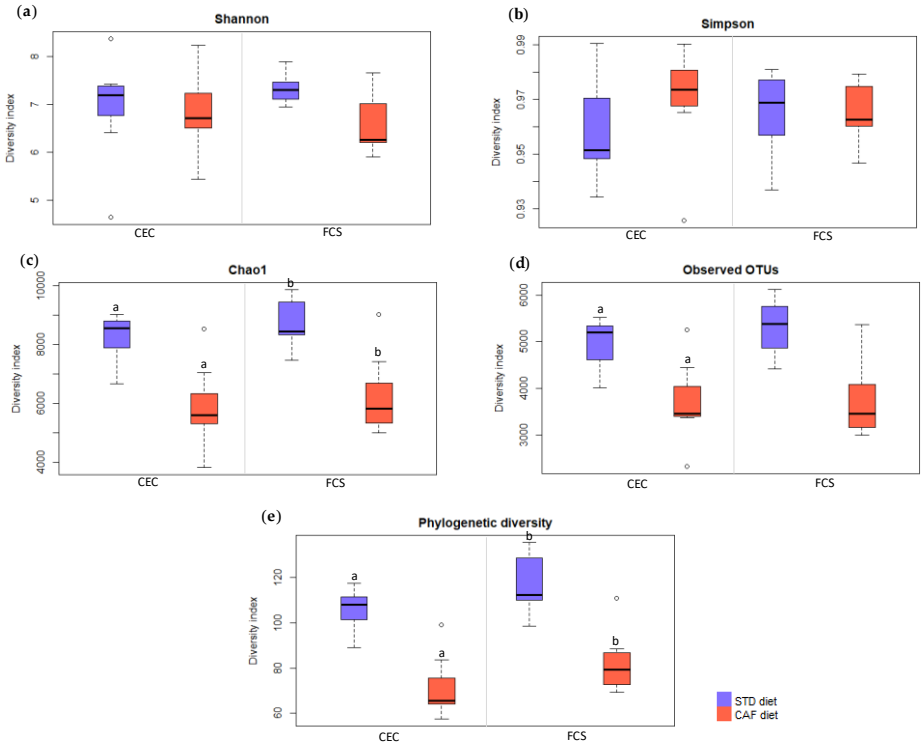

Supplementary figure 1. Characterization of the alpha diversity indices derived from the QIIME command α rarefaction of rats fed with a STD (blue boxplots) and CAF diet (red boxplots) in different metagenomic biofluids (CEC and FCS). (a) Shannon index, (b) Simpson index, (c) Chao1, (d) Observed OTUs, (e) Phylogenetic diversity. Different lowercase letters a and b indicate significant ($p < 0.05$) changes between diets.

Supplementary table 1. Summary of metagenomics in the STD-D and the CAF-D groups in CEC and FCS focusing on taxonomic data. Taxonomic data presented as the mean ± SEM (*n* = 7) per group shorted by *q*-value of CEC. The summary of univariant analysis is shown including *p*-value, *q*-value and FC, the statistically significant *p*-values and *q*-values (< 0.05) are highlighted in bold.

					CEC					FCS				
Phylum	**Class**	**Order**	**Family**	**Genus**	**STD-D (%)**	**CAF-D (%)**	***p*-value**	***q*-value**	**FC**	**STD-D (%)**	**CAF-D (%)**	***p*-value**	***q*-value**	**FC**
Firmicutes	*Clostridia*	*Clostridiales*	-	-	53.47 ± 5.66	9.31 ± 3.54	**<0.01**	**<0.01**	0.17	29.73 ± 4.17	5.59 ± 1.84	**<0.01**	**0.02**	0.19
Firmicutes	*Clostridia*	*Clostridiales*	*Lachnospiraceae*	*Ruminococcus*	0.69 ± 0.19	1.96 ± 0.2	**<0.01**	**0.01**	2.83	0.55 ± 0.1	1.05 ± 0.18	**0.03**	0.13	1.93
Firmicutes	*Bacilli*	*Turicibacterales*	*Turicibacteraceae*	*Turicibacter*	0.14 ± 0.03	0.02 ± 0.01	**<0.01**	**0.02**	0.13	0.15 ± 0.06	0.26 ± 0.12	0.42	0.58	1.76
Bacteroidetes	*Bacteroidia*	*Bacteroidales*	*Porphyromonadaceae*	*Parabacteroides*	0.22 ± 0.08	3.92 ± 0.81	**<0.01**	**0.03**	17.86	0.42 ± 0.1	3.44 ± 0.75	**0.01**	0.05	8.15
Firmicutes	*Clostridia*	*Clostridiales*	*Lachnospiraceae*	*Blautia*	0.12 ± 0.02	2.63 ± 0.62	**0.01**	**0.04**	21.65	0.08 ± 0.02	2.59 ± 0.81	**0.02**	0.1	32.14
Bacteroidetes	*Bacteroidia*	*Bacteroidales*	*S24-7*	-	9.61 ± 2.04	23.43 ± 4.04	**0.01**	0.07	2.44	33.08 ± 4.8	33.9 ± 3.51	0.89	0.93	1.02
Firmicutes	*Clostridia*	*Clostridiales*	*Peptostreptococcaceae*	-	0.58 ± 0.15	0.12 ± 0.05	**0.02**	0.09	0.2	0.53 ± 0.34	0.63 ± 0.2	0.82	0.92	1.17
Bacteroidetes	*Bacteroidia*	*Bacteroidales*	*Bacteroidaceae*	*Bacteroides*	0.65 ± 0.14	5.98 ± 1.81	**0.03**	0.09	9.13	1.62 ± 0.33	1.96 ± 0.27	0.44	0.58	1.21
Firmicutes	*Clostridia*	*Clostridiales*	*Peptococcaceae*	*rc4-4*	0.39 ± 0.1	0.96 ± 0.2	**0.03**	0.11	2.48	0.25 ± 0.04	0.22 ± 0.06	0.65	0.79	0.86
Proteobacteria	*Gammaproteobacteria*	*Enterobacteriales*	*Enterobacteriaceae*	-	0.29 ± 0.18	3.06 ± 1.08	**0.04**	0.12	10.68	1.13 ± 0.86	2.72 ± 0.78	0.2	0.42	2.4
Verrucomicrobia	*Verrucomicrobiae*	*Verrucomicrobiales*	*Verrucomicrobiaceae*	*Akkermansia*	1.21 ± 0.36	12.01 ± 4.5	**0.05**	0.12	9.94	2.28 ± 0.75	11.11 ± 3.82	0.06	0.21	4.88
Firmicutes	*Erysipelotrichi*	*Erysipelotrichales*	*Erysipelotrichaceae*	*Eubacterium*	0	0.11 ± 0.04	**0.05**	0.12	76.02	0	0.17 ± 0.09	0.1	0.27	39.76
Tenericutes	*Mollicutes*	*RF39*	-	-	0.25 ± 0.05	0.09 ± 0.05	0.06	0.13	0.38	0.6 ± 0.18	0.43 ± 0.15	0.48	0.61	0.72
Firmicutes	*Clostridia*	*Clostridiales*	*Ruminococcaceae*	*Oscillospira*	5.62 ± 0.84	3.55 ± 0.72	0.09	0.17	0.63	5.03 ± 0.63	1.93 ± 0.54	**<0.01**	**0.02**	0.38
Firmicutes	*Clostridia*	*Clostridiales*	*Lachnospiraceae*	*Dorea*	0.1 ± 0.01	0.24 ± 0.07	0.11	0.2	2.42	0.13 ± 0.03	0.28 ± 0.09	0.16	0.38	2.15
Firmicutes	*Clostridia*	*Clostridiales*	*Clostridiaceae*	*SMB53*	0.2 ± 0.05	0.08 ± 0.04	0.12	0.2	0.43	0.22 ± 0.14	0.42 ± 0.19	0.43	0.58	1.88
Firmicutes	*Clostridia*	*Clostridiales*	*Clostridiaceae*	-	0.07 ± 0.01	0.03 ± 0.02	0.12	0.21	0.42	0.11 ± 0.04	0.11 ± 0.05	0.93	0.93	1.06
Firmicutes	*Bacilli*	*Lactobacillales*	*Lactobacillaceae*	*Lactobacillus*	4.42 ± 1.23	9.81 ± 3.32	0.17	0.26	2.22	4.95 ± 2.17	16.25 ± 5.8	0.11	0.27	3.29
Bacteroidetes	*Bacteroidia*	*Bacteroidales*	*Rikenellaceae*	-	2.25 ± 0.46	1.41 ± 0.37	0.18	0.26	0.63	2.17 ± 0.26	0.83 ± 0.13	**<0.01**	**0.03**	0.38
Firmicutes	*Clostridia*	*Clostridiales*	*Ruminococcaceae*	-	4.79 ± 0.73	3.21 ± 0.94	0.21	0.29	0.67	5.2 ± 0.48	3.53 ± 1.42	0.3	0.56	0.68
Firmicutes	*Clostridia*	*Clostridiales*	*Dehalobacteriaceae*	*Dehalobacterium*	0.31 ± 0.05	0.19 ± 0.07	0.22	0.29	0.62	0.16 ± 0.02	0.05 ± 0.02	**0.01**	**0.05**	0.34
Firmicutes	*Clostridia*	*Clostridiales*	*Lachnospiraceae*	*Roseburia*	0.24 ± 0.09	1.79 ± 1.25	0.26	0.33	7.56	0.21 ± 0.12	0.16 ± 0.1	0.76	0.89	0.77
Firmicutes	*Clostridia*	*Clostridiales*	*Lachnospiraceae*	*Coprococcus*	3.04 ± 0.74	4.46 ± 1.04	0.29	0.35	1.47	2.08 ± 0.5	3.35 ± 1.27	0.38	0.58	1.61

Firmicutes	*Erysipelotrichi*	*Erysipelotrichales*	*Erysipelotrichaceae*	*Allobaculum*	0	1.71 ± 1.65	0.34	0.4	3220.5	0	0.3 ± 0.23	0.24	0.48	1024.8
Firmicutes	*Clostridia*	*Clostridiales*	*Lachnospiraceae*	-	9.04 ± 2.13	7.17 ± 1.01	0.45	0.5	0.79	6.36 ± 1.38	6.04 ± 1.78	0.89	0.93	0.95
Firmicutes	*Clostridia*	*Clostridiales*	*Mogibacteriaceae*	-	0.12 ± 0.03	0.15 ± 0.03	0.49	0.53	1.22	0.22 ± 0.06	0.1 ± 0.03	0.1	0.27	0.46
Firmicutes	*Clostridia*	*Clostridiales*	*Ruminococcaceae*	*Ruminococcus*	1.45 ± 0.3	1.22 ± 0.39	0.65	0.67	0.84	1.08 ± 0.18	0.79 ± 0.25	0.36	0.58	0.73
Firmicutes	*Clostridia*	*Clostridiales*	*Clostridiaceae*	*Clostridium*	0.14 ± 0.11	0.18 ± 0.09	0.81	0.81	1.25	0.44 ± 0.21	0.9 ± 0.42	0.36	0.58	2.04

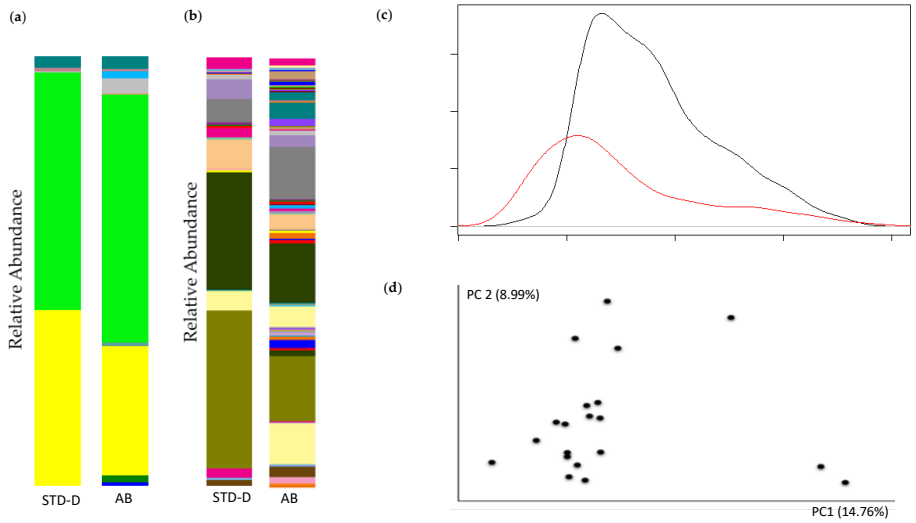

Supplementary figure 2. Microbiota analysis after the AB treatment compared with a control group (STD-D group). (a) Phyla relative abundance, (b) Genus relative abundance, (c) Density plot of OTU vs genus: STD-D (black line) and after treatment (red line) with significant differences in area (p = 0.04), (d) Analysis of beta diversity represented by scores after the AB treatment with PCoA (unweighted unifrac).

Supplementary table 2. Biometric parameters, plasma parameters and liver biochemistry of transplant model. Data are presented as the mean ± SEM (*n* = 7). The statistical comparisons among groups were conducted using Student's *t*-test, the statistically significant *p*-values ($p < 0.05$) are highlighted in bold. Abbreviations: RWAT, retroperitoneal white adipose tissue; MWAT, mesenteric white adipose tissue; TG, triglycerides; TC, total cholesterol; NEFAs, non-esterified fatty acids.

		Mean ± SEM			*p*-values		
		CNT-R	**STD-R**	**CAF-R**	**CNT-R vs STD-R**	**CNT-R vs CAF-R**	**STD-R vs CAF-R**
Biometric parameters	Initial body weight (g)	334.55 ± 17.02	341.55 ± 9.62	341.13 ± 12.16	0.37	0.42	0.94
	Final body weight (g)	415.24 ± 10.86	407.10 ± 7.56	420.47 ± 11.98	0.55	0.74	0.34
	Food intake (g)	24.06 ± 0.80	23.26 ± 1.06	23.97 ± 1.01	0.56	0.95	0.64
	RWAT weight (g)	6.73 ± 0.96	7.14 ± 0.90	9.70 ± 1.70	0.76	0.17	0.22
	MWAT weight (g)	4.40 ± 0.46	4.04 ± 0.26	5.16 ± 0.52	0.5	0.29	0.09
	Muscle weight (g)	2.49 ± 0.08	2.51 ± 0.06	2.49 ± 0.08	0.86	0.97	0.89
	Liver weight (g)	11.61 ± 0.50	11.57 ± 0.52	11.92 ± 0.59	0.96	0.69	0.66
	CEC weight (g)	8.43 ± 0.63	5.23 ± 0.26	5.33 ± 0.38	**0.002**	**0.002**	0.82
Plasma biochemistry	Glucose (mM)	74.20 ± 2.45	77.88 ± 5.81	74.46 ± 1.88	0.58	0.93	0.59
	TG (mM)	77.06 ± 4.07	80.91 ± 14.01	117.30 ± 17.12	0.8	0.07	0.13
	TC (mM)	42.34 ± 2.62	44.81 ± 9	68.19 ± 11	0.8	0.07	0.13

	NEFAs (mM)	0.35 ± 0.02	0.37 ± 0.02	0.43 ± 0.03	0.69	**0.04**	0.11
Liver biochemistry	Total lipids (mg/g)	40.98 ± 3.54	38.57 ± 2.20	28.99 ± 2.22	0.58	**0.02**	**0.01**
	TC (mg/g)	1.83 ± 0.08	1.98 ± 0.11	1.83 ± 0.08	0.28	0.97	0.27
	Phospholipids (mg/g)	12.25 ± 0.67	12.85 ± 0.60	10.67 ± 0.67	0.52	0.12	**0.03**
	TG (mg/g)	4.10 ± 0.27	4.22 ± 0.23	4.07 ± 0.34	0.75	0.94	0.72

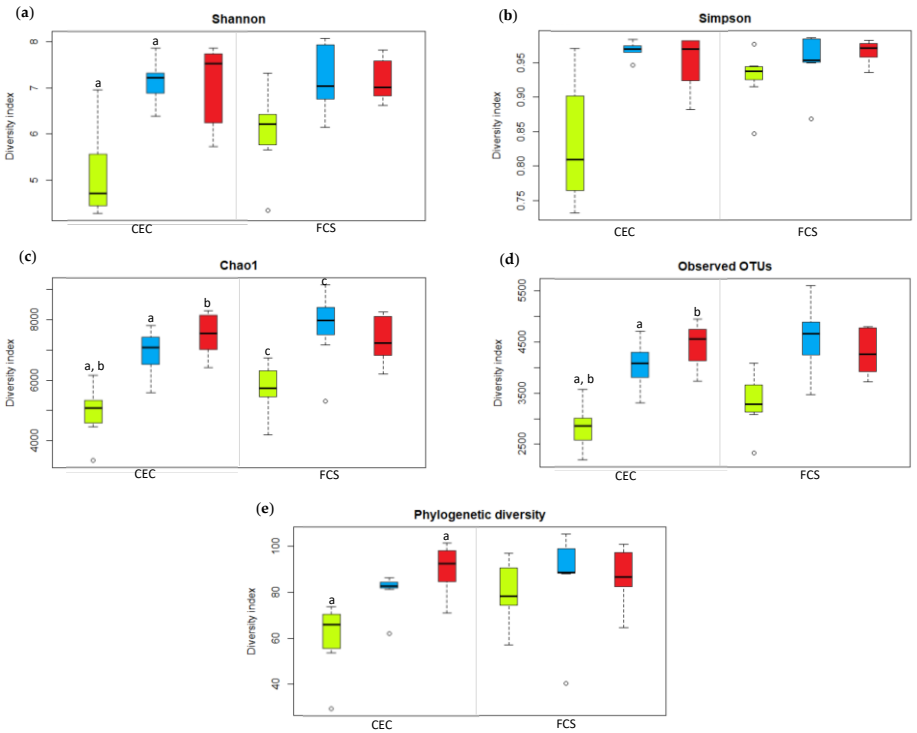

Supplementary figure 3. Characterization of the alpha diversity indices derived from the QIIME command α rarefraction after the microbiota transplant in different metagenomic biofluids (CEC and FCS). (a) Shannon index, (b) Simpson index, (c) Chao1, (d) Observed OTUs, (e) Phylogenetic diversity. Different lowercase letters a and b indicate significant ($p < 0.05$) changes between diets. Green, CNT-R; blue, STD-R; red, CAF-R.

Supplementary table 3. Summary of metagenomics in the CNT-R and the STD-R groups in CEC and FCS focusing on taxonomic data. Taxonomic data is presented as the mean ± SEM (*n* = 7) per group shorted by *q*-value of CEC. The summary of univariant analysis is shown including *p*-value, *q*-value and FC, the statistically significant *p*-values and *q*-values (< 0.05) are highlighted in bold.

					CEC					FCS				
Phylum	**Class**	**Order**	**Family**	**Genus**	**CNT-R (%)**	**STD-R (%)**	***p*-value**	***q*-value**	**FC**	**CNT-R (%)**	**STD-R (%)**	***p*-value**	***q*-value**	**FC**
Firmicutes	*Clostridia*	*Clostridiales*	*Ruminococcaceae*	*Ruminococcus*	0.68 ± 0.26	2.1 ± 0.79	**<0.01**	**<0.01**	3.09	2.41 ± 0.91	2.63 ± 1	0.85	0.92	1.09
Firmicutes	*Clostridia*	*Clostridiales*	*Lachnospiraceae*	-	3.27 ± 1.24	2.85 ± 1.08	**<0.01**	**0.01**	0.87	18.3 ± 6.91	8.59 ± 3.25	0.15	0.3	0.47
Firmicutes	*Clostridia*	*Clostridiales*	*Ruminococcaceae*	*Oscillospira*	2.51 ± 0.95	2.31 ± 0.87	**<0.01**	**0.01**	0.92	7.51 ± 2.84	4.58 ± 1.73	0.72	0.81	0.61
Firmicutes	*Clostridia*	*Clostridiales*	*Lachnospiraceae*	*Coprococcus*	1.05 ± 0.4	1.22 ± 0.46	**<0.01**	**0.02**	1.15	3.77 ± 1.43	2.72 ± 1.03	0.25	0.38	0.72
Actinobacteria	*Coriobacteriia*	*Coriobacteriales*	*Coriobacteriaceae*	*Adlercreutzia*	0.09 ± 0.04	0.09 ± 0.03	**0.01**	0.06	0.99	0.02 ± 0.01	0.06 ± 0.02	**<0.01**	**0.02**	3.33
Firmicutes	*Clostridia*	*Clostridiales*	*Lachnospiraceae*	*Roseburia*	0.07 ± 0.03	0.03 ± 0.01	**0.02**	0.08	0.47	0.38 ± 0.14	0.18 ± 0.07	0.39	0.54	0.47
Firmicutes	*Clostridia*	*Clostridiales*	*Peptococcaceae*	*rc4-4*	0.07 ± 0.03	0.17 ± 0.06	**0.02**	0.08	2.46	0.18 ± 0.07	0.47 ± 0.18	0.43	0.57	2.63
Verrucomicrobia	*Verrucomicrobiae*	*Verrucomicrobiales*	*Verrucomicrobiaceae*	*Akkermansia*	8.46 ± 3.2	12.9 ± 4.88	**0.03**	0.08	1.53	0.78 ± 0.3	2.97 ± 1.12	0.98	0.98	3.79
Bacteroidetes	*Bacteroidia*	*Bacteroidales*	*Bacteroidaceae*	*Bacteroides*	0.43 ± 0.16	5.07 ± 1.92	**0.05**	0.14	11.9	0.09 ± 0.03	0.42 ± 0.16	**0.02**	0.12	4.65
Proteobacteria	*Gammaproteobacteria*	*Enterobacteriales*	*Enterobacteriaceae*	-	0.62 ± 0.24	0.79 ± 0.3	0.06	0.16	1.26	0.21 ± 0.08	0.22 ± 0.08	0.93	0.97	1.06
Firmicutes	*Clostridia*	*Clostridiales*	*Ruminococcaceae*	-	2.52 ± 0.95	2.35 ± 0.89	0.11	0.24	0.94	4.54 ± 1.72	6.7 ± 2.53	0.63	0.75	1.48
Bacteroidetes	*Bacteroidia*	*Bacteroidales*	*S24-7*	-	17.7 ± 6.68	38.3 ± 14.5	0.15	0.31	2.17	6.96 ± 2.63	41.1 ± 15.5	0.03	0.17	5.91
Firmicutes	*Clostridia*	*Clostridiales*	*Lachnospiraceae*	*Anaerostipes*	0.03 ± 0.01	0.13 ± 0.05	0.26	0.5	3.71	0.07 ± 0.03	0.23 ± 0.09	0.21	0.37	3.37
Actinobacteria	*Actinobacteria*	*Bifidobacteriales*	*Bifidobacteriaceae*	*Bifidobacterium*	0.02 ± 0.01	0.25 ± 0.09	0.31	0.51	12.4	-	0.57 ± 0.21	**<0.01**	**<0.01**	133.67
Firmicutes	*Clostridia*	*Clostridiales*	*Clostridiaceae*	*SMB53*	0.07 ± 0.03	0.31 ± 0.12	0.29	0.51	4.49	0.19 ± 0.07	0.41 ± 0.16	0.12	0.26	2.19

Firmicutes	*Clostridia*	*Clostridiales*	*Lachnospiraceae*	*[Ruminococcus]*	1.45 ± 0.55	1.11 ± 0.42	0.33	0.51	0.76	0.91 ± 0.34	0.42 ± 0.16	0.15	0.3	0.46
Firmicutes	*Bacilli*	*Turicibacterales*	*Turicibacteraceae*	*Turicibacter*	0.06 ± 0.02	0.59 ± 0.22	0.45	0.66	9.6	0.04 ± 0.02	0.41 ± 0.15	0.06	0.18	9.86
Firmicutes	*Clostridia*	*Clostridiales*	*[Mogibacteriaceae]*	-	0.12 ± 0.04	0.2 ± 0.08	0.48	0.66	1.68	0.08 ± 0.03	0.2 ± 0.07	0.07	0.18	2.41
Firmicutes	*Bacilli*	*Lactobacillales*	*Lactobacillaceae*	*Lactobacillus*	3.46 ± 1.31	11.4 ± 4.33	0.59	0.7	3.3	2.8 ± 1.06	6.27 ± 2.37	**0.04**	0.17	2.24
Firmicutes	*Clostridia*	*Clostridiales*	-	-	55.4 ± 20.9	12.4 ± 4.68	0.55	0.7	0.22	48.8 ± 18.5	17 ± 6.42	0.06	0.18	0.35
Firmicutes	*Clostridia*	*Clostridiales*	*Clostridiaceae*	*Clostridium*	0.23 ± 0.09	0.51 ± 0.19	0.57	0.7	2.19	0.16 ± 0.06	0.73 ± 0.28	0.12	0.26	4.72
Firmicutes	*Clostridia*	*Clostridiales*	*Lachnospiraceae*	*Blautia*	0.34 ± 0.13	1.38 ± 0.52	0.65	0.74	4.13	0.28 ± 0.11	0.13 ± 0.05	0.24	0.38	0.46
Bacteroidetes	*Bacteroidia*	*Bacteroidales*	*Rikenellaceae*	-	0.69 ± 0.26	1.13 ± 0.43	0.79	0.86	1.64	0.76 ± 0.29	1.25 ± 0.47	**0.02**	0.12	1.64
Firmicutes	*Clostridia*	*Clostridiales*	*Peptostreptococcaceae*	-	0.16 ± 0.06	0.3 ± 0.11	0.91	0.95	1.9	0.17 ± 0.06	0.29 ± 0.11	0.52	0.65	1.74
Firmicutes	*Clostridia*	*Clostridiales*	*Lachnospiraceae*	*Dorea*	0.07 ± 0.02	0.18 ± 0.07	0.99	0.99	2.73	0.07 ± 0.02	0.09 ± 0.03	0.28	0.4	1.39

Supplementary table 4. Summary of metagenomics in the CNT-R and the CAF-R groups in CEC and FCS focusing on taxonomic data. Taxonomic data is presented as the mean ± SEM (*n* = 7) per group shorted by *q*-value of CEC. The summary of univariant analysis is shown including *p*-value, *q*-value and FC, the statistically significant *p*-values and q-values (< 0.05) are highlighted in bold.

					CEC					**FCS**				
Phylum	**Class**	**Order**	**Family**	**Genus**	**CNT-R (%)**	**CAF-R (%)**	***p*-value**	***q*-value**	**FC**	**CNT-R (%)**	**CAF-R (%)**	***p*-value**	***q*-value**	**FC**
Firmicutes	*Clostridia*	*Clostridiales*	*Ruminococcaceae*	*Oscillospira*	2.51 ± 0.95	7.45 ± 3.04	**<0.01**	**0.01**	2.97	2.31 ± 0.87	4.63 ± 1.75	**<0.01**	0.04	2
Firmicutes	*Clostridia*	*Clostridiales*	*Lachnospiraceae*	*Coprococcus*	1.05 ± 0.4	3.01 ± 1.23	**<0.01**	**0.04**	2.85	1.22 ± 0.46	1.79 ± 0.68	0.23	0.53	1.47
Firmicutes	*Clostridia*	*Clostridiales*	*Ruminococcaceae*	*Ruminococcus*	0.68 ± 0.26	2.24 ± 0.92	**<0.01**	**0.04**	3.3	2.1 ± 0.79	2.59 ± 0.98	0.46	0.6	1.23
Firmicutes	*Clostridia*	*Clostridiales*	*Lachnospiraceae*	-	3.27 ± 1.24	9.31 ± 3.8	**0.01**	0.06	2.85	2.85 ± 1.08	3.26 ± 1.23	0.59	0.72	1.14

Actinobacteria	*Coriobacteriia*	*Coriobacteriales*	*Coriobacteriaceae*	-	0.02 ± 0.01	-	**0.02**	0.1	0.21	0.02 ± 0.01	0.01 ± 0	0.29	0.55	0.54
Verrucomicrobia	*Verrucomicrobiae*	*Verrucomicrobiales*	*Verrucomicrobiaceae*	*Akkermansia*	8.46 ± 3.2	0.73 ± 0.3	**0.02**	0.1	0.09	12.9 ± 4.88	2.23 ± 0.84	0.03	0.24	0.17
Actinobacteria	*Coriobacteriia*	*Coriobacteriales*	*Coriobacteriaceae*	*Adlercreutzia*	0.09 ± 0.04	0.03 ± 0.01	**0.03**	0.11	0.37	0.09 ± 0.03	0.1 ± 0.04	0.79	0.82	1.11
Firmicutes	*Erysipelotrichi*	*Erysipelotrichales*	*Erysipelotrichaceae*	-	0.05 ± 0.02	0.02 ± 0.01	**0.03**	0.11	0.28	0.21 ± 0.08	0.09 ± 0.04	0.2	0.53	0.45
Firmicutes	*Clostridia*	*Clostridiales*	*Lachnospiraceae*	*Dorea*	0.07 ± 0.02	0.26 ± 0.11	0.1	0.3	4.01	0.18 ± 0.07	0.29 ± 0.11	0.22	0.53	1.61
Firmicutes	*Clostridia*	*Clostridiales*	*Peptococcaceae*	*rc4-4*	0.07 ± 0.03	0.14 ± 0.06	0.13	0.36	2.11	0.17 ± 0.06	0.27 ± 0.1	0.27	0.54	1.61
Firmicutes	*Clostridia*	*Clostridiales*	*Lachnospiraceae*	*[Ruminococcus]*	1.45 ± 0.55	0.64 ± 0.26	0.16	0.41	0.44	1.11 ± 0.42	0.42 ± 0.16	0.01	0.17	0.38
Bacteroidetes	*Bacteroidia*	*Bacteroidales*	*S24-7*	-	17.7 ± 6.68	7.94 ± 3.24	0.2	0.44	0.45	38.4 ± 14.5	41.1 ± 15.5	0.69	0.75	1.07
Tenericutes	*Mollicutes*	*RF39*	-	-	0.03 ± 0.01	0.39 ± 0.16	0.2	0.44	15.41	0.12 ± 0.04	0.58 ± 0.22	0.14	0.5	5.02
Proteobacteria	*Gammaproteobacteria*	*Enterobacteriales*	*Enterobacteriaceae*	-	0.62 ± 0.24	0.33 ± 0.14	0.24	0.47	0.54	0.79 ± 0.3	0.52 ± 0.2	0.34	0.58	0.66
Bacteroidetes	*Bacteroidia*	*Bacteroidales*	*Porphyromonadaceae*	*Parabacteroides*	0.05 ± 0.02	0.13 ± 0.06	0.26	0.49	2.65	0.15 ± 0.06	0.69 ± 0.26	0.02	0.22	4.48
Firmicutes	*Clostridia*	*Clostridiales*	*Ruminococcaceae*	-	2.52 ± 0.95	3.65 ± 1.49	0.28	0.5	1.45	2.35 ± 0.89	4.52 ± 1.71	0.05	0.25	1.92
Firmicutes	*Clostridia*	*Clostridiales*	*Lachnospiraceae*	*Blautia*	0.34 ± 0.13	0.21 ± 0.09	0.38	0.59	0.63	1.38 ± 0.52	0.13 ± 0.05	0.12	0.48	0.09
Firmicutes	*Clostridia*	*Clostridiales*	*Peptostreptococcaceae*	-	0.16 ± 0.06	0.11 ± 0.04	0.36	0.59	0.66	0.3 ± 0.11	0.68 ± 0.26	0.25	0.53	2.27
Firmicutes	*Clostridia*	*Clostridiales*	*Clostridiaceae*	*SMB53*	0.07 ± 0.03	0.05 ± 0.02	0.51	0.75	0.76	0.31 ± 0.12	0.55 ± 0.21	0.42	0.58	1.78
Bacteroidetes	*Bacteroidia*	*Bacteroidales*	*Bacteroidaceae*	*Bacteroides*	0.43 ± 0.16	0.33 ± 0.13	0.66	0.84	0.77	5.07 ± 1.92	1 ± 0.38	0.24	0.53	0.2
Firmicutes	*Bacilli*	*Turicibacterales*	*Turicibacteraceae*	*Turicibacter*	0.06 ± 0.02	0.04 ± 0.02	0.6	0.84	0.67	0.59 ± 0.22	1.22 ± 0.46	0.35	0.58	2.08
Firmicutes	*Clostridia*	*Clostridiales*	*Lachnospiraceae*	*Anaerostipes*	0.03 ± 0.01	0.03 ± 0.01	0.65	0.84	0.77	0.13 ± 0.05	0.16 ± 0.06	0.67	0.75	1.25
Firmicutes	*Clostridia*	*Clostridiales*	*Clostridiaceae*	*Clostridium*	0.23 ± 0.09	0.18 ± 0.07	0.72	0.88	0.78	0.51 ± 0.19	1.25 ± 0.47	0.05	0.25	2.46

Firmicutes	*Bacilli*	*Lactobacillales*	*Lactobacillaceae*	*Lactobacillus*	3.46 ± 1.31	3.16 ± 1.29	0.82	0.95	0.91	11.4 ± 4.3	12.7 ± 4.81	0.69	0.75	1.11
Firmicutes	*Clostridia*	*Clostridiales*	-	-	55.3 ± 20.9	57.4 ± 23.4	0.86	0.96	1.04	12.3 ± 4.6	16.3 ± 6.15	0.37	0.58	1.31
Bacteroidetes	*Bacteroidia*	*Bacteroidales*	*Rikenellaceae*	-	0.69 ± 0.26	0.72 ± 0.3	0.9	0.97	1.05	1.13 ± 0.43	1.14 ± 0.43	0.98	0.98	1.01
Actinobacteria	*Actinobacteria*	*Bifidobacteriales*	*Bifidobacteriaceae*	*Bifidobacterium*	0.02 ± 0.01	0.02 ± 0.01	0.98	0.98	0.97	0.25 ± 0.09	0.44 ± 0.17	0.4	0.58	1.76
Firmicutes	*Clostridia*	*Clostridiales*	*[Mogibacteriaceae]*	-	0.12 ± 0.04	0.12 ± 0.05	0.95	0.98	1.03	0.2 ± 0.08	0.27 ± 0.1	0.47	0.6	1.35

Supplementary table 5. Summary of metagenomics in the STD-R and the CAF-R groups in CEC and FCS focusing on taxonomic data. Taxonomic data is presented as the mean ± SEM (*n* = 7) per group shorted by *q*-value of CEC. The summary of univariant analysis is shown including *p*-value, *q*-value and FC; the statistically significant *p*-values and *q*-values (< 0.05) are highlighted in bold.

					CEC					FCS				
Phylum	**Class**	**Order**	**Family**	**Genus**	**STD-R (%)**	**CAF-R (%)**	***p*-value**	***q*-value**	**FC**	**STD-R (%)**	**CAF-R (%)**	***p*-value**	***q*-value**	**FC**
Firmicutes	*Clostridia*	*Clostridiales*	*Lachnospiraceae*	-	18.29 ± 6.91	9.31 ± 3.8	**0.02**	0.46	0.51	8.59 ± 3.25	3.26 ± 1.23	**0.01**	0.1	0.38
Bacteroidetes	*Bacteroidia*	*Bacteroidales*	*Porphyromonadaceae*	*Parabacteroides*	0.03 ± 0.01	0.13 ± 0.06	0.08	0.65	4.69	0.16 ± 0.06	0.69 ± 0.26	**0.01**	0.1	4.28
Firmicutes	*Clostridia*	*Clostridiales*	*Lachnospiraceae*	*Dorea*	0.07 ± 0.02	0.26 ± 0.11	0.09	0.65	3.99	0.09 ± 0.03	0.29 ± 0.11	**0.02**	0.1	3.16
Firmicutes	*Clostridia*	*Clostridiales*	*Lachnospiraceae*	*Roseburia*	0.38 ± 0.14	0.75 ± 0.31	0.09	0.65	1.97	0.18 ± 0.07	0.29 ± 0.11	0.37	0.61	1.6
Bacteroidetes	*Bacteroidia*	*Bacteroidales*	*Bacteroidaceae*	*Bacteroides*	0.09 ± 0.03	0.33 ± 0.13	0.17	0.67	3.65	0.42 ± 0.16	1 ± 0.38	0.06	0.23	2.41
Firmicutes	*Clostridia*	*Clostridiales*	*[Mogibacteriaceae]*	-	0.08 ± 0.03	0.12 ± 0.05	0.24	0.67	1.5	0.2 ± 0.07	0.27 ± 0.1	0.2	0.44	1.36
Firmicutes	*Clostridia*	*Clostridiales*	*Peptostreptococcaceae*	-	0.17 ± 0.06	0.11 ± 0.04	0.2	0.67	0.64	0.29 ± 0.11	0.68 ± 0.26	0.22	0.44	2.38
Tenericutes	*Mollicutes*	*RF39*	-	-	0.07 ± 0.03	0.39 ± 0.16	0.26	0.67	5.33	0.26 ± 0.1	0.58 ± 0.22	0.29	0.51	2.26
Firmicutes	*Clostridia*	*Clostridiales*	*Lachnospiraceae*	*Anaerostipes*	0.07 ± 0.03	0.03 ± 0.01	0.18	0.67	0.38	0.23 ± 0.09	0.16 ± 0.06	0.46	0.71	0.68
Firmicutes	*Clostridia*	*Clostridiales*	*Clostridiaceae*	*SMB53*	0.19 ± 0.07	0.05 ± 0.02	0.25	0.67	0.28	0.41 ± 0.16	0.55 ± 0.21	0.62	0.86	1.32

Firmicutes	*Clostridia*	*Clostridiales*	-	-	48.8 ± 18.45	57.49 ± 23.47	0.25	0.67	1.18	16.99 ± 6.42	16.28 ± 6.15	0.81	0.98	0.96
Firmicutes	*Clostridia*	*Clostridiales*	*Lachnospiraceae*	*[Ruminococcus]*	0.91 ± 0.34	0.64 ± 0.26	0.3	0.69	0.71	0.42 ± 0.16	0.42 ± 0.16	0.99	0.99	1
Firmicutes	*Clostridia*	*Clostridiales*	*Lachnospiraceae*	*Coprococcus*	3.77 ± 1.43	3.01 ± 1.23	0.36	0.77	0.8	2.72 ± 1.03	1.79 ± 0.68	0.18	0.44	0.66
Firmicutes	*Clostridia*	*Clostridiales*	*Ruminococcaceae*	-	4.54 ± 1.72	3.65 ± 1.49	0.44	0.78	0.81	6.7 ± 2.53	4.52 ± 1.71	0.08	0.28	0.67
Proteobacteria	*Gammaproteobacteria*	*Enterobacteriales*	*Enterobacteriaceae*	-	0.21 ± 0.08	0.33 ± 0.14	0.44	0.78	1.6	0.22 ± 0.08	0.52 ± 0.2	0.12	0.33	2.35
Actinobacteria	*Actinobacteria*	*Bifidobacteriales*	*Bifidobacteriaceae*	*Bifidobacterium*	-	0.02 ± 0.01	0.39	0.78	4.63	0.57 ± 0.21	0.44 ± 0.17	0.65	0.86	0.78
Firmicutes	*Clostridia*	*Clostridiales*	*Peptococcaceae*	*rc4-4*	0.18 ± 0.07	0.14 ± 0.06	0.49	0.79	0.79	0.47 ± 0.18	0.27 ± 0.1	**0.02**	0.1	0.56
Firmicutes	*Clostridia*	*Clostridiales*	*Clostridiaceae*	-	0.04 ± 0.01	0.07 ± 0.03	0.53	0.79	2.05	0.19 ± 0.07	0.46 ± 0.17	0.24	0.45	2.44
Firmicutes	*Clostridia*	*Clostridiales*	*Lachnospiraceae*	*Blautia*	0.28 ± 0.11	0.21 ± 0.09	0.51	0.79	0.76	0.13 ± 0.05	0.13 ± 0.05	0.94	0.99	0.98
Firmicutes	*Clostridia*	*Clostridiales*	*Dehalobacteriaceae*	*Dehalobacterium*	0.19 ± 0.07	0.21 ± 0.09	0.63	0.88	1.09	0.09 ± 0.04	0.05 ± 0.02	**0.02**	0.1	0.52
Firmicutes	*Bacilli*	*Lactobacillales*	*Lactobacillaceae*	*Lactobacillus*	2.8 ± 1.06	3.16 ± 1.29	0.73	0.9	1.13	6.27 ± 2.37	12.73 ± 4.81	**0.01**	0.1	2.03
Firmicutes	*Clostridia*	*Clostridiales*	*Ruminococcaceae*	*Ruminococcus*	2.41 ± 0.91	2.24 ± 0.92	0.74	0.9	0.93	2.63 ± 1	2.59 ± 0.98	0.94	0.99	0.98
Bacteroidetes	*Bacteroidia*	*Bacteroidales*	*S24-7*	-	6.96 ± 2.63	7.94 ± 3.24	0.7	0.9	1.14	41.15 ± 15.55	41.04 ± 15.51	0.98	0.99	1
Firmicutes	*Clostridia*	*Clostridiales*	*Clostridiaceae*	*Clostridium*	0.16 ± 0.06	0.18 ± 0.07	0.8	0.93	1.17	0.73 ± 0.28	1.25 ± 0.47	0.12	0.33	1.7
Verrucomicrobia	*Verrucomicrobiae*	*Verrucomicrobiales*	*Verrucomicrobiaceae*	*Akkermansia*	0.78 ± 0.3	0.73 ± 0.3	0.9	0.97	0.93	2.97 ± 1.12	2.23 ± 0.84	0.57	0.83	0.75
Bacteroidetes	*Bacteroidia*	*Bacteroidales*	*Rikenellaceae*	-	0.76 ± 0.29	0.72 ± 0.3	0.88	0.97	0.95	1.25 ± 0.47	1.14 ± 0.43	0.7	0.89	0.91
Firmicutes	*Bacilli*	*Turicibacterales*	*Turicibacteraceae*	*Turicibacter*	0.04 ± 0.02	0.04 ± 0.02	0.99	0.99	1.01	0.41 ± 0.15	1.22 ± 0.46	0.21	0.44	3.02
Firmicutes	*Clostridia*	*Clostridiales*	*Ruminococcaceae*	*Oscillospira*	7.51 ± 2.84	7.45 ± 3.04	0.96	0.99	0.99	4.58 ± 1.73	4.63 ± 1.75	0.96	0.99	1.01

Supplementary table 6. Statistical analysis of plasma metabolites in the STD-R and the CAF-R groups. 139 metabolites presented as the mean ± SEM per group shorted by *p*-value. The summary of univariant analysis is shown including *p*-value, *q*-value and FC; the statistically significant *p*-values and *q*-values (< 0.05) are highlighted in bold. Abbreviations: DG, diacylglycerol; LPC, lysophospholipid; PC, phosphatidylcholine; ChoE, cholesterol ester; SM, sphingomyelin; TG, triglyceride; PE, phosphatidylethanolamine.

Metabolite	STD-R	CAF-R	*p*-value	*q*-value	FC
DG 34:2	0.42 ± 0.04	0.72 ± 0.04	**<0.01**	**0.05**	0.09
DG 34:3	0.08 ± 0.02	0.17 ± 0.02	**0.01**	0.58	0.23
DG 36:2	0.9 ± 0.09	1.31 ± 0.12	**0.01**	0.64	0.14
DG 36:4	0.7 ± 0.07	0.96 ± 0.06	**0.02**	0.72	0.09
LPC 20:0	0.35 ± 0.02	0.3 ± 0.01	**0.03**	0.74	0.03
DG 34:1	0.78 ± 0.05	1.02 ± 0.07	**0.03**	0.80	0.10
PC 31:0	0.04 ± 0	0.03 ± 0	**0.04**	0.88	0.12
Glyceric acid	1.22 ± 0.07	1.42 ± 0.05	0.06	0.89	0.04
PC 42:4 e	0.01 ± 0	0.01 ± 0	0.07	0.89	0.10
PC 36:3 e	0.06 ± 0	0.05 ± 0	0.07	0.89	0.05
ChoE (16:0)	2.57 ± 0.22	2.08 ± 0.15	0.10	0.89	0.06
Oleic acid	1.46 ± 0.1	1.72 ± 0.13	0.12	0.89	0.09
ChoE (18:2)	20.18 ± 1.95	16.1 ± 1.27	0.12	0.89	0.06
PC 35:2	0.42 ± 0.04	0.34 ± 0.03	0.13	0.89	0.06
Ribose	4.37 ± 0.35	3.28 ± 0.51	0.13	0.89	0.12
Fumaric acid	0.71 ± 0.07	0.88 ± 0.08	0.14	0.89	0.12
ChoE (18:1)	3.04 ± 0.29	2.5 ± 0.17	0.15	0.89	0.06
LPC 15:0	0.98 ± 0.06	0.85 ± 0.06	0.15	0.89	0.06
SM 42:3	5.67 ± 0.45	4.87 ± 0.23	0.15	0.89	0.04
TG 52:3	39.46 ± 10.4	62.08 ± 11.23	0.16	0.89	0.28
Aconitic acid	0.01 ± 0	0.01 ± 0	0.16	0.89	0.10
TG 54:6	13.27 ± 1.87	19.03 ± 3.23	0.18	0.89	0.24
Threonic acid	1.68 ± 0.27	2.13 ± 0.15	0.19	0.89	0.09
ChoE (18:0)	0.15 ± 0.01	0.12 ± 0.01	0.19	0.89	0.07
PC 33:0	0.04 ± 0	0.03 ± 0	0.19	0.89	0.07
SM 43:1	1.34 ± 0.1	1.14 ± 0.1	0.20	0.89	0.07
TG 54:4	11.42 ± 3.18	17.76 ± 3.49	0.20	0.89	0.31
Cholesterol	0.51 ± 0.1	0.37 ± 0.02	0.20	0.89	0.04
TG 48:0	1.24 ± 0.19	1.88 ± 0.43	0.23	0.89	0.35
TG 50:0	0.37 ± 0.04	0.5 ± 0.08	0.23	0.89	0.22
SM 35:1	0.18 ± 0.01	0.16 ± 0.01	0.24	0.89	0.05
PC 40:5	0.33 ± 0.07	0.53 ± 0.14	0.24	0.89	0.42
TG 54:3	4.01 ± 1.08	5.87 ± 1.15	0.26	0.89	0.29

TG 54:2	0.66 ± 0.16	0.96 ± 0.19	0.27	0.89	0.29
Glucose-6-phosphate	0.17 ± 0.02	0.14 ± 0.02	0.27	0.89	0.11
TG 54:7	4.94 ± 1.19	6.91 ± 1.18	0.27	0.89	0.24
SM 41:2	0.65 ± 0.03	0.69 ± 0.03	0.29	0.89	0.05
TG 52:1	0.63 ± 0.14	0.91 ± 0.2	0.29	0.89	0.32
Malic acid	0.38 ± 0.03	0.44 ± 0.04	0.29	0.89	0.11
TG 52:5	7.38 ± 2.04	10.47 ± 1.92	0.29	0.89	0.26
TG 52:2	13.12 ± 5.39	22.41 ± 6.39	0.30	0.89	0.49
α-Ketoglutarate	1.27 ± 0.07	1.43 ± 0.13	0.30	0.89	0.10
LPC 16:0	83.94 ± 2.63	79.81 ± 2.68	0.30	0.89	0.03
TG 48:1	1.82 ± 0.51	3.29 ± 1.13	0.30	0.89	0.62
PE 38:5 e	1.91 ± 0.32	2.78 ± 0.67	0.31	0.89	0.35
TG 50:1	3.77 ± 1.33	6.83 ± 2.45	0.32	0.89	0.65
PC 38:3	0.97 ± 0.15	1.21 ± 0.17	0.33	0.89	0.17
TG 50:2	13.23 ± 4.96	22.99 ± 7.66	0.33	0.89	0.58
TG 52:6	1.13 ± 0.36	1.61 ± 0.31	0.33	0.89	0.28
LPC 16:0 e	0.56 ± 0.04	0.51 ± 0.02	0.35	0.89	0.04
Glucose	0.77 ± 0.04	0.72 ± 0.03	0.35	0.89	0.04
ChoE (17:0)	0.16 ± 0.02	0.14 ± 0.01	0.35	0.89	0.08
TG 50:3	7.94 ± 3.58	13.26 ± 4.12	0.36	0.89	0.52
SM 40:2	0.69 ± 0.08	0.77 ± 0.04	0.38	0.89	0.05
PC 32:0	0.7 ± 0.04	0.64 ± 0.05	0.38	0.89	0.07
TG 46:1	0.63 ± 0.08	0.8 ± 0.15	0.38	0.89	0.25
Citric acid	3.9 ± 0.13	3.67 ± 0.19	0.38	0.89	0.05
SM 32:1	0.28 ± 0.02	0.32 ± 0.03	0.41	0.89	0.11
TG 50:4	1.86 ± 0.75	2.73 ± 0.69	0.41	0.89	0.37
PC 36:0	0.09 ± 0.01	0.11 ± 0.02	0.42	0.89	0.20
TG 46:0	0.85 ± 0.09	0.96 ± 0.09	0.43	0.89	0.11
ChoE (16:1)	0.77 ± 0.13	0.92 ± 0.14	0.43	0.89	0.18
TG 51:2	0.83 ± 0.26	1.16 ± 0.3	0.43	0.89	0.36
TG 48:2	1.9 ± 0.77	3.19 ± 1.29	0.43	0.89	0.68
PC 38:6 e	0.07 ± 0.01	0.06 ± 0.01	0.44	0.89	0.09
Urea	2.76 ± 0.18	2.58 ± 0.15	0.45	0.89	0.05
PE 36:4	4.09 ± 0.7	4.78 ± 0.6	0.45	0.89	0.15
ChoE (18:3)	1.55 ± 0.11	1.4 ± 0.15	0.46	0.89	0.10
PC 38:4 e	0.06 ± 0.01	0.06 ± 0	0.47	0.89	0.08
Isoleucine	0.3 ± 0.16	0.69 ± 0.45	0.49	0.89	1.49
SM 34:2	1.58 ± 0.07	1.7 ± 0.14	0.49	0.89	0.09
Leucine	0.11 ± 0.06	0.24 ± 0.16	0.49	0.89	1.53

Fructose-6-phosphate	0.16 ± 0.02	0.14 ± 0.02	0.50	0.89	0.12
ChoE (22:5)	0.82 ± 0.06	0.92 ± 0.12	0.50	0.89	0.15
TG 46:2	0.38 ± 0.06	0.46 ± 0.1	0.50	0.89	0.25
Tyrosine	0.74 ± 0.09	0.91 ± 0.21	0.50	0.89	0.28
Succinic acid	0.68 ± 0.03	0.65 ± 0.02	0.51	0.89	0.03
TG 48:3	0.6 ± 0.21	0.84 ± 0.27	0.51	0.89	0.46
Valine	0.93 ± 0.35	1.67 ± 0.93	0.51	0.89	1.00
PC 32:1	0.48 ± 0.14	0.61 ± 0.13	0.51	0.89	0.27
Pyruvic acid	13.39 ± 1.64	15.12 ± 1.88	0.52	0.89	0.14
LPC 16:1 e	0.16 ± 0.01	0.16 ± 0	0.53	0.89	0.02
SM 38:1	0.49 ± 0.09	0.56 ± 0.05	0.54	0.90	0.10
ChoE (20:2)	1.16 ± 0.12	1.06 ± 0.09	0.55	0.91	0.07
Glycine	2.42 ± 0.32	3.12 ± 1.01	0.56	0.91	0.42
LPC 18:0 e	0.11 ± 0.01	0.1 ± 0.01	0.57	0.91	0.06
PC 40:4	0.22 ± 0.03	0.24 ± 0.04	0.57	0.91	0.17
SM 33:1	0.4 ± 0.03	0.38 ± 0.03	0.58	0.91	0.06
Hydroxyproline	0.65 ± 0.11	0.81 ± 0.24	0.58	0.91	0.38
PC 36:2 e	0.01 ± 0	0.02 ± 0	0.59	0.91	0.09
Glycerol	3.33 ± 0.22	3.49 ± 0.2	0.60	0.91	0.06
PC 38:5 e	0.1 ± 0.01	0.11 ± 0.01	0.61	0.91	0.10
Phenylalanine	0.76 ± 0.09	0.9 ± 0.24	0.62	0.93	0.31
Lysine	0.98 ± 0.13	1.1 ± 0.21	0.64	0.93	0.21
PC 36:2	12.51 ± 0.71	13.16 ± 1.08	0.64	0.93	0.09
PC 38:2	0.11 ± 0.02	0.13 ± 0.02	0.65	0.93	0.20
3-hydroxybutiric acid	1.84 ± 0.26	1.7 ± 0.17	0.65	0.93	0.09
SM 36:1	1.3 ± 0.1	1.39 ± 0.15	0.66	0.93	0.11
Proline	0.27 ± 0.02	0.29 ± 0.05	0.67	0.93	0.19
LPC 18:2	37.67 ± 2.31	36.37 ± 1.77	0.67	0.93	0.05
Methionine	0.12 ± 0.02	0.14 ± 0.03	0.71	0.97	0.20
PC 34:1	4.55 ± 0.61	4.86 ± 0.53	0.72	0.97	0.12
Serine	0.3 ± 0.03	0.28 ± 0.04	0.74	0.97	0.13
PC 38:4	18.05 ± 0.86	18.77 ± 1.8	0.75	0.97	0.10
SM 41:1	4.43 ± 0.22	4.32 ± 0.25	0.75	0.97	0.06
Fructose	0.43 ± 0.02	0.44 ± 0.04	0.76	0.97	0.10
SM 42:1	16.98 ± 0.71	16.52 ± 1.2	0.76	0.97	0.07
ChoE (20:4)	80.31 ± 6.86	77.25 ± 6.67	0.76	0.97	0.08
Glutamine	1.2 ± 0.24	1.11 ± 0.2	0.78	0.97	0.16
Alanine	0.4 ± 0.07	0.45 ± 0.15	0.78	0.97	0.37
β-Alanine	0.08 ± 0.01	0.07 ± 0.02	0.79	0.97	0.28

SM 40:1	4.15 ± 0.29	4.27 ± 0.38	0.79	0.97	0.09
PC 34:3 e	0.02 ± 0	0.02 ± 0	0.80	0.97	0.08
SM 36:2	0.45 ± 0.03	0.47 ± 0.04	0.80	0.97	0.09
Histidine	0.16 ± 0.05	0.18 ± 0.05	0.81	0.97	0.33
SM 39:1	0.16 ± 0.02	0.15 ± 0.03	0.81	0.97	0.19
ChoE (17:1)	0.11 ± 0.01	0.12 ± 0.01	0.82	0.97	0.10
PC 33:1	0.09 ± 0.01	0.08 ± 0.01	0.84	0.98	0.08
ChoE (22:4)	5.71 ± 0.53	5.59 ± 0.47	0.87	0.99	0.08
PC 34:1 e	0.13 ± 0.01	0.12 ± 0.01	0.88	0.99	0.08
Threonine	1.47 ± 0.19	1.52 ± 0.27	0.88	0.99	0.19
PC 32:2	0.21 ± 0.04	0.21 ± 0.03	0.89	0.99	0.13
Asparagine	0.17 ± 0.02	0.17 ± 0.04	0.89	0.99	0.23
Ornithine	2.72 ± 0.52	2.86 ± 0.81	0.90	0.99	0.30
LPC 18:1	18.71 ± 1.24	18.91 ± 1.09	0.90	0.99	0.06
Aspartic acid	0.51 ± 0.1	0.49 ± 0.11	0.90	0.99	0.21
SM 34:1	19.47 ± 0.89	19.66 ± 1.29	0.90	0.99	0.07
Lactic acid	7.09 ± 0.55	7.17 ± 0.43	0.91	0.99	0.06
Glutamic acid	0.11 ± 0.02	0.11 ± 0.03	0.95	1.00	0.26
2-hydroxyglutaric	0.69 ± 0.06	0.7 ± 0.04	0.96	1.00	0.06
Glycolic acid	3.3 ± 0.21	3.28 ± 0.17	0.96	1.00	0.05
ChoE (22:6)	2.4 ± 0.27	2.38 ± 0.37	0.96	1.00	0.15
PC 30:0	0.05 ± 0	0.05 ± 0.01	0.97	1.00	0.11
α-tocopherol	0.91 ± 0.06	0.91 ± 0.08	0.97	1.00	0.09
LPC 18:0	59.41 ± 2.44	59.28 ± 4.04	0.98	1.00	0.07
SM 42:2	13.08 ± 0.92	13.11 ± 0.84	0.98	1.00	0.06
PC 34:0	0.35 ± 0.02	0.35 ± 0.03	0.99	1.00	0.10
PC 36:4	16.73 ± 0.54	16.72 ± 1.17	1.00	1.00	0.07
Tryptophan	1.84 ± 0.34	1.84 ± 0.39	1.00	1.00	0.21

Supplementary table 7. Plasma feature importance of Random Forest Classifier. The Random Forest Classifier was calculated to sort the most important metabolites in plasma that distinguish between the STD-R and the CAF-R groups. It is shown here only the first 10 metabolites to avoid showing long list. To test it, all metabolites were taken without any filter. Abbreviations: DG, diacylglycerol; PC, phosphatidylcholine; LPC, lysophospholipid; SM, sphingomyelin; PE, phosphatidylethanolamine.

Plasma metabolite	Feature Importance
DG 34:2	0.267
Glyceric acid	0.103
Fumaric acid	0.069
PC 31:0	0.060

DG 34:3	0.034
LPC 16:1 e	0.034
SM 34:2	0.034
SM 32:1	0.034
PE 38:5 e	0.034
DG 36:2	0.034

Supplementary table 8. Statistical analysis of urine metabolites in the STD-R and the CAF-R groups. 45 metabolites are represented as the mean ± SEM per group shorted by *p*-value. The summary of univariant analysis is shown including *p*-value, *q*-value, FC, right and left chemical shift (ppm); the statistically significant *p*-values and *q*-values (< 0.05) are highlighted in bold. Abbreviations: 3-HPPA, 3-hydroxyphenylpropionate; HPPA sulfate, hydroxyphenylpropionic acid sulfate; DMA, Dimethylamine; 4-PY, methyl-4-pyridone-5-carboxamide; NAD+, nicotinamide adenine dinucleotide; TMAO, trimethylamine N-oxide; ppm, parts-per-million.

Metabolite	STD-R	CAF-R	*p*-value	*q*-value	FC	Right (ppm)	Left (ppm)
Hippurate	295.91 ± 20.55	145.49 ± 21.45	**<0.01**	**0.01**	0.49	7.53	7.66
o-Coumaric acid	2.16 ± 0.2	6.14 ± 0.76	**<0.01**	**0.04**	2.84	6.52	6.56
3-HPPA	2.31 ± 0.6	21.3 ± 3.91	**<0.01**	**0.04**	9.24	6.79	6.81
HPPA sulfate	1.92 ± 0.32	16.32 ± 3.61	**0.01**	0.08	8.52	2.89	2.92
Tyrosine	7.81 ± 0.5	28.02 ± 6	**0.01**	0.13	3.59	6.85	6.88
Phenylacetylglycine	30.47 ± 1.63	47.65 ± 5.64	**0.02**	0.17	1.56	7.34	7.38
Malate	8.51 ± 1.31	4.8 ± 1.29	0.07	0.43	0.56	2.64	2.65
Citrate	309.65 ± 46.82	214.1 ± 33	0.12	0.66	0.69	2.52	2.58
Fumarate	2.54 ± 0.3	1.88 ± 0.28	0.13	0.66	0.74	6.51	6.53
Sarcosine	4.52 ± 0.31	3.85 ± 0.32	0.16	0.69	0.85	3.59	3.60
N-Acetylglycine	21.66 ± 1.35	19.25 ± 0.9	0.17	0.69	0.89	2.03	2.04
Valine	1.16 ± 0.11	1.43 ± 0.18	0.24	0.84	1.23	0.98	1.00
Allantoin	200.61 ± 9.28	184.5 ± 10.19	0.27	0.84	0.92	5.37	5.41
Creatinine	155.24 ± 5.74	142.99 ± 8.97	0.28	0.84	0.92	3.03	3.05
N-acetylglycoproteins	50.71 ± 3.06	47.11 ± 1.45	0.32	0.89	0.93	1.99	2.08
1-methylnicotinamide	0.11 ± 0.03	1.4 ± 1.34	0.38	0.91	12.35	9.26	9.28
DMA	40.6 ± 1.94	37.71 ± 2.58	0.39	0.91	0.93	2.71	2.73
2-Oxoglutarate	197.62 ± 41.42	151.94 ± 30.02	0.39	0.91	0.77	2.42	2.46
N.N-Dimethylglycine	10.55 ± 1.67	12.95 ± 2.38	0.43	0.91	1.23	2.92	2.93
Pseudouridine	9.96 ± 0.53	9.29 ± 0.66	0.45	0.91	0.93	7.67	7.68
3-methyl-2-oxovalerate	4.41 ± 0.33	4.79 ± 0.37	0.46	0.91	1.09	1	1.09
Trimethylamine	0.89 ± 0.21	1.09 ± 0.17	0.48	0.91	1.22	2.88	2.89
4-PY	5.17 ± 0.76	4.34 ± 0.89	0.49	0.91	0.84	8.53	8.55
Leucine	13.19 ± 1.05	12.43 ± 0.52	0.53	0.91	0.94	0.91	0.95
Acetate	8.37 ± 2.76	6.66 ± 0.82	0.57	0.91	0.80	1.91	1.92
Glycine	7.19 ± 0.63	7.61 ± 0.4	0.59	0.91	1.06	3.56	3.57
Methylamine	4.21 ± 0.39	4.44 ± 0.19	0.60	0.91	1.06	2.60	2.61
Taurine	501.98 ± 67.25	545.59 ± 47.5	0.61	0.91	1.09	3.24	3.29

3-hydroxyisovalerate	4 ± 0.34	4.24 ± 0.33	0.62	0.91	1.06	1.26	1.27
Succinate	57.3 ± 6.5	52.19 ± 7.87	0.63	0.91	0.91	2.39	2.41
2-deoxycytidine	3.41 ± 0.29	3.21 ± 0.39	0.70	0.93	0.94	6.25	6.27
NAD+	0.24 ± 0.04	0.22 ± 0.03	0.70	0.93	0.91	9.35	9.36
Fucose	8.75 ± 0.41	9.06 ± 0.69	0.71	0.93	1.03	1.24	1.26
Alanine	5.07 ± 0.75	4.82 ± 0.33	0.77	0.93	0.95	1.47	1.49
Tryptophan	6.59 ± 0.74	6.34 ± 0.55	0.80	0.93	0.96	7.69	7.72
Betaine	28.95 ± 3.53	27.5 ± 4.22	0.80	0.93	0.95	3.89	3.90
N6-Acetyllysine	23.17 ± 1.7	23.67 ± 1.27	0.82	0.93	1.02	1.97	1.99
Indoxyl Sulphate	6.51 ± 0.69	6.35 ± 0.55	0.86	0.93	0.98	7.69	7.72
TMAO	1.95 ± 0.33	1.85 ± 0.47	0.87	0.93	0.95	3.24	3.24
Formate	6.45 ± 1.4	6.23 ± 0.67	0.89	0.93	0.97	8.45	8.47
α-hydroxyhippurate	0.81 ± 0.13	0.84 ± 0.13	0.89	0.93	1.03	5.51	5.52
Lactate	12.08 ± 1.45	12.04 ± 0.69	0.98	0.99	1.00	1.32	1.34

Supplementary table 9. Urine feature importance of Random Forest Classifier. The Random Forest Classifier was calculated to sort the most important metabolites that distinguish between the STD-R and CAF-R groups. It is shown here only the first metabolites to avoid showing long list. To test it, all metabolites were taken without any filter. Abbreviations: 3-HPPA, 3-hydroxyphenylpropionate; DMA, Dimethylamine; HPPA sulfate, hydroxyphenylpropionic acid sulfate.

Urine metabolite	Feature importance
o-Coumaric acid	0.232
3-HPPA	0.196
HPPA sulfate	0.125
Hippurate	0.120
Sarcosine	0.036
Phenylacetylglycine	0.036
DMA	0.018
Tyrosine	0.018
1-methylnicotinamide	0.018

Supplementary table 10. Correlation between altered metabolites and alpha diversity. None of the correlations were significative using the correlation test of Spearman. Abbreviations: 3-HPPA, 3-hydroxyphenylpropionate; DG 34:2, diacylglycerol 34:2.

		Metabolites altered			
		DG 34:2	Hippurate	o-Coumaric acid	3-HPPA
Alpha diversity	Shannon	-0.181	-0.181	-0.302	-0.187
	Simpson	-0.176	-0.192	-0.324	-0.187
	Chao1	-0.148	-0.044	-0.451	-0.264
	Observed OTUs	-0.022	-0.192	-0.269	-0.121
	Phylogenetic diversity	0.044	-0.154	-0.126	-0.033

MANUSCRIPT 4

IMBALANCES IN TCA, SHORT FATTY ACIDS AND ONE-CARBON METABOLISMS AS IMPORTANT FEATURES OF HOMEOSTATIC DISRUPTION EVIDENCED BY A MULTI-OMICS INTEGRATIVE APPROACH OF LPS-INDUCED CHRONIC INFLAMMATION IN MALE WISTAR RATS

Julia Hernandez-Baixauli [1], Nerea Abasolo [4], Hector Palacios-Jordan [4], Elisabet Foguet-Romero [4], David Suñol [5], Mar Galofré [5], Antoni Caimari [1], Laura Baselga-Escudero [1], Josep M. Del Bas [1,*] and Miquel Mulero [2,6,*]

[1] Eurecat, Centre Tecnològic de Catalunya, Unitat de Nutrició i Salut, 43204 Reus, Spain
[2] Eurecat, Centre Tecnològic de Catalunya, Centre for Omic Sciences (COS), Joint Unit Universitat Rovira i Virgili-EURECAT, 43204 Reus, Spain
[3] Eurecat, Centre Tecnològic de Catalunya, Digital Health, 08005 Barcelona, Spain
[4] Department of Biochemistry and Biotechnology, Universitat Rovira i Virgili, 43007 Tarragona, Spain
[5] Nutrigenomics Research Group, Department of Biochemistry and Biotechnology, Universitat Rovira i Virgili, 43007 Tarragona, Spain

* Correspondence: josep.delbas@eurecat.org; miquel.mulero@urv.cat

Published by International Journal of Molecular Science

Int. J. Mol. Sci. 2022, 23(5), 2563; https://doi.org/10.3390/ijms23052563

Received: 21 December 2021 / Revised: 21 February 2022 / Accepted: 23 February 2022 / Published: 25 February 2022

(This article belongs to the Special Issue Signalling Pathways in Inflammation and Its Resolution: New Insights and Therapeutic Challenges)

UNIVERSITAT ROVIRA I VIRGILI
MULTI-OMICS BIOMARKERS OF METABOLIC HOMEOSTASIS OF RISK FACTORS ASSOCIATED TO NON-COMMUNICABLE DISEASES
Julia Hernandez Baixauli

Abstract: Chronic inflammation is an important risk factor in a broad variety of physical and mental disorders leading to highly prevalent non-communicable diseases (NCDs). However, there is a need for a deeper understanding of this condition and its progression to the disease state. For this reason, it is important to define metabolic pathways and complementary biomarkers associated with homeostatic disruption in chronic inflammation. To achieve that, male Wistar rats were subjected to intraperitoneal and intermittent injections with saline solution or increasing lipopolysaccharide (LPS) concentrations (0.5, 5 and 7.5 mg/kg) thrice a week for 31 days. Biochemical and inflammatory parameters were measured at the end of the study. To assess the omics profile, GC-qTOF and UHPLC-qTOF were performed to evaluate plasma metabolome; 1H-NMR was used to evaluate urine metabolome; additionally, shotgun metagenomics sequencing was carried out to characterize the cecum microbiome. The chronicity of inflammation in the study was evaluated by the monitoring of monocyte chemoattractant protein-1 (MCP-1) during the different weeks of the experimental process. At the end of the study, together with the increased levels of MCP-1, levels of interleukin-6 (IL-6), tumour necrosis factor alpha (TNF-α) and prostaglandin E2 (PGE2) along with 8-isoprostanes (an indicative of oxidative stress) were significantly increased (p-value < 0.05). The leading features implicated in the current model were tricarboxylic acid (TCA) cycle inter-mediates (i.e., alpha-ketoglutarate, aconitic acid, malic acid, fumaric acid and succinic acid); lipids such as specific cholesterol esters (ChoEs), lysophospholipids (LPCs) and phosphatidylcholines (PCs); and glycine, as well as N, N-dimethylglycine, which are related to one-carbon (1C) metabolism. These metabolites point towards mitochondrial metabolism through TCA cycle, β-oxidation of fatty acids and 1C metabolism as interconnected pathways that could reveal the metabolic effects of chronic inflammation induced by LPS administration. These results provide deeper knowledge concerning the impact of chronic inflammation on the disruption of metabolic homeostasis.

Keywords: chronic inflammation, lipopolysaccharide, biomarker, metabolome, microbiome, energy metabolism, one-carbon metabolism, mitochondria.

1. Introduction

Inflammation is a part of a complex biological process characterized by the activation of immune and non-immune cells that protect the host from bacteria, viruses, toxins and infections, eliminating pathogens and promoting tissue repair and recovery [1]. Chronic inflammation is defined as a long-term inflammation lasting for prolonged periods, from several months to years in humans, and is characterized by the sustained elevation of inflammatory cytokines in serum due to the failure to resolve acute inflammation, oxidative stress or metabolic dysfunction [2]. Generally, the extent and effects of chronic inflammation vary depending on the cause of the injury and the ability of the body to repair and overcome the damage [3]. One of the most remarkable medical discoveries of the past two decades has been that the inflammatory processes are intimately involved in the onset of numerous NCDs such as cardiovascular diseases (CVDs), neurodegenerative processes, diabetes, cancer, auto-immune disease, non-alcoholic fatty liver disease (NAFLD) as the main liver disease and renal disease, among others [3]. Thus, chronic inflammation might be understood as a main risk factor, and, consequently, we have a long way to go before achieving full understanding about the role that chronic inflammation plays in disease risk, biological aging and NCDs evolution and mortality [4].

Current research on inflammation has focused on the causes of chronic inflammation, the discovery of inflammation-associated biomarkers and the associations between inflammation and disease. Nevertheless, further research is needed to better understand this condition and its progression towards the development of individual disease status [5]. In line with this, different studies have shown that current biomarkers of inflammation need complementary information to be applied for the monitoring of chronic inflammation. For example, monitoring the levels of general biomarkers of inflammation has been shown as a promising strategy for the prediction of morbidity and mortality in cross-sectional and longitudinal studies related to inflammation in aging [6]. However, alteration of cytokines (e.g., interleukin-1 (IL-1) and interleukin-6 (IL-6)) was discordant between studies [7–9]. Hereby, the assessment of chronic inflammation as a risk factor requires novel biomarkers and approaches to complement the information provided by the classical ones.

Consequently, there is an increasing demand for novel and growing sources of potentially promising biomarkers, such as adipokines, cytokines, metabolites and microRNAs, that are related to inflammation, as well as for a multi-dimensional approach/integration of them. This could bring huge improvements in the personalized prevention and treatment of some inflammatory-related pathologies [10]. In this regard, metabolomics is a very powerful tool for the study of the living organism thanks to the direct involvement of metabolite homeostasis in the final phenotype, which in turn is affected by the proper functioning of higher levels of biochemical organization, including the genome, the transcriptome and the proteome

[11]. Recently, the field of integrative omics has been growing as an important tool for the prognosis and diagnosis of different diseases by investigating the endogenous levels of metabolites of different biofluids (i.e., plasma/serum and urine) [11,12].

Additionally, besides the need for a deeper understanding of chronic inflammation, there is a strong need to target accurate animal models that reflect the biochemical and metabolic manifestations of the homeostatic disruption, which is generated by chronic inflammation. In this sense, a variety of studies have developed models to mimic acute or chronic inflammation using chemical or biological stimuli [13,14]. However, the isolation of chronic inflammation is challenging because it appears concomitantly with other conditions, and it does not exist separately in humans. Experimentally, one of the preferred stimuli for inducing chronic inflammation is the administration of lipopolysaccharide (LPS), a structure found in the outer membrane of gram-negative bacteria, which could be injected either intravenously or intraperitoneally, with different doses and frequency [14–17]. Furthermore, adjustment of administration, dose and frequency, together with additional approaches, allowed the development of different models of chronic inflammation diseases (e.g., CVDs or NAFLD) [18,19]. Nevertheless, it has been reported that repeated administration of LPS may reduce the ability of animals to respond to endotoxin, due to the development of endotoxin tolerance and the subsequent decrease in the inflammatory response [20]. For this reason, different procedures have been explored to overcome animal-generated endotoxin resistance, considering time and cost. One of the cutting-edge approaches consists of using LPS infusion delivered by time-release pellets for at least 60 days [19,21], but this technique failed to induce chronic inflammation, suggesting that intermittent injection of LPS on different days might be more effective in rats [14,22]. Several studies with encouraging results appeared to solve the LPS-resistance problem by means of intraperitoneal (IP) injections thrice a week, starting with doses between 1 ng/kg and 20 mg/kg and steadily increasing LPS doses [14,20,23].

In the present work, we hypothesized that chronic inflammation is accompanied by a characteristic metabolic signature that might allow the detection of a different range of inflammatory states affecting metabolism homeostasis. When applied together with classic inflammatory biomarkers, this metabolic signature might provide valuable information on chronic inflammation as a risk factor for the development of metabolic alterations leading to different diseases such as CVDs, NAFLD and neurodegeneration, among others. Therefore, the objective was to assess new metabolomic features of chronic inflammation to gain a deeper understanding of the metabolic signatures associated with inflammatory-involved diseases. To this end, we stablished a model of chronic inflammation in rodent based on injections of LPS at increasing doses. Subsequently, we interrogated the chronic inflammation model to unravel the affected metabolic pathways and identify characteristic profiles employing a multi-omics approach, including the metabolome of different biofluids (i.e., plasma and urine). Finally, we propose a biomarker/metabolic profile for the

assessment of metabolic alterations associated with chronic inflammatory states underlying different metabolic diseases. Furthermore, we highlight the corresponding metabolic pathways that might be most altered and therefore studied to understand the underlying mechanisms.

2. Results

2.1. Characterization of the LPS-Induced Inflammation Model

The stability of inflammation was evaluated during the entire experimental period thanks to the monitorization of monocyte chemoattractant protein-1 (MCP-1) during the second week, the third week and at the end of the study (Figure 1). The results indicate that MCP-1 was elevated during the entire experimental procedure, indicating a constant effect of the LPS treatment in inflammation. Thus, the recurrent administration of LPS induced a stable inflammatory state. At the end of the study, the impact of LPS treatment on inflammation was evaluated by assessing classical inflammatory biomarkers in plasma, which showed an increase in MCP-1, as well as an increase in tumour necrosis factor alpha (TNF-α), interleukin-6 (IL-6) and prostaglandin E2 (PGE2) (Table 1). These results indicate an alteration in inflammation during the experimental period and at the end of the study due to the LPS treatment. As both conditions (inflammation and oxidative stress) are often present together, the level of oxidative stress was also assessed by measuring urinary 8-isoprostanes level, which was increased by a factor of 5 in the LPS-induced inflammation model. Therefore, an alteration of oxidative levels was also observed in the LPS group.

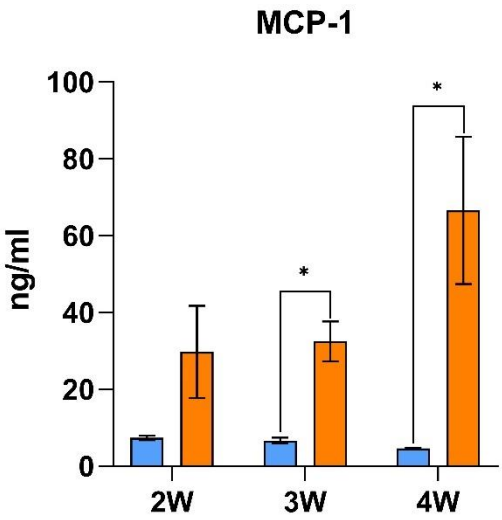

Figure 1. Assessment of inflammation levels during the experimental period by MCP-1 monitoring. The results are presented as the mean ± SEM (*n* = 10 animals per group). * Indicates significant differences using *t*-student test between CON and LPS group ($p < 0.05$). Abbreviations: MCP-1, monocyte chemoattractant protein-1; W, study's week.

Table 1. Characteristics of the LPS-induced inflammation model. The results are presented as the mean ± SEM (*n* = 10 animals per group). The biometric parameters are represented as a ratio (g/kg BW × 100) to properly compare the parameters. The statistical comparisons among groups were conducted using *t*-student test, and fold change (FC) was calculated (LPS/CON). * $p < 0.05$ (significantly different) and ** $p < 0.01$ (high significantly different) compared with control. BW, body weight; RWAT, retroperitoneal white adipose tissue; MWAT, mesenteric white adipose tissue; MCP-1, monocyte chemoattractant protein-1; IL-6, interleukin-6; PGE2, prostaglandin E2; TNF-α, tumour necrosis factor alpha; TG, triglycerides; TC, total cholesterol; NEFAs, non-esterified fatty acids.

		Control	LPS	*p*-Value	FC
Biometric parameters	Initial BW (g)	303.37 ± 4.45	306.6 ± 3.13	0.67	1
	Final BW (g)	386.33 ± 10.28	365.29 ± 10.85	0.17	0.95
	Total food consumption (AUC)	604.09 ± 16.27	492.59 ± 17.04	<0.01 **	0.82
	RWAT/BW	1.83 ± 0.13	1.57 ± 0.15	0.21	0.86
	MWAT/BW	1.07 ± 0.09	0.96 ± 0.09	0.44	0.89
	Muscle/BW	0.63 ± 0.01	0.57 ± 0.02	0.02 *	0.90
	Liver/BW	2.73 ± 0.09	3.09 ± 0.07	<0.01 **	1.13
	Cecum/BW	1.22 ± 0.05	1.2 ± 0.04	0.73	0.98
Plasma parameters	MCP-1 (ng/mL)	4.59 ± 0.21	66.53 ± 19.14	<0.01 **	14.49
	IL-6 (ng/mL)	117.37 ± 5.97	172.80 ± 51.83	0.04 *	1.47
	PGE2 (ng/mL)	2.53 ± 2.67	4.42 ± 5.29	<0.01 **	1.75
	TNF-α (pg/mL)	8.75 ± 2.13	80.43 ± 23.68	0.03 *	9.18
	Glucose (mM)	101.09 ± 4.24	104.62 ± 2.27	0.47	1.03
	TG (mM)	107.76 ± 10.11	82.46 ± 4.15	0.03 *	0.76
	TC (mM)	63.02 ± 5.16	64.36 ± 3.31	0.83	1.02
	NEFAs (mM)	0.93 ± 0.08	0.77 ± 0.04	0.11	0.83
Liver biochemistry	Total lipids (mg/g)	34.53 ± 2.23	32.67 ± 1.99	0.54	0.95
	TC (mg/g)	1.32 ± 0.07	1.50 ± 0.14	0.26	1.14
	Phospholipids (mg/g)	11.53 ± 0.61	12.16 ± 0.91	0.57	1.05
	TG (mg/g)	3.39 ± 0.14	4.51 ± 0.47	0.04 *	1.33
Urine parameters	8-isoprostane (ng/mL)	0.81 ± 0.09	4.22 ± 0.70	<0.01 **	5.21

Regarding other important characteristics of animals, body weight (BW) and food consumption were modified by LPS inoculation; thus, the decrease in BW and food consumption appeared to be related with the initial injection of LPS (Figure 2). Despite BW being similar between control (CON) group and LPS group at the end of the study (Figure 2a, Table 1), BW was significantly influenced by the LPS. During the entire experimental period, food consumption remained significantly decreased despite the different tendencies (Figure 2b, Table 1). It could be observed that BW gain was significantly decreased during the first days until a moment where the LPS group presented higher BW gain than the CON group (Figure 2c) and a corresponding improvement in feed efficiency (Figure 2d). Additionally, muscle weight was significantly decreased, while liver weight was significantly increased in the LPS group (Table 1). Among the most interesting changes in the biochemical parameters, plasma triglycerides (TG) were decreased, while liver TGs were increased (Table 1).

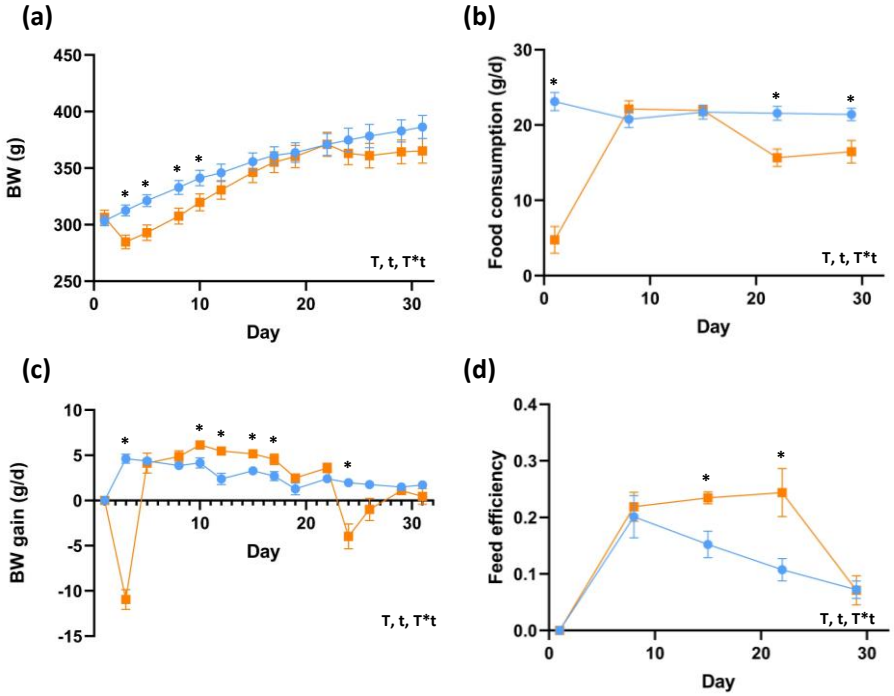

Figure 2. Body weight (BW) (a), BW gain (b), food consumption (c) and feed efficiency (d) of the LPS-induced inflammation model. Blue represents CON group and orange LPS group. Each point of represented data corresponds to the mean ± SEM (n = 10 per group). * Indicates significant differences using repeated-measures ANOVA followed by t-student test between CON and LPS group ($p < 0.05$). T indicates treatment effect; t, indicates time effect; T*t interaction between treatment and time. Abbreviations: BW, body weight.

2.2. Plasma Metabolome of the LPS-Induced Inflammation Model

The plasma metabolomic approach was based on a global multiplatform analysis including 128 metabolites (Table S1). This platform is able to discriminate between metabolites implicated in lipid metabolism as TGs, diacylglycerols (DGs), phosphatidylcholines (PCs), cholesterol esters (ChoEs), lysophospholipids (LPCs) and sphingomyelins (SMs); carbohydrate metabolism (mainly the tricarboxylic acid (TCA) cycle); and amino acid metabolism, among other interesting metabolites. The summary of analysis is shown in Table S1, including the univariate, multivariate and prediction analysis. After the Mann–Whitney (MW) test, 40 out of 128 metabolites were significantly different, and the subsequent Benjamini–Hochberg (BH) correction highlighted 24 out of 47 different metabolites (Table 2).

Table 2. Summary of the significant differential plasma metabolites in the LPS-induced inflammation model. CON and LPS groups (n = 10 animals per group) are represented by the relative abundances (AU). Relative abundances of metabolites are presented by the mean ± SEM. Plasma metabolites are sorted by p-value. The summary of the analysis is shown and includes the relative abundances of metabolites, p-value, q-value, VIP value, fold change (FC), the effect of the LPS vs. the CON group, and the related metabolic pathway. * $p < 0.05$ (significantly different) and ** $p < 0.01$ (highly significant difference) compared with control. Abbreviations: ChoE, cholesterol ester; LPC, lysophospholipid; PC, phosphatidylcholine; SM, sphingomyelin; TG, triglyceride; DG, diacylglycerol.

Metabolite	CON	LPS	p-Value	q-Value	VIP	RF	FC	Effect	Metabolic Pathway
Cholesterol	0.11 ± 0	0.15 ± 0.01	** <0.01	* 0.01	1.78	0	1.4	↑	Steroid biosynthesis
ChoE 18:0	0.09 ± 0.01	0.15 ± 0.01	** <0.01	* 0.01	1.69	0.04	1.7	↑	Fatty acids metabolism
ChoE 18:3	1.55 ± 0.12	2.48 ± 0.17	** <0.01	* 0.01	1.76	0.02	1.6	↑	
ChoE 20:4	59.73 ± 3.98	80.04 ± 3.21	** <0.01	* 0.03	1.76	0	1.3	↑	
ChoE 22:6	2.67 ± 0.19	4.28 ± 0.28	** <0.01	* 0.01	1.96	0.03	1.6	↑	
LPC 16:0 e	0.34 ± 0.03	0.52 ± 0.03	** <0.01	* 0.01	1.67	0	1.5	↑	Glycerophospholipid metabolism
LPC 18:0 e	0.07 ± 0	0.1 ± 0.01	** <0.01	* 0.01	1.61	0.03	1.4	↑	
PC 30:0	0.06 ± 0.01	0.09 ± 0.01	** <0.01	* 0.05	1.43	0.03	1.5	↑	
PC 32:0	0.7 ± 0.06	1.08 ± 0.05	** <0.01	* 0.01	1.67	0.02	1.5	↑	
PC 34:0	0.29 ± 0.02	0.46 ± 0.02	** <0.01	* 0.01	1.74	0.09	1.6	↑	
PC 34:1	4.84 ± 0.53	6.85 ± 0.44	* 0.01	* 0.03	1.36	0.04	1.4	↑	
PC 38:4	24.61 ± 1.61	35.21 ± 1.52	** <0.01	* 0.01	1.71	0.02	1.4	↑	
PC 40:4	0.25 ± 0.02	0.37 ± 0.04	** <0.01	* 0.02	1.47	0.02	1.5	↑	
SM 42:2	15.64 ± 1.49	23.35 ± 1.29	** <0.01	* 0.01	1.65	0	1.5	↑	Sphingolipid metabolism
SM 42:3	4.64 ± 0.39	7.07 ± 0.4	** <0.01	* 0.01	1.61	0.03	1.5	↑	
TG 54:7	5.21 ± 0.65	1.82 ± 0.39	** <0.01	* 0.01	1.56	0.08	0.3	↓	Lipid metabolism
DG 34:1	1.46 ± 0.08	1.84 ± 0.08	* 0.01	* 0.03	1.71	0.02	1.3	↑	
DG 36:4	3.42 ± 0.21	2.43 ± 0.11	** <0.01	* 0.02	1.89	0.02	0.7	↓	
α-ketoglutarate	2.05 ± 0.1	0.87 ± 0.09	** <0.01	* 0.01	2.05	0.06	0.4	↓	TCA cycle
Aconitic acid	0.02 ± 0	0.01 ± 0	** <0.01	* 0.02	1.64	0.04	0.5	↓	
Malic acid	0.44 ± 0.02	0.19 ± 0.02	** <0.01	* 0.01	2.02	0.08	0.4	↓	
Fumaric acid	0.63 ± 0.04	0.34 ± 0.04	** <0.01	* 0.01	1.95	0.02	0.5	↓	
Succinic acid	0.51 ± 0.02	0.41 ± 0.01	** <0.01	* 0.01	1.85	0.04	0.8	↓	
Glycine	4.57 ± 0.2	5.8 ± 0.36	* 0.03	* 0.01	1.55	0.03	1.3	↑	Glycine, serine and threonine metabolism

Principal component analysis (PCA) was performed to explore and identify the largest source of variation in the data, showing a modest clustering (Figure S1). Additionally, orthogonal partial least-squares discriminant analysis (OPLS-DA), which performs classification tasks and could predict the class, showed clear differences between groups, confirming the robustness of the LPS-induced inflammation model (Figure 3). The proportion of variance in the plasma data explained by the model (R2X) was 59.34%. The percentage of Y variability explained by the model (R2Y) was 96.6%, and the estimation of the predictive performance of the models (Q2) was 87.2%, as it is greater than 50%; thus, the model is considered to have good predictability. The highest variable importance in projection (VIP) values is shown in Table 2, with alpha-ketoglutarate and malic acid being the most important discriminative metabolites (VIP > 2) in the model, followed by other metabolites (e.g., ChoE 22:6, fumaric acid and DG 36:4, among others). Finally, the feature importance was also assessed using RF focusing on the selected metabolites, thus, PC 34:0, malic acid, TG 54:7, alpha-ketoglutarate and succinic acid presented outstanding results in the evaluation of prediction power (Table S1).

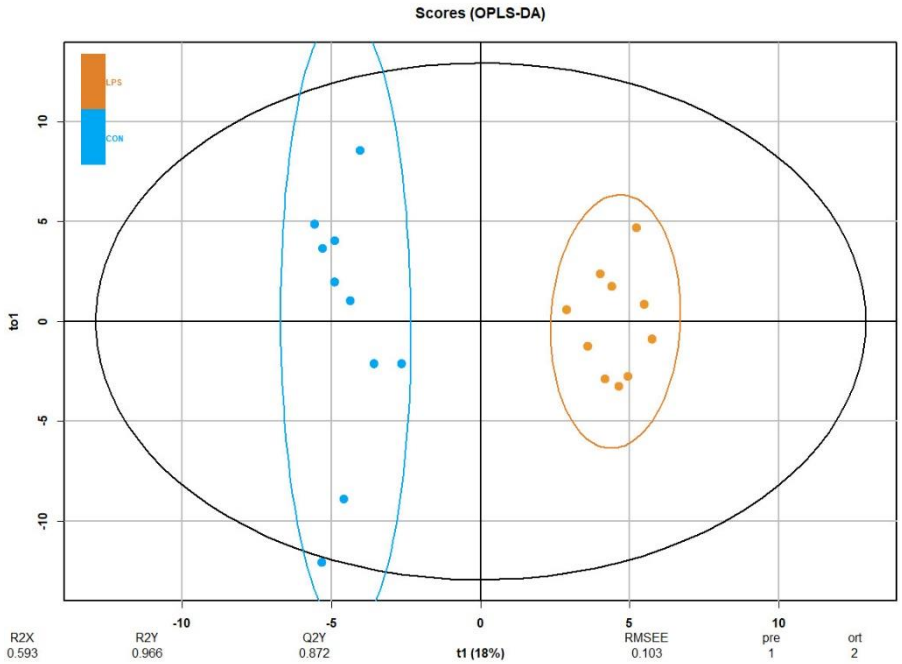

Figure 3. OPLS-DA of plasma metabolomics in the LPS-induced inflammation model. The Score plot is represented, and it includes the number of components and the cumulative R2X, R2Y and Q2Y. Blue represents CON group and orange LPS group (*n* = 10 animals per group).

2.3. Urine Metabolome of the LPS-Induced Inflammation Model

The urine metabolomic approach was based on untargeted ^{1}H-NMR methodology detecting 33 metabolites related to metabolism of amino acids (e.g., phenylalanine, tyrosine and tryptophan metabolism; glycine, serine and threonine metabolism; alanine, aspartate and glutamate metabolism; glutathione metabolism; and taurine and hypotaurine metabolism) and energetic metabolism (e.g., TCA cycle, pyruvate metabolism, and glycolysis/gluconeogenesis) (Table S2). The summary of univariate and multivariate analysis is shown in Table S2. After the MW test, N,N-dimethylglycine was significantly altered in LPS versus the CON group. After the BH correction, none of these metabolites remained significantly modified. In the case of multivariant approaches, no clustering was distinguished in PCA (Figure S2), and OPLS-DA was not significative for predictive power (data not shown). Additionally, N,N-dimethylglycine, which is almost duplicated in the LPS group, is the metabolite presenting the highest RF value, as is shown in Table S2.

2.4. Microbiome of the LPS-Induced Inflammation Model

In this research, the aim of the microbiota study was to enrich the full characterization of the effects of the LPS-induced inflammation model. The most abundant microbes were the bacterial ones, followed by virus and other microbes (less than 1%). For instance, 67% of the readings generated were assigned to bacteria and 33% to virus in CON group, and in the case of the LPS groups, the bacteria level was decreased to 58% and virus was increased to 42% in comparison to CON group. On the one hand, beta diversity, which is represented by a PCA constructed with the Aitchison distances, was not clearly clustering the different groups in bacteria (Figure 4a) and virus (Figure 4b). In the same way, PERMANOVA results were not statistically different, neither in bacteria ($F = 1.11$, p-value = 0.34) nor virus ($F = 1.10$, p-value = 0.30). On the other hand, alpha diversity, which is the measure of richness in the same group, was statistically decreased in bacteria (p-value < 0.01, Figure 4c) and virus (p-value < 0.01, Figure 4d) considering Chao1 index.

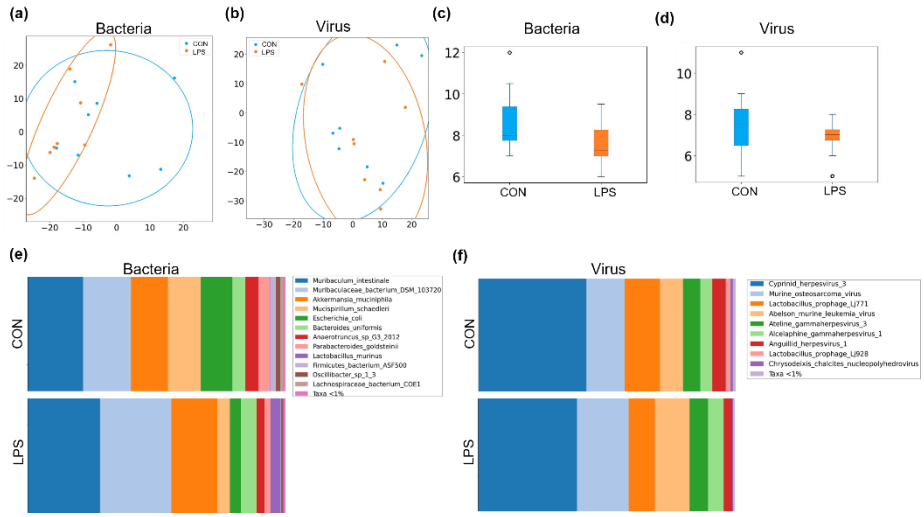

Figure 4. Summary of the microbiome statistical analysis in the LPS-induced inflammation model. Beta diversity: PCA plot calculated by Aitchison distance for bacteria (**a**) and virus (**b**). Alpha diversity (AU): chao1 index in bacteria (**c**) and virus (**d**). Taxonomic differences represented as relative distribution of species in bacteria (**e**) and virus (**f**); these figures show a bar graph at the level of both bacterial and viral species (relative %), comparing the animals in all groups. Blue represents CON group and orange LPS group (*n* = 8 animals per group).

In terms of the bacterial microbiome, the communities of both groups were mostly formed by the phyla *Bacteroidetes* (CON: 49% and LPS: 64%), *Verrucomicrobia* (CON: 14% and LPS: 18%), *Firmicutes* (CON: 11% and LPS: 9%), *Deferribacteres* (CON: 13% and LPS: 5%), *Proteobacteria* (CON: 12% and LPS: 4%) and *Actinobacteria* (CON: 1% and LPS: 0%). Focusing on bacterial species (Figure 4e), 19 species were found with a relative abundance above 0.01% (Table S3), and 3 of them were statistically different after the MW test: Muribaculum intestinale (*p*-value = 0.03, *q*-value = 0.55, CON: 21% and LPS: 28%) and *Lachnospiraceae bacterium A4* (*p*-value = 0.03, *q*-value = 0.55, CON: 0.13% and LPS: 0.32%) were increased, while *Firmicutes bacterium ASF500* was decreased (*p*-value = 0.03, *q*-value = 0.61, CON: 2.27% and LPS: 0.36%). In terms of the virus microbiome, 14 species were found with a relative abundance above 0.01% (Table S4), and 2 species were statistically increased after the MW test in LPS group, an unknown virus of *Alphabaculovirus genera* (*p*-value = 0.02, *q*-value = 0.38, CON: 0.1% and LPS: 0.27%) and an unknown virus of *Pestivirus* genera (*p*-value = 0.03, *q*-value = 0.52, CON: <0.01% and LPS: 0.23%).

2.5. Multi-Omics Data Integration

The multi-omics integrative analysis was performed with the Data Integration Analysis for Biomarker discovery using Latent cOmponents (DIABLO) method that was able to discern a multi-omic profile of eight plasma metabolites (alpha-ketoglutarate, PC 34:0, aconitic acid, LPC 16:0 e, malic acid, SM 42:3, PC 38:4, ChoE 18:3), six urine metabolites (N,N-dimethylglycine, fucose, citrate, dimethylsulfone, formate, 2-

oxoglutarate) and five microbes (*Escherichia coli*, *Pestivirus Giraffe 1*, *Anaerotruncus sp G3 2012*, *Oscillibacter sp 1 3*, *Firmicutes bacterium ASF500*). The correlation method, which is built on the Generalised Canonical Correlation Analysis (GCCA), revealed a correlation between the three data sets with coefficients above 0.6: plasma and urine metabolome (r = 0.79); plasma metabolome and microbiome (r = 0.64); and urine metabolome and microbiome (r = 0.67). The three data sets were able to discriminate between groups (Figure S3); in this case, plasma features presented major impact in the correlation between data sets (Figure S4). The variable effect in the first component, which explains the highest correlations between data, and the impact of each feature on the data sets, are shown in Figure S5a, c and e for plasma metabolomics, urine metabolomics and metagenomics, respectively.

The correlation between the features is represented in Figure 5, to show connections within and between blocks and expression levels of each variable according to each class. In the DIABLO model, the 3-HPPA sulphate (urine metabolite) was negatively correlated with several LPCs and other plasma metabolites together with some bacteria (i.e., *Oscillibacter sp 1 3* and *Escherichia coli*). Another urine metabolite, N,N-dimethylglycine, was correlated with alpha-ketoglutarate and malic acid, which are metabolites identified in plasma related to the TCA cycle. In this sense, the general correlation between plasma and urine metabolites was negative, while the correlation between microbes and plasma metabolites was positive.

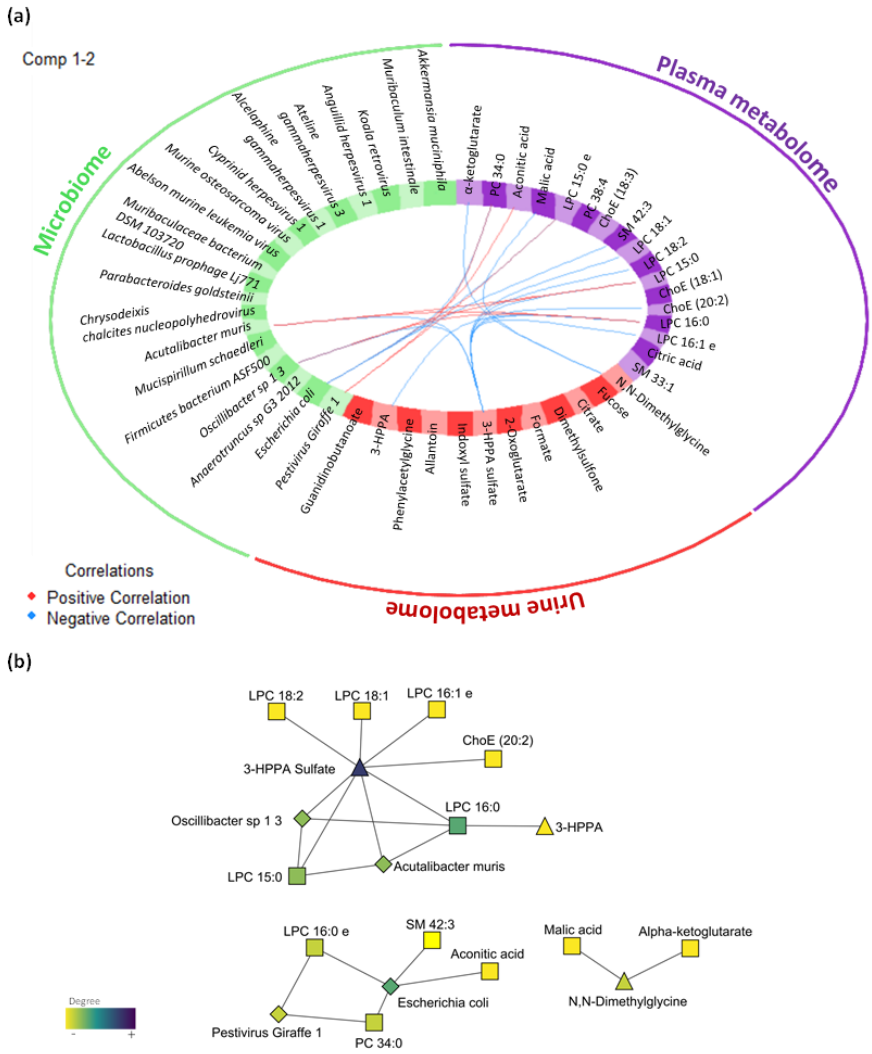

Figure 5. Multi-omics integration of plasma metabolome, urine metabolome and microbiome in the LPS-induced inflammation model. (**a**) Circos plot output from DIABLO. Each quadrant indicates the type of features: plasma metabolites (purple), urine metabolites (red), microbiome (green). (**b**) Further visualization of the network from DIABLO using Cytoscape. The shape of the features indicates the type of feature: plasma metabolites (square), urine metabolites (triangle) and metagenomics (diamond). The colour indicates the degree of each feature in the network (i.e., nodes with more connections). Abbreviations: ChoE, cholesterol ester; TG, triglyceride; PC, phosphatidylcholine; SM, sphingomyelin; LPC, lysophospholipid.

Finally, the overall error rate was calculated (0.3) for the first component to evaluate the performance of the omic profile generated by DIABLO. To give an idea, receiver operating characteristic (ROC) curve analysis showed that the optimal omic profile with the combination of eight plasma metabolites effectively separated both groups with an area under the curve (AUC) of 1 (p-value < 0.01, Figure S5b). A

combination of six plasma metabolites optimally dichotomized the groups with an AUC of 0.89 (p-value < 0.01, Figure S5d). In the microbiome, the microbes presented an AUC of 0.95 (p-value < 0.01, Figure S5f). These results support these features as key mediators of the LPS-induced inflammation model considering plasma metabolome, urine metabolome and microbiome. In this sense, the best correlations were associated with plasma metabolome, as was elucidated in the previous statistical analysis. Thus, the most optimal source of biomarkers in this study was the plasma.

3. Discussion

The evolution of chronic inflammation causes "silent" damage in the development of NCDs, partly favoured by the lack of knowledge about its mechanism and evolution. In this sense, the current study presents deeper understanding of this condition and novel insights through the use of a rodent inflammatory model induced by intermittent (1- and 2-day intervals) and increasing LPS IP injections (0.5, 5 and 7. 5 mg/kg). Hence, this approach was tried to overcome the problems related to LPS-habituation and ineffective establishment of chronic inflammation in rodent models. In previous studies, doses of 2 mg/kg reduced the survival rate to 50% compared to control groups [14], while in our case, the survival rate was 100% compared to the untreated animals. In other studies comparing the LPS in humans and rodents, LPS injections of 10 mg/kg in rodents showed similar scalable levels in humans [16], which are comparable to LPS levels in human diseases [24]. Consequently, we suggest that the rodent ability to tolerate frequent LPS challenges facilitates the dose increment up to 7.5 mg/kg, used in our approach, to carry out chronic studies related to inflammation. Furthermore, the LPS reached levels that are close to previously described LPS levels related to human diseases [20]. The intermittent and increasing LPS treatment, which resulted in BW changes due to the effect of LPS on appetite, was reflected in food consumption, which was in agreement with other studies [14,25]. The initial injection had a huge impact on BW and food consumption; then, the animals compensated for the initial response with higher feed efficiency rates, and at the end of the study, both groups presented the same pattern. These changes are not in line with the general features of NCDs, as in this chronic inflammation model, the intention was to isolate the risk factor, considering that it would not occur in a real individual.

The mechanism of inflammation induced by LPS consists of the activation of Toll-like receptors (TLRs), which lead to the activation of macrophages and lymphocytes and the production of inflammatory cytokines (i.e., TNF-α, IL-6, PGE2) [26], which is in agreement with our experimental results. Although those cytokines have several roles in different tissues and cell types related to the inflammatory response, many cytokines have other effects on neuroendocrine and metabolic functions and on the maintenance of tissue homeostasis in general [27]. In the case of MCP-1, which attracts inflammatory monocytes and stimulates the production of other cytokines, it was the selected cytokine to monitor the sustained inflammation during the

experimental procedure [28]. Those inflammatory monocytes have been involved in low-grade inflammation and altered lipid metabolism through the release of various pro-inflammatory mediators [29]. The systemic increase in oxidative stress detected in the LPS group in urine is associated with the immune response that could be attempting to kill the invading agents through the releasing of toxic content from cells (including reactive oxygen species (ROS)) [30].

As far as we know, this study is the first to evaluate the omic profile of a chronic inflammation model with the objective of elucidating the metabolic mechanism and finding potential biomarkers for early detection of metabolic alterations associated with chronic inflammation, which leads to the onset of different diseases. The study of chronic systemic inflammation is important because it can trigger and propagate metabolic inflexibility; this fact can cause a vicious circle, because such metabolic inflexibility can also trigger systemic inflammation [31]. Recent studies focused on those pathologies (CVDs [32], NAFLD [33], arthritis [34], obesity and diabetes [35]) have suggested an alteration in metabolomic and lipidomic signatures implicated in the onset of NCDs development. Nevertheless, these signatures cannot discern between chronic inflammation and other factors influencing the development of the disease. In our approach, we have detected three key pillars of metabolic disruption associated with chronic inflammation: lipidic metabolism (mainly focused on specific fatty acids (FAs) metabolism), TCA cycle and one-carbon (1C) metabolism, as summarized in Figure 6.

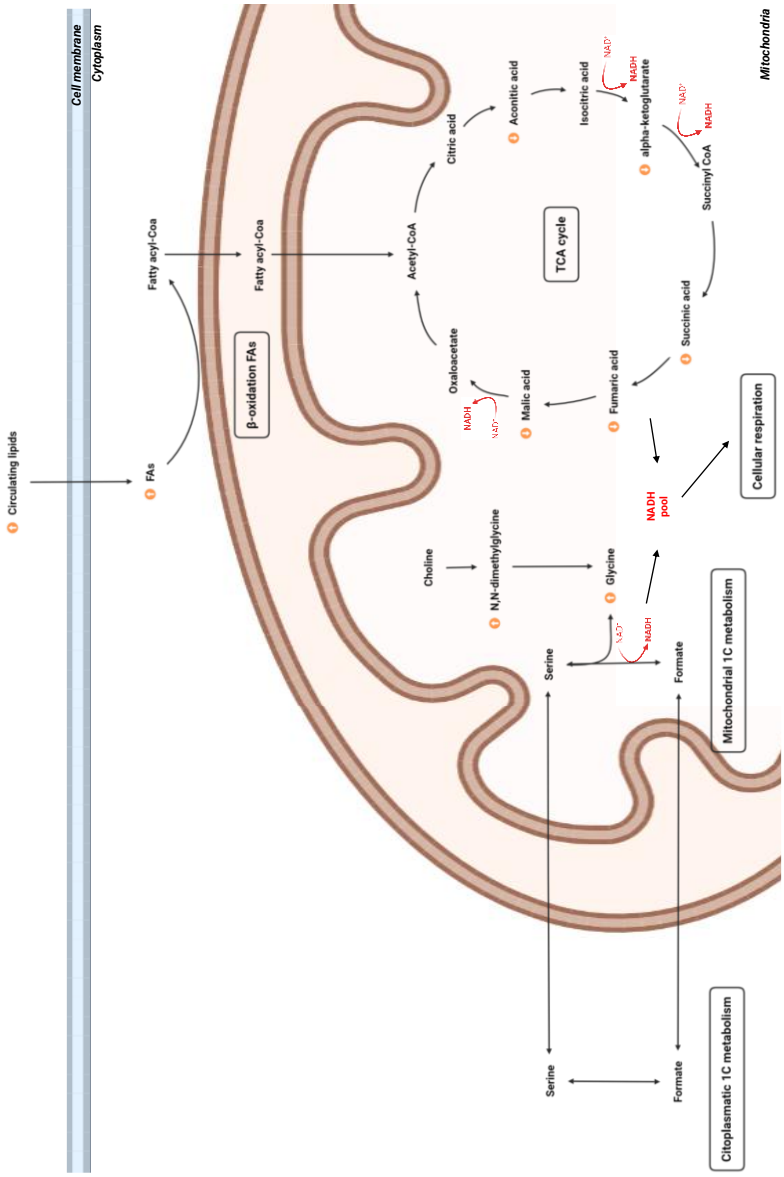

Figure 6. A schematic overview of the metabolic pathways involved in the LPS-induced inflammation model. In the context of mitochondria, TCA cycle is the nexus between FAs through β-oxidation disruption, glycine through 1C metabolism and cellular respiration. Abbreviations: FA, fatty acid; NAD+/NADH, nicotinamide adenine dinucleotide oxidized and reduced.

Lipids play an important role in the pro-inflammatory and anti-inflammatory response; thus, lipidic dynamics disruption leads to unbalanced homeostasis and the subsequent development of pathologies. In fact, lipids act as mediators on important immune receptors to induce chronic tissue inflammation that leads to adipocyte and metabolic dysfunction [36]. In our LPS-induced inflammation model, diverse types of lipids were increased. ChoEs, PCs and LPCs stand out among other lipids as the important ones, due to their influence in chronic inflammation and interactions in energetic metabolism.

Identification and quantification of circulating FAs, which are involved in critical cellular functions such as storage of energy and signalling pathways, have attracted attention as potential inflammatory status biomarkers [37]. The leading circulating FAs are made up of even-chains of 18 to 22 carbons, and regarding the saturations, we could find poly-unsaturated FAs (PUFAs) and saturated FAs (SFAs) on the LPS-induced chronic inflammation rodent model. Accumulating evidence suggests that ChoE 18:0, which is the main even SFA altered in our study, is the main even-chain SFA associated with lipid metabolism, liver function, glycaemic control and chronic inflammation leading to CVDs [38]. Additionally, ChoE (18:0) accumulation in macrophages has been related to the induction of inflammation by TLR 4/2 inducing endoplasmic reticulum stress-mediated apoptosis [39] and is considered to induce lipotoxicity in adipocytes [40]. These hypertrophied adipocytes enriched in SFAs secrete pro-inflammatory agents that promote systemic inflammation [41] and the subsequent obesity-associated adipose tissue inflammation [42].

Circulating phospholipids (LPCs and PCs) have been reported to reflect FAs metabolism, thus pointing to long-term storage of FAs indicating a long-standing exposure to FAs that are classically used as dietary biomarkers [43,44]. On the one hand, in the current experimental approach, circulating LPCs, which were composed by SFAs of 16 and 18 carbons, were also affected. Interestingly, phospholipids have been associated with pro-inflammatory and pro-atherogenic activities, which are critical factors underlying CVDs and several pathological conditions, in consistence with previous studies [38,45–47]. In fact, LPC can induce expression of COX2, a key pro-inflammatory mediator, via the p38/CREB or ATF-1 pathways in vascular endothelial cells [48]. For example, a study focused on asthma, which is a chronic inflammatory disease of the airways, presented elevated LPC 16:0 and LPC 18:0 together with activity increase in phospholipase A_2 (PLA_2) [49]. On the other hand, PCs, which carry two chains of FA, presented a predominance of chains from 16 to 20 carbons, with the SFAs predominant over MUFAs and PUFAs. This could be indicative that chronic inflammation is characterized by an increase in even SFAs between 16 and 18 carbons [50–52]. This observation suggests that chronic inflammation could induce long-term changes in the metabolism of SFAs through increasing their circulation bound to phospholipids [53]. Similarly, previous studies have shown that increased levels of PCs are positively correlated with obesity, insulin resistance, tumours and psoriasis among other inflammatory pathologies [54].

Therefore, after activation of cytosolic PLA_2, important lipid mediators of inflammatory response (FAs and LPCs) are generated, among which PUFAs are the most interesting hydrolysed FAs regarding their effects during inflammation [55]. For instance, ChoE 20:4, commonly known as arachidonic acid, is metabolized to form eicosanoids by the action of cyclooxygenases (COX1 and COX2), which generates prostaglandins and thromboxanes, or by lipoxygenases, that subsequently generate leukotrienes and lipoxins, which are associated with a pro-inflammatory response [26]. Alternatively, ChoE 18:3, commonly known as linolenic acid, is a precursor of ChoE 22:6 or docosahexaenoic acid or omega 3, and it is associated with anti-inflammatory response. The synthesis of ChoE 20:4 from ChoE 18:2 seems to be reduced in favour of the synthesis of ChoE 22:6 from ChoE 18:3 due to both syntheses competing for the same enzymes (Δ6 desaturase, elongase and Δ5 desaturase) [56]. The significant increase in ChoE 18:3 (precursor of ChoE 22:6) instead of ChoE 18:2 (precursor of ChoE 20:4) suggests that the synthesis of ChoE 22:6 reaction is favoured.

During periods of stress in the cell, intermediary metabolites of the TCA cycle, which occurs completely in mitochondria, can be released, acting as a danger signals in cytosol and regulating immune response [57]. The decrease in TCA intermediaries (i.e., alpha-ketoglutarate, aconitic acid, malic acid, fumaric acid and succinic acid) might be indicative of a systemic inhibition of the intracellular TCA cycle (Figure 6) that could be associated with the regulation of immune response and activation of other energy pathways [58]. In fact, metabolic flexibility is essential for immune function; during immune response, the immune cells shift to aerobic glycolysis for energy production, a less-efficient but fast-acting pathway [59]. Additionally, the switch to glycolysis enables glycolysis, and TCA cycle intermediates may be used as key sources of carbon molecules for biosynthesis of nucleotides, amino acids and lipids [59]. Several metabolomic studies point out the decrease in TCA cycle activity as a key characteristic of chronic inflammation, related to alterations in lipid and fatty acid metabolism [60–62]. The connection between TCA cycle and FAs could be due to the β-oxidation of FAs. In fact, FAs enter the cell to be degraded into acetyl-CoA in the mitochondria as the end product of β-oxidation; this end product is the starting point of the TCA cycle [63].

Furthermore, other metabolites could be related to the inhibition of TCA cycle activity as 1C-metabolism-related metabolites (Figure 6). Specifically, 1C metabolism consists in methionine and folate cycles, involving multiple molecules of the cytosolic and mitochondrial compartments; moreover, the folate cycle is a major player in NADPH generation. In fact, production of NADH by mitochondrial 5,10-methylene-tetrahydrofolate (THF) dehydrogenase activity links 1C metabolism to the respiratory state of the cell. Glycine (circulating in plasma) and N,N-dimethylglycine (excreted in urine), which were increased in the metabolome, are amino acids essentially involved in the modulation of oxidative stress presenting antioxidant activity. For instance, previous experimental evidence has been generated in favour of the anti-inflammatory, immunomodulatory and cytoprotective effects of glycine [64].

Regarding the secreted urine amino acids, N,N-dimethylglycine, a glycine tertiary amino acid produced by the degradation of choline, was almost duplicated in the LPS group; this fact is in agreement with other animal studies suggesting that N,N-dimethylglycine enhances immune response due to intensifying oxygen utilization by tissue and complex with free radicals, as is the case for glycine [65]. Despite the antioxidant activity of glycine, their increased metabolism related to 1C metabolism has been associated with the development of tumorigenesis [66]. Maynard and Kanarek recently discovered the association of 1C cycle and TCA cycle through the accumulation of NADH in the mitochondria [67]. The 1C cycle becomes a major source of glycine and NADH when cellular respiration is inhibited, and the accumulated NADH inhibits the TCA cycle and slows proliferation due to its toxicity in high concentrations; thus, the unbalanced concentrations of NADH condition health and the pathological state (Figure 6). Additionally, mitochondrial NAD+/NADH ratios are maintained by oxidative phosphorylation, and initial experiments in isolated mitochondria showed that formate production from serine was respiration-dependent [68].This fact could be likely suggested in the present work linked to the increase in excreted formate in urine (despite being statistically significant). Within the mitochondria, 1C units can be made from serine, glycine, sarcosine or N,N-dimethylglycine and secreted into the cytosol as formate [69]. In this regard, the elevation in urinary excretion of formate was observed in folate-deficient rats [70]. Thus, formate may play a role in some of the pathologies associated with defective 1C metabolism, but there is a need for more studies to confirm this implication [71].

Interestingly, the profile obtained by DIABLO, in trying to maximize the correlation between the different data sets, highlights feature from different data sets, although no differences were found in statistical analysis in urine metabolome and microbiome. This omic profile contemplated features that could complete the metabolic context of chronic inflammation. One of the most interesting relations is the association of N,N-dimethylglycine urine levels and TCA cycle intermediates (i.e., malic acid and alpha-ketoglutarate), which is in line with the previous discussion about the relation of 1C cycle and TCA cycle [67].

Although no major differences were found in the LPS- induced inflammation model, the microbiome has a close connection to systemic metabolism, highlighting the underlying crosstalk between the microbiome and inflammation [72]. However, the presence of these microbes or their metabolites may not represent the best source for biomarkers of inflammation, because the microbiome highly depends on the individual and the environment. Nevertheless, the microbiome can provide supplementary information indirectly related to the metabolome. In previous studies, low-grade inflammation has been related to alterations in the gut microbiota composition and increased plasma LPS levels [73]. In our case, as LPS has been administered, it is not originated by the individual's microbiota, so the effect on inflammation due to the altered microbiota may be masked. For example, *Akkermansia muciniphila* has been shown to improve metabolic profiles by reducing

chronic low-grade inflammation induced by chow diet in mice, linking this bacterium to the host immune system [74].

Finally, several shortcomings need to be taken into account in order to contextualize this experimental approach. The present study design should be considered as a pilot study due to the following factors: (1) there are limitations in obtaining a pure model of low-grade chronic inflammation, because although an attempt has been made to make the present model as close as possible to chronic inflammation, it is ultimately based on repeated induction of acute inflammation stimuli; (2) the low number of animals is not high enough (n = 10 per group) to provide a robust conclusion on biomarkers; (3) other omics approaches could be added to obtain a more robust metabolic profile; (4) urine is a complex fluid to collect in animals, as it is not possible to stablish the collecting time, which can lead to high variability of results. These issues should be considered for further experiments.

4. Materials and Methods

4.1. LPS-Induced Chronic Inflammation Model

Twenty 8-week-old male Wistar rats (Harlan Laboratories, Barcelona, Spain) were housed individually in a fully controlled environment including temperature (22 ± 2 °C), humidity (55 ± 5%) and light (12 h-light-dark cycle and lights on at 9:00 a.m.). The Animal Ethics Committee of the University Rovira i Virgili (Tarragona, Spain) approved all the procedures (code 10049). The experimental protocol followed the “Principles of Laboratory Care” and was carried out in accordance with the European Communities Council Directive (86/609/EEC).

After an acclimation period, animals were randomly assigned to two different groups considering similar average BW divided into two experimental groups (n = 10 animals per group): CON group and LPS-induced inflammation group. Regarding LPS (Sigma-Aldrich, St. Louis, MO, USA), a stock solution of 500 µg/mL was prepared in sterile saline solution (NaCl 0.9%) and stored in aliquots of 1 mL at −20 °C until administration. The experiment was conducted during the light phase (8:30–10:00 am) and was carried out for 31 days. In that period, rats were administered with increasing doses of LPS (LPS group) or saline solution (CON group) (Figure 7). The LPS group received nine IP injections of 0.5 mg/kg of LPS, four injections of 5 mg/kg and a final injection of 7. 5 mg/kg (6 h before the sacrifice).

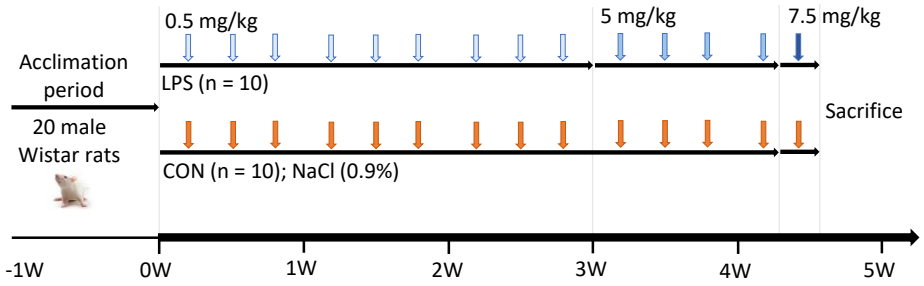

Figure 7. Schematic representation of the LPS-induced chronic inflammation model. The experimental model consisted of two groups that received intraperitoneal (IP) injections of increasing LPS and saline solution (NaCl 0.9%) for 31 days. Abbreviations: W, week; CON, control group; LPS, LPS-induced inflammation group.

To evaluate the effect of the LPS injections, mean daily BW gains were calculated for each group at each interval of three days per week and for the overall experimental period. Animals were allowed ad libitum access to food throughout the entire study period. Food consumption was measured once a week on days 1 (prior to dosing), 8, 15, 22, and 29, coinciding with the days of BW measurements. Mean food consumption was calculated for each group during each interval. Feed efficiency was also calculated for each group based on BW gain and food consumption data with the following equation: feed efficiency = food consumption (g/d)/BW gain (g/d).

4.2. Sample Collection

Blood was collected from the lateral saphenous vein in the second, third and fourth week to monitor the inflammation level. Urine was collected the day before the sacrifice following the hydrophobic sand method, which is less stressful for the animals [75]. For each rat, 300 g of hydrophobic sand was spread (LabSand, Coastline Global, Palo Alto, CA, USA) on the bottom of a mouse plastic micro-isolation cage. Urine was collected and stored with sodium azide (Sigma, St. Louis, MO, USA) as preservative every half an hour for 6 h and was finally pooled at the end of the session. On the day of the sacrifice, animals were euthanized by guillotine under anaesthesia (pentobarbital sodium, 50 mg/kg per BW) after 7 h of fasting. Blood was collected and centrifuged at 3000 g at 4 °C for 15 min to recover plasma. Tissues were rapidly removed, weighted and snap-frozen in liquid nitrogen (i.e., retroperitoneal white adipose tissue (RWAT), mesenteric white adipose tissue (MWAT), muscle, liver, and cecum). All the samples were stored at -80 °C until further analysis.

4.3. Plasma, Urine, and Liver Measurements

Enzymatic colorimetric kits were used for the determination of plasma total cholesterol (TC), TG, glucose (QCA, Barcelona, Spain) and non-esterified free fatty acids (NEFAs; WAKO, Neuss, Germany). Plasma concentrations of rat IL-6 (Cusabio Biotech Co., Wuhan, Hubei, China), MCP-1 (Thermo Fisher Scientific, Dublin, Ireland), TNF-α (Invitrogen, Vienna, Austria) and PGE2 (Bio-Techne Ltd., Minneapolis, MN, USA)

were measured by enzyme-linked immunosorbent assay (ELISA) kits according to the manufacturer's instructions. Additionally, urine 8-isoprostane was evaluated using an ELISA kit (Cayman chemical, Ann Arbor, MI, USA).

Liver lipids were extracted and quantified from a tissue piece of approximately 100 mg from the frozen liver using methods described previously [76]. Briefly, lipids were extracted with 1 mL of hexane:isopropanol (3:2, *v*/*v*), degassed with gas nitrogen before being left overnight under orbital agitation at room temperature protected from light. After an extraction with 0.3 mL of Na2SO4 (0.47 M), the lipid phase was dried with gas nitrogen and total lipids quantified gravimetrically before emulsifying as described previously [77]. TG, TC and phospholipids were assayed with commercial enzymatic kits (QCA, Barcelona, Spain).

4.4. Plasma Metabolome (GC-qTOF and UHPLC-qTOF)

Plasma metabolites were analysed by gas chromatography coupled with quadrupole time-of-flight (GC-qTOF). For the extraction, a protein precipitation extraction was performed by adding eight volumes of methanol:water (8:2, *v*/*v*) containing internal standard mixture (succinic acid-d4, myristic acid-d27, glicerol-13C3 and D-glucose-13C6) to plasma samples. Then, the samples were mixed and incubated at 4 °C for 10 min and centrifuged at 21.420 g, and the supernatant was evaporated to dryness before compound derivatization (metoximation and silylation). The derivatized compounds were analysed by GC-qTOF (model 7200 of Agilent, USA). The chromatographic separation was based on the Fiehn Method [78], using a J&W Scientific HP5-MS (30 m × 0.25 mm i.d.), 0.25 µm film capillary column and helium as carrier gas using an oven program from 60 °C to 325 °C. Ionization was done by electronic impact (EI), with electron energy of 70 eV and operated in full scan mode. The identification of metabolites was performed by matching two different parameters to a metabolomic Fiehn library (Agilent, Santa Clara, CA, USA): EI mass spectrum was considered stable and reproducible and as having good retention time. To avoid annotation errors, metabolites with very high molecular weights were cleared. After putative identification of metabolites, these were semi-quantified in terms of internal standard response ratio.

Plasma lipids were analysed by ultra-high-perfomance liquid chromatography coupled with quadrupole time-of-flight (UHPLC-qTOF). For the extraction of the hydrophobic lipids, a liquid–liquid extraction based on the Folch procedure [79] was performed by adding four volumes of chloroform:methanol (2:1, *v*/*v*) containing internal standard mixture (Lipidomic SPLASH®, Avanti Polar Lipids, Inc., Alabaster, AL, USA) to plasma. Then, the samples were mixed and incubated at −20 °C for 30 min. Afterwards, water with NaCl (0.8%) was added, and the mixture was centrifuged at 21.420 g. Lower phase was recovered, evaporated to dryness, reconstituted with methanol:methyl-tert-butyl ether (9:1, *v*/*v*) and analysed by UHPLC-qTOF (model 6550 of Agilent, Santa Clara, CA, USA) in positive electrospray ionization mode. The chromatographic consists in an elution with a ternary mobile phase containing water,

methanol, and 2-propanol with 10 mM ammonium formate and 0.1% formic acid. The stationary phase was a C18 column (Kinetex EVO C18 Column, 2.6 µm, 2.1 mm × 100 mm) that allowed the sequential elution of the more hydrophobic lipids such as TGs, DGs, PCs, ChoEs, LPCs and SMs, among others. The identification of lipid species was performed by matching their accurate mass and tandem mass spectrum, when available, to Metlin-PCDL from Agilent containing more than 40.000 metabolites and lipids. In addition, chromatographic behaviour of pure standards for each family and bibliographic information was used to ensure their putative identification. After putative identification of lipids, these were semi-quantified in terms of internal standard response ratio using one internal standard for each lipid family.

A pooled matrix of samples was generated by taking a small volume of each experimental sample to serve as a technical replicate throughout the data set. As the study took multiple days, a data normalization step was performed to correct variation resulting from instrument inter-day tuning differences. Essentially, each compound was corrected in run-day blocks through quality controls, normalizing each data point proportionately.

4.5. Urine Metabolome (^{1}H-NMR)

Urine metabolites were analysed by proton nuclear magnetic resonance (^{1}H-NMR). The urine sample was mixed (1:1, *v*/*v*) with phosphate buffered saline containing with 3-(Trimethylsilyl)propionic-2,2,3,3-d4 acid sodium salt (TSP) (Sigma Aldrich, St. Louis, MO, USA) and placed on a 5 nm NMR tube for direct analysis by ^{1}H-NMR. ^{1}H-NMR spectra were recorded at 300 K on an Avance III 600 spectrometer (Bruker®, Bremen, Germany) operating at a proton frequency of 600.20 MHz using a 5 mm PBBO gradient probe. Diluted urine aqueous samples were measured and recorded in procno 11 using a one-dimensional ^{1}H pulse. Experiments were carried out using the nuclear Overhauser effect spectroscopy (NOESY). NOESY presaturation sequence (RD–90°–t1–90°–tm–90° ACQ) suppressed the residual water peak, and the mixing time was set at 100 ms. Solvent presaturation with irradiation power of 150 µW was applied during recycling delay (RD = 5 s) and mixing time (noesypr1d pulse program in Bruker®, Bremen, Germany) to eliminate the residual water. The 90° pulse length was calibrated for each sample and varied from 11.21 to 11.38 ms. The spectral width was 9.6 kHz (16 ppm), and a total of 128 transients were collected into 64 k data points for each ^{1}H spectrum. The exponential line broadening applied before Fourier transformation was of 0.3 Hz. The frequency domain spectra were manually phased and baseline-corrected using TopSpin software (version 3.2, Bruker, Bremen, Germany). Data were normalized in two different ways: probabilistically, to avoid differences between samples due to different urine concentrations, and by ERETIC. The acquired ^{1}H-NMR were compared to references of pure compounds from the metabolic profiling AMIX spectra database (Bruker®, Bremen, Germany), HMDB and Chenomx databases for metabolite identification. In addition, we assigned metabolites by ^{1}H-^{1}H homonuclear correlation (COSY and TOCSY) and ^{1}H-^{13}C

heteronuclear (HSQC) 2D NMR experiments and by correlation with pure compounds run in-house. After pre-processing, specific ^{1}H-NMR regions identified in the spectra were integrated using MATLAB scripts run in-house. Curated identified regions across the spectra were exported to Excel spreadsheet to evaluate robustness of the different ^{1}H-NMR signals and to give relative concentrations.

4.6. Microbiome Analysis (Shotgun Metagenomics Sequencing)

DNA was extracted from faeces using the PowerSoil DNA extraction kit (MO BIO Laboratories, Carlsbad, CA, USA) following the manufacturer's protocol. Between 400 and 500 ng of total DNA was used for library preparation for Illumina sequencing employing Illumina DNA Prep kit (Illumina, San Diego, CA, USA). All libraries were assessed using a TapeStation High Sensitivity DNA kit (Agilent Technologies, Santa Clara, CA, USA) and were quantified by Qubit (Invitrogen,Waltham, MA, USA).

Validated libraries were pooled in equimolar quantities and sequenced as a paired-end 150-cycle run on an Illumina NextSeq2000. A total of 1548 million reads were generated, and raw reads were filtered for QV > 30 using an in-house phyton script. Filtered reads were aligned to unique clade-specific marker genes using MetaPhlAn 3 [80] to assess the taxonomic profile. The alignment was done indicating the closest name of species to the sequence (the best hit). The relative proportions calculated from MetaPhlAn were used to calculate relative abundances, alpha diversity measure (chao1 index) and beta diversity measures (Aitchison distance).

4.7. Statistical Analysis

4.7.1. General Statistical Analysis

Statistical analysis was performed using the R software (version 4.0.2, R Core Team 2021), and different libraries, included in Bioconductor (version 3.11, Bioconductor project), were used. The continuous variables of biological assay were showed as mean ± standard error of the mean (SEM). After the normality study, parametric unpaired t-test was used for single statistical comparisons and repeated-measures analysis of variance (ANOVA) for multiple statistical comparisons repeated during time. In all the statistical comparisons, a two-tailed value of $p < 0.05$ was considered.

4.7.2. Metabolomic Data Analysis

Individual comparisons between metabolites were determined by the MW test, because the variables follow the assumption of a non-parametric test. The p-value adjustment for multiple comparisons was carried out according to the BH correction considering a 5% false-discovery rate (FDR). The magnitude of difference between populations is presented as fold change (FC), which is relative to the control group. In parallel, a predictive analysis was done to evaluate the prediction power of the LPS-induced chronic inflammation model. On the one hand, PCA, an unsupervised

multivariate data projection method, was performed to explore the native relationship between groups. On the other hand, OPLS-DA, a supervised multivariate data projection method, was calculated to explore the possible relationships between the observable variables (X) and the predicted variables or target (Y), extracting the maximum information reflecting the variation in the dataset. No data transformation was applied before conducting the analysis. The predictive performance of the test set was estimated by the Q2Y parameter calculated through cross-validation. The values of $Q2 < 0$ suggest a model with no predictive ability, $0 < Q2 < 0.5$ suggests some predictive character and $Q2 > 0.5$ indicates good predictive ability [81]. The feature importance was calculated through the VIP, which reflects both the loading weights for each component and the variability of the response explained by the component. Additionally, the random forest classifier (RF) was calculated to sort the 10 most important metabolites that distinguish between the CON and LPS groups.

4.7.3. Metagenomic Data Analysis

Centred log-ratio (CLR) normalization was performed before any statistical test. The beta diversity was calculated from the Aitchison distance, and PERMANOVA test was performed with 100 permutations to assess the differences between groups. The alpha diversity was calculated by Chao1 index. Taxonomic abundances were compared between experimental groups using the BH adjustment on MW test that is presented by relative abundance (%). The relative abundance was filtered to only include variables that were present above 0.01% in at least 3 samples [82]. The magnitude of difference between populations was determined by the determination of FC.

4.7.4. Integration Data Analysis

Multiblock sPLS-DA is a holistic approach with the potential to find new biological insights not revealed by any single-data omics analysis, as some pathways are common to all data types, while other pathways may be specific to data. DIABLO implementation, which is built on the GCCA [83], in the mixOmics R package (version 6.18.1, mixOmics project), was used to integrate plasma and urine metabolome and microbiome [84]. The goal of the data integration with this method is to extract complementary information between omics datasets, resulting in an improved ability to associate biomarkers across multiple functional levels with the phenotype of interest. This statistical integrative framework facilitates the interpretation of complex analyses and provides significant biological insights.

To summarize, the first step is the parameter choice of the design matrix, the number of components and the number of variables to select: (1) a design matrix of 0.1 was used to focus primarily on the discrimination between the groups; (2) the perf function was used to estimate the performance of the model, and the overall error rates per component were displayed to select the optimal number of components; (3) the number of variables was chosen using the tune.block.splsda function that is run with 10-fold cross validation and repeated 10 times, and thus this tuning step led to a

selection of 8 plasma metabolites, 6 urine metabolites, and 5 microbes. Thereafter, the final model was computed, and different sample and variable plots were performed. The circosPlot function represents the correlations between variables of different types, represented on the side quadrants that are built based on a similarity matrix, which was extended to the case of multiple data sets [85]. The resulting network from circus plot with a threshold above 0.7 was further analysed using the MEtScape [86] and NetworkAnalyzer [87] packages from Cytoscape (version 3.8.2, Institute of Systems Biology, Seattle, WA, USA)[88].

The final performance of the model was evaluated by the perf function using 10-fold cross-validation repeated 10 times. The ROC curve analysis was conducted to determine the optimal metabolite combination patterns that could correctly dichotomize the stressed and healthy groups at acceptable sensitivity and specificity (defined as greater than 80% for both). The AUC value was used as a measure of the prognostic accuracy. An AUC value of 1 indicates a perfect test due to absence of overlap of the test data between the control and anxiety state; an AUC value >0.85 was considered for inclusion in the model.

4.7.5. Pathway Analysis

The resulting significant differential features were analysed through different databases to identify related pathways and elucidate the global effect on the metabolism of the LPS-induced inflammation model. The main database consulted was the Kyoto Encyclopaedia of Genes and Genomes (KEGG) [89]. To show those results, a mapping tool (version XMind 2020, XMind Ltd., Virginia, ON, Canada) was used to incorporate the information about pathway analysis.

5. Conclusions

In conclusion, intermittent (1- and 2-day intervals) and increasing (0.5, 5 and 7. 5 mg/kg) dose IP administration of LPS thrice per week for 31 days induced chronic inflammation. In general, biometric, and biochemical changes observed were in concordance to those seen in chronic inflammatory events. Thus, this model could be considered for the study of chronic inflammation in rodents, mimicking this risk for the development of inflammatory diseases.

The present study using omic approaches elucidates an altered profile associated with the current model of LPS-induced inflammation. In the metabolome, there is a clear disruption of the mitochondrial metabolism due to three key pathways in metabolism, which are β-oxidation of FAs, TCA cycle and 1C metabolism. Lipids related to β-oxidation play an important role in the unbalanced homeostasis during chronic inflammation. The main even SFA altered in our study was ChoE 18:0, which is associated with metabolic complications [38]. Other FAs related to pro-inflammatory activity such as ChoE 20:4 and anti-inflammatory activity were increased. In fact, the significant increase in ChoE 18:3 (precursor of ChoE 22:6) instead of ChoE 18:2 (precursor of ChoE 20:4) suggests that the synthesis of ChoE 22:6 reaction is favoured.

Additionally, circulating phospholipids reported the long-term storage of FAs [43,44]. The decrease in TCA intermediaries (i.e., alpha-ketoglutarate, aconitic acid, malic acid, fumaric acid and succinic acid) was indicative of a systemic inhibition of the intracellular TCA cycle that could be associated with the regulation of immune response and activation of other energy pathways [58]. Additionally, the disruption of β-oxidation plays a key role in the TCA cycle due to the end product of this pathways being the starting point of TCA cycle [63]. Additionally, 1C metabolism is mainly represented in our model by glycine (circulating in plasma) and N,N-dimethylglycine (excreted in urine), which suggests a disruption in 1C metabolism [67].

Hence, the imbalance in FAs, TCA cycle intermediates and 1C intermediates metabolites are characteristics of our rodent model of chronic inflammation that leads to the disruption of homeostasis in mitochondrial metabolism (β-oxidation, TCA cycle and 1C metabolism). Those results provide novel clues on the impact of a model of chronic inflammation in the metabolism that tries to mimic chronic low-grade inflammation in humans.

References

1. Netea, M.G.; Balkwill, F.; Chonchol, M.; Cominelli, F.; Donath, M.Y.; Giamarellos-Bourboulis, E.J.; Golenbock, D.; Gresnigt, M.S.; Heneka, M.T.; Hoffman, H.M.; et al. A guiding map for inflammation. *Nat. Immunol.* **2017**, *18*, 826–831, doi:10.1038/ni.3790.

2. Bennett, J.M.; Reeves, G.; Billman, G.E.; Sturmberg, J.P. Inflammation-Nature's Way to Efficiently Respond to All Types of Challenges: Implications for Understanding and Managing "the Epidemic" of Chronic Diseases. *Front. Med.* **2018**, *5*, 316, doi:10.3389/fmed.2018.00316.

3. Pahwa, R.; Goyal, A.; Bansal, P.; Jialal, I. *Chronic Inflammation*; StatPearls Publishing, Treasure Island (FL): National Institute of Health, 2020;

4. Furman, D.; Campisi, J.; Verdin, E.; Carrera-Bastos, P.; Targ, S.; Franceschi, C.; Ferrucci, L.; Gilroy, D.W.; Fasano, A.; Miller, G.W.; et al. Chronic inflammation in the etiology of disease across the life span. *Nat. Med.* **2019**, *25*, 1822–1832, doi:10.1038/s41591-019-0675-0.

5. Liu, C.H.; Abrams, N.D.; Carrick, D.M.; Chander, P.; Dwyer, J.; Hamlet, M.R.J.; Macchiarini, F.; PrabhuDas, M.; Shen, G.L.; Tandon, P.; et al. Biomarkers of chronic inflammation in disease development and prevention: challenges and opportunities. *Nat. Immunol.* **2017**, *18*, 1175–1180, doi:10.1038/ni.3828.

6. Arai, Y.; Martin-Ruiz, C.M.; Takayama, M.; Abe, Y.; Takebayashi, T.; Koyasu, S.; Suematsu, M.; Hirose, N.; von Zglinicki, T. Inflammation, But Not Telomere Length, Predicts Successful Ageing at Extreme Old Age: A Longitudinal Study of Semi-supercentenarians. *EBioMedicine* **2015**, *2*, 1549–1558, doi:10.1016/j.ebiom.2015.07.029.

7. Roubenoff, R.; Harris, T.B.; Abad, L.W.; Wilson, P.W.; Dallal, G.E.; Dinarello, C.A. Monocyte cytokine production in an elderly population: effect of age and inflammation. *J. Gerontol. A. Biol. Sci. Med. Sci.* **1998**, *53*, M20-6, doi:10.1093/gerona/53a.1.m20.

8. Ahluwalia, N.; Mastro, A.M.; Ball, R.; Miles, M.P.; Rajendra, R.; Handte, G. Cytokine production by stimulated mononuclear cells did not change with aging in apparently healthy, well-nourished women. *Mech. Ageing Dev.* **2001**, *122*, 1269–1279, doi:10.1016/s0047-6374(01)00266-4.

9. Beharka, A.A.; Meydani, M.; Wu, D.; Leka, L.S.; Meydani, A.; Meydani, S.N. Interleukin-6 production does not increase with age. *J. Gerontol. A. Biol. Sci. Med. Sci.* **2001**, *56*, B81-8, doi:10.1093/gerona/56.2.b81.

10. Meirow, Y.; Baniyash, M. Immune biomarkers for chronic inflammation related complications in non-cancerous and cancerous diseases. *Cancer Immunol. Immunother.* **2017**, *66*, 1089–1101, doi:10.1007/s00262-017-2035-6.

11. Jacob, M.; Lopata, A.L.; Dasouki, M.; Abdel Rahman, A.M. Metabolomics toward personalized medicine. *Mass Spectrom. Rev.* **2019**, *38*, 221–238, doi:10.1002/mas.21548.

12. Hernandez-Baixauli, J.; Quesada-Vázquez, S.; Mariné-Casadó, R.; Cardoso, K.G.; Caimari, A.; Del Bas, J.M.; Escoté, X.; Baselga-Escudero, L. Detection of early disease risk factors associated with metabolic syndrome: A new era with the NMR metabolomics assessment. *Nutrients* **2020**, *12*, 1–34, doi:10.3390/nu12030806.

13. Hamesch, K.; Borkham-Kamphorst, E.; Strnad, P.; Weiskirchen, R. Lipopolysaccharide-induced inflammatory liver injury in mice. *Lab. Anim.* **2015**, *49*, 37–46, doi:10.1177/0023677215570087.

14. Ranneh, Y.; Akim, A.M.; Hamid, H.A.; Khazaai, H.; Mokhtarrudin, N.; Fadel, A.; Albujja, M.H.K. Induction of Chronic Subclinical Systemic Inflammation in Sprague-Dawley Rats Stimulated by Intermittent Bolus Injection of Lipopolysaccharide. *Arch. Immunol. Ther. Exp. (Warsz).* **2019**, *67*, 385–400, doi:10.1007/s00005-019-00553-6.

15. Rorato, R.; Borges, B. de C.; Uchoa, E.T.; Antunes-Rodrigues, J.; Elias, C.F.; Kagohara Elias, L.L. LPS-

induced low-grade inflammation increases hypothalamic JNK expression and causes central insulin resistance irrespective of body weight changes. *Int. J. Mol. Sci.* **2017**, *18*, 1–14, doi:10.3390/ijms18071431.

16. Asgharzadeh, F.; Bargi, R.; Hosseini, M.; Farzadnia, M.; Khazaei, M. Cardiac and renal fibrosis and oxidative stress balance in lipopolysaccharide-induced inflammation in male rats. *ARYA Atheroscler.* **2018**, *14*, 71–77, doi:10.22122/arya.v14i2.1550.

17. Kudo, K.; Hagiwara, S.; Hasegawa, A.; Kusaka, J.; Koga, H.; Noguchi, T. Cepharanthine exerts anti-inflammatory effects via NF-κB inhibition in a LPS-induced rat model of systemic inflammation. *J. Surg. Res.* **2011**, *171*, 199–204, doi:10.1016/j.jss.2010.01.007.

18. Guo, H.; Diao, N.; Yuan, R.; Chen, K.; Geng, S.; Li, M.; Li, L. Subclinical-Dose Endotoxin Sustains Low-Grade Inflammation and Exacerbates Steatohepatitis in High-Fat Diet-Fed Mice. *J. Immunol.* **2016**, *196*, 2300–2308, doi:10.4049/jimmunol.1500130.

19. Smith, B.J.; Lightfoot, S.A.; Lerner, M.R.; Denson, K.D.; Morgan, D.L.; Hanas, J.S.; Bronze, M.S.; Postier, R.G.; Brackett, D.J. Induction of cardiovascular pathology in a novel model of low-grade chronic inflammation. *Cardiovasc. Pathol.* **2009**, *18*, 1–10, doi:10.1016/j.carpath.2007.07.011.

20. Liu, D.; Cao, S.; Zhou, Y.; Xiong, Y. Recent advances in endotoxin tolerance. *J. Cell. Biochem.* **2019**, *120*, 56–70, doi:10.1002/jcb.27547.

21. Smith, B.J.; Lerner, M.R.; Bu, S.Y.; Lucas, E.A.; Hanas, J.S.; Lightfoot, S.A.; Postier, R.G.; Bronze, M.S.; Brackett, D.J. Systemic bone loss and induction of coronary vessel disease in a rat model of chronic inflammation. *Bone* **2006**, *38*, 378–386, doi:10.1016/j.bone.2005.09.008.

22. Fischer, C.W.; Liebenberg, N.; Madsen, A.M.; Müller, H.K.; Lund, S.; Wegener, G. Chronic lipopolysaccharide infusion fails to induce depressive-like behaviour in adult male rats. *Acta Neuropsychiatr.* **2015**, *27*, 189–194, doi:10.1017/neu.2015.4.

23. Grinevich, V.; Ma, X.M.; Herman, J.P.; Jezova, D.; Akmayev, I.; Aguilera, G. Effect of repeated lipopolysaccharide administration on tissue cytokine expression and hypothalamic-pituitary-adrenal axis activity in rats. *J. Neuroendocrinol.* **2001**, *13*, 711–723, doi:10.1046/j.1365-2826.2001.00684.x.

24. Manco, M.; Putignani, L.; Bottazzo, G.F. Gut microbiota, lipopolysaccharides, and innate immunity in the pathogenesis of obesity and cardiovascular risk. *Endocr. Rev.* **2010**, *31*, 817–844, doi:10.1210/er.2009-0030.

25. Dudele, A.; Fischer, C.W.; Elfving, B.; Wegener, G.; Wang, T.; Lund, S. Chronic exposure to low doses of lipopolysaccharide and high-fat feeding increases body mass without affecting glucose tolerance in female rats. *Physiol. Rep.* **2015**, *3*, doi:10.14814/phy2.12584.

26. Medzhitov, R. Origin and physiological roles of inflammation. *Nature* **2008**, *454*, 428–435, doi:10.1038/nature07201.

27. Turnbull, A. V; Rivier, C.L. Regulation of the hypothalamic-pituitary-adrenal axis by cytokines: actions and mechanisms of action. *Physiol. Rev.* **1999**, *79*, 1–71, doi:10.1152/physrev.1999.79.1.1.

28. Deshmane, S.L.; Kremlev, S.; Amini, S.; Sawaya, B.E. Monocyte chemoattractant protein-1 (MCP-1): an overview. *J. Interf. cytokine Res. Off. J. Int. Soc. Interf. Cytokine Res.* **2009**, *29*, 313–326, doi:10.1089/jir.2008.0027.

29. Geng, S.; Chen, K.; Yuan, R.; Peng, L.; Maitra, U.; Diao, N.; Chen, C.; Zhang, Y.; Hu, Y.; Qi, C.-F.; et al. The persistence of low-grade inflammatory monocytes contributes to aggravated atherosclerosis. *Nat. Commun.* **2016**, *7*, 13436, doi:10.1038/ncomms13436.

30. Luc, K.; Schramm-Luc, A.; Guzik, T.J.; Mikolajczyk, T.P. Oxidative stress and inflammatory markers in prediabetes and diabetes. *J. Physiol. Pharmacol.* **2019**, *70*, doi:10.26402/jpp.2019.6.01.

31. Smith, R.L.; Soeters, M.R.; Wüst, R.C.I.; Houtkooper, R.H. Metabolic Flexibility as an Adaptation to Energy Resources and Requirements in Health and Disease. *Endocr. Rev.* **2018**, *39*, 489–517, doi:10.1210/er.2017-00211.

32. Chen, X.; Liu, L.; Palacios, G.; Gao, J.; Zhang, N.; Li, G.; Lu, J.; Song, T.; Zhang, Y.; Lv, H. Plasma metabolomics reveals biomarkers of the atherosclerosis. *J. Sep. Sci.* **2010**, *33*, 2776–2783, doi:https://doi.org/10.1002/jssc.201000395.

33. Svegliati-Baroni, G.; Pierantonelli, I.; Torquato, P.; Marinelli, R.; Ferreri, C.; Chatgilialoglu, C.; Bartolini, D.; Galli, F. Lipidomic biomarkers and mechanisms of lipotoxicity in non-alcoholic fatty liver disease. *Free Radic. Biol. Med.* **2019**, *144*, 293–309, doi:10.1016/j.freeradbiomed.2019.05.029.

34. Souto-Carneiro, M.; Tóth, L.; Behnisch, R.; Urbach, K.; Klika, K.D.; Carvalho, R.A.; Lorenz, H.-M. Differences in the serum metabolome and lipidome identify potential biomarkers for seronegative rheumatoid arthritis versus psoriatic arthritis. *Ann. Rheum. Dis.* **2020**, *79*, 499–506, doi:10.1136/annrheumdis-2019-216374.

35. Russo, L.; Muir, L.; Geletka, L.; Delproposto, J.; Baker, N.; Flesher, C.; O'Rourke, R.; Lumeng, C.N. Cholesterol 25-hydroxylase (CH25H) as a promoter of adipose tissue inflammation in obesity and diabetes. *Mol. Metab.* **2020**, *39*, 100983, doi:10.1016/j.molmet.2020.100983.

36. Iyer, A.; Fairlie, D.P.; Prins, J.B.; Hammock, B.D.; Brown, L. Inflammatory lipid mediators in adipocyte function and obesity. *Nat. Rev. Endocrinol.* **2010**, *6*, 71–82, doi:10.1038/nrendo.2009.264.

37. Tsoukalas, D.; Alegakis, A.K.; Fragkiadaki, P.; Papakonstantinou, E.; Tsilimidos, G.; Geraci, F.; Sarandi, E.; Nikitovic, D.; Spandidos, D.A.; Tsatsakis, A. Application of metabolomics part II: Focus on fatty acids and their metabolites in healthy adults. *Int. J. Mol. Med.* **2019**, *43*, 233–242, doi:10.3892/ijmm.2018.3989.

38. Zheng, J.-S.; Sharp, S.J.; Imamura, F.; Koulman, A.; Schulze, M.B.; Ye, Z.; Griffin, J.; Guevara, M.; Huerta, J.M.; Kröger, J.; et al. Association between plasma phospholipid saturated fatty acids and metabolic markers of lipid, hepatic, inflammation and glycaemic pathways in eight European countries: a cross-sectional analysis in the EPIC-InterAct study. *BMC Med.* **2017**, *15*, 203, doi:10.1186/s12916-017-0968-4.

39. Anderson, E.K.; Hill, A.A.; Hasty, A.H. Stearic acid accumulation in macrophages induces toll-like receptor 4/2-independent inflammation leading to endoplasmic reticulum stress-mediated apoptosis. *Arterioscler. Thromb. Vasc. Biol.* **2012**, *32*, 1687–1695, doi:10.1161/ATVBAHA.112.250142.

40. Spigoni, V.; Fantuzzi, F.; Fontana, A.; Cito, M.; Derlindati, E.; Zavaroni, I.; Cnop, M.; Bonadonna, R.C.; Dei Cas, A. Stearic acid at physiologic concentrations induces in vitro lipotoxicity in circulating angiogenic cells. *Atherosclerosis* **2017**, *265*, 162–171, doi:https://doi.org/10.1016/j.atherosclerosis.2017.09.004.

41. Kennedy, A.; Martinez, K.; Chuang, C.-C.; LaPoint, K.; McIntosh, M. Saturated fatty acid-mediated inflammation and insulin resistance in adipose tissue: mechanisms of action and implications. *J. Nutr.* **2009**, *139*, 1–4, doi:10.3945/jn.108.098269.

42. Engin, A. The Pathogenesis of Obesity-Associated Adipose Tissue Inflammation. *Adv. Exp. Med. Biol.* **2017**, *960*, 221–245, doi:10.1007/978-3-319-48382-5_9.

43. Ni, Y.; Zhao, L.; Yu, H.; Ma, X.; Bao, Y.; Rajani, C.; Loo, L.W.M.; Shvetsov, Y.B.; Yu, H.; Chen, T.; et al. Circulating Unsaturated Fatty Acids Delineate the Metabolic Status of Obese Individuals. *EBioMedicine* **2015**, *2*, 1513–1522, doi:https://doi.org/10.1016/j.ebiom.2015.09.004.

44. Pranger, I.G.; Corpeleijn, E.; Muskiet, F.A.J.; Kema, I.P.; Singh-Povel, C.; Bakker, S.J.L. Circulating fatty acids as biomarkers of dairy fat intake: data from the lifelines biobank and cohort study.

Biomarkers **2019**, *24*, 360–372, doi:10.1080/1354750X.2019.1583770.

45. Li, F.; Jiang, C.; Larsen, M.C.; Bushkofsky, J.; Krausz, K.W.; Wang, T.; Jefcoate, C.R.; Gonzalez, F.J. Lipidomics reveals a link between CYP1B1 and SCD1 in promoting obesity. *J. Proteome Res.* **2014**, *13*, 2679–2687, doi:10.1021/pr500145n.

46. Knuplez, E.; Marsche, G. An Updated Review of Pro- and Anti-Inflammatory Properties of Plasma Lysophosphatidylcholines in the Vascular System. *Int. J. Mol. Sci.* **2020**, *21*, doi:10.3390/ijms21124501.

47. Liu, P.; Zhu, W.; Chen, C.; Yan, B.; Zhu, L.; Chen, X.; Peng, C. The mechanisms of lysophosphatidylcholine in the development of diseases. *Life Sci.* **2020**, *247*, 117443, doi:10.1016/j.lfs.2020.117443.

48. Ruipérez, V.; Casas, J.; Balboa, M.A.; Balsinde, J. Group V phospholipase A2-derived lysophosphatidylcholine mediates cyclooxygenase-2 induction in lipopolysaccharide-stimulated macrophages. *J. Immunol.* **2007**, *179*, 631–638, doi:10.4049/jimmunol.179.1.631.

49. Yoder, M.; Zhuge, Y.; Yuan, Y.; Holian, O.; Kuo, S.; van Breemen, R.; Thomas, L.L.; Lum, H. Bioactive lysophosphatidylcholine 16:0 and 18:0 are elevated in lungs of asthmatic subjects. *Allergy. Asthma Immunol. Res.* **2014**, *6*, 61–65, doi:10.4168/aair.2014.6.1.61.

50. Dimovska Nilsson, K.; Neittaanmäki, N.; Zaar, O.; Angerer, T.B.; Paoli, J.; Fletcher, J.S. TOF-SIMS imaging reveals tumor heterogeneity and inflammatory response markers in the microenvironment of basal cell carcinoma. *Biointerphases* **2020**, *15*, 41012, doi:10.1116/6.0000340.

51. Zeng, C.; Wen, B.; Hou, G.; Lei, L.; Mei, Z.; Jia, X.; Chen, X.; Zhu, W.; Li, J.; Kuang, Y.; et al. Lipidomics profiling reveals the role of glycerophospholipid metabolism in psoriasis. *Gigascience* **2017**, *6*, 1–11, doi:10.1093/gigascience/gix087.

52. Lent-Schochet, D.; McLaughlin, M.; Ramakrishnan, N.; Jialal, I. Exploratory metabolomics of metabolic syndrome: A status report. *World J. Diabetes* **2019**, *10*, 23–36, doi:10.4239/wjd.v10.i1.23.

53. Stryjecki, C.; Roke, K.; Clarke, S.; Nielsen, D.; Badawi, A.; El-Sohemy, A.; Ma, D.W.L.; Mutch, D.M. Enzymatic activity and genetic variation in SCD1 modulate the relationship between fatty acids and inflammation. *Mol. Genet. Metab.* **2012**, *105*, 421–427, doi:10.1016/j.ymgme.2011.12.003.

54. Cole, L.K.; Vance, J.E.; Vance, D.E. Phosphatidylcholine biosynthesis and lipoprotein metabolism. *Biochim. Biophys. Acta* **2012**, *1821*, 754–761, doi:10.1016/j.bbalip.2011.09.009.

55. Balsinde, J.; Winstead, M. V; Dennis, E.A. Phospholipase A2 regulation of arachidonic acid mobilization. *FEBS Lett.* **2002**, *531*, 2–6, doi:https://doi.org/10.1016/S0014-5793(02)03413-0.

56. van Kranen, H.J.; Siezen, C.L.E. Arachidonic Acid Pathway BT - Encyclopedia of Cancer. In; Schwab, M., Ed.; Springer Berlin Heidelberg: Berlin, Heidelberg, 2011; pp. 260–265 ISBN 978-3-642-16483-5.

57. Choi, I.; Son, H.; Baek, J.-H. Tricarboxylic Acid (TCA) Cycle Intermediates: Regulators of Immune Responses. *Life (Basel, Switzerland)* **2021**, *11*, doi:10.3390/life11010069.

58. Lacourt, T.E.; Vichaya, E.G.; Chiu, G.S.; Dantzer, R.; Heijnen, C.J. The High Costs of Low-Grade Inflammation: Persistent Fatigue as a Consequence of Reduced Cellular-Energy Availability and Non-adaptive Energy Expenditure . *Front. Behav. Neurosci.* 2018, *12*, 78.

59. Donnelly, R.P.; Finlay, D.K. Glucose, glycolysis and lymphocyte responses. *Mol. Immunol.* **2015**, *68*, 513–519, doi:10.1016/j.molimm.2015.07.034.

60. Yamano, E.; Sugimoto, M.; Hirayama, A.; Kume, S.; Yamato, M.; Jin, G.; Tajima, S.; Goda, N.; Iwai, K.; Fukuda, S.; et al. Index markers of chronic fatigue syndrome with dysfunction of TCA and urea

cycles. *Sci. Rep.* **2016**, *6*, 34990, doi:10.1038/srep34990.

61. Naviaux, R.K.; Naviaux, J.C.; Li, K.; Bright, A.T.; Alaynick, W.A.; Wang, L.; Baxter, A.; Nathan, N.; Anderson, W.; Gordon, E. Metabolic features of chronic fatigue syndrome. *Proc. Natl. Acad. Sci. U. S. A.* **2016**, *113*, E5472-80, doi:10.1073/pnas.1607571113.

62. Fluge, Ø.; Mella, O.; Bruland, O.; Risa, K.; Dyrstad, S.E.; Alme, K.; Rekeland, I.G.; Sapkota, D.; Røsland, G. V; Fosså, A.; et al. Metabolic profiling indicates impaired pyruvate dehydrogenase function in myalgic encephalopathy/chronic fatigue syndrome. *JCI insight* **2016**, *1*, e89376, doi:10.1172/jci.insight.89376.

63. Martínez-Reyes, I.; Chandel, N.S. Mitochondrial TCA cycle metabolites control physiology and disease. *Nat. Commun.* **2020**, *11*, 102, doi:10.1038/s41467-019-13668-3.

64. Matilla, B.; Mauriz, J.; Culebras, J.; González-Gallego, J.; González, P. Glycine: a cell-protecting anti-oxidant nutrient. *Nutr. Hosp.* **2002**, *17*, 2–9.

65. Reap, E.A.; Lawson, J.W. Stimulation of the immune response by dimethylglycine, a nontoxic metabolite. *J. Lab. Clin. Med.* **1990**, *115*, 481–486.

66. Reina-Campos, M.; Diaz-Meco, M.T.; Moscat, J. The complexity of the serine glycine one-carbon pathway in cancer. *J. Cell Biol.* **2019**, *219*, doi:10.1083/jcb.201907022.

67. Maynard, A.G.; Kanarek, N. NADH Ties One-Carbon Metabolism to Cellular Respiration. *Cell Metab.* **2020**, *31*, 660–662, doi:10.1016/j.cmet.2020.03.012.

68. García-Martínez, L.F.; Appling, D.R. Characterization of the folate-dependent mitochondrial oxidation of carbon 3 of serine. *Biochemistry* **1993**, *32*, 4671–4676, doi:10.1021/bi00068a027.

69. Ducker, G.S.; Rabinowitz, J.D. One-Carbon Metabolism in Health and Disease. *Cell Metab.* **2017**, *25*, 27–42, doi:https://doi.org/10.1016/j.cmet.2016.08.009.

70. FRIEDMANN, B.; NAKADA, H.I.; WEINHOUSE, S. A study of the oxidation of formic acid in the folic acid-deficient rat. *J. Biol. Chem.* **1954**, *210*, 413–421.

71. Lamarre, S.G.; Morrow, G.; Macmillan, L.; Brosnan, M.E.; Brosnan, J.T. Formate: an essential metabolite, a biomarker, or more? *Clin. Chem. Lab. Med.* **2013**, *51*, 571–578, doi:10.1515/cclm-2012-0552.

72. Kramer, C.D.; Genco, C.A. Microbiota, Immune Subversion, and Chronic Inflammation. *Front. Immunol.* **2017**, *8*, 255, doi:10.3389/fimmu.2017.00255.

73. Sanz, Y.; Santacruz, A.; Gauffin, P. Gut microbiota in obesity and metabolic disorders. *Proc. Nutr. Soc.* **2010**, *69*, 434–441, doi:10.1017/S0029665110001813.

74. Zhao, S.; Liu, W.; Wang, J.; Shi, J.; Sun, Y.; Wang, W.; Ning, G.; Liu, R.; Hong, J. Akkermansia muciniphila improves metabolic profiles by reducing inflammation in chow diet-fed mice. *J. Mol. Endocrinol.* **2017**, *58*, 1–14, doi:10.1530/JME-16-0054.

75. Hoffman, J.F.; Fan, A.X.; Neuendorf, E.H.; Vergara, V.B.; Kalinich, J.F. Hydrophobic Sand Versus Metabolic Cages: A Comparison of Urine Collection Methods for Rats (Rattus norvegicus). *J. Am. Assoc. Lab. Anim. Sci.* **2018**, *57*, 51–57.

76. Caimari, A.; del Bas, J.M.; Crescenti, A.; Arola, L. Low doses of grape seed procyanidins reduce adiposity and improve the plasma lipid profile in hamsters. *Int. J. Obes. (Lond).* **2013**, *37*, 576–583, doi:10.1038/ijo.2012.75.

77. Rodriguez-Sureda, V.; Peinado-Onsurbe, J. A procedure for measuring triacylglyceride and cholesterol content using a small amount of tissue. *Anal. Biochem.* **2005**, *343*, 277–282, doi:10.1016/j.ab.2005.05.009.

78. Kind, T.; Wohlgemuth, G.; Lee, D.Y.; Lu, Y.; Palazoglu, M.; Shahbaz, S.; Fiehn, O. FiehnLib: Mass Spectral and Retention Index Libraries for Metabolomics Based on Quadrupole and Time-of-Flight Gas Chromatography/Mass Spectrometry. *Anal. Chem.* **2009**, *81*, 10038–10048, doi:10.1021/ac9019522.

79. Eggers, L.F.; Schwudke, D. Liquid Extraction: Folch BT - Encyclopedia of Lipidomics. In; Wenk, M.R., Ed.; Springer Netherlands: Dordrecht, 2016; pp. 1–6 ISBN 978-94-007-7864-1.

80. Beghini, F.; McIver, L.; Blanco-Míguez, A.; Dubois, L.; Asnicar, F.; Maharjan, S.; Mailyan, A.; Thomas, A.M.; Manghi, P.; Valles-Colomer, M.; et al. Integrating taxonomic, functional, and strain-level profiling of diverse microbial communities with bioBakery 3 2020.

81. Llorach-Asunción, R.; Jauregui, O.; Urpi-Sarda, M.; Andres-Lacueva, C. Methodological aspects for metabolome visualization and characterization: a metabolomic evaluation of the 24 h evolution of human urine after cocoa powder consumption. *J. Pharm. Biomed. Anal.* **2010**, *51*, 373–381, doi:10.1016/j.jpba.2009.06.033.

82. Fujisaka, S.; Avila-Pacheco, J.; Soto, M.; Kostic, A.; Dreyfuss, J.M.; Pan, H.; Ussar, S.; Altindis, E.; Li, N.; Bry, L.; et al. Diet, Genetics, and the Gut Microbiome Drive Dynamic Changes in Plasma Metabolites. *Cell Rep.* **2018**, *22*, 3072–3086, doi:10.1016/j.celrep.2018.02.060.

83. Tenenhaus, A.; Tenenhaus, M. Regularized Generalized Canonical Correlation Analysis. *Psychometrika* **2011**, *76*, 257, doi:10.1007/s11336-011-9206-8.

84. Rohart, F.; Gautier, B.; Singh, A.; Lê Cao, K.-A. mixOmics: An R package for 'omics feature selection and multiple data integration. *PLOS Comput. Biol.* **2017**, *13*, e1005752.

85. González, I.; Cao, K.-A.L.; Davis, M.J.; Déjean, S. Visualising associations between paired "omics" data sets. *BioData Min.* **2012**, *5*, 19, doi:10.1186/1756-0381-5-19.

86. Karnovsky, A.; Weymouth, T.; Hull, T.; Tarcea, V.G.; Scardoni, G.; Laudanna, C.; Sartor, M.A.; Stringer, K.A.; Jagadish, H. V; Burant, C.; et al. Metscape 2 bioinformatics tool for the analysis and visualization of metabolomics and gene expression data. *Bioinformatics* **2012**, *28*, 373–380, doi:10.1093/bioinformatics/btr661.

87. Assenov, Y.; Ramírez, F.; Schelhorn, S.-E.; Lengauer, T.; Albrecht, M. Computing topological parameters of biological networks. *Bioinformatics* **2008**, *24*, 282–284, doi:10.1093/bioinformatics/btm554.

88. Smoot, M.E.; Ono, K.; Ruscheinski, J.; Wang, P.-L.; Ideker, T. Cytoscape 2.8: new features for data integration and network visualization. *Bioinformatics* **2011**, *27*, 431–432, doi:10.1093/bioinformatics/btq675.

89. Kanehisa, M.; Goto, S. KEGG: kyoto encyclopedia of genes and genomes. *Nucleic Acids Res.* **2000**, *28*, 27–30, doi:10.1093/nar/28.1.27.

Annex. Supplementary Material of Manuscript 4

Supplementary table 1. Statistical analysis of plasma metabolites in the LPS-induced inflammation model. CON and LPS groups (n = 10 animals per group) are represented by the relative abundances (AU). Relative abundances of metabolites are presented by the mean ± SEM. Plasma metabolites are sorted by p-value. The summary of analysis includes *p*-value, *q*-value, VIP value, random forest classifier (RF) and fold change (FC). The statistically significant p-values and q-values are highlighted in bold. Abbreviations: DG, diacylglycerol; ChoE, cholesterol ester; TG, triglyceride; PC, phosphatidylcholine; SM, sphingomyelin; LPC, lysophospholipid; PE, phosphatidylethanolamine.

Metabolite	CON	LPS	*p*-value	*q*-value	VIP	RF	FC
Alpha-ketoglutarate	2.05 ± 0.1	0.87 ± 0.09	<0.01	0.01	2.05	0.06	0.4
Malic acid	0.44 ± 0.02	0.19 ± 0.02	<0.01	0.01	2.02	0.08	0.4
ChoE (18:3)	1.55 ± 0.12	2.48 ± 0.17	<0.01	0.01	1.76	0.02	1.6
ChoE (22:6)	2.67 ± 0.19	4.28 ± 0.28	<0.01	0.01	1.96	0.03	1.6
LPC 16:0 e	0.34 ± 0.03	0.52 ± 0.03	<0.01	0.01	1.67	0.02	1.5
PC 34:0	0.29 ± 0.02	0.46 ± 0.02	<0.01	0.01	1.74	0.09	1.6
PC 32:0	0.7 ± 0.06	1.08 ± 0.05	<0.01	0.01	1.67	0.02	1.5
SM 42:3	4.64 ± 0.39	7.07 ± 0.4	<0.01	0.01	1.61	0.03	1.5
Fumaric acid	0.63 ± 0.04	0.34 ± 0.04	<0.01	0.01	1.95	0.02	0.5
LPC 18:0 e	0.07 ± 0	0.1 ± 0.01	<0.01	0.01	1.61	0.03	1.4
PC 38:4	24.61 ± 1.61	35.21 ± 1.52	<0.01	0.01	1.71	0.02	1.4
Succinic acid	0.51 ± 0.02	0.41 ± 0.01	<0.01	0.01	1.85	0.04	0.8
ChoE (18:0)	0.09 ± 0.01	0.15 ± 0.01	<0.01	0.01	1.69	0.04	1.7
TG 54:7	5.21 ± 0.65	1.82 ± 0.39	<0.01	0.01	1.56	0.08	0.3
Cholesterol	0.11 ± 0	0.15 ± 0.01	<0.01	0.01	1.78	-	1.4
SM 42:2	15.64 ± 1.49	23.35 ± 1.29	<0.01	0.01	1.65	-	1.5
DG 36:4	3.42 ± 0.21	2.43 ± 0.11	<0.01	0.02	1.89	0.02	0.7
Aconitic acid	0.02 ± 0	0.01 ± 0	<0.01	0.02	1.64	0.04	0.5
PC 40:4	0.25 ± 0.02	0.37 ± 0.04	<0.01	0.02	1.47	0.02	1.5
ChoE (20:4)	59.73 ± 3.98	80.04 ± 3.21	<0.01	0.03	1.76	-	1.3
Glycine	4.57 ± 0.2	5.8 ± 0.36	<0.01	0.03	1.55	0.03	1.3
DG 34:1	1.46 ± 0.08	1.84 ± 0.08	0.01	0.03	1.71	0.02	1.3
PC 34:1	4.84 ± 0.53	6.85 ± 0.44	0.01	0.03	1.36	0.04	1.4
PC 30:0	0.06 ± 0.01	0.09 ± 0.01	0.01	<0.05	1.43	0.03	1.5
SM 34:1	17.9 ± 1.47	23.29 ± 0.87	0.01	0.06	1.36	0.03	1.3
Hydroxyproline	1.03 ± 0.03	0.81 ± 0.06	0.01	0.07	1.30	0.01	0.8
Alanine	0.78 ± 0.05	1.12 ± 0.13	0.02	0.08	1.43	-	1.4
ChoE (16:0)	0.94 ± 0.07	1.22 ± 0.06	0.02	0.08	1.40	-	1.3
TG 52:5	8.63 ± 1.04	5.14 ± 0.63	0.02	0.09	1.27	0.02	0.6

PC 36:2	12.78 ± 1.21	16.44 ± 1.07	0.03	0.13	1.11	-	1.3
Pyruvic acid	26.89 ± 2.5	40.27 ± 5.19	0.03	0.13	0.87	0.01	1.5
Glutamine	0.04 ± 0	0.02 ± 0.01	0.04	0.14	1.31	-	0.5
TG 52:6	1.16 ± 0.15	0.74 ± 0.09	0.04	0.14	1.03	-	0.6
Threonine	2.15 ± 0.07	2.69 ± 0.22	0.04	0.14	1.29	-	1.3
Aspartic acid	0.68 ± 0.04	0.82 ± 0.05	<0.05	0.14	1.10	-	1.2
Histidine	0.07 ± 0.01	0.1 ± 0.01	<0.05	0.14	0.70	-	1.4
Leucine	0.15 ± 0.01	0.12 ± 0.01	<0.05	0.14	0.94	-	0.8
PC 32:2	0.24 ± 0.03	0.33 ± 0.03	<0.05	0.14	1.09	0.02	1.4
PC 36:4	23.43 ± 1.55	28.01 ± 1.21	<0.05	0.14	1.05	0.01	1.2
SM 35:1	0.18 ± 0.02	0.23 ± 0.02	<0.05	0.14	1.06	-	1.3
TG 50:4	1.82 ± 0.28	1.02 ± 0.15	0.05	0.16	1.05	-	0.6
TG 54:4	14.62 ± 1.88	9.97 ± 1.44	0.05	0.16	0.93	-	0.7
LPC 18:0	40.88 ± 2.53	51.91 ± 3.4	0.06	0.19	1.19	0.01	1.3
PC 40:5	0.62 ± 0.06	0.77 ± 0.03	0.06	0.19	1.09	-	1.2
ChoE (18:2)	19.3 ± 1.52	22.57 ± 0.9	0.08	0.21	0.99	0.02	1.2
Tryptophan	0.82 ± 0.16	1.32 ± 0.18	0.08	0.21	0.91	-	1.6
ChoE (22:5)	0.94 ± 0.09	1.14 ± 0.06	0.09	0.24	1.16	-	1.2
Glucose	0.22 ± 0.01	0.24 ± 0.01	0.10	0.25	0.72	-	1.1
PC 33:0	0.04 ± 0	0.04 ± 0	0.10	0.25	0.94	-	1
PC 38:3	0.96 ± 0.12	1.14 ± 0.1	0.10	0.25	0.85	-	1.2
Proline	0.65 ± 0.04	0.57 ± 0.03	0.10	0.25	0.76	-	0.9
SM 38:1	0.44 ± 0.04	0.55 ± 0.04	0.10	0.25	1.05	-	1.3
TG 52:3	60.57 ± 6.94	43.35 ± 4.91	0.10	0.25	0.93	-	0.7
2-hydroxyglutaric	0.8 ± 0.07	0.62 ± 0.08	0.12	0.27	1.03	-	0.8
Glycolic acid	12.61 ± 0.46	11.65 ± 0.43	0.12	0.27	0.73	-	0.9
PC 31:0	0.04 ± 0	0.05 ± 0	0.12	0.27	0.84	-	1.3
SM 40:1	4.31 ± 0.35	5.17 ± 0.34	0.12	0.27	0.96	0.01	1.2
TG 48:1	1.37 ± 0.32	2.69 ± 0.77	0.12	0.27	1.00	-	2
Fructose	1.85 ± 0.16	1.54 ± 0.11	0.14	0.29	0.78	-	0.8
PC 32:1	0.77 ± 0.13	1.13 ± 0.17	0.14	0.29	1.00	-	1.5
SM 32:1	0.2 ± 0.02	0.22 ± 0.01	0.14	0.29	0.63	-	1.1
Threonic acid	1.71 ± 0.07	1.52 ± 0.1	0.14	0.29	0.98	-	0.9
LPC 18:1	13.7 ± 1.28	11.38 ± 0.55	0.16	0.33	0.74	-	0.8
DG 34:2	2.44 ± 0.08	2.51 ± 0.07	0.19	0.37	0.49	-	1
TG 54:3	6.14 ± 0.73	4.92 ± 0.59	0.19	0.37	0.55	-	0.8
PC 33:1	0.1 ± 0.01	0.12 ± 0.01	0.21	0.40	0.77	-	1.2

TG 50:1	3.92 ± 0.52	6.87 ± 1.63	0.21	0.40	1.02	-	1.8
Urea	0.92 ± 0.03	1.01 ± 0.05	0.21	0.40	0.79	-	1.1
Phenylalanine	2.08 ± 0.06	2.24 ± 0.09	0.24	0.44	0.99	0.01	1.1
SM 36:1	1.16 ± 0.09	1.41 ± 0.11	0.24	0.44	0.92	-	1.2
Beta-alanine	0.07 ± 0.01	0.09 ± 0.02	0.27	0.49	0.70	0.01	1.3
Oleic acid	1.61 ± 0.05	1.75 ± 0.09	0.27	0.49	0.86	-	1.1
Methionine	0.12 ± 0.01	0.13 ± 0.01	0.31	0.52	0.58	-	1.1
Ornithine	2.55 ± 0.24	2.78 ± 0.25	0.31	0.52	0.37	-	1.1
Tyrosine	0.26 ± 0.05	0.33 ± 0.06	0.31	0.52	0.72	-	1.3
Lactic acid	5.28 ± 0.22	4.95 ± 0.21	0.34	0.57	0.56	-	0.9
LPC 18:2	40.43 ± 4.01	34.65 ± 2.35	0.34	0.57	0.58	-	0.9
SM 39:1	0.18 ± 0.02	0.19 ± 0.02	0.34	0.57	0.46	-	1.1
Isoleucine	0.43 ± 0.03	0.59 ± 0.23	0.38	0.62	0.07	-	1.4
SM 34:2	1.48 ± 0.13	1.63 ± 0.07	0.38	0.62	0.66	-	1.1
Glutamic acid	0.09 ± 0.01	0.11 ± 0.01	0.43	0.65	0.71	0.01	1.2
LPC 15:0	0.74 ± 0.08	0.67 ± 0.05	0.43	0.65	0.37	-	0.9
TG 46:1	0.11 ± 0.03	0.16 ± 0.05	0.43	0.65	0.58	-	1.5
TG 48:2	1.13 ± 0.28	1.45 ± 0.37	0.43	0.65	0.48	-	1.3
PC 35:2	0.39 ± 0.04	0.44 ± 0.04	0.47	0.70	0.44	-	1.1
SM 42:1	17.87 ± 1.52	19.93 ± 1.01	0.47	0.70	0.70	-	1.1
TG 50:2	14.09 ± 2.18	18.19 ± 3.48	0.47	0.70	0.61	-	1.3
ChoE (17:1)	0.02 ± 0.01	0.02 ± 0.01	0.52	0.75	0.23	-	1
TG 52:1	0.96 ± 0.1	1.19 ± 0.21	0.52	0.75	0.61	-	1.2
Alpha-tocopherol	0.42 ± 0.04	0.48 ± 0.06	0.57	0.77	0.43	-	1.1
Asparagine	0.18 ± 0.03	0.16 ± 0.02	0.57	0.77	0.50	-	0.9
ChoE (22:4)	9.95 ± 0.84	11.14 ± 0.74	0.57	0.77	0.69	-	1.1
Glucose-6-phosphate	0.67 ± 0.08	0.82 ± 0.15	0.57	0.77	0.29	-	1.2
TG 46:0	0.1 ± 0.01	0.15 ± 0.04	0.57	0.77	0.65	-	1.5
Valine	1.25 ± 0.05	1.38 ± 0.13	0.57	0.77	0.61	-	1.1
ChoE (18:1)	2.65 ± 0.23	2.51 ± 0.14	0.62	0.82	0.20	-	0.9
DG 36:2	1.63 ± 0.07	1.66 ± 0.07	0.62	0.82	0.44	-	1
ChoE (20:2)	1.81 ± 0.19	1.67 ± 0.16	0.68	0.84	0.30	-	0.9
Lysine	0.11 ± 0.03	0.12 ± 0.03	0.68	0.84	0.44	-	1.1
SM 33:1	0.34 ± 0.03	0.37 ± 0.01	0.68	0.84	0.63	-	1.1
TG 48:0	0.67 ± 0.08	0.92 ± 0.22	0.68	0.84	0.62	-	1.4
TG 50:0	0.17 ± 0.05	0.22 ± 0.06	0.68	0.84	0.42	-	1.3
TG 50:3	8.63 ± 1.48	7.69 ± 1.39	0.68	0.84	0.14	-	0.9

Glyceric acid	0.92 ± 0.06	0.98 ± 0.1	0.73	0.89	0.13	-	1.1
TG 46:2	0.06 ± 0.02	0.07 ± 0.02	0.73	0.89	0.28	-	1.2
TG 48:3	0.32 ± 0.07	0.28 ± 0.06	0.73	0.89	0.07	-	0.9
3-hydroxybutiric acid	2.04 ± 0.13	2.08 ± 0.19	0.79	0.92	0.01	-	1
ChoE (17:0)	0.02 ± 0.01	0.02 ± 0.01	0.79	0.92	0.27	-	1
LPC 20:0	0.26 ± 0.02	0.27 ± 0.01	0.79	0.92	0.16	-	1
TG 54:2	3.67 ± 0.47	3.45 ± 0.45	0.79	0.92	0.01	-	0.9
PC 38:2	0.2 ± 0.02	0.21 ± 0.01	0.85	0.95	0.41	-	1.1
Serine	0.5 ± 0.03	0.56 ± 0.08	0.85	0.95	0.25	-	1.1
TG 51:2	0.86 ± 0.13	0.78 ± 0.12	0.85	0.95	0.09	-	0.9
TG 52:2	19.11 ± 2.93	18.4 ± 2.94	0.85	0.95	0.08	-	1
TG 54:6	21.68 ± 2.17	20.48 ± 1.86	0.85	0.95	0.24	-	0.9
Fructose-6-phosphate	0.46 ± 0.06	0.54 ± 0.12	0.91	0.98	0.01	-	1.2
Ribose	26.67 ± 3.59	26.14 ± 3.57	0.91	0.98	0.05	-	1
SM 41:1	4.85 ± 0.35	5.1 ± 0.3	0.91	0.98	0.39	0.01	1.1
SM 41:2	1.18 ± 0.11	1.19 ± 0.05	0.91	0.98	0.19	-	1
Citric acid	3.93 ± 0.12	3.94 ± 0.24	0.97	1.00	0.02	-	1
Glycerol	3.6 ± 0.28	3.56 ± 0.26	0.97	1.00	0.05	-	1
LPC 16:0	73.27 ± 5.3	75 ± 3.44	0.97	1.00	0.19	-	1
SM 36:2	0.42 ± 0.04	0.43 ± 0.02	0.97	1.00	0.24	-	1
ChoE (16:1)	0.59 ± 0.09	0.58 ± 0.08	1.00	1.00	0.13	-	1
DG 34:3	0.73 ± 0.06	0.7 ± 0.05	1.00	1.00	0.11	-	1
LPC 16:1 e	0.11 ± 0.01	0.12 ± 0.01	1.00	1.00	0.43	-	1.1
SM 40:2	0.77 ± 0.07	0.78 ± 0.04	1.00	1.00	0.18	-	1
SM 43:1	1.59 ± 0.14	1.61 ± 0.07	1.00	1.00	0.20	0.01	1

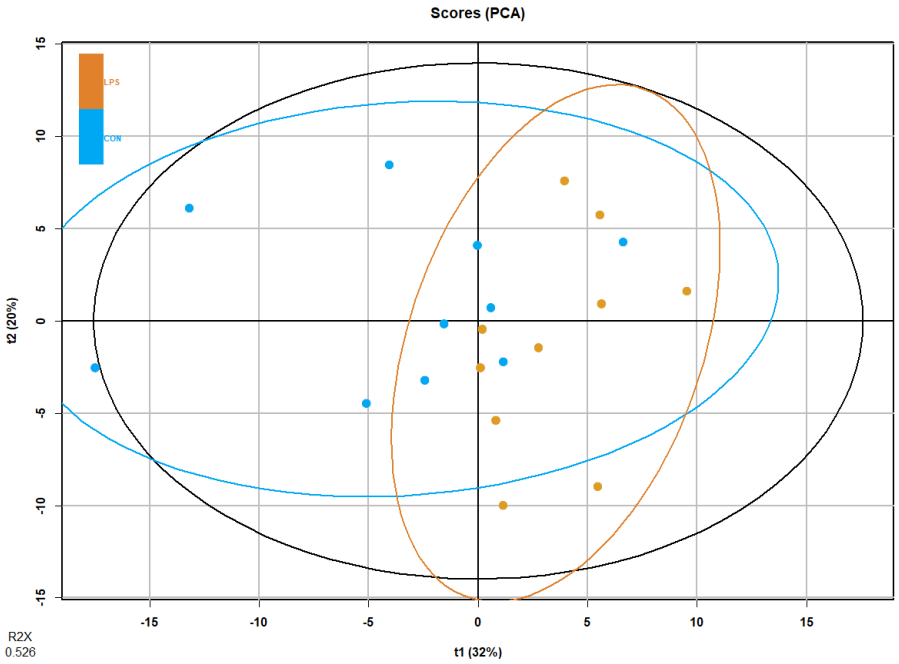

Supplementary Figure 1. PCA of plasma metabolomics in the LPS-induced inflammation model. Blue represents CON group and orange LPS group (*n* = 10 animals per group).

Supplementary Table 2. Statistical analysis of urine metabolites in the LPS-induced inflammation model. CON and LPS groups (n = 10 animals per group) are represented by the relative abundances (AU). Relative abundances of metabolites are presented by the mean ± SEM. Plasma metabolites are sorted by p-value. The summary of univariant and multivariate analysis is shown including p-value, q-value, random forest classifier (RF) and fold change (FC) The statistically significant *p*-values and *q*-values (< 0.05) are highlighted in bold. Abbreviations: 3-HPPA, 3-hydroxyphenylpropionate.

Metabolite	CON	LPS	*p*-value	*q*-value	RF	FC
N,N-Dimethylglycine	3.59 ± 0.41	7.47 ± 1.44	<0.01	0.25	0.17	2.1
Dimethylsulfone	14.66 ± 1.11	11.93 ± 0.67	0.07	0.78	0.09	0.8
Fucose	2.64 ± 1.44	2.02 ± 0.33	0.13	0.78	0.06	0.8
Fumarate	3.87 ± 0.35	5.08 ± 0.82	0.13	0.78	0.06	1.3
Citrate	291.02 ± 26.18	234.34 ± 20.97	0.18	0.78	0.05	0.8
Formate	2.77 ± 0.22	3.72 ± 0.55	0.21	0.78	0.04	1.3
Succinate	31.64 ± 2.28	35.55 ± 2.06	0.24	0.78	0.04	1.1
Choline	6.41 ± 0.8	7.9 ± 0.76	0.31	0.78	0.04	1.2
Hippurate	79.56 ± 5.07	72.33 ± 5.2	0.31	0.78	0.04	0.9
Isoleucine	14.69 ± 0.78	16.18 ± 1.45	0.31	0.78	0.04	1.1
N-Acetylglycoproteins	102.1 ± 4.33	106.23 ± 5.52	0.31	0.78	0.03	1
Glucose	3.23 ± 0.4	2.94 ± 0.17	0.35	0.78	0.03	0.9

3-HPPA Sulfate	4.01 ± 0.7	5.83 ± 1.28	0.39	0.78	0.03	1.5
4-Guanidinobutanoate	12.38 ± 0.66	13.04 ± 0.47	0.39	0.78	0.03	1.1
Lactate	9.66 ± 1.16	9.76 ± 1.61	0.39	0.78	0.03	1
Methylamine	4.32 ± 0.7	3.69 ± 0.38	0.39	0.78	0.02	0.9
Trigonelline	1.26 ± 0.07	1.15 ± 0.06	0.44	0.82	0.02	0.9
2-Oxoglutarate	373.05 ± 42.57	341.04 ± 34.71	0.49	0.82	0.02	0.9
Alanine	5.44 ± 0.57	6.03 ± 0.41	0.54	0.82	0.02	1.1
Allantoin	213.8 ± 14.49	229.6 ± 9.79	0.54	0.82	0.02	1.1
Pseudouridine	9.32 ± 0.79	10.07 ± 0.51	0.54	0.82	0.02	1.1
Glyoxylic acid	0.33 ± 0.04	0.33 ± 0.04	0.60	0.87	0.02	1
Acetate	5.55 ± 0.89	6.43 ± 1.72	0.65	0.87	0.01	1.2
Phenylacetylglycine	55.78 ± 6.22	58.17 ± 5.19	0.65	0.87	0.01	1
3-HPPA	14.37 ± 1.45	14.22 ± 1.52	0.78	0.89	0.01	1
Creatinine	347.25 ± 13.61	346.44 ± 17.76	0.78	0.89	0.01	1
1-Methylnicotinamide	0.12 ± 0.04	0.14 ± 0.04	0.84	0.89	0.01	1.2
Indoxyl sulfate	5.51 ± 0.46	5.59 ± 0.56	0.84	0.89	0.01	1
Pyruvate	4.81 ± 0.48	5.37 ± 0.82	0.84	0.89	0.01	1.1
Taurine	389.61 ± 66.45	372.46 ± 40.77	0.84	0.89	0.01	1
Glycine	11.22 ± 1.78	11.04 ± 1.57	0.90	0.93	-	1
Betaine	16.7 ± 2.4	16.23 ± 1.3	0.97	0.99	-	1

Supplementary Figure 2. PCA of urine metabolomics in the LPS-induced inflammation model. Blue represents CON group and orange LPS group (*n* = 10 animals per group).

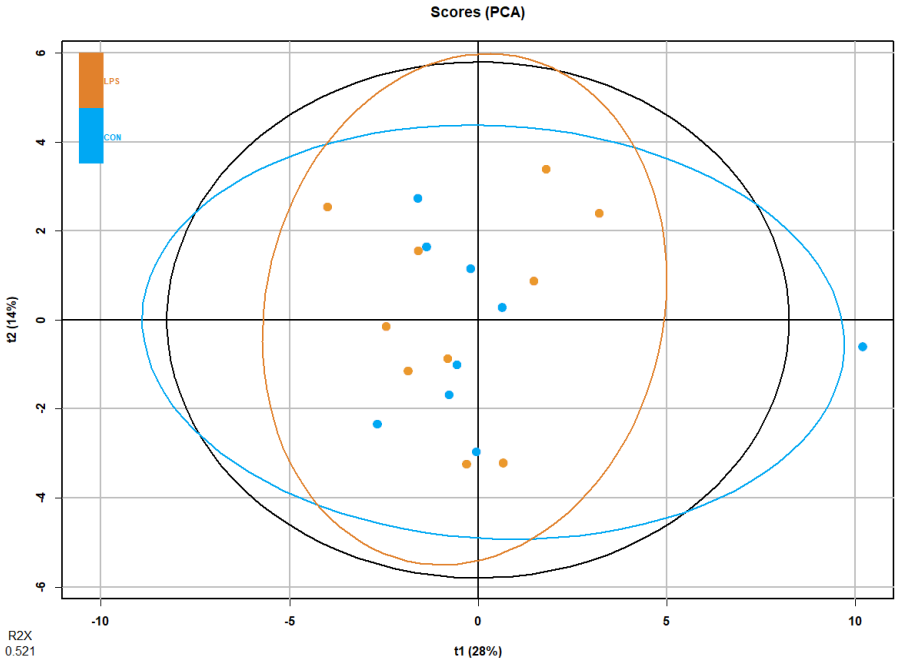

Supplementary table 3. Summary of bacteria species in the LPS-induced inflammation model. The summary of univariant analysis of CON group and LPS group (n = 8 animals per group) includes the results of MW test (*p*-value), MW corrected by BH (*q*-value) and FC. The alignment was done indicating the closest name of specie to the sequence (the best hit). Taxonomic data is presented by the mean of relative abundance (%) and shorted by p-value. The statistically significant values (< 0.05) are highlighted in bold.

Specie	CON	LPS	*p*-value	*q*-value	FC
Muribaculum intestinale	21.46%	28.03%	0.03	0.55	1.3
Lachnospiraceae bacterium A4	0.13%	0.32%	0.03	0.55	2.6
Firmicutes bacterium ASF500	2.27%	0.36%	0.03	0.61	0.2
Akkermansia muciniphila	14.42%	17.86%	0.05	0.76	1.2
Muribaculaceae bacterium DSM 103720	18.50%	27.66%	0.06	0.82	1.5
Bacteroides uniformis	4.94%	6.21%	0.09	0.82	1.3
Lachnospiraceae bacterium COE1	1.06%	0.09%	0.11	0.82	0.1
Anaerotruncus sp G3 2012	5.25%	2.99%	0.16	0.90	0.6
Romboutsia ilealis	0.14%	0.25%	0.16	0.90	1.8
Oscillibacter sp 1 3	1.66%	0.68%	0.25	0.96	0.4
Bifidobacterium pseudolongum	0.54%	<0.01%	0.25	0.96	-
Lachnospiraceae bacterium 10 1	0.08%	<0.01%	0.25	0.96	-
Acutalibacter muris	0.03%	<0.01%	0.25	0.96	-

Escherichia coli	12.23%	4.16%	0.28	0.96	0.3
Parabacteroides goldsteinii	4.27%	2.33%	0.32	0.96	0.5
Bacteroides caecimuris	0.11%	0.27%	0.32	0.96	2.5
Mucispirillum schaedleri	12.74%	4.89%	0.36	0.96	0.4
Lactobacillus murinus	0.14%	3.90%	0.48	0.96	27.2
Enterorhabdus caecimuris	0.02%	<0.01%	0.48	0.96	-

Supplementary table 4. Summary of virus species in the LPS-induced inflammation model. The summary of univariant analysis of CON group and LPS group (n = 8 animals per group) includes the results of MW test (*p*-value), MW corrected by BH (*q*-value) and FC. The alignment was done indicating the closest name of specie to the sequence (the best hit). Taxonomic data is presented by the mean of relative abundance (%) and shorted by p-value. The statistically significant values (< 0.05) are highlighted in bold.

Genera	Specie	CON	LPS	*p*-value	*q*-value	FC
Alphabaculovirus	*Chrysodeixis chalcites nucleopolyhedrovirus*	1.00%	0.27%	0.02	0.38	0.3
Siphoviridae unclassified	*Lactobacillus prophage Lj928*	1.73%	0.00%	0.11	0.92	-
Gammaretrovirus	*Abelson murine leukemia virus*	8.95%	13.57%	0.16	0.97	1.5
Gammaretrovirus	*Murine osteosarcoma virus*	15.00%	20.02%	0.16	0.97	1.3
Simplexvirus	*Human alphaherpesvirus 2*	0.14%	<0.01%	0.22	0.99	-
Myoviridae unclassified	*Lactobacillus prophage Lj771*	13.61%	10.29%	0.28	1.00	0.8
Cyprinivirus	*Anguillid herpesvirus 1*	5.18%	3.38%	0.28	1.00	0.7
Cyprinivirus	*Cyprinid herpesvirus 3*	41.97%	38.53%	0.32	1.00	0.9
Rhadinovirus	*Alcelaphine gammaherpesvirus 1*	4.74%	6.10%	0.28	1.00	1.3
Herpesviridae unclassified	*Ateline gammaherpesvirus 3*	6.79%	7.04%	0.32	1.00	1.0
Gammaretrovirus	*Koala retrovirus*	0.34%	0.40%	0.40	1.00	1.2
Potyvirus	*Zantedeschia mild mosaic virus*	<0.01%	0.06%	0.32	1.00	-
Varicellovirus	*Bovine alphaherpesvirus 1*	0.56%	0.10%	0.48	1.00	0.2

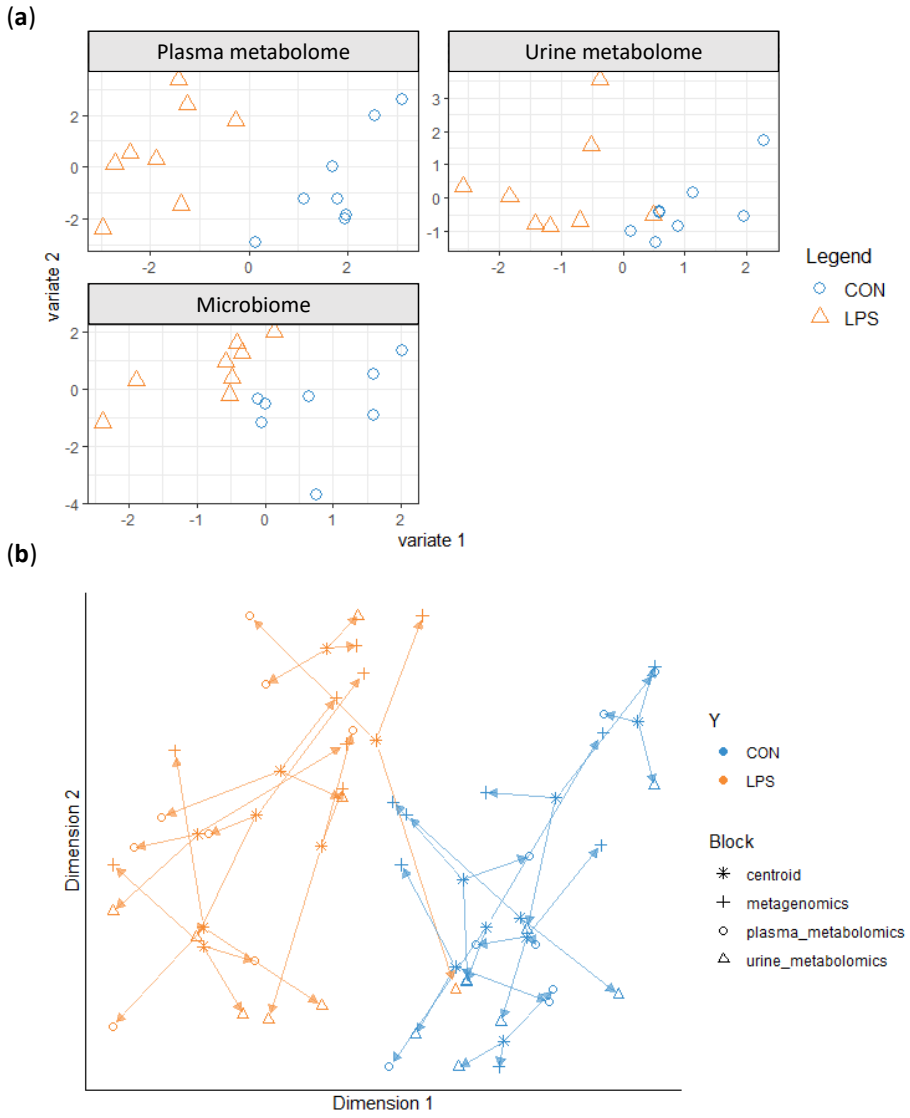

Supplementary figure 3. Integration of plasma metabolomics, urine metabolomics and metagenomics data using DIABLO in the LPS-induced inflammation model. (a) The sample plot projects each sample into the space spanned by the components of each block. The first components from each data set are highly correlated to each other. (b) Arrow plot: the start of the arrow indicates the centroid between all data sets for a given sample and the tips of the arrows the location of that sample in each omic, highlighting the agreement between the 3 data sets at the sample level. LPS in orange and CON in blue.

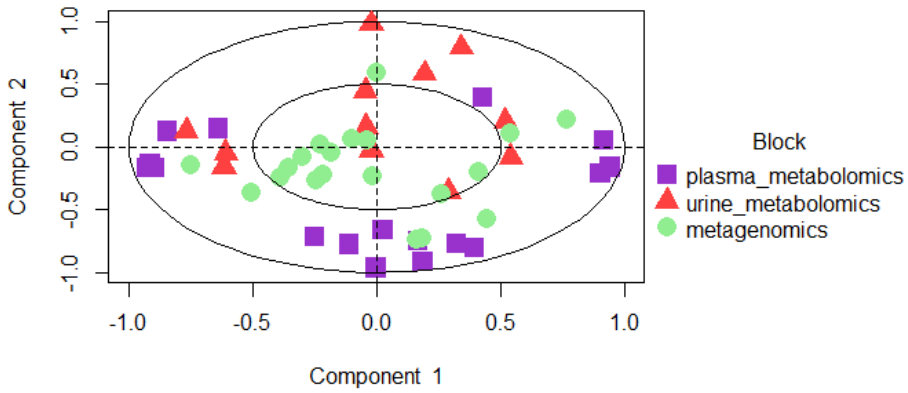

Supplementary figure 4. Correlation circle plot in the LPS-induced inflammation model (DIABLO). This plot highlights the contribution of each selected variable to component 1 and 2. Clusters of points indicate a strong correlation between variables. Each colour and shape indicate the type of features: i.e., plasma metabolites (purple square), urine metabolites (red triangle) and finally, bacteria and virus species (green circle).

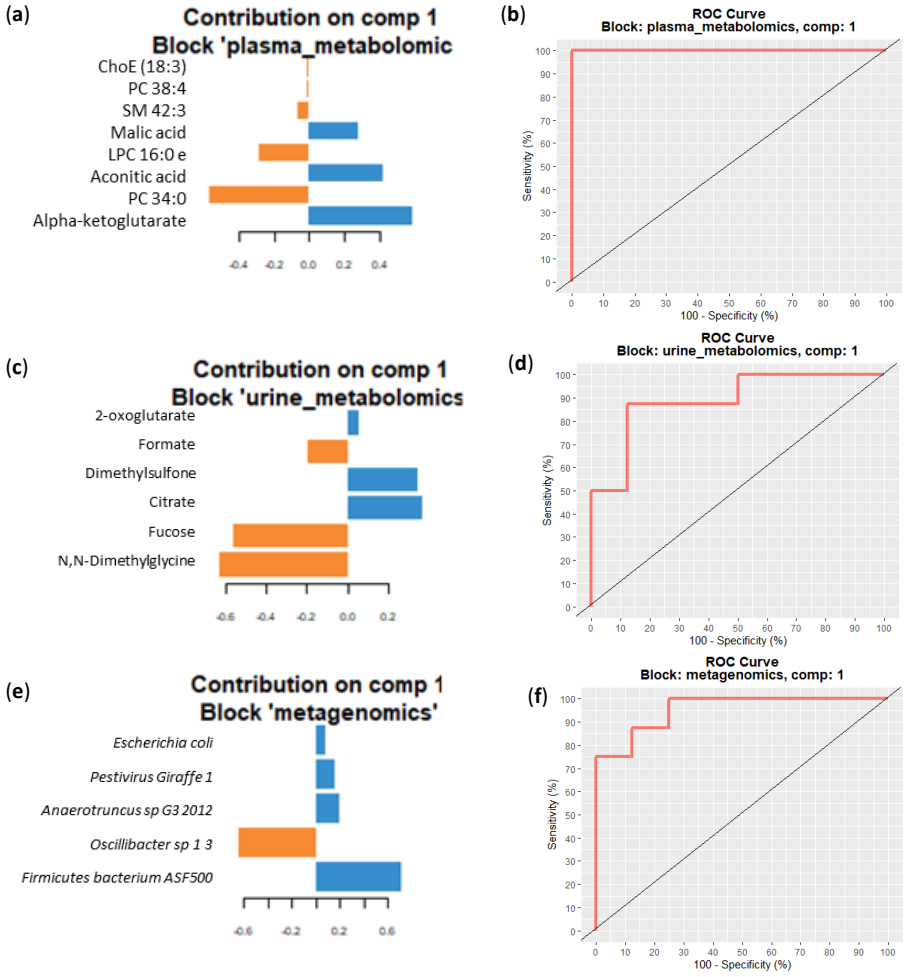

Supplementary figure 5. Feature integration in plasma metabolomics, urine metabolomics and metagenomics in the LPS-induced inflammation model (DIABLO). (a) (c) (e) Feature impact in each data set in component 1. (b) (d) (f) ROC curve and AUC averaged using one-vs-all comparisons in the different data set. LPS in orange and CON in blue.

UNIVERSITAT ROVIRA I VIRGILI
MULTI-OMICS BIOMARKERS OF METABOLIC HOMEOSTASIS OF RISK FACTORS ASSOCIATED TO NON-COMMUNICABLE DISEASES
Julia Hernandez Baixauli

MANUSCRIPT 5

METABOLIC IMPACT OF MITOCHONDRIAL OXIDATIVE STRESS IN A PARAQUAT-INDUCED MALE WISTAR RAT MODEL BASED ON INCREASED HYDROGEN PEROXIDE: A MULTI-OMICS INTEGRATIVE APPROACH

Julia Hernandez-Baixauli [1], Antonio J Cortés-Espinar [2], Javier Ávila-Román [2,3], Nerea Abasolo [4], Hector Palacios-Jordan [4], Elisabet Foguet-Romero [4], David Suñol [5], Mar Galofré [5], Antoni Caimari [1], Laura Baselga-Escudero [1], Josep M Del Bas [1 *], and Miquel Mulero [2 *]

[1] Eurecat, Centre Tecnològic de Catalunya, Unitat de Nutrició i Salut, 43204 Reus, Spain
[2] Nutrigenomics Research Group, Department of Biochemistry and Biotechnology, Universitat Rovira i Virgili, 43007 Tarragona, Spain
[3] Department of Pharmacology, Universidad de Sevilla, 41012 Seville, Spain
[4] Eurecat, Centre Tecnològic de Catalunya, Centre for Omic Sciences (COS), Joint Unit Universitat Rovira i Virgili-EURECAT, 43204 Reus, Spain
[5] Eurecat, Centre Tecnològic de Catalunya, Digital Health, 08005 Barcelona, Spain

***** Correspondence: josep.delbas@eurecat.org; miquel.mulero@urv.cat

Pending submission to Free Radical Biology and Medicine

UNIVERSITAT ROVIRA I VIRGILI
MULTI-OMICS BIOMARKERS OF METABOLIC HOMEOSTASIS OF RISK FACTORS ASSOCIATED TO NON-COMMUNICABLE DISEASES
Julia Hernandez Baixauli

Abstract: Oxidative results in the progression of major health problems in humans. Despite this fact, it is difficult to track, and it is only detected with the presence of developed diseases. For this reason, the characterisation of the metabolic profile of oxidative stress might be of considerable importance for the prevention and diagnosis of this risk factor before the onset of diseases. To determine the metabolic effects of oxidative stress, male Wistar rats were subjected to a single intraperitoneal injection of paraquat (PQ) of 15 and 30 mg/kg. To confirm and characterize the model, biochemical and oxidative biomarkers were measured at the end of the study. To assess the omics profile, GC-qTOF and UHPLC-qTOF were performed to evaluate plasma metabolome; ^{1}H-NMR was used to evaluate urine metabolome; and shotgun metagenomics sequencing was carried out to study the gut microbiome. The classical biomarkers of oxidative stress were different between the groups treated with PQ and the control group. Both PQ groups were characterized by an excess of intracellular SOD, that leads to an increase of hydrogen peroxide (H_2O_2). The metabolome is highlighted by 3-hydroxibutiric acid, SMs and LPCs that were altered in a dose-dependent manner in all groups, thus those metabolites could be considered key features for monitoring mitochondrial oxidative stress. Thus, β-oxidation of fatty acids together with other related lipid pathways are important in this experimental approach. Additionally, disrupted tricarboxylic acid (TCA) cycle and one-carbon metabolism seems to play an important role in this metabolic profile. Collateral effects on gut microbiome indicated different sensibility of microbes to H_2O_2. Overall, these results indicate the complexity of the metabolic profile depending on the PQ-dose, being different across different metabolic pathways, with some potential shared metabolites.

Keywords: oxidative stress, biomarkers, animal model, paraquat, metabolomics, metagenomics.

1. Introduction

Recent milestones in scientific research have shown that oxidative stress is implicated in the progression of major health problems in humans by inactivating metabolic enzymes, damaging important cellular components or oxidising nucleic acids, that leads to non-communicable diseases (NCD) such as cardiovascular disease, neurological diseases, atherosclerosis, and cancer, among others [1]. However, oxidative stress is difficult to track epidemiologically in the population. This is due there is a lack of tools to diagnose it clinically as an isolated risk factor, thus it is currently detected when it is associated with diseases. A reflection of this fact is the example of epidemiological studies in humans that have shown a close association between chronic oxidative conditions and carcinogenesis, where the latter does have a high incidence in the population [2].

Indeed, oxidative stress is a set of reactions that occurs when there is an imbalance between oxygen and nitrogen reactive species (ROS/RNS) generation and the body's antioxidant defence systems [3]. Many types of agents (chemical, physical and microbial) can cause oxidative stress in tissues and cells, as the case of increasing environmental pollutants that are considered a growing threat to global health [4]. In addition, oxidative stress is involved in many fundamental aspects of life processes, such as cellular respiration (mitochondria), lipid synthesis, metal metabolism, lysosomes, phagocytosis of foreign bodies (immunity and inflammation) and xenobiotic biotransformation of organic compounds. Concretely, ROS are mainly produced by mitochondria under both physiological and pathological conditions. Generally, superoxide radical ($O_2^{\bullet -}$) is formed by cellular respiration through the activity of lipoxygenases (LOX) and cyclooxygenases (COX) during arachidonic acid metabolism, and by endothelial and inflammatory cells [5]. Although these organelles have an intrinsic ROS scavenging capacity [6], it should be noted that this is not sufficient to cope with the cellular need to remove the amount of ROS produced by mitochondria [7]. ROS have divergent effects on cellular function and contribute to disease through different mechanism [8]. The first mechanism involves the production of reactive species during oxidative stress such as hydroxyl radical ($HO^{\bullet}$) or peroxynitrite anion ($ONOO^-$) that oxidize molecules (e.g., proteins, lipids, and nucleic acids) leading to disrupted homeostasis of cell function and death. The second mechanism involves aberrant redox signalling as the case of the oxidant hydrogen peroxide (H_2O_2) that can act as second messenger [9]. On the other hand, the antioxidant system of cells is based mainly on enzymatic components, such as superoxide dismutase (SOD), catalase (CAT), glutathione reductase (GR) and glutathione peroxidase (GPx), to protect themselves from ROS-induced cellular damage [10].

Due to the great impact of oxidative stress on the development of disease, oxidative stress markers are taking more importance as a tool to assess the biological redox status, disease state and progression, and the health-enhancing effects of

antioxidants in humans [1]. The identification of biomarkers has been the focus of many studies, and several biomarkers from various biomolecule sources have been proposed over the past decades. However, there is a lack of consensus concerning validation, standardization, and reproducibility for some of them. Within the current biomarkers, 8-hydroxy-2′-deoxyguanosine (8-OHdG), 8-isoprostane, 3-nitrotyrosine, malondialdehyde (MDA) and oxidized low-density lipoprotein (oxLDL) are the main biomarkers for monitoring oxidative status over time [11]. All these determinations until the date are performed with expensive kits and sometimes the fine-tune determination depends on the storage time. Regarding the novel approaches for the identification of new potential biomarkers, omics profiling seems to be a promising methodology for the identification of early biochemical changes in disease. Thereby, omics approaches provides an opportunity to discriminate a profile of candidate features that can provide valuable tools to prevent the development of diseases [12,13].

Since oxidative stress is not isolated in humans, this fact is a handicap for monitoring this risk factor before the onset of disease. For this reason, animal models of oxidative stress are adopted to study the biochemical and metabolic alterations of the homeostasis disruption. Current animal models of oxidative stress depend on the rate of prooxidant generation and the effects of antioxidants, thus experimental oxidative models can target either production of ROS or suppression of antioxidants [14]. Therefore, treatments that increase ROS production are particularly useful to evaluate oxidative stress through ingestion or injection of oxidative stress generating molecules such as diazinon [15], diquat [16] or paraquat (PQ) [17–23]. Concretely, PQ (1,10-dimethyl-4,40-bipyridinium dichloride) is the most commonly used oxidative stress inducer, it should be noted that it is a very toxic herbicide when absorbed by ingestion, skin contact or inhalation [24–26]. Despite lung is the primary organ affected, PQ toxicity affects other organs such as the liver that has a high potential for generating ROS and has considered a key target for PQ [27]. However, PQ alternatives, as inducers of oxidative stress, present more drawbacks than PQ administration due to their greater toxicological effects.

The systemic effect of PQ is related to its redox cycle [25]. PQ is reduced, mainly by NADPH-cytochrome P-450 reductase [28], NADPH-cytochrome c reductase [29] and the mitochondrial complex I [30] to form a monocation free radical of PQ ($PQ^{\bullet+}$). The $PQ^{\bullet+}$ is then rapidly re-oxidised in the presence of oxygen generating $O_2^{\bullet-}$ [31], that is physiologically generated by the activity of LOX and COX during cellular respiration and arachidonic metabolism, respectively [5]. Then, it follows the well-known cascade leading to the generation of other ROS such as H_2O_2 and $HO^{\bullet}$ generating the subsequent effects on homeostasis. This high ROS production induces a non-selective oxidation of biomolecules such as lipids, proteins and nucleic acids that lead to cell damage and eventually result in death [26]. In fact, $HO^{\bullet}$ have been implicated in the initiation of membrane damage by lipid peroxidation during the exposure to PQ [31,32]. Besides the administration of PQ by intragastric administration is widely

related to PQ poisoning [17], single or periodically intraperitoneal injection (IP) of PQ induce oxidative stress in different degree from a risk factor to a toxic effect depending on the rodent model and the dosage [18–23]. Therefore, this oxidative stress model is the most suitable experimental approach that should be evaluated with caution as it is associated with a some complications: such as localized damage to lungs; interacts with microglia to induce increased neural damage, particularly to dopaminergic neurons [14]. In this line, this model is widely adopted and studied as a factor of different diseases such as the case of Parkinson's disease [33,34] and lung diseases [35].

In this study, we hypothesized that oxidative stress is associated by a characteristic metabolic signature that might allow the detection of oxidative stress states affecting homeostasis. This metabolic signature along with classic oxidative biomarkers could provide valuable information about oxidative stress as a risk factor the onset of diseases. To achieve that, we explore and interrogate the oxidative model based on the use of low doses of PQ to mimic the systemic influence of oxidative stress in our rodent model. Different omic sources were performed to obtain a metabolic profile of biomarkers, which included the metabolome of different biofluids (plasma and urine) and the microbiome. This approximation enriches the knowledge related to disrupted homeostasis due to this stressor effect on metabolism.

2. Materials and Methods

2.1. LPS-Induced Chronic Inflammation Model

Thirty 8-week-old male Wistar rats (Harlan Laboratories, Barcelona, Spain) were housed individually under a fully controlled condition including temperature (22 ± 2°C), humidity (55± 5%) and light (12 h-light-dark cycle and lights on at 9:00 a.m.). The Animal Ethics Committee of the University Rovira i Virgili (Tarragona, Spain) approved all the procedures (code 10049). The experimental protocol followed the "Principles of Laboratory Care" and was carried out in accordance with the European Communities Council Directive (86/609/EEC).

After an acclimation period, rodents were randomly divided into 3 groups (n = 10 animals per group) consisting of the control group (CON, 0.9% NaCl solution), the oxidative stress dose A group (OXS A, 15 mg/kg of BW of PQ) and the oxidative stress dose B group (OXS B, 30 mg/kg of BW of PQ). Focusing on the treatment, PQ (Sigma-Aldrich, St. Louis, MO, USA) was dissolved in 0.9% NaCl saline solution and a single IP dose depending on BW. Control rats were treated with saline solution (0.9% NaCl) depending on BW.

2.2. Sample Collection

Urine samples were collected the day before the sacrifice with the hydrophobic sand method [36]. For each rat, 300 g of hydrophobic sand was spread (LabSand, Coastline Global, Palo Alto, CA, USA) on the bottom of a mouse plastic micro-isolation cage. Urine was collected with sodium azide (Sigma-Aldrich, St Louis, MO, USA) as preservative every half hour for 6 hours and was finally pooled at the end of the session.

On the last day of the study, animals were euthanized by guillotine under anaesthesia (pentobarbital sodium, 50 mg/kg per body weight) after 7 hours of fasting. Blood was collected and centrifuged at 3,000 g at 4 °C for 15 min to recover plasma. Tissues were rapidly removed, weighted and snap-frozen in liquid nitrogen (i.e., retroperitoneal white adipose tissue (RWAT), mesenteric white adipose tissue (MWAT), muscle, liver, and cecum). All the samples were stored at -80°C until further analysis.

2.3. Pl General measurements for the characterization of the experimental approach

2.3.1. General determinations

Enzymatic colorimetric kits were used for the general determination of plasma total cholesterol (TC), triglycerides (TG), glucose (QCA, Barcelona, Spain) and non-esterified free fatty acids (NEFAs, WAKO, Neuss, Germany).

For the determination of oxidative stress, we measured the markers of lipid oxidative damage with the measure of malondialdehyde (MDA, TBARS assay kit, Cayman Chemical Company, Ann Arbor, MI, USA) and 8-isoprostane (8-Isoprostane ELISA Kit, Cayman Chemical Company, Ann Arbor, MI, USA). To know the antioxidant capacity of the subjects, we quantified the activity of the main antioxidant enzyme that is the superoxide dismutase (SOD, SOD Colorimetric Activity Kit, Thermo Fisher Scientific, Waltham, MA, USA). The overall inflammatory response was measured with the level of the monocyte chemoattractant protein-1 (MCP-1, MCP-1 Rat Instant ELISA™ Kit, Thermo Fisher Scientific, Waltham, MA, USA) one of the main pro-inflammatory cytokines. The manufacture's protocol was followed in all the determinations.

2.3.2. RNA extraction and qPCR

Total RNA was obtained from liver samples using TriPure reagent (Roche Diagnostic, Barcelona, Spain) and RNeasy Mini Kit (QIAgen, Madrid, Spain) as described in supplier's protocol. RNA concentration and purity were measured by the determination of the absorbance at 260 and 280 nm with a nanophotometer (Implen, Munich, Germany). RNA was converted to cDNA using a High-Capacity cDNA Reverse Transcription Kit (Applied Biosystems, Wilmington, DE, USA) with a RNase Inhibitor (Applied Biosystems, Wilmington, DE, USA) as described in manufacturer's protocol.

The expression of genes related with oxidative stress (i.e., Cu/Zn SOD, Mn SOD, CAT, GPx1) were evaluated by quantitative polymerase chain reaction (qPCR). For this purpose, cDNAs samples were diluted 1:10 before being incubated with commercial LightCycler® 480 SYBR Green I Master on a LightCycler® 480 II (Roche Diagnostics, Manheim, Germany). Table 1 shows a list of primers used and verified with Primer-Blast software (National Centre for Biotechnology Information, Bethesda, MD, USA) and the selected housekeeping gene was PPIA. Thermal cycling comprised an initial step at 95 °C for 5 min and a cycling step with the following conditions: 45 cycles of denaturation at 90 °C for 10 s, annealing at 60 °C for 10 s and extension at 72 °C for 10 s. Fluorescence data were acquired at 72 °C of cycling step.

Table 1. Detailed sequences of the oligonucleotides used in q-PCR.

Gene	Forward Primer (5'-3')	Reverse Primer (5'-3')	Accession number	Size (bp)
Cu/Zn SOD	GGTGGTCCACGAGAAACAAG	CAATCACACCACAAGCCAAG	NM_017050.1	98
Mn SOD	AAGGAGCAAGGTCGCTTACA	ACACATCAATCCCCAGCAGT	NM_017051.2	94
Catalase	GAATGGCTATGGCTCACACA	CAAGTTTTTGATGCCCTGGT	NM_012520.2	100
GPx1	TGCAATCAGTTCGGACATC	CACCTCGCACTTCTCAAACA	NM_030826.4	120
PPIA	CCTCGAGCTGTTTGCAGACAA	AAGTCACCACCCTGGCACATG	NM_017101.1	138

2.3.3. Protein Extraction and Western Blot Analysis

Liver samples were homogenated in RIPA buffer (50 mM Tris-HCL, 150 mM NaCl; pH 7.4, 1% Tween 20, 0,25% Na-deoxycholate) containing PMSF (Sigma-Aldrich, Madrid, Spain), phosphatase cocktails 2 and 3 (Sigma-Aldrich, Madrid, Spain) and protease inhibitor cocktail (Sigma-Aldrich, Madrid, Spain) with TissueLyser LT (QIAgen, Madrid, Spain) for 50 s. After shaking samples for 30 min at 4 °C, the lysates were centrifuged at 16,300 g for 15 min at 4 °C. Finally, protein concentration was measured by BCA protein assay (Thermo Fisher Scientific, Madrid, Spain).

50 µg of protein per sample were electrophoretically separated on 10% SDS-polyacrylamide gels (TGX FastCast Acrylamide Kit, Bio-Rad, Madrid, Spain) and transferred to PVDF membranes (Trans-Blot Turbo System, Bio-Rad, Barcelona, Spain). Protein transfer efficiency was evaluated by Pounceau-S stain. Then, membranes were blocked with 5% non-fat milk in TBS-Tween (0.2%) for one hour at room temperature. After blocking, membranes were blotted overnight at 4 °C with rabbit or ¿mouse? antibodies (dilution 1:1,000): Monoclonal antibody for Glutathione Reductase and Monoclonal antibody for β-Actine were used. After 3 washings with TBS-Tween, membranes were hybridized with anti-rabbit secondary antibody (Amersham, Cytiva, Barcelona, Spain) (dilution 1:10,000) conjugated with horseradish peroxidase for 1 h at room temperature. After 3 more washings, immunoreactive proteins were visualized using a chemiluminescence substrate kit (Amersham ECL Select, Cytiva, Barcelona, Spain) following the supplier's protocol. Digital images were obtained with

a G:BOX Chemi XL1.4 (Syngene, Cambridge, UK) and densitometry analysis were evaluated using ImageJ Software (NIH, Bethesda, MD).

2.4. Plasma metabolomics (GC-qTOF and UHPLC-qTOF)

Plasma metabolites were analysed by gas Chromatography coupled with Quadrupole Time-of-Flight (GC-qTOF). For the extraction, a protein precipitation extraction was performed by adding eight volumes of methanol:water (8:2, *v*/*v*) containing internal standard mixture (succinic acid-d4, myristic acid-d27, glicerol-13C3 and D-glucose-13C6) to plasma samples. Then, the samples were mixed and incubated at 4 °C for 10 min, centrifuged at 21,420 g and supernatant was evaporated to dryness before compound derivatization (metoximation and silylation). The derivatized compounds were analysed by GC-qTOF (model 7200 of Agilent, Santa Clara, CA, USA). The chromatographic separation was based on the Fiehn Method, using a J&W Scientific HP5-MS (30 m x 0.25 mm i.d.), 0.25 µm film capillary column and helium as carrier gas using an oven program from 60 °C to 325 °C. Ionization was done by electronic impact (EI), with electron energy of 70 eV and operated in full Scan mode. The identification of metabolites was performed by matching their EI mass spectrum and retention time to metabolomic Fiehn library (Agilent, Santa Clara, CA, USA) which contains more than 1,400 metabolites. After putative identification of metabolites, these were semi-quantified in terms of internal standard response ratio.

Plasma lipids were analysed by Ultra High Perfomance Liquid Chromatography coupled with Quadrupole Time-of-Flight (UHPLC-qTOF). For the extraction of the hydrophobic lipids, a liquid-liquid extraction based on the Folch procedure [37] was performed by adding four volumes of chloroform:methanol (2:1, v/v) containing internal standard mixture (Lipidomic SPLASH®, Avanti Polar Lipids, Inc., Alabaster, AL, USA) to plasma. Then, the samples were mixed and incubated at -20 °C for 30 min. Afterwards, water with NaCl (0.8 %) was added and the mixture was centrifuged at 21,420 g. Lower phase was recovered, evaporated to dryness and reconstituted with methanol:methyl-tert-butyl ether (9:1, *v*/*v*) and analysed by UHPLC-qTOF (model 6550 of Agilent, Santa Clara, CA, USA) in positive electrospray ionization mode. The chromatographic consists in an elution with a ternary mobile phase containing water, methanol, and 2-propanol with 10 mM ammonium formate and 0.1% formic acid. The stationary phase was a C18 column (Kinetex EVO C18 Column, 2.6 µm, 2.1 mm x 100 mm) that allows the sequential elution of the more hydrophobic lipids such as triglycerides (TGs), diacylglycerols (DGs), cholesterol ester (ChoEs), phosphatidylcholines (PCs), phosphatidylethanolamine (PE), lysophospholipids (LPCs) and sphingomyelins (SMs), among others.

The identification of lipid species was performed by matching their accurate mass and tandem mass spectrum, when available, to Metlin-PCDL from Agilent containing more than 40,000 metabolites and lipids. In addition, chromatographic behaviour of pure standards for each family and bibliographic information was used to ensure their putative identification. After putative identification of lipids, these were semi

quantified in terms of internal standard response ratio using one internal standard for each lipid family. A pooled matrix of samples was generated by taking a small volume of each experimental sample serving as a technical replicate throughout the data set. As the study took multiple days, a data normalization step was performed to correct variation resulting from instrument inter-day tuning differences. Essentially, each compound was corrected in run-day blocks through quality controls, normalizing each data point proportionately.

2.5. Urine metabolome (^{1}H-NMR)

Urine metabolites were analysed by proton nuclear magnetic resonance (^{1}H-NMR). The urine sample was mixed (1:1, *v*/*v*) with phosphate buffered saline containing with 3-(Trimethylsilyl)propionic-2,2,3,3-d4 acid sodium salt (TSP) (Sigma-Aldrich, St. Louis, MO, USA) and placed on a 5 nm NMR tube for direct analysis by ^{1}H-NMR. ^{1}H-NMR spectra were recorded at 300 K on an Avance III 600 spectrometer (Bruker®, Bremen, Germany) operating at a proton frequency of 600.20 MHz using a 5 mm PBBO gradient probe. Diluted urine aqueous samples were measured and recorded in procno 11 using a One-dimensional ^{1}H pulse experiments were carried out using the nuclear Overhauser effect spectroscopy (NOESY). NOESY presaturation sequence (RD–90°–t1–90°–tm–90° ACQ) to suppress the residual water peak, and the mixing time was set at 100 ms. Solvent presaturation with irradiation power of 150 µW was applied during recycling delay (RD = 5 s) and mixing time. (noesypr1d pulse program in Bruker®) to eliminate the residual water. The 90° pulse length was calibrated for each sample and varied from 11.21 to 11.38 ms. The spectral width was 9.6 kHz (16 ppm), and a total of 128 transients were collected into 64 k data points for each ^{1}H spectrum. The exponential line broadening applied before Fourier transformation was of 0.3 Hz. The frequency domain spectra were manually phased and baseline-corrected using TopSpin software (version 3.2, Bruker). Data has been normalized by two different ways, by probabilistic to avoid differences between sample due to different urine concentration, and by ERETIC. The acquired ^{1}H-NMR were compared to references of pure compounds from the metabolic profiling AMIX spectra database (Bruker®), HMDB, and Chenomx databases for metabolite identification. In addition, we assigned metabolites by ^{1}H-^{1}H homonuclear correlation (COSY and TOCSY) and ^{1}H-^{13}C heteronuclear (HSQC) 2D NMR experiments and by correlation with pure compounds run in-house. After pre-processing, specific ^{1}H-NMR regions identified in the spectra were integrated using MATLAB scripts run in house. Curated identified regions across the spectra were exported to excel spreadsheet to evaluate robustness of the different ^{1}H-NMR signals and to give relative concentrations.

2.6. Shotgun metagenomics sequencing

DNA was extracted from faeces using the PowerSoil DNA extraction kit (MO BIO Laboratories, Carlsbad, CA, USA) following the manufacturer's protocol. Between 400 and 500 ng of total DNA was used for library preparation for Illumina sequencing

employing Illumina DNA Prep kit (Illumina, San Diego, CA, USA). All libraries were assessed using a TapeStation High Sensitivity DNA kit (Agilent Technologies, Santa Clara, CA, USA) and were quantified by Qubit (Invitrogen, Waltham, MA, USA).

Validated libraries were pooled in equimolar quantities and sequenced as a paired-end 150-cycle run on an Illumina NextSeq2000. A total of 1548 million reads were generated, and raw reads were filtered for QV > 30 using an in-house phyton script. Filtered reads were aligned to unique clade-specific marker genes using MetaPhlAn 3 [38] to assess the taxonomic profile. The alignment was done indicating the closest name of specie to the sequence (the best hit). The relative proportions calculated from MetaPhlAn were used to calculate relative abundances, alpha diversity measure (chao1 index) and beta diversity measures (Aitchison distance).

2.7. Statistical Analysis

2.7.1. General statistical analysis

The results were expressed as the mean ± SEM and statistical comparisons were carried out using one-way ANOVA, followed by Tukey's multiple comparison test after the study of the normality. In all the statistical comparisons, a two-tailed *p*-value < 0.05 was considered. Across the different statistical analysis, the magnitude of difference between populations is presented as fold change (FC). The statistical analysis was performed using different software: (1) the R statistical software v4.0.2 (R Core Team 2021) and different libraries, included in Bioconductor v3.11 (Bioconductor project) as rolps and mixOmics; (2) SPSS v25.0 (SPSS Inc, Chicago, IL, USA); (3) GraphPad Prism v8.0.0 (GraphPad Software, San Diego, CA, USA).

2.7.2 Metabolomic data analysis

Individual comparisons between metabolites were determined by the Kruskal-Wallis H-test, a non-parametric version of ANOVA, due to the variables follow the assumption of a non-parametric test. The p-value adjustment for multiple comparisons was carried out according to the Benjamin-Hochberg (BH) correction method with a false discovery rate (FDR) of 5%, and a Post-hoc Dunn. In parallel, a predictive analysis was done to evaluate the prediction power of the oxidative stress model. On the one hand, principal component analysis (PCA), an unsupervised multivariate data projection method, was performed to explore the native variance of the samples. On the other hand, partial least squares discriminant analysis (PLS-DA) was performed to determine the prediction power that supervised multivariate data projection method explores, possible relationships between the observable variables (X) and the predicted variables or target (Y) by regression extensions. The predictive performance of the test set was estimated by the Q2Y parameter calculated through cross-validation. The values of Q2 < 0 suggests a model with no predictive ability, 0 < Q2 < 0.5 suggests some predictive character and Q2 > 0.5 indicates good predictive ability [39]. The feature importance was calculated through the variable importance in projection (VIP), which reflects both the loading weights for each component and the variability of the response explained by the component.

2.7.3. Metagenomic data analysis

Centred log-ratio (CLR) normalization was performed before any statistical test. The beta diversity was calculated from the Aitchison distance and PERMANOVA test was performed with 100 permutations to assess de differences between groups. The alpha diversity was calculated by Chao1 index. Taxonomic abundances, which are presented by relative abundance (%), were compared between experimental groups using the Holm-Šídák (HS) post-hoc adjustment on Kruskal-Wallis test. The relative abundance was filtered to only include variables that were present above 0.01% in at least 3 samples [40].

2.7.4. Integration data analysis

Multiblock sPLS-DA, which is also known as Data Integration Analysis for Biomarker discovery using Latent cOmponents (DIABLO), is a holistic approach with the potential to find new biological insights not revealed by any single-data omics analysis, as some pathways are common to all data types, while other pathways may be specific to data. DIABLO is built on the Generalised Canonical Correlation Analysis (GCCA) [41] in the mixOmics R package (version 6.18.1, mixOmics project) and in our case it was used to integrate plasma and urine metabolome and microbiome [42].

To summarize, the first step is the parameter choice of the design matrix, the number of components and the number of variables to select: (1) a design matrix based on pairwise correlations was used to be more accurate; (2) the perf function was used to estimate the performance of the model and the balanced error rate (BER) and overall error rates per component were displayed to select the optimal number of components; (3) the number of variables was chosen using the tune.block.splsda function that is run with 10-fold cross validation and repeated 10 times. Thereafter, the final model was computed, and different sample and variable plots were performed. The circosPlot function represents the correlations between variables of different types, represented on the side quadrants that is built based on a similarity matrix, which was extended to the case of multiple data sets [43].

The final performance of the model was evaluated by the perf function using 10-fold cross-validation repeated 10 times. The receiver operating characteristic (ROC) curve analysis was conducted to determine the optimal metabolite combination patterns that could correctly dichotomize the stressed and healthy groups at acceptable sensitivity and specificity (defined as greater than 80% for both). The area under the ROC curve (AUC) value was used as a measure of the prognostic accuracy.

2.7.5. Pathway Analysis

The resulting significant differential features were analysed through different data bases to identify related pathways and elucidate the global effect in the metabolism of the LPS-induced inflammation model. The main data base consulted was the Kyoto Encyclopaedia of Genes and Genomes (KEGG) [44], among others. To show those results, a mapping tool (XMind 2020, version XMind 2020, XMind Ltd.,

Virginia, ON, Canada) was used to incorporate the information about pathway analysis.

3. Results

3.1. Characterization and validation of the PQ model

3.1.1. General changes

The effect of the PQ dose had repercussions on the animal through body changes and biochemical changes that are summarized in Table 2. Initially, a decrease in BW together with a decrease of food consumption was observed in the OXS A and OXS B group versus controls. In this line, different tissues weights were decreased as liver, muscle, and cecum while the dose increases. Other interesting general parameters, as plasma TG were decreased in both treated groups while TC was increased.

Focusing on the plasma biomarkers of oxidative stress, MDA was increased in both doses while SOD was only decreased in OXS B. For liver, MDA and SOD was increased in the OXS B group with statistical differences. The increasing level of 8-isoprostane correlates with the increasing dose of PQ. For the characterization of inflammation response, MCP-1 was increased in the two treated groups in contrast to the CON group.

Table 2. General characteristics of the oxidative stress model. The results are presented as the mean ± SEM (*n* = 10 animals per group). The biometric parameters are represented as a ratio (g/ kg BW * 100) to properly compare the parameters. The statistical comparisons among groups were conducted using 1-way ANOVA and post hoc (Tukey) test. * Denotes $p < 0.1$ (tendency), ** $p < 0.05$ (significantly different) and *** $p < 0.01$ (high significantly different) compared with control. Abbreviations: BW, body weight; MWAT, mesenteric white adipose tissue; RWAT, retroperitoneal white adipose tissue; MDA, malondialdehyde; SOD, superoxide dismutase; MCP-1, monocyte chemoattractant protein-1; TG, triglycerides; TC, total cholesterol; NEFAs, non-esterified fatty acids.

		Control	OXS A	OXS B	*p*-value	CON vs OXS A	CON vs OXS B	OXS A vs OXS B
Biometric parameters	Inicial BW (g)	286.21 ± 4.24	286.37 ± 3.24	300.85 ± 8.28	0.11	0.94	0.7	0.33
	Final BW (g)	293.77 ± 3.90	271.59 ± 5.54	263.35 ± 7.37	<0.01***	0.03**	<0.01***	0.58
	Total food consumption (g)	21.19 ± 0.77	11.47 ± 1.44	0.65 ± 0.20	<0.01***	<0.01***	<0.01***	<0.01***
	MWAT/BW	0.86 ± 0.02	0.87 ± 0.5	0.71 ± 0.06	0.05*	0.99	0.09*	0.76
	RWAT/BW	1.09 ± 0.5	1.03 ± 0.09	0.88 ± 0.13	0.36	0.91	0.31	0.55
	Muscle/BW	0.63 ± 0.01	0.60 ± 0.01	0.56 ± 0.01	<0.01***	0.17	<0.01***	<0.01***
	Liver/BW	3.61 ± 0.04	3.26 ± 0.10	2.55 ± 0.06	<0.01***	<0.01***	<0.01***	<0.01***
	Cecum/BW	1.55 ± 0.09	1.37 ± 0.07	0.97 ± 0.11	<0.01***	0.37	<0.01***	0.13
Plasma parameters	MDA (µM)	11.62 ± 0.33	12.73 ± 1.25	17.66 ± 2.23	0.01**	0.83	0.01**	0.04**
	SOD (U/ml)	7.33 ± 0.31	7.15 ± 0.27	4.48 ± 0.33	<0.01***	0.91	<0.01***	<0.01***
	MCP-1 (pg/ml)	6.48 ± 1.10	9.94 ± 0.59	9.72 ± 1.13	0.03**	0.04**	0.05*	0.98
	Glucose (mM)	114.39 ± 1.63	108.47 ± 3.74	119.10 ± 5.33	0.17	0.53	0.67	0.14
	TG (mM)	81.05 ± 7.96	55.29 ± 12.11	57.12 ± 5.70	0.09*	0.13	0.16	0.98
	TC (mM)	67.44 ± 3.09	76.62 ± 5.55	94.33 ± 4.83	<0.01***	0.35	<0.01***	0.03**
	NEFAs (mM)	0.70 ± 0.04	0.63 ± 0.03	0.68 ± 0.05	0.39	0.39	0.95	0.56
Liver biochemistry	MDA (µM)	9.50 ± 0.56	8.90 ± 0.29	12.61 ± 0.70	<0.01***	0.72	<0.01***	<0.01***
	SOD (U/ml)	62.80 ± 3.90	66.97 ± 6.26	78.86 ± 4.55	0.08*	0.82	0.07*	0.23
Urine parameters	Isoprostanes (µM)	1.14 ± 0.12	1.35 ± 0.34	5.95 ± 0.99	<0.01***	0.97	<0.01***	<0.01***

3.1.2. PQ altered the oxidative stress state in liver tissue

To further understand how the oxidative stress produced by PQ affects the liver tissue, we assessed an expression analysis of some of the most important enzymes involved in the detoxification of ROS by qPCR in this tissue. On the one hand, as shown in Figure 1a, the cytoplasmatic SOD (SOD1 or Cu/Zn SOD), responsible for approximately 90% of the SOD activity in eukaryotic cells, shows a significant increase at both doses of PQ, being statistically significant at the higher dose. Moreover, a similar result is presented by mitochondrial SOD (SOD2 or Mn SOD), which shows statistically significant differences at the highest dosage, confirming that described by Krall et al. (Figure 1b) [45]. On the other hand, the expression of the CAT gene, responsible for detoxifying hydrogen peroxide, decreased statistically in both doses regarding with control group (Figure 1c). For its part, the expression levels of GPx1, responsible for detoxifying hydrogen peroxide but from a different biochemical pathway, also changed showing a decrease for the lowest dose of PQ with respect to the control group, while it is at the same level at the highest dose with respect to the control group (Figure 1d). However, there were no significant differences between groups. These results could suggest PQ effects are related, at least partially, with the accumulation of hydrogen peroxide caused by the reduction of the expression of the enzymes responsible for its detoxification.

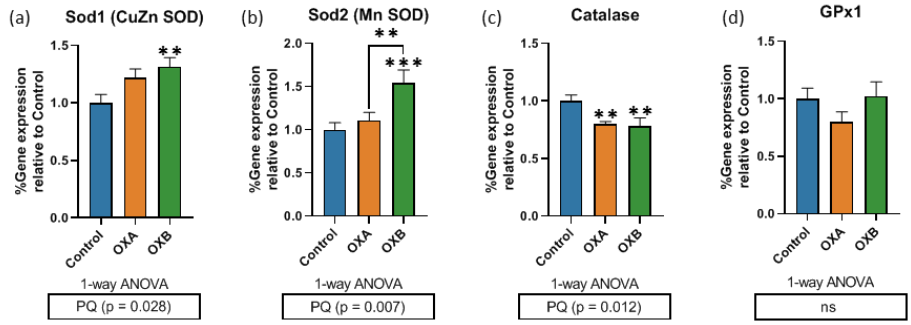

Figure 1. PQ induces altered expression of oxidative stress-related genes. The values represented are the mean ± SEM (n = 6-7 animals per group). Comparison among the three groups were analyzed by a one-way ANOVA test, followed by a Tukey's post-hoc test. The limit of statistical significance was set at $p < 0.05$. * Denotes $p < 0.1$ (tendency), ** $p < 0.05$ (significantly different) and *** $p < 0.01$ (high significantly different) compared with control. Statistical differences between treated groups are indicated by lines. Abbreviation: ns, no significant differences.

3.1.3. PQ increased the amount of GR, and thus GSH available to detoxify ROS

As it is well known, the glutathione (GSH), a tripeptide formed by the amino acids glutamate, cysteine and glycine, plays an important role in the defense against ROS-induced damage. To carry out its functions, the enzyme glutathione reductase (GR) must catalyze the reduction of glutathione disulfide (GSSG) to obtain GSH. For this reason, we assessed a Western blotting analysis of GR, determinant enzyme for the GSSG/GSH ratio. The results obtained showed treatment with PQ significantly

increased the total amount of GR enzyme, obtaining a similar response after both doses of treatment (Figure 2).

3.2 Plasma metabolic profiling and biomarker identification

Our plasma metabolomics approach is based on a multiplatform global analysis (GC-qTOF and UHPLC-qTOF) that determined the relative abundance (AU) of 128 metabolites (Table S1). We obtained 109 metabolites with a different mean between groups by Kruskal-Wallis H-test. Then, we corrected the multiple hypothesis testing *p*-values with False discovery rate Benjamin/Hochberg method and we obtained 107 metabolites having at least two groups with different means. After the post-Hoc test to check from which of the 3 relations is coming the difference in the mean, 74 metabolites were different between CON and OXS A; 70 metabolites were different between CON and OXS B; 58 metabolites were different between OXS A and OXS B (Figure S1).

As it is shown in Figure 3, 12 metabolites were significantly different between all groups (CON, OXS A and OXS B) that are aconitic acid, fructose, cholesterol, citric acid, 3-hydroxybutiric acid, serine, LPCs (LPC 18:1 and LPC 15:0) and SMs (SM 34:1, SM 34:2, SM 36:2 and SM 36:1) (Figure 3a). The distribution of the 12 metabolites were visualized with boxplot graphs to analyse the distribution of them in the different groups (Figure 3a). The expected pattern considering the dose-effect was a decrease or an increase starting in the control group. However, we found that aconitic acid, citric acid, serine, cholesterol, and fructose did not follow this patron. Further comparisons between groups are necessary to understand the metabolic profile.

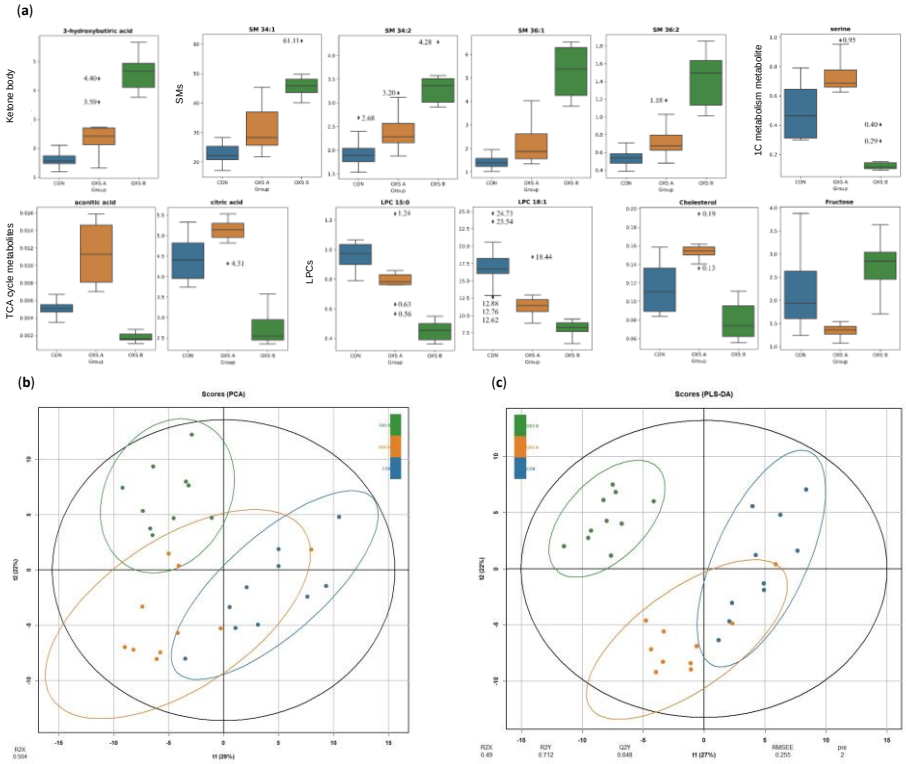

Figure 3. Graphical summary of plasma metabolome analysis. (a) Boxplot of the 12 metabolites significantly different between CON, OXS A and OXS B. Blue, CON; orange, OXS A; green, OXS B. Box denotes 25th and 75th percentiles; line within box denotes 50th percentile (median); whisker denotes standard deviation. (b) PCA scores of plasma metabolome. (c) PLS-DA scores of plasma metabolome. The Score plot is represented, and it includes the number of components, the cumulative R2X, R2Y and Q2Y. Groups (*n* = 10 animals per group): CON, blue; OXSA, orange; OXSB, green. Abbreviations: SM, sphingomyelin; LPC, lysophospholipid.

In the case of control versus OXS A, 10 metabolites altered with high impact were lipids that include mainly a group of TGs (TG 48:3, TG 48:1, TG 48:2, TG 46:1, TG 46:0, TG 52:6, TG 50:4) and specific lipids as DG 34:3, PC 38:3 and SM 35:1. In the case of control versus OXS B, the 10 metabolites altered with high impact were two groups of lipids, which are LPCs (LPC 18:1, LPC 18:2 and LPC 15:0) and SMs (SM 34:1, SM 34:2, SM 36:1, SM 36:2, SM 38:1), and a ketone body (i.e., 3-hydroxybutiric acid). Focusing on the differential metabolites between OXS A and OXS B, there were intermediate metabolites of TCA cycle (i.e., aconitic acid, citric acid and fumaric acid), cholesterol, serine, fructose, glycolytic acid and ChoE (22:5) among others.

The PCA explains the variance in the plasma metabolome showing that the data tend to be segregated in the three different groups (Figure 3b). Additionally, PLS-DA was performed to assess the discriminative power of the different groups (Figure 3c). The proportion of variance explained by the model (R2X) was 47% in the plasma data.

The percentage of Y variability explained by the model (R2Y) was 65,5% and, the estimation of the predictive performance of the models (Q2) was 57,8%. A model is considered to have good predictability when the Q2 is greater than 50% [46], thus the predictive power of the model in plasma was good. The main metabolites with the highest VIP values, which reflects both the loading weights for each component and the variability of the response explained by this component, coincide with the 12 differential metabolites between groups and presented values near to 2 (Table S1).

3.3 Urine metabolome profiling

Our urine metabolomics approach is based on H^1-NMR that method determined the relative abundance (AU) of 21 metabolites (Table S2). We obtained 15 metabolites having at least two groups with different means by Kruskal-Wallis H-test and corrected by Benjamin/Hochberg method. After the post-Hoc test to check from which of the 3 relations is coming the difference in the mean, 4 metabolites were different between CON and OXS A; 13 metabolites were different between CON and OXS B; 10 metabolites were different between OXS A and OXS B (Figure S2).

The common metabolites between the pair-wise comparisons are shown in Figure 4a. The differences between CON and OXS A groups were attributed to the levels of creatinine, pseudouridine, 1-methylmicotinamide and N-acetylglycoproteins. The differences between CON and OXS B groups were attributed to common metabolites previously differentiated in CON *vs* OXS A (creatinine and N-acetylglycoproteins), TCA intermediates (fumaric acid, citric acid and succinic acid), nicotinamide intermediates (1-methylnicotinamide and trigonelline), amino acids (tryptophan, glycine, alanine and hippurate) and lactate. Finally, the differences associated to the different doses (OXS A and OXS B group) were similar to the differences of CON against OXS B group including the TCA intermediates, nicotinamide intermediates, some previously described amino acids (tryptophan, glycine and hippurate) including a derivate of glycine (N,N-dimethylglycine) and pseudouridine.

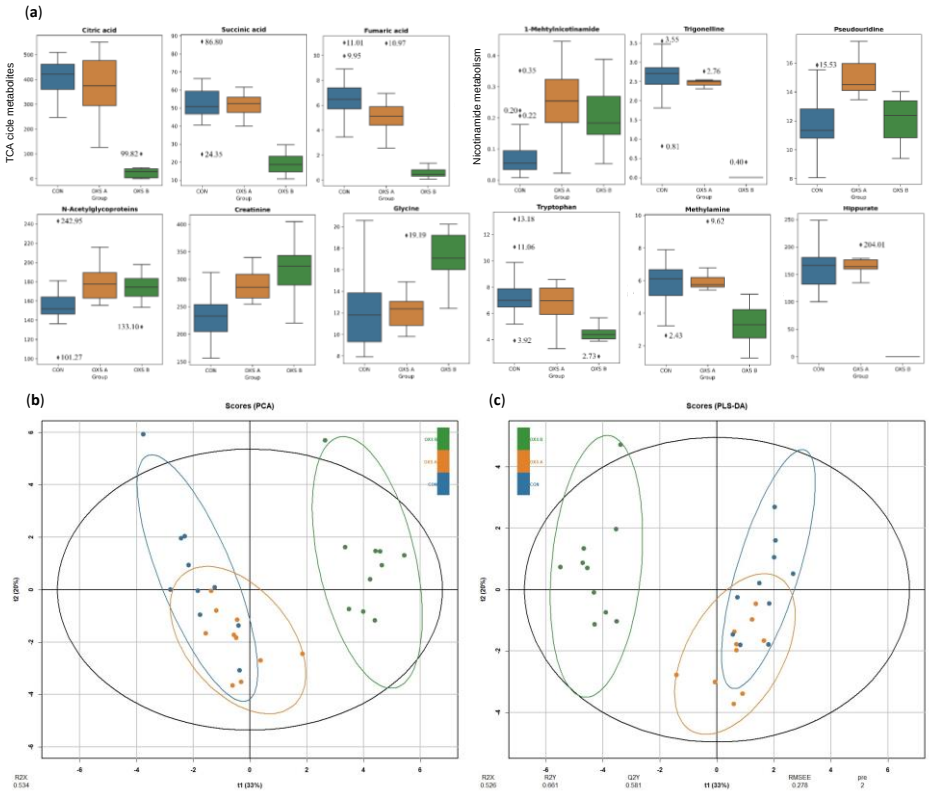

Figure 4. Graphical summary of urine metabolome analysis. (a) Boxplot of the 12 metabolites significantly different in pair-wise comparisons between CON, OXS A and OXS B. Box denotes 25th and 75th percentiles; line within box denotes 50th percentile (median); whisker denotes standard deviation. (b) PCA scores of urine metabolome. (c) PLS-DA scores of urine metabolome. The Score plot is represented, and it includes the number of components, the cumulative R2X, R2Y and Q2Y. Groups (*n* = 10 animals per group): CON, blue; OXSA, orange; OXSB, green.

PCA shows that the variance of the data was able to discriminate the OXS B group in front the others (Figure 4b). Furthermore, PLS-DA was performed to assess the discriminative power of the different groups (Figure 4c). The proportion of variance in the urine data explained by the model (R2X) is 52.6%. The percentage of Y variability explained by the model (R2Y) is 66.1% and, the estimation of the predictive performance of the models (Q2) is 58.1%. A model is considered to have good predictability when the Q2 is greater than 50%, [46], thus the predictive power of the model in urine was good. However, we observed the same tendency as PCA showing that OXS B segregates and OXS A and CON are close. The main metabolites with the highest VIP values, which reflects both the loading weights for each component and the variability of the response explained by this component (Table S2).

3.4 Microbiome profiling

The metagenomic analysis characterized the effect of oxidative stress on the microbiome of the cecum section to evaluate the highest variability and diversity of the gut tract. The taxonomic assignment has made possible to detect the presence of bacteria and viruses. In the case of the control group, 76% of readings generated have been assigned to bacteria and the rest to viruses; following the same pattern as control group, 73% of readings were assigned to bacteria in the OXS A; in contrast, 95% of readings were associated to bacteria in the OXS B group. The differences between the OXS B group and the rest were statistically significant (p-value < 0.02).

The representation of the bacterial communities in the PCA (beta diversity) shows that the communities of the OXS B group are remarkably different from the other groups (Figure 5a). Additionally, PERMANOVA showed statistical differences (F = 13.51, p-value < 0.01) indicating differences in bacteria composition/beta diversity, those differences are clearly associated with the OXS B group. The comparison of alpha diversity values (index that measures the richness of the sample) showed a clear decrease in chao 1 index in the OXS B group (Figure 5b), as it has been already observed in the beta diversity (Figure 5a).

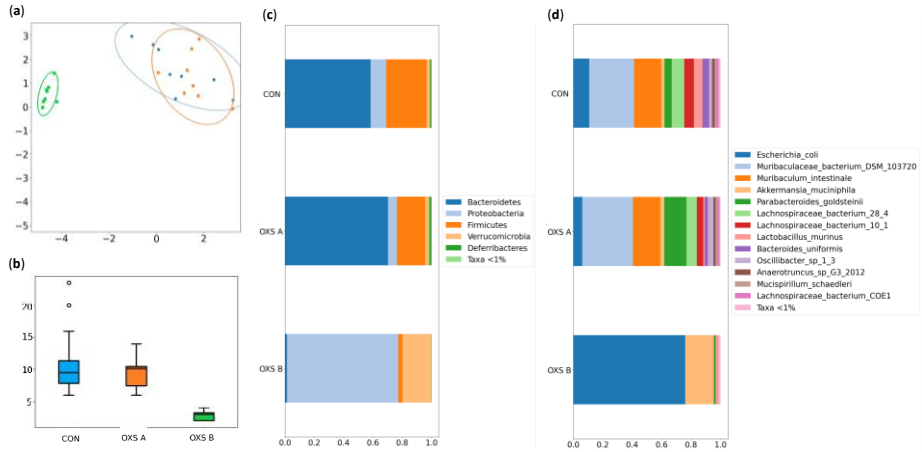

Figure 5. Summary of the bacteria statistical analysis in the oxidative stress model. (a) Beta diversity: PCA plot calculated by Aitchison distance. (b) Alpha diversity (AU): Chao1 index. (c) Relative distribution of bacterial phylum. (d) Relative distribution of bacterial species. Groups (n = 8 animals per group): CON, blue; OXSA, orange; OXSB, green.

In terms of bacterial diversity, the communities of the CON and OXS A groups are mainly formed by the phylum *Bacteroidetes* (CON: 58% and OXS A: 70%) and *Firmicutes* (CON: 27% and OXS A: 19%) while the OXS B group is dominated by *Proteobacteria* (76%) and *Verrucomicrobes* (19%) (Figure 5c). The relative proportions of all phyla reported by the OXS B group are statistically different from those reported in the other groups (Table S3). Focusing on species, 27 species were found with a relative abundance above 0.01% at least in one group (Figure 5d, Table S4). In the CON

and OXS A groups the species *Muribaculum intestinale* and *Murobaculaceae bacterium* predominate above the others. In contrast, *Escherichia coli* and *Akkermansia muciniphila* predominate in the OXS B group that could be explained by a decrease of the other species. Overall, the OXS B group is very different from the other two groups, with the main statistically significant differences that are indicated in table 3.

Table 3. Taxonomic statistical analysis of bacterial species between the CON, OXS A and OXS B group. Taxonomic data is presented as the mean of relative abundance (%). The summary of the analysis is shown including results of Kruskal-Wallis corrected by HS. * Denotes $p < 0.1$ (tendency), ** $p < 0.05$ (significantly different) and *** $p < 0.01$ (high significantly different).

	Corrected *p*-value				**Relative abundance (%)**		
Specie	CON vs OXS A vs OXS B	OXS A vs OXS B	CON vs OXS B	CON vs OXS A	CON	OXS A	OXS B
Muribaculaceae bacterium DSM 103720	< 0.01***	0.02**	< 0.01***	1.00	30.40%	34.43%	0.03%
Akkermansia muciniphila	< 0.01***	0.02**	< 0.01***	1.00	2.30%	2.75%	19.31%
Muribaculum intestinale	< 0.01***	0.02**	< 0.01***	1.00	18.49%	18.51%	-
Bifidobacterium pseudolongum	0.01**	0.02**	< 0.01***	1.00	-	-	0.15%
Anaerotruncus sp G3 2012	0.01**	0.02**	< 0.01***	1.00	1.87%	1.44%	0.04%
Escherichia coli	0.01**	0.02**	< 0.01***	1.00	10.79%	6.09%	76.00%
Oscillibacter sp 1 3	0.01**	0.02**	0.08*	0.55	1.90%	3.80%	0.09%
Lactobacillus johnsonii	0.02**	0.03**	0.01**	1.00	0.07%	0.01%	0.16%
Bacteroides uniformis	0.03**	0.28	0.01**	0.92	4.55%	2.18%	0.10%
Ruthenibacterium lactatiformans	0.03**	0.02**	0.04**	1.00	0.23%	0.03%	0.69%
Faecalibaculum rodentium	0.04**	0.05*	0.04**	1.00	-	-	0.04%

The representation of the virus communities in the PCA (beta diversity) shows that the communities of the different groups were similar (Figure S3a). In this line, the PERMANOVA test (F = 0.80, *p*-value > 0.05) indicates that there were no differences in bacteria composition/beta diversity. The comparison of Chao1 (index that measures the richness of the sample) indicated that the different groups presented similar alpha diversity (Figure S3b) following the same tendency as beta-diversity (Figure S3a). In terms of virus diversity, the communities of virus are mainly formed by the order of *Herpesvirales*, *Ortevirales* and *Caudovirales* (Figure S3c) without reporting differences between groups (data not shown). Focusing on species, 18 species were found with a relative abundance above 0.01% at least in one group (Table S5). We observed that some residual virus trend to differ between group, however these differences were

not considered due to beta diversity was not different and those residual differences could be associated to technical variability. In this case, *Cyprinid hespervirus 3* was the highest represented virus in all groups.

Furthermore, 37 functions were detected with a representation higher than 1% at least in one group, standing out the fermentation of pyruvate, which is the most abundant in the three groups. The groups present different distribution of the other functions with statistically significant differences, especially the OXS B group with respect to the rest (Table S6).

3.5 Multi-omics data integration

Previously, regression analyses were performed with PLS to further understand the cross-correlation between different omics. The data sets taken in a pairwise manner are highly correlated: plasma and urine metabolome (r = 0.93); plasma metabolome and microbiome (r = 0.97); urine metabolome and microbiome (r = 0.91). These correlations are used to tune the final DIABLO model that is constructed with 2 components (low error rate) and the selection of the optimal number of variables based on these 2 components: this selection includes 6 and 9 plasma metabolites; 20 and 5 urine metabolites; and 5 and 30 microbes for the 1-2 component, respectively.

The final model was able to discriminate between the different omics in Figure S4a and S4b, as it is observed there are some dissimilarities between animals across data sets (Figure S4b). The variables with higher impact were represented in Figure S4c. In general, the correlation structure in component 1 shows correlation between specific variables at different omics, while some plasma and urine metabolites seem to highly contribute to component 2. Focusing on component 1, the most important variables are LPC 18:2 (plasma metabolite), succinic acid (urine metabolite) and *Escherichia Coli* (microbes) among others (Figure 6a). Focusing on the multi-omics signature selected on component 2, the most important variables are a group of TGs plasma metabolites and a group of urine metabolites as Pseudouridine, 1-Methylnicotinamide and N,N-Dimethylglycine (Figure 6a). Additionally, the cross-correlations between omics, and the nature of these correlations are represented in Figure 6b, thus we can observe that correlations are between plasma metabolites and some urine metabolites and microbes. The majority negative correlations are observed between Pseudouridine and plasma metabolites. Additionally in plasma, LPCs and two amino acids (proline and hydroxyproline) are positive correlated with other omics as succinic acid and fumaric acid in urine. *Escherichia coli* and *Muribaculaceae bacterium DSM 103720* targets the negative and positive correlations between the other omics.

Finally, the performance of the model was assessed indicating a BER of 0.12. This error rate is almost null in the OXSB group, while CON presents the highest error. To complement the analysis, ROC and AUC shows that OXSA is the most difficult group to classify with DIABLO compared to the other groups (Figure S5). Thus, multi-omics

data integrations present a high prediction power highlighting the discrimination of OXSB versus CON and OXSA groups.

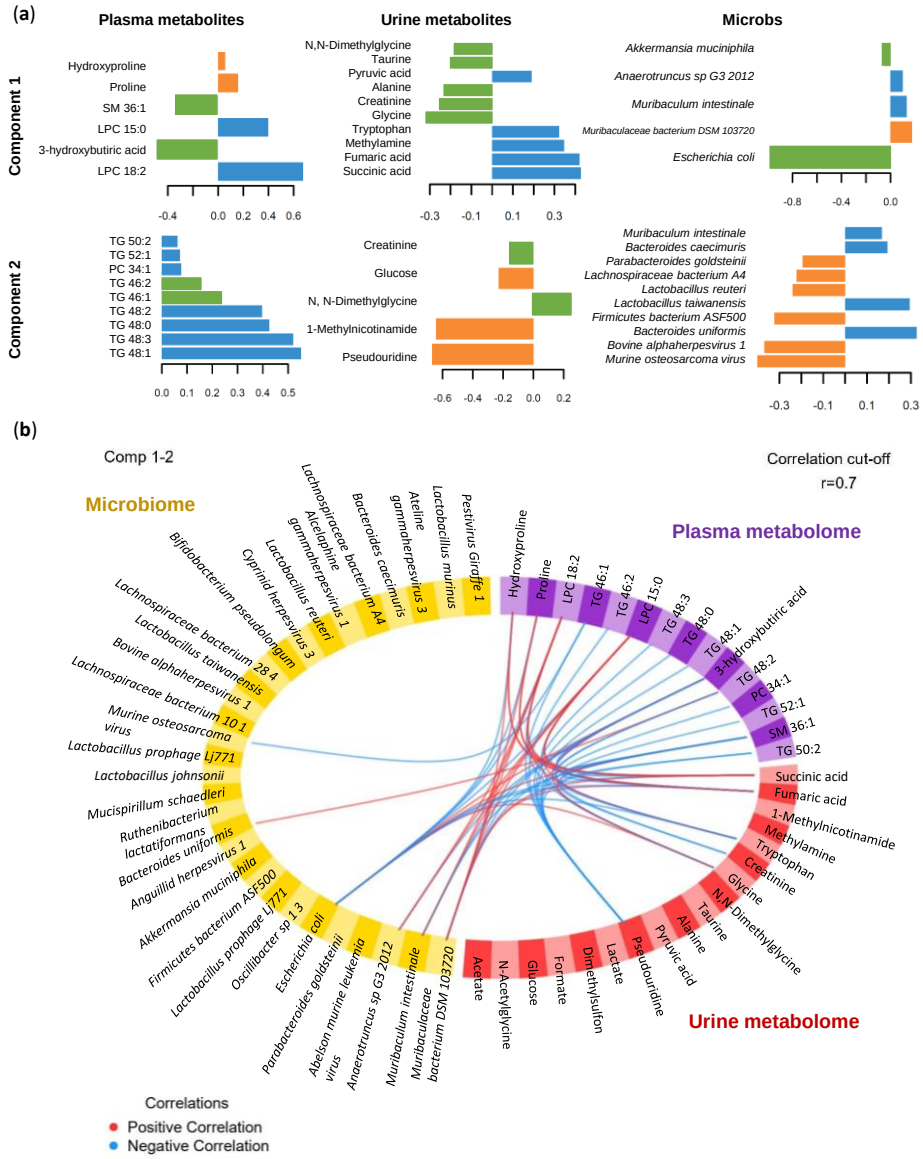

Figure 6. Multi-omics data integration of plasma metabolome, urine metabolome and microbiome using DIABLO in the oxidative stress model. (a) Loading plot for the variables selected in each data set and the 2 components. The most important variables are ordered from bottom to top. Colours indicate the group for which the median expression value is the highest for each feature: CON, blue; OXSA, orange; OXSB, green. (b) Circos plot. The plot represents the correlations greater than 0.7 between variables of different omics. Each quadrant indicates the type of features: plasma metabolites (purple), urine metabolites (red), microbes (yellow). The lines show the positive (red) and negative (blue) correlations. Abbreviations: LPC, lysophospholipid; PC, phosphatidylcholine; SM, sphingomyelin; TG, triglyceride.

4. Discussion

To determine the metabolic effects of oxidative stress, we explored the response of a PQ model in male Wistar rats with different degrees of oxidative stress. We generated oxidative stress chemically through a single IP administration of 15 and 30 mg/kg PQ [19,21]. Initially, the animals showed a decrease in BW as the dose increased, thus suggesting that increasing the dose of PQ is directly related to a greater impact on weight. The same weight observation carries over to the weight of specific tissues such as liver, which is the target of PQ [27], and food consumption, having a dose-dependent relationship.

Focusing on the classical biomarkers related to oxidative stress, an alteration in lipid peroxidation was observed both in liver and in plasma, represented by the high levels of MDA, as it is previously reported in PQ animal models [31,32]. Furthermore, trying to observe the systemic effect on other biofluid available, urine 8-isoprostanes were also increased in a dose-dependent manner as observed in previous studies [47]. Related to the PQ mechanism, the H_2O_2 accumulation is evidenced because both mitochondrial (SOD1) and cytoplasmic (SOD2) SOD expression are elevated in liver suggesting the increment of dismutation of $O_2^{\bullet-}$ to H_2O_2. Additionally, elevated levels of expression of CAT were observed indicating that the decomposition of H_2O_2 was reduced in liver. Those results were in the line of previous studies that indicate increase of SOD activity as a main characteristic of the oxidative model with PQ administration [48]. To further confirm our results, SOD activity was measured indicating an increase in liver, while SOD activity was not altered in plasma. One of the major antioxidant elements is GSH that plays an important role in the defence against oxidative stress damage due to the increment of GR that catalyse the reduction of GSSG to obtain GSH. Its major antioxidant properties are further manifested in direct scavenging of hydroxyl radicals and singlet oxygen, while it can also detoxify H_2O_2 and lipid peroxides in tandem with enzymatic action of GPx and glutathione transferases [49]. Finally, H_2O_2 decomposition is not increased because GPx1 values have not changed, therefore, it is another feature indicating H_2O_2 accumulation along with the decrease of CAT.

NLRP3 inflammasome plays a key role in sensing mitochondrial stress and responding with the activation and secretion of inflammatory cytokines such as interleukin 1 beta (IL-1β) to trigger inflammation [50,51]. The mechanism of PQ induces elevated mitochondrial H_2O_2 leading to mitochondrial stress and plays a key role in mediating PQ-induced NLRP3 inflammasome activation and elevation of brain inflammation [52]. Thus, circulating levels of IL-1β and MCP-1 were previously proposed as biomarkers for monitoring PQ-mediating inflammation [53]. In concordance, elevated levels of MCP-1 were assented in both groups independently to the dosage. Additionally to elevated levels of MCP-1, the treated groups presented higher excretion levels of N-acetylglycoproteins in urine that are biomarkers of systemic inflammation [13]. Those results suggest that the levels of oxidative stress

led to the activation of systemic inflammation as a consequence of the level of oxidative stress.

The mitochondrial stress generated by PQ administration, which has been confirmed by classical biomarkers such as MDA, SOD, CAT, GR and GPx1, was also observed in the plasma metabolic profile. Therefore, the plasma metabolic profile is characterised by altered metabolites associated with mitochondrial metabolism along with other related pathways, as summarised in Figure 7. In fact, it has long been recognized that energy metabolism is linked to the production of ROS and critical metabolites allied to metabolic pathways can be affected by redox reactions [54]. Mammals produce the majority metabolic energy from carbohydrates, with glucose as the principal substrate for energy production (ATP), that is produced through three well-known pathways: glycolysis, tricarboxylic acid (TCA) cycle and the electron transport chain.

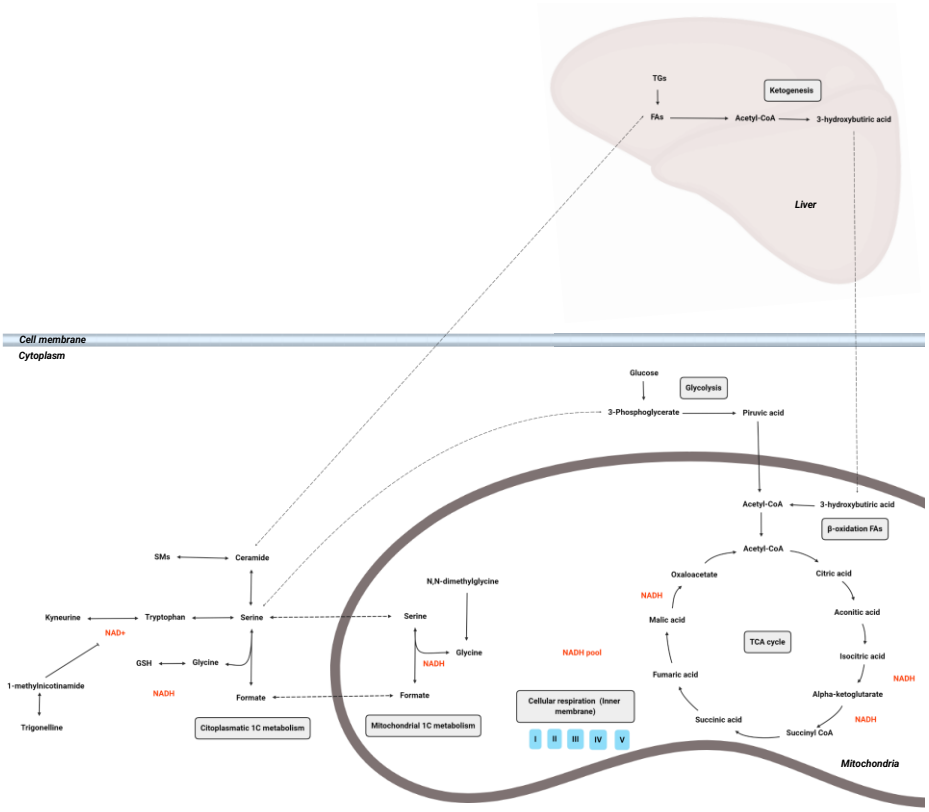

Figure 7. Overview of the candidate biomarkers and the main metabolic pathways implicated in the oxidative stress model. Abbreviations: TG, triacylglycerol; FA, fatty acid; SM, sphingomyelin; GSH, glutathione; NAD, nicotinamide adenine dinucleotide.

The TCA cycle, which constitutes an epicentre in cell metabolism because multiple substrates can feed into it, is one of the main altered pathways in the mitochondria that is considered a key cycle controlling physiology and diseases [55]. In the current research, citric acid and aconitic acid, which are intermediates of TCA cycle, were increased in the OXS A group while they were decreased in the OXS B. Thereby, our experimental approach suggests that in early oxidative stages (OXS A), TCA cycle increases in parallel to ketonic bodies accumulation; while in advanced oxidative stages (OXS B), the TCA cycle was disrupted, and the ketone bodies accumulation continue increasing. The H_2O_2 accumulation leads to the suppression of TCA cycle through the inhibition of enzymes implicated in the process that limits the availability of reduced nicotinamide adenine dinucleotide (NADH) for the respiratory chain under oxidative stress. On the assumption that H_2O_2 levels determine their effect on the TCA cycle and taking into account the results obtained for dose A and B, we can suggest two states for each dose in the line of previous studies [56,57]: (1) low H_2O_2 concentrations inactivate aconitase that is the most sensitive enzyme in the TCA cycle to H_2O_2 inhibition, thus glutamate fuels the TCA cycle and NADH generation is unaltered (OXS A), (2) high H_2O_2 concentrations also inhibits α-ketoglutarate dehydrogenase limiting the amount of NADH available for the respiratory chain (OXS B). This disruption of TCA cycle is shown also in urine metabolites of the group OXS B.

A crucial key metabolite linking TCA cycle and glycolysis is acetyl-CoA, a fundamental intermediate for ATP production as a main characteristic [58]. In fact, acetyl-CoA is the major product of fatty acid catabolism, thus plays a major role in ketogenesis that is the formation of ketone bodies [58]. The main altered ketone body in our animal model was 3-hydroxybutiric acid that functions as a stress molecule response and helps organisms to overcome stressful/pathological situations by triggering a molecular program for stress resistance similar to calorie restriction [59]. In fact, prolonged fasting events cause a decrease of glucose levels while the production of ketone bodies increases at the expense of liver β-oxidation of adipose tissue-derived fatty acids [60]. In our study, the oxidative stress response leads to a decrease of calorie intake mimicking a fasting reaction to overcome the increase of ROS. Thus, it has been shown a clear relation between the calorie restriction mechanism and stress resistance, however the exact mechanism linking calorie restriction to enhanced stress resistance, and particularly of reducing oxidative stress, is still missing [59]. It has been suggested that 3-hydroxybutiric acid mediates the beneficial effects of calorie restriction through its antioxidant activity: (1) acts as a direct antioxidant [61]; (2) inhibits mitochondrial ROS production through NADH oxidation [62]; (3) and promotes transcriptional activity of antioxidant defences [63].

In fasting episodes, ketone bodies are the alternative energy source of brain. However this shift to ketogenic metabolism is associated to the mitochondrial respiration dysfunction and an increase in H_2O_2 production in different neurodegenerative diseases [64]. These changes in mitochondrial function and shift to ketone body utilization in brain, have been linked to a mechanistic pathway that

connects early decline in mitochondrial respiration and H_2O_2 production to activation of pathway to catabolize myelin lipids (myelin to SMs, SMs to ceramide, ceramide to FAs and FAs to ketone bodies) resulting in white matter degeneration [65]. These lipids act as a local source of ketone body generation via astrocyte mediated β-oxidation of fatty acids. Astrocyte derived ketone bodies can then be transported to neurons where they undergo ketolysis to generate acetyl-CoA for TCA derived ATP generation required for synaptic and cell function [65]. This mechanism suggests a similar effect in our model due to the same pattern of increasing expression of 3-hydroxybutiric acid linked to the increase of SMs in both doses.

Indeed, the generation of ROS regulates SMs pathways, specifically this pathway is reversibly activated by H_2O_2 and reversibly inhibited by GSH. In our experimental approach, we suggest that the SMs pathway is up-regulated due to the high amount of H_2O_2 as well as GSH could not inhibit the activation of the pathway due to the large amount of H_2O_2 available. In previous studies, SM signalling cascade has been connected to oxidation in cell cycle and apoptotic signalling [66]. The SMs are recognized as a ubiquitous signalling system that links specific cell-surface receptors and environmental stresses to the nucleus [67]. Thus, the crosstalk between oxidation system and SM metabolism could have important implication for developing apoptosis which plays important role in NCD. In concordance, our data reflects an increase of total SMs in the treated groups being more pronounced in the OXS B group following a dose-dependent pattern.

Serine, which was increased in OXS A and decreased in OXS B, is a key amino acid acting as a central node linking glycolysis to GSH synthesis and one-carbon (1C) metabolic cycle, which are closely related to its antioxidant capacity [68]. 1C metabolism intermediate metabolites regulates oxidative stress with the production of NADH and GSH, which have an intrinsic ROS scavenging capacity, as has been previously described those metabolites are potential biomarker for oxidative stress [13]. In previous studies, serine decreases when oxidative rises, thus favouring the development of metabolic syndrome and obesity [69,70]. In this line, our results are the line with the decreased values of serine for OXS B group while we suggest that the increased levels of serine in the OXS A group were trying to regulate the ROS production in our experimental study. In addition, in vitro study declares that serine deficiency causes a higher response to oxidative stress and higher ROS content as is shown in group B [71].

Generally, elevated levels of LPC are associated with oxidative stress through the generation of ROS and systemic inflammation [72]. Interestingly, the LPC levels were decreased in the animals suffering oxidative stress in our model. LPC, which is the main component of oxLDL, originates from the cleavage of the membrane PC by phospholipase A2 (PLA_2). In this sense, inactivation of PLA_2, which could explain the low LPC levels, was detected in PQ exposed rats attributed to Fenton reaction as it is previous report [73]. Additionally, it has been be proposed that LPC-induced oxidative

stress may have a dual effect depending upon the amount and type of ROS, the duration of exposure and the type cell [74].

In this experimental approach, plasma metabolome provides a superior picture of the metabolic changes compared to urine metabolome, nonetheless there are interesting metabolites that could be discussed and linked to the plasma metabolic profile. Related to energy metabolism, the TCA cycle was decreased in group OXS B as it is previously described for plasma. For instance, 1-methylnicotinamide, a major urinary product of nicotinamide metabolism, was increased in animals with oxidative stress. This key metabolite was shown to inhibit NAD+ synthesis participating in redox homeostasis, making it central to energy metabolism [75]. Additionally, trigonelline a methylated 1-methylnicotinamide was decreased in the OXS B group. In the context of NAD+ synthesis, tryptophan is degraded to produce NAD+ in the kynurenine pathway that can be activated by stress and immunocytokines. The decrease of tryptophan in OXS B groups suggest that the tryptophan was displaced to generate NAD+. Those altered metabolites reflects the importance of NADH metabolism in energy metabolism and the subsequent development of metabolic disorders [76]. In previous studies, pseudouridine has been considered a secreted urinary oxidative stress biomarker, reflecting RNA turnover due to it is originated mainly from degraded rRNA and tRNA [77]. The OXS A group followed the general tendency of increased pseudouridine related to oxidative stress [78], while the OXS B group presented similar values to CON group. That fact could be explained due to pseudouridine could be accumulated in other tissue as it is previous report in the case of renal failure [79], and it is in consistence with the heterogenous results obtained in urine metabolomics across studies [13].

Our microbiome results, indicate a systemic alteration of microbes in the higher dose (OXS B group) due to the only difference was the injection of PQ and the diet was the same, as is in concordance with previous studies focused on injected insecticides [80,81] and their transfer to gastrointestinal track [82]. We suggest that the transfer of oxidative stress elevated H_2O_2 in the gut microbiome, leading to high dose killing of some microbes that are sensitive to different doses, which would explain the lack of homogeneous decrease of microbes in the gut microbiome. For example, one of the latest studies on early PQ exposure indicated that PQ reduced gut microbiota diversity and altered the structure of gut microbiota in adulthood in a murine model [83]. In this study, relative abundance of Firmicutes decreased, which is widely associated with obesity, as it was shown in the OXS A group while in OXS B group the relative abundance of Firmicutes and Bacteroidetes dramatically decreased in favour of Proteobacteria and Verrucomicrobia. Those changes suggested that Proteobacteria and Verrucomicrobia have efficient mechanism to manage oxidative stress in comparison to other phyla. For example, *Escherichia coli*, which was the main specie altered in Proteobacteria, has several major regulators activated during oxidative stress that are functionally conserved in a broad range of bacterial groups in Proteobacteria (SoxRS and RpoS), probably reflecting positive selection of these

regulators [84]. This could explain that *Escherichia coli* presented a different pattern being the most resistant in the OXS B group.

5. Conclusions

We have used a PQ-induced oxidative model to examine the metabolic effects of oxidative stress and have drawn a metabolic profile looking at specifically changed metabolites and the related pathways. Both groups were characterized by an excess of ROS, specifically H_2O_2, and mainly an excess of intracellular SOD, but each group presented some differences and similarities.

In both groups, 3-hydroxibutiric acid, SMs and LPCs were altered in a dose-dependent manner being key metabolites for monitoring the mitochondrial oxidative stress produced by PQ. Those metabolites are linked to lipid peroxidation, which was represented by high levels of MDA and 8-isoprostane, that are related to lipid metabolism as β-oxidation of fatty acids. Mitochondrial oxidative stress influences the membrane degradation and could be a key point to monitor the ROS impact on the individual before the onset of diseases. In fact, SMs degradation is related to neurobiological disorders as Parkinson or Alzheimer disease.

In contrast, TCA cycle was altered in both group but following different patterns that are related to the effort to return to homeostasis. In fact, the dose A was able to overcome the inhibition of TCA cycle by H_2O_2 and even increased, while dose B was found to inhibit both plasma and urine metabolites. Additionally, 1C cycle followed the same tendency has TCA Cycle being related to the effect of H_2O_2 and the available pool of NADH. In fact, 1C metabolism is involved in GDH synthesis a key redox molecule as the case of NADH. Collateral effects on gut microbiome were detected. The observed effect was based in the resistance of each microbe to ROS presenting different killing patterns depending on the dosage.

These findings provide an overview of systematic responses to PQ exposure and metabolomic insight into the oxidative stress mechanism induced by different doses of PQ. Although PQ is considered to be relatively toxic, it is a very close approximation to a hypothetical model of oxidative stress that is useful for exploring the impact of stress on the metabolome. Further research on oxidative stress is needed to develop more accurate models trying to avoid single chemical and toxicological procedures to confirm those results.

References

1. Pizzino, G.; Irrera, N.; Cucinotta, M.; Pallio, G.; Mannino, F.; Arcoraci, V.; Squadrito, F.; Altavilla, D.; Bitto, A. Oxidative Stress: Harms and Benefits for Human Health. *Oxid. Med. Cell. Longev.* **2017**, *2017*, 8416763, doi:10.1155/2017/8416763.

2. Toyokuni, S. Molecular mechanisms of oxidative stress-induced carcinogenesis: from epidemiology to oxygenomics. *IUBMB Life* **2008**, *60*, 441–447, doi:10.1002/iub.61.

3. Sies, H.; Cadenas, E. Oxidative stress: damage to intact cells and organs. *Philos. Trans. R. Soc. London. Ser. B, Biol. Sci.* **1985**, *311*, 617–631, doi:10.1098/rstb.1985.0168.

4. Kim, D.; Chen, Z.; Zhou, L.-F.; Huang, S.-X. Air pollutants and early origins of respiratory diseases. *Chronic Dis. Transl. Med.* **2018**, *4*, 75–94, doi:https://doi.org/10.1016/j.cdtm.2018.03.003.

5. Al-Gubory, K.H.; Garrel, C.; Faure, P.; Sugino, N. Roles of antioxidant enzymes in corpus luteum rescue from reactive oxygen species-induced oxidative stress. *Reprod. Biomed. Online* **2012**, *25*, 551–560, doi:10.1016/j.rbmo.2012.08.004.

6. Hansen, J.M.; Go, Y.-M.; Jones, D.P. Nuclear and mitochondrial compartmentation of oxidative stress and redox signaling. *Annu. Rev. Pharmacol. Toxicol.* **2006**, *46*, 215–234, doi:10.1146/annurev.pharmtox.46.120604.141122.

7. Glasauer, A.; Chandel, N.S. Targeting antioxidants for cancer therapy. *Biochem. Pharmacol.* **2014**, *92*, 90–101, doi:10.1016/j.bcp.2014.07.017.

8. Forman, H.J.; Zhang, H. Targeting oxidative stress in disease: promise and limitations of antioxidant therapy. *Nat. Rev. Drug Discov.* **2021**, *20*, 689–709, doi:10.1038/s41573-021-00233-1.

9. Forman, H.J.; Maiorino, M.; Ursini, F. Signaling functions of reactive oxygen species. *Biochemistry* **2010**, *49*, 835–842, doi:10.1021/bi9020378.

10. Deponte, M. Glutathione catalysis and the reaction mechanisms of glutathione-dependent enzymes. *Biochim. Biophys. Acta* **2013**, *1830*, 3217–3266, doi:10.1016/j.bbagen.2012.09.018.

11. Asmat, U.; Abad, K.; Ismail, K. Diabetes mellitus and oxidative stress—A concise review. *Saudi Pharm. J.* **2016**, *24*, 547–553, doi:https://doi.org/10.1016/j.jsps.2015.03.013.

12. Humer, E.; Pieh, C.; Probst, T. Metabolomic Biomarkers in Anxiety Disorders. *Int. J. Mol. Sci.* **2020**, *21*, 4784, doi:10.3390/ijms21134784.

13. Hernandez-Baixauli, J.; Quesada-Vázquez, S.; Mariné-Casadó, R.; Cardoso, K.G.; Caimari, A.; Del Bas, J.M.; Escoté, X.; Baselga-Escudero, L. Detection of early disease risk factors associated with metabolic syndrome: A new era with the NMR metabolomics assessment. *Nutrients* **2020**, *12*, 1–34, doi:10.3390/nu12030806.

14. Koch, R.E.; Hill, G.E. An assessment of techniques to manipulate oxidative stress in animals. *Funct. Ecol.* **2017**, *31*, 9–21.

15. Karimani, A.D.V.M.; Mamashkhani, Y.D.V.M.; Moghadam Jafari, A.P.; Akbarabadi, M.D.V.M.; Heidarpour, M.P. Captopril Attenuates Diazinon-Induced Oxidative Stress: A Subchronic Study in Rats. *Iran. J. Med. Sci.* **2018**, *43*, 514–522.

16. Zhang, H.; Chen, Y.; Chen, Y.; Jia, P.; Ji, S.; Xu, J.; Li, Y.; Wang, T. Comparison of the effects of resveratrol and its derivative pterostilbene on hepatic oxidative stress and mitochondrial dysfunction in piglets challenged with diquat. *Food Funct.* **2020**, *11*, 4202–4215, doi:10.1039/d0fo00732c.

17. Wang, Z.; Ma, J.; Zhang, M.; Wen, C.; Huang, X.; Sun, F.; Wang, S.; Hu, L.; Lin, G.; Wang, X. Serum Metabolomics in Rats after Acute Paraquat Poisoning. *Biol. Pharm. Bull.* **2015**, *38*, 1049–1053,

doi:10.1248/bpb.b15-00147.

18. Novaes, R.D.; Gonçalves, R.V.; Marques, D.C.S.; Cupertino, M. do C.; Peluzio, M. do C.G.; Leite, J.P.V.; Maldonado, I.R.D.S.C. Effect of bark extract of Bathysa cuspidata on hepatic oxidative damage and blood glucose kinetics in rats exposed to paraquat. *Toxicol. Pathol.* **2012**, *40*, 62–70, doi:10.1177/0192623311425059.

19. Novaes, R.D.; Gonçalves, R. V; Cupertino, M.C.; Santos, E.C.; Bigonha, S.M.; Fernandes, G.J.M.; Maldonado, I.R.S.C.; Natali, A.J. Acute paraquat exposure determines dose-dependent oxidative injury of multiple organs and metabolic dysfunction in rats: impact on exercise tolerance. *Int. J. Exp. Pathol.* **2016**, *97*, 114–124, doi:10.1111/iep.12183.

20. El-Boghdady, N.A.; Abdeltawab, N.F.; Nooh, M.M. Resveratrol and Montelukast Alleviate Paraquat-Induced Hepatic Injury in Mice: Modulation of Oxidative Stress, Inflammation, and Apoptosis. *Oxid. Med. Cell. Longev.* **2017**, *2017*, 9396425, doi:10.1155/2017/9396425.

21. Ahmed, M.A.E.; El Morsy, E.M.; Ahmed, A.A.E. Protective effects of febuxostat against paraquat-induced lung toxicity in rats: Impact on RAGE/PI3K/Akt pathway and downstream inflammatory cascades. *Life Sci.* **2019**, *221*, 56–64, doi:10.1016/j.lfs.2019.02.007.

22. Ranjbar, A.; Soleimani Asl, S.; Firozian, F.; Heidary Dartoti, H.; Seyedabadi, S.; Taheri Azandariani, M.; Ganji, M. Role of Cerium Oxide Nanoparticles in a Paraquat-Induced Model of Oxidative Stress: Emergence of Neuroprotective Results in the Brain. *J. Mol. Neurosci.* **2018**, *66*, 420–427, doi:10.1007/s12031-018-1191-2.

23. Liu, M.-W.; Su, M.-X.; Tang, D.-Y.; Hao, L.; Xun, X.-H.; Huang, Y.-Q. Ligustrazin increases lung cell autophagy and ameliorates paraquat-induced pulmonary fibrosis by inhibiting PI3K/Akt/mTOR and hedgehog signalling via increasing miR-193a expression. *BMC Pulm. Med.* **2019**, *19*, 35, doi:10.1186/s12890-019-0799-5.

24. Dasta, J.F. Paraquat poisoning: a review. *Am. J. Hosp. Pharm.* **1978**, *35*, 1368–1372.

25. Bismuth, C.; Garnier, R.; Baud, F.J.; Muszynski, J.; Keyes, C. Paraquat poisoning. An overview of the current status. *Drug Saf.* **1990**, *5*, 243–251, doi:10.2165/00002018-199005040-00002.

26. Blanco-Ayala, T.; Andérica-Romero, A.C.; Pedraza-Chaverri, J. New insights into antioxidant strategies against paraquat toxicity. *Free Radic. Res.* **2014**, *48*, 623–640, doi:10.3109/10715762.2014.899694.

27. Costa, M.D.; de Freitas, M.L.; Dalmolin, L.; Oliveira, L.P.; Fleck, M.A.; Pagliarini, P.; Acker, C.; Roman, S.S.; Brandão, R. Diphenyl diselenide prevents hepatic alterations induced by paraquat in rats. *Environ. Toxicol. Pharmacol.* **2013**, *36*, 750–758, doi:10.1016/j.etap.2013.07.009.

28. Clejan, L.; Cederbaum, A.I. Synergistic interactions between NADPH-cytochrome P-450 reductase, paraquat, and iron in the generation of active oxygen radicals. *Biochem. Pharmacol.* **1989**, *38*, 1779–1786, doi:10.1016/0006-2952(89)90412-7.

29. Fernandez, Y.; Subirade, I.; Anglade, F.; Periquet, A.; Mitjavila, S. Microsomal membrane peroxidation by an Fe3+/paraquat system. Consequences of phenobarbital induction. *Biol. Trace Elem. Res.* **1995**, *47*, 9–15, doi:10.1007/BF02790096.

30. Fukushima, T.; Yamada, K.; Isobe, A.; Shiwaku, K.; Yamane, Y. Mechanism of cytotoxicity of paraquat. I. NADH oxidation and paraquat radical formation via complex I. *Exp. Toxicol. Pathol. Off. J. Gesellschaft fur Toxikologische Pathol.* **1993**, *45*, 345–349, doi:10.1016/S0940-2993(11)80424-0.

31. Dicker, E.; Cederbaum, A.I. NADH-dependent generation of reactive oxygen species by microsomes in the presence of iron and redox cycling agents. *Biochem. Pharmacol.* **1991**, *42*, 529–535, doi:10.1016/0006-2952(91)90315-v.

32. Burk, R.F.; Lawrence, R.A.; Lane, J.M. Liver necrosis and lipid peroxidation in the rat as the result

of paraquat and diquat administration. Effect of selenium deficiency. *J. Clin. Invest.* **1980**, *65*, 1024–1031, doi:10.1172/JCI109754.

33. Miller, G.W. Paraquat: The Red Herring of Parkinson's Disease Research. *Toxicol. Sci.* **2007**, *100*, 1–2, doi:10.1093/toxsci/kfm223.

34. Castello, P.R.; Drechsel, D.A.; Patel, M. Mitochondria are a major source of paraquat-induced reactive oxygen species production in the brain. *J. Biol. Chem.* **2007**, *282*, 14186–14193, doi:10.1074/jbc.M700827200.

35. Xu, Y.; Tai, W.; Qu, X.; Wu, W.; Li, Z.; Deng, S.; Vongphouttha, C.; Dong, Z. Rapamycin protects against paraquat-induced pulmonary fibrosis: Activation of Nrf2 signaling pathway. *Biochem. Biophys. Res. Commun.* **2017**, *490*, 535–540, doi:https://doi.org/10.1016/j.bbrc.2017.06.074.

36. Hoffman, J.F.; Fan, A.X.; Neuendorf, E.H.; Vergara, V.B.; Kalinich, J.F. Hydrophobic Sand Versus Metabolic Cages: A Comparison of Urine Collection Methods for Rats (Rattus norvegicus). *J. Am. Assoc. Lab. Anim. Sci.* **2018**, *57*, 51–57.

37. Eggers, L.F.; Schwudke, D. Liquid Extraction: Folch BT - Encyclopedia of Lipidomics. In; Wenk, M.R., Ed.; Springer Netherlands: Dordrecht, 2016; pp. 1–6 ISBN 978-94-007-7864-1.

38. Beghini, F.; McIver, L.J.; Blanco-Míguez, A.; Dubois, L.; Asnicar, F.; Maharjan, S.; Mailyan, A.; Manghi, P.; Scholz, M.; Thomas, A.M.; et al. Integrating taxonomic, functional, and strain-level profiling of diverse microbial communities with bioBakery 3. *Elife* **2021**, *10*, doi:10.7554/eLife.65088.

39. Llorach-Asunción, R.; Jauregui, O.; Urpi-Sarda, M.; Andres-Lacueva, C. Methodological aspects for metabolome visualization and characterization: a metabolomic evaluation of the 24 h evolution of human urine after cocoa powder consumption. *J. Pharm. Biomed. Anal.* **2010**, *51*, 373–381, doi:10.1016/j.jpba.2009.06.033.

40. Fujisaka, S.; Avila-Pacheco, J.; Soto, M.; Kostic, A.; Dreyfuss, J.M.; Pan, H.; Ussar, S.; Altindis, E.; Li, N.; Bry, L.; et al. Diet, Genetics, and the Gut Microbiome Drive Dynamic Changes in Plasma Metabolites. *Cell Rep.* **2018**, *22*, 3072–3086, doi:10.1016/j.celrep.2018.02.060.

41. Tenenhaus, A.; Tenenhaus, M. Regularized Generalized Canonical Correlation Analysis. *Psychometrika* **2011**, *76*, 257, doi:10.1007/s11336-011-9206-8.

42. Rohart, F.; Gautier, B.; Singh, A.; Lê Cao, K.-A. mixOmics: An R package for 'omics feature selection and multiple data integration. *PLOS Comput. Biol.* **2017**, *13*, e1005752.

43. González, I.; Cao, K.-A.L.; Davis, M.J.; Déjean, S. Visualising associations between paired "omics" data sets. *BioData Min.* **2012**, *5*, 19, doi:10.1186/1756-0381-5-19.

44. Kanehisa, M.; Goto, S. KEGG: kyoto encyclopedia of genes and genomes. *Nucleic Acids Res.* **2000**, *28*, 27–30, doi:10.1093/nar/28.1.27.

45. Weydert, C.J.; Cullen, J.J. Measurement of superoxide dismutase, catalase and glutathione peroxidase in cultured cells and tissue. *Nat. Protoc.* **2010**, *5*, 51–66, doi:10.1038/nprot.2009.197.

46. Worley, B.; Powers, R. PCA as a practical indicator of OPLS-DA model reliability. *Curr. Metabolomics 4*, 97–103, doi:10.2174/2213235X04666160613122429.

47. Göcgeldi, E.; Uysal, B.; Korkmaz, A.; Ogur, R.; Reiter, R.J.; Kurt, B.; Oter, S.; Topal, T.; Hasde, M. Establishing the use of melatonin as an adjuvant therapeutic against paraquat-induced lung toxicity in rats. *Exp. Biol. Med. (Maywood).* **2008**, *233*, 1133–1141, doi:10.3181/0802-RM-65.

48. Krall, J.; Bagley, A.C.; Mullenbach, G.T.; Hallewell, R.A.; Lynch, R.E. Superoxide mediates the toxicity of paraquat for cultured mammalian cells. *J. Biol. Chem.* **1988**, *263*, 1910–1914.

49. Marí, M.; Morales, A.; Colell, A.; García-Ruiz, C.; Kaplowitz, N.; Fernández-Checa, J.C.

Mitochondrial glutathione: Features, regulation and role in disease. *Biochim. Biophys. Acta - Gen. Subj.* **2013**, *1830*, 3317–3328, doi:https://doi.org/10.1016/j.bbagen.2012.10.018.

50. Kepp, O.; Galluzzi, L.; Kroemer, G. Mitochondrial control of the NLRP3 inflammasome. *Nat. Immunol.* **2011**, *12*, 199–200, doi:10.1038/ni0311-199.

51. Zhou, R.; Yazdi, A.S.; Menu, P.; Tschopp, J. A role for mitochondria in NLRP3 inflammasome activation. *Nature* **2011**, *469*, 221–225, doi:10.1038/nature09663.

52. Chen, L.; Na, R.; Boldt, E.; Ran, Q. NLRP3 inflammasome activation by mitochondrial reactive oxygen species plays a key role in long-term cognitive impairment induced by paraquat exposure. *Neurobiol. Aging* **2015**, *36*, 2533–2543, doi:https://doi.org/10.1016/j.neurobiolaging.2015.05.018.

53. Yen, J.-S.; Wang, I.-K.; Liang, C.-C.; Fu, J.-F.; Hou, Y.-C.; Chang, C.-C.; Gu, P.-W.; Tsai, K.-F.; Weng, C.-H.; Huang, W.-H.; et al. Cytokine changes in fatal cases of paraquat poisoning. *Am. J. Transl. Res.* **2021**, *13*, 11571–11584.

54. Frisard, M.; Ravussin, E. Energy metabolism and oxidative stress. *Endocrine* **2006**, *29*, 27–32, doi:10.1385/ENDO:29:1:27.

55. Martínez-Reyes, I.; Chandel, N.S. Mitochondrial TCA cycle metabolites control physiology and disease. *Nat. Commun.* **2020**, *11*, 102, doi:10.1038/s41467-019-13668-3.

56. Tretter, L.; Adam-Vizi, V. Inhibition of Krebs cycle enzymes by hydrogen peroxide: A key role of [alpha]-ketoglutarate dehydrogenase in limiting NADH production under oxidative stress. *J. Neurosci.* **2000**, *20*, 8972–8979, doi:10.1523/JNEUROSCI.20-24-08972.2000.

57. Nulton-Persson, A.C.; Szweda, L.I. Modulation of mitochondrial function by hydrogen peroxide. *J. Biol. Chem.* **2001**, *276*, 23357–23361, doi:10.1074/jbc.M100320200.

58. Pietrocola, F.; Galluzzi, L.; Bravo-San Pedro, J.M.; Madeo, F.; Kroemer, G. Acetyl coenzyme A: a central metabolite and second messenger. *Cell Metab.* **2015**, *21*, 805–821, doi:10.1016/j.cmet.2015.05.014.

59. Rojas-Morales, P.; Pedraza-Chaverri, J.; Tapia, E. Ketone bodies, stress response, and redox homeostasis. *Redox Biol.* **2020**, *29*, 101395, doi:https://doi.org/10.1016/j.redox.2019.101395.

60. Puchalska, P.; Crawford, P.A. Multi-dimensional Roles of Ketone Bodies in Fuel Metabolism, Signaling, and Therapeutics. *Cell Metab.* **2017**, *25*, 262–284, doi:10.1016/j.cmet.2016.12.022.

61. Haces, M.L.; Hernández-Fonseca, K.; Medina-Campos, O.N.; Montiel, T.; Pedraza-Chaverri, J.; Massieu, L. Antioxidant capacity contributes to protection of ketone bodies against oxidative damage induced during hypoglycemic conditions. *Exp. Neurol.* **2008**, *211*, 85–96, doi:10.1016/j.expneurol.2007.12.029.

62. Maalouf, M.; Sullivan, P.G.; Davis, L.; Kim, D.Y.; Rho, J.M. Ketones inhibit mitochondrial production of reactive oxygen species production following glutamate excitotoxicity by increasing NADH oxidation. *Neuroscience* **2007**, *145*, 256–264, doi:10.1016/j.neuroscience.2006.11.065.

63. Luo, H.; Chiang, H.-H.; Louw, M.; Susanto, A.; Chen, D. Nutrient Sensing and the Oxidative Stress Response. *Trends Endocrinol. Metab.* **2017**, *28*, 449–460, doi:10.1016/j.tem.2017.02.008.

64. Jensen, N.J.; Wodschow, H.Z.; Nilsson, M.; Rungby, J. Effects of Ketone Bodies on Brain Metabolism and Function in Neurodegenerative Diseases. *Int. J. Mol. Sci.* **2020**, *21*, 8767, doi:10.3390/ijms21228767.

65. Klosinski, L.P.; Yao, J.; Yin, F.; Fonteh, A.N.; Harrington, M.G.; Christensen, T.A.; Trushina, E.; Brinton, R.D. White Matter Lipids as a Ketogenic Fuel Supply in Aging Female Brain: Implications for Alzheimer's Disease. *EBioMedicine* **2015**, *2*, 1888–1904, doi:10.1016/j.ebiom.2015.11.002.

66. Alessenko, A. V; Shupik, M.A.; Gutner, U.A.; Bugrova, A.E.; Dudnik, L.B.; Shingarova, L.N.; Mikoyan, A.; Vanin, A.F. The relation between sphingomyelinase activity, lipid peroxide oxidation and NO-releasing in mice liver and brain. *FEBS Lett.* **2005**, *579*, 5571–5576, doi:https://doi.org/10.1016/j.febslet.2005.08.085.

67. Hannun, Y.A.; Luberto, C.; Argraves, K.M. Enzymes of sphingolipid metabolism: from modular to integrative signaling. *Biochemistry* **2001**, *40*, 4893–4903, doi:10.1021/bi002836k.

68. Zhou, X.; He, L.; Wu, C.; Zhang, Y.; Wu, X.; Yin, Y. Serine alleviates oxidative stress via supporting glutathione synthesis and methionine cycle in mice. *Mol. Nutr. Food Res.* **2017**, *61*, doi:10.1002/mnfr.201700262.

69. Ducker, G.S.; Chen, L.; Morscher, R.J.; Ghergurovich, J.M.; Esposito, M.; Teng, X.; Kang, Y.; Rabinowitz, J.D. Reversal of Cytosolic One-Carbon Flux Compensates for Loss of the Mitochondrial Folate Pathway. *Cell Metab.* **2016**, *23*, 1140–1153, doi:10.1016/j.cmet.2016.04.016.

70. Palmnäs, M.S.A.; Kopciuk, K.A.; Shaykhutdinov, R.A.; Robson, P.J.; Mignault, D.; Rabasa-Lhoret, R.; Vogel, H.J.; Csizmadi, I. Serum metabolomics of activity energy expenditure and its relation to metabolic syndrome and obesity. *Sci. Rep.* **2018**, *8*, 1–12.

71. Maddocks, O.D.K.; Berkers, C.R.; Mason, S.M.; Zheng, L.; Blyth, K.; Gottlieb, E.; Vousden, K.H. Serine starvation induces stress and p53-dependent metabolic remodelling in cancer cells. *Nature* **2013**, *493*, 542–546, doi:10.1038/nature11743.

72. Liu, P.; Zhu, W.; Chen, C.; Yan, B.; Zhu, L.; Chen, X.; Peng, C. The mechanisms of lysophosphatidylcholine in the development of diseases. *Life Sci.* **2020**, *247*, 117443, doi:10.1016/j.lfs.2020.117443.

73. Giulivi, C.; Lavagno, C.C.; Lucesoli, F.; Bermüdez, M.J.; Boveris, A. Lung damage in paraquat poisoning and hyperbaric oxygen exposure: Superoxide-mediated inhibition of phospholipase a2. *Free Radic. Biol. Med.* **1995**, *18*, 203–213, doi:https://doi.org/10.1016/0891-5849(94)00111-V.

74. Kim, E.A.; Ae Kim, J.; Park, M.H.; Jung, S.C.; Suh, S.H.; Pang, M.-G.; Kim, Y.J. Lysophosphatidylcholine induces endothelial cell injury by nitric oxide production through oxidative stress. *J. Matern. Neonatal Med.* **2009**, *22*, 325–331, doi:10.1080/14767050802556075.

75. Ostrakhovitch, E.A.; Tabibzadeh, S. Chapter Two - Homocysteine in Chronic Kidney Disease. In; Makowski, G.S.B.T.-A. in C.C., Ed.; Elsevier, 2015; Vol. 72, pp. 77–106 ISBN 0065-2423.

76. Okabe, K.; Yaku, K.; Tobe, K.; Nakagawa, T. Implications of altered NAD metabolism in metabolic disorders. *J. Biomed. Sci.* **2019**, *26*, 34, doi:10.1186/s12929-019-0527-8.

77. Topp, H.; Fusch, G.; Schoch, G.; Fusch, C. Noninvasive markers of oxidative DNA stress, RNA degradation and protein degradation are differentially correlated with resting metabolic rate and energy intake in children and adolescents. *Pediatr. Res.* **2008**, *64*, 246–250, doi:10.1203/PDR.0b013e31817cfca6.

78. Miccheli, A.; Capuani, G.; Marini, F.; Tomassini, A.; Praticò, G.; Ceccarelli, S.; Gnani, D.; Baviera, G.; Alisi, A.; Putignani, L.; et al. Urinary 1H-NMR-based metabolic profiling of children with NAFLD undergoing VSL#3 treatment. *Int. J. Obes.* **2015**, *39*, 1118–1125, doi:10.1038/ijo.2015.40.

79. Dzúrik, R.; Lajdová, I.; Spustová, V.; Opatrný, K.J. Pseudouridine excretion in healthy subjects and its accumulation in renal failure. *Nephron* **1992**, *61*, 64–67, doi:10.1159/000186836.

80. Gao, B.; Chi, L.; Tu, P.; Gao, N.; Lu, K. The Carbamate Aldicarb Altered the Gut Microbiome, Metabolome, and Lipidome of C57BL/6J Mice. *Chem. Res. Toxicol.* **2019**, *32*, 67–79, doi:10.1021/acs.chemrestox.8b00179.

81. Liang, Y.; Zhan, J.; Liu, D.; Luo, M.; Han, J.; Liu, X.; Liu, C.; Cheng, Z.; Zhou, Z.; Wang, P. Organophosphorus pesticide chlorpyrifos intake promotes obesity and insulin resistance through impacting gut and gut microbiota. *Microbiome* **2019**, *7*, 19, doi:10.1186/s40168-019-0635-4.

82. Daniel, J.W.; Gage, J.C. Absorption and excretion of diquat and paraquat in rats. *Occup. Environ. Med.* **1966**, *23*, 133–136.

83. Li, Y.; Zuo, Z.; Zhang, B.; Luo, H.; Song, B.; Zhou, Z.; Chang, X. Impacts of early-life paraquat exposure on gut microbiota and body weight in adult mice. *Chemosphere* **2021**, 133135, doi:https://doi.org/10.1016/j.chemosphere.2021.133135.

84. Chiang, S.M.; Schellhorn, H.E. Regulators of oxidative stress response genes in Escherichia coli and their functional conservation in bacteria. *Arch. Biochem. Biophys.* **2012**, *525*, 161–169, doi:10.1016/j.abb.2012.02.007.

Annex. Supplementary Material of Manuscript 5

Supplementary table 1. Statistical analysis of plasma metabolites in the oxidative stress model. CON, OXS A and OXS B groups (*n* = 10 animals per group) are represented by relative abundances (AU). Relative abundances of metabolites are presented by the mean ± SEM. Plasma metabolites are shorted by VIPs. The summary of univariant and multivariate analysis is shown including *p*-value (Kruskal-Wallis test), *q*-value (correction with False discovery rate Benjamini-Hochberg test), post-Hoc test between groups if there are significant differences in Krustal-Wallis test and VIP value of PLS-DA. The statistically significant values (< 0.05) are highlighted in bold. Abbreviations: DG, diacylglycerol; ChoE, cholesterol ester; TG, triglyceride; PC, phosphatidylcholine; SM, sphingomyelin; LPC, lysophospholipid; PE, phosphatidylethanolamine.

Metabolite	CON	OXS A	OXS B	*p*-value	*q*-value	CON vs OXS A	CON vs OXS B	OXSA vs OXS B	VIP
Aconitic acid	0.005 ± 0.0002	0.011 ± 0.0011	0.002 ± 0.0002	**<0.01**	**<0.01**	**<0.01**	**<0.01**	**<0.01**	1.7
Citric acid	4.41 ± 0.11	5.09 ± 0.11	2.75 ± 0.14	**<0.01**	**<0.01**	**<0.01**	**<0.01**	**<0.01**	1.6
SM 36:1	1.39 ± 0.05	2.19 ± 0.28	5.28 ± 0.34	**<0.01**	**<0.01**	**0.02**	**<0.01**	**0.02**	1.6
3-hydroxybutiric acid	1.61 ± 0.06	2.54 ± 0.29	4.58 ± 0.19	**<0.01**	**<0.01**	**0.02**	**<0.01**	**0.02**	1.6
LPC 20:0	0.31 ± 0.01	0.34 ± 0.02	0.14 ± 0.01	**<0.01**	**<0.01**	0.39	**<0.01**	**<0.01**	1.6
LPC 15:0	0.96 ± 0.02	0.81 ± 0.06	0.45 ± 0.02	**<0.01**	**<0.01**	**0.02**	**<0.01**	**0.02**	1.6
SM 36:2	0.53 ± 0.02	0.74 ± 0.07	1.41 ± 0.09	**<0.01**	**<0.01**	**0.02**	**<0.01**	**0.02**	1.6
ChoE (22:6)	5.09 ± 0.41	5.16 ± 0.58	13.07 ± 0.66	**<0.01**	**<0.01**	0.83	**<0.01**	**<0.01**	1.6
SM 34:1	22.72 ± 0.67	31.58 ± 2.67	46.87 ± 1.81	**<0.01**	**<0.01**	**0.01**	**<0.01**	**0.03**	1.6
Serine	0.5 ± 0.04	0.74 ± 0.04	0.16 ± 0.03	**<0.01**	**<0.01**	**0.02**	**<0.01**	**<0.01**	1.5
SM 34:2	1.93 ± 0.06	2.42 ± 0.14	3.36 ± 0.13	**<0.01**	**<0.01**	**0.02**	**<0.01**	**0.03**	1.5
SM 38:1	0.56 ± 0.02	0.88 ± 0.11	1.49 ± 0.09	**<0.01**	**<0.01**	**0.01**	**<0.01**	0.06	1.5
LPC 18:1	17.22 ± 0.7	11.85 ± 0.83	8.15 ± 0.35	**<0.01**	**<0.01**	**0.01**	**<0.01**	**0.03**	1.5
LPC 18:2	52.7 ± 1.09	46.39 ± 4.11	24.49 ± 1.2	**<0.01**	**<0.01**	0.08	**<0.01**	**0.01**	1.5
Cholesterol	0.11 ± 0.01	0.16 ± 0	0.08 ± 0.01	**<0.01**	**<0.01**	**<0.01**	**0.02**	**<0.01**	1.5

Urea	0.77 ± 0.02	0.8 ± 0.03	1.11 ± 0.05	**<0.01**	**<0.01**	0.76	**<0.01**	**<0.01**	1.4
PC 32:2	0.36 ± 0.02	0.21 ± 0.04	0.12 ± 0.01	**<0.01**	**<0.01**	**<0.01**	**<0.01**	0.09	1.4
SM 35:1	0.23 ± 0.01	0.39 ± 0.04	0.42 ± 0.03	**<0.01**	**<0.01**	**<0.01**	**<0.01**	0.33	1.4
DG 34:3	0.79 ± 0.06	0.36 ± 0.03	0.41 ± 0.04	**<0.01**	**<0.01**	**<0.01**	**<0.01**	0.54	1.4
Fumaric acid	0.9 ± 0.04	0.6 ± 0.04	1.12 ± 0.08	**<0.01**	**<0.01**	**<0.01**	0.07	**<0.01**	1.4
PC 33:1	0.13 ± 0.01	0.08 ± 0.01	0.06 ± 0	**<0.01**	**<0.01**	**<0.01**	**<0.01**	0.25	1.3
ChoE (20:4)	103.57 ± 11.17	71 ± 3.79	171.05 ± 4.16	**<0.01**	**<0.01**	0.37	**<0.01**	**<0.01**	1.3
PC 38:2	0.28 ± 0.01	0.25 ± 0.02	0.15 ± 0.01	**<0.01**	**<0.01**	0.13	**<0.01**	**0.01**	1.3
ChoE (16:1)	0.59 ± 0.06	0.27 ± 0.04	0.15 ± 0.01	**<0.01**	**<0.01**	**<0.01**	**<0.01**	0.06	1.3
SM 42:3	6.6 ± 0.23	8.87 ± 0.83	11.52 ± 0.86	**<0.01**	**<0.01**	**0.02**	**<0.01**	0.06	1.3
LPC 16:0	80.8 ± 1.99	83.7 ± 3.85	61.2 ± 1.08	**<0.01**	**<0.01**	0.67	**<0.01**	**<0.01**	1.3
Fructose	2.17 ± 0.17	1.34 ± 0.05	2.76 ± 0.17	**<0.01**	**<0.01**	**<0.01**	0.05	**<0.01**	1.3
SM 33:1	0.38 ± 0.01	0.47 ± 0.03	0.54 ± 0.03	**<0.01**	**<0.01**	**0.01**	**<0.01**	0.14	1.3
LPC 16:1 e	0.13 ± 0	0.16 ± 0.01	0.17 ± 0.01	**<0.01**	**<0.01**	**<0.01**	**<0.01**	0.44	1.2
PC 38:3	1.45 ± 0.11	0.76 ± 0.18	0.68 ± 0.06	**<0.01**	**<0.01**	**<0.01**	**<0.01**	0.91	1.2
TG 46:0	0.35 ± 0.06	0.05 ± 0.02	0.44 ± 0.03	**<0.01**	**<0.01**	**<0.01**	0.49	**<0.01**	1.2
ChoE (22:5)	1.46 ± 0.12	1.1 ± 0.1	2.13 ± 0.15	**<0.01**	**<0.01**	0.06	**0.01**	**<0.01**	1.2
ChoE (16:0)	1.18 ± 0.06	1.6 ± 0.09	1.04 ± 0.12	**<0.01**	**<0.01**	**<0.01**	0.44	**<0.01**	1.2
DG 34:2	2.62 ± 0.11	2.01 ± 0.07	2.52 ± 0.09	**<0.01**	**<0.01**	**<0.01**	0.88	**<0.01**	1.2
PC 32:1	0.96 ± 0.12	0.4 ± 0.08	0.35 ± 0.04	**<0.01**	**<0.01**	**<0.01**	**<0.01**	0.72	1.2
SM 40:1	5.74 ± 0.23	7.6 ± 0.7	8.33 ± 0.44	**<0.01**	**<0.01**	**0.02**	**<0.01**	0.19	1.1
SM 40:2	0.93 ± 0.03	1.2 ± 0.09	1.34 ± 0.1	**<0.01**	**<0.01**	**<0.01**	**<0.01**	0.35	1.1
DG 34:1	1.45 ± 0.06	1.07 ± 0.07	1.23 ± 0.06	**<0.01**	**<0.01**	**<0.01**	0.10	0.10	1.1

Oleic acid	1.38 ± 0.04	1.6 ± 0.08	1.25 ± 0.03	**<0.01**	**<0.01**	0.06	**0.03**	**<0.01**	1.1
TG 46:1	0.2 ± 0.04	0.03 ± 0.02	0.18 ± 0.01	**<0.01**	**<0.01**	**<0.01**	0.89	**<0.01**	1.1
DG 36:2	1.6 ± 0.09	1.16 ± 0.06	1.22 ± 0.05	**<0.01**	**<0.01**	**<0.01**	**0.01**	0.66	1.1
TG 46:2	0.13 ± 0.02	0.02 ± 0.01	0.11 ± 0.01	**<0.01**	**<0.01**	**<0.01**	0.90	**<0.01**	1.1
PC 38:4	26.42 ± 0.86	33.53 ± 3.19	35.9 ± 1.41	**<0.01**	**<0.01**	0.06	**<0.01**	0.13	1.1
ChoE (18:1)	3.2 ± 0.13	3.84 ± 0.21	2.81 ± 0.16	**<0.01**	**<0.01**	**0.04**	0.08	**<0.01**	1.0
Glycolic acid	12.88 ± 0.44	13.1 ± 0.58	28.56 ± 5.95	**<0.01**	**<0.01**	0.89	**<0.01**	**<0.01**	1.0
Alpha-ketoglutarate	2.46 ± 0.13	1.85 ± 0.11	1.9 ± 0.1	**<0.01**	**<0.01**	**<0.01**	**0.01**	0.66	1.0
Glucose-6-phosphate	0.6 ± 0.05	0.77 ± 0.07	0.38 ± 0.06	**<0.01**	**<0.01**	0.10	**0.02**	**<0.01**	1.0
TG 50:4	1.99 ± 0.3	0.74 ± 0.41	0.4 ± 0.09	**<0.01**	**<0.01**	**<0.01**	**<0.01**	0.89	1.0
SM 39:1	0.22 ± 0.01	0.28 ± 0.04	0.36 ± 0.03	**<0.01**	**<0.01**	0.09	**<0.01**	0.09	1.0
TG 52:6	1.29 ± 0.17	0.56 ± 0.26	0.34 ± 0.06	**<0.01**	**<0.01**	**<0.01**	**<0.01**	0.89	1.0
PC 40:5	0.83 ± 0.04	0.81 ± 0.08	1.12 ± 0.05	**<0.01**	**<0.01**	0.64	**<0.01**	**<0.01**	1.0
ChoE (22:4)	12.04 ± 0.8	11.08 ± 1.02	17.31 ± 1.43	**<0.01**	0.01	0.60	**0.01**	**0.01**	1.0
TG 48:3	0.39 ± 0.07	0.09 ± 0.06	0.13 ± 0.02	**<0.01**	**<0.01**	**<0.01**	0.06	0.08	1.0
SM 32:1	0.25 ± 0.01	0.22 ± 0.02	0.32 ± 0.02	**<0.01**	0.01	0.26	**0.02**	**0.01**	1.0
ChoE (18:0)	0.1 ± 0.01	0.16 ± 0.01	0.14 ± 0.02	**<0.01**	**<0.01**	**<0.01**	0.09	0.21	1.0
PC 30:0	0.07 ± 0	0.05 ± 0.01	0.05 ± 0.01	**<0.01**	**<0.01**	**0.01**	**0.01**	0.88	1.0
SM 41:2	1.39 ± 0.04	1.74 ± 0.11	1.79 ± 0.15	**<0.01**	**<0.01**	**0.01**	**0.01**	0.97	1.0
Glyceric acid	1.1 ± 0.08	0.84 ± 0.06	0.72 ± 0.06	**<0.01**	**<0.01**	0.06	**<0.01**	0.28	1.0
TG 54:7	6.07 ± 0.67	3.3 ± 1.26	2.19 ± 0.36	**<0.01**	**<0.01**	**<0.01**	**<0.01**	0.77	1.0
PC 32:0	0.9 ± 0.03	1.03 ± 0.08	1.16 ± 0.05	**<0.01**	**<0.01**	0.22	**<0.01**	0.13	1.0
TG 50:3	8.43 ± 1.46	2.71 ± 1.61	2.55 ± 0.71	**<0.01**	**<0.01**	**<0.01**	**0.01**	0.41	0.9

LPC 18:0 e	0.08 ± 0	0.09 ± 0	0.08 ± 0.01	**<0.01**	**0.01**	**0.02**	0.41	**0.01**	0.9
SM 42:2	22.62 ± 0.86	28.47 ± 2.98	30.21 ± 1.78	**<0.01**	**<0.01**	0.11	**<0.01**	0.24	0.9
PC 34:0	0.4 ± 0.02	0.44 ± 0.03	0.52 ± 0.02	**<0.01**	**<0.01**	0.29	**<0.01**	0.05	0.9
TG 48:2	1.26 ± 0.25	0.34 ± 0.21	0.37 ± 0.06	**<0.01**	**<0.01**	**<0.01**	**0.03**	0.13	0.9
TG 48:1	1.57 ± 0.3	0.41 ± 0.2	0.71 ± 0.11	**<0.01**	**<0.01**	**<0.01**	0.09	0.06	0.9
LPC 16:0 e	0.4 ± 0.01	0.47 ± 0.02	0.43 ± 0.03	**0.02**	**0.02**	**0.01**	0.24	0.23	0.9
TG 54:4	14.67 ± 1.6	8.1 ± 3.06	6.04 ± 0.91	**<0.01**	**<0.01**	**<0.01**	**<0.01**	0.97	0.9
PC 35:2	0.56 ± 0.02	0.52 ± 0.05	0.4 ± 0.02	**<0.01**	**<0.01**	0.15	**<0.01**	**0.04**	0.9
ChoE (20:2)	2.46 ± 0.16	1.75 ± 0.26	1.69 ± 0.16	**<0.01**	**<0.01**	**0.02**	**0.02**	0.88	0.9
Malic acid	0.44 ± 0.02	0.33 ± 0.02	0.42 ± 0.03	**0.01**	**0.02**	**0.02**	0.89	**0.03**	0.9
SM 41:1	6.17 ± 0.21	7.73 ± 0.61	7.43 ± 0.58	**0.02**	**0.03**	0.05	0.06	0.76	0.9
TG 48:0	0.97 ± 0.1	0.52 ± 0.15	0.79 ± 0.06	**0.02**	**0.02**	**0.01**	0.39	0.13	0.9
TG 52:5	9.05 ± 1.17	4.73 ± 1.96	3.68 ± 0.73	**<0.01**	**<0.01**	**0.01**	**0.01**	0.80	0.9
ChoE (18:3)	2.39 ± 0.21	1.82 ± 0.14	1.53 ± 0.1	**<0.01**	**<0.01**	0.06	**<0.01**	0.24	0.9
Histidine	0.09 ± 0.01	0.16 ± 0.02	0.08 ± 0.03	**<0.01**	**<0.01**	**0.02**	0.26	**<0.01**	0.9
PC 34:1	6.84 ± 0.45	4.93 ± 0.55	6.71 ± 0.48	**0.02**	**0.02**	**0.02**	0.91	**0.02**	0.9
TG 51:2	0.81 ± 0.11	0.41 ± 0.17	0.35 ± 0.06	**<0.01**	**<0.01**	**<0.01**	**0.01**	0.62	0.9
2-hydroxyglutaric	0.76 ± 0.05	0.73 ± 0.06	1.22 ± 0.22	**0.04**	0.05	0.77	**0.04**	**0.04**	0.9
TG 54:3	4.82 ± 0.51	3.48 ± 1.18	1.67 ± 0.23	**<0.01**	**<0.01**	**0.03**	**<0.01**	0.17	0.8
SM 42:1	23.01 ± 0.85	27.7 ± 1.9	25.74 ± 1.4	0.06	0.07	-	-	-	0.8
SM 43:1	1.79 ± 0.08	2.16 ± 0.15	1.8 ± 0.1	0.07	0.08	-	-	-	0.8
TG 50:2	14.57 ± 2.28	6.37 ± 2.89	7.49 ± 1.7	**<0.01**	**<0.01**	**<0.01**	0.08	0.19	0.8
PC 40:4	0.29 ± 0.02	0.27 ± 0.04	0.38 ± 0.02	**0.01**	**0.01**	0.25	**0.03**	**0.01**	0.8

PC 33:0	0.04 ± 0	0.05 ± 0.01	0.03 ± 0	0.05	0.06	-	-	-	0.8
LPC 18:0	48.71 ± 1.03	55.14 ± 3.51	49.58 ± 1.05	0.31	0.33	-	-	-	0.8
Pyruvic acid	30.87 ± 2.02	23.77 ± 1.8	31.08 ± 1.56	**0.02**	**0.02**	**0.02**	0.84	**0.02**	0.8
TG 50:1	3.83 ± 0.55	1.89 ± 0.84	2.07 ± 0.48	**<0.01**	**<0.01**	**<0.01**	0.07	0.25	0.8
TG 54:6	19.84 ± 1.92	12.89 ± 3.24	22.01 ± 3.29	0.05	0.06	-	-	-	0.7
TG 52:2	15.48 ± 2.48	7.62 ± 3.91	7.4 ± 1.85	**<0.01**	**<0.01**	**<0.01**	0.05	0.30	0.7
TG 54:2	2.05 ± 0.3	2.1 ± 0.72	0.49 ± 0.07	**<0.01**	**<0.01**	0.60	**<0.01**	**<0.01**	0.7
Threonic acid	1.86 ± 0.16	2.1 ± 0.12	1.43 ± 0.13	**0.02**	**0.03**	0.15	0.12	**0.02**	0.7
TG 52:3	54.19 ± 6.72	29.27 ± 12.27	36.46 ± 8.08	**0.02**	**0.03**	**0.02**	0.22	0.22	0.7
Beta-alanine	0.23 ± 0.07	0.11 ± 0.01	1.02 ± 0.54	**<0.01**	**<0.01**	0.12	**0.02**	**<0.01**	0.7
Phenylalanine	1.77 ± 0.14	2.33 ± 0.09	3.74 ± 1.31	**0.01**	**0.02**	**0.01**	0.17	0.17	0.6
Isoleucine	0.95 ± 0.5	0.8 ± 0.14	14.07 ± 9.56	**<0.01**	**<0.01**	**0.02**	**<0.01**	0.41	0.6
Valine	1.91 ± 0.83	1.56 ± 0.1	20.64 ± 13.75	**<0.01**	**<0.01**	**0.01**	**0.01**	0.76	0.6
PC 31:0	0.06 ± 0	0.06 ± 0	0.05 ± 0	0.05	0.06	-	-	-	0.6
Leucine	0.33 ± 0.18	0.28 ± 0.04	4.39 ± 2.99	**<0.01**	**<0.01**	**0.01**	**0.01**	0.83	0.6
Glycerol	2.87 ± 0.16	2.53 ± 0.14	2.47 ± 0.12	0.16	0.17	**-**	**-**	-	0.6
Aspartic acid	1.19 ± 0.4	1.14 ± 0.08	4.7 ± 2.76	**0.01**	**0.01**	**0.03**	0.22	**0.01**	0.6
Glutamine	0.31 ± 0.18	0.15 ± 0.01	1.63 ± 1.11	0.08	0.09	-	-	-	0.5
Tyrosine	1.08 ± 0.32	0.76 ± 0.05	3.21 ± 1.81	0.45	0.47	-	-	-	0.5
ChoE (18:2)	29.79 ± 1.56	26 ± 1.42	28.56 ± 1.48	0.30	0.32	-	-	-	0.5
Methionine	0.22 ± 0.05	0.23 ± 0.01	0.72 ± 0.43	**<0.01**	**0.01**	**0.03**	0.13	**<0.01**	0.5
Glycine	6.48 ± 1.36	8.09 ± 0.27	19.98 ± 11.45	**0.01**	**0.01**	**0.01**	0.51	**0.01**	0.5
Tryptophan	2.13 ± 0.46	2.51 ± 0.17	6.45 ± 3.69	**0.02**	**0.02**	**0.03**	0.44	**0.02**	0.5

TG 50:0	0.22 ± 0.04	0.15 ± 0.07	0.25 ± 0.02	**0.04**	0.05	0.06	0.47	0.05	0.5
TG 52:1	0.8 ± 0.08	0.55 ± 0.24	0.58 ± 0.11	**0.04**	0.05	0.05	0.15	0.52	0.5
Ribose	30.94 ± 3.05	26.44 ± 3.09	38.01 ± 6.78	0.44	0.46				0.5
Lactic acid	4.52 ± 0.13	4.61 ± 0.15	4.91 ± 0.21	0.32	0.34				0.5
Ornithine	6.18 ± 1.64	6.41 ± 0.32	17.84 ± 10.54	**<0.01**	**<0.01**	**0.03**	0.10	**<0.01**	0.5
Alanine	1.42 ± 0.32	1.4 ± 0.08	3.43 ± 1.92	**0.01**	**0.02**	0.08	0.08	**0.01**	0.5
Asparagine	0.17 ± 0.03	0.31 ± 0.02	0.43 ± 0.27	**<0.01**	**<0.01**	**0.02**	0.17	**<0.01**	0.5
DG 36:4	3.79 ± 0.15	3.52 ± 0.17	3.87 ± 0.05	0.27	0.30				0.5
ChoE (17:1)	0.03 ± 0.01	0.02 ± 0.01	0.04 ± 0.02	0.42	0.43				0.4
Lysine	0.49 ± 0.13	0.53 ± 0.05	1.05 ± 0.51	0.13	0.14				0.4
Threonine	2.31 ± 0.24	2.93 ± 0.12	4.22 ± 2.13	**<0.01**	**0.01**	0.07	0.07	**<0.01**	0.4
ChoE (17:0)	0.07 ± 0.03	0.03 ± 0	0.06 ± 0.02	0.88	0.88				0.4
PC 36:4	25.43 ± 0.81	27.26 ± 2.13	26.93 ± 1.04	0.62	0.63				0.4
Hydroxyproline	3.82 ± 1.27	2.9 ± 0.23	6.8 ± 4.06	**0.01**	**0.02**	0.43	**0.02**	**0.02**	0.3
Glutamic acid	0.16 ± 0.03	0.24 ± 0.01	0.23 ± 0.13	**<0.01**	**<0.01**	**0.01**	0.09	**<0.01**	0.3
Proline	0.65 ± 0.06	0.83 ± 0.07	0.67 ± 0.34	**0.01**	**0.01**	0.16	**0.04**	**0.01**	0.3
Fructose-6-phosphate	0.47 ± 0.05	0.48 ± 0.05	0.41 ± 0.06	0.40	0.42				0.3
Alpha-tocopherol	0.55 ± 0.06	0.63 ± 0.06	0.54 ± 0.14	0.17	0.18				0.3
Glucose	0.22 ± 0.01	0.24 ± 0.01	0.22 ± 0.05	**0.04**	0.05	0.14	0.22	**0.03**	0.2
PC 36:2	18.99 ± 0.64	18.62 ± 2.1	17.96 ± 0.65	0.37	0.39				0.2
Succinic acid	0.49 ± 0.01	0.49 ± 0.02	0.48 ± 0.03	0.78	0.78				0.2

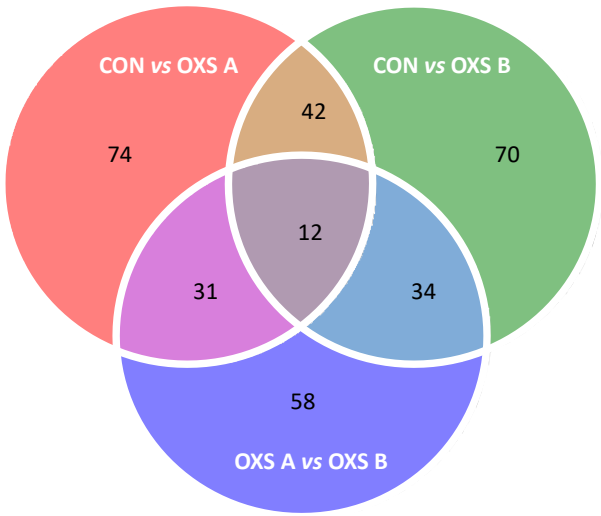

Supplementary figure 1. Venn-diagram of plasma metabolites with statistical differences. The numbers correspond to the total of metabolites presenting statistical differences

Supplementary table 2. Statistical analysis of urine metabolites in the oxidative stress model. CON, OXS A and OXS B groups (*n* = 10 animals per group) are represented by relative abundances (AU). Relative abundances of metabolites are presented by the mean ± SEM. Urine metabolites are shorted by VIPs. The summary of univariant and multivariate analysis is shown including *p*-value (Kruskal-Wallis test), *q*-value (correction with False discovery rate Benjamini-Hochberg test), post-Hoc test between groups if there are significant differences in Krustal-Wallis test and VIP value of PLS-DA. The statistically significant values (< 0.05) are highlighted in bold.

Metabolite	CON	OXS A	OXS B	*p*-value	*q*-value	CON vs OXS A	CON vs OXS B	OXSA vs OXS B	VIP
Hippurate	160.93 ± 8.42	166.66 ± 6.1	-	**<0.01**	**<0.01**	0.79	**<0.01**	**<0.01**	1.52
Trigonelline	2.59 ± 0.13	2.48 ± 0.04	0.04 ± 0.04	**<0.01**	**<0.01**	0.24	**<0.01**	**<0.01**	1.44
Fumaric acid	6.62 ± 0.42	5.44 ± 0.75	0.59 ± 0.13	**<0.01**	**<0.01**	0.15	**<0.01**	**<0.01**	1.39
Succinic acid	53 ± 2.82	51.42 ± 2.07	18.94 ± 1.86	**<0.01**	**<0.01**	0.80	**<0.01**	**<0.01**	1.34
Creatinine	228.98 ± 8.09	290.18 ± 9.37	319.77 ± 16.44	**<0.01**	**<0.01**	**<0.01**	**<0.01**	0.46	1.25
Pseudouridine	12 ± 0.47	14.98 ± 0.43	12.11 ± 0.49	**<0.01**	**<0.01**	**<0.01**	0.94	**<0.01**	1.18
1-Mehtylnicotinamide	0.09 ± 0.02	0.25 ± 0.04	0.21 ± 0.03	**<0.01**	**<0.01**	**<0.01**	**0.01**	0.66	1.14
Methylamine	5.87 ± 0.33	6.24 ± 0.4	3.28 ± 0.4	**<0.01**	**<0.01**	0.93	**<0.01**	**<0.01**	1.05
Tryptophan	7.46 ± 0.47	6.67 ± 0.54	4.41 ± 0.26	**<0.01**	**<0.01**	0.57	**<0.01**	**0.01**	0.97
Citric acid	405.1 ± 17.52	375.34 ± 42.58	29.56 ± 9.7	**<0.01**	**<0.01**	0.67	**<0.01**	**<0.01**	0.92
Alanine	6.44 ± 0.32	7.46 ± 0.47	9.36 ± 0.68	**<0.01**	**<0.01**	0.11	**<0.01**	0.11	0.91
Glycine	12.06 ± 0.74	12.7 ± 0.87	17.19 ± 0.75	**<0.01**	**<0.01**	0.50	**<0.01**	**0.01**	0.90
Lactate	13.52 ± 0.77	15.94 ± 0.84	17.76 ± 0.88	**<0.01**	**0.01**	0.12	**<0.01**	0.19	0.87
Dimethylsulfone	15.41 ± 0.54	21.67 ± 2.94	17.27 ± 1.73	0.20	0.21	-	-	-	0.81
N-Acetylglycoproteins	157.07 ± 5.95	178.33 ± 6.24	171.61 ± 5.94	**0.01**	**0.01**	**0.01**	**0.04**	0.57	0.80
Formate	2.27 ± 0.21	18.35 ± 11.88	4.36 ± 0.76	0.09	0.10	-	-	-	0.79
N,N-Dimethylglycine	11.18 ± 1.16	7.75 ± 1.2	17.49 ± 3.34	**0.03**	**0.04**	0.12	0.20	**0.03**	0.72
Taurine	201.52 ± 22.06	236.57 ± 23.81	278.47 ± 28.9	0.08	0.10	-	-	-	0.64

Glucose	7.63 ± 1.63	8.57 ± 0.73	6.11 ± 0.83	0.08	0.10	-	-	-	0.50
Pyruvic acid	6.88 ± 0.41	6.93 ± 0.3	5.91 ± 0.33	0.10	0.11	-	-	-	0.43
Acetate	5.62 ± 0.37	6.05 ± 0.51	5.51 ± 0.3	0.80	0.80	-	-	-	0.30

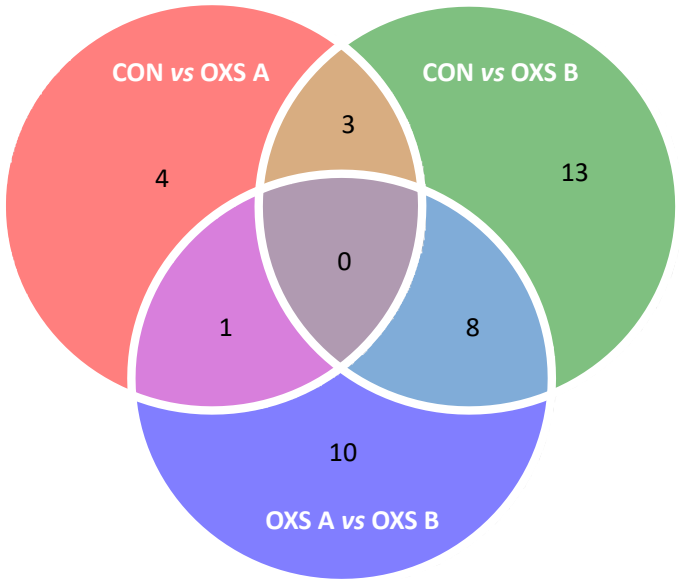

Supplementary figure 2. Venn-diagram of urine metabolites with statistical differences. The numbers correspond to the total of metabolites presenting statistical differences.

Supplementary table 3. Summary of bacteria phyla in the CON, OXS A and OXS B group (*n* = 8 animals per group). The summary of univariant analysis is shown including results of Kruskal-Wallis (p-value), Kruskal-Wallis corrected by HS (q-value) and FC, the statistically significant values (< 0.05) are highlighted in bold. Taxonomic data is presented as the mean of relative abundance (%).

	CON vs OXS A vs OXS B		**OXS A vs OXS B**			**CON vs OXS B**			**CON vs OXS A**			**Relative abundance (%)**		
Phylum	*p*-value	*q*-value	*p*-value	*q*-value	FC	*p*-value	*q*-value	FC	*p*-value	*q*-value	FC	CON	OXS A	OXS B
Bacteroidetes	**<0.01**	**<0.01**	**<0.01**	**<0.01**	0.02	**<0.01**	**<0.01**	0.02	0.90	0.95	1.20	58	70	1
Firmicutes	**<0.01**	**<0.01**	**<0.01**	**0.01**	0.15	**<0.01**	**<0.01**	0.10	0.14	0.53	0.70	27	19	3
Proteobacteria	**<0.01**	**0.01**	**0.01**	**0.01**	12.48	**<0.01**	**0.02**	7.05	0.76	0.95	0.56	11	6	76
Verrucomicrobia	**<0.01**	**<0.01**	**<0.01**	**0.01**	7.02	**<0.01**	**<0.01**	8.38	0.62	0.95	1.19	2	3	19
Deferribacteres	**0.02**	**0.02**	**0.03**	**0.01**	0.20	**0.01**	**0.05**	0.33	0.22	0.63	1.60	1	2	0.3
Actinobacteria	**0.01**	**0.01**	**0.02**	**0.01**	-	**0.01**	**0.05**	2.16	0.06	0.30	-	0.1	0.0	0.2

Supplementary table 4. Summary of bacteria species in the CON, OXS A and OXS B group (*n* = 8 animals per group). The summary of univariant analysis is shown including results of Kruskal-Wallis (*p*-value), Kruskal-Wallis corrected by Holm-Šídák (*q*-value) and FC, the statistically significant values (< 0.05) are highlighted in bold. Taxonomic data is presented as the mean of relative abundance (%).

	CON vs OXS A vs OXS B		**OXS A vs OXS B**			**CON vs OXS B**			**CON vs OXS A**			**Relative abundance (%)**		
Specie	*p*-value	*q*-value	*p*-value	*q*-value	FC	*p*-value	*q*-value	FC	*p*-value	*q*-value	FC	CON	OXS A	OXS B
Muribaculaceae bacterium DSM 103720	**<0.01**	**<0.01**	**<0.01**	**0.02**	-	**<0.01**	**<0.01**	-	0.46	1.00	1.1	30.40	34.43	0.03
Muribaculum intestinale	**<0.01**	**<0.01**	**<0.01**	**0.02**	-	**<0.01**	**<0.01**	-	0.71	1.00	1	18.49	18.51	-
Escherichia coli	**<0.01**	**0.01**	**<0.01**	**0.02**	12.4	**<0.01**	**<0.01**	7-	0.81	1.00	0.6	10.79	6.09	76.00
Lachnospiraceae bacterium 28 4	0.35	0.82	0.17	0.66	0.1	0.50	0.97	-	0.30	1.00	0.8	8.60	6.94	0.32
Lachnospiraceae bacterium 10 1	**0.01**	0.10	0.34	0.66	-	**<0.01**	**0.02**	-	0.16	0.98	0.7	6.44	4.46	0.06
Lactobacillus murinus	**0.02**	0.17	0.14	0.66	1.3	0.20	0.83	0.2	**0.01**	0.19	0.1	5.88	0.84	1.07
Parabacteroides goldsteinii	**0.03**	0.22	**0.02**	0.24	0.1	0.27	0.89	0.2	**0.04**	0.71	3.2	4.80	15.13	1.15
Bacteroides uniformis	**<0.01**	**0.03**	**0.04**	0.28	-	**<0.01**	**0.01**	0.02	0.10	0.92	0.5	4.55	2.18	0.10
Akkermansia muciniphila	**<0.01**	**<0.01**	**<0.01**	**0.02**	7	**<0.01**	**<0.01**	8.4	0.50	1.00	1.2	2.30	2.75	19.31
Oscillibacter sp 1 3	**<0.01**	**0.01**	**<0.01**	**0.02**	-	**0.01**	0.08	0.1	**0.03**	0.55	2	1.90	3.80	0.09
Anaerotruncus sp G3 2012	**<0.01**	**0.01**	**<0.01**	**0.02**	-	**<0.01**	**<0.01**	-	0.85	1.00	0.8	1.87	1.44	0.04
Lachnospiraceae bacterium COE1	0.35	0.82	0.14	0.66	-	0.62	0.97	-	0.30	1.00	0.7	1.63	1.12	0.00
Mucispirillum schaedleri	0.08	0.43	0.05	0.31	0.2	0.27	0.89	0.3-	0.09	0.90	1.6	1.00	1.60	0.33
Lactobacillus taiwanensis	**0.01**	0.12	**<0.01**	**0.02**	-	0.07	0.50	1	0.18	0.99	-	0.26	-	0.27
Ruthenibacterium lactatiformans	**<0.01**	**0.03**	**<0.01**	**0.02**	22	**<0.01**	**0.04**	3	0.58	1.00	0.1	0.23	0.03	0.69
Firmicutes bacterium ASF500	**0.01**	0.14	**0.01**	0.11	0.10	0.06	0.48	0.2	0.08	0.88	1.9	0.21	0.39	0.04
Lachnospiraceae bacterium A4	0.77	0.82	0.29	0.66	-	0.76	0.97	-	0.90	1.00	1	0.17	0.17	-

Bacteroides caecimuris	0.41	0.82	0.29	0.66	2.02	0.54	0.97	0.4	0.24	1.00	0.2	0.13	0.03	0.05
Lactobacillus reuteri	0.24	0.74	0.14	0.66	0.39	0.13	0.70	0.3	1.00	1.00	0.7	0.11	0.08	0.03
Enterorhabdus caecimuris	**0.01**	0.14	**0.01**	0.11	-	**0.01**	0.14	0.4	0.58	1.00	-	0.08	-	0.03
Lactobacillus johnsonii	**<0.01**	**0.02**	**<0.01**	**0.03**	31.23	**<0.01**	**0.01**	2.2	0.50	1.00	0.1	0.07	0.01	0.16
Romboutsia ilealis	**0.02**	0.17	**0.03**	0.24	0.48	**0.01**	0.10	0.2	0.50	1.00	0.3	0.04	0.01	0.01
Acutalibacter muris	0.12	0.55	**0.02**	0.24	-	0.67	0.97	-	0.20	0.99	-	0.04	-	-
Bifidobacterium pseudolongum	**<0.01**	**0.01**	**<0.01**	**0.02**	-	**<0.01**	**<0.01**	-	0.54	1.00	-	-	-	0.15
Enterococcus faecalis	**<0.01**	0.09	**0.02**	0.24	-	**<0.01**	**0.04**	-	0.54	1.00	-	-	-	0.01
Blautia coccoides	**0.01**	0.10	**0.02**	0.24	-	**<0.01**	**0.04**	-	0.54	1.00	-	-	-	0.02
Faecalibaculum rodentium	**<0.01**	**0.04**	**<0.01**	0.05	-	**<0.01**	**0.04**	-	0.54	1.00	-	-	-	0.04

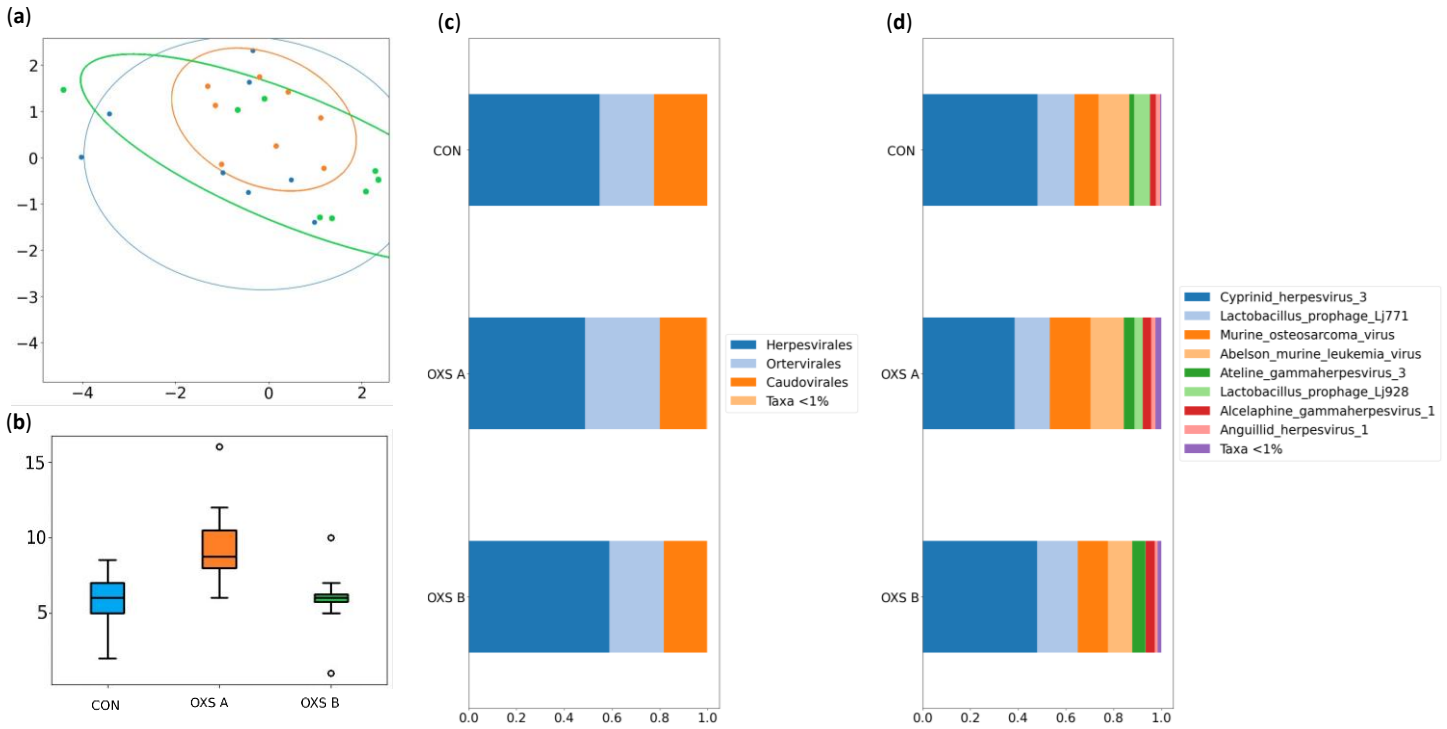

Supplementary figure 3. Summary of the virus statistical analysis in the oxidative stress model. (a) Beta diversity: PCA plot calculated by Aitchison distance. (b) Alpha diversity (AU): Chao1 index. (c) Relative distribution of virus phylum. (d) Relative distribution of virus species. Groups (n = 8 animals per group): CON, blue; OXSA, orange; OXSB, green.

Supplementary table 5. Summary of virus species in the CON, OXS A and OXS B group (*n* = 8 animals per group). The summary of univariant analysis is shown including results of Kruskal-Wallis (*p*-value), Kruskal-Wallis corrected by Holm-Šídák (*q*-value) and FC, the statistically significant values (< 0.05) are highlighted in bold. Taxonomic data is presented as the mean of relative abundance (%).

	CON vs OXS A vs OXS B		**OXS A vs OXS B**			**CON vs OXS B**			**CON vs OXS A**			**Relative abundance (%)**		
Specie	*p*-value	*q*-value	*p*-value	*q*-value	FC	*p*-value	*q*-value	FC	*p*-value	*q*-value	FC	CON	OXS A	OXS B
Cyprinid herpesvirus 3	**<0.01**	0.06	**0.02**	0.29	1.5	0.46	0.99	1	**<0.01**	**0.02**	0.8	48.08	38.45	47.96
Lactobacillus prophage Lj771	0.25	0.90	0.17	0.78	1.2	0.13	0.93	1.1	0.85	0.97	1	15.51	14.80	16.99
Abelson murine leukemia virus	0.79	0.96	1.00	1.00	0.7	0.81	0.99	0.8	0.43	0.97	1	12.82	14.10	10.23
Murine osteosarcoma virus	0.78	0.96	0.40	0.88	0.7	0.95	0.99	1.3	0.62	0.97	1.7	10.12	16.98	12.61
Lactobacillus prophage Lj928	0.07	0.53	**0.03**	0.34	-	0.08	0.82	-	0.39	0.97	0.5	6.68	3.53	0.16
Alcelaphine gammaherpesvirus 1	0.57	0.96	0.29	0.88	1.1	0.43	0.99	1.6	0.76	0.97	1.5	2.41	3.56	3.83
Ateline gammaherpesvirus 3	0.08	0.58	0.14	0.75	1.3	0.04	0.58	3	0.36	0.97	2	2.06	4.32	5.53
Anguillid herpesvirus 1	0.55	0.96	0.60	0.88	0.6	0.39	0.99	0.6	0.39	0.97	1	1.91	1.85	1.17
Pestivirus Giraffe 1	0.15	0.77	0.07	0.66	0.8	0.24	0.99	2.2	0.22	0.89	2.5	0.16	0.40	0.34
Human alphaherpesvirus 2	**<0.01**	**0.02**	**0.01**	0.17	-	0.10	0.89	-	**<0.01**	**0.02**	-	0.14	0.00	0.00
Bovine alphaherpesvirus 1	0.39	0.92	0.17	0.78	0.8	0.39	0.99	3	0.50	0.97	3.6	0.13	0.45	0.37
Salmonella phage RE 2010	**0.04**	0.41	0.07	0.66	-	0.22	0.99	-	0.02	0.26	-	-	0.67	-
Enterobacteria phage mEp460	**0.04**	0.41	0.07	0.66	-	0.22	0.99	-	0.02	0.26	-	-	0.22	-
Enterococcus phage phiEf11	**<0.01**	**0.04**	0.01	0.14	-	0.71	0.99	-	**<0.01**	**0.02**	-	-	0.00	0.81
Feline leukemia virus	**0.04**	0.41	0.07	0.66	-	0.22	0.99	-	0.02	0.26	-	-	0.21	-
Koala retrovirus	0.25	0.90	0.34	0.88	-	0.22	0.99	-	0.18	0.88	-	-	0.14	-
Chrysodeixis chalcites nucleopolyhedrovirus	0.25	0.90	0.34	0.88	-	0.22	0.99	-	0.18	0.88	-	-	0.26	-
Molluscum contagiosum virus	**0.04**	0.41	0.07	0.66	-	0.22	0.99	-	0.02	0.26	-	-	0.04	-

Supplementary table 6. Statistically significant differences in functions between the experimental groups of the oxidative stress model. In this table, the most abundant functions are represented in CON, OXS A and OXS B groups (*n* = 8 animals per group). The summary of analysis is shown including results of Kruskal-Wallis corrected by HS (*q*-value) and % relative of each function, the statistically significant values (< 0.05) are highlighted in bold.

	Corrected *p*-value				**Relative %**		
	CON vs OXS A vs OXS B	CON vs OXS A	OXS A vs OXS B	CON vs OXS B	CON	OXS A	**OXS B**
PWY-7111: pyruvate fermentation to isobutanol (engineered)	**0.001**	0.462	**0.001**	**0.001**	3.60	2.44	**1.31**
PWY-7219: adenosine ribonucleotides de novo biosynthesis	**0.001**	0.854	**0.001**	**0.001**	2.95	2.04	**0.65**
PWY-6122: 5-aminoimidazole ribonucleotide biosynthesis II	**0.001**	0.582	**0.001**	**0.001**	2.56	2.15	**0.69**
PWY-6277: superpathway of 5-aminoimidazole ribonucleotide biosynthesis	**0.001**	0.582	**0.001**	**0.001**	2.56	2.15	**0.69**
DTDPRHAMSYN-PWY: dTDP-L-rhamnose biosynthesis I	**0.001**	0.540	**0.001**	**0.001**	2.43	1.65	**0.14**
VALSYN-PWY: L-valine biosynthesis	**0.004**	0.854	**0.001**	**0.004**	2.30	2.45	**1.21**
ILEUSYN-PWY: L-isoleucine biosynthesis I (from threonine)	**0.003**	0.582	**0.001**	**0.003**	2.21	2.32	**1.21**
PWY-6609: adenine and adenosine salvage III	**<0.001**	0.270	**0.001**	**0.000**	1.86	1.50	**0.41**
PWY-1042: glycolysis IV (plant cytosol)	**0.002**	0.501	**0.001**	**0.003**	1.81	2.02	**0.67**
SER-GLYSYN-PWY: superpathway of L-serine and glycine biosynthesis I	**0.000**	0.245	**0.001**	**0.001**	1.80	1.52	**0.48**
TRNA-CHARGING-PWY: tRNA charging	**0.002**	0.358	**0.001**	**0.004**	1.70	1.98	**0.55**
PWY-6121: 5-aminoimidazole ribonucleotide biosynthesis I	**0.002**	0.391	**0.001**	**0.003**	1.67	1.87	**0.64**
BRANCHED-CHAIN-AA-SYN-PWY: superpathway of branched amino acid biosynthesis	**0.003**	0.713	**0.001**	**0.003**	1.64	1.68	**0.94**
PWY-3841: folate transformations II	**0.001**	0.111	**0.001**	**0.004**	1.57	1.92	**0.40**
PWY-5103: L-isoleucine biosynthesis III	**0.003**	0.668	**0.001**	**0.003**	1.52	1.54	**0.90**
PWY-5104: L-isoleucine biosynthesis IV	**0.004**	0.713	**0.001**	**0.004**	1.37	1.46	**0.51**

CALVIN-PWY: Calvin-Benson-Bassham cycle	**0.002**	0.854	**0.001**	**0.002**	1.33	1.44	**0.67**
PWY-6123: inosine-5'-phosphate biosynthesis I	**0.003**	0.759	**0.001**	**0.004**	1.25	1.43	**0.45**
PWY-7400: L-arginine biosynthesis IV (archaebacteria)	**0.002**	0.713	**0.001**	**0.003**	1.19	1.29	**0.49**
ARGSYN-PWY: L-arginine biosynthesis I (via L-ornithine)	**0.002**	0.759	**0.001**	**0.003**	1.18	1.28	**0.49**
GLYCOGENSYNTH-PWY: glycogen biosynthesis I (from ADP-D-Glucose)	**0.003**	0.759	**0.001**	**0.004**	1.18	1.25	**0.42**
PWY-6124: inosine-5'-phosphate biosynthesis II	**0.003**	0.624	**0.001**	**0.003**	1.17	1.34	**0.44**
PWY-7229: superpathway of adenosine nucleotides de novo biosynthesis I	**0.002**	0.178	**0.001**	**0.005**	1.17	1.46	**0.51**
PWY0-1296: purine ribonucleosides degradation	**0.001**	0.426	**0.015**	**0.000**	1.17	0.68	**0.40**
PWY-5686: UMP biosynthesis	**0.003**	0.854	**0.001**	**0.004**	1.14	1.27	**0.52**
ARGSYNBSUB-PWY: L-arginine biosynthesis II (acetyl cycle)	**0.004**	0.713	**0.001**	**0.006**	1.07	1.14	**0.63**
PWY-6700: queuosine biosynthesis	**0.002**	0.327	**0.001**	**0.004**	1.04	1.28	**0.45**
PWY-6126: superpathway of adenosine nucleotides de novo biosynthesis II	**0.005**	**0.221**	**0.001**	**0.016**	**1.01**	**1.27**	**0.45**

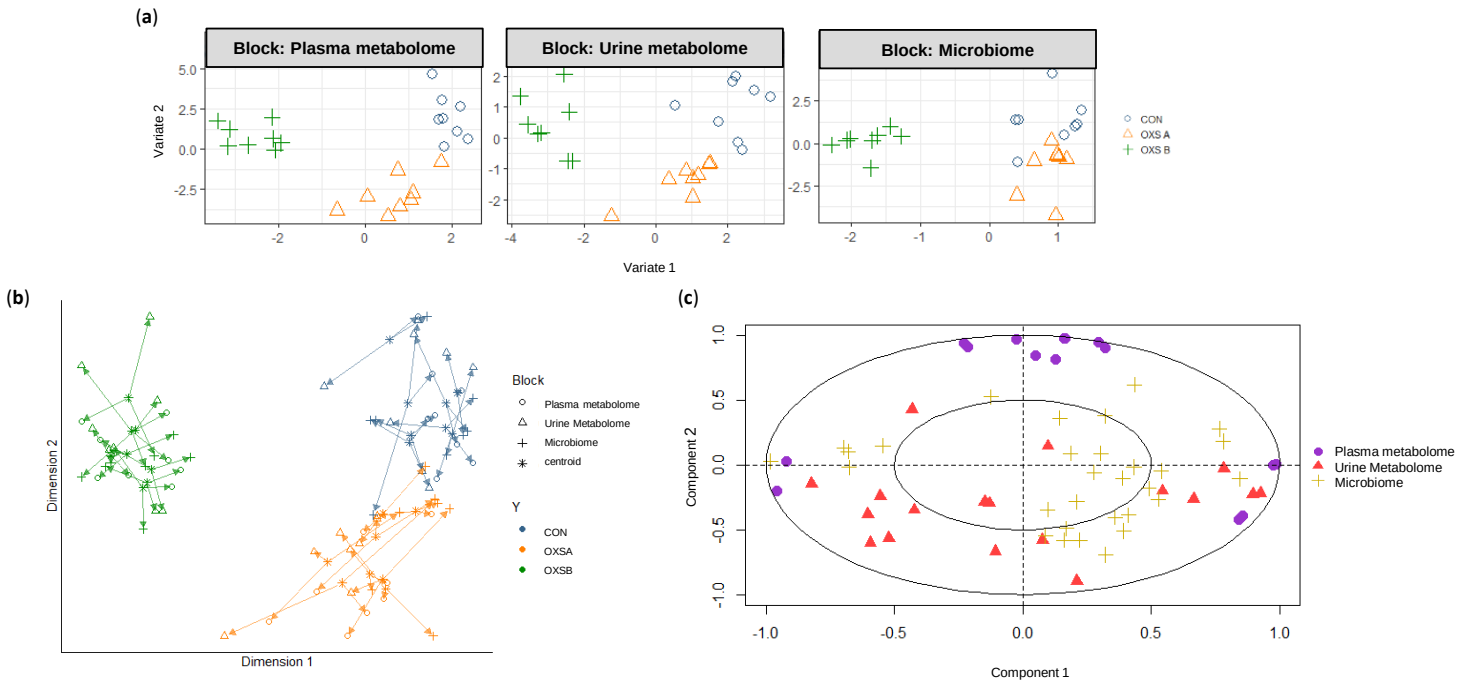

Supplementary figure 4. Multi-omics data integration of plasma metabolome, urine metabolome and microbiome using DIABLO in the oxidative stress model. (a) Sample plot. The samples, which are plotted according to their scores on the 2 components for each data set, are associated showing the degree of agreement between the different data sets and the discriminative ability of each data set. Samples are coloured by group: CON is blue, OXSA is orange and OXSB is green. (b) Arrow plot. The samples are projected into the space spanned by the first 2 components for each data set then overlaid across data sets. The start of the arrow indicates the centroid between all data sets for a given sample and the tip of the arrow the location of the same sample in each block. Arrows further from their centroid indicate some disagreement between data sets. Samples are coloured by group (CON is blue, OXSA is orange and OXSB is green) and data sets are shaped (plasma metabolome is a circle, urine metabolome is a triangle and microbiome is a cross). (c) Correlation circle plot. The plot highlights the potential associations within and between different variable types. Clusters of points indicate a strong correlation between variables. Each colour and shape indicate the type of features: plasma metabolome (purple circle), urine metabolites (red triangle) and finally, microbiome (yellow cross).

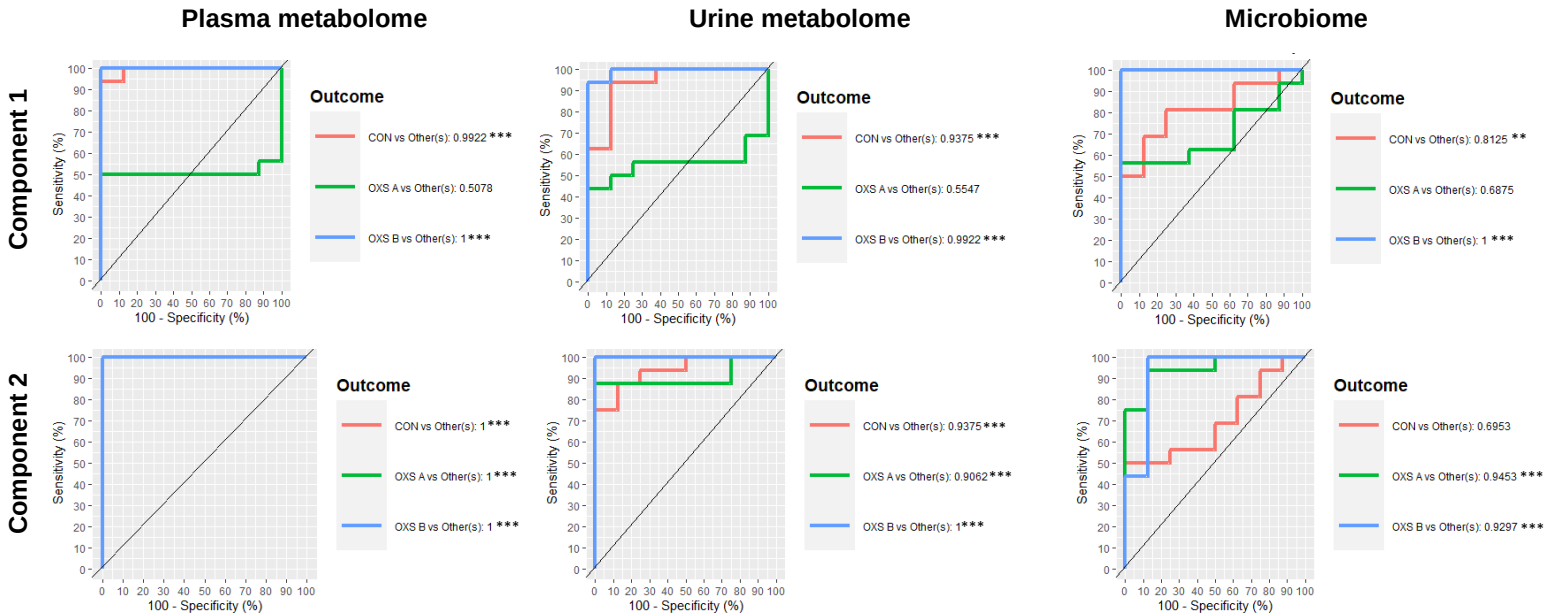

Supplementary figure 5. ROC and AUC based on DIABLO performed on the oxidative stress model. This figure shows the ROC curve and AUC for one class versus the others for each data set (plasma metabolome, urine metabolome and microbiome) and the 2 components. The Wilcoxon test p-value is calculated to assess the differences between the predicted components from one class versus the others. * Denotes $p < 0.1$ (tendency), ** $p < 0.05$ (significantly different) and *** $p < 0.01$ (high significantly different).

UNIVERSITAT ROVIRA I VIRGILI
MULTI-OMICS BIOMARKERS OF METABOLIC HOMEOSTASIS OF RISK FACTORS ASSOCIATED TO NON-COMMUNICABLE DISEASES
Julia Hernandez Baixauli

MANUSCRIPT 6

ALTERATIONS IN METABOLOME AND MICROBIOME ASSOCIATED WITH AN EARLY STRESS STAGE IN MALE WISTAR RATS: A MULTI-OMICS APPROACH

Julia Hernandez-Baixauli [1], Pere Puigbò [1,2,3], Nerea Abasolo [4], Hector Palacios-Jordan [4], Elisabet Foguet-Romero [4], David Suñol [5], Mar Galofré [5], Antoni Caimari [1], Laura Baselga-Escudero [1], Josep M. Del Bas [1,*] and Miquel Mulero [2,6,*]

[1] Eurecat, Centre Tecnològic de Catalunya, Unitat de Nutrició i Salut, 43204 Reus, Spain
[2] Department of Biochemistry and Biotechnology, Universitat Rovira i Virgili, 43007 Tarragona, Spain
[3] Department of Biology, University of Turku, 20014 Turku, Finland
[4] Eurecat, Centre Tecnològic de Catalunya, Centre for Omic Sciences (COS), Joint Unit Universitat Rovira i Virgili-EURECAT, 43204 Reus, Spain
[5] Eurecat, Centre Tecnològic de Catalunya, Digital Health, 08005 Barcelona, Spain
[6] Nutrigenomics Research Group, Department of Biochemistry and Biotechnology, Universitat Rovira i Virgili, 43007 Tarragona, Spain

* Correspondence: josep.delbas@eurecat.org; miquel.mulero@urv.cat

Published by International Journal of Molecular Science

Int. J. Mol. Sci. 2021, 22(23), 12931; https://doi.org/10.3390/ijms222312931

Received: 29 October 2021; Revised: 22 November 2021; Accepted: 23 November 2021; Published: 29 November 2021

UNIVERSITAT ROVIRA I VIRGILI
MULTI-OMICS BIOMARKERS OF METABOLIC HOMEOSTASIS OF RISK FACTORS ASSOCIATED TO NON-COMMUNICABLE DISEASES
Julia Hernandez Baixauli

Abstract: Stress disorders have dramatically increased in recent decades becoming the most prevalent psychiatric disorder in the United States and Europe. However, the diagnosis of stress disorders is currently based on symptom checklist and psychological questionnaires, thus making the identification of candidate biomarkers necessary to gain better insights into this pathology and its related metabolic alterations. Regarding the identification of potential biomarkers, omic profiling and metabolic footprint arise as promising approaches to recognize early biochemical changes in such disease and provide opportunities for the development of integrative candidate biomarkers. Here, we studied plasma and urine metabolites together with metagenomics in a 3 days Chronic Unpredictable Mild Stress (3d CUMS) animal approach that aims to focus on the early stress period of a well-established depression model. The multi-omics integration showed a profile composed by a signature of eight plasma metabolites, six urine metabolites and five microbes. Specifically, threonic acid, malic acid, alpha-ketoglutarate, succinic acid and cholesterol were proposed as key metabolites that could serve as key potential biomarkers in plasma metabolome of early stages of stress. Such findings targeted the threonic acid metabolism and the tricarboxylic acid (TCA) cycle as important pathways in early stress. Additionally, an increase in opportunistic microbes as virus of the *Herpesvirales* spp. was observed in the microbiota as an effect of the primary stress stages. Our results provide an experimental biochemical characterization of the early stage of CUMS accompanied by a subsequent omic profiling and a metabolic footprinting that provide potential candidate biomarkers.

Keywords: early stress, biomarker, animal model, chronic unpredictable mild stress, metabolome, microbiome, energy disruption.

1. Introduction

Psychological stress disorders have dramatically increased in recent decades, becoming a prevalent global health problem. Nowadays, it affects the lives of almost 300 million people worldwide suffering from a range of different stress disorders [1]. In line with this, the World Health Organization (WHO) estimates that stress disorders, anxiety and depression cost to the global economy around USD 1 trillion each year due to lost productivity [1]. Generally, stressful events are thought to influence the pathogenesis of other non-communicable diseases (NCDs) by causing negative affective states (e.g., feelings of anxiety and depression) [2]. During stressful events, two endocrine response systems are activated: the hypothalamic–pituitary–adrenocortical axis (HPA) and the sympathetic–adrenal–medullary (SAM) system. Thus, prolonged or repeated activation of the HPA and SAM systems can interfere with a broad range of physiological processes, resulting in an increased risk of NCDs, particularly cardiovascular diseases, in addition to the traditional psychiatric disorders related with stressful events [3].

The diagnosis of stress disorders, like all psychiatric disorders, is mainly based on symptom checklists and psychological questionnaires referring to a single diagnosis, while patients commonly present symptoms that fit multiple diagnoses [4]. Therefore, the identification of biomarkers and altered metabolic pathways in stress disorders are necessary to gain better insights into the mechanisms that promote metabolic alterations that usually come along with stressful events. This knowledge will allow either: (a) early and accurate diagnosis (by means of biomarkers discovery) and/or, (b) prevention treatments, tailored interventions and general treatments based on the direct or indirect restoration of metabolic parameters.

Regarding the novel approaches for the identification of new potential biomarkers, omics profiling seems to be a promising methodology for the identification of early biochemical changes in disease and thus provides an opportunity to discriminate a footprint of candidate biomarkers that can favour the initiation of earlier interventions; for example, through personalized nutrition and life-style modifications to avoid future drug treatments [5,6]. In this sense, the most relevant biological material for the study of biomarkers in psychiatric disorders derives from the brain [7]. Nevertheless, human brain samples are only available for post-mortem analysis; in consequence, animal models are essential for translating these results to more feasible tissues for the detection of molecular pathways implicated in the pathology and for finding candidate biomarkers of stress disorders [8]. Thus, the use of plasma, serum and urine has been increasing in the metabolomic study of mental disorders, which also provides valuable information about the effect of the disorder throughout the body, as the brain is engaged in all physiological functions of the body [9].

Metabolomic approaches point out that oxidative stress, alterations in lipid and energy metabolism (i.e., mitochondrial regulation), glutamine metabolism and neurotransmitters metabolism could be involved in stress disorders [10]. These

metabolic alterations could overlap with depressive disorder—which often occur simultaneously in individuals with stressful events—where changes in the glutamate–glutamine cycle, as well as changes in lipid and energy metabolism, have been found to be related to the pathogenesis of major depressive disorder [11]. For this reason, it could be interesting to study the early stress episodes to further differentiate between depression and psychological stress. The Chronic Unpredictable Mild Stress (CUMS) model is an experimental approach commonly used to simulate the core behavioural characteristics of human depression for investigating the pathophysiology and assisting in diagnosis [12]. Therefore, the study of CUMS during an initial short period could provide a valuable tool for studying the effects of early stressful events before the animals develop depression disorder. Previous metabolomic studies have fully profiled the metabolic patterns of the rodent CUMS model [13]; nevertheless, it is of interest to distinguish between a classical CUMS and an early CUMS to determine early biomarkers of nerve-wracking events.

To summarize, depressive-related states are the most prevalent psychiatric disorder, but no early metabolic biomarkers have been clearly identified for their early diagnosis, accurate patient subcategorization, treatment or effective prevention. In this study, we explore and interrogate a CUMS experimental model during a period of 3 days (3d) to unravel the neurobiological underpinnings and to identify candidate biomarkers and affected pathways of harsh stress episodes, using the metabolome of different biofluids (plasma and urine) and the microbiome.

2. Results

2.1. Characterization of the Early Stress Stage in Male Wistar Rats

Thigmotaxis is “wall-hugging” behaviour. For example, this conduct is frequently exhibited by humans when they enter an elevator with strangers. In an open field experiment, rodents will typically exhibit less thigmotaxis as they become acclimatized to the chamber. In this regard, the anxiety-like behaviour level of the animals was measured on the open field test (OFT) and is summarised in Figure 1. The number of entries and the total time in the zones were determined to analyse such behaviour (anxious or fearful animals will spend less time in the centre of the field and more time next to the walls, yielding a decreased centre-to-total time ratio). Interestingly, the number of crosses between zones decreased in the 3d CUMS group (p-value = 0.02), indicating less motor activity than in the control (CON) group (Figure 1a). Generally, the total time in the outer zone was lower than the total time spent in the inner zone in all the animals. However, the total time in the inner zone was not statistically different (data not shown). Additionally, to further evidence an anxiety-like behaviour, we observed that the 3d CUMS group exhibited a significant increase in fecal boli deposits (p-value = 0.02, Figure 1b), and the rearing pattern was significantly decreased in 3d CUMS group (p-value < 0.01, Figure 1c); such rearing evaluation

consisted in the assessment of the total number of erect postures, thorough the full test period, adopted by the rodent with the intention of exploring

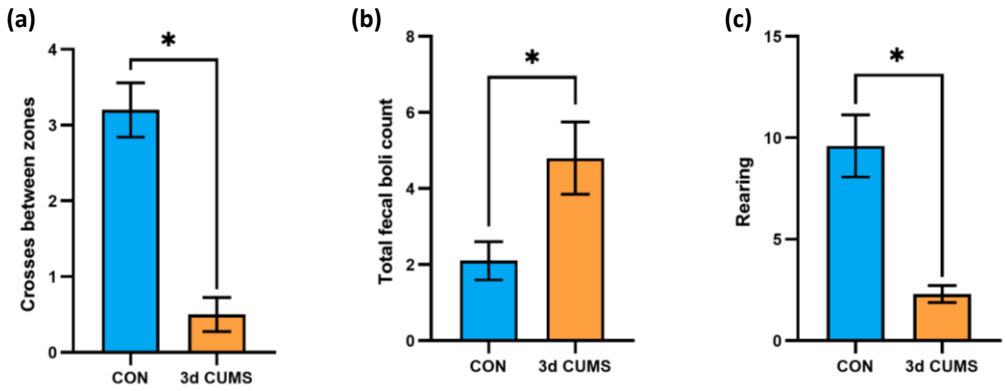

Figure 1. Evaluation of the anxiety-like behaviour on the OFT test in the early stress stage. CON and 3d CUMS (*n* = 10 animals per group) rats were subjected to the OFT for 5 min. (a) Number of crosses between inner and outer zone. (b) Total number of fecal boli deposits. The number of defecations was counted by the researcher after the rats were removed. (c) Rearing behaviour. The statistical comparisons among groups were conducted using Student's t test; the statistically significant *p*-values versus CON ($p < 0.05$) are highlighted with an asterisk (*).

The main endocrine hormones related to the stress response were measured in plasma (i.e., corticosterone and serotonin) (Table 1). The results showed that both hormones were significantly increased in the 3d CUMS group. In this regard, corticosterone (*p*-value < 0.01) and serotonin (*p*-value = 0.01) were increased in the 3d CUMS group approximately more than six times and four times, respectively.

To obtain a broader description of the rodent, the biometric and plasma parameters were also measured (Table 1). The body weight was constant during the three days of the experiment, and no differences were observed in food intake. Furthermore, no differences were observed in the weight of the analysed tissues. Focusing on the plasma parameters, the 3d CUMS group presented an increase in glucose concentration (*p*-value < 0.01), as well as a rise in triglycerides (TG, *p*-value = 0.2), total cholesterol (TC, *p*-value = 0.06) and non-esterified fatty acids (NEFAs, *p*-value = 0.02).

Table 1. **Biometric and plasma parameters of the early stress stage.** Data are presented as the mean ± SEM (*n* = 10 animals per group). (*) Represent statistically significant differences among groups ($p < 0.05$) using Student's *t*-test (*p*-value), and the FC represents the change magnitude. Abbreviations: RWAT, retroperitoneal white adipose tissue; MWAT, mesenteric white adipose tissue; TG, triglycerides; TC, total cholesterol; NEFAs, non-esterified fatty acids.

		CON	3d CUMS	*p*-Value	FC
Biometric parameters	Initial body weight (g)	476.67 ± 10.99	467.29 ± 12.04	0.57	0.98
	Final body weight (g)	476.50 ± 10.69	468.26 ± 10.44	0.59	0.98
	Food intake (g)	21.23 ± 0.76	20.71 ± 0.7	0.63	0.98
	RWAT weight (g)	11.33 ± 1.22	12.11 ± 1.3	0.67	1.07

	MWAT weight (g)	5.96 ± 0.52	7.28 ± 0.73	0.16	1.22
	Muscle weight (g)	2.97 ± 0.33	2.84 ± 0.45	0.67	0.96
	Liver weight (g)	12.26 ± 0.43	11.51 ± 0.3	0.17	0.94
	Cecum weight (g)	4.95 ± 0.26	4.51 ± 0.22	0.22	0.91
Plasma biochemistry	Corticosterone (ng/mL)	58 ± 6.6	374.5 ± 24.8	<0.01 *	6.46
	Serotonin (ng/mL)	49.99 ± 9.95	211.55 ± 50.95	0.01 *	4.32
	Glucose (mM)	67.56 ± 1.71	82.63 ± 2.60	<0.01 *	1.22
	TG (mM)	71.15 ± 4.34	82.75 ± 7.89	0.2	1.16
	TC (mM)	67.12 ± 2.92	79.30 ± 5.09	0.06	1.18
	NEFAs (mM)	0.42 ± 0.03	0.56 ± 0.04	0.02 *	1.33

2.2. Plasma Metabolic Profiling and Biomarker Identification

The plasma metabolomic approach was based on a global multiplatform analysis including 138 metabolites (Table S1). This platform was associated with the following biochemical processes: the lipid metabolism (represented as a wide diversity of different triacyclglycerols (TGs), diacylglycerols (DGs), phosphatidylcholines (PCs), cholesterol esters (ChoEs), lysophospholipids (LPCs) and sphingomyelins (SMs), among others); the carbohydrate metabolism (where the main metabolites of tricarboxylic acid cycle (TCA cycle) were included); and the amino acid metabolism. The summaries of the univariate and multivariate analyses are shown in the Table S1. After the Mann–Whitney (MW) test, 23 out 138 metabolites were significantly different, and the subsequent Benjamin–Hochberg (BH) correction highlighted 6 out of 23 different metabolites that were as follows: succinic acid, malic acid, threonic acid, alpha-ketoglutarate, pyruvic acid, cholesterol, oleic acid and 3-hydroxybutitic acid (Table 2).

Table 2. Summary of the significant differential plasma metabolites in the early stress stage. CON and 3d CUMS groups (*n* = 10 animals per group) are represented by the relative abundances (AU). Relative abundances of metabolites are presented by the mean ± SEM. Plasma metabolites are sorted by *p*-value. The summary of the analysis is shown and includes the relative abundances of metabolites, *p*-value, *q*-value, VIP value, RF, FC, the effect of the 3d CUMS versus the CON group and the related metabolic pathway.

Metabolite	CON	3d CUMS	*p*-Value	*q*-Value	VIP	RF	FC	Effect	Metabolic Pathway
Malic acid	0.36 ± 0.03	0.74 ± 0.07	<0.01	0.03	2.4	0.03	2.1	↑	TCA cycle
Threonic acid	2.55 ± 0.21	0.8 ± 0.17	<0.01	0.03	2.6	0.03	0.3	↓	Ascorbate and aldarate metabolism
Alpha-ketoglutarate	1.21 ± 0.08	1.94 ± 0.13	<0.01	0.03	2.3	0.03	1.6	↑	TCA cycle
Succinic acid	0.61 ± 0.04	0.86 ± 0.04	<0.01	0.03	2.3	0.03	1.4	↑	TCA cycle

Pyruvic acid	14.68 ± 0.85	25.39 ± 3.14	<0.01	0.03	2.1	0.03	1.7	↑	Glycolysis
Cholesterol	0.33 ± 0.02	0.6 ± 0.05	<0.01	0.05	2.4	0.05	1.8	↑	Steroid biosynthesis

The distribution of the six metabolites were visualized with boxplots to evaluate the distribution between groups and the impact in the early stress stage (Figure 2): Threonic acid was decreased more than three times in the 3d CUMS group, while the other metabolites were increased.

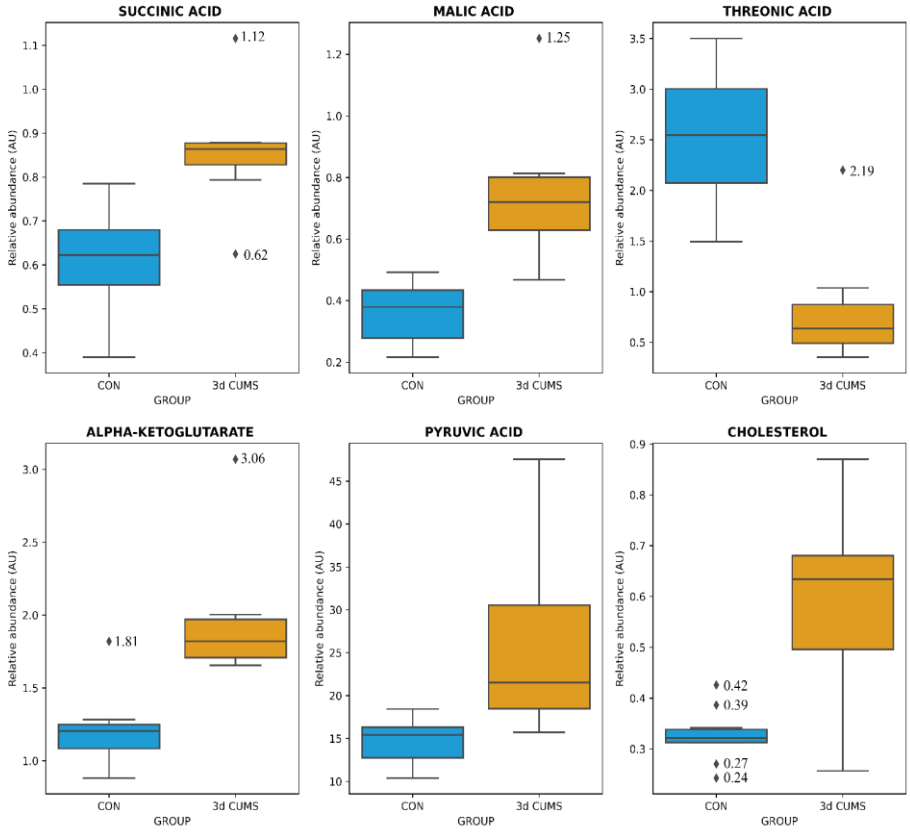

Figure 2. Box-whisker plots of the differential metabolites in the early stress stage. Relative abundance of metabolites (AU) is represented: blue represents CON group and orange the 3d CUMS group (*n* = 10 animals per group). Box denotes 25th and 75th percentiles; line within box denotes 50th percentile (median); whisker denotes standard deviation.

Despite no clustering being distinguished in the principal component analysis (PCA, Figure S1), differences in orthogonal the partial least squares discriminant analysis (OPLS-DA) were observed between groups (Figure 3). OPLS-DA was performed in parallel to the statistical analysis to assess the prediction power of the key plasma metabolites. The proportion of variance explained by the model (R2X) was 45.1% in the plasma data. The percentage of Y variability explained by the model (R2Y) was 95.1% and the estimation of the predictive performance of the models (Q2) was

67.8%; as it is greater than 50%, the model is considered to have good predictability. The highest variable importance in projection (VIP) values are shown in Table 2, threonic acid (2.6) being the most important metabolite in the model, followed by malic acid, cholesterol, alpha-ketoglutarate and succinic acid. Finally, the feature importance was also assessed using a random forest classifier (RF) to complete the evaluation of the prediction power (Table S1). In this case, the most important feature was the malic acid followed by threonic acid, oleic acid and alpha-ketoglutarate, with values above 0.1.

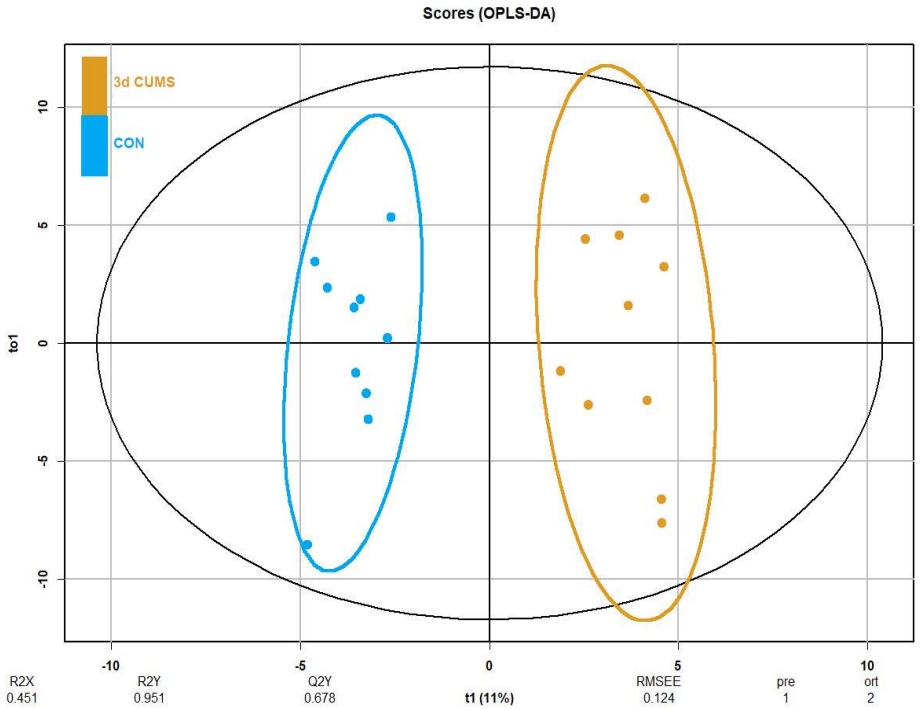

Figure 3. OPLS-DA of plasma metabolomics in the early stress stage. Blue represents the CON group and orange the 3d CUMS group (*n* = 10 animals per group). The Score plot is represented, and it includes the number of components, the cumulative R2X, R2Y and Q2Y.

2.3. Urine Metabolic Profiling and Biomarker Identification

The urine metabolomic approach, which was based on the untargeted 1H-NMR methodology, detected 42 metabolites mainly belonging to the amino acid metabolism (e.g., phenylalanine, tyrosine and tryptophan metabolism; glycine, serine and threonine metabolism; alanine, aspartate and glutamate metabolism; glutathione metabolism; and taurine and hypotaurine metabolism) and the energetic metabolism (e.g., TCA cycle, pyruvate metabolism and glycolysis/gluconeogenesis) (Table S2). The summary of the univariate and multivariate analysis is shown in the Table S2. After the MW test, N,N-dimethylglycine and taurine were significantly altered in the 3d CUMS group versus the CON group. After the BH correction, none of these metabolites

remained significantly modified. The distribution was also analysed, noticing a decrease in N,N-dimethylglycine and an increase in taurine (Figure 4a).

Differences were observed between groups in OPLS-DA (Figure 4b), despite no clustering being distinguished in the PCA (Figure S2). The proportion of variance explained by the OPLS-DA model (R2X) was 32.3% in the urine data. The percentage of Y variability (R2Y) was 91.3% and the estimation of the predictive performance (Q2) was 41.8%. In this case, the predictive power in urine metabolites is not strong enough to discriminate between groups. The highest VIP values are shown in Table S2, being the before-mentioned metabolites the most important in urine with higher VIP values. In this case, the most important features were also N,N-dimethylglycine (0.21) and taurine (0.18) applying RF to elucidate the evaluation of this metabolites (Table S2).

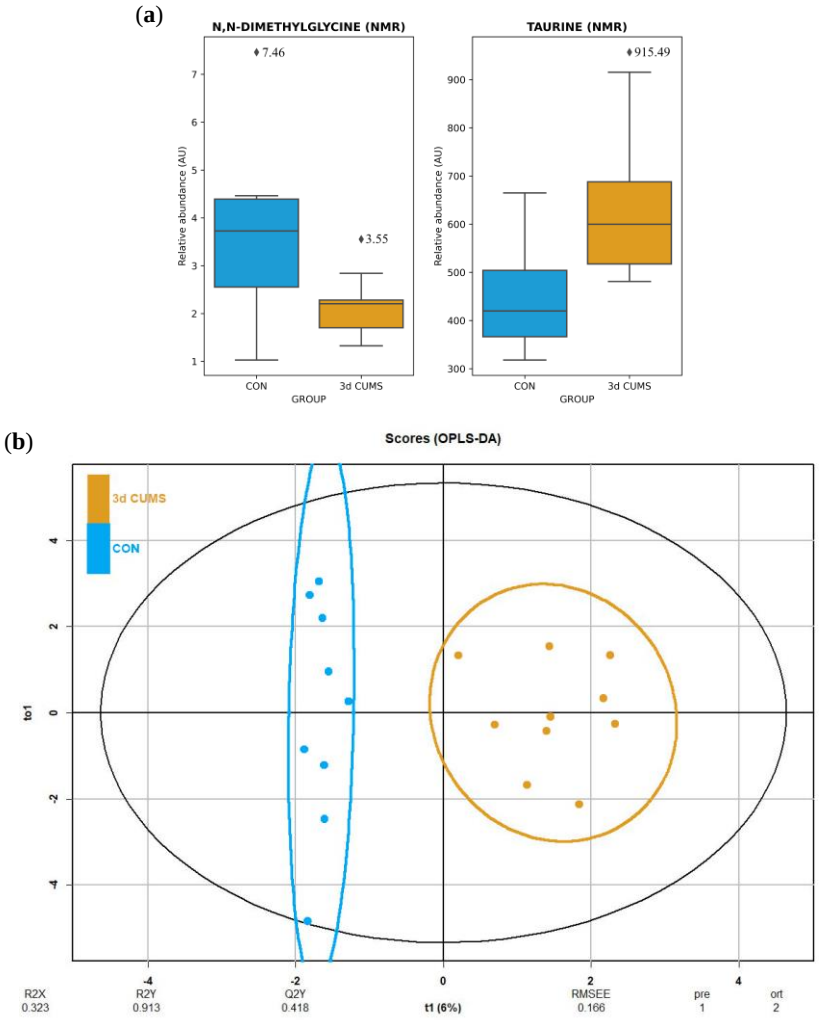

Figure 4. Box-whisker plots and OPLS-DA representation of urine metabolomics in the early stress stage. Blue represents the CON group and orange the 3d CUMS group (*n* = 10 animals per group). (a) Box-whisker plots of the major impact metabolites in urine represented by the relative abundance of metabolites (AU).

Box denotes 25th and 75th percentiles; line within box denotes 50th percentile; whisker denotes standard deviation. (b) OPLS-DA of plasma metabolomics. The score plot that is represented includes the number of components, and the cumulative R2X, R2Y and Q2Y (indicated below the plot).

2.4. Microbiome Profiling

The taxonomic assignment detected the presence of the most abundant microbes in the cecum section to evaluate the highest variability and diversity of the gut tract (i.e., bacteria, viruses and <1% of other microbes). Making a general overview related to the abundance of microbes, we can see that 78% of the generated readings were assigned to bacteria and 22% to viruses in the CON group, and in the case of the 3d CUMS group, the readings assigned to bacteria were slightly decreased to 69% and the viruses were increased to 31% in comparison to CON (not statistically significant). The beta diversity, which is represented by a PCA of Aitchison distances, were highly overlapped between bacterial groups (Figure 5a) and between viruses (Figure 5b). In this regard, the PERMANOVA showed a tendency in bacteria (F = 1.89, *p*-value = 0.09) indicating differences in bacteria composition/beta diversity, while there were no significant differences in viruses (F = 0.93, *p*-value = 0.5). The alpha diversity (measure of richness in the same group) showed a tendency to decrease in the microbiome of the 3d CUMS group, without being statistically significant in neither bacteria (Figure 5c) nor viruses (Figure 5d).

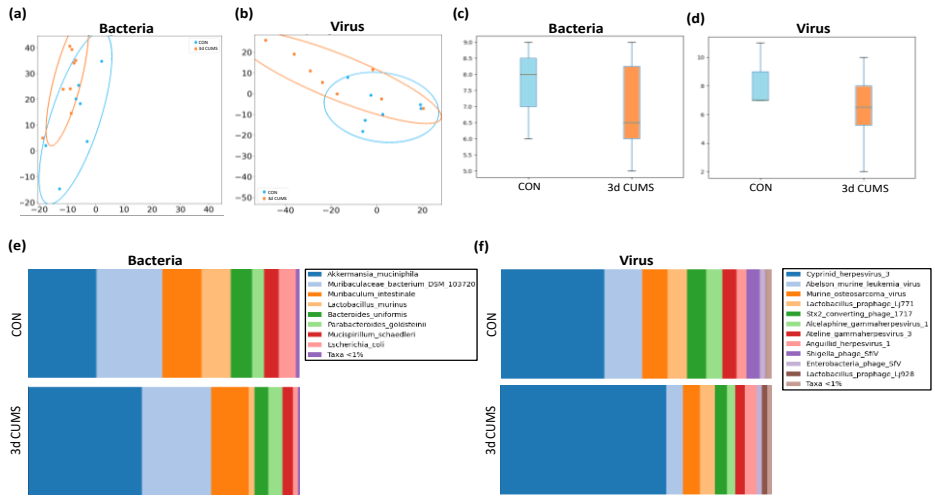

Figure 5. Summary of the microbiome statistical analysis in the early stress stage. Blue represents the CON group and orange the 3d CUMS group (*n* = 8 animals per group). Beta diversity: PCA plot calculated by Aitchison distance for bacteria (a) and viruses (b). Alpha diversity (AU): chao1 index in bacteria (c) and viruses (d). Taxonomic differences represented as relative distribution of species in bacteria (e) and viruses (f); these figures show a bar graph at the level of both bacterial and viral species (relative %) comparing the animals in all groups.

Regarding the bacterial microbiome, the communities of both groups were mostly formed by the phyla Bacteroidetes (CON: 51% and 3d CUMS: 49%), Verrucomicrobia (CON: 26% and 3d CUMS: 42%), Firmicutes (CON: 12% and 3d CUMS: 4%), Proteobacteria (CON: 6% and 3d CUMS: 2%), and Deferribacteres (CON: 5% and

3d CUMS: 4%). Although these differences were not statistically significant, interesting results could be found on the magnitude of the different phyla. Thus, the relative abundance of Verrumicrobia was increased almost twice, while Firmicutes and Proteobacteria decreased three times in the 3d CUMS group. Focusing on bacterial species (Figure 5e), 12 species were found to have a relative abundance above 0.01% (Table S3). Interestingly, the *Akkermansia muciniphila* species was the most abundant one (CON: 26% and 3d CUMS: 42%), being the main species implicated in the increase in the Verrucomicrobia phylum in both groups (Figure 5a). However, the difference was not significant, even though the values almost doubled (p-value = 0.1 and q-value = 0.4). The higher increase in *Akkermansia muciniphila* indirectly affects the relative abundance of other species, for example, Lactobacillus murinus (CON: 11% and 3d CUMS: 2%), *Escherichia coli* (CON: 6% and 3d CUMS: 2%) or *Bacteroides uniformis* (CON: 8% and 3d CUMS: 5%) (Figure 5a).

In the case of the virus microbiome, the communities of both groups were mostly formed by the following orders: *Herpesvirales* (CON: 54% and 3d CUMS: 73%), *Ortervirales* (CON: 24% and 3d CUMS: 12%) and *Caudovirales* (CON: 23% and 3d CUMS: 14%). Thus, the relative abundance of *Herpesvirales* increased almost 1.5 times in the 3d CUMS group; however, *Ortervirales* and *Caudovirales* decreased twice in the same group. Focusing on virus species (Figure 5f), 13 species were found to have a relative abundance above 0.01% (Table S4). In both groups, the most represented virus was an uncharacterized herpesvirus (CON: 39% and 3d CUMS: 61%) that was increased in the 3d CUMS group (p = 0.02). This virus is the main species implicated in the *Herpesvirales* order (Figure 5b). Other relative abundant species were *Abelson murine leukemia* virus (CON: 14% and 3d CUMS: 6%), *Murine osteosarcoma virus* (CON: 9% and 3d CUMS: 6%), *Lactobacillus prophage Lj771* (CON: 7% and 3d CUMS: 5%), *Stx2 converting phage 1717* (CON: 7% and 3d CUMS: 4%), *Alcelaphine gammaherpesvirus* (CON: 6% and 3d CUMS: 3%) and *Ateline gammaherpesvirus* (CON: 5% and 3d CUMS: 4%), among others (Figure 5b).

2.5. Multi-Omics Data Integration

The multi-omics integrative analysis with Data Integration Analysis for Biomarker discovery using Latent cOmponents (DIABLO) identified a highly associated profile of eight plasma metabolites (threonic acid, alpha-ketoglutarate, malic acid, 3-hydroxybutiric acid, DG 34:2, succinic acid, aspartic acid and cholesterol); six urine metabolites (taurine, α-hydroxyhippurate, N-acetylglycine, malic acid, N,N-dimethylglycine and betaine); and five microbes, including bacteria and viruses (*Escherichia coli*, *Lactobacillus murinus*, *Akkermansia muciniphila*, uncharacterized *Herpesvirus* and *Bacteroides uniformis*). This analysis revealed a high correlation between data sets with coefficients above 0.6 (Figure S3a), specifically between the plasma metabolome that correlated with the urine metabolome (r = 0.82) and microbiome (r = 0.81). Moreover, the data sets were able to discriminate between groups (Figure S3b), highlighting the relationship between plasma and the urine metabolome (Figure S3c). The variable effect in the first component and the impact of each feature in the data set are shown in Figure S4 a,c,e for plasma metabolomics,

urine metabolomics and metagenomics, respectively. The correlation between the variables from the three different blocks is shown in Figure 6a (cut-off was set at 0.7). Further visualization in Cytoscape revealed the highest correlations between the different omics (Figure 6b).

To evaluate the performance of the proposed omics profile, the overall error was calculated as 0.2 in the first component. Additionally, the receiver operating characteristic (ROC) curve analysis showed that the optimal omics profile with the combination of eight plasma metabolites effectively separated both groups with an area under the ROC curve (AUC) of 1 (p-value < 0.01, Figure S4b). A combination of six plasma metabolites optimally dichotomized the groups with an AUC of 0.86 (p-value = 0.02, Figure S4d). In the metagenomics data, the combination of five bacteria and viruses grouped the animals with an AUC of 0.92 (p-value < 0.01, Figure S4f). These results support the above-selected features as a representative omics profile of the early stress stage.

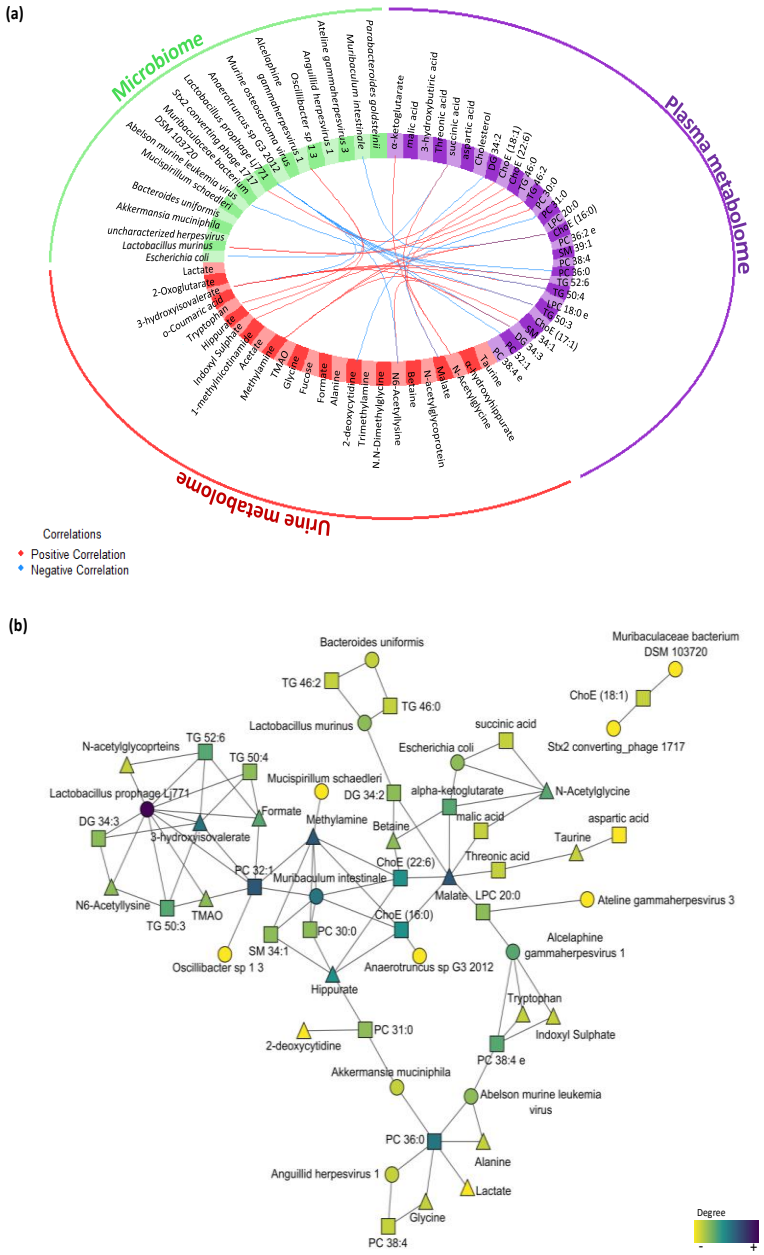

Figure 6. Multi-omics integration of plasma metabolome, urine metabolome and microbiome in the early stress stage. (a) Circos plot output from DIABLO. Each quadrant indicates the type of features: plasma metabolites (purple), urine metabolites (red), bacteria species (green) and virus species (orange); lines indicate measure of association (correlation), either positive or negative. (b) Further visualization of the network from DIABLO using Cytoscape. The shape of the features indicates the type of feature: plasma metabolites (square), urine metabolites (triangle) and metagenomics (circle). The colour indicates the degree of each feature in the network (i.e., nodes with more connections). Abbreviations: DG, diacylglycerol; ChoE, cholesterol ester; TG, triglyceride; PC, phosphatidylcholine; SM, sphingomyelin; LPC, lysophospholipid.

3. Discussion

In the present study, differences in the patterns of anxiety-like behaviour were found in 5–6 months old male Wistar rats in the early stress stage. Generally, younger animals (with ages between 6 and 9 weeks) have been used for these kinds of experiments. These animals could be more resilient and adaptive to stressful events than the older ones [14,15]. Interestingly, even rat and mice pups have also been used to study anxiety-like behaviour [16]. However, it is not until 5–6 months old that rats are fully grown in terms of social competence, brain development and musculoskeletal maturity [17]. Therefore, the use of adult animals is especially interesting because a lot of physiological and molecular phenomena are still changing over the first 3 months of age [18]. Thus, increasing data indicate that important changes in the emotional behaviour occur with aging [19]. The evaluation of exploratory behaviour and general activity was evaluated showing an alteration in anxiety-like behaviour that was characterized by a decrease in motor activity (decrease in the number of crosses between zones in the OFT) in the 3d CUMS group [20]. Furthermore, defecation was increased and was inversely correlated with rearing, suggesting adverse conditions as an initial depressive behaviour [21]. The increased levels of corticosterone and serotonin confirmed the activation of the HPA axis and thus a high increase in the activity of endocrine pathways that could lead to NCDs [3]. In this regard, it has been found in different studies that corticosterone has an impact on hepatic lipid metabolism, energy metabolism and the subsequent metabolite profile [22,23]. Moreover, some biochemical parameters were increased (i.e., glucose concentration) in the 3d CUMS group, as other evidence of the activation of the endocrine response from a metabolic point of view.

The metabolome was investigated for the elucidation of neurobiological underpinnings and for the identification of candidate biomarkers in the affected pathways in this early stress stage approach (summarized in Figure 7). Interestingly, one main impact on the metabolome was characterized by a decrease in threonic acid, which is the major breakdown product of ascorbate, being a distinctive metabolite of the 3d CUMS approach compared to other metabolomic classic CUMS studies [13]. In this sense, the presence of high levels of ascorbate in neurons seems to be related to high levels of aerobic respiration rates that could lead to superoxide production and prooxidant effects in mitochondria [24]. Additionally, the control of threonic acid levels have been described as a promising strategy for predicting the subtypes of depressive disorders [25]. In line with this, different strategies have been tailored, focusing on threonic acid, to try to improve multiple brain disorders (e.g., dietary treatment with magnesium-L-threonate) [26].

Several studies have demonstrated a potential link of stressful events with the alteration of energy metabolism thought the stress response [27]. In the 3d CUMS group, increased key intermediate products of the TCA cycle are indicative of the overstimulation of this cycle (i.e., alpha-ketoglutarate, malic acid and succinic acid) due to the stress response. This fact differentiates the 3d CUMS from the classical

CUMS that is associated with energy disruption or deficiency (being one of the most represented depressive symptoms associated to the reduction of the activity and curiosity in animal models) [26]. These results supports the idea that, lately, mitochondrial organelles and the energetic metabolism are emerging as modulators of anxiety-related behaviour both in rodent and human studies [28]. One of the intermediate products of the TCA cycle, alpha-ketoglutarate, is an important source of neurotransmitters (i.e., glutamate and gamma aminobutyric acid (GABA)), which are the major brain neurotransmitters mediating excitatory and inhibitory signalling, respectively [29]. Moreover, the alpha-ketoglutarate pathway can synthesize other important amino acids, including proline, hydroxyproline and ornithine, which tend to be increased in the 3d CUMS group as in the case of CUMS model [13]. Related to the energy metabolism, pyruvic acid, which is increased in the 3 CUMS group, is the end-product of glycolysis, a major substrate for oxidative metabolism and a branching point for glucose, lactate, fatty acid and amino acid synthesis [30]. In previous CUMS studies, pyruvic acid was disturbed without being significant, and for this reason, we suggest that the increased pyruvic acid is related to the early response to stress instead of depression when pyruvic acid returns to its normal levels, leading to other metabolic changes [31].

Figure 7. Metabolic profiling of candidate biomarkers and the main metabolic pathways implicated in the early stress stage. It is presented the metabolites with highest influence on the model (match in all the statistical methods, green dot), influence on metabolites (partial match in the statistical methods, yellow dot) and other metabolites presenting an impact on metabolism. The up- and downregulated metabolites are indicated with up and down arrows, respectively. Abbreviations: DG, diacylglycerol; ChoE, cholesterol ester; TMAO, trimethylamine N-oxide; TMA, trimethylamine; GABA, gamma aminobutyric acid.

The slightly plasmatic increase in 3-hydroxybutiric acid, a known ketone body, reflects an increase in energy production through fatty acid oxidation, supporting the idea that the disruption of carbohydrate and energy metabolism might be disrupted in the 3d CUMS group. Hereof, the production of ketone bodies has been shown to have a positive influence on the production of GABA, which is illustrated by reduced

plasma levels in depressed patients [25]. In contrast, in the present study, we suggest that, paradoxically to depression, an increment in ketone bodies could be associated with stress states. Furthermore, the increased urine excretion of taurine has been highly related to the stress response [32]. This amino acid plays a vital role in the central nervous system acting as a neurotransmitter and in the regulation of oxidative and energy metabolism. In this regard, taurine raises fatty acid oxidation and ketone bodies levels, which is connected with the increase in fatty acids and other related lipids and the increase in 3-hydroxybutiric acid, as has been previously discussed [33]. According to previous studies, taurine embraces antidepressant and anxiolytic activities in different animal models using different doses and types of administration [34].

In studies focused on lipidomics, the connection between lipids, neuronal signalling, and NCDs stands out [35]. In our case, we observed an increase in this group of metabolites characterized by the cholesterol increase, as well as others lipids less relevant in the experimental statistical approach, such as the case of complex lipids (i.e., DG 34:2) and polyunsaturated fatty acids (PUFAs) (i.e., ChoE (18:3), also known as linolenic acid, and ChoE (18:2), also known as linoleic acid) and monounsaturated fatty acid (MUFA) (i.e., ChoE (18:1), also known as oleic acid). Those fatty acids are precursors of other important fatty acids, supporting the evidence of a potential crucial role of membrane lipids and lipid oxidation in mental disorders [24]. In fact, disturbances in those PUFAs, precursors of arachidonic acid and docosahexaenoic acid, were associated with inflammation response and further complications as type 2 diabetes and cardiovascular diseases that were also altered in CUMS studies [31].

Interestingly, a major finding regarding the metabolites excreted in urine is their relation to methylamine metabolism that has been critically related to stressed phenotype through the decrease in choline (precursor of neurotransmitters in the brain) [36]. Furthermore, methylamines have been defined as microbiota-derived metabolites [37]. N,N-dimethylglycine and related metabolites of methylamine metabolism are mainly produced when choline is catabolized into other metabolites via gut microbiota [38], and they are finally excreted in urine. This fact could suggest that the proposed early stress stage may be associated with alterations on the intestinal microorganism populations.

Accordingly, the gut microbiota has been widely studied in psychological disorders, and it has been proposed as a pivotal axis in the regulation of anxiety-like behaviour. Even though the 3d CUMS group was absent of important differences in the gut microbiome, there were some microbes and metabolites that were altered related to a hypothetical gut microbiome disruption. Recent studies in rats subjected to CUMS revealed that the changes in the gut microbiome were associated with the dysregulation of plasma metabolites related to the metabolism of glycerophospholipids, glycerolipids, fatty acyls and sterols [39]. In consequence, this metabolite alteration could be caused by the synergistic effect of the altered microbiome and the stress response. Blacher and colleagues identified that

nicotinamide (a vitamin enrolled in the production of steroid hormones synthesized by the adrenal gland and stress-related hormones) is produced by *Akkermansia muciniphila*, and when it was injected into diseased mice, it improved their anxiety-like behaviour [40]. This vitamin may be involved in minimizing oxidative stress and the consequent preservation of neuronal health. Accumulating evidence suggests that gut microbes can also produce metabolites with high neuroactive potential (neurotransmitters) [41]. The interaction between gut microbiota and gut hormones has been greatly evidenced in gut–brain cross-talk [42]. Recently, *Bacteroides* spp. have been confirmed as producers of GABA as a mechanism of stress tolerance in humans [43]. Furthermore, other bacteria taxa, which were altered in our experimental approach, such as *Escherichia coli* and lactic acid bacteria have been found to also produce neurotransmitters such as serotonin [44] and GABA [45], respectively. Interestingly, it has been described an increment in opportunistic microbes [46] as in the case of some bacteria (e.g., *Lactobacillus*) and some viruses (e.g., *Herpesvirus* order) as consequence of stressful events.

Finally, previous studies that profiled stress for finding potential candidate biomarkers presented some drawbacks when trying to obtain pure stress biomarkers because of the existing similarities between early stress stages and the development of depressive disorder [8,11,47–51]. In our study, a comparison between univariate and multivariate analyses, RF and multi-omics integration was performed to check the robustness among methods of the candidate biomarkers and try to determine the essence of stress (Table S5). The full matching metabolites are malic acid, threonic acid, alpha-ketoglutarate, succinic acid and cholesterol in plasma metabolomics (Figure 7), showing their importance as key metabolites in the 3d CUMS study. Additionally, pyruvic acid and 3-hydroxibutiric acid in plasma metabolomics and N,N-dimethylglycine and taurine in urine metabolomics match as candidate biomarkers in two different statistical methodologies (Figure 7). Globally, considering the results of the present 3d CUMS study and previous CUMS studies, we have observed that energy metabolism has a greater impact together with fatty acids, while in CUMS, energy metabolism does not have much impact while there is greater alteration of amino acids associated with the monitoring of depression [31,52].

4. Materials and Methods

4.1. Animal Experimental Design

A total of 20 22-week-old male Wistar rats (Harlan Laboratories, Barcelona, Spain) were housed individually with a shelter (i.e., cardboard tube) to enrich the cage environment, under fully controlled conditions including temperature (22 ± 2 °C), humidity (55 ± 5%) and light (12 h light–dark cycle and lights on at 9:00 am). All rats were given standard chow diet and tap water ad libitum. The Animal Ethics Committee of the University Rovira i Virgili (Tarragona, Spain) approved all the procedures (code 10049). The experimental protocol followed the “Principles of Laboratory Care” and

was carried out in accordance with the European Communities Council Directive (86/609/EEC).

Animals with similar body weight were randomly assigned to two different groups (*n* = 10 animals per group): the CON group and the 3d CUMS group. The early stress approach is a short-adapted version of the classical CUMS model of behavioural stress to mimic a short stressor effect during the first 3 days of the CUMS model (Figure 8). Animals from the CON group were not subjected to any stress, and they were only handled to habituate them to the manipulator contact. Animals from the 3d CUMS group were subjected to different stressors for three consecutive days. The stressors included in the protocol were physical restriction for 30 min and 5 min; bedding wetting for 12 h (consisting of mixing 300 mL of water with 1 L of sawdust bedding); light flashes (120 flashes/minute for 15 s, followed by one minute of rest, and this procedure was repeated 5 times); 45° cage tilt for 15 h; and the combination of light flashes and physical restriction before the sacrifice.

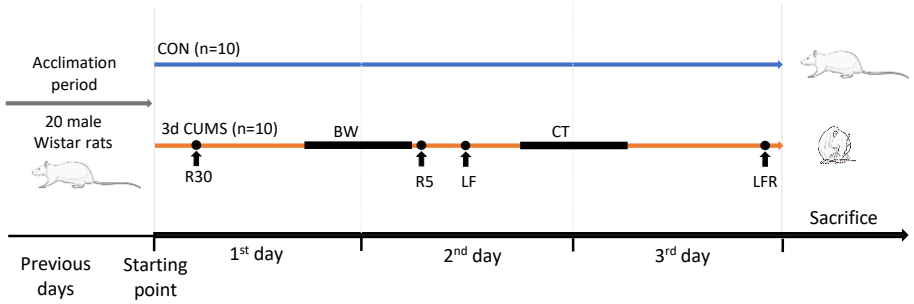

Figure 8. Schematic representation of an early stress stage based on a 3 days CUMS showing the CON and 3d CUMS groups (*n* = 10 animals per group) during the 3 experimental days. The different stressors are represented with a dot if they are punctual or with a line if they last for a period. Abbreviations: R30, restriction during 30 min; BW, bedding wetting; R5, restriction during 30 min; LF, light flashes; CT, cage tilt; LFR, light flashes with restriction.

4.2. OFT

To assess anxiety-like behaviour, at the end of the 3d CUMS (7 h before sacrifice) rats were individually placed in a grey wooden box (70 × 45 × 45 cm) and allowed to explore it for 5 min. A central area (20 × 40 cm) was considered for scoring time and number of entries in the inner zone. Locomotor activity, fecal boli deposits and rearing were also recorded and analysed using a tracking system (ANY-Maze, version 4.82, Stoelting Co., Wood Dale, Il, USA). The box was wiped clean with 70% ethanol before testing each animal.

4.3. Sample Collection

Urine samples were collected the day before the sacrifice through hydrophobic sand method, which is less stressful for the animals than others classical methodologies [53]. For each rat, 300 g of hydrophobic sand was spread (LabSand, Coastline Global, Palo Alto, CA, USA) on the bottom of a mouse plastic micro-isolation cage. Urine was collected every half hour for 6 h with sodium azide (Sigma, St Louis,

MO, USA) as preservative and was finally pooled at the end of the session. On the day of the sacrifice, animals were killed by guillotine under anaesthesia (sodium pentobarbital, 50 mg/kg per body weight) after 7 h of fasting. Blood was collected and centrifuged at 3000× g at 4 °C for 15 min to recover plasma. Tissues were rapidly removed, weighted and snap-frozen in liquid nitrogen (i.e., RWAT, MWAT, muscle, liver and cecum). All the samples were stored at −80 °C until further analysis.

4.4. Plasma Biochemistry

Concentrations of serotonin (#ab133053, Abcam, Cambridge, UK) and corticosterone (#EIACORT, Invitrogen, Carlsbad, CA, USA) were measured in plasma by ELISA according to the manufacturer's protocol. Enzymatic colorimetric kits were used for the plasma determination of TC, TG, glucose (QCA, Barcelona, Spain) and NEFAs (WAKO, Neuss, Germany).

4.5. Metabolome Analysis

4.5.1. Plasma Metabolome (GC-qTOF and UHPLC-qTOF)

Plasma metabolites were analysed by gas Chromatography coupled with Quadrupole Time-of-Flight (GC-qTOF). For the extraction, a protein precipitation extraction was performed by adding eight volumes of methanol:water (8:2, *v*/*v*) containing internal standard mixture (succinic acid-d4, myristic acid-d27, glicerol-13C3 and D-glucose-13C6) to plasma samples. Then, the samples were mixed and incubated at 4 °C for 10 min, centrifuged at 21,420× g and the supernatant was evaporated to dryness before compound derivatization (metoximation and silylation). The derivatized compounds were analysed by GC-qTOF (model 7200 of Agilent, Santa Clara, CA, USA). The chromatographic separation was based on the Fiehn Method, using a J&W Scientific HP5-MS (30 m × 0.25 mm i.d.), 0.25 µm film capillary column and helium as carrier gas using an oven program from 60 °C to 325 °C. Ionization was performed by electronic impact (EI), with electron energy of 70 eV and operated in full Scan mode. The identification of metabolites was performed matching two different parameters to metabolomic Fiehn library (Agilent, Santa Clara, CA, USA): EI mass spectrum, considered stable and reproducible and retention time. To avoid annotation errors, metabolites with very high molecular weights were cleared. After the putative identification of metabolites, these were semi-quantified in terms of the internal standard response ratio.

Plasma lipids were analysed by Ultra-High-Performance Liquid Chromatography coupled with Quadrupole Time-of-Flight (UHPLC-qTOF). For the extraction of the hydrophobic lipids, a liquid–liquid extraction based on the Folch procedure [54] was performed by adding four volumes of chloroform:methanol (2:1, *v*/*v*) containing internal standard mixture (Lipidomic SPLASH®, Avanti Polar Lipids, Inc., Alabaster, AL, USA) to plasma. Then, the samples were mixed and incubated at −20 °C for 30 min. Afterwards, water with NaCl (0.8%) was added, and the mixture was centrifuged at 21,420× g. Lower phase was recovered, evaporated to dryness and reconstituted with methanol:methyl-tert-butyl ether (9:1, *v*/*v*) and analysed by UHPLC-qTOF (model 6550 of Agilent, Santa Clara, CA, USA) in positive electrospray ionization mode. The

chromatographic consists in an elution with a ternary mobile phase containing water, methanol, and 2-propanol with 10 mM ammonium formate and 0.1% formic acid. The stationary phase was a C18 column (Kinetex EVO C18 Column, 2.6 µm, 2.1 mm × 100 mm) that allows the sequential elution of the more hydrophobic lipids such as TGs, DGs PCs, ChoEs, LPCs and SMs, among others. The identification of lipid species was performed by matching their accurate mass and tandem mass spectrum, when available, to Metlin-PCDL from Agilent containing more than 40,000 metabolites and lipids. In addition, chromatographic behaviour of pure standards for each family and bibliographic information was used to ensure their putative identification. After putative identification of lipids, these were semi-quantified in terms of internal standard response ratio using one internal standard for each lipid family.

A pooled matrix of samples was generated by taking a small volume of each experimental sample serving as a technical replicate throughout the data set. As the study took multiple days, a data normalization step was performed to correct variation resulting from instrument inter-day tuning differences. Essentially, each compound was corrected in run-day blocks through quality controls, normalizing each data point proportionately.

4.5.2. Urine Metabolome (^{1}H-NMR)

Urine metabolites were analysed by proton nuclear magnetic resonance (^{1}H-NMR). The urine sample was mixed (1:1, *v*/*v*) with phosphate buffered saline containing with 3-(Trimethylsilyl)propionic-2,2,3,3-d4 acid sodium salt (TSP) (Sigma Aldrich) and placed on a 5 nm NMR tube for direct analysis by ^{1}H-NMR. ^{1}H-NMR spectra were recorded at 300 K on an Avance III 600 spectrometer (Bruker®, Bremen, Germany) operating at a proton frequency of 600.20 MHz using a 5 mm PBBO gradient probe. Diluted urine aqueous samples were measured and recorded in procno 11 using one-dimensional ^{1}H pulse experiments and were carried out using the nuclear Overhauser effect spectroscopy (NOESY). NOESY presaturation sequence (RD–90°–t1–90°–tm–90° ACQ) was used to suppress the residual water peak, and the mixing time was set at 100 ms. Solvent presaturation with irradiation power of 150 µW was applied during recycling delay (RD = 5 s) and mixing time (noesypr1d pulse program in Bruker®) to eliminate the residual water. The 90° pulse length was calibrated for each sample and varied from 11.21 to 11.38 ms. The spectral width was 9.6 kHz (16 ppm), and a total of 128 transients were collected into 64 k data points for each ^{1}H spectrum. The exponential line broadening applied before Fourier transformation was of 0.3 Hz. The frequency domain spectra were manually phased and baseline-corrected using TopSpin software (version 3.2, Bruker). Data were normalized by two different ways, by the probabilistic method to avoid differences between samples due to different urine concentration and by ERETIC. The acquired ^{1}H-NMR were compared to references of pure compounds from the metabolic profiling AMIX spectra database (Bruker®), HMDB and Chenomx databases for metabolite identification. In addition, we assigned metabolites by ^{1}H-^{1}H homonuclear correlation (COSY and TOCSY) and ^{1}H-^{13}C heteronuclear (HSQC) 2D NMR experiments and by correlation with pure compounds run in-house. After pre-processing, specific ^{1}H-NMR regions identified in

the spectra were integrated using MATLAB scripts run in-house. Curated identified regions across the spectra were exported to an Excel spreadsheet to evaluate robustness of the different ^{1}H-NMR signals and to give relative concentrations.

4.6. Microbiome Analysis (Shotgun Metagenomic Sequencing)

The shotgun metagenomic sequencing was performed in 8 animals per group. DNA was extracted from cecum content using the PowerSoil DNA extraction kit (MO BIO Laboratories, Carlsbad, CA, USA) following the manufacturer's protocol. Between 400 and 500 ng of total DNA was used for library preparation for Illumina sequencing employing Illumina DNA Prep kit (Illumina, San Diego, CA, USA). All libraries were assessed using a TapeStation High Sensitivity DNA kit (Agilent Technologies, Santa Clara, CA, USA) and quantified by Qubit (Invitrogen, Waltham, MA, USA).

Validated libraries were pooled in equimolar quantities and sequenced as a paired-end 150-cycle run on an Illumina NextSeq2000. A total of 1548 million reads were generated, and raw reads were filtered for QV > 30 using an in-house phyton script. Filtered reads were aligned to unique clade-specific marker genes using MetaPhlAn 3 [55] to assess the taxonomic profile. The alignment was performed indicating the closest name of species to the sequence (the best hit). The relative proportions calculated from MetaPhlAn were used to calculate relative abundances, alpha diversity measure (chao1 index) and beta diversity measure (Aitchison distance).

4.7. Statistical Analysis

4.7.1. General Statistical Analysis

The statistical analysis was performed using the R statistical software (version 4.0.2, R Core Team 2021) and different libraries included in Bioconductor (version 3.11, Bioconductor project) were used [56]. The continuous variables of biological assay were shown as mean ± standard error of the mean (SEM) per group. After the normality study, parametric unpaired t-test was used for single statistical comparisons; thus, a two-tailed value of p-value < 0.05 was considered.

4.7.2. Metabolomic Data Analysis

For metabolomics, the MW test was performed in this case because the variables follow the assumption of a non-parametric test. The p-value adjustment for multiple comparisons was carried out according to the BH correction considering a 5% of FDR. The magnitude of difference between populations was presented as fold change (FC) relative to the control group. In parallel, a predictive analysis was conducted to evaluate the prediction power of the experimental model. On the one hand, PCA, an unsupervised multivariate data projection method, was performed to explore the native relationship between groups. On the other hand, OPLS-DA, a supervised multivariate data projection method, was calculated to explore the possible relationships between the observable variables (X) and the predicted variables or target (Y), reflecting the variation in the data set. No data transformation has been

applied before conducting the analysis. The predictive performance of the test set was estimated by the Q2Y parameter calculated through cross-validation. The values of Q2 < 0 suggests a model with no predictive ability, 0 < Q2 < 0.5 suggests some predictive character and Q2 > 0.5 indicates good predictive ability [57]. The feature importance was calculated through the VIP values that reflect both the loading weights for each component and the variability in the response explained by the component.

In this case, we followed a pipeline, which was previously described [58,59], considering statistical significance and predicting capability of individual metabolites to capture the major differences in the experimental study: (1) the metabolites reflecting general metabolic differences were selected according to the MW statistical test (p-value < 0.05) and the VIP (>1.0) values to present an overview of the impact in the metabolism of early stress stage; (2) the individual discriminating metabolites associated with stress and controls were selected primarily according to the MW statistical test (p-value < 0.01) and the BH correction (q-value < 0.05) and the VIP (>1.5) values to propose candidate biomarkers.

Additionally, RF was calculated to sort the most important metabolites that distinguish between the CON and 3d CUMS groups. The whole data set was used without rejecting the metabolites where no differences were observed using the MW test. Therefore, the 10 most relevant metabolites were presented.

4.7.3. Metagenomic Data Analysis

For microbiome data, centred log-ratio (CLR) was performed before any statistical test. The beta diversity was calculated from the Aitchison distance, and PERMANOVA test was performed with 100 permutations to assess the differences between groups (n = 8 animals per group). The alpha diversity was calculated by Chao1 index. Taxonomic abundances were compared between experimental groups using the BH adjustment on MW test that is presented by relative abundance (%). The relative abundance was filtered to only include variables that were present above 0.01% in at least 3 samples [60]. The magnitude of difference between populations was determined by the determination of FC.

4.7.4. Integration Data Analysis

For multi-omics data integration, DIABLO implementation in the mixOmics R package (version 6.18.1, mixOmics project) was used to integrate plasma and urine metabolome and microbiome [61]. The R script was added as supplementary data with the steps to perform all the integration analysis. To summarize, the first step is the parameter choice of the design matrix, the number of components and the number of variables to select: (1) a design matrix of 0.1 was used to focus primarily on the discrimination between the groups; (2) the perf function was used to estimate the performance of the model and the balanced error rate (BER) and overall error rates per component were displayed to select the optimal number of components; and (3) the number of variables was chosen using the tune.block.splsda function that is run with 10-fold cross validation and repeated 10 times, thus this tuning step led to a selection of 8 plasma metabolites, 6 urine metabolites and 5 microbes. Thereafter,

the final model was computed, and different sample and variable plots were performed. In Figure 6a, the correlations greater than 0.7 between variables of different types were represented using the function circosPlot. In Figure 6b, the resulting network, which was calculated with the network function, was further analysed using Cytoscape (version 3.8.2, Institute of Systems Biology, Seattle, WA, USA) [62].

The final performance of the model was evaluated by the perf function using 10-fold cross-validation repeated 10 times. Additionally, the ROC curve analysis was conducted to evaluate the metabolite combination patterns that could correctly dichotomize the stressed and healthy groups at acceptable sensitivity and specificity (defined as greater than 80% for both). The AUC value was used as a measure of the prognostic accuracy, thus, an AUC value of 1 indicates a perfect test due to the absence of overlap of the test data between the groups. In this case, an AUC value above >0.85 was considered for inclusion in the model.

4.7.5. Pathway Analysis

Finally, a comparison between univariate (MW test adjusted by BH) and multivariate analyses (PCA and OPLS-DA), RF and multi-omics integration (DIABLO) was performed to check the robustness among methods of the candidate biomarkers. The weights of the methods can be 0 (no influence) or 1 (influence), and the final value is a summatory of the weights of the different methods of analysis: Features with a weight of 3 (positive in all the methods) presented the highest impact on the model followed by weights of 2. The key features were analysed through different databases to identify related pathways and elucidate the global effect in the metabolism of an early stress stage. The main database consulted was the Kyoto Encyclopaedia of Genes and Genomes (KEGG) [63], among others. To show those results, XMind (version XMind 2020, XMind Ltd., Virginia, ON, Canada) was used to incorporate the information about pathway analysis (Figure 7).

5. Conclusions

In summary, differences between the groups were observed in the behaviour, biochemical parameters and metabolic patterns. Specifically, an omics profile was elucidated and was composed by a signature of eight plasma metabolites (threonic acid, alpha-ketoglutarate, malic acid, 3-hydroxybutiric acid, DG 34:2, succinic acid, aspartic acid and cholesterol); six urine metabolites (taurine, α-hydroxyhippurate, N-acetylglycine, malic acid, N,N-dimethylglycine and betaine); and five microbes, including bacteria and viruses (*Escherichia coli*, *Lactobacillus murinus*, *Akkermansia muciniphila*, uncharacterized *Herpesvirus* and *Bacteroides uniformis*). Finally, seven metabolites may be considered a metabolic footprint from plasma (malic acid, threonic acid, alpha-ketoglutarate, succinic acid, cholesterol and pyruvic acid) and urine metabolomics (N,N-dimethylglycine). Furthermore, the full matching metabolites are malic acid, threonic acid, alpha-ketoglutarate, succinic acid and cholesterol in plasma metabolomics, these being the key metabolites of the early

stress stage based on a 3d CUMS approach targeting the TCA cycle and energy metabolism. In addition, more studies profiling the early stress stage are recommended for the further exploration and validation of these omics profiles, metabolic footprints and potential candidate biomarkers.

References

1. World Health Organization Mental Health in the Workplace Available online: http://www.who.int/mental_health/world-mental-health-day/2017/en/ (accessed on Apr 12, 2021).

2. Cohen, S.; Kessler, R.C.; Gordon, L.U. Strategies for measuring stress in studies of psychiatric and physical disorders. In *Measuring stress: A guide for health and social scientists.*; Oxford University Press: New York, NY, US, 1995; pp. 3–26 ISBN 0-19-508641-4 (Hardcover).

3. Turner, A.I.; Smyth, N.; Hall, S.J.; Torres, S.J.; Hussein, M.; Jayasinghe, S.U.; Ball, K.; Clow, A.J. Psychological stress reactivity and future health and disease outcomes: A systematic review of prospective evidence. *Psychoneuroendocrinology* **2020**, *114*, 104599, doi:https://doi.org/10.1016/j.psyneuen.2020.104599.

4. Battle, D.E. Diagnostic and Statistical Manual of Mental Disorders (DSM). *CoDAS* 2013, *25*, 191–192.

5. Humer, E.; Pieh, C.; Probst, T. Metabolomic Biomarkers in Anxiety Disorders. *Int. J. Mol. Sci.* **2020**, *21*, 4784, doi:10.3390/ijms21134784.

6. Hernandez-Baixauli, J.; Quesada-Vázquez, S.; Mariné-Casadó, R.; Cardoso, K.G.; Caimari, A.; Del Bas, J.M.; Escoté, X.; Baselga-Escudero, L. Detection of early disease risk factors associated with metabolic syndrome: A new era with the NMR metabolomics assessment. *Nutrients* **2020**, *12*, 1–34, doi:10.3390/nu12030806.

7. Martin, E.I.; Ressler, K.J.; Binder, E.; Nemeroff, C.B. The neurobiology of anxiety disorders: brain imaging, genetics, and psychoneuroendocrinology. *Psychiatr. Clin. North Am.* **2009**, *32*, 549–575, doi:10.1016/j.psc.2009.05.004.

8. Filiou, M.D.; Zhang, Y.; Teplytska, L.; Reckow, S.; Gormanns, P.; Maccarrone, G.; Frank, E.; Kessler, M.S.; Hambsch, B.; Nussbaumer, M.; et al. Proteomics and Metabolomics Analysis of a Trait Anxiety Mouse Model Reveals Divergent Mitochondrial Pathways. *Biol. Psychiatry* **2011**, *70*, 1074–1082, doi:https://doi.org/10.1016/j.biopsych.2011.06.009.

9. Guest, P.C.; Guest, F.L.; Martins-de Souza, D. Making Sense of Blood-Based Proteomics and Metabolomics in Psychiatric Research. *Int. J. Neuropsychopharmacol.* **2016**, *19*, doi:10.1093/ijnp/pyv138.

10. Donati, R.J.; Rasenick, M.M. G protein signaling and the molecular basis of antidepressant action. *Life Sci.* **2003**, *73*, 1–17.

11. Wood, P.L. Mass Spectrometry Strategies for Clinical Metabolomics and Lipidomics in Psychiatry, Neurology, and Neuro-Oncology. *Neuropsychopharmacology* **2014**, *39*, 24–33, doi:10.1038/npp.2013.167.

12. Antoniuk, S.; Bijata, M.; Ponimaskin, E.; Wlodarczyk, J. Chronic unpredictable mild stress for modeling depression in rodents: Meta-analysis of model reliability. *Neurosci. Biobehav. Rev.* **2019**, *99*, 101–116, doi:10.1016/j.neubiorev.2018.12.002.

13. Li, Z.-Y.; Zheng, X.-Y.; Gao, X.-X.; Zhou, Y.-Z.; Sun, H.-F.; Zhang, L.-Z.; Guo, X.-Q.; Du, G.-H.; Qin, X.-M. Study of plasma metabolic profiling and biomarkers of chronic unpredictable mild stress rats based on gas chromatography/mass spectrometry. *Rapid Commun. Mass Spectrom.* **2010**, *24*, 3539–3546, doi:10.1002/rcm.4809.

14. Zhong, F.; Liu, L.; Wei, J.-L.; Hu, Z.-L.; Li, L.; Wang, S.; Xu, J.-M.; Zhou, X.-F.; Li, C.-Q.; Yang, Z.-Y.; et al. Brain-Derived Neurotrophic Factor Precursor in the Hippocampus Regulates Both Depressive and Anxiety-Like Behaviors in Rats . *Front. Psychiatry* 2019, *9*, 776.

15. Nishitani, N.; Nagayasu, K.; Asaoka, N.; Yamashiro, M.; Andoh, C.; Nagai, Y.; Kinoshita, H.; Kawai, H.; Shibui, N.; Liu, B.; et al. Manipulation of dorsal raphe serotonergic neurons modulates active

coping to inescapable stress and anxiety-related behaviors in mice and rats. *Neuropsychopharmacol. Off. Publ. Am. Coll. Neuropsychopharmacol.* **2019**, *44*, 721–732, doi:10.1038/s41386-018-0254-y.

16. Jin, S.; Zhao, Y.; Jiang, Y.; Wang, Y.; Li, C.; Zhang, D.; Lian, B.; Du, Z.; Sun, H.; Sun, L. Anxiety-like behaviour assessments of adolescent rats after repeated maternal separation during early life. *Neuroreport* **2018**, *29*, 643–649, doi:10.1097/WNR.0000000000001010.

17. Mengler, L.; Khmelinskii, A.; Diedenhofen, M.; Po, C.; Staring, M.; Lelieveldt, B.P.F.; Hoehn, M. Brain maturation of the adolescent rat cortex and striatum: changes in volume and myelination. *Neuroimage* **2014**, *84*, 35–44.

18. McCutcheon, J.E.; Marinelli, M. Age matters. *Eur. J. Neurosci.* **2009**, *29*, 997–1014.

19. Meyza, K.Z.; Boguszewski, P.M.; Nikolaev, E.; Zagrodzka, J. Age increases anxiety and reactivity of the fear/anxiety circuit in Lewis rats. *Behav. Brain Res.* **2011**, *225*, 192–200, doi:10.1016/j.bbr.2011.07.011.

20. Seibenhener, M.L.; Wooten, M.C. Use of the Open Field Maze to measure locomotor and anxiety-like behavior in mice. *J. Vis. Exp.* **2015**, e52434–e52434, doi:10.3791/52434.

21. Sturman, O.; Germain, P.-L.; Bohacek, J. Exploratory rearing: a context- and stress-sensitive behavior recorded in the open-field test. *Stress* **2018**, *21*, 443–452, doi:10.1080/10253890.2018.1438405.

22. Zaytsoff, S.J.M.; Brown, C.L.J.; Montina, T.; Metz, G.A.S.; Abbott, D.W.; Uwiera, R.R.E.; Inglis, G.D. Corticosterone-mediated physiological stress modulates hepatic lipid metabolism, metabolite profiles, and systemic responses in chickens. *Sci. Rep.* **2019**, *9*, 19225, doi:10.1038/s41598-019-52267-6.

23. Xie, X.; Shen, Q.; Yu, C.; Xiao, Q.; Zhou, J.; Xiong, Z.; Li, Z.; Fu, Z. Depression-like behaviors are accompanied by disrupted mitochondrial energy metabolism in chronic corticosterone-induced mice. *J. Steroid Biochem. Mol. Biol.* **2020**, *200*, 105607, doi:https://doi.org/10.1016/j.jsbmb.2020.105607.

24. Müller, C.P.; Reichel, M.; Mühle, C.; Rhein, C.; Gulbins, E.; Kornhuber, J. Brain membrane lipids in major depression and anxiety disorders. *Biochim. Biophys. Acta* **2015**, *1851*, 1052–65, doi:10.1016/j.bbalip.2014.12.014.

25. Liu, X.-J.; Zhou, Y.-Z.; Li, Z.-F.; Cui, J.; Li, Z.-Y.; Gao, X.-X.; Sun, H.-F.; Zhang, L.-Z.; Du, G.-H.; Qin, X.-M. Anti-depressant effects of Xiaoyaosan on rat model of chronic unpredictable mild stress: a plasma metabonomics study based on NMR spectroscopy. *J. Pharm. Pharmacol.* **2012**, *64*, 578–588, doi:10.1111/j.2042-7158.2011.01412.x.

26. Serretti, A.; Mandelli, L.; Lattuada, E.; Smeraldi, E. Depressive syndrome in major psychoses: a study on 1351 subjects. *Psychiatry Res.* **2004**, *127*, 85–99, doi:10.1016/j.psychres.2003.12.025.

27. Humer, E.; Probst, T.; Pieh, C. Metabolomics in Psychiatric Disorders: What We Learn from Animal Models. *Metab.* 2020, *10*.

28. Filiou, M.D.; Sandi, C. Anxiety and Brain Mitochondria: A Bidirectional Crosstalk. *Trends Neurosci.* **2019**, *42*, 573–588, doi:10.1016/j.tins.2019.07.002.

29. Wu, N.; Yang, M.; Gaur, U.; Xu, H.; Yao, Y.; Li, D. Alpha-Ketoglutarate: Physiological Functions and Applications. *Biomol. Ther. (Seoul).* **2016**, *24*, 1–8, doi:10.4062/biomolther.2015.078.

30. Gray, L.R.; Tompkins, S.C.; Taylor, E.B. Regulation of pyruvate metabolism and human disease. *Cell. Mol. Life Sci.* **2014**, *71*, 2577–2604, doi:10.1007/s00018-013-1539-2.

31. Geng, C.; Guo, Y.; Wang, C.; Liao, D.; Han, W.; Zhang, J.; Jiang, P. Systematic impacts of chronic unpredictable mild stress on metabolomics in rats. *Sci. Rep.* **2020**, *10*, 700, doi:10.1038/s41598-020-57566-x.

32. El Idrissi, A. Taurine Regulation of Neuroendocrine Function. *Adv. Exp. Med. Biol.* **2019**, *1155*, 977–985, doi:10.1007/978-981-13-8023-5_81.

33. Wang, Z.; Ohata, Y.; Watanabe, Y.; Yuan, Y.; Yoshii, Y.; Kondo, Y.; Nishizono, S.; Chiba, T. Taurine Improves Lipid Metabolism and Increases Resistance to Oxidative Stress. *J. Nutr. Sci. Vitaminol. (Tokyo).* **2020**, *66*, 347–356, doi:10.3177/jnsv.66.347.

34. Jakaria, M.; Azam, S.; Haque, M.E.; Jo, S.-H.; Uddin, M.S.; Kim, I.-S.; Choi, D.-K. Taurine and its analogs in neurological disorders: Focus on therapeutic potential and molecular mechanisms. *Redox Biol.* **2019**, *24*, 101223, doi:https://doi.org/10.1016/j.redox.2019.101223.

35. Tracey, T.J.; Steyn, F.J.; Wolvetang, E.J.; Ngo, S.T. Neuronal Lipid Metabolism: Multiple Pathways Driving Functional Outcomes in Health and Disease. *Front. Mol. Neurosci.* **2018**, *11*, 10, doi:10.3389/fnmol.2018.00010.

36. Coplan, J.D.; Mathew, S.J.; Mao, X.; Smith, E.L.P.; Hof, P.R.; Coplan, P.M.; Rosenblum, L.A.; Gorman, J.M.; Shungu, D.C. Decreased choline and creatine concentrations in centrum semiovale in patients with generalized anxiety disorder: relationship to IQ and early trauma. *Psychiatry Res.* **2006**, *147*, 27–39, doi:10.1016/j.pscychresns.2005.12.011.

37. Abdul Rahim, M.B.H.; Chilloux, J.; Martinez-Gili, L.; Neves, A.L.; Myridakis, A.; Gooderham, N.; Dumas, M.-E. Diet-induced metabolic changes of the human gut microbiome: importance of short-chain fatty acids, methylamines and indoles. *Acta Diabetol.* **2019**, *56*, 493–500, doi:10.1007/s00592-019-01312-x.

38. He, Q.; Tang, H.; Ren, P.; Kong, X.; Wu, G.; Yin, Y.; Wang, Y. Dietary supplementation with l-arginine partially counteracts serum metabonome induced by weaning stress in piglets. *J. Proteome Res.* **2011**, *10*, 5214–21, doi:10.1021/pr200688u.

39. Shan, B.; Ai, Z.; Zeng, S.; Song, Y.; Song, J.; Zeng, Q.; Liao, Z.; Wang, T.; Huang, C.; Su, D. Gut microbiome-derived lactate promotes to anxiety-like behaviors through GPR81 receptor-mediated lipid metabolism pathway. *Psychoneuroendocrinology* **2020**, *117*, 104699, doi:https://doi.org/10.1016/j.psyneuen.2020.104699.

40. Blacher, E.; Bashiardes, S.; Shapiro, H.; Rothschild, D.; Mor, U.; Dori-Bachash, M.; Kleimeyer, C.; Moresi, C.; Harnik, Y.; Zur, M.; et al. Potential roles of gut microbiome and metabolites in modulating ALS in mice. *Nature* **2019**, *572*, 474–480, doi:10.1038/s41586-019-1443-5.

41. Valles-Colomer, M.; Falony, G.; Darzi, Y.; Tigchelaar, E.F.; Wang, J.; Tito, R.Y.; Schiweck, C.; Kurilshikov, A.; Joossens, M.; Wijmenga, C.; et al. The neuroactive potential of the human gut microbiota in quality of life and depression. *Nat. Microbiol.* **2019**, *4*, 623–632, doi:10.1038/s41564-018-0337-x.

42. Sun, L.-J.; Li, J.-N.; Nie, Y.-Z. Gut hormones in microbiota-gut-brain cross-talk. *Chin. Med. J. (Engl).* **2020**, *133*, 826–833, doi:10.1097/CM9.0000000000000706.

43. Otaru, N.; Ye, K.; Mujezinovic, D.; Berchtold, L.; Constancias, F.; Cornejo, F.A.; Krzystek, A.; de Wouters, T.; Braegger, C.; Lacroix, C.; et al. GABA Production by Human Intestinal Bacteroides spp.: Prevalence, Regulation, and Role in Acid Stress Tolerance . *Front. Microbiol.* 2021, *12*, 860.

44. Capitani, G.; De Biase, D.; Aurizi, C.; Gut, H.; Bossa, F.; Grütter, M.G. Crystal structure and functional analysis of Escherichia coli glutamate decarboxylase. *EMBO J.* **2003**, *22*, 4027–4037, doi:10.1093/emboj/cdg403.

45. Cui, Y.; Miao, K.; Niyaphorn, S.; Qu, X. Production of Gamma-Aminobutyric Acid from Lactic Acid Bacteria: A Systematic Review. *Int. J. Mol. Sci.* **2020**, *21*, doi:10.3390/ijms21030995.

46. Bear, T.; Dalziel, J.; Coad, J.; Roy, N.; Butts, C.; Gopal, P. The Microbiome-Gut-Brain Axis and Resilience to Developing Anxiety or Depression under Stress. *Microorg.* 2021, *9*.

47. Pistorio, E.; Luca, M.; Luca, A.; Messina, V.; Calandra, C. Autonomic nervous system and lipid metabolism: findings in anxious-depressive spectrum and eating disorders. *Lipids Health Dis.*

2011, *10*, 192, doi:10.1186/1476-511X-10-192.

48. Zhang, Y.; Filiou, M.D.; Reckow, S.; Gormanns, P.; Maccarrone, G.; Kessler, M.S.; Frank, E.; Hambsch, B.; Holsboer, F.; Landgraf, R.; et al. Proteomic and Metabolomic Profiling of a Trait Anxiety Mouse Model Implicate Affected Pathways. *Mol. Cell. Proteomics* **2011**, *10*, M111.008110, doi:https://doi.org/10.1074/mcp.M111.008110.

49. Lieberman, H.R.; Kellogg, M.D.; Kramer, F.M.; Bathalon, G.P.; Lesher, L.L. Lipid and other plasma markers are associated with anxiety, depression, and fatigue. *Heal. Psychol. Off. J. Div. Heal. Psychol. Am. Psychol. Assoc.* **2012**, *31*, 210–216, doi:10.1037/a0026499.

50. Demirkan, A.; Isaacs, A.; Ugocsai, P.; Liebisch, G.; Struchalin, M.; Rudan, I.; Wilson, J.F.; Pramstaller, P.P.; Gyllensten, U.; Campbell, H.; et al. Plasma phosphatidylcholine and sphingomyelin concentrations are associated with depression and anxiety symptoms in a Dutch family-based lipidomics study. *J. Psychiatr. Res.* **2013**, *47*, 357–362, doi:https://doi.org/10.1016/j.jpsychires.2012.11.001.

51. Puurunen, J.; Tiira, K.; Vapalahti, K.; Lehtonen, M.; Hanhineva, K.; Lohi, H. Fearful dogs have increased plasma glutamine and γ-glutamyl glutamine. *Sci. Rep.* **2018**, *8*, 15976, doi:10.1038/s41598-018-34321-x.

52. Zhang, Y.; Yuan, S.; Pu, J.; Yang, L.; Zhou, X.; Liu, L.; Jiang, X.; Zhang, H.; Teng, T.; Tian, L.; et al. Integrated Metabolomics and Proteomics Analysis of Hippocampus in a Rat Model of Depression. *Neuroscience* **2018**, *371*, 207–220, doi:https://doi.org/10.1016/j.neuroscience.2017.12.001.

53. Hoffman, J.F.; Fan, A.X.; Neuendorf, E.H.; Vergara, V.B.; Kalinich, J.F. Hydrophobic Sand Versus Metabolic Cages: A Comparison of Urine Collection Methods for Rats (Rattus norvegicus). *J. Am. Assoc. Lab. Anim. Sci.* **2018**, *57*, 51–57.

54. Eggers, L.F.; Schwudke, D. Liquid Extraction: Folch BT - Encyclopedia of Lipidomics. In; Wenk, M.R., Ed.; Springer Netherlands: Dordrecht, 2016; pp. 1–6 ISBN 978-94-007-7864-1.

55. Beghini, F.; McIver, L.J.; Blanco-Míguez, A.; Dubois, L.; Asnicar, F.; Maharjan, S.; Mailyan, A.; Manghi, P.; Scholz, M.; Thomas, A.M.; et al. Integrating taxonomic, functional, and strain-level profiling of diverse microbial communities with bioBakery 3. *Elife* **2021**, *10*, doi:10.7554/eLife.65088.

56. Marini, F.; Linke, J.; Binder, H. ideal: an R/Bioconductor package for interactive differential expression analysis. *BMC Bioinformatics* **2020**, *21*, 565, doi:10.1186/s12859-020-03819-5.

57. Llorach-Asunción, R.; Jauregui, O.; Urpi-Sarda, M.; Andres-Lacueva, C. Methodological aspects for metabolome visualization and characterization: a metabolomic evaluation of the 24 h evolution of human urine after cocoa powder consumption. *J. Pharm. Biomed. Anal.* **2010**, *51*, 373–381, doi:10.1016/j.jpba.2009.06.033.

58. Wang, H.; Liang, S.; Wang, M.; Gao, J.; Sun, C.; Wang, J.; Xia, W.; Wu, S.; Sumner, S.J.; Zhang, F.; et al. Potential serum biomarkers from a metabolomics study of autism. *J. Psychiatry Neurosci.* **2016**, *41*, 27–37, doi:10.1503/jpn.140009.

59. To, K.K.W.; Lee, K.-C.; Wong, S.S.Y.; Sze, K.-H.; Ke, Y.-H.; Lui, Y.-M.; Tang, B.S.F.; Li, I.W.S.; Lau, S.K.P.; Hung, I.F.N.; et al. Lipid metabolites as potential diagnostic and prognostic biomarkers for acute community acquired pneumonia. *Diagn. Microbiol. Infect. Dis.* **2016**, *85*, 249–254, doi:10.1016/j.diagmicrobio.2016.03.012.

60. Fujisaka, S.; Avila-Pacheco, J.; Soto, M.; Kostic, A.; Dreyfuss, J.M.; Pan, H.; Ussar, S.; Altindis, E.; Li, N.; Bry, L.; et al. Diet, Genetics, and the Gut Microbiome Drive Dynamic Changes in Plasma Metabolites. *Cell Rep.* **2018**, *22*, 3072–3086, doi:10.1016/j.celrep.2018.02.060.

61. Rohart, F.; Gautier, B.; Singh, A.; Lê Cao, K.-A. mixOmics: An R package for 'omics feature selection and multiple data integration. *PLOS Comput. Biol.* **2017**, *13*, e1005752.

62. Smoot, M.E.; Ono, K.; Ruscheinski, J.; Wang, P.-L.; Ideker, T. Cytoscape 2.8: new features for data

integration and network visualization. *Bioinformatics* **2011**, *27*, 431–432, doi:10.1093/bioinformatics/btq675.

63. Kanehisa, M.; Goto, S. KEGG: kyoto encyclopedia of genes and genomes. *Nucleic Acids Res.* **2000**, *28*, 27–30, doi:10.1093/nar/28.1.27.

Annex. Supplementary Material of Manuscript 6

Supplementary table 1. Statistical analysis of plasma metabolites in the early stress stage. CON and 3d CUMS groups (*n* = 10 animals per group) are represented by relative abundances (AU). Relative abundances of metabolites are presented by the mean ± SEM. Plasma metabolites are sorted by *p*-value. The summary of univariant and multivariate analysis is shown including *p*-value, *q*-value, VIP value, RF and FC. The statistically significant *p*-values and *q*-values are highlighted in bold. Abbreviations: DG, diacylglycerol; ChoE, cholesterol ester; TG, triglyceride; PC, phosphatidylcholine; SM, sphingomyelin; LPC, lysophospholipid; PE, phosphatidylethanolamine.

Metabolite	CON	3d CUMS	*p*-value	*q*-value	VIP	RF	FC
Malic acid	0.36 ± 0.03	0.74 ± 0.07	**<0.01**	**0.03**	2.42	0.23	2.1
Threonic acid	2.55 ± 0.21	0.8 ± 0.17	**<0.01**	**0.03**	2.63	0.15	0.3
Alpha-ketoglutarate	1.21 ± 0.08	1.94 ± 0.13	**<0.01**	**0.03**	2.30	0.10	1.6
Succinic acid	0.61 ± 0.04	0.86 ± 0.04	**<0.01**	**0.03**	2.25	0.04	1.4
Pyruvic acid	14.68 ± 0.85	25.39 ± 3.14	**<0.01**	**0.03**	2.09	0.05	1.7
Cholesterol	0.33 ± 0.02	0.6 ± 0.05	**<0.01**	**0.05**	2.38	0.05	1.8
Oleic acid	1.71 ± 0.09	2.47 ± 0.22	**<0.01**	0.06	1.80	0.12	1.4
3-hydroxybutiric acid	2.03 ± 0.19	2.76 ± 0.08	**0.01**	0.09	1.91	0.04	1.4
Citric acid	3.04 ± 0.14	3.8 ± 0.2	**0.01**	0.10	1.89	0.01	1.3
Phenylalanine	0.87 ± 0.15	0.55 ± 0.11	**0.01**	0.16	1.44	0.01	0.6
Threonine	1.35 ± 0.13	0.97 ± 0.11	**0.01**	0.16	1.56	-	0.7
DG 34:2	1 ± 0.05	0.84 ± 0.05	**0.02**	0.19	1.28	0.01	0.8
Glucose	0.78 ± 0.04	0.9 ± 0.04	**0.02**	0.19	1.53	0.01	1.2
Valine	1.69 ± 0.64	0.94 ± 0.42	**0.02**	0.19	0.85	-	0.6
Aspartic acid	0.53 ± 0.1	0.68 ± 0.04	**0.03**	0.21	1.49	0.02	1.3
Fructose	0.4 ± 0.02	0.3 ± 0.02	**0.03**	0.21	1.94	-	0.8
Glyceric acid	1.75 ± 0.12	1.33 ± 0.11	**0.03**	0.24	1.84	0.02	0.8
2-hydroxyglutaric	0.69 ± 0.07	0.51 ± 0.02	**0.05**	0.32	1.56	-	0.7
Asparagine	0.17 ± 0.02	0.24 ± 0.02	**0.05**	0.32	1.55	-	1.4
ChoE (18:2)	13.81 ± 0.53	15.18 ± 0.6	**0.05**	0.32	1.13	-	1.1
ChoE (18:3)	1.27 ± 0.09	1.74 ± 0.18	**0.05**	0.32	1.19	0.02	1.4
Hydroxyproline	0.54 ± 0.1	0.7 ± 0.07	**0.05**	0.32	1.35	0.01	1.3
Methionine	0.12 ± 0.02	0.17 ± 0.02	0.08	0.44	1.41	-	1.4
Tyrosine	0.9 ± 0.15	0.72 ± 0.09	0.09	0.49	0.57	-	0.8
Beta-alanine	0.08 ± 0.01	0.1 ± 0.02	0.10	0.52	0.80	-	1.3
TG 46:0	0.77 ± 0.05	0.66 ± 0.03	0.10	0.52	1.35	-	0.9
ChoE (16:0)	1.8 ± 0.06	1.97 ± 0.09	0.12	0.52	0.93	-	1.1
Histidine	0.14 ± 0.01	0.11 ± 0.01	0.12	0.52	1.10	-	0.8
Ornithine	3.12 ± 0.6	3.71 ± 0.36	0.12	0.52	0.90	-	1.2
Proline	0.26 ± 0.02	0.29 ± 0.01	0.12	0.52	1.06	0.02	1.1
Serine	0.26 ± 0.02	0.22 ± 0.01	0.12	0.52	1.06	-	0.8
ChoE (22:6)	1.67 ± 0.12	2.08 ± 0.17	0.14	0.54	1.38	-	1.2
DG 36:4	1.97 ± 0.13	1.88 ± 0.07	0.14	0.54	0.09	-	1
TG 52:1	0.98 ± 0.46	0.45 ± 0.05	0.14	0.54	1.32	-	0.5
TG 54:2	1.06 ± 0.52	0.48 ± 0.05	0.14	0.54	1.22	-	0.5
Glucose-6-phosphate	0.14 ± 0.02	0.18 ± 0.02	0.16	0.55	0.94	-	1.3
Glutamic acid	0.09 ± 0.01	0.12 ± 0.01	0.16	0.55	1.36	-	1.3
Lysine	1 ± 0.17	0.76 ± 0.1	0.16	0.55	0.71	-	0.8
PC 42:4 e	0.01 ± 0	0.01 ± 0	0.16	0.55	0.66	-	1
SM 33:1	0.34 ± 0.02	0.38 ± 0.02	0.16	0.55	0.92	-	1.1
ChoE (18:0)	0.11 ± 0.02	0.14 ± 0.01	0.19	0.60	0.89	-	1.3
TG 50:0	0.44 ± 0.13	0.28 ± 0.02	0.19	0.60	1.25	-	0.6
LPC 16:1 e	0.13 ± 0	0.14 ± 0	0.21	0.65	0.99	-	1.1
LPC 15:0	0.68 ± 0.03	0.74 ± 0.04	0.24	0.65	0.81	-	1.1

LPC 16:0	67.34 ± 1.75	71.03 ± 1.93	0.24	0.65	0.81	-	1.1
PC 33:1	0.04 ± 0.01	0.06 ± 0.01	0.24	0.65	0.83	-	1.5
PC 34:1	3.07 ± 0.26	3.59 ± 0.28	0.24	0.65	0.63	-	1.2
SM 34:2	1.65 ± 0.07	1.75 ± 0.1	0.24	0.65	0.44	-	1.1
SM 43:1	1.13 ± 0.04	1.03 ± 0.05	0.24	0.65	1.15	0.01	0.9
TG 52:5	13.23 ± 6.44	6.29 ± 1.23	0.24	0.65	1.18	-	0.5
LPC 18:2	31.95 ± 1.27	34.19 ± 1.03	0.27	0.67	0.80	-	1.1
TG 46:1	0.67 ± 0.15	0.5 ± 0.03	0.27	0.67	1.12	-	0.7
TG 48:1	1.64 ± 0.43	1.22 ± 0.17	0.27	0.67	1.03	-	0.7
TG 54:3	6.28 ± 3.07	2.83 ± 0.34	0.27	0.67	1.19	-	0.5
Fumaric acid	1.04 ± 0.15	1.25 ± 0.1	0.31	0.67	0.91	-	1.2
PC 35:2	0.38 ± 0.02	0.4 ± 0.02	0.31	0.67	0.26	-	1.1
Ribose	4.05 ± 0.33	3.66 ± 0.39	0.31	0.67	0.88	-	0.9
SM 35:1	0.16 ± 0.01	0.17 ± 0.01	0.31	0.67	0.80	-	1.1
TG 48:0	1.24 ± 0.31	0.86 ± 0.04	0.31	0.67	1.19	-	0.7
TG 54:4	17.8 ± 8.18	8.52 ± 1.28	0.31	0.67	1.17	-	0.5
Tryptophan	1.75 ± 0.26	1.55 ± 0.26	0.31	0.67	0.44	-	0.9
ChoE (20:4)	62.3 ± 3.02	67.79 ± 3.27	0.34	0.67	0.92	-	1.1
ChoE (22:4)	4.72 ± 0.26	5.18 ± 0.3	0.34	0.67	0.59	-	1.1
PE 38:5 e	2.07 ± 0.36	2.64 ± 0.56	0.34	0.67	0.63	-	1.3
SM 32:1	0.24 ± 0.01	0.27 ± 0.02	0.34	0.67	0.47	-	1.1
TG 46:2	0.39 ± 0.08	0.3 ± 0.02	0.34	0.67	1.05	-	0.8
TG 51:2	1.03 ± 0.45	0.58 ± 0.08	0.34	0.67	1.01	-	0.6
TG 52:3	52.41 ± 16.39	33.45 ± 5.31	0.34	0.67	1.09	-	0.6
TG 52:6	1.91 ± 1.01	0.94 ± 0.22	0.34	0.67	1.04	-	0.5
TG 54:7	8.71 ± 4.11	4.34 ± 0.75	0.34	0.67	1.16	-	0.5
Alanine	0.39 ± 0.07	0.45 ± 0.08	0.38	0.70	0.63	-	1.2
ChoE (18:1)	2.35 ± 0.07	2.43 ± 0.18	0.38	0.70	0.09	-	1
PC 34:3 e	0.02 ± 0	0.02 ± 0	0.38	0.70	0.83	-	1
ChoE (17:0)	0.13 ± 0.01	0.13 ± 0	0.43	0.70	0.48	-	1
ChoE (20:2)	0.86 ± 0.05	0.91 ± 0.06	0.43	0.70	0.08	-	1.1
DG 36:2	1.39 ± 0.06	1.45 ± 0.06	0.43	0.70	0.66	-	1
LPC 18:0	49.81 ± 1.79	51.54 ± 2.09	0.43	0.70	0.35	-	1
PC 36:2	12.64 ± 0.81	13.17 ± 0.67	0.43	0.70	0.17	-	1
TG 50:2	15.37 ± 7.15	8.76 ± 1.9	0.43	0.70	0.95	-	0.6
TG 52:2	21.51 ± 13.25	8.94 ± 1.76	0.43	0.70	0.84	-	0.4
TG 54:6	16.71 ± 3.96	12.25 ± 1.56	0.43	0.70	1.04	-	0.7
ChoE (17:1)	0.07 ± 0	0.07 ± 0	0.47	0.70	0.40	-	1
Fructose-6-phosphate	0.14 ± 0.02	0.16 ± 0.02	0.47	0.70	0.38	-	1.1
PC 32:0	0.58 ± 0.03	0.6 ± 0.03	0.47	0.70	0.11	-	1
PC 38:6 e	0.05 ± 0	0.06 ± 0	0.47	0.70	0.81	-	1.2
SM 34:1	17.31 ± 0.65	18.33 ± 0.97	0.47	0.70	0.57	-	1.1
SM 36:1	1.14 ± 0.05	1.21 ± 0.07	0.47	0.70	0.54	-	1.1
SM 36:2	0.42 ± 0.02	0.44 ± 0.02	0.47	0.70	0.63	-	1
TG 48:2	2.31 ± 1.29	1.17 ± 0.25	0.47	0.70	0.87	-	0.5
TG 48:3	0.7 ± 0.37	0.37 ± 0.07	0.47	0.70	0.87	-	0.5
TG 50:1	6.36 ± 3.98	2.51 ± 0.48	0.47	0.70	0.96	-	0.4
TG 50:4	2.91 ± 1.73	1.3 ± 0.32	0.47	0.70	0.94	-	0.4
Alpha-tocopherol	0.56 ± 0.04	0.53 ± 0.03	0.52	0.73	0.45	-	0.9
ChoE (22:5)	0.55 ± 0.03	0.58 ± 0.04	0.52	0.73	0.25	-	1.1
LPC 20:0	0.31 ± 0.01	0.32 ± 0.01	0.52	0.73	0.53	-	1
PC 34:1 e	0.11 ± 0	0.11 ± 0.01	0.52	0.73	0.41	-	1
PC 36:4	15.99 ± 0.86	16.57 ± 0.89	0.52	0.73	0.12	-	1
PC 38:3	0.61 ± 0.12	0.68 ± 0.08	0.52	0.73	0.47	-	1.1
DG 34:3	0.37 ± 0.02	0.4 ± 0.03	0.57	0.76	0.50	-	1.1
LPC 18:1	12.68 ± 0.59	13.55 ± 0.61	0.57	0.76	0.66	-	1.1

PC 32:1	0.26 ± 0.04	0.3 ± 0.06	0.57	0.76	0.03	-	1.2
PC 36:2 e	0.01 ± 0	0.01 ± 0	0.57	0.76	0.68	-	1
DG 34:1	1.14 ± 0.03	1.12 ± 0.03	0.62	0.77	0.38	-	1
PC 40:4	0.13 ± 0.01	0.14 ± 0.01	0.62	0.77	0.07	-	1.1
SM 38:1	0.49 ± 0.02	0.51 ± 0.03	0.62	0.77	0.32	-	1
SM 39:1	0.16 ± 0.03	0.14 ± 0.02	0.62	0.77	0.75	-	0.9
SM 40:1	3.58 ± 0.08	3.83 ± 0.18	0.62	0.77	0.70	-	1.1
SM 40:2	0.79 ± 0.06	0.81 ± 0.06	0.62	0.77	0.07	-	1
SM 42:1	13.2 ± 0.37	13.47 ± 0.68	0.62	0.77	0.07	-	1
TG 50:3	11.1 ± 6.87	5.07 ± 1.39	0.62	0.77	0.85	-	0.5
ChoE (16:1)	0.38 ± 0.03	0.4 ± 0.03	0.68	0.81	0.18	-	1.1
Isoleucine	0.71 ± 0.32	0.41 ± 0.19	0.68	0.81	0.34	-	0.6
LPC 18:0 e	0.08 ± 0	0.08 ± 0	0.68	0.81	0.12	-	1
PE 36:4	3.24 ± 0.31	2.98 ± 0.3	0.68	0.81	0.68	-	0.9
Lactic acid	6.9 ± 0.46	7.11 ± 0.36	0.73	0.85	0.40	-	1
PC 32:2	0.15 ± 0.02	0.16 ± 0.01	0.73	0.85	0.10	-	1.1
PC 38:2	0.11 ± 0.01	0.09 ± 0.01	0.73	0.85	0.92	-	0.8
PC 38:4 e	0.05 ± 0	0.05 ± 0	0.73	0.85	0.10	0.01	1
Leucine	0.26 ± 0.12	0.14 ± 0.08	0.79	0.89	0.51	-	0.5
PC 33:0	0.03 ± 0	0.03 ± 0	0.79	0.89	0.48	-	1
SM 42:2	8.38 ± 0.2	8.27 ± 0.47	0.79	0.89	0.34	-	1
Urea	2.94 ± 0.11	2.86 ± 0.12	0.79	0.89	0.42	-	1
Glycine	2.74 ± 0.55	2.25 ± 0.36	0.85	0.92	0.37	-	0.8
PC 36:3 e	0.05 ± 0	0.05 ± 0	0.85	0.92	0.13	-	1
PC 38:5 e	0.09 ± 0.01	0.09 ± 0.01	0.85	0.92	0.05	-	1
PC 40:5	0.16 ± 0.03	0.14 ± 0.01	0.85	0.92	0.45	-	0.9
SM 41:1	3.49 ± 0.09	3.59 ± 0.14	0.85	0.92	0.28	-	1
Glutamine	1.13 ± 0.17	1.03 ± 0.19	0.91	0.95	0.29	-	0.9
Glycolic acid	3.79 ± 0.12	4 ± 0.35	0.91	0.95	0.02	-	1.1
PC 30:0	0.04 ± 0	0.04 ± 0	0.91	0.95	0.41	-	1
PC 36:0	0.09 ± 0	0.09 ± 0.01	0.91	0.95	0.15	-	1
LPC 16:0 e	0.39 ± 0.02	0.39 ± 0.02	0.97	0.98	0.10	-	1
PC 38:4	19.45 ± 1.2	19.4 ± 0.93	0.97	0.98	0.14	-	1
SM 41:2	0.66 ± 0.04	0.65 ± 0.04	0.97	0.98	0.23	-	1
SM 42:3	3.95 ± 0.16	3.97 ± 0.17	0.97	0.98	0.07	-	1
PC 31:0	0.03 ± 0	0.03 ± 0	1.00	1.00	0.82	-	1
PC 34:0	0.31 ± 0.01	0.32 ± 0.02	1.00	1.00	0.05	-	1

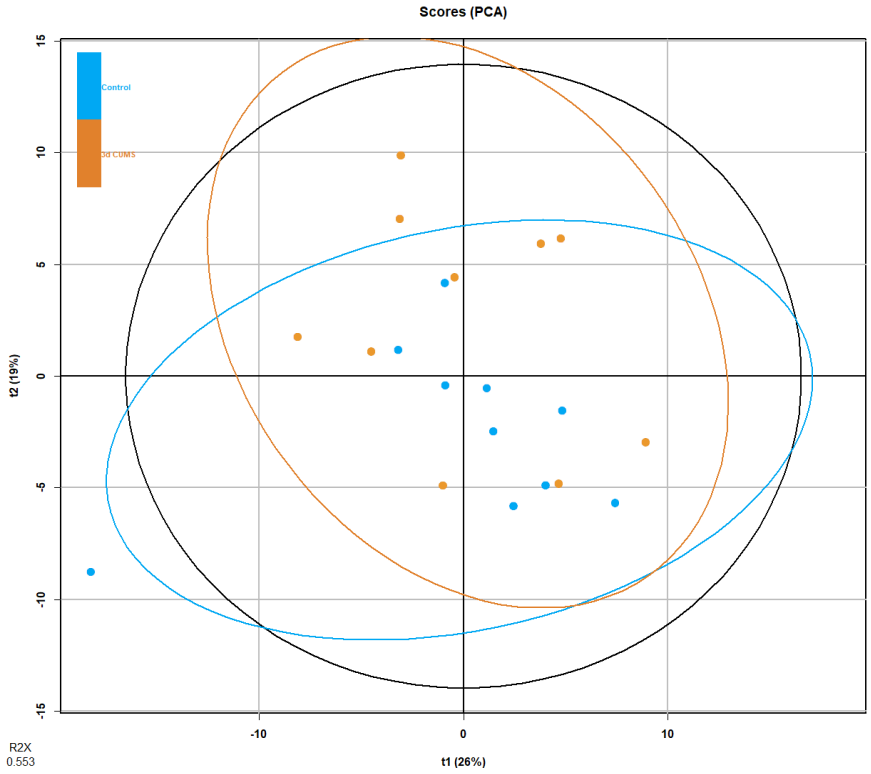

Supplementary Figure 1. PCA of plasma metabolomics in the early stress stage. Blue represents CON group and orange 3d CUMS group (*n* = 10 animals per group).

Supplementary table 2. Statistical analysis of urine metabolites in the early stress stage. CON and 3d CUMS groups (*n* = 10 animals per group) are represented by relative abundances (AU). Relative abundances of metabolites are presented by the mean ± SEM. Urine metabolites are sorted by *p*-value. The summary of univariant and multivariate analysis is shown including *p*-value, *q*-value, VIP value and FC. The statistically significant *p*-values and *q*-values (< 0.05) are highlighted in bold. Abbreviations: TMAO, trimethylamine N-oxide; 3-HPPA, 3-hydroxyphenylpropionate; 4-PY, methyl-4-pyridone-5-carboxamide; DMA, Dimethylamine; NAD+, nicotinamide adenine dinucleotide.

Metabolite	CON	3d CUMS	*p*-value	*q*-value	VIP	RF	FC
Taurine	442.78 ± 38.45	644.38 ± 53.46	**0.01**	0.38	2.57	0.18	1.5
N.N-Dimethylglycine	3.71 ± 0.59	2.18 ± 0.21	**0.02**	0.38	2.27	0.21	0.6
Methylamine	5.09 ± 0.44	4.15 ± 0.37	0.08	0.88	1.52	0.07	0.8
N-Acetylglycine	29.45 ± 1.25	31.9 ± 2.26	0.11	0.88	0.69	0.07	1.1
Glycine	7.75 ± 0.65	6.39 ± 0.43	0.13	0.88	1.78	0.04	0.8
TMAO	3 ± 0.21	2.52 ± 0.16	0.13	0.88	1.98	-	0.8
Pseudouridine	9.09 ± 0.81	9.42 ± 0.68	0.21	0.88	0.08	-	1
2-Oxoglutarate	292.51 ± 36.51	244.45 ± 36.43	0.24	0.88	0.72	0.09	0.8
Betaine	28.54 ± 3.05	32.05 ± 2.64	0.24	0.88	0.50	-	1.1

Malate	6.94 ± 1.01	8.84 ± 0.73	0.24	0.88	1.21	-	1.3
Alanine	4.3 ± 0.48	3.56 ± 0.27	0.31	0.88	1.31	-	0.8
Hippurate	235.99 ± 18.29	211.23 ± 13.23	0.31	0.88	1.12	0.02	0.9
α-hydroxyhippurate	0.74 ± 0.1	0.89 ± 0.11	0.31	0.88	0.59	-	1.2
Citrate	336.66 ± 36.14	320.26 ± 32.95	0.35	0.88	0.12	0.01	1
Phenylacetylglycine	34.25 ± 6.33	40.12 ± 4.67	0.35	0.88	0.39	0.01	1.2
N-acetylglycoprteins	63.31 ± 2.81	64.9 ± 4.13	0.39	0.88	0.02	0.05	1
Trimethylamine	0.51 ± 0.14	0.89 ± 0.25	0.39	0.88	1.62	0.05	1.7
Tyrosine	7.43 ± 1.49	8.06 ± 1.24	0.39	0.88	0.09	0.03	1.1
NAD+	0.35 ± 0.07	0.31 ± 0.05	0.44	0.90	0.47	0.01	0.9
2-deoxycytidine	1.24 ± 0.16	1.36 ± 0.16	0.49	0.90	0.49	-	1.1
Creatinine	185.21 ± 10.84	166.45 ± 11.89	0.49	0.90	1.54	-	0.9
Leucine	13.3 ± 0.73	12.25 ± 0.83	0.49	0.90	1.15	0.01	0.9
Formate	2.33 ± 0.37	2.08 ± 0.28	0.54	0.90	0.44	-	0.9
Fumarate	3.02 ± 0.45	2.57 ± 0.43	0.54	0.90	0.60	0.01	0.9
Succinate	41.36 ± 2.33	43.83 ± 3.83	0.54	0.90	0.68	-	1.1
1-methylnicotinamide	0.11 ± 0.08	0.07 ± 0.03	0.60	0.90	0.43	0.04	0.6
Allantoin	196.28 ± 11.94	181.57 ± 10.82	0.60	0.90	1.25	0.02	0.9
o-Coumaric acid	1.57 ± 0.4	1.77 ± 0.39	0.65	0.90	0.30	-	1.1
Sarcosine	10.39 ± 1.27	9.73 ± 1.09	0.65	0.90	0.60	-	0.9
Dimethylamine (DMA)	14.68 ± 3.03	11.5 ± 1.22	0.71	0.90	0.16	0.01	0.8
Indoxyl Sulphate	5.19 ± 0.4	5.5 ± 0.6	0.71	0.90	0.13	-	1.1
3-methyl-2-oxovalerate	4.92 ± 0.39	5.7 ± 0.83	0.78	0.90	0.69	-	1.2
N6-Acetyllysine	30.2 ± 2.44	31.7 ± 2.03	0.78	0.90	0.37	-	1
3-HPPA	4.86 ± 2.09	2.77 ± 0.71	0.84	0.90	0.96	-	0.6
3-hydroxyisovalerate	3.65 ± 0.33	3.53 ± 0.25	0.84	0.90	0.40	-	1
4-PY	5.86 ± 0.64	6.31 ± 0.39	0.84	0.90	0.38	-	1.1
Acetate	5.31 ± 0.76	6.29 ± 1.19	0.84	0.90	0.57	-	1.2
HPPA sulfate	3.44 ± 0.95	2.63 ± 0.37	0.84	0.90	0.94	-	0.8
Tryptophan	5.21 ± 0.4	5.5 ± 0.6	0.84	0.90	0.08	-	1.1
Valine	1.16 ± 0.1	1.32 ± 0.2	0.84	0.90	0.45	-	1.1
Lactate	11.55 ± 1.09	11.25 ± 0.7	0.90	0.94	0.26	-	1
Fucose	8.57 ± 0.55	8.48 ± 0.5	1.00	1.00	0.39	0.01	1

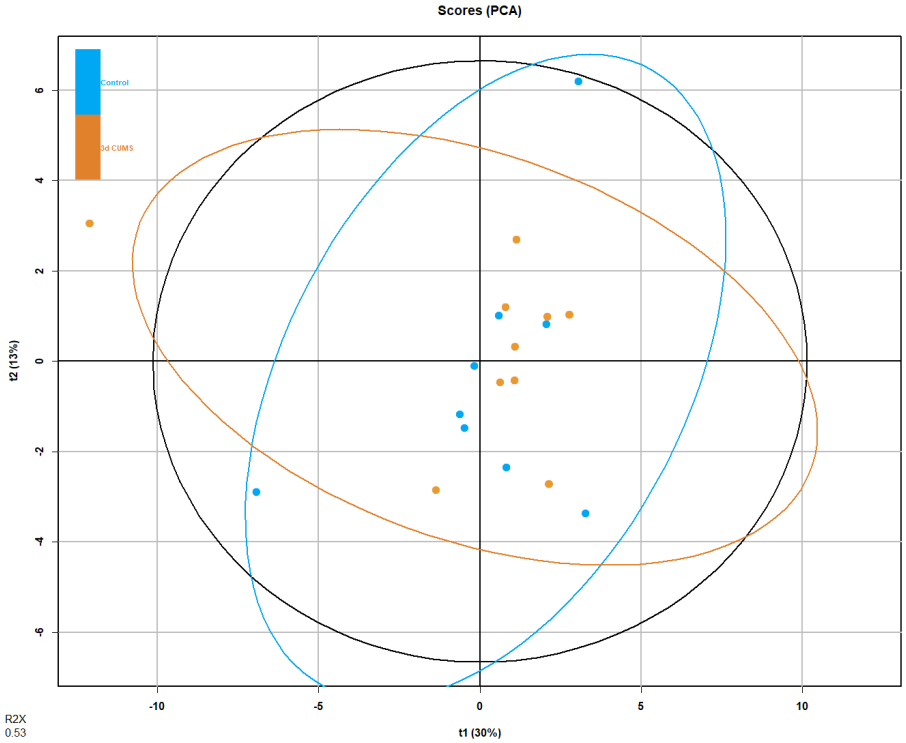

Supplementary Figure 2. PCA of urine metabolomics in the early stress stage. Blue represents CON group and orange 3d CUMS group (*n* = 10 animals per group).

Supplementary table 3. Summary of bacteria species in the early stress stage. The summary of univariant analysis includes the results of MW test (*p*-value), MW corrected by BH (*q*-value) and FC; between CON group and 3d CUMS group (*n* = 8 animals per group). The alignment was done indicating the closest name of specie to the sequence (the best hit). Taxonomic data is presented by the mean of relative abundance (%) and shorted by p-value. The statistically significant values (< 0.05) are highlighted in bold.

Specie	CON	3d CUMS	p-value	q-value	FC
Bacteroides uniformis	7.71%	4.93%	**0.05**	0.32	0.6
Escherichia coli	6.27%	1.75%	**0.05**	0.32	0.3
Lactobacillus murinus	10.68%	2.24%	0.06	0.32	0.2
Akkermansia muciniphila	25.84%	41.66%	0.11	0.42	1.6
Firmicutes bacterium ASF500	0%	0.03%	0.28	0.43	10.0
Muribaculaceae bacterium DSM 103720	24.09%	25.33%	0.30	0.43	1.1
Muribaculum intestinale	14.31%	13.61%	0.30	0.43	1.0
Mucispirillum schaedleri	5.26%	3.81%	0.34	0.43	0.7
Bacteroides caecimuris	0.02%	0.03%	0.34	0.43	1.7
Anaerotruncus sp G3 2012	0.89%	0.98%	0.41	0.44	1.1
Oscillibacter sp 1 3	0.46%	0.41%	0.41	0.44	0.9
Parabacteroides goldsteinii	4.47%	5.21%	0.48	0.48	1.2

Supplementary table 4. Summary of virus species in the early stress stage. The summary of univariant analysis includes results of MW test (*p*-value), MW corrected by BH (*q*-value) and FC; between CON group and 3d CUMS group (*n* = 8 animals per group). The alignment was done indicating the closest name of specie to the sequence (the best hit). Taxonomic data is presented by the mean of relative abundance (%) and shorted by p-value. The statistically significant values (< 0.05) are highlighted in bold.

Specie	CON	3d CUMS	p-value	q-value	FC
uncharacterized *herpesvirus*	38.50%	61.01%	**0.02**	0.31	1.6
Human alphaherpesvirus 2	0%	0.33%	**0.05**	0.40	-
Alcelaphine gammaherpesvirus 1	5.94%	3.05%	0.07	0.40	0.5
Lactobacillus prophage Lj928	0.14%	2.02%	0.13	0.40	14.9
Koala retrovirus	0.33%	0.06%	0.25	0.50	0.2
Lactobacillus prophage Lj771	7.11%	5.48%	0.30	0.50	0.8
Abelson murine leukemia virus	13.90%	6.14%	0.34	0.50	0.4
Pestivirus Giraffe 1	0.18%	0.30%	0.34	0.50	1.6
Murine osteosarcoma virus	9.29%	6.15%	0.41	0.50	0.7
Ateline gammaherpesvirus 3	5.29%	3.62%	0.43	0.50	0.7
Stx2 converting phage 1717	6.93%	4.40%	0.45	0.50	0.6
Bovine alphaherpesvirus 1	0.33%	0.78%	0.47	0.50	2.4
Anguillid herpesvirus 1	3.57%	4.21%	0.50	0.50	1.2

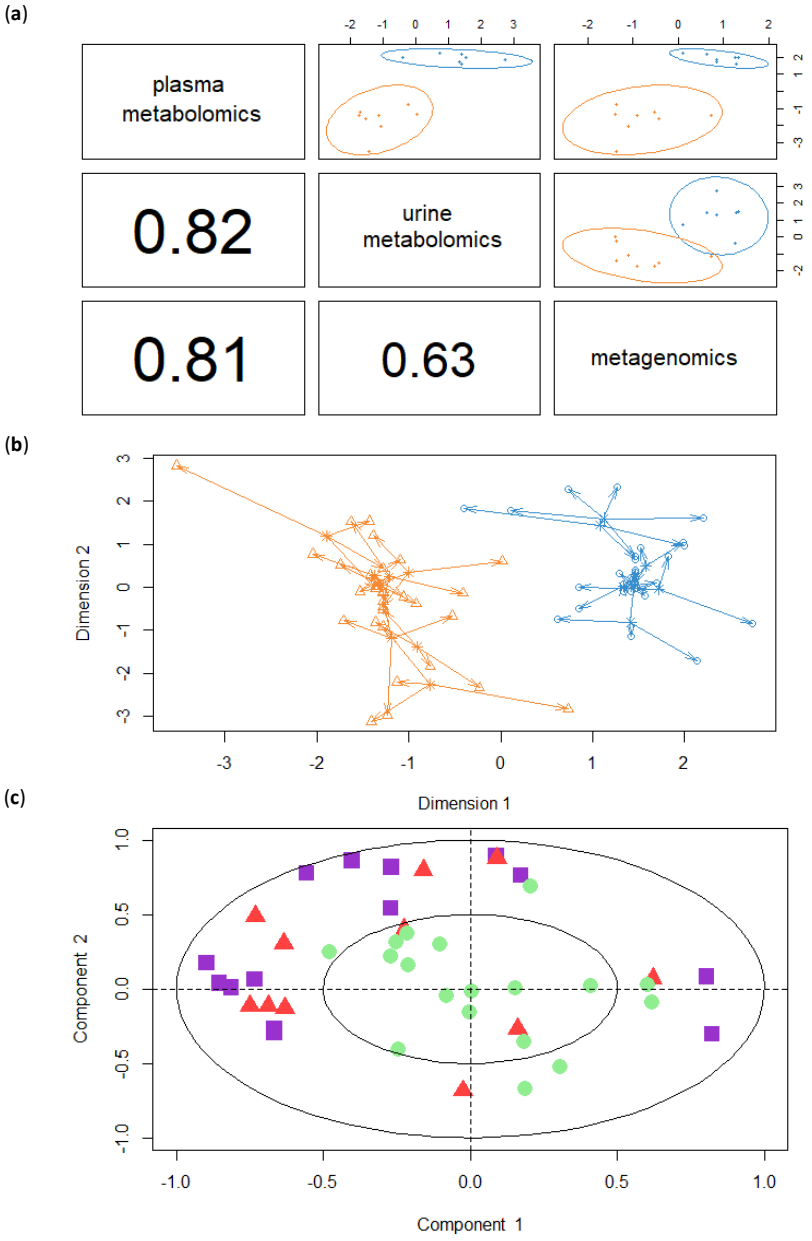

Supplementary figure 3. Integration of plasma metabolomics, urine metabolomics and metagenomics data using DIABLO in the early stress stage. (a) Global overview: correlation values between data at the component level (component 1). The first components from each data set are highly correlated to each other. (b) Arrow plot: the start of the arrow indicates the centroid between all data sets for a given sample and the tips of the arrows the location of that sample in each omic, highlighting the agreement between the 3 data sets at the sample level. In the figure (a) and (b) the group 3d CUMS is represented by orange and the CON group by blue. (c) Correlation circle plot: This plot highlights the contribution of each selected variable to component 1 and 2. Clusters of points indicate a strong correlation between variables. Each colour and shape indicate the type of features, i.e., plasma metabolites (purple square), urine metabolites (red triangle) and finally, bacteria and virus species (green circle). 3d CUMS in orange and CON in blue.

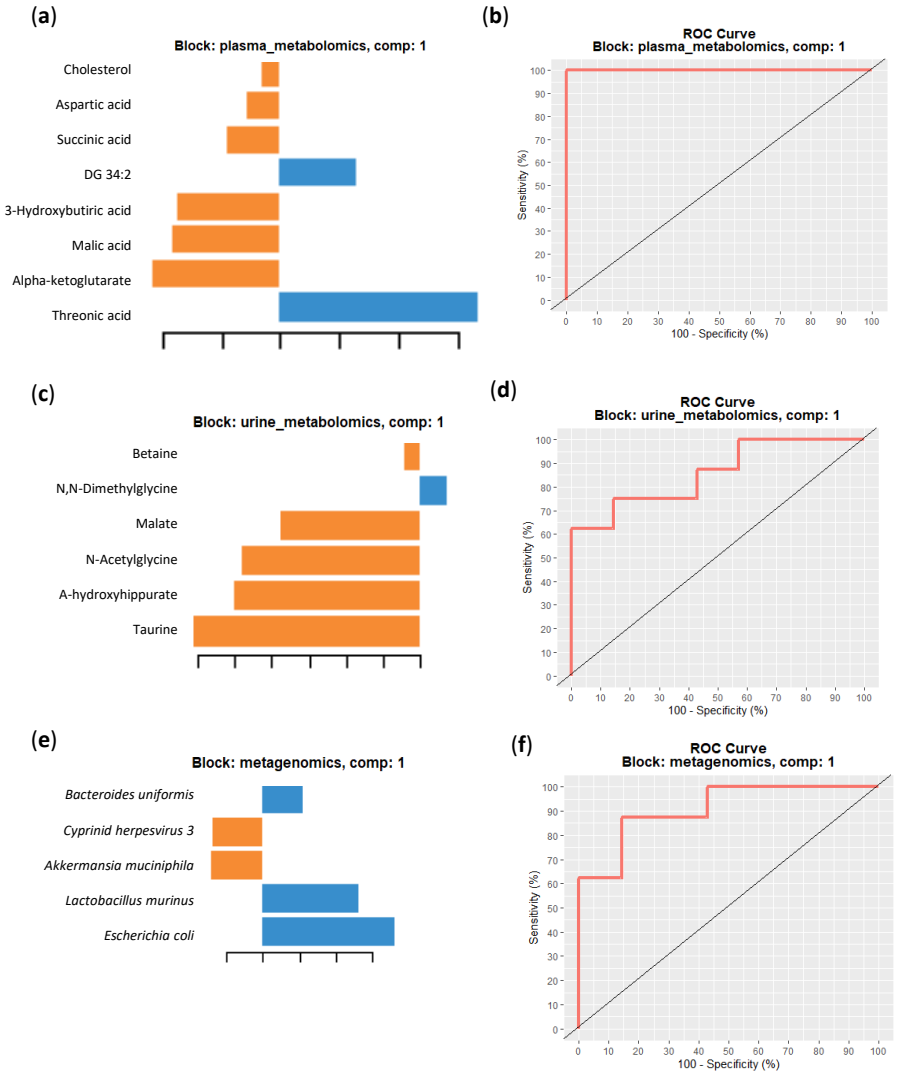

Supplementary figure 4. Feature integration in plasma metabolomics, urine metabolomics and metagenomics in the early stress stage. (a) (c) (e) Feature impact in each data set in component 1. 3d CUMS in orange and CON in blue. (b) (d) (f) ROC curve and AUC averaged using one-vs-all comparisons in the different data set.

Supplementary table 5. Summary of the comparison between univariate and multivariate analysis, random forest, and multi-omics integration in the early stress stage. The different methods of analysis are represented in the table - univariate and multivariate (U/M) analysis, random forest (RF) and the multi-omics integration (DIABLO) – and the weights of the features in the different omic approaches. The values of the methods can be 0 (no influence) or 1 (influence). The final value is the summatory of the weights of the different methods of analysis: features with weight of 3 (green) presented the highest impact on the model followed by weights of 2 (yellow). Abbreviations: DG, diacylglycerol; ChoE, cholesterol ester.

Source	Feature	U/M analysis	RF	DIABLO	Weight
Plasma metabolomics	Malic acid	1	1	1	3
	Threonic acid	1	1	1	3
	Alpha-ketoglutarate	1	1	1	3
	Succinic acid	1	1	1	3
	Cholesterol	1	1	1	3
	3-hydroxybutiric acid	0	1	1	2
	Pyruvic acid	1	1	0	2
	Oleic acid	0	1	0	1
	ChoE (18:3)	0	1	0	1
	Glyceric acid	0	1	0	1
	Aspartic acid	0	0	1	1
	DG 34:2	0	0	1	1
Urine metabolomics	N,N-Dimethylglycine	0	1	1	2
	Taurine	0	1	1	2
	2-Oxoglutarate	0	1	0	1
	N-Acetylglycine	0	0	1	1
	Methylamine	0	1	0	1
	Trimethylamine	0	1	0	1
	N-acetylglycoprteins	0	1	0	1
	2-oxoglutarate	0	1	0	1
	1-methylnicotinamide	0	1	0	1
	Glycine	0	1	0	1
	α-hydroxyhippurate	0	0	1	1
	Malic acid	0	0	1	1
	Betaine	0	0	1	1
Metagenomics	*Escherichia coli*	0	0	1	1
	Lactobacillus murinus	0	0	1	1
	Akkermansia muciniphila	0	0	1	1
	uncharacterized *herpesvirus*	0	0	1	1
	Bacteroides uniformis	0	0	1	1

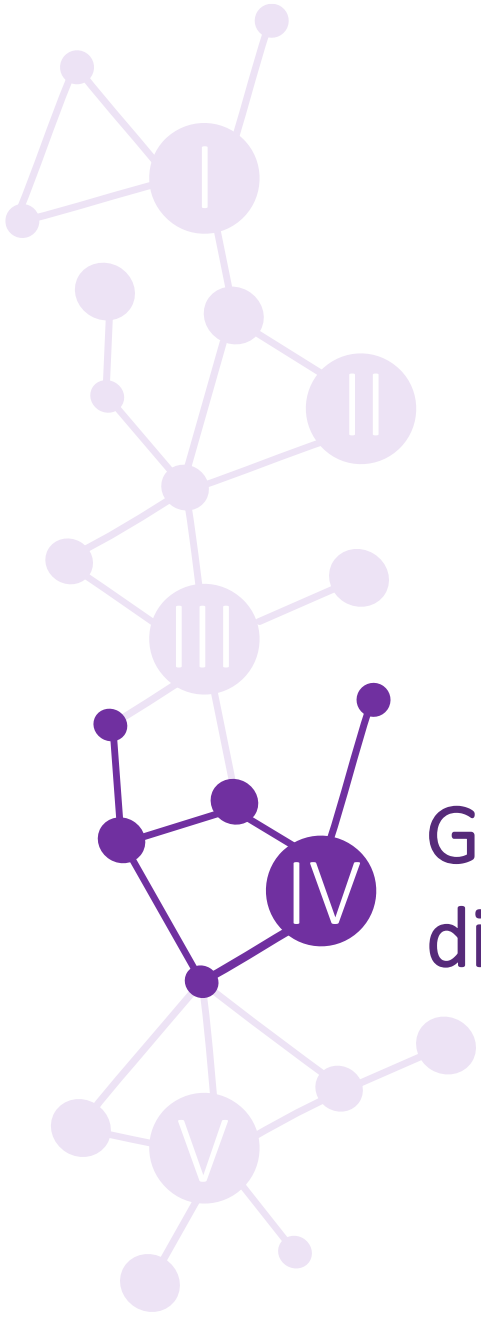

General discussion

UNIVERSITAT ROVIRA I VIRGILI
MULTI-OMICS BIOMARKERS OF METABOLIC HOMEOSTASIS OF RISK FACTORS ASSOCIATED TO NON-COMMUNICABLE DISEASES
Julia Hernandez Baixauli

IV. General discussion

NCDs is the umbrella term that covers a set of diseases that are developed mainly as a consequence of the accumulation and persistence of different risk factors over long periods of time [1]. As Van Ommen *et al*., proposed, the onset of NCDs arises from the imbalance of a few overarching processes that are mainly metabolic stress, inflammatory stress, oxidative stress and psychological stress [2]. This premise has offered new opportunities to discern early alterations that are responsible for onset of NCDs. Thus, the present work unfolds a characteristic metabolic signature that can be measured by omics technologies for specific risk factors associated to general processes. These include the deregulation of carbohydrate metabolism, lipid metabolism, hypertension, and gut dysbiosis, as representative of metabolic stress; inflammation stress; oxidative stress and psychological stress.

In this sense, it has been feasible to isolate 7 risk factors in rodent models which usually in the pathological state tend to occur in concomitantly. These metabolic profiles have been previously discussed in the results section, except the carbohydrates disfunction risk factor. In this regard, carbohydrate dysfunction has been excluded from the results section due to time issues. In addition, the proposed experimental model (based on STZ administration) [3] has also been extensively studied at the metabolic level and, consequently, it has been one of the less likely to provide new relevant information [4]. To date, STZ preclinical model is the closest approach to human carbohydrate dysfunction. Besides this inconvenient, other risk factors have been developed by: (a) for the induction of early stages of hyperlipidaemia, a low dose of P407 was administered [5]; (b) for hypertension, which is a risk factor similar to the preceding conditions, we used the genetically well-established SHR model in which rats are spontaneously hypertensive [6]; (c) in the case of gut dysbiosis, it was achieved by the transplantation of microbiota from rats with obesity (induced by cafeteria diet treatment to healthy rats) [7]; (d) the inflammation stress model was generated by the intermittent and increasing administration of LPS that caused a chronic inflammation model [8]; (e) the oxidative stress model was obtained by the administration of two increasing doses of the pesticide PQ [9]; finally, (**f**) the psychological stress was achieved by the adaptation of a model of depression (CUMS) [10]. In general, the different preclinical models were based on those that have been widely used before by the scientific community, and their mechanism of action are widely known. In this case, animal models are the means to underline the metabolic alterations associated to the different risk factors that are associated to overarching processes.

In the current work, different metabolic profiles have been analysed for different risk factors presenting both common and different characteristics between them. Therefore, each risk factor has been analysed in an isolated way. Additionally, we have further deep into the results with the intention of integrating their metabolic signature into a general predictive model. To do that, a final analysis has been

performed in order to identify a metabolomic signature that can be used to detect early alterations for different risk factors in plasma. Although the metabolomic analysis of urine samples has been successfully used to identify a variety of metabolomic profiles and potential biomarkers under a range of different conditions, our results are not powerful enough to obtain a specific metabolic profile for urine. On the other hand, despite the microbiome profiling has provided new opportunities to further characterise the metabolic state of several animal models, there are no conclusive results of promising biomarkers regarding the microbiome. Thus, this deep integrative analysis has been performed only with the plasma metabolome from the different experimental models due to the success on obtaining significant reliable biomarkers in the different risk factor modelling studies.

Regarding the data integration, we have carried out a previous step which consisted of data harmonization before the integrative analysis. Thus, since experiments for each risk factor were conducted independently, the metabolomics values of each risk factor were normalized by their respective control groups in order to avoid the inter-experiment variability. The first step consisted of an unsupervised analysis based on T-SNE to determine the variance between groups and studies (**Figure 1**). Results show that: (1) as expected, there are profound differences in the plasma metabolome between control groups and risk factors' animals; (2) a closer view on risk factors alone (**Figure 1 inset**) shows that inflammation, oxidative and psychological stress almost fully segregates from the metabolic stressors (i.e., dyslipidemia, carbohydrate dysregulation, hypertension, microbiota dysbiosis). Metabolic stress-related risk factors tend to present greater clustering between them except for hypertension; this segregation could be explained by the genetic background of the models [6]. In fact, these results reflect reality and highlight the difficulty of isolating a risk factor, as they tend to appear concomitantly. However, considering that this is an unsupervised unbiased method, these results suggest that the initial hypothesis, based on the idea that overarching processes present a distinctive metabolomic signature, is confirmed.

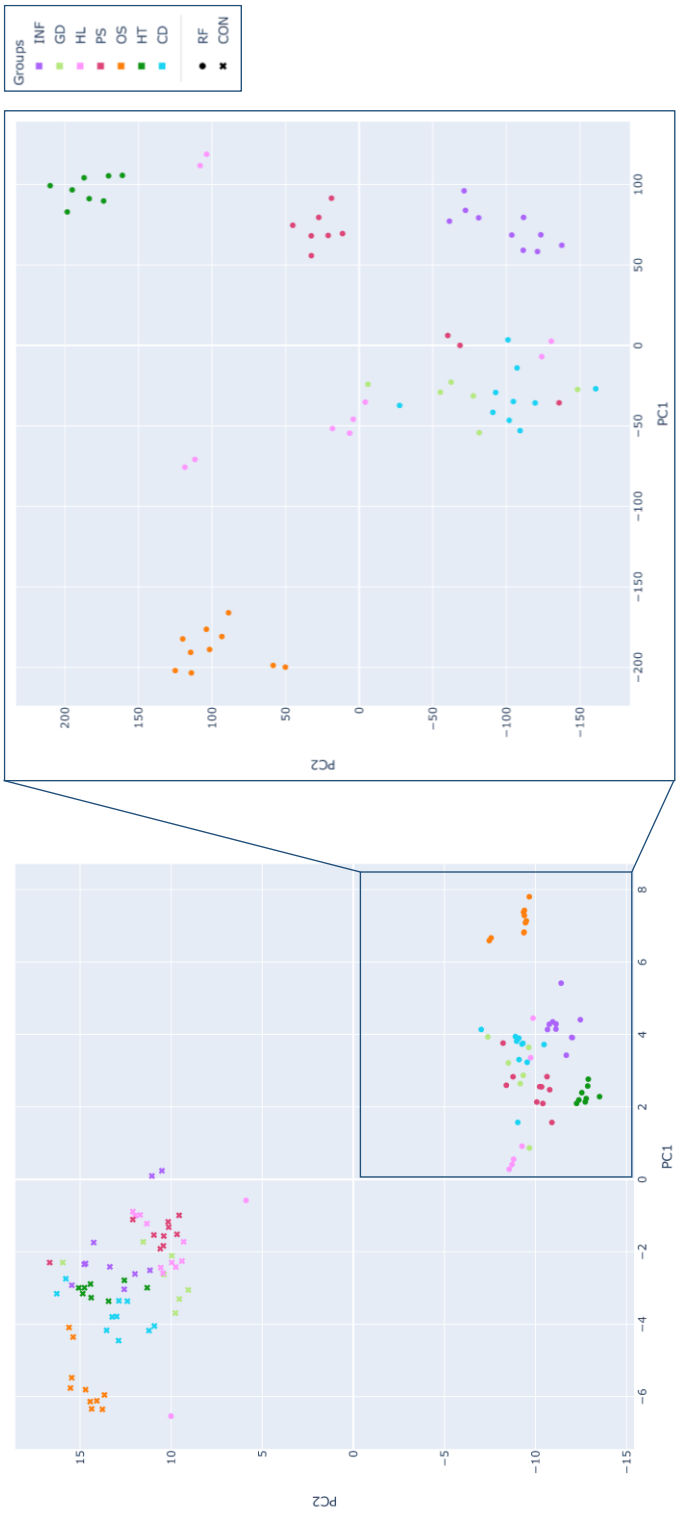

Figure 1. T-SNE plot of the analysis of all the risk factors including controls and focusing on risk factors. The first plot was calculated with all available data. Once we observed that CON and RF segregate differently, the analysis was performed only with RF. Abbreviations: NF, inflammation; GD, gut dysbiosis; HL, hyperlipidaemia; PS, psychological stress; OS, oxidative stress; HT, hypertension; CD, carbohydrate dysfunction. Groups: control; CON, control; RF, risk factor.

The second step has been to identify a metabolic profile that can discriminate between the different isolated risk factors. For this purpose, a random forest approach (a supervised machine learning method) has been used. Thus, we have been able to elucidate a metabolic profile that is able to predict the presence of the different risk factors. The model has been trained with 51 animals that showed 95 % accuracy during the training phase and tested with 13 animals that showed 92 % accuracy in the testing phase (**Figure 2**). In general, this predictive model could differentiate each risk factor by means of metabolomic data. Among the 13 animals tested, the prediction of inflammation, oxidative stress and psychological stress was 100% accurate. On the other hand, interestingly the only mismatching has been derived from animals of the risk factor associated with metabolic stress. More precisely, one animal was grouped as hypertension, but it really corresponded to the gut dysbiosis risk factor (**Figure S1**). Despite this mismatch, the model has obtained very good results and is therefore a good initial and robust approximation.

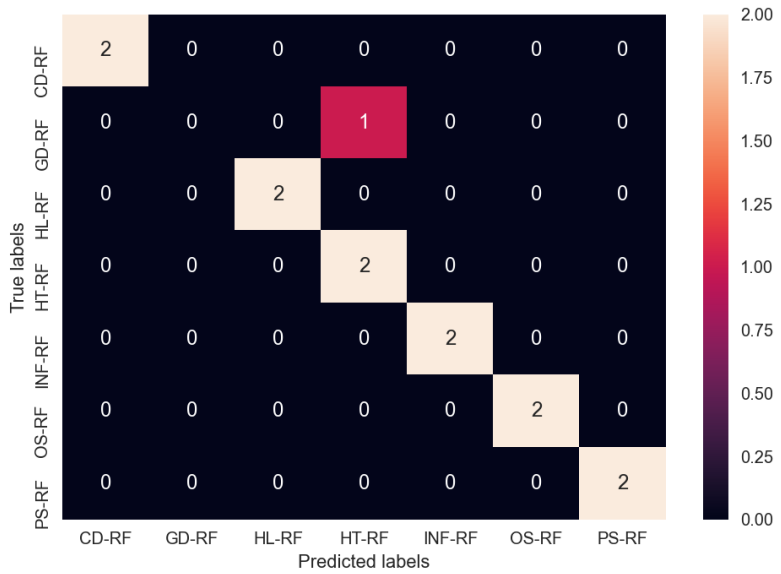

Figure 2. Confusion matrix of random forest test for risk factors. On the X-axis the predicted labels and on the y-axis the true labels are represented. Thirteen variables have been used for training, of which two do not coincide with the real ones. Abbreviations: NF, inflammation; GD, gut dysbiosis; HL, hyperlipidaemia; PS, psychological stress; OS, oxidative stress; HT, hypertension; CD, carbohydrate dysfunction.at control; CON, control; RF, risk factor.

The efficiency of the predictive model can be explained by the 20 metabolites presented in **Figure 3**; the results show that DG 36:4, followed by alpha-ketoglutarate and glycerol present the highest predictive power in almost all groups. These metabolites provided an interesting metabolic profile for monitoring the progression of different risk factors. Additionally, it has been possible to determine the metabolites that most influence the modelling for each risk factor (**Figure S2-S8**).

Altogether, the results of this thesis suggest that the monitoring of DGs along with other lipids such as phospholipids and derived lysophospholipids, as well as TCA cycle intermediates, can be used to differentiate the status of different overarching processes.

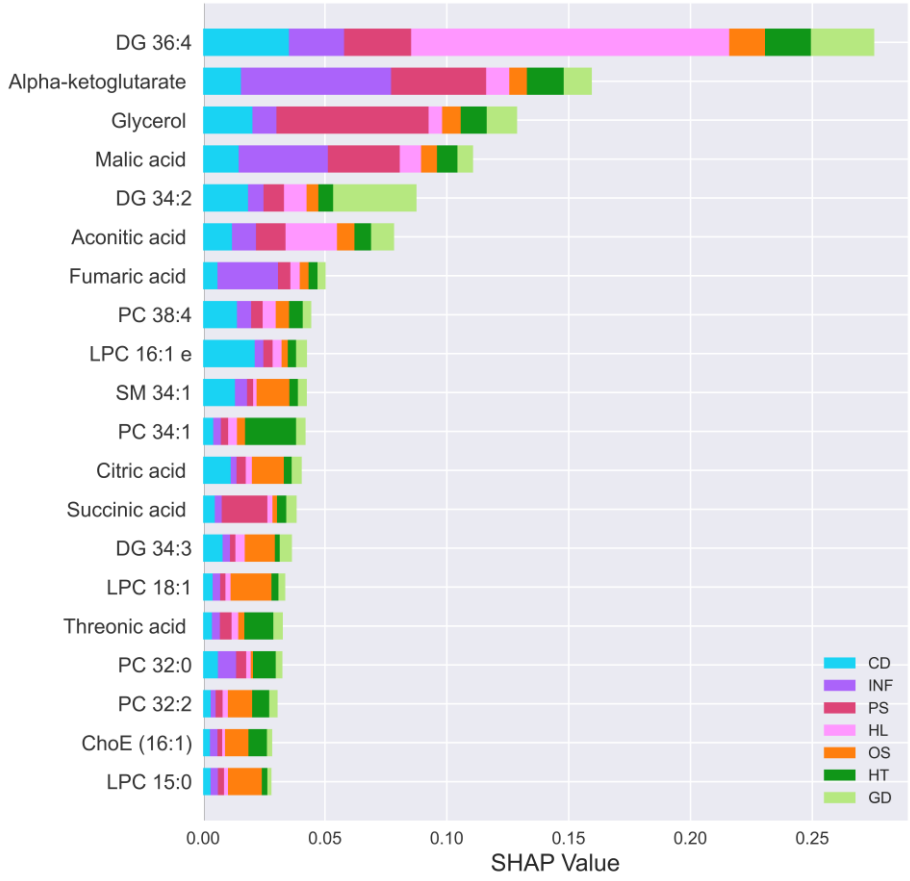

Figure 3. Variable importance plot of random forest (SHAP values) for risk factors. The following variable importance plot lists the most significant biomarkers in descending order for the RF model. The top biomarkers contribute more to the model than the bottom ones and thus have high predictive power. Abbreviations: INF, inflammation; GD, gut dysbiosis; HL, hyperlipidaemia; PS, psychological stress; OS, oxidative stress; HT, hypertension; CD, carbohydrate dysfunction.at control; CON, control; RF, risk factor.

The introduction of lipids as biomarkers has gained importance over the last couple of decades. Many lipids have been closely implicated in the onset and progression of different diseases. In fact, almost 35,000 articles have been published in the last two decades (a search in Pubmed using “lipid”, “biomarkers” and “disease” as keywords was performed). Of these, although it can be intuitively assumed that the vast majority are related to CVDs [11], lipid biomarkers have been also found to be discriminative for other important conditions. Recent evidence indicates that lipid metabolism is affected in numerous neurodegenerative diseases including Alzheimer’s [12] or Parkinson’s disease [13]. These dysfunctions lead to abnormal

levels of certain lipids in the brain, cerebrospinal fluid and plasma that are of interest to establish lipid profiles in neurodegenerative diseases [14]. Another case would be cancer in which these biomarkers have been of great utility, as they contribute to the monitoring of tumours and could also provide some information about tumoral heterogeneity [15]. These results postulate the lipidomic approach as a way for the discovery of integrative biomarkers capable to overcome the intricacy of pathological conditions and could help on the diagnosis as well as on the understanding of such complex pathologies.

Specifically, DGs are the lipids with the greatest impact on the models used in the present work, either in the analysis of the different risk factors or in the integrative analysis discussed above. Structurally, a DG is a glyceride consisting of two fatty acid chains covalently bonded to a glycerol. Functionally, its small size and simple composition confer exceptional properties to DG as: a basic component of biological membranes, an intermediate in lipid metabolism and a second messenger in lipid mediated signalling [16]. In fact, DGs are tightly regulated because of the critical structural and signalling roles. Focusing on their structural functions, DGs are precursors of other lipids (i.e., glycerophospholipids and triacylglycerols (TGs)), which are required in the Golgi apparatus for the formation of vesicles for outer transport; and are also fundamental in the structuration endoplasmic reticulum and nuclear envelope [16]. Regarding their signal transduction, DGs can modulate nuclear signal transduction via activation of protein kinase C (PKC) that was the first receptor to be described for DG [17]. Although PKC is the most recognizable target of DG, there are other DG receptors that have also been discovered, including chimaerins, Ras guanyl-releasing proteins (RasGRPs), Munc13, protein kinase Ds (PKDs) and DG kinases [18]. Additionally, it has been described that immune function is also modulated by the action of DG [19]. Given such diverse roles and functions of DGs, slight alterations in these tightly regulated systems can yield dramatic effects on normal cell processes. Thus, DGs have been described as a key molecule with severe effects on organ development and cell growth associated with diseases such as cancer, diabetes, immune system disorders and Alzheimer's disease [16].

Specifically, DG 36:4 and DG 34:2 are the DGs with the greatest impact on the integrative analysis and in the different risk factors studied in this work. Although the structure of the carbons and saturations has not been identified by our methodology, based on the scientific literature it is likely to think that DG 36:4 could be composed by palmitic acid (C16:0) and arachidonic acid (AA, C20:4) while DG 34:2 share palmitic acid with DG 36:4 and the second FFA could be linoleic acid (C18:2). AA is a long-chain polyunsaturated FFA of the omega-6 group and represents 7-10 % of total circulating FFAs; it is the second most abundant omega-6 fatty acid in the human body, with linoleic acid being the first [20]. Endogenous AA generation mainly occurs via the release of AA from cell membrane phospholipids. It has been described that multiple stimulus lead to the release of membrane-bound AA via the activation of cellular phospholipases, principally the phospholipase A_2 (PLA_2) family [21]. This cleavage step is rate limiting on the production of biologically relevant arachidonate metabolites. In

the case of PLA_2 activation, membrane receptors activate guanine nucleotide-binding (G) proteins, leading to the release of AA directly from membrane phospholipids. On the other hand, activation of phospholipase C (PLC) or phospholipase D (PLD) releases AA via the sequential action of the phospholipase-mediated production of DG, with the subsequent release of AA from DG by the action of DG lipase [22]. For instance, AA is metabolized to form eicosanoids by the action of cyclooxygenases (COX1 and COX2), which generates prostaglandins and thromboxanes; or by lipoxygenases, that subsequently generate leukotrienes and lipoxins, which are associated with the pro-inflammatory response [23]. Additionally, AA can be synthesized in the body from linoleic acid through three steps mediated by two enzymes, desaturase and elongase, and may also be derived from the diet. Thus, our results suggest a relation between the altered DGs and AA metabolism, which is the major precursor of a series of bioactive metabolites (eicosanoids), which regulate several physiological processes.

In line with of our results, there are studies that suggest that DG composition reflects differences in underlying lipid metabolism between healthy and several pathological conditions. On the one hand, DG 36:4 was decreased in hypertension, inflammation, and oxidative stress model which could suggest, as it has been previously stated, that they are being hydrolysed in favour of metabolites related to the AA metabolism [11]. On the other hand, DG 36:4 and DG 34:2 were increased in hyperlipidaemia and gut dysbiosis suggesting a role in body lipid storage as it has been previously described for FFAs containing molecules, such as DG [24,25]. Thus, DGs could play important roles in inflammatory processes and oxidative stress-related pathologies as well as in obesity and disrupted metabolic conditions and, consequently, could be considered a good candidate for this set of biomarkers that form part of the metabolic signature unfolded in this thesis. Altogether, DGs circulation could be important for the monitoring of FFAs, because pathways of FFA elongation and desaturation are differentially regulated during disease progression. However, the mechanism by which the DGs are altered in the risk factors studied is currently unknown.

Additionally, glycerol, which is the backbone in glycerides (e.g., DGs or TGs) and is a precursor of TGs and phospholipids in liver and adipose tissue [26], have appeared as an important metabolite in the integration analysis. Glycerol along with FFAs are released into the bloodstream when fats are metabolised, thus the alteration of this three-carbon metabolite might indicate lipid disfunction. In fact, elevated levels of glycerol are related to the progression of diabetes. For example, a large population-based study showed that serum levels of glycerol and FFAs are biomarkers associated to an increased risk of development of hyperglycemia and T2DM in Finnish men [27]. Although it has no major impact on the risk factors studies at the individual level, subtle variations in glycerol may be a sign of altered lipid metabolism, which also supports the variations on DGs previously discussed. Furthermore, glycerol is an important metabolite in the human body, connecting the metabolic pathways of carbohydrates (glycolysis and gluconeogenesis) and lipids.

Moreover, TCA cycle intermediates, which are also implicated in the oxidative phosphorylation pathway of mitochondria, plays an important role controlling physiology and disease [28]. In fact, mitochondria are cellular organelles that generate ATP and metabolites for survival and growth, respectively. In addition, several metabolic processes are associated with TCA cycle as gluconeogenesis, lipogenesis, cholesterol and heme biosynthesis, urea cycle, and inter-conversion of amino acids. This means that monitoring TCA cycle intermediates provide a large amount of information about the individuals' status, and therefore might be considered as an important source of biomarkers [28]. For example, TCA cycle intermediates have been linked to ageing. This link could have an important role in translating basic knowledge of the biology of aging into health and disease status [29]. In line with this, BMI, a risk factor for CVDs, is associated to metabolites included in the TCA cycle (i.e., alpha-ketoglutarate and aconitic acid) [30]. In fact, these metabolites are directly related to diabetes alterations. Thus, the serum profiling of TCA intermediates has emerged as a key approach for its early diagnosis [31]. For example, perturbations in serum and urine TCA cycle intermediaries (citric acid, malic, acid, succinic acid, and aconitic acid) was observed in diabetic db/db mice and could be considered as an early diagnosis tool for diabetes and associated alteration (e.g. nephropathy) [32]. Additionally, the relative abundance of TCA intermediates in urine relative to those in serum were suggested as an index of metabolic damage [32]. Moreover, TCA intermediates play an important role in cancer monitoring for glioma [33], colorectal cancer [34] or lung cancer [35], among others.

Interestingly, the risk factors presenting major alterations in the metabolic profile related to the TCA cycle are inflammation, oxidative and psychological stress. In this sense, those studies presented alterations in the TCA cycle intermediates in the independent and in the integrative analysis. In fact, 6 metabolites out of the top 20 are intermediates of the TCA cycle.

During periods of stress in the cell, intermediary metabolites of the TCA cycle can be released acting as a danger signals in cytosol and regulating immune response [36]. In the case of the inflammation model, the decrease of TCA intermediaries (i.e., alpha-ketoglutarate, aconitic acid, malic acid, fumaric acid and succinic acid) might be indicative of a systemic inhibition of the intracellular TCA cycle that could be associated with the regulation of immune response and activation of other energy pathways [37]. In fact, metabolic flexibility is essential for immune function. During immune response, the immune cells shift to aerobic glycolysis for energy production, a less-efficient, but fast-acting pathway [38]. Additionally, the switch to glycolysis enables TCA cycle intermediates to be used as key sources of carbon molecules for biosynthesis of nucleotides, amino acids, and lipids [38]. In this sense, several metabolomic studies point out the decrease of TCA cycle activity as a key characteristic of chronic inflammation, related to alterations in lipid and FFA metabolism as has been previously discussed [39–41]. In the case of the oxidative stress model, TCA intermediates tend to decrease or increase depending on the degree of the stressor. In this sense, the TCA cycle is intimately linked to oxidative

phosphorylation which implicates multiple reactions of oxidation and reduction that are closely related to oxidative stress [28].

It is noteworthy to mention that, as has been observed in the inflammatory and oxidative stress, several studies have demonstrated a potential link between stressful events and the alteration of energy metabolism [42]. More concisely, the stress response induced an increase on key intermediate products of the TCA cycle which are indicative of the overstimulation of this cycle (i.e., alpha-ketoglutarate, malic acid, and succinic acid). This fact differentiates the early psychological stress model from the classical CUMS model of depression. Thus, CUMS model is associated with energy disruption or deficiency (being one of the most represented depressive symptoms associated with the reduction of the activity and curiosity in animal models) [43]. These results supports the idea that mitochondria and the energetic metabolism are emerging as modulators of behaviour both in rodent and human studies [44].

Within the TCA cycle, alpha-ketoglutarate is one of the most promising intermediates that could be considered as a biomarker, due to its occurrence as one of the metabolites with the highest predictive power both in the isolated risk factors and in integrative analysis. In addition, due to its crucial role in the TCA cycle, alpha-ketoglutarate plays a critical role in multiple metabolic processes in experimental animals and humans. Alpha-ketoglutarate is a co-substrate for 2-oxoglutarate-dependent dioxygenases (2-OGDD), which catalyse hydroxylation reactions on various types of substrates, including proteins, nucleic acids, lipids, and metabolic intermediates producing CO_2 and succinic acid. The activity of 2-OGDD is dependent on the intracellular ratio of alpha-ketoglutarate to succinic acid or other inhibitors. Thus, the disruption of homeostasis of 2-OGDD and alpha-ketoglutarate have consequences for health status [28]. The availability of alpha-ketoglutarate has a direct impact on gene expression due to its role in regulating epigenetic changes, and thus can modulate cellular fate decision by regulating histones and DNA demethylases [28]. In macrophages, an important functional role has been attributed to alpha-ketoglutarate. In this sense, alpha-ketoglutarate favours the anti-inflammatory profile while represses the pro-inflammatory responses [45]. Additionally, alpha-ketoglutarate is an important source of neurotransmitters (i.e., glutamate, glutamine and gamma aminobutyric acid (GABA)), which are the major brain neurotransmitters mediating excitatory and inhibitory signalling, respectively [46]. As a precursor of glutamate and glutamine, alpha-ketoglutarate acts as an antioxidant agent as it directly reacts with H_2O_2 with formation of CO_2 and succinic acid [47]. In fact, due to its characteristics it is considered a key metabolite regulating aging [48], thus it has been proposed as an effective supplement for improving metabolism and reducing biological aging (e.g., “Rejuvant” supplement) [49].

Nowadays, metabolomic profiling is becoming a promising tool for the screening, the diagnosis, and the prognosis of NCDs. In our case, the next steps to be followed would be the use of the metabolomic data to integrate human data into a predictive model containing the metabolomic signatures of the overarching processes. Such

approach would allow to determine the global processes mostly altered in a person. Hence, nutritional, or medical personalisation strategies could be established based on this stratification. To do so, the preclinical results showed herein would need to be translated to human metabolome. But the first step, which is the proof of concept about the feasibility of such approach has already been achieved here with promising results.

Currently, there are important projects related to the search of robust health biomarkers and metabolic profiles to overcome the limitations to understand the onset and development of NDCs. In fact, Food and Drug Administration (FDA) and the National Institutes of Health (NIH) have worked together to create a set of definitions that should guide researchers in developing needed evidence and practitioners in the application of biomarkers in health care [50]. Whilst other organizations, such as the Clinical Trials Transformation Initiative and the Foundation for the National Institutes of Health Biomarkers Consortium, are following these recommendations [50]. For example, euCanSHare that is a joint EU-Canada project aimed to establish a cross-border data sharing and multi-cohort cardiovascular research platform. It is composed by more than 35 cohorts that include biomarkers from omics data (e.g., metabolomics).

In the case of personalized nutrition, there are different research groups working on the research of biomarkers for personalized nutrition that are useful for the food industry. One of these projects is PREVENTOMICS, a project funded by the European Union's program Horizon 2020 under the call of Personalized Nutrition, that aims to use health biomarkers for dietary advice applications directed to consumers. Other initiative is BIOCLAIMS, a collaborative research project carried out at the European level, which has established the principles to identify, establish and validate robust biomarkers to quantify the health status.

Despite the advantages and opportunities, there are various limitations in the present thesis. For example, the modelling of risk factors in an isolated way is challenging because this situation would not exist in nature, and this entails that only relatively mild "close-to-reality" models can be developed. On the other hand, the size of our cohort is other of the main limitations of our work because this modest animal numbers can certainly limit the power of the statistical and predictive analysis that could somehow limit our conclusions. Additionally, the results are limited to the selected omic approaches but we must consider that there is other possible combination of methodologies that could cover a higher range of features.

The use of metabolic profiling in the future seems promising because of the valuable findings that are emerging from current studies. Furthermore, it seems likely that future applications will include novel innovations that brings metabolic profiling into the nutritionist and physician's office or even into the surgeon's hands in the operating room (e.g., smart knife) [51]. Altogether, the contributions of this thesis provide a novel approach about the metabolic profiling of risk factors in different animal models, which we hope will stimulate both interest and future applications.

References

1. Stolk, R.P.; Rosmalen, J.G.M.; Postma, D.S.; de Boer, R.A.; Navis, G.; Slaets, J.P.J.; Ormel, J.; Wolffenbuttel, B.H.R. Universal risk factors for multifactorial diseases. *Eur. J. Epidemiol.* **2008**, *23*, 67–74, doi:10.1007/s10654-007-9204-4.

2. van Ommen, B.; Keijer, J.; Heil, S.G.; Kaput, J. Challenging homeostasis to define biomarkers for nutrition related health. *Mol. Nutr. Food Res.* **2009**, *53*, 795–804, doi:10.1002/mnfr.200800390.

3. Islam, M.S.; Loots, D.T. Experimental rodent models of type 2 diabetes: a review. *Methods Find. Exp. Clin. Pharmacol.* **2009**, *31*, 249–261, doi:10.1358/mf.2009.31.4.1362513.

4. Chen, R.; Zeng, Y.; Xiao, W.; Zhang, L.; Shu, Y. LC-MS-Based Untargeted Metabolomics Reveals Early Biomarkers in STZ-Induced Diabetic Rats With Cognitive Impairment. *Front. Endocrinol. (Lausanne).* **2021**, *12*, 665309, doi:10.3389/fendo.2021.665309.

5. Chaudhary, H.R.; Brocks, D.R. The single dose poloxamer 407 model of hyperlipidemia; systemic effects on lipids assessed using pharmacokinetic methods, and its effects on adipokines. *J. Pharm. Pharm. Sci.* **2013**, *16*, 65–73, doi:10.18433/j37g7m.

6. Doris, P.A. Genetics of hypertension: an assessment of progress in the spontaneously hypertensive rat. *Physiol. Genomics* **2017**, *49*, 601–617, doi:10.1152/physiolgenomics.00065.2017.

7. Hernandez-Baixauli, J.; Puigbò, P.; Torrell, H.; Palacios-Jordan, H.; Ripoll, V.J.R.; Caimari, A.; Del Bas, J.M.; Baselga-Escudero, L.; Mulero, M. A Pilot Study for Metabolic Profiling of Obesity-Associated Microbial Gut Dysbiosis in Male Wistar Rats. *Biomolecules* **2021**, *11*, doi:10.3390/biom11020303.

8. Ranneh, Y.; Akim, A.M.; Hamid, H.A.; Khazaai, H.; Mokhtarrudin, N.; Fadel, A.; Albujja, M.H.K. Induction of Chronic Subclinical Systemic Inflammation in Sprague-Dawley Rats Stimulated by Intermittent Bolus Injection of Lipopolysaccharide. *Arch. Immunol. Ther. Exp. (Warsz).* **2019**, *67*, 385–400, doi:10.1007/s00005-019-00553-6.

9. Ahmed, M.A.E.; El Morsy, E.M.; Ahmed, A.A.E. Protective effects of febuxostat against paraquat-induced lung toxicity in rats: Impact on RAGE/PI3K/Akt pathway and downstream inflammatory cascades. *Life Sci.* **2019**, *221*, 56–64, doi:10.1016/j.lfs.2019.02.007.

10. Hernandez-Baixauli, J.; Puigbò, P.; Abasolo, N.; Palacios-Jordan, H.; Foguet-Romero, E.; Suñol, D.; Galofré, M.; Caimari, A.; Baselga-Escudero, L.; Bas, J.M. Del; et al. Alterations in Metabolome and Microbiome Associated with an Early Stress Stage in Male Wistar Rats: A Multi-Omics Approach. *Int. J. Mol. Sci.* **2021**, *22*, doi:10.3390/ijms222312931.

11. Sonnweber, T.; Pizzini, A.; Nairz, M.; Weiss, G.; Tancevski, I. Arachidonic Acid Metabolites in Cardiovascular and Metabolic Diseases. *Int. J. Mol. Sci.* **2018**, *19*, doi:10.3390/ijms19113285.

12. Zarrouk, A.; Debbabi, M.; Bezine, M.; Karym, E.M.; Badreddine, A.; Rouaud, O.; Moreau, T.; Cherkaoui-Malki, M.; El Ayeb, M.; Nasser, B.; et al. Lipid Biomarkers in Alzheimer's Disease. *Curr. Alzheimer Res.* **2018**, *15*, 303–312, doi:10.2174/1567205014666170505101426.

13. Sinclair, E.; Trivedi, D.K.; Sarkar, D.; Walton-Doyle, C.; Milne, J.; Kunath, T.; Rijs, A.M.; de Bie, R.M.A.; Goodacre, R.; Silverdale, M.; et al. Metabolomics of sebum reveals lipid dysregulation in Parkinson's disease. *Nat. Commun.* **2021**, *12*, 1592, doi:10.1038/s41467-021-21669-4.

14. Wood, P.L.; Cebak, J.E.; Woltjer, R.L. Diacylglycerols as biomarkers of sustained immune activation in Proteinopathies associated with dementia. *Clin. Chim. Acta* **2018**, *476*, 107–110, doi:https://doi.org/10.1016/j.cca.2017.11.009.

15. Holzlechner, M.; Eugenin, E.; Prideaux, B. Mass spectrometry imaging to detect lipid biomarkers and disease signatures in cancer. *Cancer reports (Hoboken, N.J.)* **2019**, *2*, e1229, doi:10.1002/cnr2.1229.

16. Carrasco, S.; Mérida, I. Diacylglycerol, when simplicity becomes complex. *Trends Biochem. Sci.* **2007**, *32*, 27–36, doi:10.1016/j.tibs.2006.11.004.

17. Violin, J.D.; Zhang, J.; Tsien, R.Y.; Newton, A.C. A genetically encoded fluorescent reporter reveals oscillatory phosphorylation by protein kinase C. *J. Cell Biol.* **2003**, *161*, 899–909, doi:10.1083/jcb.200302125.

18. Toker, A. The biology and biochemistry of diacylglycerol signalling. Meeting on molecular advances in diacylglycerol signalling. *EMBO Rep.* **2005**, *6*, 310–314, doi:10.1038/sj.embor.7400378.

19. Wattenberg, B.W.; Raben, D.M. Diacylglycerol kinases put the brakes on immune function. *Sci. STKE* **2007**, *2007*, pe43, doi:10.1126/stke.3982007pe43.

20. Risé, P.; Tragni, E.; Ghezzi, S.; Agostoni, C.; Marangoni, F.; Poli, A.; Catapano, A.L.; Siani, A.; Iacoviello, L.; Galli, C. Different patterns characterize Omega 6 and Omega 3 long chain polyunsaturated fatty acid levels in blood from Italian infants, children, adults and elderly. *Prostaglandins. Leukot. Essent. Fatty Acids* **2013**, *89*, 215–220, doi:10.1016/j.plefa.2013.06.009.

21. Dennis, E.A.; Cao, J.; Hsu, Y.-H.; Magrioti, V.; Kokotos, G. Phospholipase A2 enzymes: physical structure, biological function, disease implication, chemical inhibition, and therapeutic intervention. *Chem. Rev.* **2011**, *111*, 6130–6185, doi:10.1021/cr200085w.

22. Reisenberg, M.; Singh, P.K.; Williams, G.; Doherty, P. The diacylglycerol lipases: structure, regulation and roles in and beyond endocannabinoid signalling. *Philos. Trans. R. Soc. Lond. B. Biol. Sci.* **2012**, *367*, 3264–3275, doi:10.1098/rstb.2011.0387.

23. Medzhitov, R. Origin and physiological roles of inflammation. *Nature* **2008**, *454*, 428–435, doi:10.1038/nature07201.

24. Turinsky, J.; O'Sullivan, D.M.; Bayly, B.P. 1,2-Diacylglycerol and ceramide levels in insulin-resistant tissues of the rat in vivo. *J. Biol. Chem.* **1990**, *265*, 16880–16885.

25. Polewski, M.A.; Burhans, M.S.; Zhao, M.; Colman, R.J.; Shanmuganayagam, D.; Lindstrom, M.J.; Ntambi, J.M.; Anderson, R.M. Plasma diacylglycerol composition is a biomarker of metabolic syndrome onset in rhesus monkeys. *J. Lipid Res.* **2015**, *56*, 1461–1470, doi:10.1194/jlr.M057562.

26. Funahashi, T.; Nagasawa, A.; Hibuse, T.; Maeda, N. Impact of glycerol gateway molecule in adipocytes. *Cell. Mol. Biol. (Noisy-le-grand).* **2006**, *52*, 40–45.

27. Mahendran, Y.; Cederberg, H.; Vangipurapu, J.; Kangas, A.J.; Soininen, P.; Kuusisto, J.; Uusitupa, M.; Ala-Korpela, M.; Laakso, M. Glycerol and fatty acids in serum predict the development of hyperglycemia and type 2 diabetes in Finnish men. *Diabetes Care* **2013**, *36*, 3732–3738, doi:10.2337/dc13-0800.

28. Martínez-Reyes, I.; Chandel, N.S. Mitochondrial TCA cycle metabolites control physiology and disease. *Nat. Commun.* **2020**, *11*, 102, doi:10.1038/s41467-019-13668-3.

29. Sharma, R.; Ramanathan, A. The Aging Metabolome-Biomarkers to Hub Metabolites. *Proteomics* **2020**, *20*, e1800407, doi:10.1002/pmic.201800407.

30. Ho, J.E.; Larson, M.G.; Ghorbani, A.; Cheng, S.; Chen, M.-H.; Keyes, M.; Rhee, E.P.; Clish, C.B.; Vasan, R.S.; Gerszten, R.E.; et al. Metabolomic Profiles of Body Mass Index in the Framingham Heart Study Reveal Distinct Cardiometabolic Phenotypes. *PLoS One* **2016**, *11*, e0148361, doi:10.1371/journal.pone.0148361.

31. Zhang, Y.; Zhao, H.; Liu, B.; Shu, H.; Zhang, L.; Bao, M.; Yi, W.; Tan, Y.; Ji, X.; Zhang, C.; et al. Human serum metabolomic analysis reveals progression for high blood pressure in type 2 diabetes mellitus. *BMJ open diabetes Res. care* **2021**, *9*, doi:10.1136/bmjdrc-2021-002337.

32. Li, M.; Wang, X.; Aa, J.; Qin, W.; Zha, W.; Ge, Y.; Liu, L.; Zheng, T.; Cao, B.; Shi, J.; et al. GC/TOFMS analysis of metabolites in serum and urine reveals metabolic perturbation of TCA cycle in db/db

mice involved in diabetic nephropathy. *Am. J. Physiol. Renal Physiol.* **2013**, *304*, F1317-24, doi:10.1152/ajprenal.00536.2012.

33. Feng, S.; Liu, Y. Metabolomics of Glioma. *Adv. Exp. Med. Biol.* **2021**, *1280*, 261–276, doi:10.1007/978-3-030-51652-9_18.

34. Hashim, N.A.A.; Ab-Rahim, S.; Suddin, L.S.; Saman, M.S.A.; Mazlan, M. Global serum metabolomics profiling of colorectal cancer. *Mol. Clin. Oncol.* **2019**, *11*, 3–14, doi:10.3892/mco.2019.1853.

35. Peng, F.; Liu, Y.; He, C.; Kong, Y.; Ouyang, Q.; Xie, X.; Liu, T.; Liu, Z.; Peng, J. Prediction of platinum-based chemotherapy efficacy in lung cancer based on LC-MS metabolomics approach. *J. Pharm. Biomed. Anal.* **2018**, *154*, 95–101, doi:10.1016/j.jpba.2018.02.051.

36. Choi, I.; Son, H.; Baek, J.-H. Tricarboxylic Acid (TCA) Cycle Intermediates: Regulators of Immune Responses. *Life (Basel, Switzerland)* **2021**, *11*, doi:10.3390/life11010069.

37. Lacourt, T.E.; Vichaya, E.G.; Chiu, G.S.; Dantzer, R.; Heijnen, C.J. The High Costs of Low-Grade Inflammation: Persistent Fatigue as a Consequence of Reduced Cellular-Energy Availability and Non-adaptive Energy Expenditure . *Front. Behav. Neurosci.* 2018, *12*, 78.

38. Donnelly, R.P.; Finlay, D.K. Glucose, glycolysis and lymphocyte responses. *Mol. Immunol.* **2015**, *68*, 513–519, doi:10.1016/j.molimm.2015.07.034.

39. Yamano, E.; Sugimoto, M.; Hirayama, A.; Kume, S.; Yamato, M.; Jin, G.; Tajima, S.; Goda, N.; Iwai, K.; Fukuda, S.; et al. Index markers of chronic fatigue syndrome with dysfunction of TCA and urea cycles. *Sci. Rep.* **2016**, *6*, 34990, doi:10.1038/srep34990.

40. Naviaux, R.K.; Naviaux, J.C.; Li, K.; Bright, A.T.; Alaynick, W.A.; Wang, L.; Baxter, A.; Nathan, N.; Anderson, W.; Gordon, E. Metabolic features of chronic fatigue syndrome. *Proc. Natl. Acad. Sci. U. S. A.* **2016**, *113*, E5472-80, doi:10.1073/pnas.1607571113.

41. Fluge, Ø.; Mella, O.; Bruland, O.; Risa, K.; Dyrstad, S.E.; Alme, K.; Rekeland, I.G.; Sapkota, D.; Røsland, G. V; Fosså, A.; et al. Metabolic profiling indicates impaired pyruvate dehydrogenase function in myalgic encephalopathy/chronic fatigue syndrome. *JCI insight* **2016**, *1*, e89376, doi:10.1172/jci.insight.89376.

42. Humer, E.; Probst, T.; Pieh, C. Metabolomics in Psychiatric Disorders: What We Learn from Animal Models. *Metab.* 2020, *10*.

43. Serretti, A.; Mandelli, L.; Lattuada, E.; Smeraldi, E. Depressive syndrome in major psychoses: a study on 1351 subjects. *Psychiatry Res.* **2004**, *127*, 85–99, doi:10.1016/j.psychres.2003.12.025.

44. Filiou, M.D.; Sandi, C. Anxiety and Brain Mitochondria: A Bidirectional Crosstalk. *Trends Neurosci.* **2019**, *42*, 573–588, doi:10.1016/j.tins.2019.07.002.

45. Liu, P.-S.; Wang, H.; Li, X.; Chao, T.; Teav, T.; Christen, S.; Di Conza, G.; Cheng, W.-C.; Chou, C.-H.; Vavakova, M.; et al. α-ketoglutarate orchestrates macrophage activation through metabolic and epigenetic reprogramming. *Nat. Immunol.* **2017**, *18*, 985–994, doi:10.1038/ni.3796.

46. Wu, N.; Yang, M.; Gaur, U.; Xu, H.; Yao, Y.; Li, D. Alpha-Ketoglutarate: Physiological Functions and Applications. *Biomol. Ther. (Seoul).* **2016**, *24*, 1–8, doi:10.4062/biomolther.2015.078.

47. Liu, S.; He, L.; Yao, K. The Antioxidative Function of Alpha-Ketoglutarate and Its Applications. *Biomed Res. Int.* **2018**, *2018*, 3408467, doi:10.1155/2018/3408467.

48. Rhoads, T.W.; Anderson, R.M. Alpha-Ketoglutarate, the Metabolite that Regulates Aging in Mice. *Cell Metab.* **2020**, *32*, 323–325, doi:https://doi.org/10.1016/j.cmet.2020.08.009.

49. Demidenko, O.; Barardo, D.; Budovskii, V.; Finnemore, R.; Palmer, F.R.; Kennedy, B.K.; Budovskaya, Y. V Rejuvant®, a potential life-extending compound formulation with alpha-ketoglutarate and vitamins, conferred an average 8 year reduction in biological aging, after an

average of 7 months of use, in the TruAge DNA methylation test. *Aging (Albany. NY).* **2021**, *13*, 24485–24499, doi:10.18632/aging.203736.

50. Califf, R.M. Biomarker definitions and their applications. *Exp. Biol. Med. (Maywood).* **2018**, *243*, 213–221, doi:10.1177/1535370217750088.

51. Balog, J.; Sasi-Szabó, L.; Kinross, J.; Lewis, M.R.; Muirhead, L.J.; Veselkov, K.; Mirnezami, R.; Dezső, B.; Damjanovich, L.; Darzi, A.; et al. Intraoperative tissue identification using rapid evaporative ionization mass spectrometry. *Sci. Transl. Med.* **2013**, *5*, 194ra93, doi:10.1126/scitranslmed.3005623.

Annex I. General discussion: Methods for analysis of all risk factors

7 studies were included in the analysis and each risk factors were standardized regarding its control to be able to compare the different studies. Once the standardization was done, we work with two groups of data: (1) the whole data including controls (CON) and risk factors (RF) that is composed of 129 animals and 124 variables; (2) and a subset that includes only the RF, thus, this subset is composed of 64 animals and 124 variables.

First, unsupervised learning was performed to show how the data is distributed in the space and determine if the internal grouping in a set of unlabelled data are the samples corresponding to the same risk factor. For this purpose, we used t-distributed Stochastic Neighbour Embedding (t-SNE) instead of PCA because it is a non-linear Dimensionality reduction technique, involves hyperparameters such as perplexity, can handle outliers and is a non-deterministic or randomised algorithm.

Once the data has been visualized with unsupervised learning, we proceed to use a supervised learning technique to be able to interpret our data and see which biomarkers are the most influential in separating the different groups. For this purpose, the Random Forest classifier was used that is a machine learning method that creates decision trees on randomly selected data samples, obtains a prediction from each tree, and selects the best solution. It is also a good indicator of the feature importance so that we can obtain the most important biomarkers in predicting the presence of the different risk factors. In this case, only the RF's subset was used, thus 51 animals were used for training the model and 13 for test it. To increase the model transparency and explain the output of our random forest model (trained with rodent data), we have used the SHAP (SHapley Additive exPlanations) values. SHAP values interpret the impact of having a certain value for a given variable in comparison to the prediction we had make if that variable took the baseline value.

Annex II. General discussion: results analysis

Supplementary figure 1. Individual SHAP value for the gut dysbiosis individual tested in the random forest. This plot evaluates each prediction indicating the output value, the base value and the features that push the prediction higher (red), and those pushing the prediction lower (blue). In this case the gut dysbiosis (GD) rodent is predicted to be associated to hypertension (HT) with higher output value followed by carbohydrate dysfunction (CD) and hyperlipidemia (HL). This plot shows the importance of each variable in the prediction in which it is observed that the difference between the prediction and the real value is minimal: (1) the two factors are favoured in the prediction by alpha-ketoglutarate and glycerol; (2) the predicted risk factor is also pushed by DG 36:4 and SM 34:2 and decreased by 34:2 and PC 34:1; (3) the real value is favoured by DG 34:2. Thus, the main differences in the prediction are associated to DG 34:2 and DG 36:4. Abbreviations: SM, sphingomyelin; DG, diacylglycerol; PC, phosphatidylcholine; LPC, lysophospholipid.

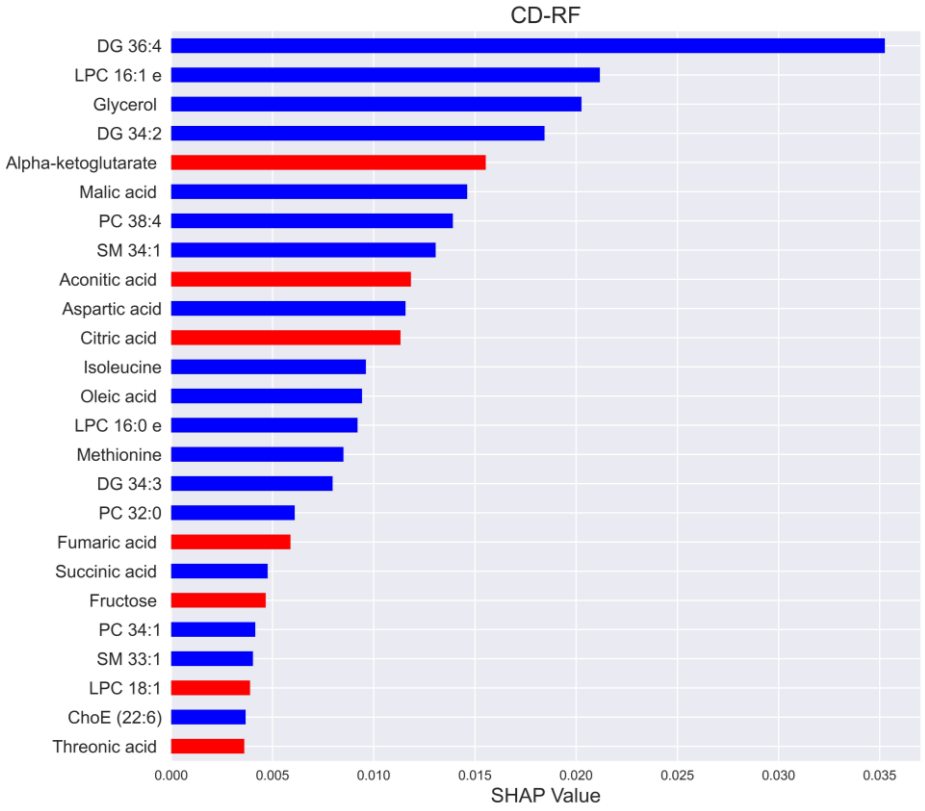

Supplementary figure 2. Variable importance of random forest (SHAP values) for carbohydrate dysfunction (CD-RF). The 25 variables with the highest SHAP values are represented in the figure that can further show the positive and negative relationships of the variables. It demonstrates the following information: (1) feature importance: variables are ranked in descending order; (2) impact, the horizontal location shows whether the effect of that value is associated with a higher or lower prediction. The red colour means a biomarker is positively correlated with the target variable. The blue colour means a biomarker negatively correlated. Abbreviations: DG, diacylglycerol; LPC, lysophospholipid; PC, phosphatidylcholine; SM, sphingomyelin; ChoE, cholesterol ester.

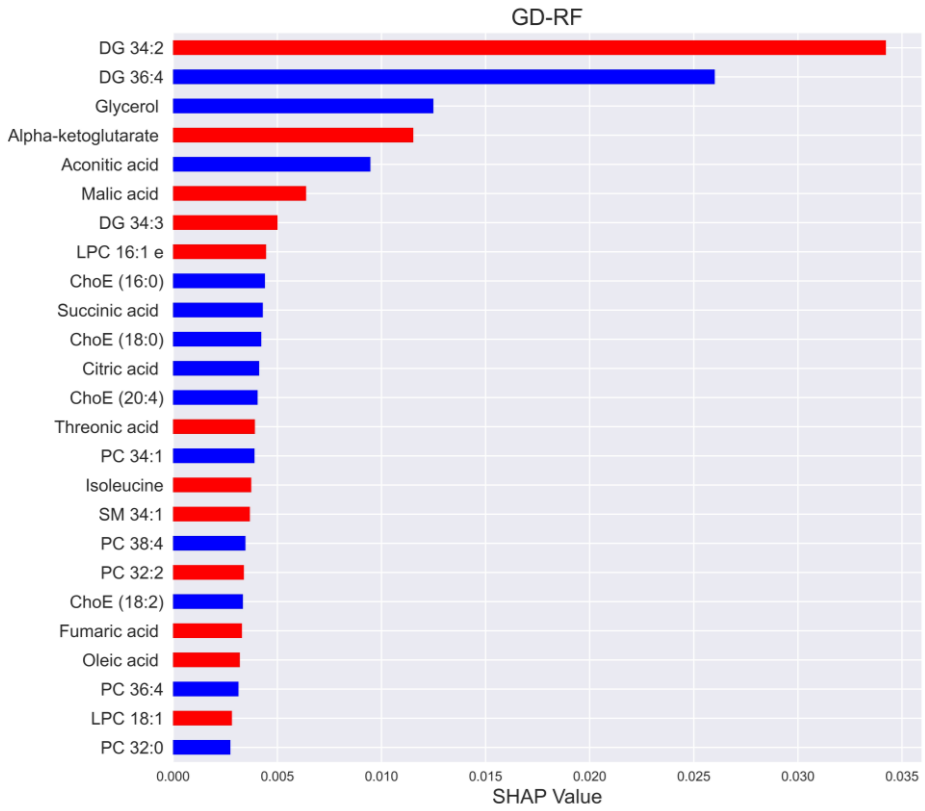

Supplementary figure 3. Variable importance of random forest (SHAP values) for gut dysbiosis (GD-RF). The 25 variables with the highest SHAP values are represented in the figure that can further show the positive and negative relationships of the variables. It demonstrates the following information: (1) feature importance: variables are ranked in descending order; (2) impact, the horizontal location shows whether the effect of that value is associated with a higher or lower prediction. The red colour means a biomarker is positively correlated with the target variable. The blue colour means a biomarker negatively correlated. Abbreviations: DG, diacylglycerol; LPC, lysophospholipid; ChoE, cholesterol ester; PC, phosphatidylcholine; SM, sphingomyelin.

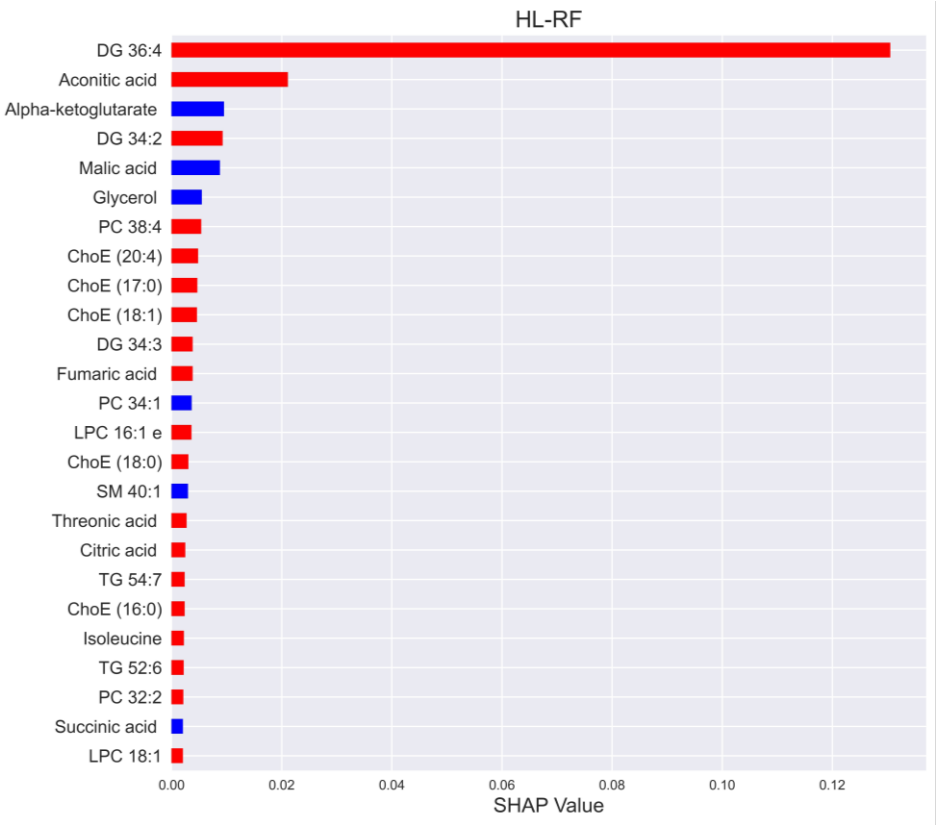

Supplementary figure 4. Variable importance of random forest (SHAP values) for hyperlipidaemia (HL-RF). The 25 variables with the highest SHAP values are represented in the figure that can further show the positive and negative relationships of the variables. It demonstrates the following information: (1) feature importance: variables are ranked in descending order; (2) impact, the horizontal location shows whether the effect of that value is associated with a higher or lower prediction. The red colour means a biomarker is positively correlated with the target variable. The blue colour means a biomarker negatively correlated. Abbreviations: DG, diacylglycerol; PC, phosphatidylcholine; ChoE, cholesterol ester; LPC, lysophospholipid; TG, triacylglycerol.

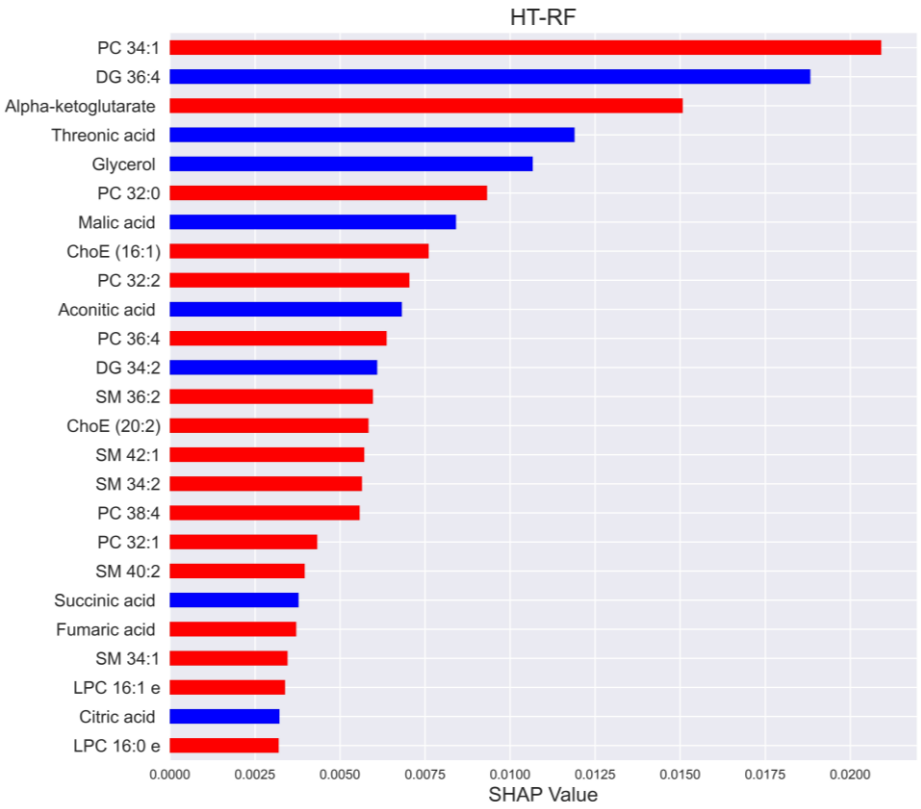

Supplementary figure 5. Variable importance of random forest (SHAP values) for hypertension (HT-RF). The 25 variables with the highest SHAP values are represented in the figure that can further show the positive and negative relationships of the variables. It demonstrates the following information: (1) feature importance: variables are ranked in descending order; (2) impact, the horizontal location shows whether the effect of that value is associated with a higher or lower prediction. The red colour means a biomarker is positively correlated with the target variable. The blue colour means a biomarker negatively correlated. Abbreviations: DG, diacylglycerol; PC, phosphatidylcholine; ChoE, cholesterol ester; LPC, lysophospholipid; TG, triacylglycerol.

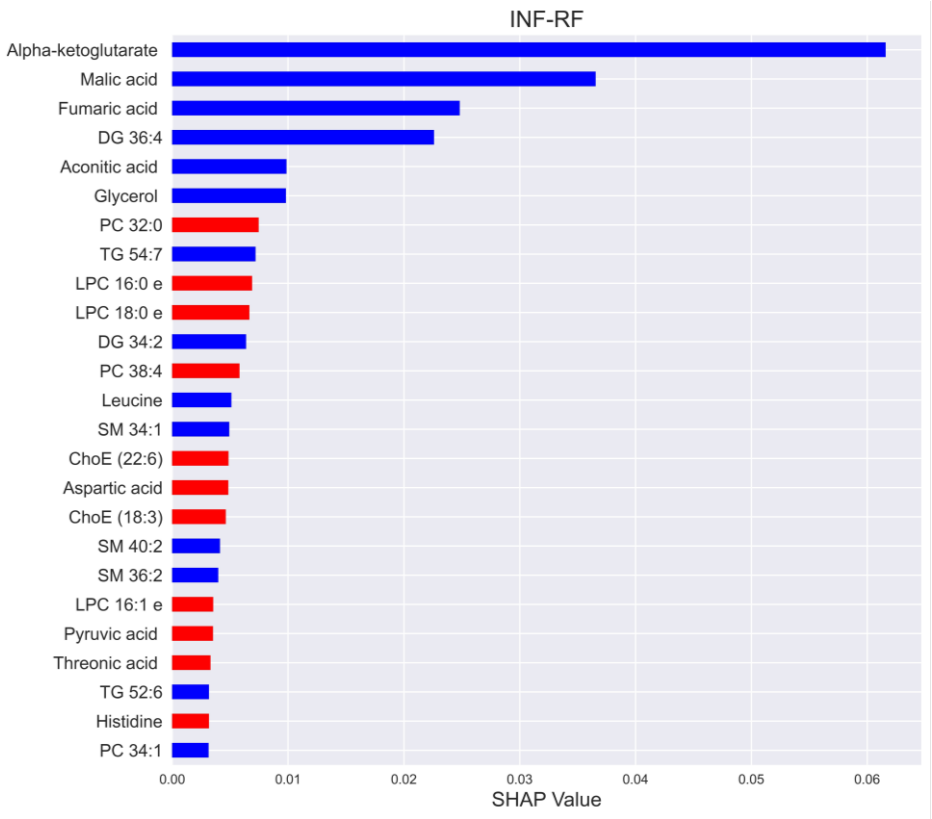

Supplementary figure 6. Variable importance of random forest (SHAP values) for inflammation (INF-RF). The 25 variables with the highest SHAP values are represented in the figure that can further show the positive and negative relationships of the variables. It demonstrates the following information: (1) feature importance: variables are ranked in descending order; (2) impact, the horizontal location shows whether the effect of that value is associated with a higher or lower prediction. The red colour means a biomarker is positively correlated with the target variable. The blue colour means a biomarker negatively correlated. Abbreviations: DG, diacylglycerol; PC, phosphatidylcholine; TG, triacylglycerol; LPC, lysophospholipid; SM, sphingomyelin; ChoE, cholesterol ester.

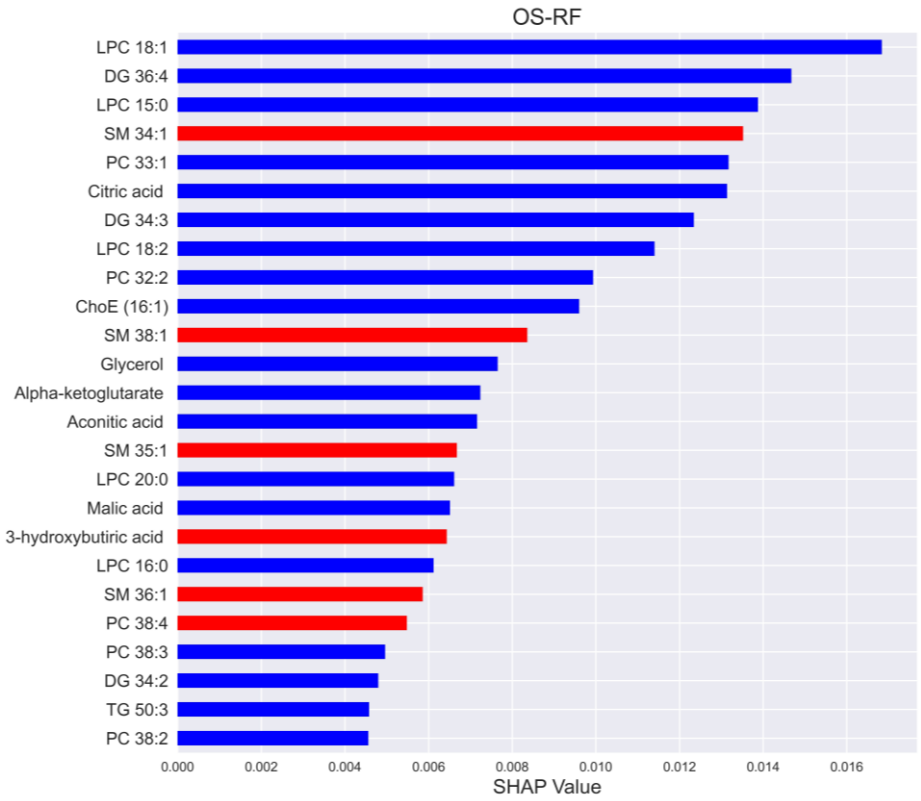

Supplementary figure 7. Variable importance of random forest (SHAP values) for oxidative stress (OS-RF). The 25 variables with the highest SHAP values are represented in the figure that can further show the positive and negative relationships of the variables. It demonstrates the following information: (1) feature importance: variables are ranked in descending order; (2) impact, the horizontal location shows whether the effect of that value is associated with a higher or lower prediction. The red colour means a biomarker is positively correlated with the target variable. The blue colour means a biomarker negatively correlated. Abbreviations: LPC, lysophospholipid; DG, diacylglycerol; SM, sphingomyelin; PC, phosphatidylcholine; ChoE, cholesterol ester; TG, triacylglycerol.

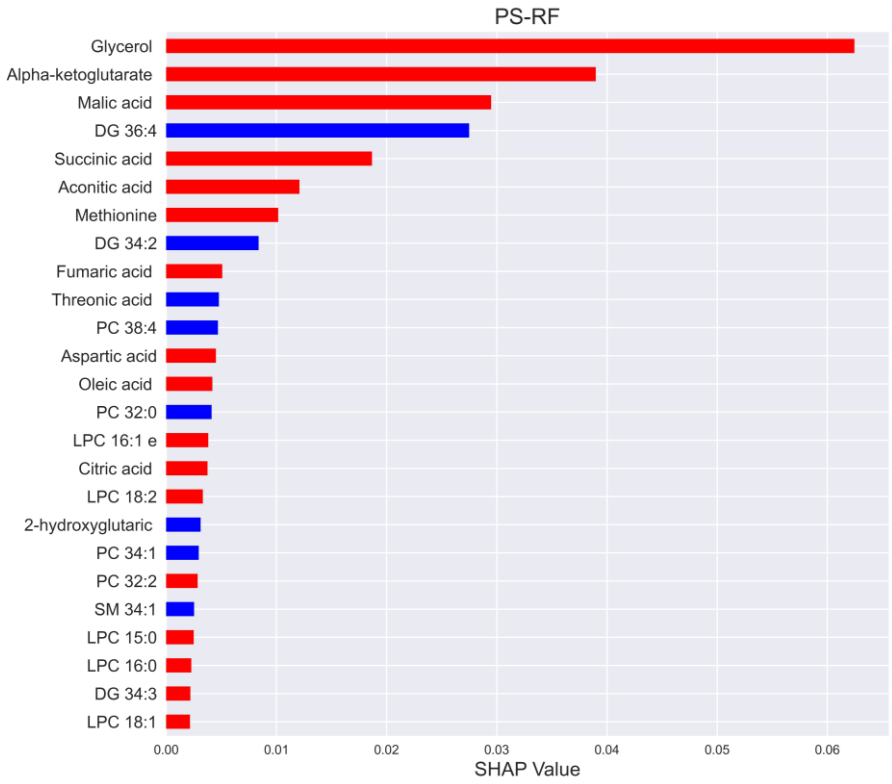

Supplementary figure 8. Variable importance of random forest (SHAP values) for psychological stress (PS-RF). The 25 variables with the highest SHAP values are represented in the figure that can further show the positive and negative relationships of the variables. It demonstrates the following information: (1) feature importance: variables are ranked in descending order; (2) impact, the horizontal location shows whether the effect of that value is associated with a higher or lower prediction. The red colour means a biomarker is positively correlated with the target variable. The blue colour means a biomarker negatively correlated. Abbreviations: DG, diacylglycerol; PC, phosphatidylcholine; LPC, lysophospholipid; SM, sphingomyelin.

UNIVERSITAT ROVIRA I VIRGILI
MULTI-OMICS BIOMARKERS OF METABOLIC HOMEOSTASIS OF RISK FACTORS ASSOCIATED TO NON-COMMUNICABLE DISEASES
Julia Hernandez Baixauli

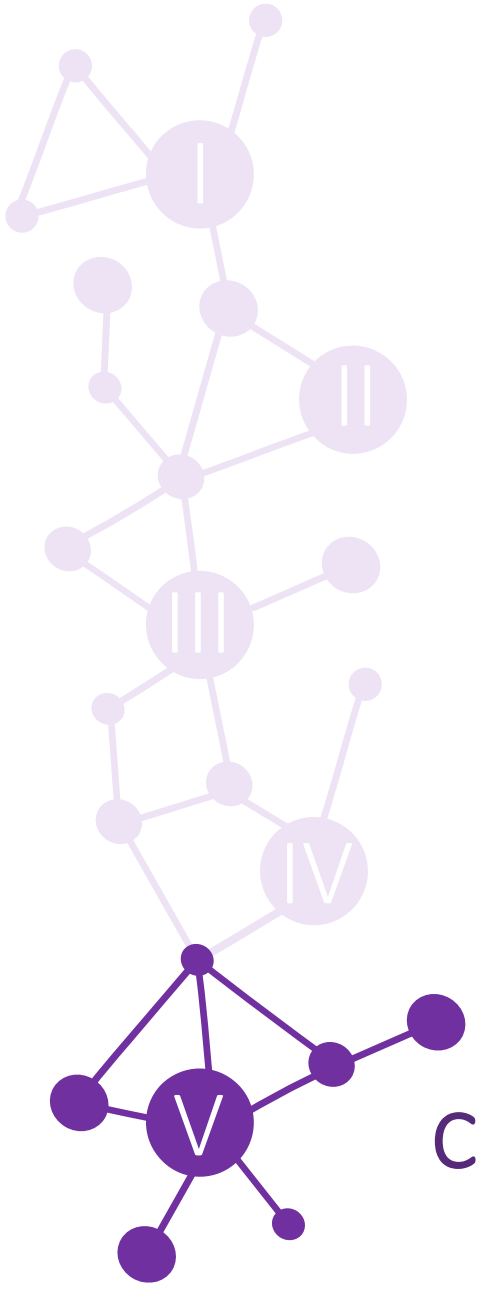

Conclusions

UNIVERSITAT ROVIRA I VIRGILI
MULTI-OMICS BIOMARKERS OF METABOLIC HOMEOSTASIS OF RISK FACTORS ASSOCIATED TO NON-COMMUNICABLE DISEASES
Julia Hernandez Baixauli

V. Conclusions

- **The different rodent models based on the overarching processes present the targeted characteristics for each risk factor and different omic profiles.** These include the deregulation of carbohydrate metabolism, lipid metabolism, hypertension, and gut dysbiosis, as representative of metabolic stress; chronic inflammation; oxidative stress and psychological stress.

- **Hyperlipidaemia** has been induced by a single IP injection of 150 mg/kg of P407 in male Wistar rats. This model is characterized by elevated levels of TGs and TC that confirms the state of dyslipidaemia. In addition to the total levels of TGs and TC, specific lipids are altered in the metabolic profile of hyperlipidaemia (TGs, PCs, LPCs, DGs, and ChoEs) in plasma.

- SHR and its normotensive control (WKY) have been selected to establish the **hypertension** rodent model. Being threonic acid and several lipids (SMs, PCs, LPCs and ChoEs) characteristics of the hypertension's metabolic profile of this model.

- **Gut dysbiosis** has been achieved through the transference of gut microbiota from obese to non-obese male Wistar rats. The study of the metabolome, in an obesity-associated gut dysbiosis model, provides a relevant way for the discrimination on the different biomarkers in the obesity onset that are characterised by lipid alteration being DG 34:2 a key discriminative feature.

- **Chronic Inflammation** has been established by IP and intermittent injections with saline solution or increasing LPS concentrations (0.5, 5 and 7.5 mg/kg) thrice a week for 31 days in male Wistar rats. The chronicity of inflammation throughout the study has been evaluated by the monitoring of MCP-1, and other inflammatory biomarkers confirming the inflammation state at the endpoint. The leading metabolites implicated in the current model are TCA cycle intermediates (i.e., alpha-ketoglutarate, aconitic acid, malic acid, fumaric acid and succinic acid); specific lipids (ChoEs, LPCs and PCs); and glycine that is related to one-carbon (1C) metabolism. Those metabolites point out to mitochondrial metabolism through TCA cycle, β-oxidation of FFA and 1C metabolism, as interconnected pathways revealing the metabolic effects of chronic inflammation induced by LPS administration.

- **Oxidative stress** has been caused by intraperitoneal administration of PQ (15 and 30 mg/kg) that is characterized by high amounts of H_2O_2 in male Wistar rats. The metabolic profile is highlighted by 3-hydroxibutiric acid, SMs and LPCs that are altered in a dose-dependent manner in all groups, thus those metabolites could be considered key features for monitoring mitochondrial oxidative stress.

- **Psychological stress** has been studied in a 3d CUMS rodent approach in male Wistar rats that aims to focus on the early stress period of a well-established depression model. The metabolic profiling suggests alteration in threonic acid

metabolism and TCA cycle as important pathways in early stress. Specifically, threonic acid, malic acid, alpha-ketoglutarate, succinic acid and cholesterol are key metabolites that could serve as key potential biomarkers in plasma metabolome of early stages of stress.

- **Lipids present specific features for each risk factor and stand out as a potential source of biomarkers of metabolic profiling.** Across risk factors, DGs are the determined lipids with the greatest impact on metabolic profiles. Specifically, DG 36:4 and DG 34:2 are the common features that links arachidonic acid metabolism with different risk factors.

- **TCA cycle intermediates, as well as playing a major role in energy metabolism, have emerged as potential biomarkers for inflammation, oxidative and psychological stress.** Thus, TCA cycle intermediates play an important role controlling physiology and disease through the regulation of homeostasis alteration. In fact, mitochondria disruption is attributed to these risk factors due to TCA cycle is the central metabolic pathway of mitochondria. Specifically, alpha-ketoglutarate is one of the most promising intermediates as a biomarker due to its multiple roles in mitochondrial metabolism.

- **The establishment of a metabolic profile is plausible and feasible through predictive models that allow the study of metabolic dysregulation representative of overarching processes.** In this work, the model of 7 risk factors is built by applying a predictive model capable of differentiating between their unique characteristics that make them distinguishable from each other. Theoretically, the model could be tested with problem individuals, and it could be determined to which group they pertain. Thus, this work provides a profile of metabolites that may be able to differentiate between risk factors for possible prevention through personalised nutrition or treatment.

V. Conclusions

- **Els diferents models de rosegadors basats en els processos generals presenten característiques de cada factor de risc i diferents perfils òmics.** Aquests inclouen la desregulació del metabolisme dels carbohidrats, el metabolisme dels lípids, la hipertensió i la dysbiosis intestinal, com a representant de l'estrès metabòlic; inflamació crònica; estrès oxidatiu i estrès psicològic.

- La **hiperlipèmia** ha estat induïda per una única injecció IP de 150 mg/kg de P407 en rates Wistar mascles. Aquest model es caracteritza per nivells elevats de TGs i TC que confirmen l'estat de la dislipèmia. A més dels nivells totals de TGs i TC, els lípids específics presenten alteracions específics en el perfil metabòlic plasmàtic (TGs, PCs, LPCs, DGs i ChoEs).

- S'han seleccionat rates SHR i el seu control normo-tensiu (WKY) per establir el model de rosegador d'**hipertensió**. L'àcid treònic i diversos lípids (SMs, PCs, LPCs i ChoEs) són característics del perfil metabòlic de la hipertensió en aquest model.

- La **dysbiosis intestinal** s'ha aconseguit mitjançant la transferència de microbiota intestinal de rates de Wistar mascles obeses a no-obeses. L'estudi del metaboloma, en el model de dysbiosis intestinal associada a l'obesitat, proporciona una forma rellevant per a la discriminació dels diferents biomarcadors a l'inici de l'obesitat, que es caracteritzen per alteració de lípids com el DG 34:2.

- La **inflamació crònica** ha estat establerta per injeccions IP, intermitents i incrementades de LPS (0,5, 5 i 7,5 mg/kg) tres cops a la setmana durant 31 dies en rates Wistar mascle. La cronicitat de la inflamació al llarg de l'estudi ha estat avaluada pel seguiment del MCP-1, posteriorment, altres biomarcadors inflamatoris que confirmen l'estat d'inflamació al punt final. Els metabòlits principals implicats en el model actual són els intermediaris del cicle del TCA (per exemple, l'alfa-cetoglutarat, l'àcid aconític, l'àcid màlic, l'àcid fumàric i l'àcid succínic), els lípids específics (ChoEs, LPCs i PCs) i la glicina relacionada amb el metabolisme d'1C. Aquests metabòlits apunten al metabolisme mitocondrial a través del cicle de TCA, l'oxidació dels FFA i el metabolisme d'1C, com a vies interconnectades que revelen els efectes metabòlics de la inflamació crònica induïda per l'administració de LPS.

- L'**estrès oxidatiu** ha estat causat per l'administració IP de PQ (15 i 30 mg/kg) que es caracteritza per altes quantitats de H2O2 en rates Wistar mascles. El perfil metabòlic es destaca per l'àcid 3-hidroxibutíric, SMs i LPC que s'alteren de manera dosi-dependent en tots els grups, de manera que aquests metabòlits es podrien considerar característiques clau per controlar l'estrès oxidatiu mitocondrial.

- L'**estrès psicològic** s'ha estudiat en un enfocament de rosegador de 3d CUMS en rates de Wistar mascles que té com a objectiu centrar-se en el període d'estrès primerenc d'un model de depressió ben establert. L'elaboració de perfils

metabòlics suggereix alteració en el metabolisme de l'àcid treònic i el cicle TCA com a rutes importants en l'estrès primerenc. Específicament, l'àcid treònic, l'àcid màlic, l'alfa-cetoglutarat, l'àcid succínic i el colesterol són metabòlits clau que podrien servir com a biomarcadors potencials clau en el metaboloma del plasma de les primeres etapes de l'estrès.

- **Els lípids presenten característiques específiques per a cada factor de risc i destaquen com una font potencial de biomarcadors del perfil metabòlic.** A través dels factors de risc, les DG són els lípids amb major impacte en els perfils metabòlics. Concretament, el DG 36:4 i el DG 34:2 són característics relacionant el metabolisme de l'àcid araquidònic amb diferents factors de risc.

- **Els intermediaris del cicle del TCA, a més de tenir un paper important en el metabolisme energètic, han sorgit com a potencials biomarcadors per a la inflamació, l'estrès oxidatiu i psicològic.** Degut a que aquests metabòlits tenen un paper important en el control de la fisiologia i la malaltia mitjançant la regulació de l'homeòstasi. De fet, un mal funcionament dels mitocondris s'atribueix a aquests factors de risc a causa d'alteracions del cicle de TCA ja que és la ruta metabòlica central dels mitocondris. En concret, l'alfa-cetoglutarat és un dels intermediaris més prometedors com a biomarcador a causa dels seus múltiples rols en el metabolisme mitocondrial.

- **L'establiment d'un perfil metabòlic és plausible i factible a través de models predictius que permeten l'estudi de la desregulació metabòlica representativa dels factors de risc.** En aquest treball, el model de 7 factors de risc es construeix aplicant un model predictiu capaç de diferenciar entre les seves característiques úniques que les fan distingibles entre si. Teòricament, el model es pot provar amb individus problema, i es podia determinar a quin grup pertanyen. Per tant, aquest treball proporciona un perfil de metabòlits que poden ser capaços de diferenciar entre factors de risc per a la possible prevenció mitjançant nutrició o tractament personalitzat.

UNIVERSITAT ROVIRA I VIRGILI
MULTI-OMICS BIOMARKERS OF METABOLIC HOMEOSTASIS OF RISK FACTORS ASSOCIATED TO NON-COMMUNICABLE DISEASES
Julia Hernandez Baixauli

Research activity

Papers included in the thesis

- **Hernandez-Baixauli J**, Quesada-Vázquez S, Mariné-Casadó R, Gil Cardoso K, Caimari A, Del Bas JM, Escoté X, Baselga-Escudero L. Detection of Early Disease Risk Factors Associated with Metabolic Syndrome: A New Era with the NMR Metabolomics Assessment. Nutrients. 2020 Mar 18;12(3):806. doi: 10.3390/nu12030806. PMID: 32197513; PMCID: PMC7146483.

- **Hernandez-Baixauli J**, Puigbò P, Torrell H, Palacios-Jordan H, Ripoll VJR, Caimari A, Del Bas JM, Baselga-Escudero L, Mulero M. A Pilot Study for Metabolic Profiling of Obesity-Associated Microbial Gut Dysbiosis in Male Wistar Rats. Biomolecules. 2021 Feb 18;11(2):303. doi: 10.3390/biom11020303. PMID: 33670496; PMCID: PMC7922951

- **Hernandez-Baixauli J**, Puigbò P, Abasolo N, Palacios-Jordan H, Foguet-Romero E, Suñol D, Galofré M, Caimari A, Baselga-Escudero L, Bas JMD, Mulero M. Alterations in Metabolome and Microbiome Associated with an Early Stress Stage in Male Wistar Rats: A Multi-Omics Approach. Int J Mol Sci. 2021 Nov 29;22(23):12931. doi: 10.3390/ijms222312931. PMID: 34884735; PMCID: PMC8657954.

- **Hernandez-Baixauli J**, Abasolo N, Palacios-Jordan H, Foguet-Romero E, Suñol D, Galofré M, Caimari A, Baselga-Escudero L, Del Bas JM, Mulero M. Imbalances in TCA, Short Fatty Acids and One-Carbon Metabolisms as Important Features of Homeostatic Disruption Evidenced by a Multi-Omics Integrative Approach of LPS-Induced Chronic Inflammation in Male Wistar Rats. Int. J. Mol. Sci. 2022, 23, 2563. https://doi.org/10.3390/ijms23052563

Other papers

- Pusceddu MM, **Hernandez-Baixauli J**, Puiggrós F, Arola L, Caimari A, Del Bas JM, Baselga L. Mediterranean natural extracts improved cognitive behavior in zebrafish and healthy rats and ameliorated lps-induced cognitive impairment in a sex dependent manner. Behav Brain Funct. 2022 Feb 25;18(1):5. doi: 10.1186/s12993-022-00190-8. PMID: 35216588; PMCID: PMC8876132.

Book Chapters

- Sergio Quesada-Vázquez*, **Julia Hernandez-Baixauli***, Elia Navarro-Masip* and Xavier Escoté [1]. NMR metabolomics for marker discovery of metabolic syndrome. Book: Biomarkers in Disease: Methods, Discoveries and Applications. Springer. **ACCEPTED.**

Conference contributions

- **Julia Hernandez Baixauli**, Miquel Mulero Abellan, Josep Maria Del Bas, Laura Baselga Escudero. PREVENTOMICS: Application of the omic technologies to detect disease risk factors for their prevention through personalized nutrition. JIPI 2019. Jornada d'Investigadors Predoctorals Interdisciplinària. 2019. Barcelona, Spain. **POSTER PRESENTATION**.

- **Julia Hernandez Baixauli**. Metabolic risk factor assessment through an integrative metabolomic approach: a personalized nutrition tool. VII Spanish Nutrition Society Young Researchers' Meeting. SOCIEDAD ESPAÑOLA DE NUTRICION. 2020. **ORAL PRESENTATION.**

- **Julia Hernandez Baixauli**, Pere Puigbó, Nerea Abosolo, Hector Palacios Jordan, Elisabet Foguet Romero, David Suñol, Mar Galofré, Antoni Caimari, Laura Baselga Escudero, Josep Maria Del Bas, Miquel Mulero. The metabolic footprint of the Short Unpredictable Variable Stress model in male Wistar rat. 43rd Annual meeting of the Spanish society of biochemistry & molecular biology. Spanish society of biochemistry & molecular biology. 2021. Barcelona, Spain. **POSTER PRESENTATION.**

UNIVERSITAT ROVIRA I VIRGILI
MULTI-OMICS BIOMARKERS OF METABOLIC HOMEOSTASIS OF RISK FACTORS ASSOCIATED TO NON-COMMUNICABLE DISEASES
Julia Hernandez Baixauli

UNIVERSITAT ROVIRA I VIRGILI
MULTI-OMICS BIOMARKERS OF METABOLIC HOMEOSTASIS OF RISK FACTORS ASSOCIATED TO NON-COMMUNICABLE DISEASES
Julia Hernandez Baixauli

Non-communicable diseases, such as obesity, metabolic syndrome, cardiovascular diseases, cancer and neurodegenerative diseases, are considered multifactorial diseases. For this reason, it has been proposed that the occurrence of these diseases is due to an imbalance of overarching processes (i.e., metabolic, inflammatory, oxidative, and psychological stress). Monitoring these overarching processes opens the door to the possibility of modulating them, and thus preventing the occurrence of different process through the design of more precise personalised interventions or treatments. However, current biomarkers of disease cannot assess early alterations that could lead to the development of disease, highlighting the need to define new biomarkers. Thus, the present work presents a characteristic metabolic signature for the detection of specific processes using omic technologies: carbohydrate dysfunction, hyperlipidaemia, hypertension and intestinal dysbiosis, as representative of metabolic stress; inflammatory stress; oxidative stress and psychological stress.